A
MATERIALS CHARACTERISATION
OF
LAMINITIC DONKEY HOOF HORN

SIMON NICHOLAS COLLINS

THESIS PRESENTED FOR THE DEGREE OF

DOCTOR OF PHILOSOPHY

DE MONTFORT UNIVERSITY

JANUARY 2004

FRONTISPIECE

"I make no apology for bringing so common a disease before your notice, because I think it is doubly important that we should be as nearly perfect as may be in those affections we meet with oftenest,

and because the pain of laminitis is of so excruciating a character and the sequela of such permanent injury to the animal, that if we can by discussion learn something ..... the night will not by any means have been spent in vain."

M. Woods, Jun. (1889)

ABSTRACT

A multidisciplinary approach was adopted to complete a comprehensive materials characterisation of the *Stratum medium* (*SM*) of laminitic donkey hoof wall. The structural organisation and material properties of the *SM* were evaluated, and the relationship between these characteristics and the radiographic anatomy of the laminitic foot were assessed. In addition, the structure-function relationships of the SM were explored and the potential effects upon hoof wall function were investigated.

New, unbiased quantitative methods for the assessment of the radiography anatomy of the foot, the structural organisation of the *SM*, and the material properties of the hoof wall were devised. In addition sophisticated computer modelling techniques were employed to assess the gross anatomic, macro- and micromechanics of the hoof wall, and investigate the potential effects of the laminitic condition. These methods were used to:-

1. Assess the radiographic anatomy of the laminitic foot and to compare this with that of the normal donkey.
2. Define the morphological and morphometric characteristics of the laminitic *SM*.
3. Evaluate resistance to deformation and energy absorption within the hoof wall.
4. Model hoof wall deformation and assess stress and strain distribution within the hoof wall in response to static loading.

The radiographic anatomy of the normal donkey foot was found to be different from that reported for the horse, in terms of the absolute values of key radiographic parameters used to define the lateromedial radiograph. The anatomy of the laminitic foot also differed from that of the normal donkey foot, and displayed a wide range of anatomical variation. Dislocation of distal phalanx (DP) was evident with the laminitic foot, however, the nature and extent of the DP dislocation varied between individual. Statistically significant differences ($P<0.05$) were recorded in the radiographic anatomy between the normal and laminitic foot. Multivariate statistical analysis techniques indicated a two-fold categorisation of the laminitic donkey based upon the anatomy of the foot, and in particular, the nature of the of the DP dislocation. Laminitic Group 1 was characterised by capsular rotation and/or DP dislocation, whereas Group 2 was characterised by phalangeal rotation. Statistically significant differences in the radiographic anatomy of the foot were recorded between laminitic sub-groups, and between these sub-groups and the normal donkey foot.

The *SM* of the laminitic donkey hoof wall was found to consist of three morphologically distinct zones across the dorso-palmar hoof wall depth (HWD), based upon differences in the structural organisation of the tubular and intertubular horn.

This zonation pattern divided the *SM* into:

- *Z*1 the outer region of the *SM*
- *Z*2 the middle region of the *SM*
- *Z*3 the inner region of the *SM*

The three-fold zonation pattern differed from that previously reported for the horse in respect of the relative dorso-palmar depth of the respective zones. Three morphologically distinct horn tubule types were observed within the *SM* of the laminitic donkey. 'Irregularities' in the structural organisation of the *SM* were also observed. The morphological appearance of these structural irregularities was described, and their zonal location recorded.

The morphometric characteristics of zonal structure within the *SM* of the laminitic donkey hoof wall were objectively assessed, in terms of linear and area, 'field' and 'feature' specific structural characteristics relevant to hoof wall function. Statistically significant differences were recorded between zones. Significant differences between laminitic sub-groups were evident in the morphometric characteristics of *Z*1. In particular, absolute area measurements of the horn tubules were smaller in Laminitic Group 1, and the area fraction, relative proportion, of tubular horn was lower than in Group 2.

The material properties of laminitic hoof horn were characterised. The resistance to deformation (modulus of elasticity – E) was assessed under test conditions of uniaxial compression ($_C$), for both full HWD and zonal material at maximal hydration levels. In addition, elastic strain energy absorption (Resilience) was recorded for the full HWD. The donkey hoof wall displayed a dorso-palmar decrease in zonal E_C. Significant 'between sub-group' differences were recorded in median *Z*1 E_C, with Group 1 lower than Group 2.

Computer modelling of the hoof wall, using the technique of Finite Element Analysis, indicated that the structural and material property characteristics of the *SM* affected stress and strain distribution within the hoof wall, and that the laminitic condition was associated with increased levels of stress acting upon the laminar interface.

Pearson product moment correlation, partial correlation, and linear regression analyses revealed important associations between the radiographic anatomy of the laminitic foot, and the structural organisation and material properties in Z1.

The materials characterisation presented in this thesis indicates that the laminitic condition may be associated with changes in structure and material properties that affect the normal process of force transfer within the hoof wall. Indeed predicted stress at the laminar interface may reach levels that threaten the functional integrity of the suspensory apparatus of the DP. These changes may have important consequences to the biomechanics of the foot, and directly contribute to the lameness observed in the afflicted donkey.

DECLARATION OF ORIGINALITY

This is to certify that I am responsible for the work in this thesis. The work is my own unless otherwise acknowledged. Neither this thesis nor the original work reported therein has been submitted to this nor any other institution for a higher degree. The work carried out in the Faculty of Applied Sciences at De Montfort University, Leicester and was supervised by Prof. R.J. Latham and Dr. J.D. Reilly.

Signed:	.....	Simon Nicholas Collins (Candidate)
Signed:	.....	Prof. R.J. Latham (Supervisor)
Signed:	.....	Lt. Col J.D. Reilly (Supervisor)

DEDICATION

This thesis is dedicated to the memory of my father,

Mr George Collins

And also to that

'Very Special Person'

ACKNOWLEGEMENTS

I gratefully acknowledge Dr E.D. Svendsen MBE, and the Trustees of The Donkey Sanctuary, Sidmouth, Devon for the financial sponsorship of this PhD project.

I am especially grateful for the help and assistance received from the staff at The Donkey Sanctuary, especially from:

Mr A. Trawford BVSc, MSc, MRCVS, CVMA, Director of Veterinary Studies, for his personal involvement and enthusiasm as External Advisor to this project.

Mr M. Crane BVM & S, MRCVS. for his thoughts regarding the laminitic condition in the donkey.

Mr N. Bell MA VetMB, MRCVS for his assistance, enthusiasm and perseverance in obtaining the digital radiographs used in this project.

Miss C. Morriss BSc (Hons), MSc for organising the provision of medical histories for the laminitic donkeys used throughout this study.

In addition, I would like to thank all those people whose generosity supports the work of The Donkey Sanctuary in improving the welfare and management of the donkey.

I acknowledge the foresight shown by De Montfort University (DMU) in providing the opportunity to develop a multidiseiplinary approach in this area of scientific research, especially Professor Roger Linford, who was instrumental in establishing the Hoof Research Group within the Faculty.

I thank all those people at DMU who have helped during this project, in particular:

To Professor Roger Latham for his unrelenting drive and commitment to this project, and for his loyal personal support. Above all, for believing in me, when I personally doubted myself.

To Dr John Reilly for his encouragement, passion and intellectual stimulation – a true mentor in every sense. Long may we be able to continue our 'keratinous crusade' to the benefit of all Equids.

To Dr Hugh Newlyn (Dept of Mechanical and Manufacturing Engineering), Internal Advisor to this project, for his guidance in engineering principles and the Finite Element technique, assistance with modelling and data interpretation, and also for his enthusiasm, support and friendship throughout.

To Dr Ralf Dahm (Formerly Dept of Chemistry) for the many hours spent with me, in the translation and interpretation from original German manuscripts.

To Drs Paul Hagan (Formerly Dept of Chemistry) and Nick Longford (Faculty of Computing) for introducing me to the subject of multivaraite statistical analysis.

To Dr John Williams (Dept of Textile Research) for 'letting me loose' on his Instron Material Testing Machine.

To Mike Simmonds and his staff (Lens Media Department) for their help and advise in obtaining the photomicrographs presented in this thesis.

To Rohit Tailor (Inter-Library Loans Department) for his untiring endeavours in tracing obscure references around the world.

To Brett Howard and his staff in the Faculty's Computer Node, especially Michelle Johnson, for their IT and logistical support.

To Pam Payne (IT Services) for help and assistance in achieving the final layout of this thesis.

To Yve Shaw (Former Head of Animal Sciences) for giving me the opportunity to embark upon my university studies, to Alan Lee (Head Warden) for providing the means to financially support these studies, and to Dr Daniel Milles for introducing me to Dr John Reilly during the final year of my undergraduate studies.

I would also like to express my thanks to Mr John Horrell and fellow Directors of Dodson & Horrell Ltd. for their funding of the Image Analysis System commissioned for this project.

To Bob Fleming, Roslin Research Institute Edinburgh, for help received in establishing the Image Analysis System.

To Professors Chris Pollitt (University of Queensland) and David Hood (Texas A&M) for sharing their passion, enthusiasm and knowledge.

To the members of the Biomimetics Newsgroup, in particular, to Professors Julian Vincent, John Bertram, Steven Vogel, and Stephen Wainwright, for their advice and comments during the initial planning phase of this project.

A special thank you is extended to my colleges, both past and present, within the Hoof Research Group, especially to Dr Lyn Hopegood and Teresa Hollands, for their friendship and support during the past years. I am forever indebted.

Finally I am indebted to my Mother and eldest Sister, who have provided unstinting support as I went through the 'trials and tribulations' of the PhD process. I am truly grateful.

PAGE NUMBERING AS ORIGINAL

TABLE OF CONTENTS

LIST OF APPENDICIES

LIST OF ABBREVIATIONS

AB-PAS – Alcian Blue, Periodic Acid, Schiff Reagent
AF – Area Fraction
Ang H – Angle H
Ang R – Angle R
ANOVA – Analysis of Variance

BB – Bearing Border
Bwt – Bodyweight
BM – Basement Membrane

CB – Coronary Band
CE – Cell Envelope
CET – Common Extensor Tendon
CH – Cap Horn
Co – Cortex
Co Area – Cortical Cross Sectional Area
CoAF – Cortical Area Fraction
CV – Coefficient of Variation

Da – Dalton
DDFT – Deep Digital Flexor Tendon
DHWA – Dorsal Hoof Wall Angle
DIP – Distal Interphalangeal Joint
DP – Distal Phalanx
DW – Dry Weight

E – Modulus of Elasticity
Subscripts:
C – Compressive
F – Flexural
T – Tensile
f – Fibre
m - Matrix

F – Force
FE – Finite Element
FEA – Finite Element Analysis

HPA – Hoof Pastern Axis
HWD – Hoof Wall Depth

I – Second Moment of Area
IAS – Image Analysis System
ICC – Inter Cellular Cement
IF – Intermediate Filament
IFAP – Intermediate Filament Associated Protein
IQ Range – Inter-Quartile Range
IT – Intertubular Horn

K – Stiffness

K – Moduli ratio

LF – Left Fore

MA – Major Axis
Ma – Marrow/Medulla
Ma Area – Marrow Cross Sectional Area
MaAF – Marrow Area Fraction
MC – Moisture Content
Subscripts:
0 – 0% Hydration
F – '*In vivo*' Hydration Level
M – 100% Maximal Hydration Level
RH – Relative Humidity
MCG – Membrane Coating Granule
MDC – Midline Dead Centre
MI – Minor Axis
MR – Moisture Regain
Subscripts:
0 – 0% Hydration
F – '*In vivo*' Hydration Level
M – 100% Maximal Hydration Level
RH – Relative Humidity

N – Newton
NAV – Nomina Anatomica Veterinaria
NSD – No significant Difference

P Axis – Phalangeal Axis
Pa – Pascal
PC – Principle Component
PCA – Principle Component Analysis
PcaSco – Principle Component Score
Pers Com. – Personal Communication
Pers Obs. – Personal Observation
PIP – Proximal Interphalangeal Joint

RDA – Regularised Discriminative Analysis
RF – Right Fore
ROI – Region of Interest

S – Dorsal Hoof Wall Angle
SADP – Suspensory Apparatus of the Distal Phalanx
SD – Sole Depth
sd – Standard Deviation
SE – *Stratum externum*
SI – *Stratum internum*
SM – *Stratum medium*
STTM – Soft Tissue Thickness at the Midpoint of the Dorsal Aspect of the Distal Phalanx

T – Angle of the Dorsal Aspect of the Distal Phalanx
TD – Tubule Density
Tu – Tubule

Tu Area – Tubule Cross Sectional Area
TuAF – Tubular Horn Area Fraction

U – Angle of Pastern Axis

V – Volume Fraction
Subscripts:
f – Fibre
m - Matrix

WW – Wet Weight
Subscripts:
F – '*In vivo*' Hydration Level
M – 100% Maximal Hydration Level
w/v – Weight per Volume
w/w – Weight per Weight

X – Displacement
Subscripts:
APP – Apparent
COR – Corrected
MAC – Machine
x-ray – Radiography

%CH – Percentage Capsular Height
%HWD –Percentage Hoof Wall Depth
%HWH – Percentage Hoof Wall Height
%S – Percentage Saturation
Subscript:
R – Moisture Regain

ε – Strain
Subscripts:
F – Failure
Y – Yield

σ – Stress
Subscripts:
F – Failure (Ultimate Strength)
Y – Yield (Yield Strength)

ν – Poisson Ratio

1. INTRODUCTION

1.1 GENERAL INTRODUCTION

Degenerative conditions of the foot are a major cause of lameness within the donkey population in the UK (Crane 2001), and hence constitute an area of particular management and welfare concern (Whitehead *et al.* 1991). Despite this fact, little is known about the impact of these conditions upon the anatomical organisation of the foot or its functionality. Due to the stoical nature of the donkey and the absence of overt signs of pain (Trawford and Crane 1995, Mathews *et al.* 1997), these conditions are often not detected until an advanced stage of degenerative change (Trawford 1999 – Pers Com.).

The evolution of the family *Equidae* during the Tertiary period was marked by adaptive changes that enabled the equids to exploit the plains environment (MacFadden 1988, Bennett 1980, 1992). These changes included the specialisation of the appendicular skeleton and its associated musculature, especially within the distal limb and foot (Hildebrand 1987, MacFadden 1988, Bennett 1980, 1992). Foremost amongst these anatomical adaptations were the: -

- Emergence of a perissodactyl organisation within the foot, following the progressive reduction in the digit number to a single digit or distal phalanx (MacFadden 1988)
- Development of an unguligrade stance (Bennett 1992), in which the entire bodyweight acts through the hoof capsule via the distal phalanx (DP)

These adaptive, cursorial changes (see Figure 1.1) have afforded the family *Equidae* considerable biomechanical advantage (Hildebrand 1959, 1987, Bennett 1992). These have, in part, enabled the equids to develop outstanding athletic qualities of stamina and speed, characterised by the ability to stand for long periods, traverse long distances and accelerate rapidly over short distances (Thomason *et al.* 1992). All of these have been central to the survival of the genus (Bolliger 1991). In this respect, Reilly *et al.* (1996) asserted that the equids represent a pinnacle of evolutionary selection.

Concurrent increases in height and bodyweight have, however, placed significant biomechanical demands upon the musculoskeletal system of the limb and the foot in particular (Leach 1990a). The foot represents the functional platform for 'athletic' performance (Balch *et al.* 1991, 1997). Hence it must possess the ability to accommodate and ultimately resist the forces associated with static and dynamic loading (Douglas 1994). Any loss of functional capability within the foot may directly result in gross anatomical lesions, secondary infection, and/or degenerative changes, leading to pain and ultimately lameness (Geyer and Tagweker 1986).

Bridges (1752), recognised not only the importance of the foot to the well-being of the horse, but also the debilitating consequences of disruption to its functional integrity, simply stated:

"No foot no horse."

The donkey has adapted to thrive in arid environments, browsing upon sparse, low quality vegetation and travelling many miles each day often over abrasive surfaces, in search of food (Seegmiller and Ohmart 1981, Groves 1986, Svendsen 1995). In this way, hoof growth and wear are compensatory, and the biomechanical forces acting on the foot are maintained in 'optimal' balance.

In contrast, domestication in Northern Europe places the donkey in a moist temperate environment, restricted to small paddocks, and with access to lush vegetation (Crane 2002a). This raises concerns as to whether the donkey is adaptive to the prevailing conditions of the temperate grassland environment (Collins *et al.* 2002). These management conditions can result in dietary overload, increased bodyweight and overgrown feet. All of which are recognised as potential risk factors associated with degenerative conditions of the equid foot (Eley 1998, Alford *et al.* 2001). In fact there is a tendency for donkeys in this country to be more prone to problems of the foot than in their native environment (Trawford 1997 - Pers. Com, Crane 2000, 2002a).

Laminitis is one such degenerative condition of the foot, which can lead to acute and/or chronic lameness in the affected animal. Hunt (1991) stated that of the wide array of equid diseases, laminitis was:

….. "among the most devastating and permanently crippling"

The prevalence of laminitis in this country is in marked contrast with the low prevalence levels in the donkey's native environment reported by Bolbol and Saleh (1987). Fowler (1995) and Reilly (1997) have interpreted this difference in terms of a lack of evolutionary adaptation to the temperate environment. Conversely Crane (1998 - Pers Com., 2000, 2002b) and Eley (1998) have suggested that the high prevalence of the condition may be related to the longevity of donkeys in the UK which has lead to the emergence of a significant geriatric population. Crane (2001, 2002a,b) argued that laminitis may form part of a natural degenerative foot/hoof syndrome directly related to the ageing process.

Figure 1.1 The Perissodactyl organisation of the unguligrade equid digit. (After Banks 1993)

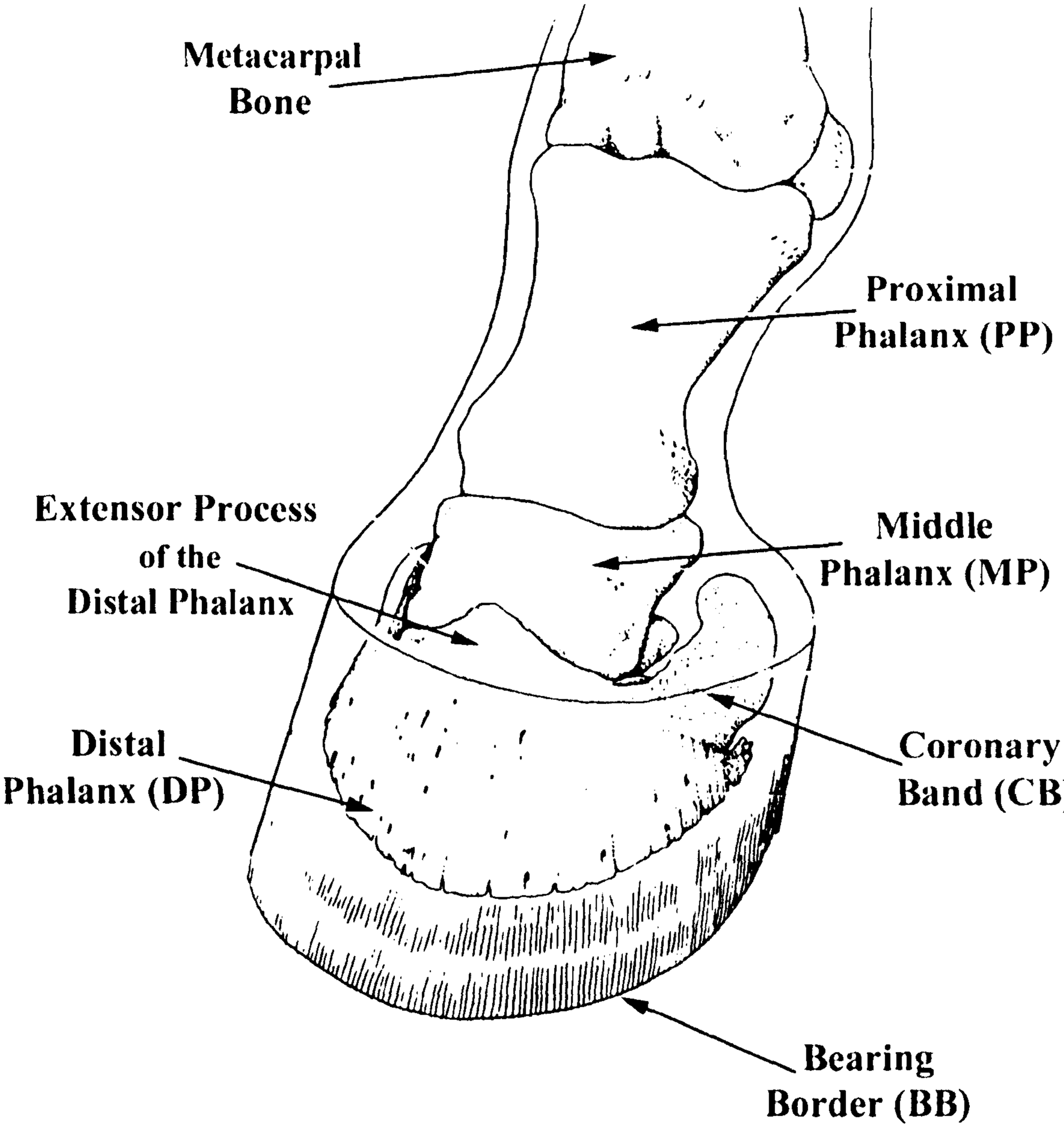

This may be of particular significance as it is widely accepted that laminitis is a predisposing cause of other problems of the foot (Weaver 1971, Bradley *et al.* 1989) including haemorrhage, sole ulcers (Nilsson 1963), hoof wall separation, and white line disease (Redden 1990). Hence the laminitic condition represents a significant threat to the donkey population within temperate grassland environments.

Despite the fact that the donkey accounts for ~36% of the worldwide domestic equine population, with global numbers estimated at 48 million (F.A.O. Database - 2001), little information exists regarding the laminitic condition in this species (Mostafa 1988, Walker *et al.* 1995). As a consequence of the paucity of information relating to this species, Svendsen (1995) stated that there has been a tendency to:

"view the *donkey as a small horse.*"

Hence diagnostic and therapeutic strategies have tended to be based upon the assumption of an equine model. However Collins *et al.* (2002) stressed the importance of recognising that the donkey and horse are two distinct equid species. Indeed mitochondrial DNA analysis by George and Ryder (1986), Ishida *et al.* (1995) and Xu *et al.* (1996) suggest that evolutionary divergence occurred between these two equid species approximately 3-10 million years ago.

Collins *et al.* (2002) have highlighted anatomical differences between the two species throughout the distal limb, and hence questioned the validity of applying an equine model to the distal limb of the donkey without further research. Indeed French (2000) and Collins *et al.* (2002) were of the opinion that the donkey must be viewed as a unique equid.

1.2 BIOMECHANICS OF THE EQUID FOOT

The biomechanical demands placed upon the equid foot are immense (Leach 1980). During locomotion, the foot strikes the ground with great force and frequency. Quddus *et al.* (1978) reported ground reaction forces (GRF) in the horse of ~ 9000 Newton during gallop. That is equivalent to approximately twice the animal bodyweight. The GRF develops during a stance, when the foot is in contact with the ground, of ~0.1 sec (Geary 1975), and occurs at a frequency of up to 120 strides per minute (Lekeux and Art 1994). Therefore the foot must be capable both of withstanding and dissipating high velocity shock waves (Dyhre-Poulson *et al.* 1994), and facilitating the smooth and painless cyclic transmission of forces between the ground and the axial skeleton (Leach 1980, Bertram and Gosline 1986). This must be achieved without damage to the sensitive structures of the foot (Leach 1980). Indeed, Pollitt (1990b) stated that in achieving this, evolution has produced in the equid foot:

" a miracle of bioengineering."

However despite the biomechanical importance of the equid foot our knowledge of the way in which it achieves these objectives is limited, as indeed is our understanding of those factors that directly affect its finer functioning (Bragulla *et al.* 1992, Reilly 1995, Reilly *et al.* 1996).

1.2.1 HOOF FUNCTION – AN OVERVIEW

The importance of the fully functioning hoof capsule to the well being of the equid has long been recognised. Indeed Xenophon in ~300 BC stated:

"Just as a house would be good for nothing If it were very handsome above but lacked the proper foundations, so too a horse if he had bad feet (sic- hooves): for he could not use one of his fine points."

The anatomical organisation of the unguligrade foot is such that the hoof capsule must: -

- Support the axial skeleton (Budras *et al.* 1989)
- Provide locomotive traction (Hickman and Humphrey 1987)
- Withstand high velocity ground impacts (Thomason *et al.* 1992)
- Transfer loading forces and absorb energy (Leach 1980)
- Resist excessive wear (Reilly 1995)
- Possibly allow controlled cracking (Reilly *et al.* 1996, 1998)
- Regenerate itself, so that wear is compensated by hoof horn formation (Hahn *et al.* 1986)
- Protect against infectious agents (Budras *et al.* 1998a)
- Prevent excessive moisture loss (Emery *et al.* 1987)
- Assist in venous blood return (Pollitt 1995)
- Contribute to the thermoregulation of the foot (Pollitt 1992)

Commenting upon these issues, Reilly (1995) stated that all equids are therefore totally reliant upon the hoof capsule for effective locomotion.

1.2.2 HOOF QUALITY

There has been a tendency within the scientific literature to assess the hoof in terms of 'horn quality' (Vermunt and Greenough 1995). Dietz and Prietz (1981) stated that 'claw quality' was determined by the 'degree of resistance' to imposed mechanical demands, with 'deficiencies' in the hoof being indicative of 'poor quality' hoof horn.

The implication of this is that 'horn quality' is not a finite property, and that variation exists. Greenough (1982, 1985), Reilly and Kempson (1992), and Bragulla *et al.* (1992) stated that

'horn quality' was influenced by genetic, nutritional, and management factors, and also by disease status.

Although various references to hoof 'quality' are to be found within the scientific literature, it has not been defined precisely in objective terms. Hence its use is both arbitrary and highly subjective, and also lacks the required scientific basis of definition, and means of characterisation.

Politiek *et al.* (1986) recognised the need to determine a scientific basis for the characterisation of 'claw quality', and consequently defined high 'claw quality' as that which displayed a '*low susceptibility to claw disorders*'. Although this definition did not fully resolve this issue it did however, draw attention to the significance of structure-function interactions. Reilly and Kempson (1992) were the first to attempt to define quality in terms of structure-function relationships, stating that:

"Good quality horn is that which allows proper function to be fulfilled. Whereas, poor quality hoof horn is that which does not fulfil its function and leads to structural and functional weakness."

These authors argued that it was essential to identify those measurable and repeatable hoof horn characteristics that represent normality, and establish how these were related to hoof horn quality, in terms of objective measures of the hoof's functional capabilities.

By achieving this, Reilly and Kempson (1992) stated that subjective term 'quality' could be replaced by an objective means of hoof horn assessment based upon precisely defined and measurable hoof horn characteristics. However establishing such measures poses a particular intellectual challenge.

1.2.3 STRUCTURE-FUNCTION INTERACTIONS

Vogel and Wainwright (1969) highlighted the importance of structure to function in biological materials and argued that an intimate and intrinsic inter-relationship exists. In this regard they stated that:

"Structure without function is a corpse, and function without structure is a ghost."

The implication of this statement is far reaching. It implies that the integrated functioning of an organ is inextricably linked to its structural organisation. Thus the means by which functionality is achieved can only be realistically assessed with a thorough knowledge of structural organisation. In addition, changes in structural organisation will affect the functionality of an organ.

Hence a detailed investigation of structure-function inter-relationships will afford a valuable insight into the design hierarchy of the hoof, and thereby provide a better understanding of hoof

function. This will in turn form a basis of understanding from which the impact of pathological change can be assessed.

1.3 THE ANATOMY OF THE EQUID FOOT

1.3.1 NOMENCLATURE

The anatomical nomenclature, presented in italics throughout this review, follows the convention advocated by Nomina Anatomica Veterinaria (Anon 1994).

1.3.2 OVERVIEW

The equine foot (See Figure 1.2) is a highly evolved locomotor organ (Bolliger 1991, Reilly *et al.* 1996). It has a complex three-dimensional structure and consists of a 'horny capsule' (*ungula*), which encases bones, joints, ligaments, tendons, bursae, nerves, blood vessels, and connective and fatty tissues (Schummer *et al.* 1981, Dyce *et al.* 1987). The integument or outer layer of the foot displays the same basic three-fold anatomical structure as common integument (*Integumentum commune*) seen elsewhere in the body (Schummer et al. 1981).

This consists of the subcutis, the dermis and the epidermis (Trautmann and Fiebiger 1957, Schummer *et al.* 1981). The hoof capsule itself is a highly modified structure of epidermal origin (Dellman 1971, Talukar *et al.* 1972, Budras *et al.* 1995).

1.3.3 THE SUBCUTIS

The subcutis of the foot is of variable thickness. It is expansive at the height of the coronary band (CB) and deep to the frog, where it forms the perioplic and coronary cushion, and the digital cushion, respectively. These cushions adjoin the periosteum of the distal phalanx (DP) or pedal bone (Trautmann and Fiebiger 1957, Budras *et al.* 1995). In certain parts of the equid foot however, the subcutis is very thin or absent.

1.3.4 THE CORIA OF THE FOOT AND THE TOPOGRAPHICAL MODIFICATION OF THE DERMIS

The dermis of the foot is a highly vascular and innervated tissue composed of collagenous material rich in elastic fibres. It forms a continuation of the common dermis of the skin (Dyce *et al.* 1987). Although the dermis of the foot forms a continuous structural unit, it can be divided topographically into 6 regions, namely the perioplic, coronary, laminar or parietal, bulbar, solear and frog coria (Trautmann and Fiebiger 1957, Schummer *et al.* 1981).

Figure 1.2 Sagittal section of the equid foot to show the anatomical relationship between the osseous and exosseous structures of the foot (Modified after Geyer 1980, Bolliger 1991).

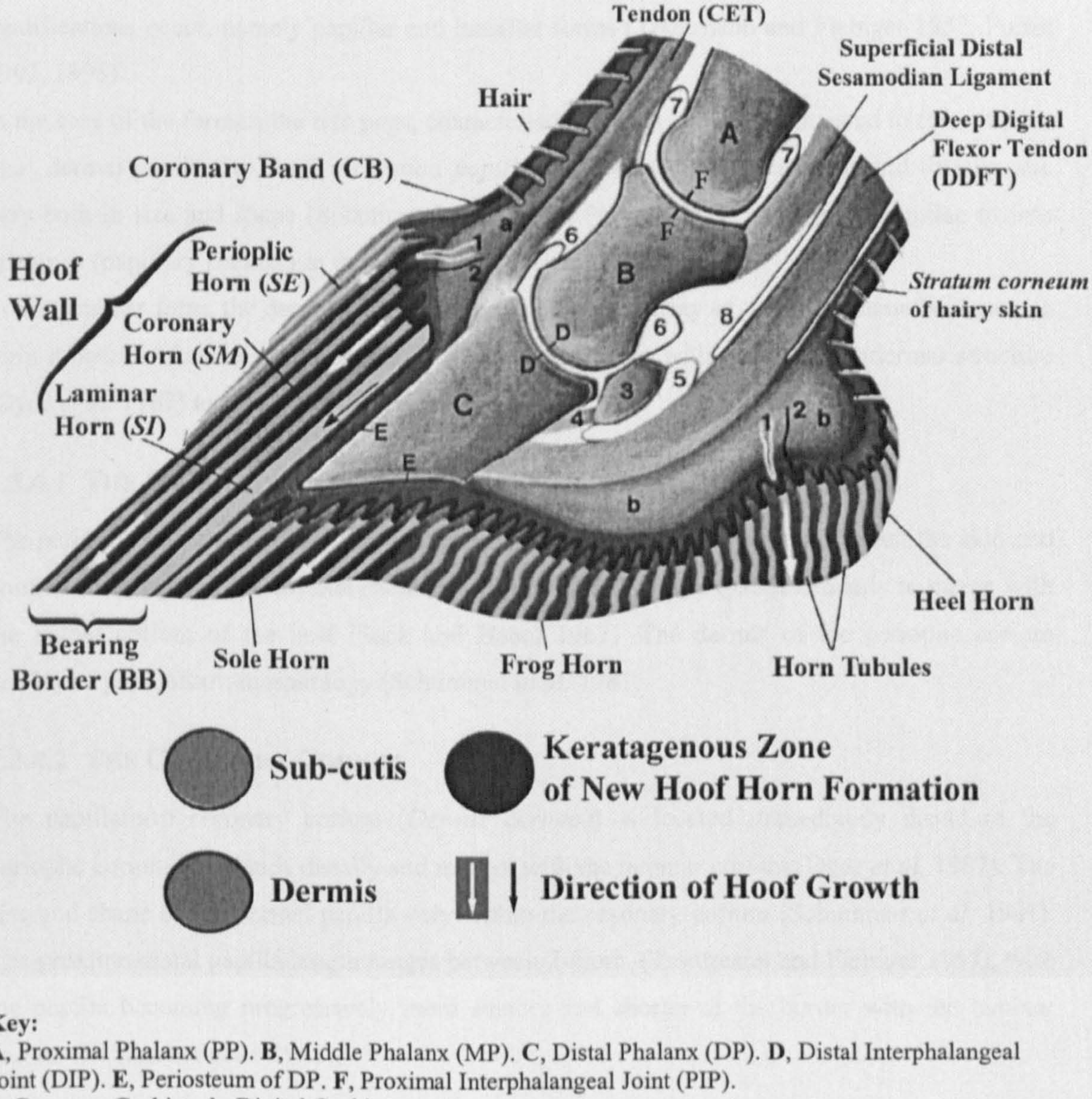

Key:

A, Proximal Phalanx (PP). **B**, Middle Phalanx (MP). **C**, Distal Phalanx (DP). **D**, Distal Interphalangeal Joint (DIP). **E**, Periosteum of DP. **F**, Proximal Interphalangeal Joint (PIP).

a, Coronary Cushion. **b**, Digital Cushion.

1, Blood Vessels. **2**, Nerves. **3**, Navicular Bone. **4**, T Ligament. **5**, Bursa. **6**, DIP Joint Capsule. **7**, PIP Joint Capsule. **8**, Tendon Sheath.

It is the topographical division of the dermis that the German anatomists, including Budras *et al.* (1995, 1998a), Budras and Patan (2003), Paton and Budras (2003), and Bragulla (2003) refer to as the 'segment-specific' nature of the dermis of the foot. Where present, the underlying subcutis merges into the dermal layer. Elsewhere, the dermis directly overlies the periosteum of the DP (Dyce *et al.* 1987, Budras *et al.* 1995).

The dermis of the foot is highly modified (Dyce *et al.* 1987). Two distinct morphological modifications occur, namely papillar and lamellar forms (Trautmann and Fiebiger 1957, Pollitt 1992, 1995).

In the case of the former, the rete pegs, characteristic of thick skin, are elongated to form 'finger like' dermal papillae to form a *Stratum papillare*. These dermal papillae extend distally and vary both in size and shape (Schummer *et al.* 1981, Pollitt 1992). The dermal papillae fit into openings (papillary sockets) in the subjacent epidermal structure.

In the lamellar form, the dermis is organised into a parallel array of 'leaf like' lamella planes, to form a *Stratum laminae*. The dermal lamellae interdigitate with subjacent epidermal structure (Dyce *et al.* 1987) to form the *Stratum lamellatum*.

1.3.4.1 The Perioplic Corium

The perioplic corium (*Dermis limbi*) forms a narrow band at the junction between the skin and hoof, at the height of the coronet (Schummer *et al.* 1981). This expands caudally to merge with the bulbar corium of the heel (Sack and Habel 1967). The dermis of the perioplic corium displays a papillaform morphology (Schummer *et al.* 1981).

1.3.4.2 The Coronary Corium

The papillaform coronary corium (*Dermis coronae*) is located immediately distad to the perioplic corium. It extends distally and merges with the laminar corium (Dyce *et al.* 1987). The size and shape of the dermal papilla vary within the coronary corium (Schummer *et al.* 1981). The proximo-distal papilla length ranges between 2-6mm. (Trautmann and Fiebiger 1957), with the papilla becoming progressively more slender and shorter at the border with the laminar corium (Schummer *et al.* 1981).

1.3.4.3 The Laminar Corium

The laminar (parietal) corium (*Lamellae dermalis parietis*) is continuous, proximally, with the coronary corium, and distally, with the solear corium (Schummer *et al.* 1981). The laminar corium can be divided morphologically into a deep, *Stratum reticulare* and a peripheral, *Stratum laminae*.

The *Stratum reticulare* has been referred to as sub-lamellar connective tissue by Pollitt and Daradka (1998), and the submural dermis by Hood (1999a). The *Stratum reticulare* is a highly vascular connective tissue, comprising an extracellular matrix of collagen and elastin (Pellmann 1995, Westerfeld 2003).

The *Stratum laminae* is characterised by the presence of dermal lamellae which are arranged in a proximo-distal direction, from the proximal junction with the coronary corium to the distal junction with the solear corium. There are approximately 600 primary lamellae present in the horse's foot, (Leach 1980, Dyce *et al.* 1987). Each primary lamella is invaginated in a proximo-distal direction to form ~100-200 secondary lamellae. The secondary lamellae arise distad to the proximal limit of the primary lamella (Leach 1980, Budras *et al.* 1989). This complex modification of the laminar corium serves to significantly increase the surface area of the dermo-epidermal (laminar) interface.

Proximally, at their boundary with the coronary corium, the primary lamellae appear as shallow ridges (Schummer *et al.* 1981). These lamellae increase rapidly in height in the proximal third of the corium attaining a height of ~ 4mm. (Budras *et al.* 1989). Distally, accessory (Budras *et al.* 1985) or cap (Hirschberg *et al.* 2001) papillae (*Papillae dermalis galeares*) arise from the apical crest of the primary laminae (Dirks 1985). The distal margin of each primary lamella is also marked by the presence of terminal papillae (*Papillae termalis parietis*) (Trautmann and Fiebiger 1957, Pollitt 1992, 1995).

1.3.4.4 The Coria of the Sole, Frog and Bulbs of the Heels

The respective coria of the sole (*Dermis soleae*), the frog (*Dermis cunei*), and the bulbs of the heel (*Dermis tori*) each exhibit papillaform modification of the dermis (Trautmann and Fiebiger 1957, Schummer *et al.* 1981).

1.3.5 THE BASEMENT MEMBRANE

The dermis is separated from the overlying epidermis by the basal membrane (BM) or basal lamina (Pollitt 1994). This anatomical structure forms the dermo-epidermal junction within the integument (Alberts *et al.* 1994). A dense matrix of fibres connects the basal membrane to the periosteum of the DP, thereby forming a cohesive bond that attaches the integument to the appendicular skeleton (Pellmann 1995, Pellmann *et al.* 1997).

1.3.6 THE EPIDERMIS

A single layer of epidermal basal cells or keratinocytes, that is, the *Stratum basale* or *Stratum germinativum* covers the basal membrane (Stump 1996, 1967, Leach 1980). These cells are anchored to the basal membrane by means of hemidesmosomal attachments (Budras *et al.* 1989,

Pollitt 1992). These basal cells are in turn, linked to each other by desmosomes, to form a cohesive germinative cell layer (Leach 1980). In this way the various anatomical structures of the foot are united into a single functional entity via the basement membrane. This association which Pollitt (1992, 1994) referred to as the hoof / pedal bone (*sic* distal phalanx – DP) bond, forms the Suspensory Apparatus of the Distal Phalanx (Müller 1936, Pellmann 1995) and is discussed in detail in Section 1.6.

1.3.7 HOOF HORN FORMATION

Cell division within this basal layer results in proliferative hoof horn formation or growth (Stump 1996, 1967). The subsequent processes associated with the terminal differentiation of the keratinocyte results in the production of a fully keratinized, mature hoof horn cell or corneocyte (Bragulla *et al.* 1992). It is this process of cornification that ultimately gives rise to the formation of the hoof capsule.

The differentiation, maturation and eventual atresia of the keratinocyte are associated with a complex series of biochemical processes, in which a sequential expression of structural and matrix molecules occurs within the cell (Leach 1980, Grosenbaugh and Hood 1992, Bragulla *et al.* 1992). These events lead to a progressive changes in the morphological appearance of the keratinocyte and in the nature of the intercellular attachments (Mülling 1993, Mülling *et al.* 1994a,b,c).

These processes are thought to directly influence cellular strength and rigidity, and the level of intercellular cohesion, and hence contribute to the mechanical properties of the epidermis (Mülling *et al.* 1994b).

Bowden *et al.* (1987) and Suter *et al.* (1997) have extensively reviewed these processes within the mammalian epidermis. Whereas the pioneering work of Larsson *et al.* (1956), Ekfalck (1991) and Wattle (1998, 2000, 2001) have specifically investigated the biochemistry associated with equid hoof horn formation in both the normal, and the laminitic states.

The cornification processes can be summarised as: -

- Synthesis and assembly of intracellular keratin proteins to form a cytoskeletal structure of Intermediate Filaments – the process of Keratinization
- Synthesis and exocytosis of membrane coating granules (MCG)
- Formation of Intercellular cement (ICC)
- Formation of the cell envelope (CE)

It is important to note that cornification and keratinization are not synonymous terms. Keratinization refers only to those metabolic process involved in the formation and assembly of the cytoskeleton. Conversely, the process of cornification refers to all process involved in the

formation of the corneocyte. Thus keratinization represents one component of the cornification process.

At the cellular level, the cornification processes result in the formation of several morphologically distinct layers or strata (see Figure 1.3).

Basal cells mitosis gives rise to a population of undifferentiated daughter cells within the immediate suprabasal layers of the epidermis. As these cells undergo terminal differentiation, they are progressively removed from the suprabasal layer by ongoing cellular proliferation within the stratum basale (Leach 1980). This results in the formation of a zone of cornification (Larsson *et al.* 1956) or keratagenous zone (Ekfalck 1991). Cells at different levels within this zone are at different stages of cellular maturation and appear as morphologically distinct layers or strata (Leach 1980).

In those regions of the hoof characterised by the presence of 'hard' horn three such layers occur. These are: -

- The *Stratum basale* and its immediate suprabasal layer of daughter cells
- The *Stratum spinosum*
- The *Stratum corneum*

However in those region of the hoof where 'soft horn' is generated, for example, the periople, an additional layer is present, namely the *Stratum granulosum*. This layer is found between that of the *Stratum spinosum* and the *Stratum corneum* (Leach 1980).

In the manner described above, the events associated with the cornification processes combine to produce a highly keratinised and cohesive cellular solid. The cornification process serves both to strengthen the individual keratinocyte and establish a cohesive functional hoof unit with structural integrity (Bolliger 1991). Indeed, Galvin *et al.* (1989) and Fuchs (1993) stated that the protective function of the epidermis is generally dependent upon the cellular arrangement within the epidermis, and the cytoskeletal network present with the horn cells.

The mature hoof horn cell or corneocyte representing the material basis of the hoof capsule.

The hoof, in common with all epidermal structures, is dependent upon the underlying dermis to support hoof horn formation (Leach 1980). The metabolic processes associated with hoof horn formation are supported by diffusion from the vascular dermal tissues across the basal membrane (Leach 1980, Bolliger 1991, Bragulla *et al.* 1992). The modification of the dermis increases the surface area available for diffusion (Pollitt 1992). Indeed the dermal tissues of the foot are highly vascular with extensions of the capillary network reaching deep into both the papillae and lamellae (Mishra and Leach 1983a,b, Pollitt and Molyneux 1990, Hirschberg *et al.* 2001).This anatomical organisation significantly reduces the diffusion distance to the metabolically active epidermal layers (Bragulla *et al.* 1992, Budras *et al.* 1998a).

Figure 1.3 Diagrammatic representation of the process of hoof horn formation. (Modified after Reilly 2001).

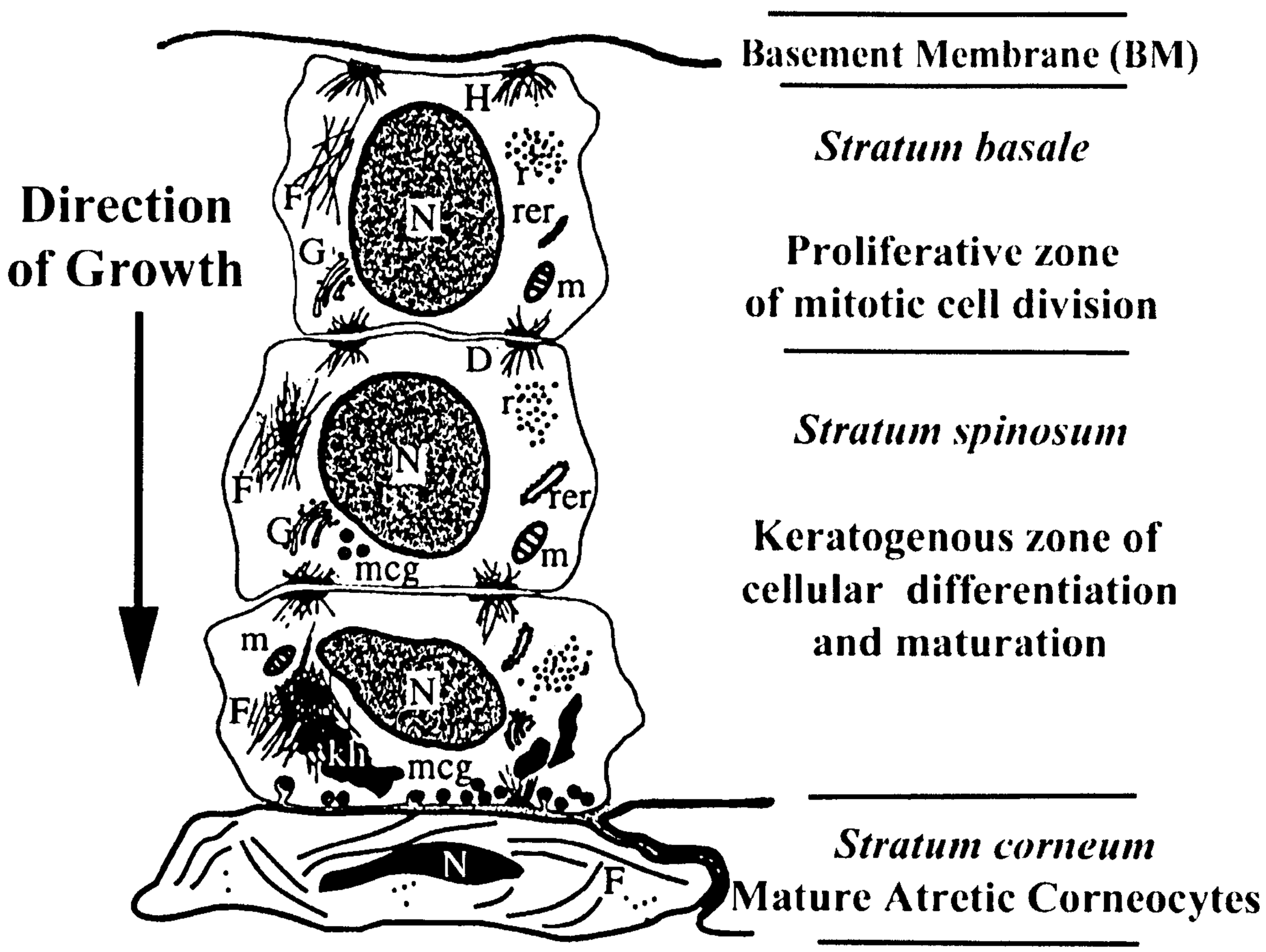

Key:
F, Keratin filaments. **G**, Golgi apparatus. **H**, Hemidesmosomes. **N**, Nucleus.
kh, Ketatahyaline granules. **m**, Mitochondria. **mcg**, Membrane coating granules. **r**, Ribosomes.
rer, Rough endoplasmic reticulum.

The BM is also thought to play a critical role in horn formation. Recent work has suggested that the BM is vital for mediating controlled and co-ordinated epidermal growth (Pollitt 2002- Pers Com.). In addition, the BM form the spatial template by which the structural organisation of the epidermis is maintained (Pollitt 1994)

1.4 THE STRUCTURAL ORGANISATION OF HOOF HORN MATERIAL

The modification of the dermis into papillar and lamellar forms gives a distinct structural organisation to the hoof horn material within the capsule (Fleming 1871, Mettam 1896, Trautmann and Feibiger 1957, Schummer *et al.* 1981). The intimate relationship that exists between the modification of the dermis, and its associated vascular supply, and also, the structural organisation of the hoof horn material which they support are illustrated in Figures 1.4, 1.5, 1.6 and 1.7.

1.4.1 PAPILLAFORM MODIFICATION OF THE DERMIS

Papillaform modification of the dermis gives rise to the formation of tubular and intertubular horn fractions (Chauveau 1853, Bruhnke 1931, Nickel 1938a,b, 1939, Trautmann and Feibiger 1957). Each horn tubule consists of a central marrow or medullary cavity surrounded by a cellular cortex, and the individual horn tubules are separated by intertubular horn (Tautmann and Fiebiger 1957, Banks 1993, Schummer at al 1981).

Hoof horn formation from the basal epidermal cells overlying the dermal papillae produces the individual horn tubules, whilst that from the basal cells within the interpapillary regions gives rise to the intertubular horn fraction (Chauveau 1853, Fleming 1871, Nickel 1938a,b, 1939, Banks 1993) – see Figure 1.4. Horn Formation from the basal cells overlying the apical papillary tip (the suprapapillary region) produces the tubule marrow, whereas the tubule cortex is generated by horn formation from the walls of the papillae (the peripapillary region). These two horn components combine with the intertubular horn fraction, distad to the apical tip of the papillae, to form the structural organisation of tubular and intertubular horn.

As the hoof horn material is moved progressively distad to the *Stratum papillare*, diffusion deficiencies occurring in the suprapapillary region may adversely affect the cornification of the marrow horn cells (Budras *et al.* 1998a). The resultant loss of cellular cohesion within the marrow can lead to cell shrinkage and degradation, with the formation of a central void or medullary cavity, within the horn tubule (Trautmann and Fiebiger 1957, Geyer and Leu 1984, Budras *et al.* 1998a).

1.4.2 LAMELLAFORM MODIFICATION OF THE DERMIS

Horn formation from the basal epidermal cells overlying different topographical regions of the dermal lamellae give rise to three distinct hoof horn components (Budras *et al.* 1989, Reilly *et al.* 1998b) – see Figure 1.5. These are: -

- The Laminar Horn of the epidermal lamellae (LH)
- The Cap Horn of the epidermal lamellae (CH)
- The Terminal Horn - interlaminar or interdigitating horn of the epidermal lamellae (TH)

Figure 1.4 Diagrammatic representation of the papillarform modification of the dermis and the associated microcirculation, that supports tubular and intertubular horn production. (After Collins and Reilly 2004a, modified after Banks 1993).

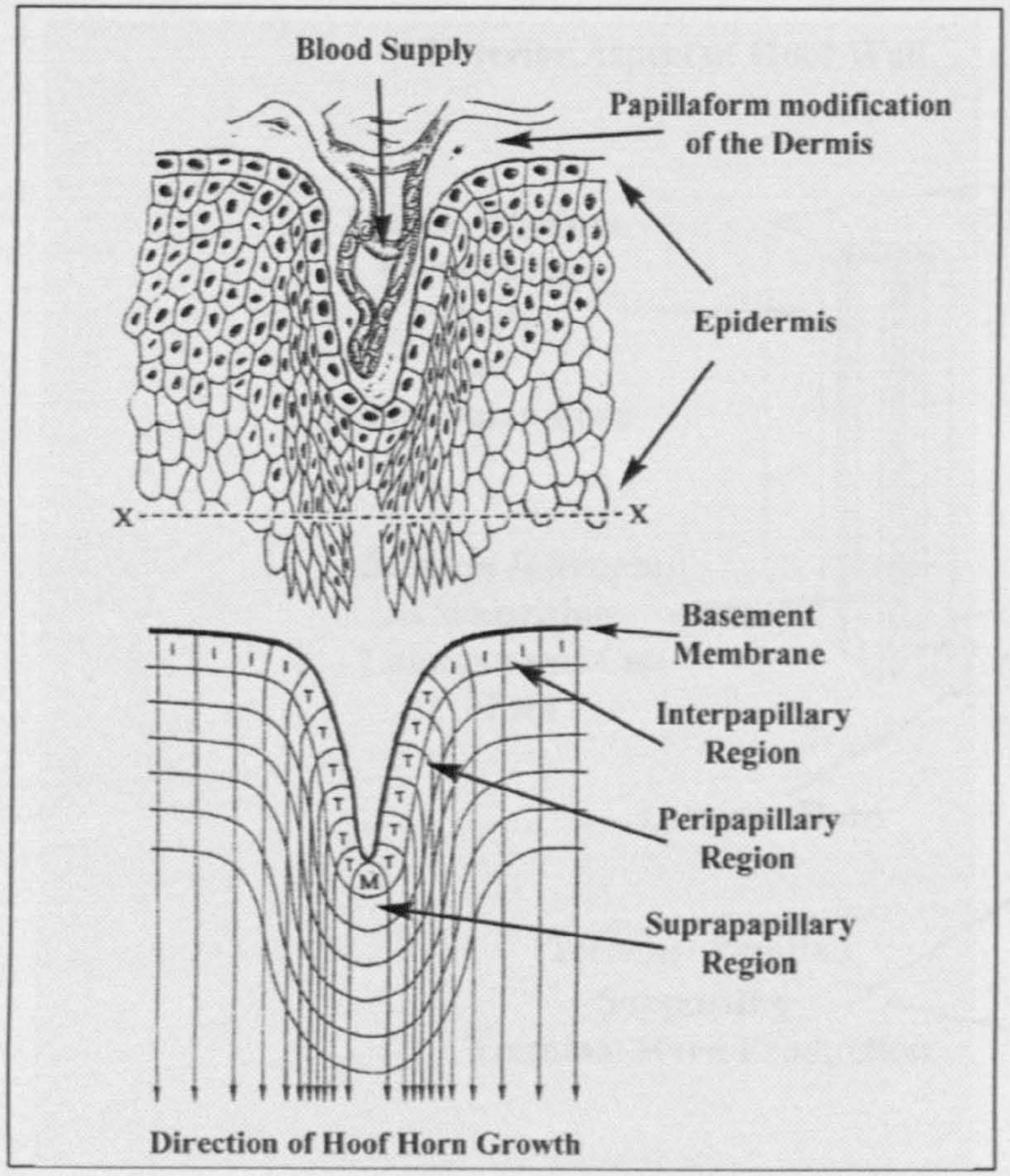

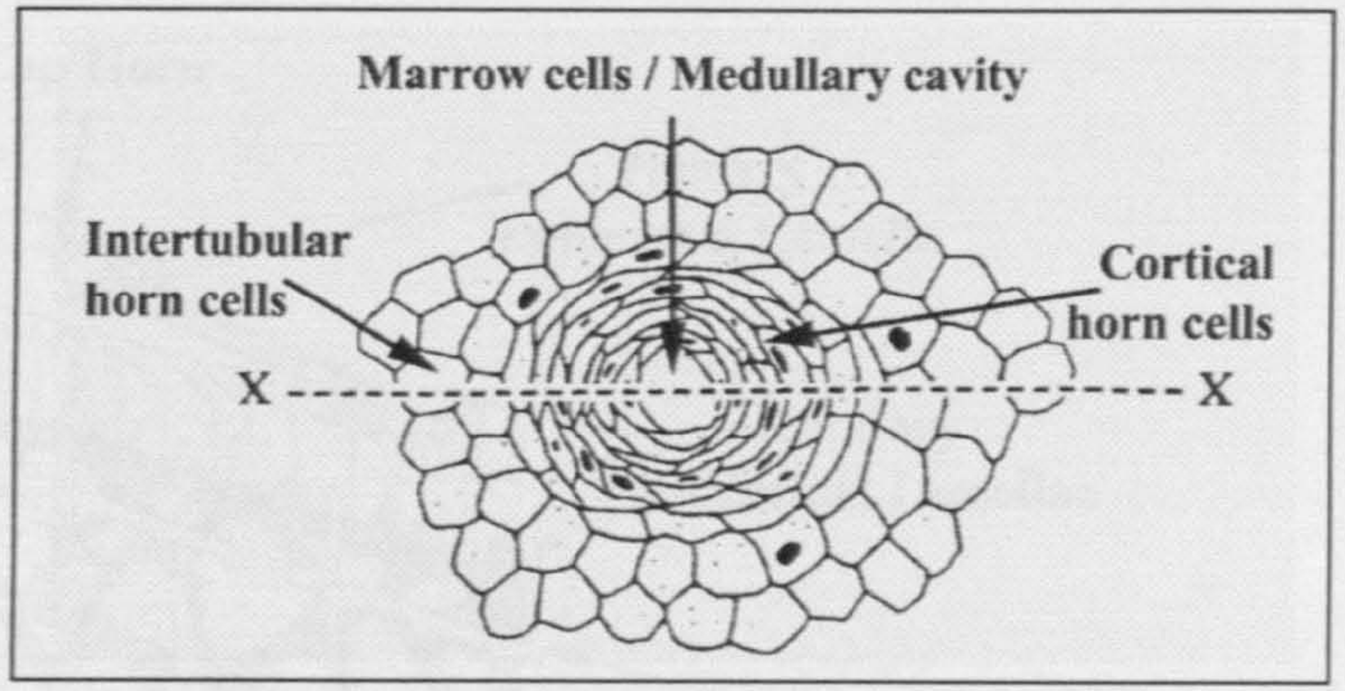

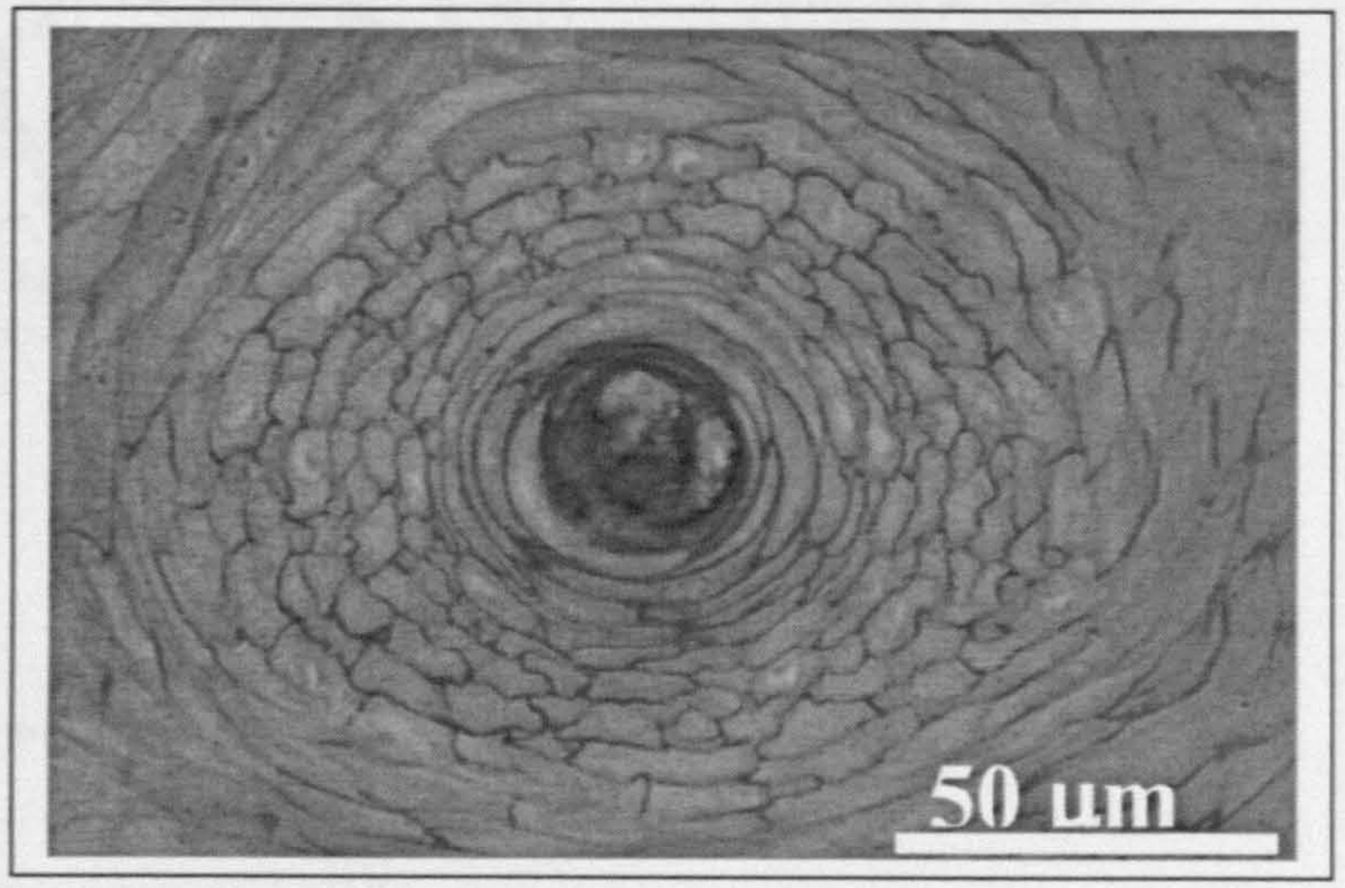

Key: A. Longitudinal section through the dermo-epidermal junction to show papillaform modification of the dermis, papillar microcirculation, basement membrane and epidermis. Schematic of hoof horn production in longitudinal section, to show the production of the intertubular horn fraction, and the marrow and cortical horn components. **B**. Transverse section to show the structural organisation of the tubular and intertubular horn fractions. **C**. Photomicrograph of the tubular and intertubular horn fractions in the donkey hoof wall.

Figure 1.5 Diagrammatic representation of the lamellarform modification of the dermis and its associated microcirculation that supports laminar, cap and terminal horn production. (Modified after Pollitt and Molyneux 1990).

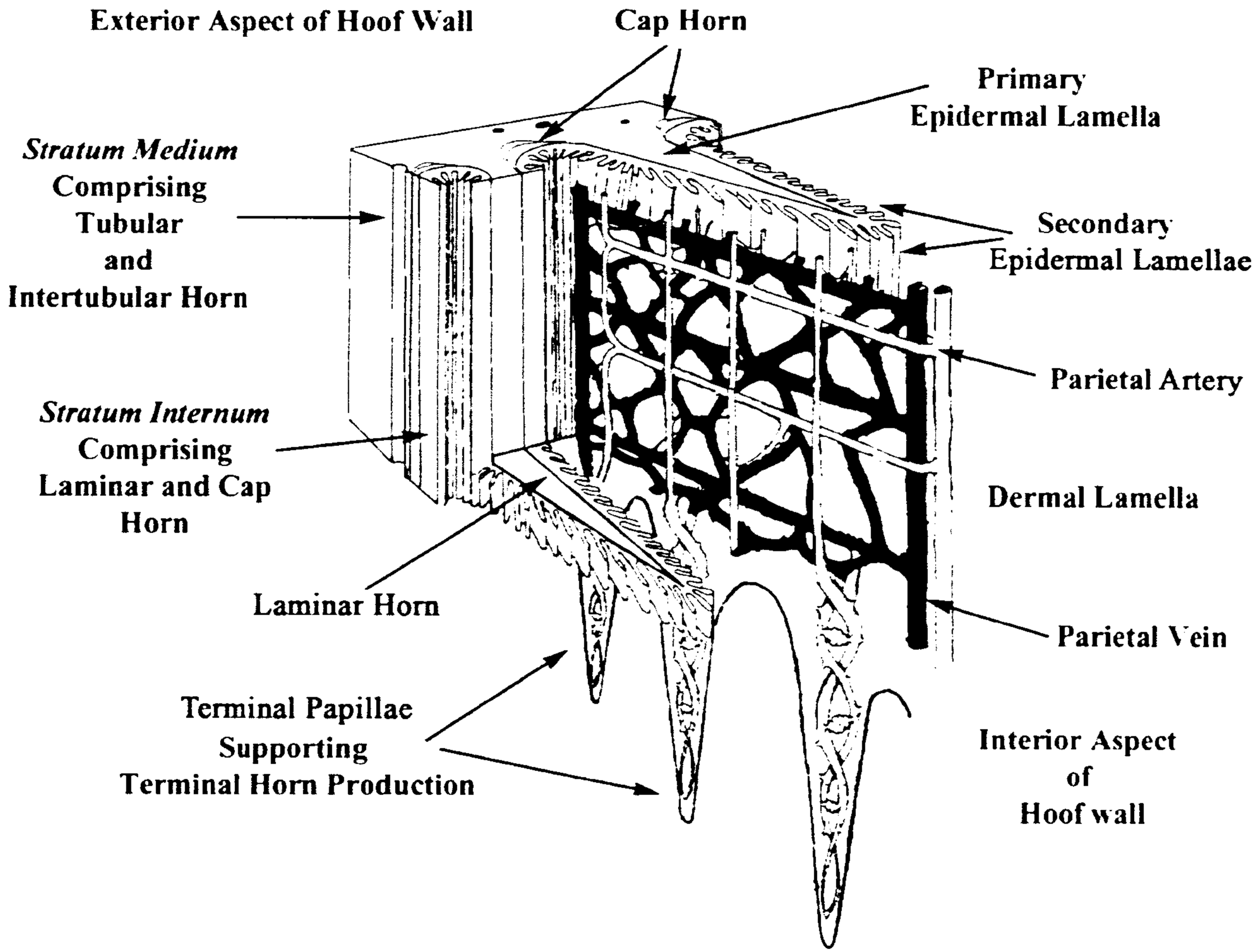

Figure 1.6 Anatomical organisation of the coronary and laminar coria and the horn components of the hoof wall which they support (Adapted after Pollitt 2001, Pollitt 2002 – Pers Com.).

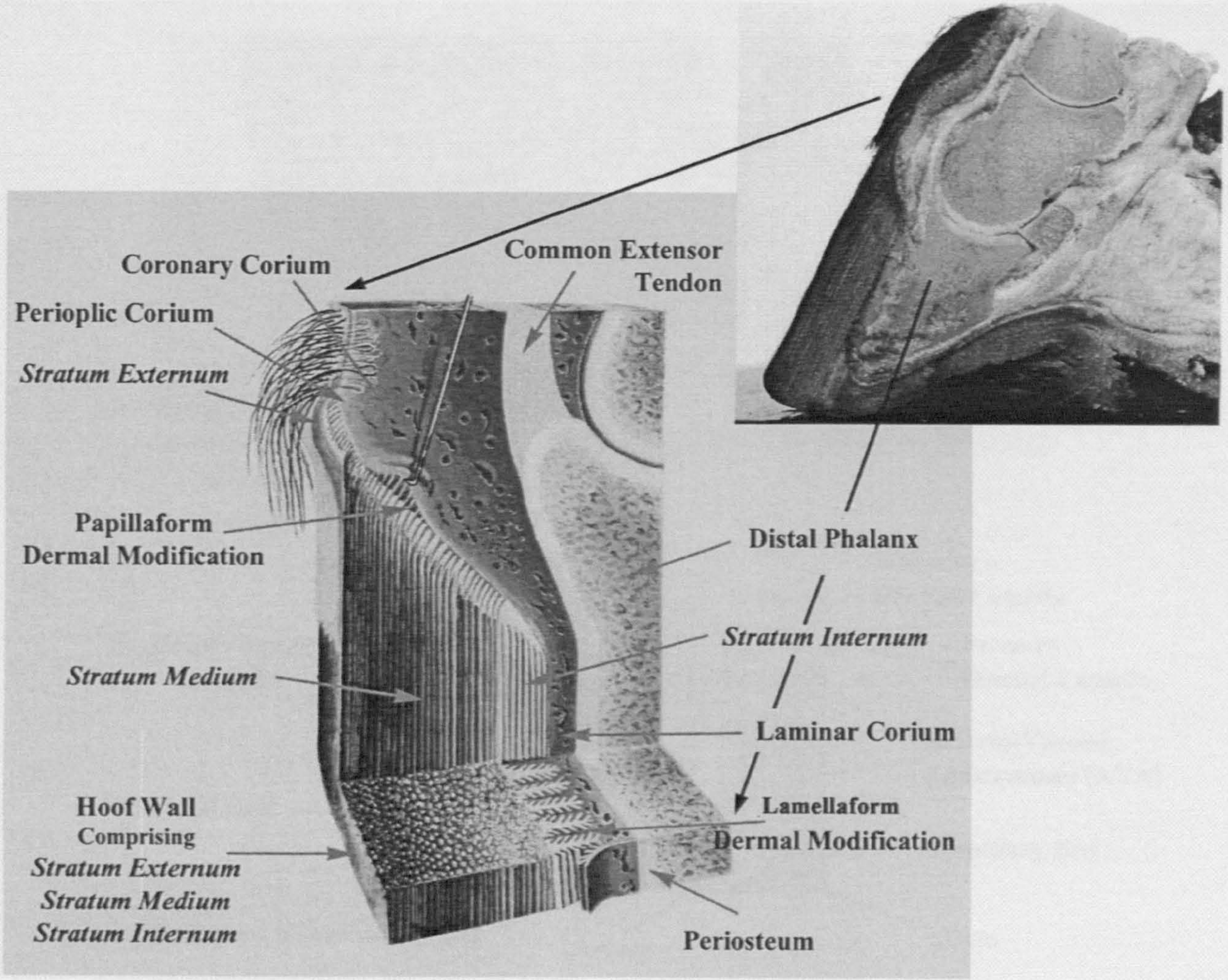

Figure 1.7 Diagrammatic representation of the intimate dermo-epidermal association at the laminar interface and the laminar microcirculation (Adapted after Pollitt 2001, Pollitt 2002 – Pers Com.).

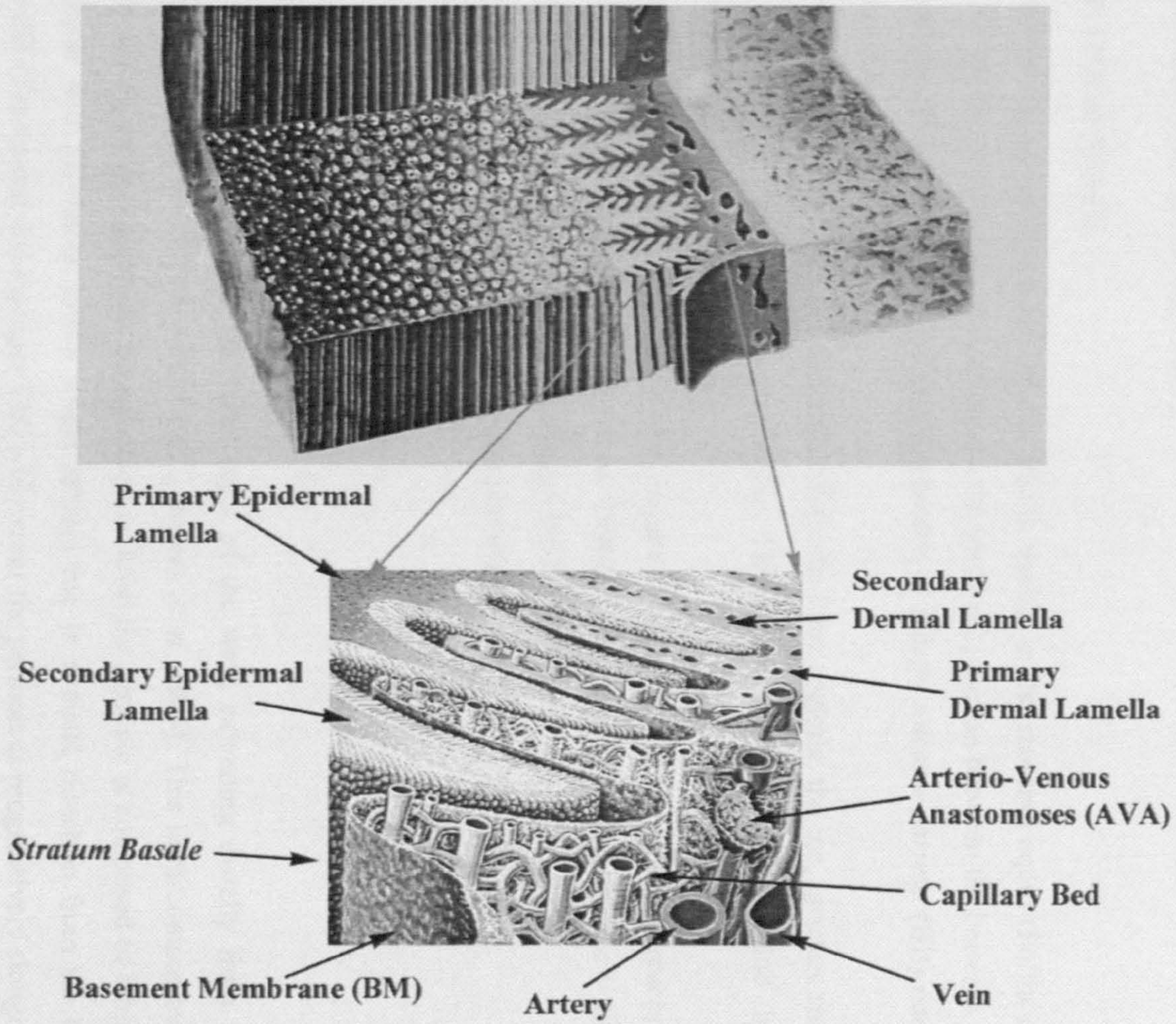

1.5 THE DESIGN COMPLEXITY OF THE EQUID HOOF CAPSULE

1.5.1 OVERVIEW

The hoof capsule displays a complex 3-dimensional geometric form that has a distinct structural organisation of hoof horn material. The hoof capsule can be divided topographically into the wall, frog, sole and white line (Stump 1967).

1.5.2 THE HOOF WALL

The hoof wall is the part of the hoof capsule that is visible in the standing equid (Pollitt and Molyneux 1990). The coronary band (CB) marks the proximal junction between the between the hoof wall and the skin, whilst the distal bearing border or *Margo solearis parietis* (BB) marks the hoof ground interface.

The hoof wall itself can be divided topographically into three regions: the toe, quarters (both lateral and medial) and the heels (Bruhnke 1931). The wall is thickest at the toe and thins caudally towards the heel (Tscherne 1910).

Within the wall, a structural hierarchy (see Figure 1.8) is evident at the macroscopic, microscopic and ultrastuctural level (Reilly *et al.* 1996). At the macroscopic level, the wall is composed of three layers (Trautmann and Feirbiger 1957). These are the: -

- *Stratum externum* - Periople and *Stratum tectorium* (*SE*)
- *Stratum medium* (*SM*)
- *Stratum internum* (*SI*)

1.5.2.1 THE *STRATUM EXTERNUM*

The *Stratum externum* (*SE*) forms the outer layer of the wall, extending distally from the coronary band (CB) (Nickel 1938b, Leach 1980, Budras *et al.* 1995). This horn component is supported by the perioplic corium. At the microscopic level the periople is composed of tubular and intertubular horn (Klemola 1933). These tubules run in a distal direction from the CB towards the BB (Trautmann and Fiebiger 1957). However the periople is progressively sloughed off from the wall to leave a thin layer of flat cells, the *Stratum tectorium* (Trautmann and Feibiger 1957, Schummer *et al.* 1981, Dyce *et al.* 1987). The *SE* is important because it is considered to play a vital role in controlling hydration levels within the capsule (Leach 1980, Schummer *et al.* 1981) and in affording protection to the coronary coria (Schummer *et al.* 1981).

1.5.2.2 THE *STRATUM MEDIUM*

The *SM* constitutes the bulk of the hoof wall and is produced by horn production supported by the coronary corium. It extends from the CB to the BB and, like the *SE*, it is composed of tubular horn and intertubular horn (Schummer *et al.* 1981). The horn tubules are also arranged in a parallel array and extend distally from the CB (Bertram and Gosline 1987).

1.5.2.3 THE *STRATUM INTERNUM*

The *Stratum internum* (*SI*) is the inner layer of the hoof wall and forms form a continuous structural unit with the *SM* of the hoof wall (Budras *et al.* 1989). The *SI* is composed of epidermal lamellae, consisting of LH and CH components (see Section 1.4.2). The epidermal lamellae interdigitate with their dermal counterparts to form a complex dermo-epidermal anatomical association (Leach 1980) that Trautmann and Feibiger (1957) referred to as, the *Stratum lamellatum* (see Figure 1.7).

Figure 1.8 Hierarchical design of the equid hoof wall to show the material basis of the hoof at the ultrastructural level, the structural organisation at the micro and macroscopic levels, and the geometric shape at the gross anatomical level. (Modified after Reilly 2001).

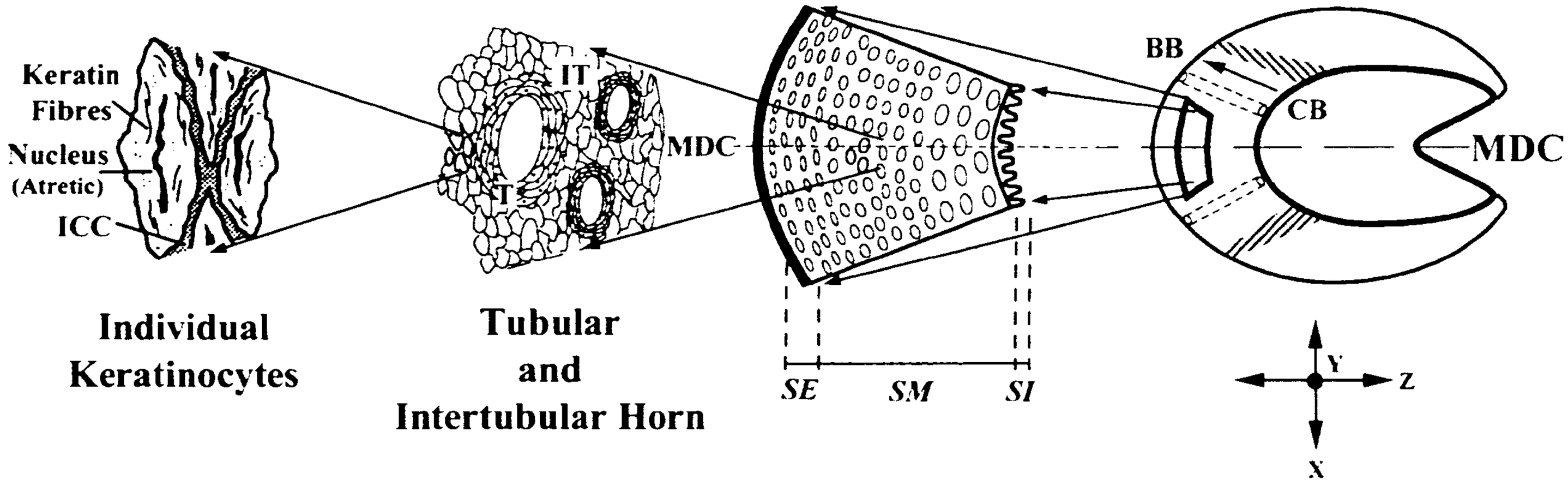

Individual Keratinocytes	Tubular and Intertubular Horn		
Ultrastructural Level	**Microscopic Level**	**Macroscopic Level**	**Gross Anatomical Level**
X10,000	**X100**	**X10**	**X1**

Key:

CB, Coronary Band
BB, Bearing Border
MDC, Plane of Midline Dead Centre

SE, *Stratum externum*
SM, *Stratum medium*
SI, *Stratum internum*

Tu, Horn Tubule
IT, Intertubular Horn
ICC, Intercellular Cement

1.5.3 THE FROG

The frog (*Epidermis cunei*) is a wedge-shaped structure composed of tubular and intertubular horn situated on the solear aspect of the hoof capsule (Trautmann and Feibiger 1957). The palmar aspect of the frog merges into the bulbous heels (Dyce *et al.* 1987). The apex of the frog is visible on the solar surface of the hoof. The frog is separated from the sole by collateral sulci. The centre axis of the frog is marked by the central sulcus.

1.5.4 THE SOLE

The sole (*Epidermis soleae*) is a concave structure occupying the space between the frog and the BB of the hoof wall. The sole is similarly composed of tubular and tubular horn. The tubules of the sole are arranged in parallel alignment with those of the hoof wall (Bolliger 1991). The sole is separated from the hoof wall by the white line.

1.5.5 THE WHITE LINE

The white line (*Zona alba*) forms the junction between the sole and the hoof wall. It extends from the distal margin of the dermal lamellae to the BB (Bolliger 1991, Warzecha 1993). The white line is formed by horn production supported by the laminar corium. It displays a lamellated structural organisation that incorporates the *SI* of the hoof wall, distad to the distal margin of the dermal lamellae, and unites this to the sole. It is believed that that the white line allows independent movement of wall and sole during loading and thus prevents catastrophic failure of the hoof capsule (Reilly 1997).

1.5.6 SUMMARY

An intimate relationship exists between the dermal and epidermal tissues of the foot. The nature of the hoof horn material is determined by the cornification and keratinisation processes that the dermis supports, and the BM mediates. In addition, the structural organisation of this hoof horn material is dictated by the nature of the dermal modification within the respective topographical coria of the foot. This is summarised in Table 1.1.

Table 1.1 Summary table of the topographical modification of the dermis of the equid foot, the keratinisation process that the dermis supports, and the resultant structural organisation of the epidermis.

Coria	Dermal Modification	Keratinisation process	Epidermal Structural Organisation
Perioplic	Papillaform	Soft Keratinisation	Tubular and Intertubular Horn
Coronary	Papillaform	Hard Keratinisation	Tubular and Intertubular Horn
Laminar	Lamella- and Papillaform	Hard Keratinisation	Lamellar, Tubular and Intertubular Horn
Solear	Papillaform	Hard Keratinisation	Tubular and Intertubular Horn
Frog	Papillaform	Hard Keratinisation	Tubular and Intertubular Horn
Bulbs of Heel	Papillaform	Soft Keratinisation	Tubular and Intertubular Horn

Finally, the geometric form, or shape of the hoof capsule is governed by the spatial disposition of the respective coria within the foot. In this way the design complexity of the hoof capsule is derived.

Hence the convention adopted in this thesis is that the hoof horn cells forms the material basis of the hoof capsule. The arrangement of this material within the respective capsular components constitutes its structural organisation. Finally, the spatial disposition of the capsular components collectively represents the geometric form or shape of the hoof capsule.

However to gain an insight into the design hierarchy of the hoof there is a need to appraise the biomechanical forces associated with its function. This is because the structural organisation evident within the hoof is likely to be determined by the external and internal forces that act upon the hoof. Similarly the precise response of the hoof capsule to these forces will itself be governed by hierarchical nature of its design.

1.6 THE SUSPENSORY APPARATUS OF THE DISTAL PHALANX

The distal limb of the equid is totally suspended within the laminar region of the hoof capsule via the suspensory apparatus of the distal phalanx (SADP) (Müller 1936, Budras *et al.* 1989, Pellmann 1995). This suspensory device is formed by the interdigitation of the dermal and epidermal lamellae within the *Stratum lamellatum, and the Stratum reticulare.* This association is facilitated by the BM, and its structural linkage to the periosteum of the distal phalanx, via the network of connective fibres contained within the extracellular matrix of the laminar dermis (Budras *et al.* 1996). This complex anatomical association, which is illustrated in Figure 1.9, unites the hoof wall to the DP (Pellmann 1995, Budras *et al.* 1996, Pellmann *et al.* 1997), and results in the equid foot acting as a single functional entity (Budras and Huskamp 1999, Hood 1999b, Pollitt 2001, 2002).

Figure 1.9 Diagrammatic representation of the equid foot to illustrate the suspensory apparatus of the distal phalanx (SADP).

A. Sagittal section of the foot to show transect line X-X.
B. Transverse section along the transect X-X to show the anatomical organisation of the SADP
(After Müller 1936, modified after Pellmann 1995, Budras et al. 1998a, Budras and Huskamp 1999).

A

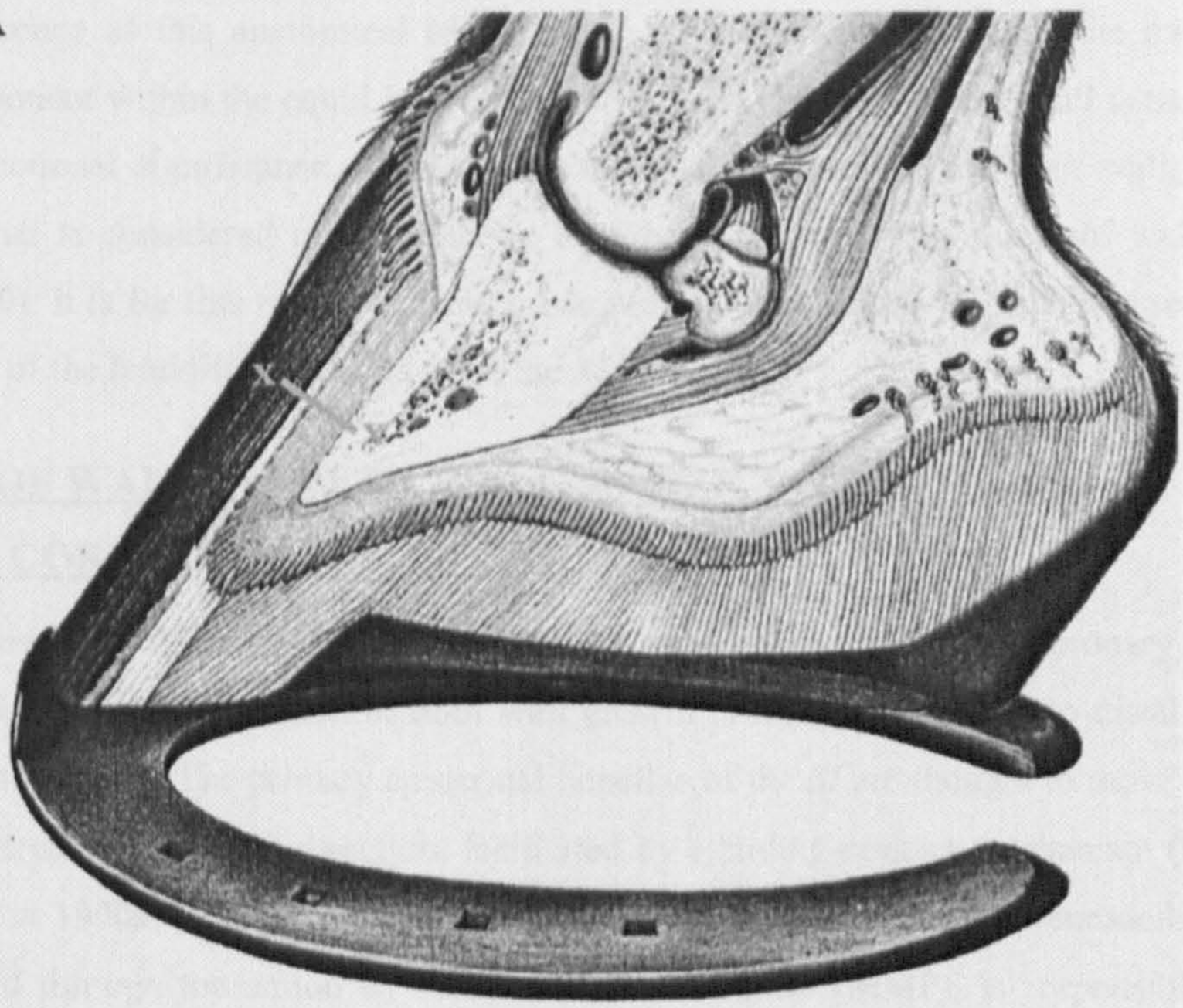

B

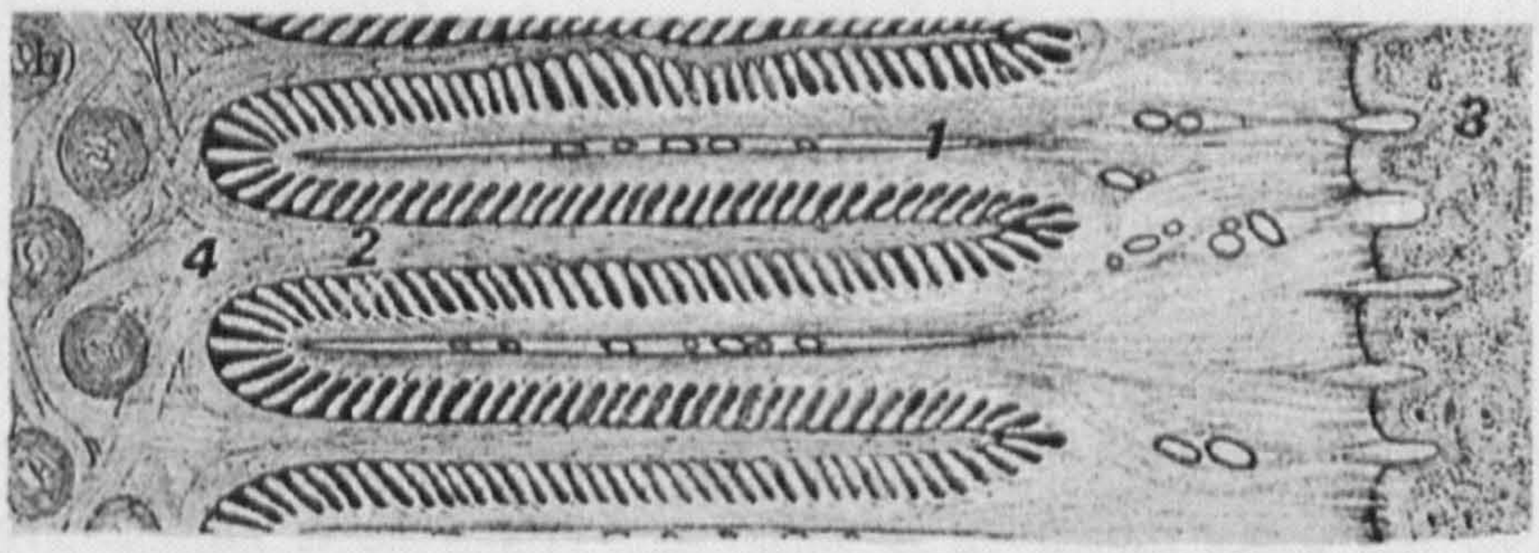

Stratum lamellatum
comprising interdigitating Dermal (1) and Epidemal 92) Lamellae

Stratum reticulare
containing network of collagenous fibres

Suspensory Apparatus of the Distal Pahalanx (SADP)
comprising the *Stratum lamellatum* and the *Stratum reticulare.*

The SADP unites the Distal Phalanx (3) and the *Stratum medium* of the hoof wall (4) into a single functional entity.

This anatomical organisation is thought to results in a unique mode of weight bearing within the equid (Pollitt 2002). In this regard, the forces associated with weight bearing do not act through the digital cushion and the sole, as is the case in digitigrade and plantigrade foot. Instead, they are redirected to the hoof wall via the laminar interface (Coleman 1805, Peters 1883). Hence the SADP is central to the transfer of forces between the ground and the axial skeleton (Pellmann 1995, Pellmann *et al.* 1997).

As a consequence of this anatomical organisation, the hoof wall represents the major load-bearing component within the equid hoof capsule (Nickel 1938a). The hoof wall is therefore of particular functional significance. As the *SM* constitutes the bulk of the hoof wall, it is this component that is considered to be principle load bearing element of the hoof wall (Nickel 1938a,b, 1939). It is for this reason that the predominant focus of this thesis is an investigation of the impact of the laminitic condition upon the *SM*.

1.7 3D HOOF WALL GROWTH AND ITS ASSOCIATION WITH THE LAMINAR CORIUM

Hoof wall growth results from the ongoing cellular proliferation within the coronary region of the hoof wall. Hence the direction of hoof wall growth proceeds in a proximo-distal direction from the CB to the BB. The primary epidermal lamellae of the *SI* are thought to move past their dermal counterparts in a distal direction, facilitated by a sliding-contact mechanism (Budras *et al.* 1989, Pollitt 1990a, Bolliger 1991) – see Figure 1.10. The physiological remodelling of the BM, mediated through the action of matrix metalloproteinase (MMP), is responsible for the sliding-contact within the laminar interface (Pollitt 2002 - Pers Com.). In this way, the hoof wall can move distally from the CB, as a single anatomical entity, whilst maintaining the functional integrity of the SADP.

1.8 THE HOOF PASTERN AXIS

Efficient locomotor function, devoid of pain, is reliant upon optimal stress and strain distribution within the distal limb (Collins and Reilly 2004b – Submitted). In this regard, Balch *et al.* (1991), Stashak *et al.* (2002) and Tachio *et al.* (2002) stated that the anatomical conformation of the distal limb was central in achieving correct foot balance, and that a balanced foot was an essential prerequisite in achieving efficient locomotor function. These authors also argued that the Hoof Pastern Axis (HPA) was a key determinant of dorso-palmar balance within the equid foot.

The HPA summarises the spatial relationship, in the sagittal plane, between the following anatomical elements of the distal limb: -

- The proximal phalanx or *Phalanx proximalsis* (PP)
- The middle phalanx or *Phalanx media* (MP)
- The distal phalanx or *Phalanx distalis* (DP)
- The hoof capsule

The HPA describes the angular relationship between the Pastern and Hoof axes, during static weight bearing, when the longitudinal axis of the metacarpal bone is perpendicular to the ground surface – see Figure 1.11.

The anatomic reference points that determine these axes are: -

1. The Pastern Axis formed by:-
    - The alignment of the phalanges (PP-MP)

and its angular relationship with: -

- The dorsal aspect of the DP
- The scapular spine

2. The Hoof Axis formed by:-
    - The dorsal aspect of the hoof wall

According to accepted dogma three distinct anatomical configurations may occur during static loading when the metacarpal is in perpendicular alignment to the ground. These are summarised in Table 1.2.

1.8.1 THE HOOF PASTERN AXIS IN THE LAMINITIC EQUINE

The development of a 'Broken Forward' HPA is of particular significance with regard to the laminitic condition, and is discussed in Section 1.11.1.2. Conversely events associated with the laminitic condition can also result in the development of an apparent 'Broken Back' HPA. This is characterised by an obtuse angular difference between the pastern axis and the dorsal aspect of the hoof wall (Collins – Pers Obs.). This configuration differs, however, from the recognised 'Broken Back' HPA axis in that it is not centred upon the DIP joint. Hence an obtuse angular relationship between the Pastern Axis and the dorsal aspect of the DP is not pathognomonic. The biomechanical consequences of this anatomical configuration are poorly defined. The development of this apparent 'Broken Back' HPA is also discussed further in Section 1.11.1.2.

Figure 1.10 Diagrammatic representation of the sliding mechanism by which proximo-distal hoof wall growth occurs whilst maintaining the functional integrity of the SADP. (Modified after Pollitt 1990).

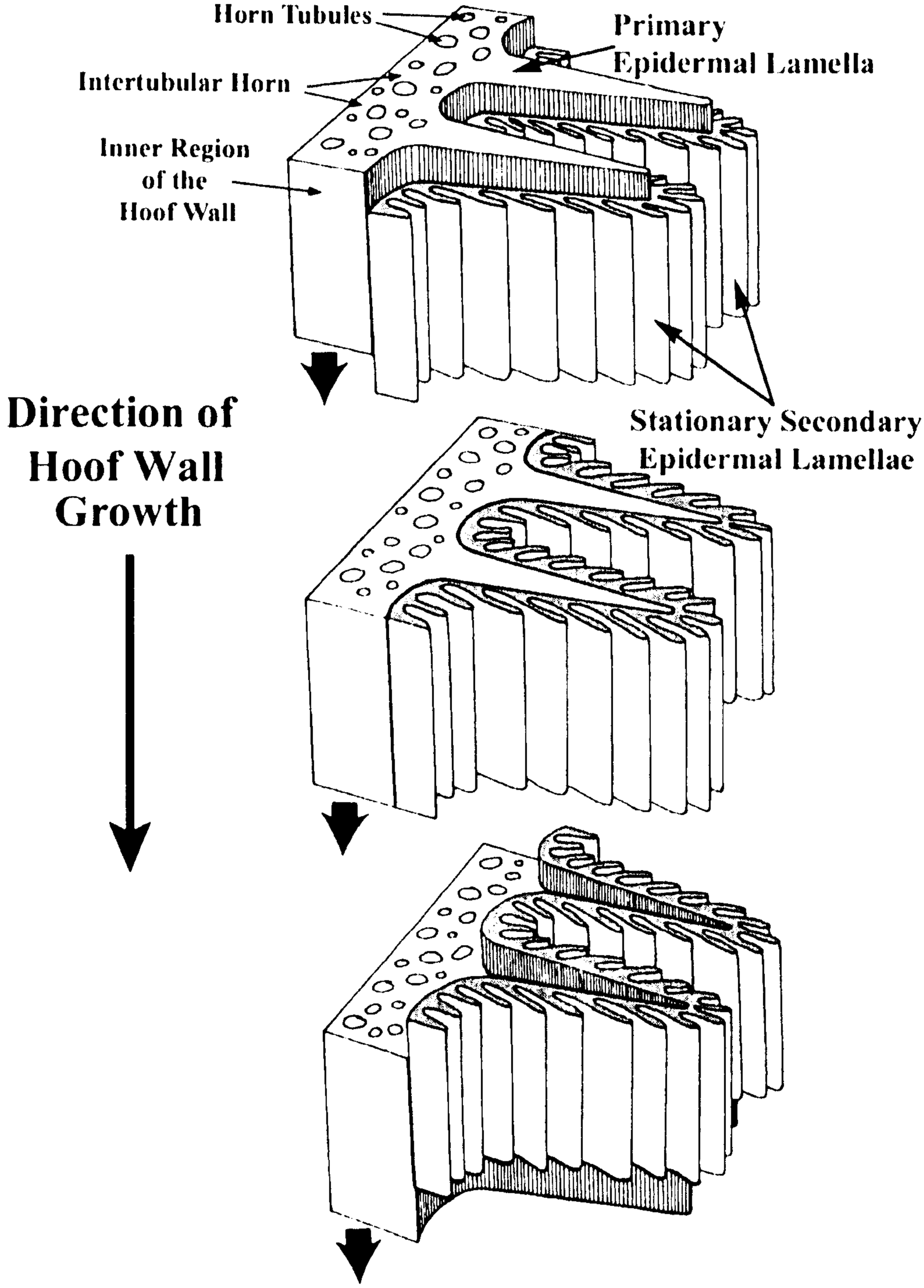

Figure 1.11 Schematic representation of the artiodactyl anatomy of the distal limb of the equid foot to show the anatomical reference axes used to determine the hoof pastern axis (Modified after Eley 1998).

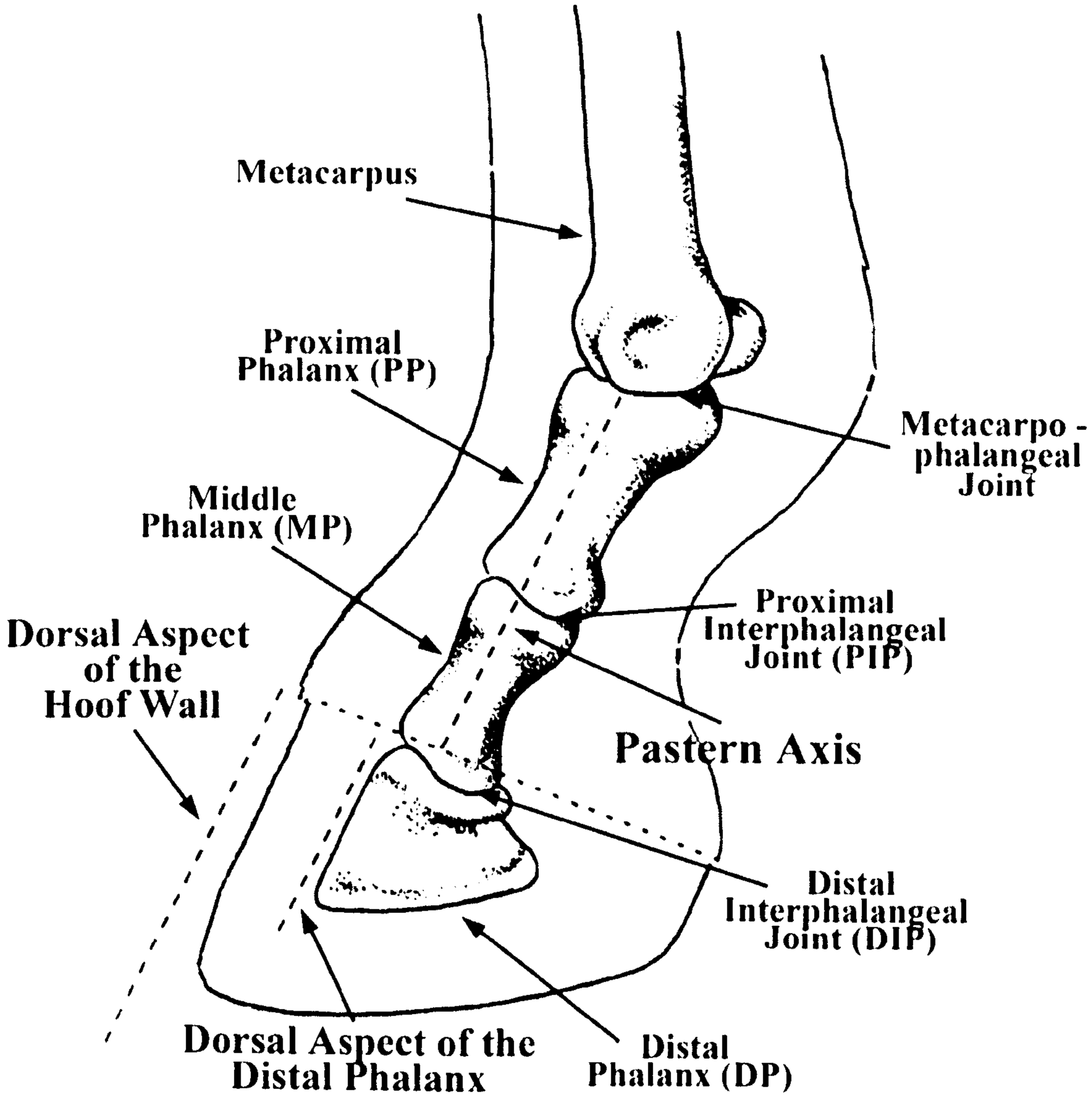

Table 1.2 Summary table of the anatomical configuration of the Hoof Pastern Axis (HPA) evident within the equine and their biomechanical implications.

Configuration of the Hoof Pastern Axis (HPA)	Anatomical Description	Causes	Biomechanical implications
The Theoretical Ideal or 'Straight' HPA	Characterised by:- • Pastern Axis parallel to the dorsal aspect of the DP to form straight Phalangeal Axis (PP-MP-DP) • No angular deviation at either the PIP or DIP Joint • Pastern Axis forming an angle with the ground of ~45-50° • Pastern Axis parallel with the dorsal aspect of the hoof wall, and the scapular spine	N/A	• Ensures 'correct' dorso-palmar foot balance (Curtis 1999) • Optimal force distribution within the foot • Growth and wear compensatory • Aids effective locomotor function
'Broken Forward' HPA	Characterised by: - • Misalignment of Pastern Axis with the dorsal aspect of the DP and the hoof wall, centred at the DIP joint • Acute angular difference exists between the Pastern Axis and the dorsal aspect of both the hoof wall, and the DP • Angular misalignment centred at the DIP • Hoof capsules with 'high heels' and 'short toes' (Curtis 1999)	• Poor farriery • Contracted DDFT (Stashak *et al.* 2002) • Palmar solear pain • Laminitis (Hood 1999a,b)	• Places excess stress upon the distal limb (Curtis 1999) • Subjects the joints of the limb to increased concussive forces (Curtis 1999)
'Broken Back' HPA	Characterised by:- • Obtuse angular misalignment between the Pastern Axis and the dorsal aspect of the DP and the dorsal aspect of the hoof wall • Angular misalignment centred at the DIP • Hoof capsules with 'long heels' and excessively 'long toes' (Curtis 1999)	• 'Long toe, Short heel' Syndrome • Abnormal weightbearing • Poor farriery	• Deleterious strain upon the palmar aspect of the foot • Redistribution of forces within the phalangeal axis • Abnormal wear patterns in the hoof capsule

Key: DP, Distal phalanx. **MP**, Middle phalanx. **PP**, Proximal phalanx. **PIP**, Proximal interphalangeal joint. **DIP**, Distal interphalangeal joint.

1.9 HOOF FUNCTION

1.9.1 FINER FUNCTIONING OF THE HOOF

As the hoof represents the platform for dynamic performance (Balch *et al.* 1991), it must accommodate and ultimately resist the forces associated with weight bearing (Leach 1980). The hoof must also achieve the smooth and painless cyclic transfer of these forces between the ground and the axial skeleton (Reilly and Kempson 1992). This must be achieved without excessive deformation or catastrophic failure of the hoof capsule in order to afford protection to the underlying sensitive structures of the foot (Leach and Zoerb 1983). Hence it can be argued that without a fully functioning hoof capsule there can be no healthy or painless foot (Newlyn *et al.* 1999, Collins and Reilly 2004a – Submitted).

Despite these facts, our knowledge of the factors that govern the functional capabilities of the hoof is limited, as is our understanding of the impact of specific pathological conditions of the foot (Reilly 1995). This is of particular concern as deficiencies in the functional capability of the hoof lead to reduced performance, pain and lameness (Geyer and Tagweker 1986). These issues raise particular welfare concerns to those involved in equid management (Reilly 1995, Collins *et al.* 2002).

Despite these facts there is distinct lack of basic and applied research concerning lameness within the unguligrade foot (Payne 1966, Greenough 1978). Indeed research in this field has been criticised in view of its subjectivity and lack of rigor (Slater *et al.* 1995).

Reilly (1995) recognised these facts and stated that there was a need to adopt a new research approach. This author proposed a measurement-driven scientific rational for further hoof research.

This thesis has followed the principles outlined by Reilly (1995). It has sought to establish an appropriate scientific basis by which the pathology of the hoof, associated with the laminitic condition, can be investigated.

The eminent Victorian pathologist Rudolf Virchow stated that pathologic change can be defined as:

"alterations in structure and function in response to injury"

(cited by Ranther 1966)

Indeed this author stated that pathological processes represent quantitative changes in, or the degeneration of, existing structures, rather than the formation of completely new structures. Hence the study of pathological degenerative change can be placed on a quantitative basis. However Reid (1980) argued that the study of biological structures, even in quantitative terms, is a sterile and obsolete science unless specifically related to function.

1.9.2 STRUCTURE-FUNCTION INTERACTIONS OF THE HOOF

The ability of the hoof to bring about smooth and painless force transfer will depend upon the biomechanical characteristics of the capsule, and the nature of the forces acting upon the hoof. In this respect, Politiek *et al.* (1986) suggested that the functional capabilities of the capsule were likely to be determined by both the hoof horn characteristics, and the geometric shape of the capsule.

According to first engineering principles, Gordon (1976) stated that the response of a solid body to mechanical loading is governed by: -

- The material/s that forms the body
- The geometric form of the body

Geometric shape dictates the nature of the deformation in response to loading, whilst the size of the object, and the material/s that form the object will govern the magnitude of the deformation. However Vincent (1992), highlighted that mechanical properties are determined not only by the material/s that form the object, but also by the structural organisation of the material/s within the object.

Indeed the structural organisation of the hoof wall has been suggested to be important both in terms of stress transfer and energy absorption (Nickel 1938a,b), and force distribution within the wall (Bertram and Gosline 1986). Reilly *et al.* (1996) argued that the structural organisation of the hoof ultimately affects the horse's ability to:

"transmit the forces of locomotion".

It can therefore be concluded that the functionality of the hoof is likely dependent upon: -

- The hoof horn material from which it is composed
- The structural organisation of the hoof horn material
- The 3-dimensional geometric shape of the capsule

Thus it is to be expected that the design complexity of the hoof capsule *per se* determines the functional capabilities of the capsule, with the functional capabilities of the hoof wall governed by its design hierarchy (Bragulla *et al.* 1992, Reilly *et al.* 1996). Rooney (1978, 1980) stated that the design of hoof wall reflects directly the need both for force resistance and energy absorption.

In this regard, Bragulla *et al.* (1992) and Reilly *et al.* (1996) stated that the finer function of the hoof wall was dependent upon: -

- Intracellular Factors
- Intercellular Factors
- Architectural Factors

Reilly *et al.* (1996) also emphasised that the functional properties of the hoof wall were also likely to be modulated by the level of hydration.

In order to determine the structure-function relationships within the hoof, Reilly (1995) argued that there is a need to further develop our knowledge of: -

- The mechanical functioning of the hoof
- The relationship between the forces generated during loading and the structural organisation and material properties of the hoof

Studies have been conducted, using a variety of different scientific techniques, to define hoof characteristics at the gross anatomic level (Josseck *et al.* 1995), the macroscopic and microscopic levels (Pellmann *et al.* 1993, Reilly *et al.* 1996, 1998a), and the ultrastructural level (Pellmann *et al.* 1993, Wattle 1998).

Several studies including Leach (1980), Pellmann *et al.* (1993), Geyer and Schulze (1994), Zenker (1991), Zenker *et al.* (1995), Kasapi and Gosline (1997), Collins *et al.* (1998) and Reilly (2001) have also variably correlated these findings with defining mechanical properties. These have included ultimate strength, modulus of elasticity, and fracture toughness.

However progress to date has been limited (Reilly 1995). There is a need to continue with this approach, and seek additional imaging, analytical and material testing techniques to complete the characterisation of the hoof capsule. In addition, new methods of objectively assessing capsular performance and modelling hoof function need to be established. It is only through this approach that progress towards unravelling the design complexity of the hoof can be achieved (Reilly 1995, Collins *et al.* 2002).

Only in this way, can a comprehensive

'materials characterisation'

of the hoof be conducted, and the design complexity of the hoof truly understood (Collins *et al.* 2002).

Commenting upon this approach, Reilly (1995), Reilly *et al.* (1998b) and Collins *et al.* (2002) concluded that if this can be achieved, then it will be possible to: -

- Identify those hoof horn characteristics affected in pathologically challenged hoof
- Assess the effects of these changes on the mechanical properties of the hoof
- Model the potential impact of these changes on hoof function
- Model the effects of therapy

In this way we can further develop our understanding of the impact of degenerative conditions of the foot such as laminitis, and provide a scientific basis for the management and treatment of the affected animal (Reilly 1995, Reilly *et al.* 1998b, Collins *et al.* 2002).

These issues are of fundamental importance in interpreting the effects of the laminitic condition on the biomechanics of the foot, and hence affect our ability to effectively manage the afflicted animal. Therefore these issues form the basis of the elements of work covered in this thesis.

Chapter 3 specifically deals with the impact of the laminitic condition on the radiographic anatomy of the laminitic foot. Chapter 4 investigates the effects of these changes upon the structural organisation of the *SM* of the hoof wall, whilst Chapters 5 assess critical material characteristics of particular biomechanical significance. Chapter 6 seeks to explore the structure-function relationships of the hoof, and also evaluates the potential effects of the laminitic condition upon biomechanical hoof function. The final chapter investigates the structure-function interactions within the laminitic donkey hoof.

1.9.3 HOOF FUNCTION – A BIOMECHANICAL OVERVIEW

Despite the fact that the hoof capsule is fundamental to equid performance it has largely been overlooked in terms of biomechanical assessment and modelled function (Newlyn *et al.* 1998). Newton's third law of motion states 'for every reaction there is an equal and opposite reaction'. Thus a solid object deform in response to loading to generate internal forces that counter the applied load (Gordon 1976).

In a similar manner, the hoof deforms upon loading in order to accommodate and resist the forces associated with weightbearing (Leach 1980, Douglas *et al.* 1996). During static and dynamic weightbearing the hoof deforms in a consistent pattern (Douglas *et al.* 1996). This results in: -

- Inward movement of the proximal margin of the hoof wall
- Decrease in the proximo-distal height of the capsule
- Dorso-concavity of the dorsal aspect of the hoof wall
- Medio-lateral heel expansion
- Flattening of the sole

Leach (1980) stated that the nature of this deformation reflects the complex interaction between external forces that act against the ground during weight bearing, force changes that occur internally within the foot. Knowledge of the capsule's response to loading is however limited, as is the finer detail of the respective forces that act upon the hoof during weight bearing. A detailed summary of our present understanding of capsular response to weight bearing was published as part of the initial work associated with this thesis by Newlyn *et al.* (1998). This is included in Appendix VII of this thesis.

Figure 1.12 summarises the biomechanical response of the equid foot to static weight bearing.
It is widely accepted that the foot responds to loading in accordance with the depression theory described by Coleman (1805) and Peters (1883).
In accordance with Newton's third law of motion, a vertically directed ground reaction force (G) is directed through the centre of the solear aspect of the hoof, to counter the weight of the horse (W) that acts through the DP. However, as the distal margin of the hoof wall (BB) represent the weightbearing element of the hoof, components of the ground reaction force (g) act via the BB. A resolved compressive force vector (c) is directed in a disto-proximal direction, from the BB to the CB. The magnitude of the resultant vector, at any point around the BB, is dependent upon the inclination of the hoof wall relative to the GRF. The action of the force vectors (c) result in the generation of tensile forces (T) within the SADP.
The DP is subjected to 4 additional loading forces. These are: -

- Compressive forces at the DIP due to the body weight of the animal
- Tensile forces at the extensor process due to the insertion and action of the Common Extensor Tendon (CET)
- Tensile forces on the palmar surface due to the insertion and action of the DDFT
- Compressive forces generated against the sole

The pliant nature of the dermis allows semi-independent movement of the DP relative to the hoof wall and sole (dislocation) in response to these forces. The dislocation of the DP is dependent on the anatomical organisation of the foot, and the complex interaction of force vectors. As the foot acts as a unified functional entity, the dislocation of the DP is both influenced by, and influences, the hoof wall through the action of the SADP. At ground contact, the DP is dislocated vertically away from the wall towards the sole. This initial movement generates tensile forces within the SADP. As the loading forces increase the DP begins to act directly upon the hoof capsule. This results in the initial distal displacement of the sole. Eventually a point is reached at which the sole can not be displaced further. At this stage the sole acts as a fulcrum about which the DP rotates. The palmar aspect of the DP rotates distally further flattening the solear surface, whilst the apex of the DP rotates towards the dorsal aspect of the hoof wall. This rotation displaces the proximo-dorsal aspect of the DP and, as a consequence of its intimate attachment via the SADP, the proximal hoof wall. It is this action that induces the dorso-concavity of the hoof wall observed during weight bearing. The associated lowering of the MP, which results as a consequence of DP dislocation, leads to a concurrent medio-lateral expansion of the heels.
This kinematic response within the hoof wall occurs in a recognisable and repeatable manner, and reflects the complex interaction of forces that are generated during weight bearing.

Figure 1.12 Diagrammatic summary of the force interaction within the distal limb during static weightbearing, and the resultant force distribution and displacements within the hoof wall (Modified after Leach 1980, Thomason *et al.* 1992, Newlyn *et al.* 1998, Reilly 2001).

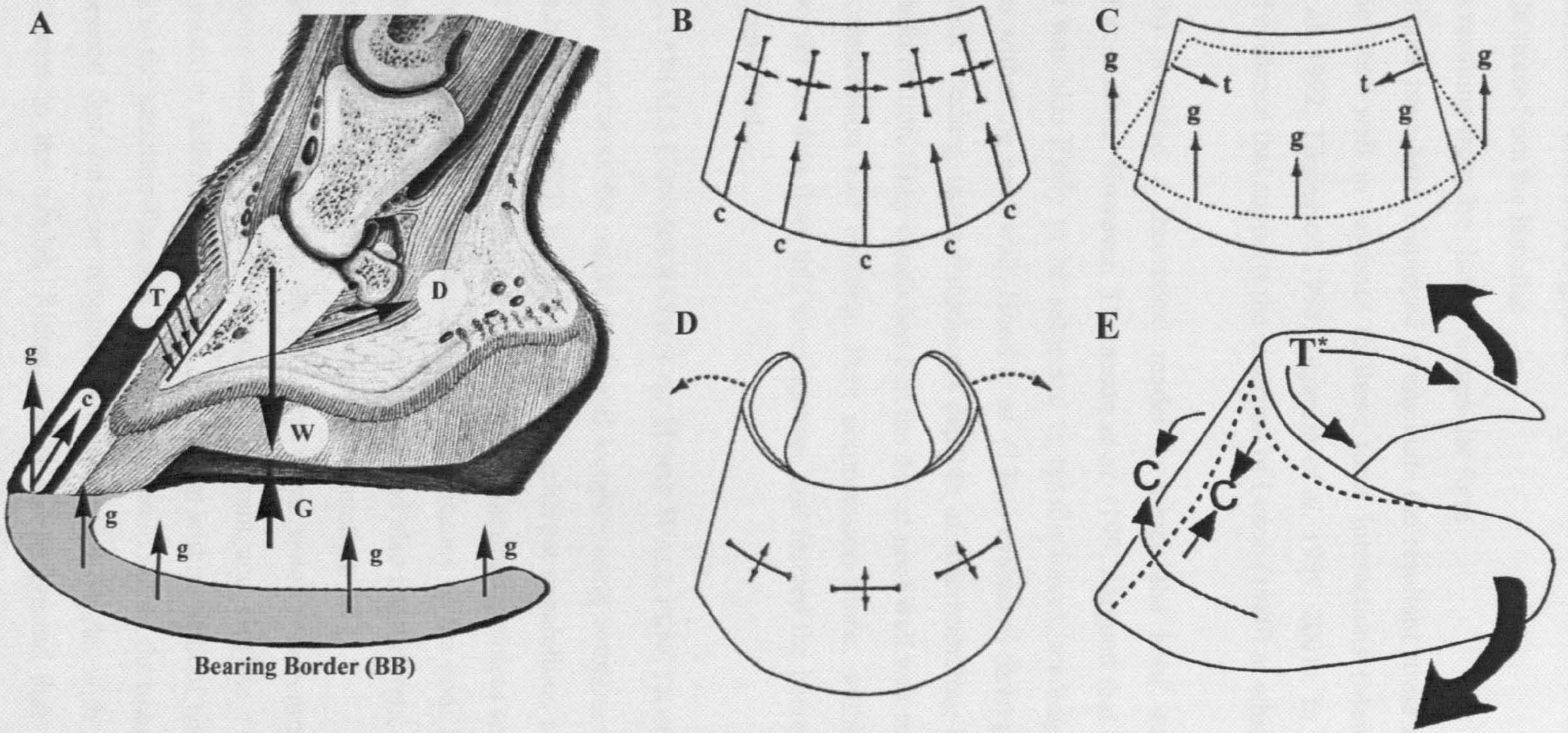

A. Schematic to illustrate the force interaction in the sagittal plane of the foot. **B**. Schematic to show direction of principle stresses induced within the hoof wall as a consequence of the resolved compressive component of the ground reaction force. **C**. Schematic to show the deformation occurring within the hoof wall as a consequence of the interaction between the components of the GRF (g) that act around the bearing border, and the tensile forces (**t**) generated within the SADP. **D**. Schematic to show direction of principle stresses induced within the hoof wall as a consequence of the heel expansion. **E**. Schematic to show the overall pattern of hoof wall deformation, and the nature and direction of the forces generated by this deformation.

Key: W, Weight of horse acting through the centre of the hoof. **G**, Ground reaction force (GRF) generated in response to W. **g**. Component of the GRF acting upon the bearing border. c, Resolved compressive component of g acting in a disto-proximal direction within the hoof wall. **T**, Tensile forces acting across the SADP. **D**. Action of DDFT. **t**, Tensile reaction force in the heels. **C**. Biaxial compression acting on the dorsal aspect of the hoof wall at the MDC. **T***. Tensile forces generated in the inner aspect of the hoof wall at the MDC.

Leach (1980) theorised that the hoof wall was likely to be subjected to forces originating from three sources in response to weight bearing. These are: -

- Compressive stress from the ground
- Tensile stress from the lamellae
- Stress resulting from the change in capsular form

Various techniques have been employed to elucidate the resultant stress and strain distribution patterns in the hoof wall in response to these force interactions (Mair 1974, Colles 1989, Thomason *et al.* 1992, Thomason 1998, Dejardin *et al.* 1999, 2001). In general, these studies have provided evidence that supports the assertion of Leach (1980) in which compressive forces predominate.

Nickel (1938b) proposed a theoretical model in which the hoof wall was subjected to compressive forces alone. However, Thomason *et al.* (1992) argued that as the inner aspect of the hoof wall was also likely to be subjected to tensile forces, leading to the generation of bending forces within the hoof wall. Hood *et al.* (1991) evaluated force generation in the hoof wall during static loading, using transducers capable of discriminating between bending and compressive deformation. They concluded that the dorsal hoof wall was subjected to either pure bending, or compression and bending. Pure compression alone, within the wall, was not recorded. However the data from this investigation, that formed the basis of these conclusions, have yet to be published.

1.9.3.1 A Materials Consideration of Hoof Wall function

As the hoof wall represents the major functional weightbearing component of the hoof capsule (Nickel 1938a,b, Parker 1973) it must posses the inherent capabilities to dampen concussive ground impact forces, resist weightbearing forces, and facilitate painless stress transfer.

This has raised issues relating to the functional significance of the hoof horn material and the structural organisation evident within the hoof wall, and also the different mechanisms that may exist within the design hierarchy that facilitates hoof function.

Nickel (1938a,b, 1939) argued that the structural organisation was central to the processes of force transference and energy absorption, and Bertram and Gosline (1986) stated that the structural organisation determined the force distribution within the hoof wall.

Speculating as to the structure-function interactions present within the hoof wall, Nickel (1938b, 1939) hypothesised that the horn tubules acted as vertical struts, with the intertubular horn transferring stresses to the tubules. Klema (1937) also suggested that the intertubular horn would serve to prevent horn tubule buckling. If the horn tubules acted in this manner, it would be anticipated that the modulus of elasticity would be greater to in the direction of the horn

tubules i.e. parallel to long axis of the horn tubule. Several studies have been conducted in order to evaluate Nickel's theory, including Leach (1980), Leach and Zoreb (1983) and Kasapi and Gosline (1997), however the results of these studies are equivocal. Whilst both Douglas *et al.* (1996), Kasapi and Gosline (1997) and Douglas (1998) reported moduli values consistent with Nickel's theory, neither Leach (1980), nor Leach and Zoerb (1983), were unable to detect such an association.

More recently, Bertram and Gosline (1986), Kasapi and Gosline (1996, 1997), Reilly *et al.* (1996, 1998a), Cope *et al.* (1998), Collins *et al.* (1998), and Newlyn *et al.* (1999) have speculated as to whether the structural organisation of the hoof wall, can be interpreted in terms of composite material theory.

At the microscopic level of the design hierarchy Collins *et al.* (1998), Reilly *et al.* (1998a), and Newlyn *et al.* (1999) suggested that, the horn tubules might act as reinforcing fibres within a matrix of intertubular horn, in a similar manner to synthetic unidirectional fibre composites. Newlyn *et al.* (1999) stated that composite material theory at this level in the hierarchy could prove to be a fruitful approach to elucidating both normal and abnormal hoof function. In this regard, these authors argued that the functional capabilities of the *SM* would be determined by the: -

- Tubule density
- Material properties of the tubular and intertubular horn components
- Absolute areas of the marrow (medullary cavity), cortices and tubules
- Cross sectional shape of the tubules and the medullary cavity
- Volume fraction of tubular and intertubular horn
- Volume fraction of the medullary and cortical contribution to the tubular horn

Reilly *et al.* (1996) and Kasapi and Gosline (1997) have suggested that the hoof wall may also act as a multi-laminated composite, at a macroscopic level of the design hierarchy.

Strain energy absorbed both in the separation of different material phases, and also the laminar ply, would increase the work of fracture (Gordon 1976, Vogel 1988). This complex design would produce a "tortuous jagged path" to inward crack propagation (Reilly *et al.* 1998a). In addition, separation along the tubular-intertubular interface would produce an effective crack stopping mechanism (Bertram and Gosline 1986, Kasapi and Gosline 1997). Differences in the structural organisation between the respective laminar ply would allow different crack diversion mechanisms to exist across the HWD of the *SM*. This would afford additional protection against crack propagation originating in different directional planes (Kasapi and Gosline 1997). Finally, delamination along these laminar interfaces would also serve to absorb strain energy, and

provide an additional means of preventing catastrophic failure (Bertram and Gosline 1986, Reilly *et al.* 1996, Kasapi and Gosline 1996).

If hoof wall function can be interpreted successfully in terms of composite material theory, then the measurement of specific hoof horn parameters would provide an appropriate basis for objective hoof horn characterisation. This would enable the effective quantification of pathologic change, and facilitate the functional interpretation of change. These issues are explored within Chapters 4, 6 and 7 of this thesis.

1.10 THE DONKEY AND HORSE FOOT – HOMOLOGOUS LOCOMOTOR ORGANS?

Despite the importance of the donkey in the developing nations, there is a paucity of information relating to the donkey (Walker *et al.* 1995) and the foot in particular (Doguer 1943). Hence there has been a tendency to assume that the distal limb and foot of the donkey represents homologous anatomical structures to those of the equine (Collins *et al.* 2002).

Preliminary work associated with this thesis sought to comprehensively review the comparative anatomy of the distal limb and foot for the horse and donkey, and culminated in the publication of Collins *et al.* (2002). These findings are summarised in Table 1.3. Fundamental differences between these species are apparent both in the anatomical organisation of the distal limb, the foot, and within the design hierarchy of the hoof.

Collins *et al.* (2002) argued that these differences, which are discussed below, suggest that the donkey must properly be viewed as a unique equid species, and hence the application of an equine model to the donkey foot is not justified.

1.10.1 THE HPA OF THE DONKEY

It is widely accepted that the HPA of the donkey is steeper than that of the horse (Crane 2000). However debate exists as to whether the donkey naturally exhibits a 'Straight' HPA like the horse, or due to anatomical differences between the two species, a 'Broken Forward' HPA – (Reilly 1997) – See Figure 1.13. This issue is of particular biomechanical significance as the HPA determines the nature and magnitude of force generation within the foot, and hence, affects those internal forces that the hoof wall must accommodate. The accepted management practice of dressing the donkey foot to the theoretically 'ideal' equine HPA (Fowler 1995, Eley 1998, Crane 2001) may have deleterious consequences within the donkey foot if a 'Broken Forward' HPA occurs naturally. Indeed this would significantly increase the biomechanical force that the deep digital flexor tendon (DDFT) exerts upon the DP, and thereby the SADP, but answers to these questions remain unresolved.

Table 1.3 Summary of comparative anatomy of the distal limb of the horse and donkey with specific regard to the evolutionary adaptation and biomechanics of the foot (Modified after Collins *et al.* 2002).

Parameter	Horse *Equus caballus*	Donkey *Equus asinus*
Evolutionary progenitor (1,10,12)	• Native Horse Breeds[1, 12]	• African Wild Ass?[1,10,12]
Environmental adaptation (1,12,13,31,32)	• Adapted to the grassland plains of the temperate Steppe environment[1, 12, 13] • Trickle feeding on quality grasses[12] • Athleticism[13]	• Adapted to the rocky terrain of the Arid plains[12, 13] • Browsing on low quality herbage[31, 32] • Surefootedness and athleticism[13]
Survival strategy (1,10,12,13,16,24)	• Highly evolved locomotor flight response[1,12,13,16]	• Locomotive flight response?[10,13] Stoical nature[10], Tendency to 'freeze'[10,24]
Anatomical adaptation of distal limb (1,12,13,16,24)	• Perissodactyl organisation[1,12,16] • Unguligrade stance[1,12,13,16]	• Perissodactyl organisation[1,12,13] • Unguligrade stance[1,12,13] • Additional accessory check ligament[24]
Hoof Pastern Axis (3,8,9,26)	• 'Straight' HPA[3,26]	• 'Straight'[8,9] / 'Broken Forward'?[26] HPA – Axis masked by developed CB?[26] • HPA is more upright[9]
Capsular shape (5,7,9,11,12,14,20,26)	• Circular solear profile[20] • Capsule inclined[20] • Truncated cone?[5,20]	• 'U' shaped profile with flare at heels[7,9,26] • Capsule of upright, 'boxy'[12] / quadrilateral appearance[11]. Proportionally narrower than horse[7,14] • Truncated cylinder?[5]
Dorsal Hoof Wall Angle (3,7,14,20)	• Fore 45-50°[3, 7,14,20]	• Fore @ ~55°[7,14] More upright by 5-10°[14]
Lateral/medial angles (7, 14, 20)	• Inclined[20] Lateral 101.5°[14] Medial 101.5°[14]	• Almost perpendicular[7,14] Lateral 91°[14] Medial 88.5°[14]
Capsular Dimensions Height ratio (7,10,14,25)	• Relatively large hoof capsule[10,25] Midline: Quarters : Heel Ratio 3:2:1[7,14]	• Relatively small hoof capsule[10,25] Midline: Quarters : Heel Ratio 3:3:1.5[7,14]
Heel (3,7,9,33)	• Sloping heel[3]	• Strongly developed heel buttress[7,9,33] to give upright appearance[9]
Solear weight bearing (9,14)	• Sole does not normally bear weight[9] • Sole height up to 10mm[14]	• Evidence of solear weight bearing?[9] • Sole height up to 13mm[14]
Frog (11)	• Intimate association with capsule. Contained within the other structures of the capsule[11]	• Frog appears to be separate from the other structures of the capsule[11]
Perioplic groove (5, 7, 14)	• Merges with coronary groove[7]	• Widens at heel and fuses with frog[7,14] • Perioplic hyperplasia?[5]

White line (2,9)	• 2 - 3.5mm dorso-palmar depth Dependant upon bodyweight[2]	• No greater than 1 mm dorso-palmar depth[9]
Dorso-palmar hoof wall depth (HWD) (17,26,30)	• Tapers from the midline to the heel[30] • HWD at MDC ~ 10mm[17]	• Does not appear to taper[26] • HWD at MDC > than the horse?[17]
SADP (2,14)	• Approx. 600 Dermal lamellae[2,14]	• Approx. 350 Dermal lamellae[14] • Lamellae broader than the horse[14]
Zona nonpigmentosa (5,17)	• Evident within the horse[5,17] Functional significance unknown	• Not present[5,17]
Tubule Density (17,19,27,28,29,34)	•Dorso-palmar decrease in horn tubule numbers per unit area (TD)[17,19,27,28] • 4 TD regions or TD Zones[27,28] • Zonal Boundaries @ ~25, 50, and 75 %HWD[27,28] • Stepped pattern[27,28]	•Dorso-palmar decrease in horn tubule numbers per unit area (TD)[17,29] • 3 TD Zones?[17,29] • Zonal Boundaries @ ~ 33, and 50 %HWD[17] • Curvilinear pattern[17,29]
Tubular horn organization of the *SM* (5,6,14,19,26,30,34)	• Distinct tubules types[13, 22,30] • Tubule types vary 'across and around' the HWD[13,22] • Distinct regional populations of tubule types[13]	• Broadly similar tubule types[5,14] • Tubule types vary 'across and around' the HWD[5,6,26] • Distinct regional populations of tubule types[5,6] • Pattern of regional distribution of tubule types (Tubule Zonation) different to the horse[5,30,34]
Moisture content of the *SM* in temperate environment (4,17,18)	• Physiological moisture content in the order of ~ 25%[17,18] • Dorso-palmar decrease across HWD[17] • Zonal variation across the HWD[17]	• Greater than the horse @ ~33%[17,18] • Dorso-palmar decrease across HWD[17] • Zonal variation across the HWD[17] Z1 23%, Z2 33%, Z3 38%[5,17]
Mechanical Properties (4, 15,17,19,21)	• Modulus of Elasticity at physiological moisture levels @ ~ 450 MPa[17,19] • Zonal moduli decreases across HWD[15,17,19]	• Comparable values for the donkey are significantly lower @ ~180 MPa,[4,17] • Zonal moduli decreases across the HWD[17] • Zonal values < horse[17]
Hoof Function (22,25,34)	• Recognised pattern of deformation during loadbearing[22]	• Pattern not known • Modelled deformation indicates differences[25] • Deformation not as pronounced?[34]

Key:

1 Bennett (1980, 1992)
2 Budras and Schiel (1996)
3 Colles (1983)
4 Collins *et al.* (1998)
5 Collins *et al.* (2002)
6 Collins and Reilly 2004a,b)
7 Doguer (1943)
8 Eley (1988)
9 Fowler (1995)
10 French (2000)
11 Getty (1975)
12 Groves (1974)
13 Groves (1986)
14 Hifny and Misk (1983)
15 Hinterhofer (1996)
16 Hildebrand (1987)
17 Hopegood (2002)
18 Hopegood *et al.* (2003b)
19 Kasapi and Gosline (1999)
20 Leach (1990b)
21 Leach and Zoerb (1983)
22 Lungwitz (1891)
23 Mathews (2000, 2002)
24 Mathews (2002 - Pers Com)
25 Newlyn *et al.* (1998)
26 Reilly (1997)
27 Reilly *et al.* (1996)
28 Reilly *et al.* (1998a)
29 Reilly *et al.* (2003)
30 Schummer *et al.* (1981)
31 Seegmiller and Ohmart (1981)
32 Svendsen (1995)
33 Symons (1994)
34 Tohara (1948)

1.10.2 CAPSULAR SHAPE

Distinct differences in capsular shape exist between the donkey and the horse – see Figure 1.14. The donkey is characterised by the presence of an 'upright boxy' hoof compared with the 'inclined rounded' capsule of the horse (Doguer 1943, Groves 1974, Reilly 1995). The hoof of the donkey displays a u-shaped (Getty 1975), or staple (French 2000), solear profile in which the dorso-palmar depth exceeds the medio-lateral width (Doguer 1943). The hoof wall of the donkey is also characterised by the presence of a marked flare, and by the development of a heel buttress. These characteristics are in marked contrast with the circular solear profile, and tapering heel of the horse hoof, and also the shallow inclined equine heel angle.

Summarising these differences, Collins *et al.* (2002) suggested that by first approximation the donkey hoof capsule could be considered as an inclined and truncated cylinder. Whereas the hoof capsule of the horse, resembles that of an inclined and truncated cone or frustum.

1.10.3 STRUCTURAL ORGANISATION OF THE HOOF WALL

Although the anatomical organisation the hoof capsule the donkey and the horse are broadly similar (Hifny and Misk 1983), Tohara (1948) stated that differences in the structural organisation existed between the two species – see Figure 1.15. Reilly (1997) provided photomicrographs that highlighted visual differences between the donkey and horse hoof wall. More recently Hopegood (2002), Collins *et al.* 2002, and Reilly *et al.* (2002a) have reported objective differences in pattern of tubule density, the number of horn tubules per unit area (TD) across the HWD at the midline of the hoof capsule – see Figure 1.16. Reilly *et al.* (1996) referred to this anatomical site as the midline dead centre of the hoof wall (MDC).

Collins *et al.* (2002) also commented upon the fact that the macroscopic appearance of the donkey hoof wall, was in marked contrast to that previously reported for the horse by Kasapi and Gosline (1997) – see Figure 1.15. The macroscopic appearance of the hoof wall reflects the structural organisation of tubular and intertubular horn. Collins and Reilly (2004a – Submitted) reported the presence of three distinct tubule types within the *SM* of the donkey hoof wall. These authors argued that it was possible to sub-divide the dorso-palmar depth of the *SM* into discrete morphological regions, or zones, based upon the regional distribution of these tubule types. This issue is discussed in detail in Chapter 4 of this thesis. Hence the differences noted in regional distribution of tubule types, between the donkey and the horse indicate the presence of a 'species specific' zonation pattern (Collins *et al.* 2002). The zonation pattern evident in the *SM* of the donkey hoof wall at the MDC, and the region distribution of the different Donkey Tubule Types, are illustrated in Figure 1.17.

Figure 1.13 Photograph of the distal of the donkey showing a 'Broken Forward' hoof pastern axis (HPA) characterised by an angular relationship between the dorsal hoof wall and the pastern axes.

Figure 1.14 Photographic summary of the geometric differences in the gross anatomical shape of the donkey (left) and horse (right) hoof capsule.

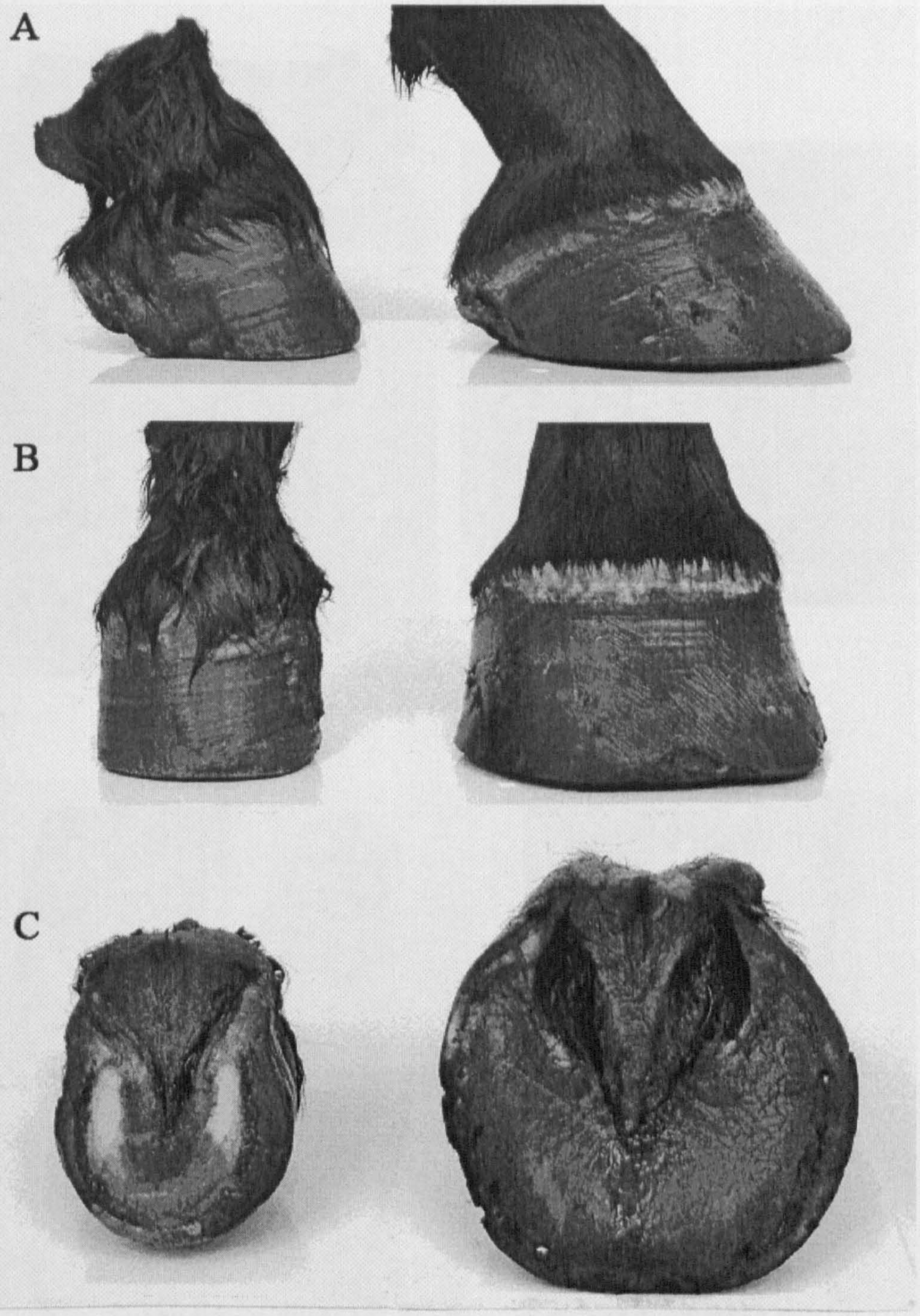

A. lateral view of the hoof capsule to highlight difference in dorsal hoof wall angle, and heel development and angulation. **B**. Dorsal view of the hoof capsule to highlight differences in the medial and lateral angulation of the hoof wall. **C**. solear view of the hoof capsule to highlight differences in the solear profile of the hoof, and the anatomical relationship between the sole and frog.

Figure 1.15 Photographic comparison of differences in structural organisation of the hoof wall at the macroscopic level in the design hierarchy between the donkey (above) and horse (below).

A.

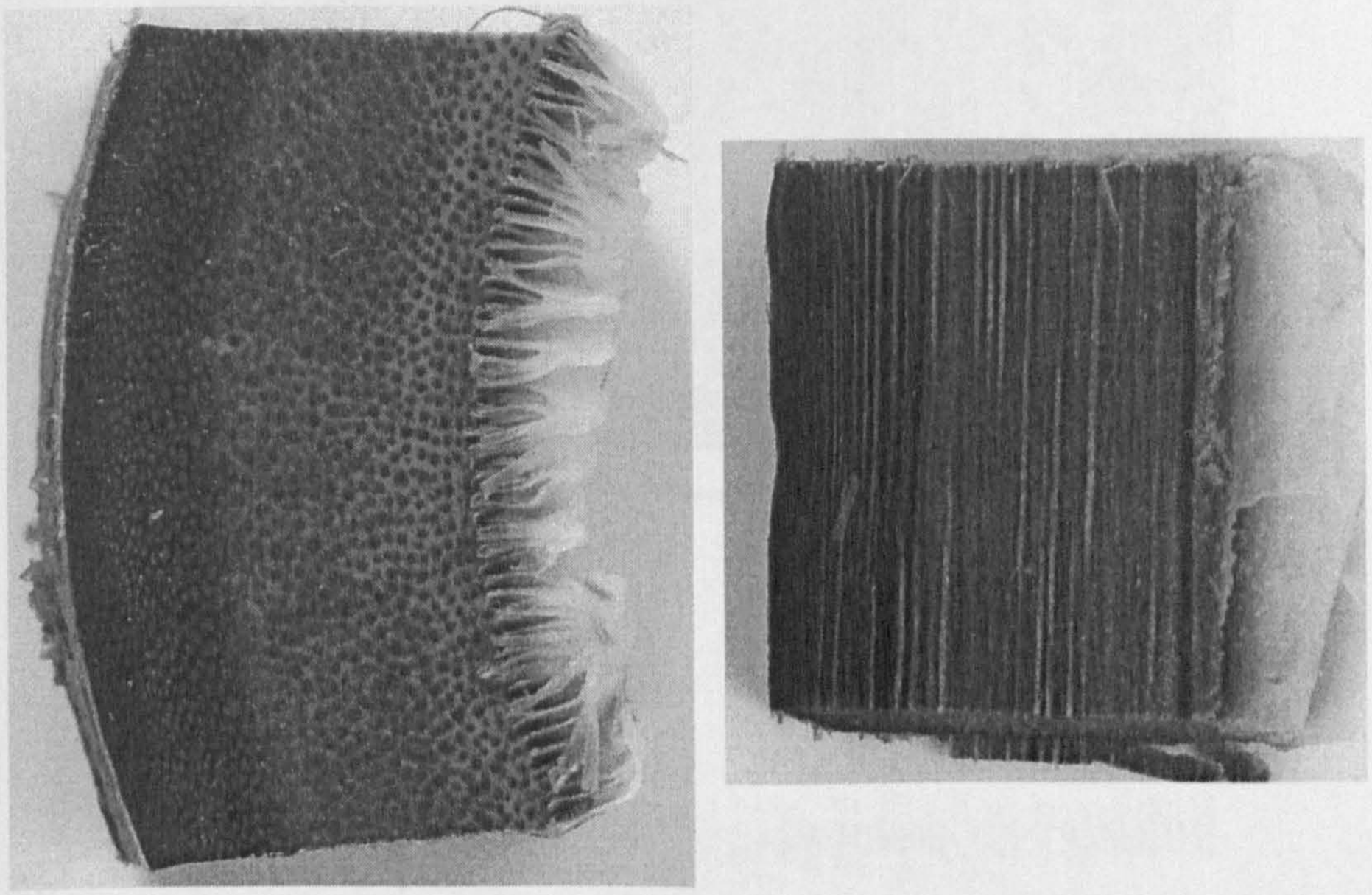

B.

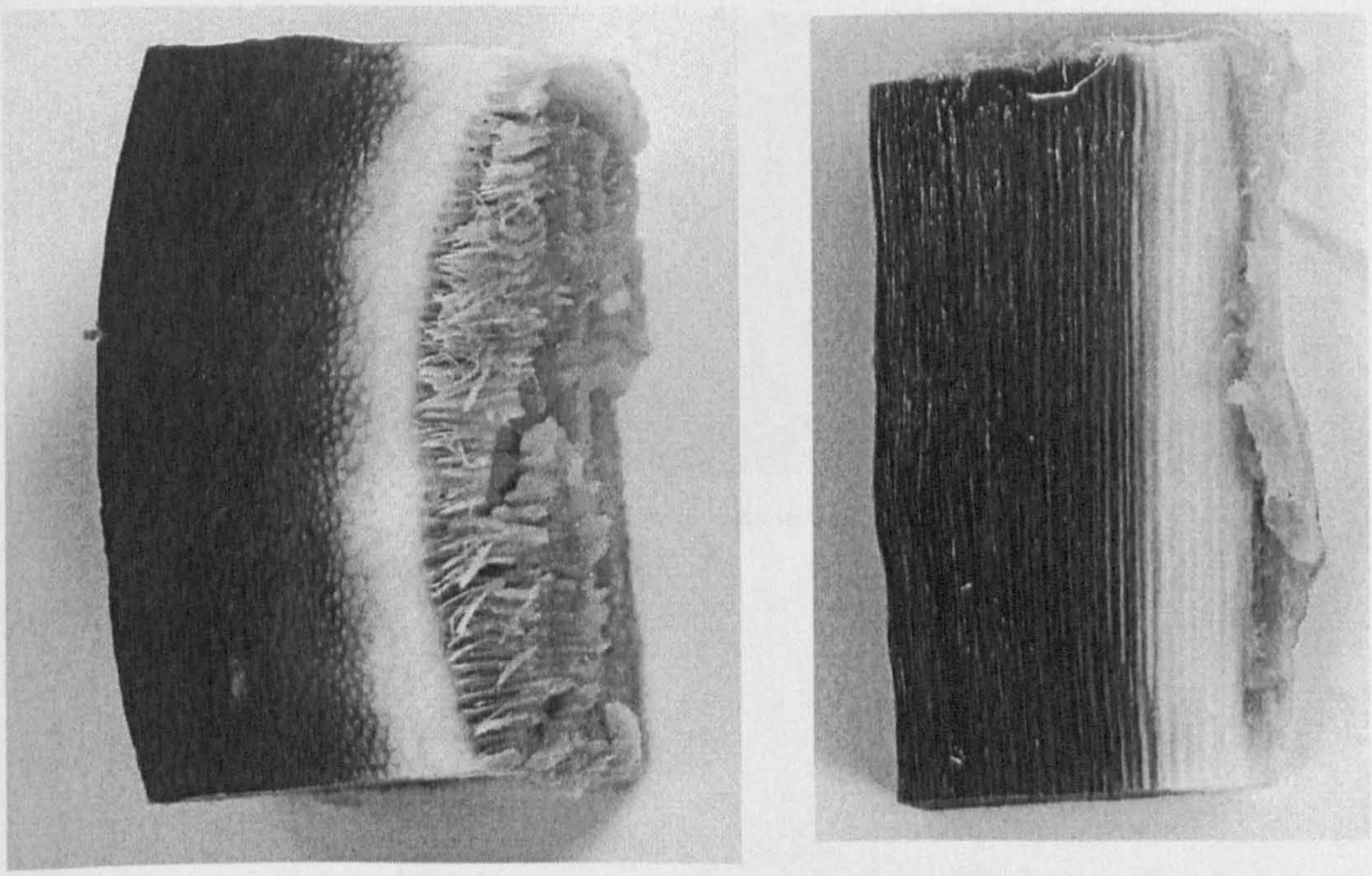

A. Donkey hoof wall at the midline of the hoof capsule in transverse (left) and longitudinal (right) section. **B.** Horse hoof wall at the midline of the hoof capsule in transverse (left) and longitudinal (right) section.

Figure 1.16 Comparison of differences in the dorso-palmar variation in tubule density (The number of horn tubules per unit area) across the hoof wall depth, at the midline of the donkey (top) and horse (bottom) hoof capsule (AB – PAS Staining).

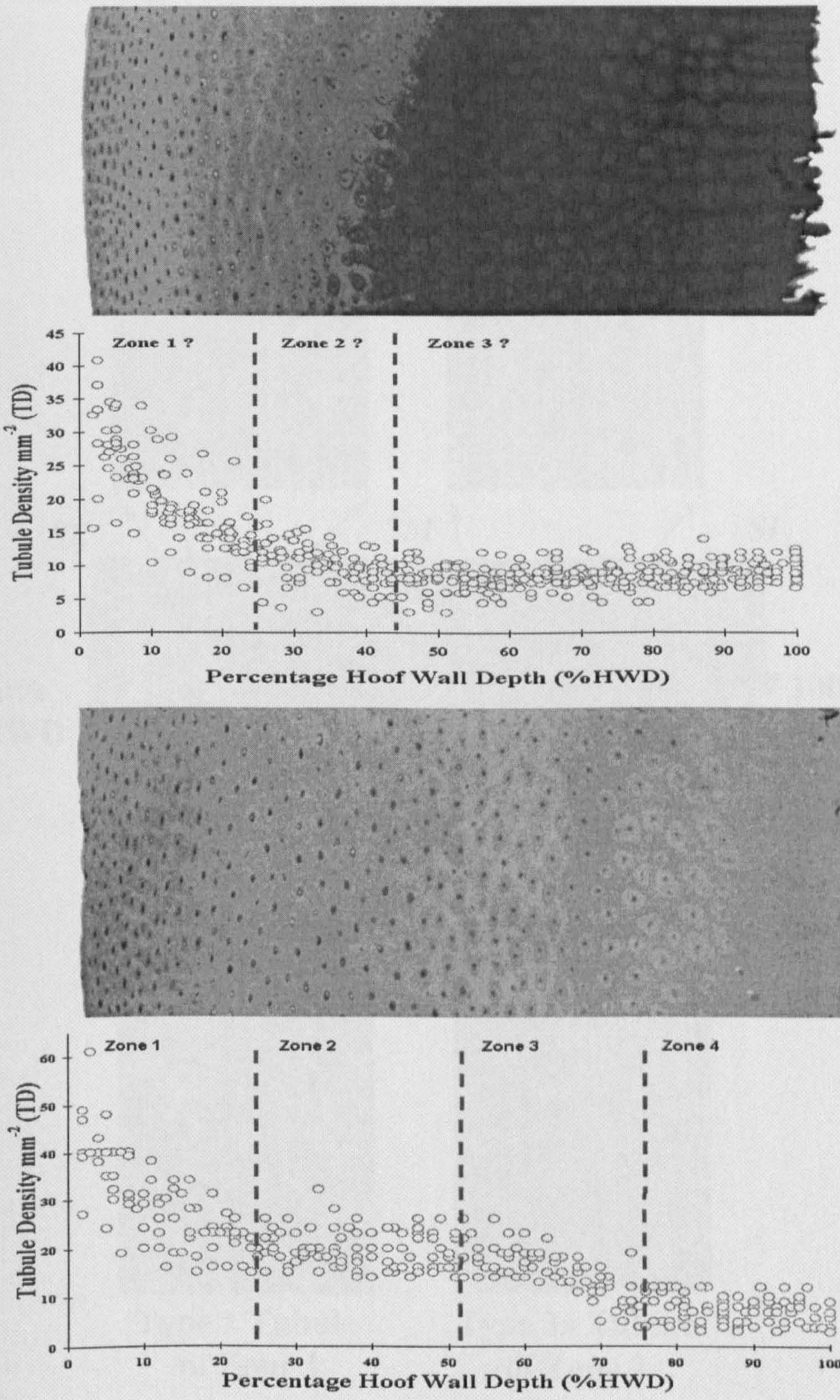

Figure 1.17 Photomicrograph of the transverse section of the donkey hoof wall at the midline dead centre (MDC) to show the three morphologically distinct Donkey Tubule Types, and the zonation of the *Stratum medium* by regional distribution of tubule types (AB – PAS Staining).

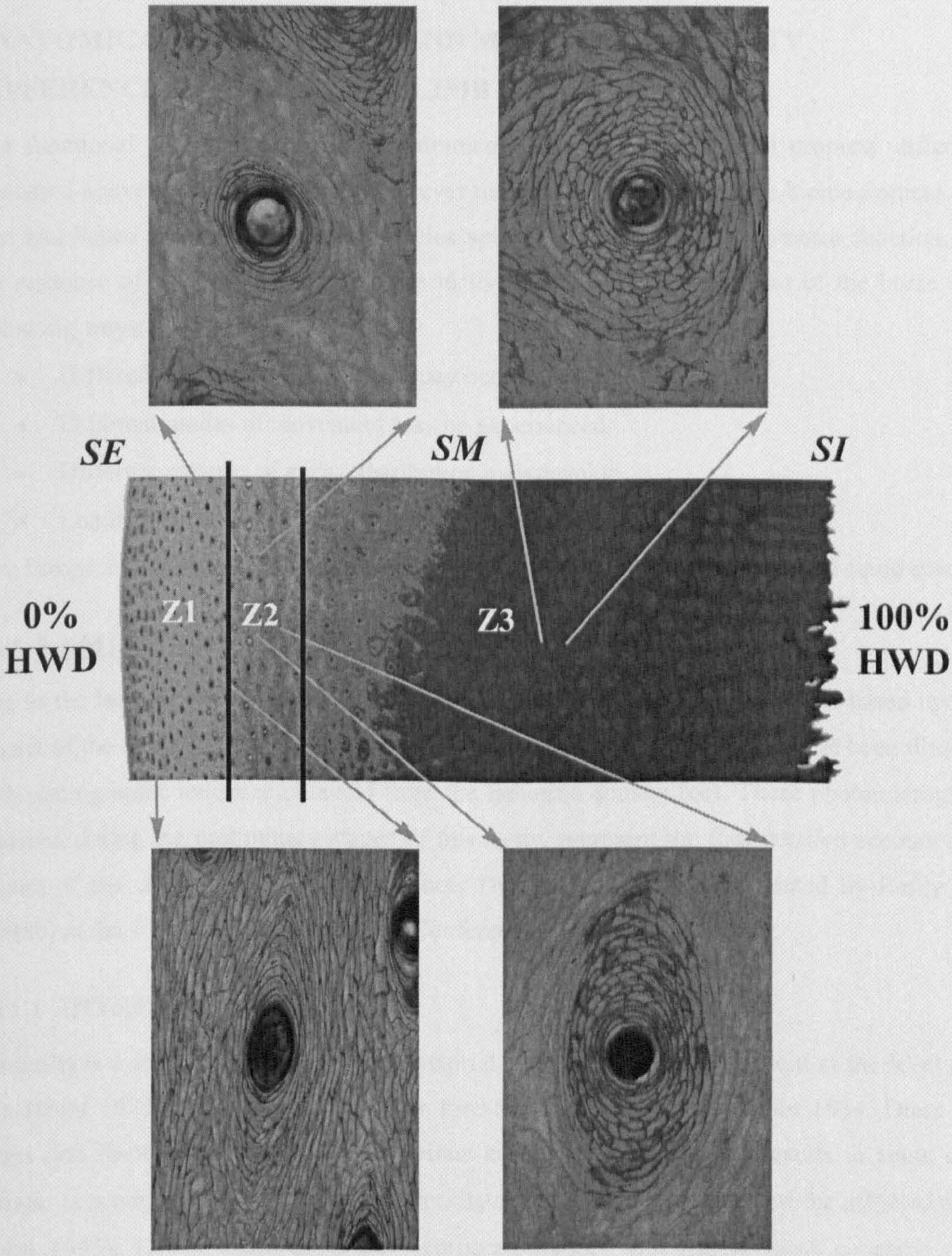

1.10.4 MATERIAL PROPERTIES OF THE HOOF WALL

Collins *et al.* (1998), Hopegood (2002) and Collins *et al.* (2002) have reported differences in the modulus of elasticity (E) of the hoof wall between the donkey and the horse.

1.10.5 BIOMECHANICAL CONSEQUENCES TO HOOF FUNCTION OF ANATOMICAL, STRUCTURAL AND MATERIAL PROPERTY DIFFERENCES IN THE DISTAL LIMB OF THE DONKEY

The functional consequences of the anatomical, structural and material property differences discussed above are poorly defined. However these are likely to affect the biomechanical of the foot and hence represent important 'species specific' differences in locomotor function. Thus the response of the donkey hoof capsule to loading may differ from that of the horse in the following ways: -

- Different amounts of movement may occur.
- Different modes of movement may be experienced.
- Different patterns of stress distribution may develop.
- Loading forces may be accommodated differently.

This brings into question the validity of applying an equine model to this unique equid species.

1.11 LAMINITIS

Due to the lack of information regarding laminitis in the donkey, this review is based upon the impact of the condition in the horse. However the events covered in review have been illustrated with photographic evidence obtained from the laminitic donkey foot. These photomicrographs, obtained during the preliminary stages of this study, represent the first detailed account of the impact of the condition in the donkey foot. This information was presented by Reilly *et al.* (1998b) at the 1st International Research Conference on Equine Laminitis.

1.11.1 INTRODUCTION

Laminitis is a complex disease of multifactorial origin that becomes evident at the level of the foot (Hunt 1993), that poses a particular threat to all *Equidae* (Åkerblom 1934, Dietz 1977, Riggs and Knottenbelt 2000). It is a serious and painful disease that results in acute and/or chronic lameness. Indeed it may even necessitate the humane destruction of the afflicted animal (Hunt 1993). Hence laminitis raises significant welfare and management concerns (Hood 1999a).

The most commonly reported causal factors for laminitis are carbohydrate overload, overlong feet, trauma on hard ground, retained placenta, stress, concurrent diseases and pituitary tumour. Although the predisposing causes of laminitis are varied, they induce disturbances within the digital circulation leading to vascular compromise, focal anoxia, tissue damage and inflammatory responses that lead to degenerative changes within the foot (Hood *et al.* 1993a).

The unique character of the equid digital, which is marked by numerous arteriovenous anastomoses, counter-current mechanisms and low systolic pressure, is well documented (Allen *et al.* 1988, Pollitt and Molyneux, 1990, Hunt 1991, Hood *et al.* 1994, Molyneux *et al.* 1994, Moore and Allen 1995, and Hirschberg *et al.* 2001). Indeed Hood (1999a,b) stated that the nature of the anatomy, and physiology, of the equid digital circulation actually predisposes the genus to vascular compromise. Hence the significant threat that laminitis poses to all equids.

The major focus of laminitic research in the equid has centred upon aetiology (cause) and pathophysiology (effects) within the dermal tissues of the foot, during the developmental stage. Research efforts have concentrated on the laminar corium in particular, which lends its name to the term laminitis, the inflammation of the dermal lamella (Reilly *et al.* 1998b).

Consequently little is known about the nature of degenerative changes evident elsewhere within the dermis of the foot, or the impact upon hoof horn material that the dermis supports (Reilly *et al.* 1998b). Similarly there is little information as to the long-term effect of these degenerative changes upon the hoof (Hunt 1996). These issues are clearly of fundamental concern given the biomechanical importance of the hoof (Reilly *et al.* 1998b).

Hence it can be argued that the chronic lameness often associated with laminitis is more likely to reflect upon the degenerative consequences of these pathophysiologic events, rather than the specific causal events themselves. In this regard, Hood *et al.* (1993b, Hunt 1996) stated that in spite of widespread knowledge of the inductive aetiologic mechanisms of laminitis, further research was required to assess the consequences of the pathophysiologic events within the chronically affected foot.

It is therefore more appropriate to refer restrict the use of the term laminitis to those pathophysiologic events associated with the initiation of the developmental and acute inflammatory phase within the dermis. Hence the convention adopted in this thesis is to use the broader generic term of the 'laminitic condition' to encompass both the developmental and acute inflammatory stage, and the degenerative changes that occur within the foot as a consequence of laminitis.

1.11.1.1 THE AETIOLOGY OF LAMINITIS

Three distinct aetiological hypotheses have been proposed, and have been extensively reviewed by Moore *et al.* (1989), Baxter (1994), and Hood (1999c). These are: -

1. The vascular hypothesis

This hypothesis argues that all pathological events, including metabolic dysplasias, inflammatory processes and tissue damage, stem from an ischaemic crisis, or infarction, within the foot.

2. The toxic/metabolic hypothesis

This theory suggests that the vascular, structural and inflammatory changes follow directly from metabolic dysfunction within the foot, induced by the action of toxic agents.

These two distinct mechanistic processes suggest that laminitis develops secondary to a systemic insult within the affected animal.

3. The traumatic hypothesis

This hypothesis proposes that vascular, metabolic and inflammatory responses within the foot develop as a direct consequence of digital trauma.

1.11.1.2 THE PROGRESSION OF THE LAMINITIC CONDITION

The onset of the acute phase of the condition is marked by changes in stance and gait of the afflicted animal (Obel 1948, Hood 1999a), which are indicative of acute pain within the affected foot. Degenerative changes are initiated within the foot as a consequence of the attendant vascular disturbance (Hood *et al.* 1993a,b).

STRUCTURAL FAILURE OF THE SADP

Pathologic changes within the laminar interface compromise the structural integrity of the SADP (Marks 1984, Pellmann 1995, Pellmann *et al.* 1997, Pollitt 1998a,b, Johnson *et al.* 1998, 2000), and reduce the ultimate strength of this structure (Hallab *et al.* 1991, Pollitt and Daradka 1998, Hood 1999a,b). This threatens the functional ability of the SADP to effectively suspend the appendicular skeleton within the hoof capsule (Budras *et al.* 1992a,b, 1996). Biomechanical forces acting upon the compromised dermo-epidermal junction can ultimately lead to failure of the SADP (Coffman *et al.* 1970a, Stick *et al.* 1982), resulting in the dislocation of the DP (Obel 1948, Marks 1984).

Hood *et al.* (1993a), Hood (1997, 1999a,b,c) and Morgan *et al.* (1999) considered that the dislocation of the DP signified the onset of digital collapse. This event marks the progression into a distinct phase of the condition. Structural failure of the SADP results in irreversible changes to the normal anatomical organisation of the foot, which adversely affect the normal

biomechanical function of the foot. In this regard, Dietz (1977) and Hood (1997a) asserted that digital collapse should be viewed as a distinct pathological condition from that which precedes the failure of the SADP. These issues are considered in Section 1.11.3, and Appendix II.

The mechanical failure results in traumatic tearing and compression of dermal tissues relatively unaffected by the initiating pathology. It is also at this stage in the progression of the laminitic condition, that secondary pathologies are initiated within the foot.

In fact, the irreversible degenerative changes associated with progression into the chronic phase of the condition preclude a full recovery, and restoration of the normal anatomical organisation of the foot.

Regenerative processes however attempt to restore the functional integrity of the SADP (Budras *et al.* 1992a, b, Bragulla *et al.* 1992). This takes the form of cicatricial 'scar' horn production. However the resultant 'scar' horn that is produced is altered pathologically (Budras *et al.* 1992a,b).

BIOMECHANICAL CONSEQUENCES OF DIGITAL COLLAPSE

The decoupling of the DP associated with the failure of the SADP prevents the foot from acting as an integrated functional unit (Hood 1999a). This alters the manner in which forces are distributed within the hoof capsule, and results in individual components of the foot being subjected to abnormal loading conditions (Oliver 1987). Failure of the SADP leads to both osseous and exosseous alterations within the foot.

DISLOCATION OF THE DP

It has been suggested that the precise nature and extent of the dislocation of the DP has a direct bearing upon the severity of condition and hence the prognosis of the affected animal (Kameya 1973, Stick *et al.*1982, Eustace 1991, 1995, Cripps and Eustace 1999a,b).

THE NATURE OF THE DP DISLOCATION

The failure of the laminar interface results in either rotation or distal displacement of the DP within the hoof capsule. Historically these two distinct modes of DP dislocation have been referred to as 'founder' and 'sinker' respectively (Butler *et al.* 1998). However these two modes of dislocation are not mutually exclusive (Baxter 1992a,b). Goetz (1987) stated that most afflicted animals exhibit a combination of both rotation and distal displacement.

ROTATIONAL DISLOCATION OF THE DP – 'FOUNDER'

Eustace (1992), Fergusson (1994) and Herthel and Hood (1999) have commented upon the varied nature of rotational dislocation that may occur within the affected foot. Cripps and

Eustace (1999a) stated that there is a clinical need to accurately establish the precise nature of the rotational dislocation. In this regard, three distinct rotational events can be identified. These are: -

1. Capsular Rotation

Capsular rotation is characterised by the unequal dislocation of the dorsal aspect of the DP relative to the dorsal aspect of the hoof wall, such that the two surfaces are not in parallel alignment. In addition, the phalangeal axis exhibits a straight alignment. This dislocation event is what Stick *et al.* (1982) referred to as pedal bone (*sic* DP) rotation.

The mechanism responsible for the development of capsular rotation is unknown, and remains an area of conjecture. Herthel and Hood (1999) considered that leverage of the dorsal aspect of the hoof wall against the weakened SADP, which occurs as the toe rolls over during locomotion, leads directly to the physical separation of the DP from the hoof wall, to produce this unequal dislocation. Alternatively, Stick *et al.* (1982) suggested that the action of the DDFT upon the DP, in those cases where compromise to the SADP was localised to the dorsal aspect of the laminar interface, led to this type of dislocation. Ryan (1999, 2000a) however considered that capsular rotation resulted from differential rates of hoof horn growth between the dorsal aspect of the hoof wall and the heels, which result as a *sequela* of the acute phase of the condition.

2. Phalangeal Rotation

Phalangeal rotation is characterised by the dorso-palmar dislocation of the DP around the DIP to produce a 'broken' phalangeal axis. The dorsal aspect of the hoof wall is in parallel alignment with the dorsal aspect of the DP, hence this type of rotation is also characterised by the presence of a 'Broken Forward' HPA.

A satisfactory explanation for the development of Phalangeal Rotation is lacking. However several contributing factors have been suggested. Rotation of the DP around the DIP joint may arise as a consequence of the as a consequence of the action of the DDFT on the DP. The reluctance of the animal to bear weight fully on the afflicted foot may result in the rotation of the DP around the DIP joint in response to the action of the DDFT. This may be further exacerbated overtime as a consequence of DDFT contraction that can result from a prolonged absence of normal tendon loading. Weight shifting away from the afflicted foot, may also result in reduced heel wear, which combined with the differential rates of hoof horn growth (see Section 1.8, may lead to development of a 'Broken Forward' HPA. Conversely (Herthel and Hood 1999) suggested that differential hoof horn growth could result in a tendency for heel height to increase, and thus induce flexure of the DIP joint.

3. Combined Rotation

This type of dislocation involves both capsular and phalangeal rotation within the afflicted foot. It is characterised by both flexure of the DIP joint, resulting in a 'broken' phalangeal axis, and the absence of parallelism between the dorsal aspect of the hoof wall and the dorsal aspect of the DP. The mechanisms involved in the development of combined rotation are also unclear. In fact, it is not known whether combined rotation arises as a consequence of the same mechanisms that are responsible for phalangeal and capsular rotational dislocation, which occur either sequentially or concurrently within the foot, or whether it represents a distinct *sequela* of degenerative change.

Herthel and Hood (1999), commenting upon the contributing factors relating to phalangeal rotation, described two mechanistic scenarios that would actually result in the development of combined rotation, rather that phalangeal rotation alone.

Firstly Hood (1999a) stated that laminar compromise might adversely affect the resistance afforded by the SADP to the action of the DDFT on the DP, leading to palmar rotation of the DP around the DIP joint. This author also stated that is a tendency for the apex of the DP to displace distally in response to a loss of functional integrity within the SADP, due to the fat that the sole preferentially supports the palmar aspect of the DP.

Both of these events would result in development of a 'broken' phalangeal axis, and also, the unequal dislocation of the dorsal aspect of the DP relative to the dorsal aspect of the hoof wall, that is, the characteristic of combined rotation.

DISTAL DISPLACEMENT OF THE DP – 'SINKER'

Distal displacement of the DP (DP displacement) is characterised by the distal dislocation of the DP relative to the hoof wall. Parallelism is maintained between the dorsal aspect of the DP and the dorsal aspect of the hoof wall. DP displacement is marked both by an increased linear distance between the proximal limits of the two structures, in a distal direction, and also an increased orthogonal distance between the dorsal aspect of the hoof wall and the dorsal aspect of the DP.

DP displacement is generally thought to indicate structural compromise throughout the entire laminar interface (Baxter 1986, Herthel and Hood 1999). The resultant loss of laminar support is such that the vertical GRF, imposed upon the foot during static loading, predominates in the process of digital collapse. This effectively forces the hoof wall up the limb and displaces the DP and sole towards the ground, thereby shearing the SADP.

Baxter (1986) concluded that DP displacement represented a severe form of digital collapse that often necessitates euthanasia, and hence reflected a guarded prognosis for the animal. However Hood (1999a) challenged this assertion, stating that this misconception had arisen due to inherent difficulties in detecting modest DP displacement. Hood (1999a) stated that DP displacement frequently accompanies rotational dislocation. Indeed O'Brien and Baker (1986) argued that an increase in the orthogonal linear distance, between the dorsal aspect of the hoof wall and the dorsal aspect of the DP was pathognomonic of the initial stages of the dislocation of the DP *per se*. Linford (1987, 1990) and Linford *et al.* 1993 suggested that this resulted from 'laminar' *sic* lamellar swelling associated with inflammatory responses during the acute phase of the condition.

ROENTGENIC CHANGE WITHIN THE DP

Osseous changes (roentgenic change) in the DP have been widely reported in association with the laminitic condition (Chandra *et al.* 1982, McNeel 1986, Linford 1990, 1996, Butler *et al.* 1998, Thrall 1998). These include new bone formation, and bone resorption and demineralisation. These in turn result in changes to the bone contour, density and shape of the DP. These degenerative processes reflect changes in the biomechanical forces acting upon the DP during the progression of the condition (Colles and Jeffcott 1977, Colles1983). O'Brien and Baker (1986) and Baxter (1992a, 1994) stated that mild bony reaction along the dorsal aspect of the DP is one of the earliest diagnostic signs of the laminitic condition. In the chronic phase of the condition, a distinct 'dorsal hump' may occur due to new bone formation along the dorsal aspect of the DP (O'Brien and Baker 1986). In addition, a 'ski-tip' profile may arise due to bone spur formation at the apex of the DP (Baxter 1992a,b). Butler *et al.* (1998) stated that this is most notable in those cases that have taken 'pressure' on the sole. Excessive pressure on the sole can lead to bone fracture at the apex of the DP (Linford 1987), or degenerative resorption of the DP. The nature of the roentgenic changes evident within the afflicted foot, are widely accepted to be related to the severity of the condition, and to be of prognostic significance (Eustace 1995, Hemker 2001, Glöckner 2002).

1.11.1.3 THE IMPACT OF DIGITAL COLLAPSE UPON THE INTEGUMENT OF THE FOOT

Digital collapse has a profound effect upon the intimate association that exists between the dermal and epidermal components of the foot, and leads to the development of specific pathophysiologic sequelae. These include vascular malperfusion (Hood et al. 1994), metabolic dysfunction (Grosenbaugh and Hood 1992, 1993, Grosenbaugh *et al.* 1999), and altered patterns of hoof horn formation (Grosenbaugh *et al.* 1991, Ryan 1995, 1999, 2000a, b) within the

afflicted foot. Dietz (1977) stated that the events following digital collapse should be viewed as a discrete pathology.

As the nature and extent of the DP dislocation varies within the foot, then the resultant pathophysiologic changes are also likely to be different (Reilly *et al.* 1998b). This may in part account for varied nature of the clinical presentation of the chronically affected laminitic animal reported by Morgan *et al.* (1999).

THE IMPACT AT THE LEVEL OF THE CORONARY BAND

Changes in the appearance of the coronary band are frequent and varied in the laminitic condition (Hood 1999a). During the early stage of the condition, the coronary band appears swollen and oedematous. As digital collapse occurs, the coronary band is displaced distally. This displacement results in the development of a palpable depression or 'sunken coronary band', which is detectable at the distal hairline. It is believed that the extent of this depression is related directly to the degree of laminar compromise, and the nature of the DP dislocation (Linford 1990). This is restricted to the midline of the hoof, in the case of DP rotation (Linford 1990, 1996) whereas, the depression extends from the midline towards the heels if DP displacement has occurred (Baxter 1986). The development of this depression affects the normal anatomical organisation of the coronary corium. In the normal foot, the extensor process of the DP extends above the height of the coronary groove. However following digital collapse, the extensor process may be displaced distally behind the coronary sulcus, displacing and compressing the dermal tissues of the coronary corium behind the hoof wall (see Figure 1.18).

This anatomical re-organisation distorts the coronary corium, increasing its dorso-palmar depth (Eustace 1993, Hood *et al.* 1994, Hood 1999a) and altering the papillae orientation (Goetz 1987, Eustace 1993). This displacement (see Figure 1.19) is associated with papilla hypoplasia, and blunting of the apical tips (Hood *et al.* 1994). This displacement is also believed to result in the generation of tensile and/or shear forces within the dermis. This can lead to a physical separation of the hoof wall from the dermis, and can result in retraction of the dermal papillae from the papillary sockets (see Figure 1.20 and Figure 1.22). Subsequent horn production no longer maintains parallel alignment with the dorsal aspect of the DP.

These anatomical changes also lead to the development of negative interstitial pressure within the dermal tissues of the corium (Oliver 1987), that may account for the vascular malperfusion reported by Hood (1984) and Hood *et al.* (1994).

The coronary corium is normally protected from traumatic damage during weight bearing by energy absorption within the wall (Dyhre-Poulson *et al.* 1994) and by stress transfer across the laminar interface (Oliver 1987).

Figure 1.18 Schematic of the sagittal section of the equid foot to illustrate the effects of DP dislocation upon the integumentary structures of the coronary corium (Modified after Goetz 1987).

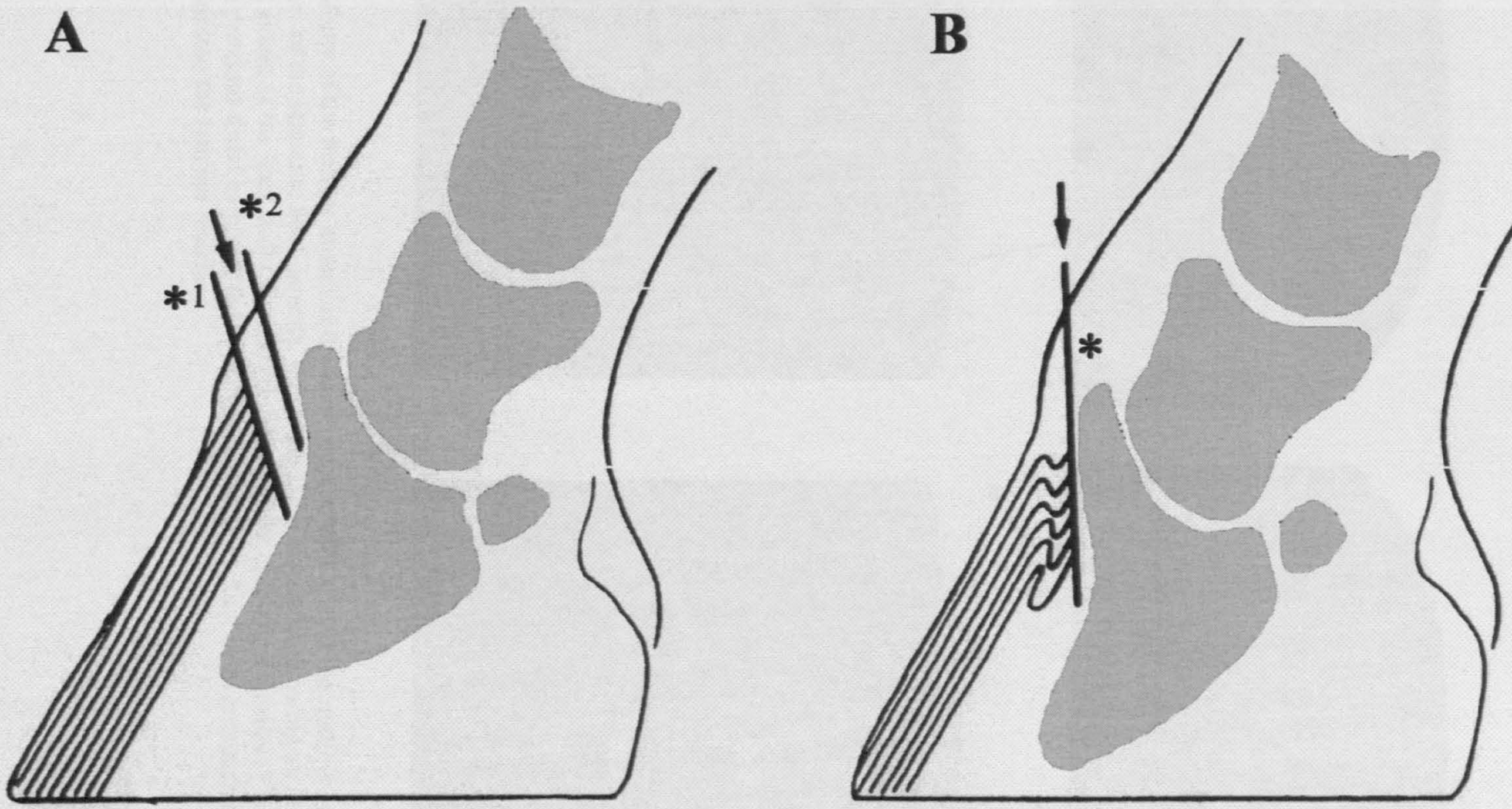

A. Normal anatomical organisation of the foot to show the relationship between the extensor process of the DP, the dermal tissues of the coronary corium, and the tubule orientation of the hoof wall. Parallel lines, marked $*^{1,2}$ show the boundary, and orientation, of the proximal and distal limits of the dermis of the coronary corium, in relation to the DP and the hoof wall.

B. Anatomical organisation of the foot following DP dislocation, showing displacement of the extensor process of the DP and the resultant compression, stretching and anatomical displacement of the coronary corium, and the reorientation, 'kinking', of the horn tubules. Line marked * indicates compression of the proximal and distal dermal limits, elongation of the coronary corium, and reorientation of the corium in relation to the extensor process and the hoof wall.

Figure 1.19 Photographs of the interio aspect of the donkey hoof capsule, at the height of the CB, to illustrate the increase in the proximo-distal extent of the hoof wall at the midline of the capsule, which results from the stretching of the coronary corium following DP dislocation.

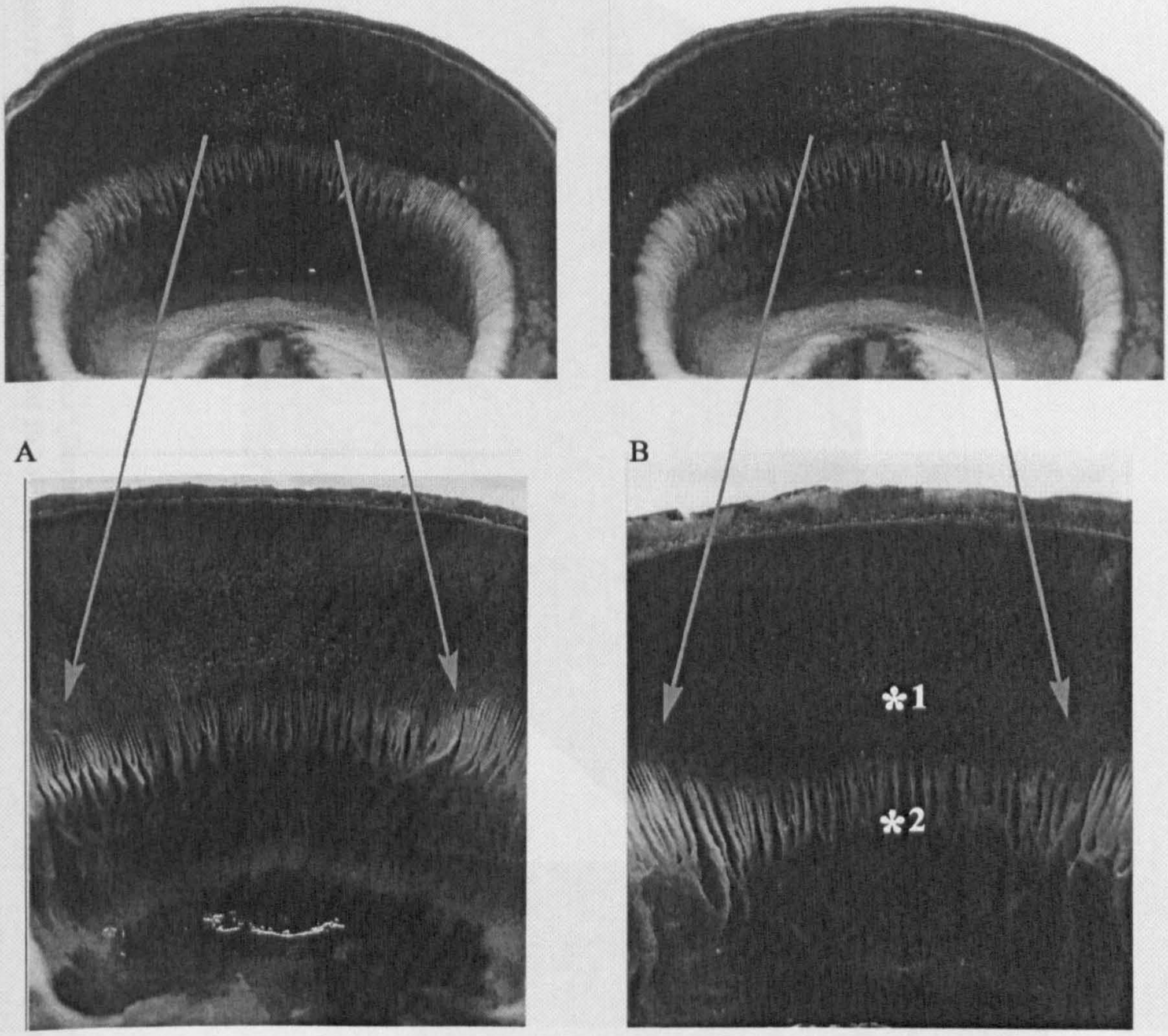

A. Normal anatomy of the interior aspect of the hoof capsule hoof wall at the midline of the hoof capsule. **B** Interior aspect of the laminitic hoof capsule, following DP dislocation, showing an increase in the proximo-distal extent of the hoof wall ($*^1$), and stretching of the epidermal lamella ($*^2$). Note also, the decrease in the proximo-distal height of the epidermal lamella resulting from encroachment of the coronary corium into the laminar interface.

Figure 1.20 Photograph of a sagittal section of the laminitic donkey foot to show evidence of papillary retraction and separation from the former hoof wall. The separation is marked by a shear lesion (*) in the wall. Note 'kinking', reorientation of the horn tubules proximad to the shear lesion.

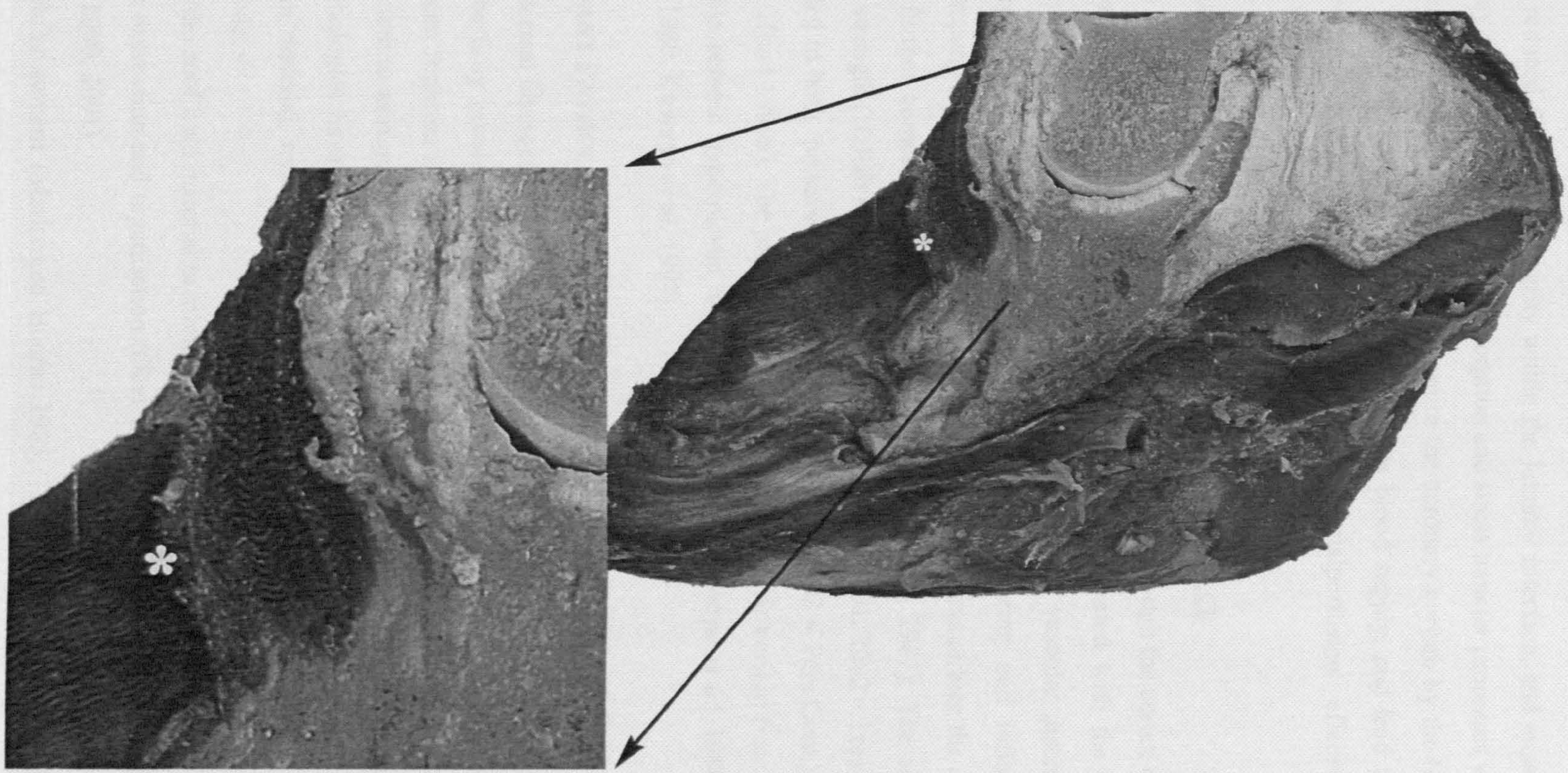

However encroachment of the coronary corium into the laminar interface reduces the effective proximo-distal extent of the SADP (Hood *et al.* 1994, Hood 1999a,b). This encroachment, combined with the reduced functional integrity within the laminar interface, and misalignment of the hoof wall, may adversely affect energy absorption and stress transfer processes within the hoof wall, thus reducing the level of protection given to the coronary corium by the hoof wall. This may result in traumatic damage to the dermis and its blood supply, and lead to further inflammatory responses, pressure necrosis and vascular malperfusion effects, which subsequently affect hoof horn formation.

THE IMPACT ON THE LAMINAR CORIUM AND THE LAMINAR INTERFACE

The laminar dermis is, in part, supported by vasculature that passes through the cortex of the DP (Hood *et al.* 1994). Dislocation of the DP (see Figure 1.21) associated with the laminitic condition compromises the blood supply to the coria. This resultant vascular disturbance is further compounded by lamellar stretching, submural lamellar tearing and inflammatory responses that accompany this dislocation. These events are thought to exacerbate the challenge to the SADP and further compromise its functional integrity (Goetz 1987). The associated reduction in tensile strength (Hallab *et al.* 1991, Hood 1999a, Pollitt 2001, 2002 – Pers Com.) is believed to be related to both the severity of the condition (Pollitt 2002 – Pers Com.), and the treatment outcome (Hood 1999a). The physical separation of the laminar corium from the hoof wall induces variable ectopic hyperplastic hoof horn formation (Kameya *et al.* 1980, Marks 1984, Budras *et al.* 1989, Kuwano *et al.* 1998).

1.11.1.4 ATTENDANT PATHOLOGIES IN THE CHRONIC LAMINITC HOOF

The effects of the dermal changes associated with digital collapse upon the epidermis that they support are yet to be fully investigated (Reilly *et al.* 1998b). However a number of attendant pathologies have been reported in the chronically affected hoof. In fact Dietz (1977) viewed these changes sufficient to warrant the specific generic pathologic term of 'Laminitis Hoof'.

Attendant hoof pathologies have been described at every level in the design hierarchy, and affect the hoof horn material, its structural organisation and the geometric form of the hoof capsule. These include: -

- Changes to the hoof horn material involving:
  - Keratin expression and organisation (Obel 1948, Larsson *et al.* 1956, Marks 1984, Wattle 2000, 2001)
  - Intercellular cement (Marks and Budras 1985, 1986, Budras and Bragulla 1990, Bragulla *et al.* 1992 Mülling 1993)

  - Moisture levels (Goetz 1987, 1989)
  - Ectopic/hyperplastic 'scar horn' formation (Wortley-Axe 1912, Marks 1984, Budras *et al.* 1989, Kuwano *et al.* 1998, Reilly *et al.* 1998b) see Figure 1.22, and Figure 1.24
  - Hyperplasia/hypertrophy of the periople (Wortley-Axe 1912, Reilly *et al.* 1998b) – see Figure 1.25
- Changes to the structural organisation at the macro- and microscopic level including:
  - 'Kinked'/'Crimped' horn tubules (Lungwitz and Adams 1913, Goetz 1987, 1989, Eustace 1991, Pollitt 1995) see Figure 1.23 and Figure 1.24
  - 'Tubule irregularities' (Said *et al.* 1992, Nakade *et al.* 1992, Mostafa 1986, Reilly *et al.* 1998b, Collins *et al.* 2002)
  - Changes in the structural organisation of the white line (Marks 1984, Budras and Huskamp 1990, Budras and Schiel 1996, Reilly *et al.* 1998b)
- Changes of geometric form
  - Dorso-concavity of the hoof wall (Lungwitz and Adams 1913, Dietz 1977)
  - 'Angulation' of the hoof wall (Hood 1999a)
  - Divergent growth rings (Lungwitz and Adams 1913, Colles and Jeffcott 1977) see Figure 1.26
  - Irregular thickening of the hoof wall (Eustace 1993)
  - Dimensional changes to the white line (Budras *et al.* 1989, Budras and Huskamp 1990 Reilly *et al.* 1998b)
  - Flattening/Bulging of the sole (Linford 1990, Pollitt 1995, Morgan *et al.* 1999)

Bragulla *et al.* (1992) considered that the pathophysiology of the laminitic condition results in the production of poor 'quality' hoof horn, and Maclean (1971a) stated that resultant hoof horn was less able to afford protection to the sensitive structures of the foot. In this regard, Hendry *et al.* (1997, 1998) argued that the laminitic condition should be correctly considered as a:

"consequence of poor 'quality' hoof horn".

This statement implies that the debilitating effects of the laminitic condition are inextricably linked to epidermal changes, and their resultant effect upon hoof function. It therefore follows that the attendant epidermal changes may be related to the severity of the condition, and directly affects the recovery outcome of the laminitic equid.

This statement further highlights the important role of hoof horn research in developing a comprehensive understanding as to the impact of the laminitic condition on the affected animal. However in order to place this research on a proper scientific basis, quantitative assessment of the structure-function relationships within laminitic hoof horn is now required.

Figure 1.21 Photograph of a sagittal section of the laminitic donkey foot to show distortion of the lamina (*), solear corium (*[1]) caused by the rotation of the apex of the distal phalanx following DP dislocation. Note reorientation of the horn tubules of the sole (*[2]).

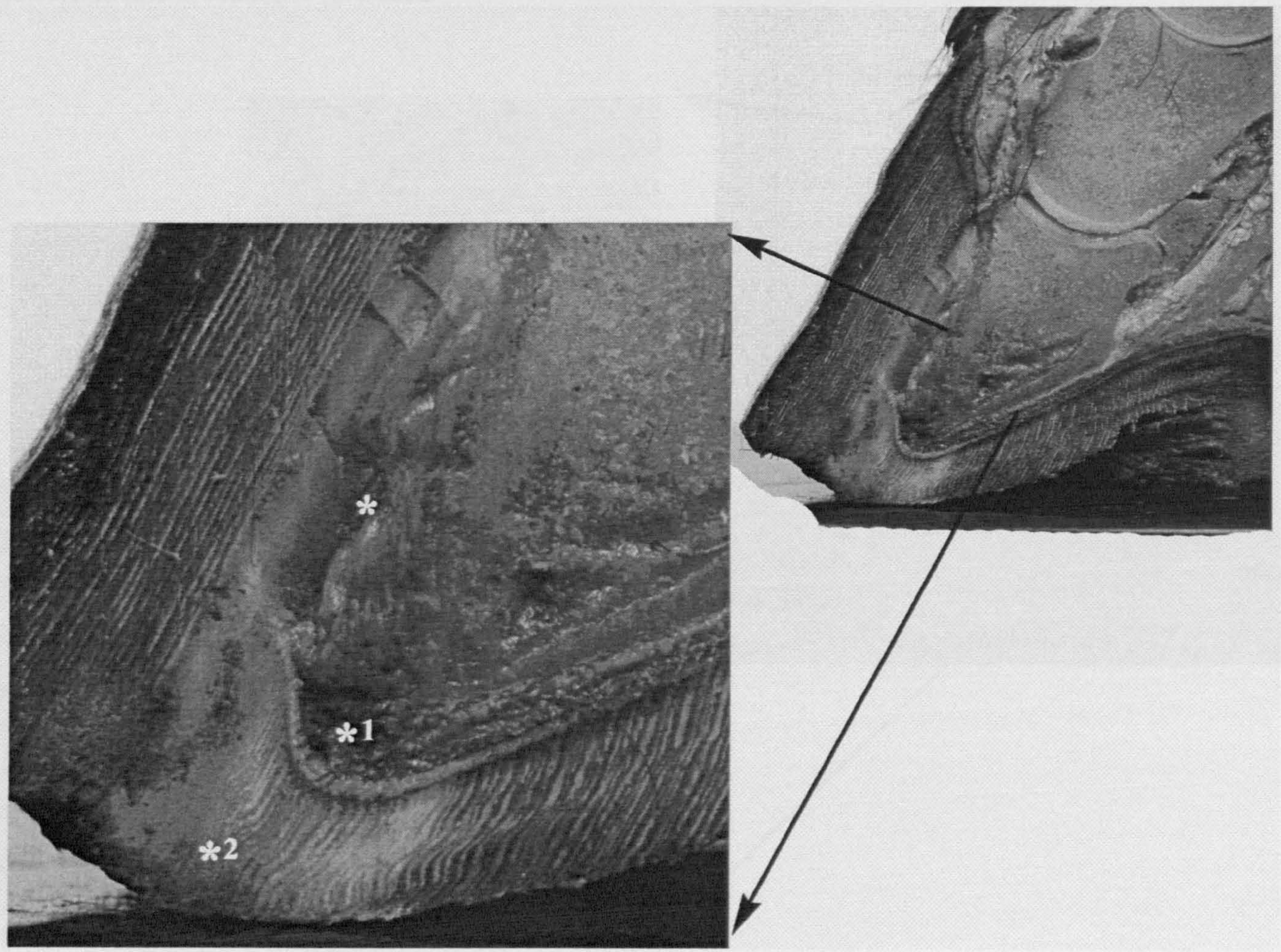

Figure 1.22 Photograph of a sagittal section of the laminitic donkey foot to show ectopic 'scar' horn formation in the laminar region of the foot (*1). Note dorso-palmar elongation (stretching) of the coronary corium (*2) resulting in an increase in dorso palmar hoof wall depth (*3), and encroachment of the corium into the laminar interface.

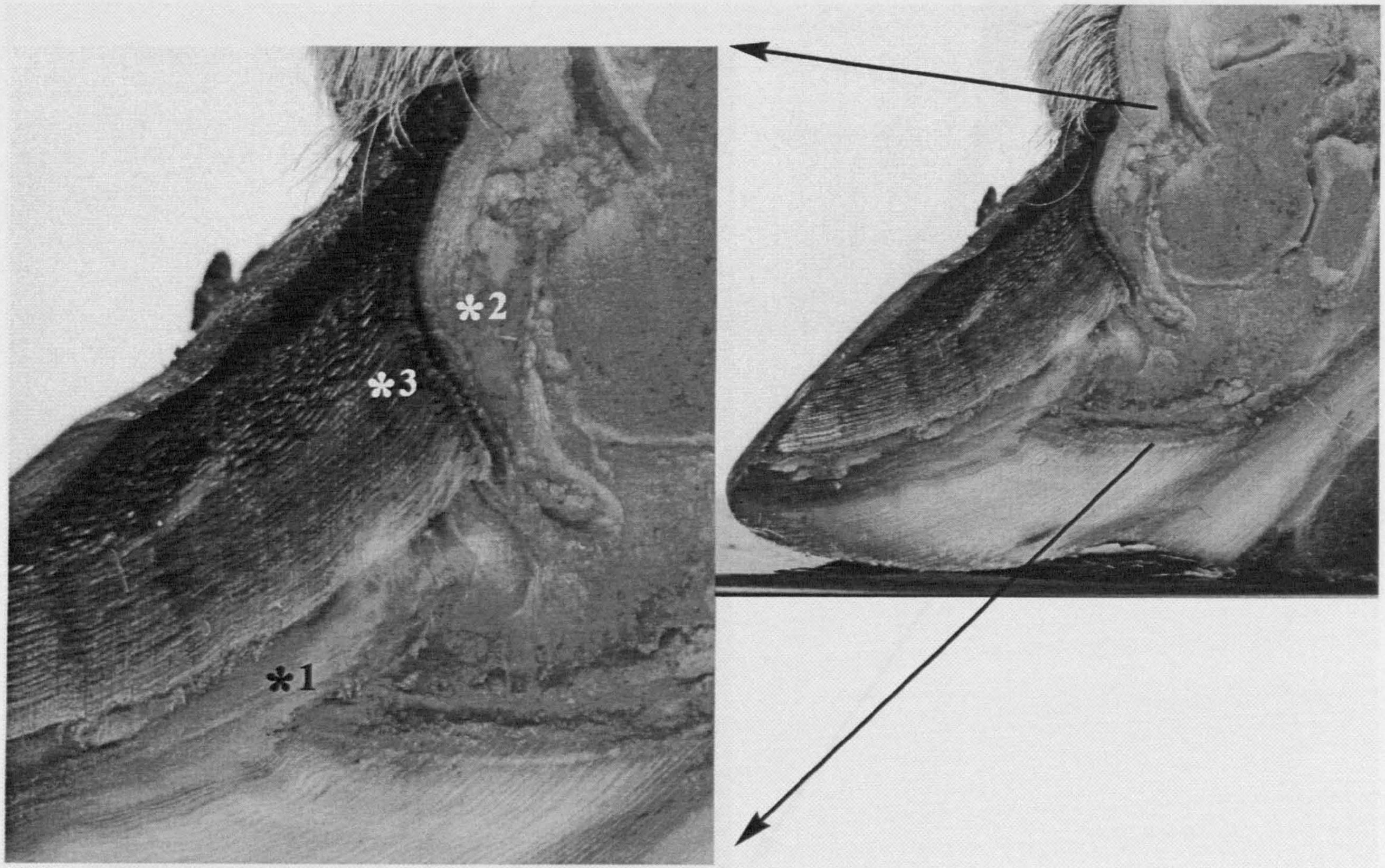

Figure 1.23 Photograph of a sagittal section of the laminitic donkey foot showing 'crimping' of the horn tubules along the proximo-distal extent of the hoof wall.

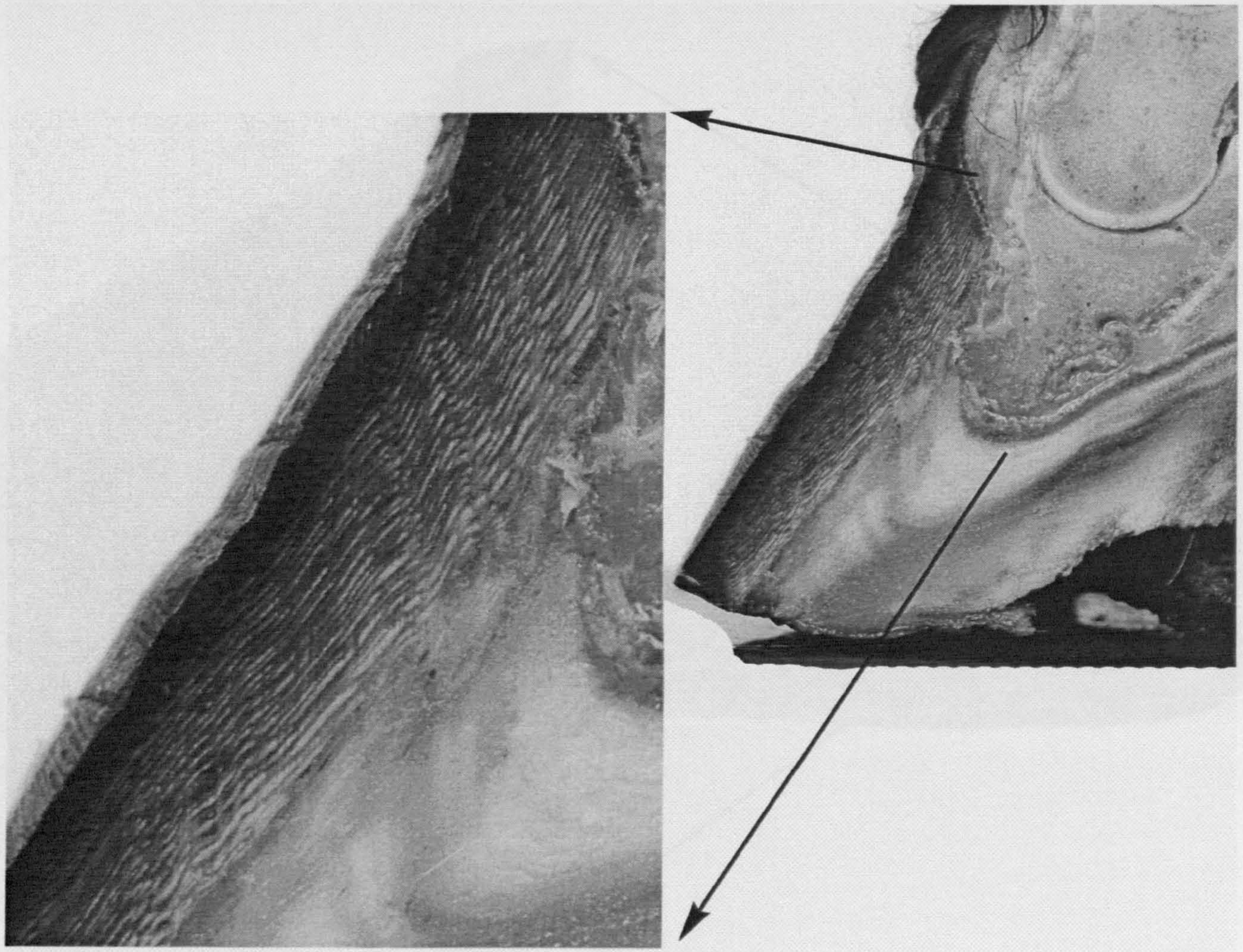

Figure 1.24 Photograph of a sagittal section of the laminitic donkey foot to show tubule crimping in the immediate proximity of the coronary corium (*1). Note the absence of proximo-distal elongation (stretching) of the coronary corium. Ectopic 'scar horn production in the laminar region of the foot is also evident (*2).

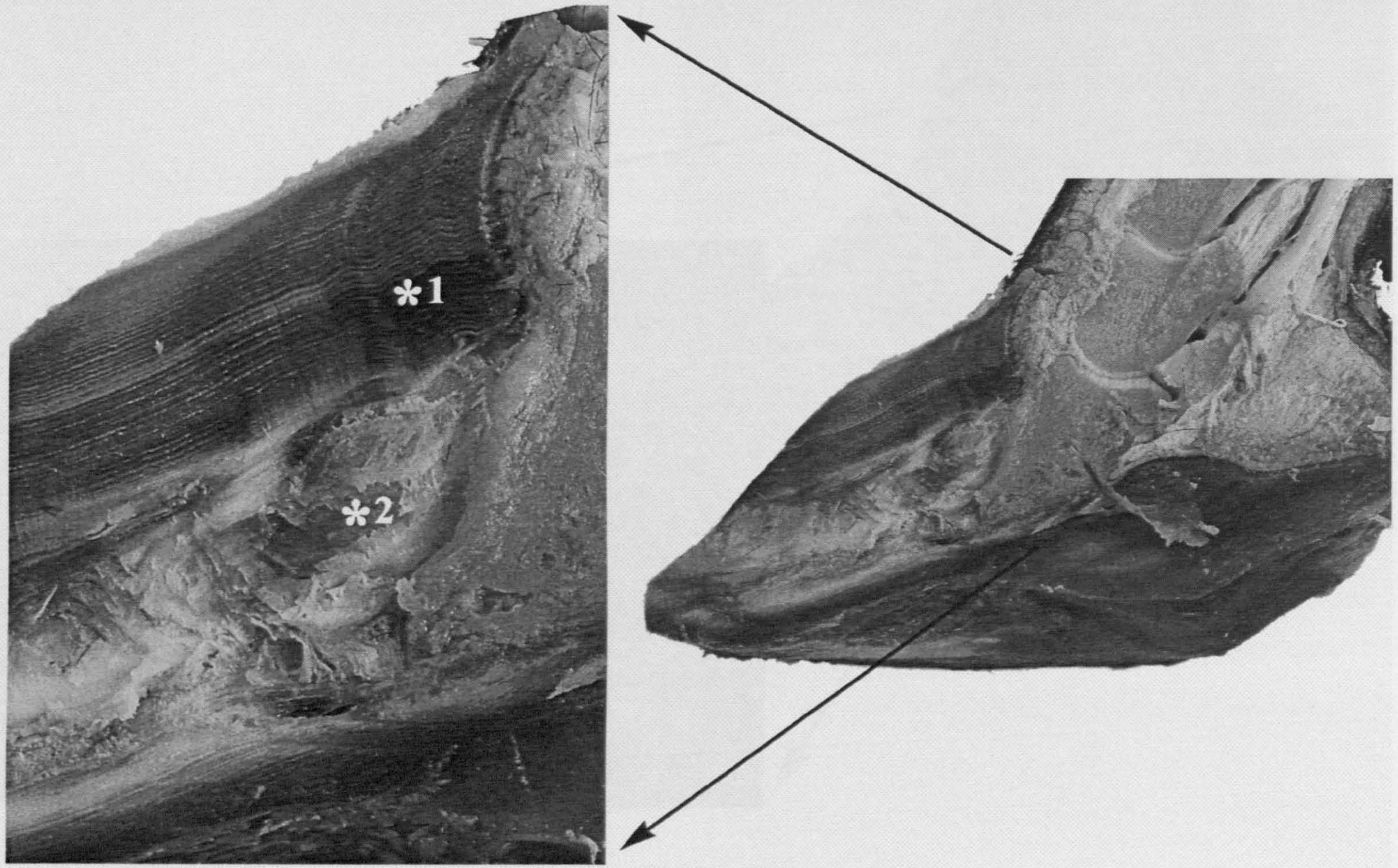

Figure 1.25 Photograph of the lateral aspect of the laminitic donkey hoof capsule to show hyperproliferation of the perioplic horn (*).

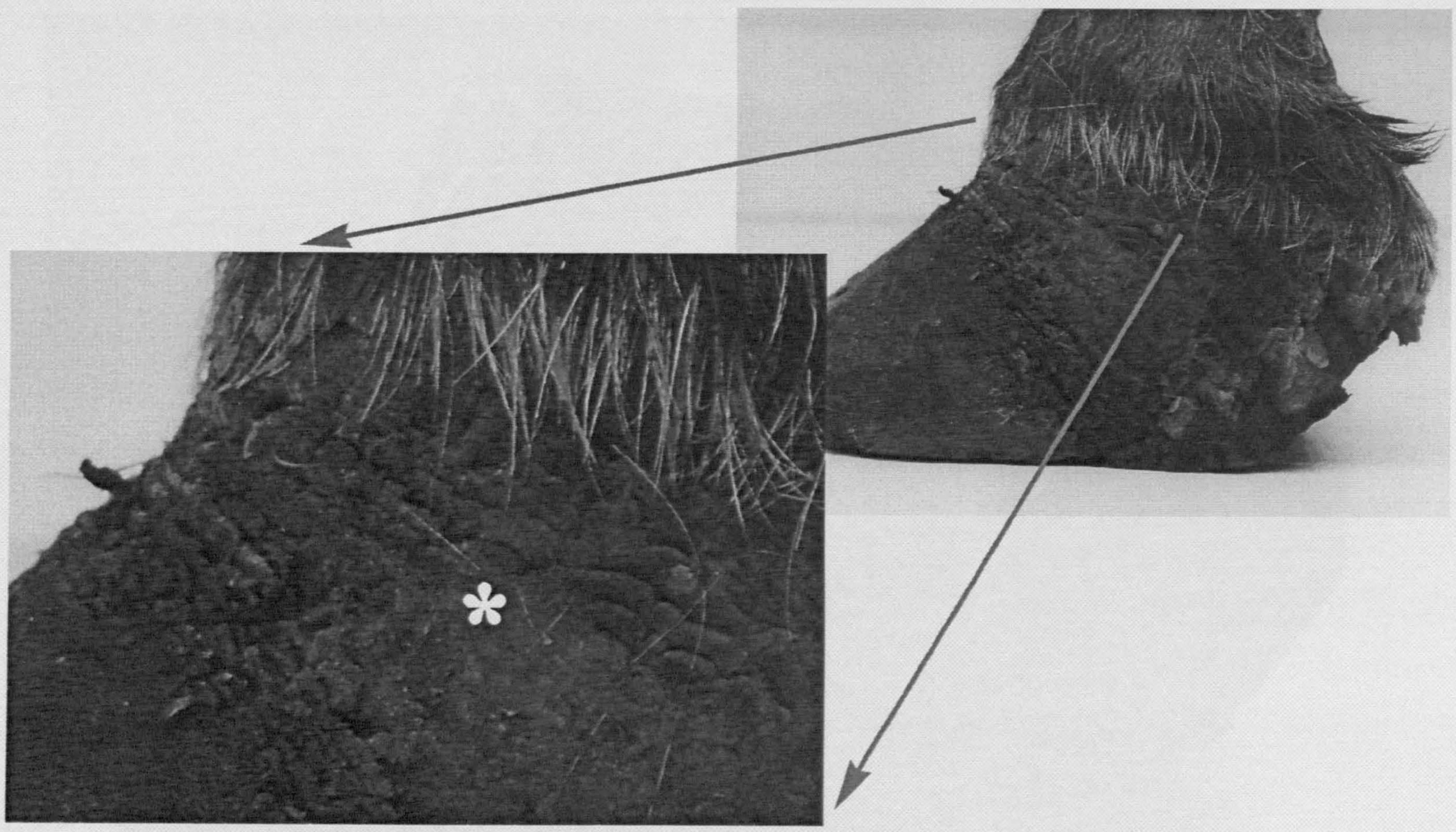

Figure 1.26 Photograph of a lateral aspect of a dressed laminitic hoof capsule to show divergent growth rings (arrows) caused by differential growth rates between the midline and the heels, and irregular thickening of the hoof wall (*).

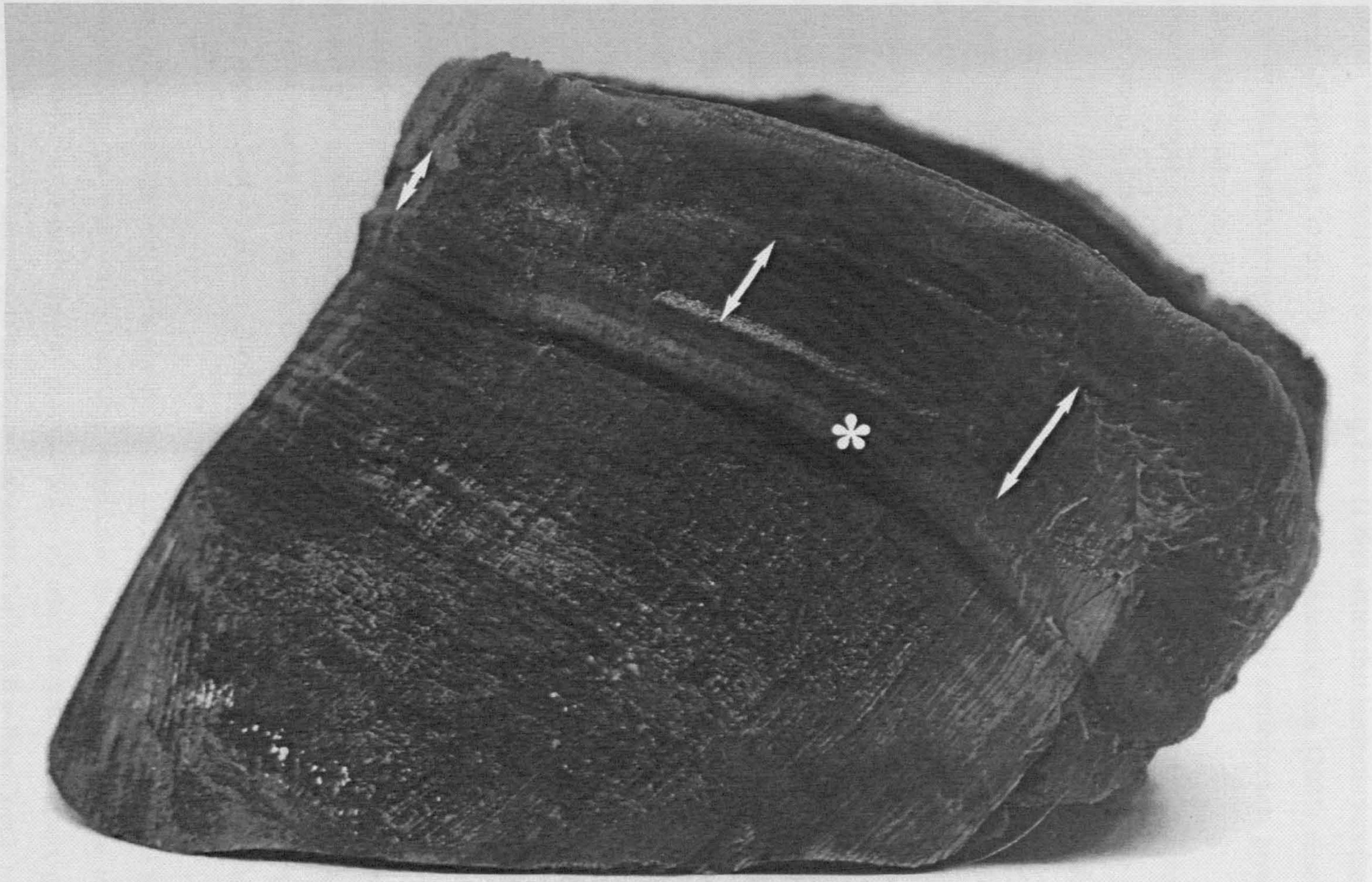

1.11.2 LAMINITIS AND THE DONKEY

The significance of the threat posed by the laminitic condition to the donkey in temperate environments has been highlighted in Section 1.1. Eley (1998) stated that laminitis was the most common cause of lameness in the UK donkey population. Indeed Crane (2001) raised the question as to whether laminitis was an inevitable and unavoidable consequence, given the longevity of the UK donkey, and the prevailing management regime.

The life expected life span of the donkey in the UK far exceeds far exceeds that of the working donkey (10-16 years) in its native environment, with many individuals reaching 30+ years (Crane 2002b). This is of particular relevance as the incidence of laminitis in the donkey increases significantly with age (Eley and French 1983a, Eley 1998, Crane 1998 – Pers Com.). Eley (1998) reported that 35% of donkeys between 10 and 20 years surveyed in a cross sectional epidemiological study were suffering from chronic effects of laminitis. This compared with less that 4% in donkeys under 10 years of age. Crane (2002a) suggested that laminitis formed part of a continuum of degenerate and dysfunctional geriatric foot conditions.

Eley (1998) also identified that inadequate foot trimming, history of overgrown feet, free access to lush pasture, and high body condition scores were also common risk factors for the condition. These factors may indicate that inappropriate management conditions exist in the UK for a species adapted to an arid environment. This clearly raises significant welfare concerns.

However despite these facts little is known about the impact of the laminitic condition upon the donkey foot, either in terms of its effect upon the anatomy of the foot, or hoof function. In the absence of baseline data for the donkey it is assumed that the progression of the condition is similar to that observed in the horse. This has resulted in diagnoses and prognoses based upon information gained from the horse (Collins *et al.* 2002).

Empirical evidence however suggests that this assumption may be inappropriate. For example, Eley (1998) and Bell (2001– Pers Com.) stated that the donkey foot can withstand the DP displacement more readily than rotational events. This is in marked contrast to the response reported in the equine foot by Baxter (1986), Linford (1990, 1996), and Cripps and Eustace (1999b).

Effective therapeutic management of the chronic laminitic donkey is further complicated by the fact that considerable variation exists between individuals in the clinical response to the condition. Whilst some individuals display minimal signs of overt lameness and pain, others encounter repeated bouts of 'acute' pain and severe lameness (Bell 2000 – Pers Com.). Indeed Hunt (1993) highlighted the present inability to predict the clinical course of the condition with certainty in the wider equid population, due to the lack of 'useful' prognostic indicators.

1.11.3 CLASSIFICATION OF LAMINITIS

The broad spectrum of clinical presentation of the laminitic equid necessitates a reliable classification system for the condition (Morgan *et al.* 1999). However despite this fact, a universally accepted system has not yet been achieved. Progress towards this end has been hampered both by fundamental differences of approach, and the inconsistent application of terminology.

Various systems have been proposed to provide an effective basis for classification. These have included systems based upon aetiology, clinical presentation, clinical pathology, and/or progression of the condition. A comprehensive critique of these different classification systems is given in Appendix II.

Table 1.4 highlights the fact that an effective and fully comprehensive mode of classification for the laminitic condition is yet to be achieved, and also draws specific attention to the inconsistent use of terminology between systems. This represents an unsatisfactory state of affairs. An effective classification system for the laminitic condition represents a key research priority if improvements in the management of the affected animal are ultimately to be achieved, and the welfare of the laminitic animal improved. Appropriate diagnostic and prognostic criteria must be considered. Hence classification must reflect the anatomic or pathologic alterations within the foot, and the biomechanical consequences of these alterations. Assessment of impaired biomechanical function by indirect methods alone is of questionable value.

The degree of functional compromise evident within the foot is likely to be determined by the occurrence, nature and extent of DP dislocation, and the attendant digital pathologies that arise as a consequence of digital collapse. These issues are considered in Section 1.11.4.

An effective classification system for the laminitic condition also requires standardised terminology. The terminology adopted must then be consistently used in related research. Definitions must be unambiguous, and limit the possibility for confusion within the wider community.

Hence the convention adopted in this thesis is in accordance with Marks (1984). The terms acute and chronic are used to signify, respectively, the absence or presence of DP dislocation within the affected foot. This system is preferred as it reflects the irreversible nature of anatomical changes within the foot, and reflects the significant biomechanical implications of this degenerative event. In addition, the terms DP displacement, and DP rotation are used to signify the nature of the DP dislocation event. These are used in preference to 'sinker' and 'founder' respectively. This avoids confusion relating to the colloquial usage of these terms and their inconsistent application evident throughout the scientific literature.

Table 1.4 Summary of the classification systems applied to the laminitic condition.

Author	Mode of classification	Nature of classification	Classification System
Obel (1948)	Clinical Presentation	Lameness Grade	Divided into 4 Lameness Grades of increasing severity: - Grades I – IV
Kameya (1973)	Radiography and Treatment Outcome	Nature and Extent of DP Dislocation and Treatment Outcome	Divided into 4 groups based upon 'Return to Former Performance Levels' and linking Occurrence, Nature and Extent of Capsular and Phalangeal Rotation: - Sound - Intermittent Lameness – Persistent Lameness - Euthanased due to Severe Lameness
Hood and Stevens* (1981) * After Nilsson (1963)	Clinical Presentation and Duration	Digital Pathology and Progression over time	Divided into 4 groups based upon the Clinical Presentation, Occurrence of DP Dislocation, and Duration: - Developmental - Acute - Subacute – Chronic
Dietz (1977)	Aetiology	Aetiologic Factor	Divided into 4 groups based upon Causal Factor(s) precipitating the condition: - Traumatic Toxic Symptomatic Rheumatic
Stick *et al.*(1982)	Radiography and Treatment Outcome	Extent of Capsular Rotation and Treatment Outcome	Divided into 4 groups based upon 'Return to Former Performance Levels' and linked to Occurrence, Extent of Capsular Rotation Sound - Intermittent Lameness – Persistent Lameness - Euthanased due to Severe Lameness
Linford (1990)	Clinical Presentation Treatment Outcome	Response to Treatment	Divided into 6 groups based upon Occurrence of DP Dislocation and Response to Treatment Acute - Refractory Exacerbative Laminitics (REL) - Chronic Remissive Laminitics (CRL)
Baxter (1992a,b)	Radiography	Nature of DP Dislocation and Roentgenic Change	Divided into 6 groups based upon Occurrence and Nature of DP Dislocation, and attendant Roentgenic Change
Eustace (1992, 1995)	Clinical Presentation Radiography Treatment Outcome	Nature of DP Dislocation, Roentgenic Change and Response to Treatment	Divided into 6 groups based upon Clinical Presentation, Occurrence and Nature of DP Rotation and DP Displacement, Duration, Roentgenic Change, and Response to Treatment Acute – Sinker - Acute Founder – Chronic Founder Type 1 - Chronic Founder Type 2
Hood *et al.* 1993a	Radiography	Nature of DP Dislocation	Divided into 2 groups based upon Colloquial use of the terms 'Founder' and 'Sinker' Type 1 (Founder) – Type 2 (Sinker)
Moore and Allen (1995)	Clinical Presentation Radiography	Digital Pathology, Lameness Grade and Nature of DP Dislocation	Divided into 6 groups based upon Occurrence and Nature of DP Dislocation, and attendant Obel Lameness Grade Earliest Changes - Mild - Moderate – DP Rotation - Severe - DP Displacement
Hood (1997a)	Clinical Presentation Treatment Outcome	Lameness Severity and Lameness Progression	2-way division into 4 groups bases upon Lameness Severity and Lameness Change over Time Compensated Versus Non compensated, and Stable Versus Progressive
Butler *et al.* (1998)	Radiography	Nature of DP Dislocation	Divided into 3 groups based on Occurrence and Nature of DP Dislocation Acute - Sinker – Founder
Cripps and Eustace (1999b)	Clinical Presentation and Radiography	Digital Pathology, Duration and Nature of DP Dislocation	Divided into 4 groups Acute - Sinker - Acute Founder – Chronic Founder

In addition, the terms phalangeal, capsular and combined rotation are used to further detail the specific nature of the rotational dislocation of the DP. With the adoption of this terminology, the impact of the laminitic condition upon the affected foot can be accurately and unambiguously described.

1.11.4 SEVERITY AND PROGNOSIS OF THE LAMINITIC CONDITION

Little is known as to the precise factors that govern the severity of the laminitic condition, or which determine prognosis in the affected animal (Hunt 1993). However it may be argued that the lameness severity and likely recovery outcome are both influenced by the degree of biomechanical compromise to the affected foot. Given the fact that the biomechanical functioning of the foot is reliant upon the smooth and painless transfer of force across the SADP (Reilly *et al.* 1996), then the degree to which the SADP is damaged may be of particular biomechanical significance. In fact Pollitt and Daradka (1998) and (Pollitt 2002 – Pers Com.) reported a positive correlation between the degree of degenerative change within the laminar interface, and the Obel lameness score in the afflicted animal.

The extent of the compromise within the SADP also dictates progression into the chronic phase of the condition (Pellmann 1995, Pellmann *et al.* 1997). In addition, it directly affects the nature and extent of the resultant dislocation of the DP (Linford 1990, Butler *et al.* 1998), and also contributes towards the occurrence of roentgenic change to the DP (Hood 1999a, Hemker and Hertsch 2002).

Thus, the severity of the laminitic condition may display a direct, though not causal, relationship with either DP dislocation and/or roentgenic change to the DP. Hence the assessment of the affected foot in respect of these specific pathologies, may serve as an effective means of severity assessment and prognosis. If a direct relationship is demonstrated, it would represent an important criterion for the classification of the laminitic condition, as this would reflect the degree of biomechanical impairment. In addition, it would enable the classification of the laminitic condition to be placed on an objective basis.

As the hoof capsules surrounds the internal structures of the foot, '*in vivo*' assessment of the anatomical organisation and morphological characteristics of these internal structure, can only be achieved with the aid of remote imaging techniques (Butler *et al.* 1998). One such imaging technique that has the ability to discern both the osseous and exosseous structures of the foot, and reveal their anatomical inter-relationship is radiography using x-rays (x-rays).

1.11.5 RADIOGRAPHY (X-RAYS) AND LAMINITIS

X-rays have been extensively employed to aid the clinician to: -

- Suggest, confirm, or refute a diagnosis
- Give information on progression and severity of a condition and hence aid prognosis
- Add information regarding size, shape, position and duration of a lesion

1.11.5.1 LATERAL RADIOGRAPHS

The lateral radiograph (lateromedial projection) represents the 'gold standard' for the assessment of degenerative change within the foot associated with the laminitic condition (Collins and Reilly 2004b – Submitted). It enables the visualisation and anatomical assessment of the dorsal and palmar surfaces of the phalanges of the distal limb, and the DIP and PIP joints (O'Brien and Baker 1986, McNeel 1986). In addition, the relationship between the DP and the exosseous tissues of the foot, including the hoof wall, may be evaluated (Colles1983). Hence pastern and hoof pastern axes can be determined, DP dislocation events detected, and quantified (Herthel and Hood 1999), and roentgenic change recorded (Linford 1987). On this basis, Kameya (1973) and Chandra *et al.* (1982) argued that the lateral radiographic projection was ideally suited for the diagnostic assessment of the laminitic condition.

However in order to recognise and interpret pathological change within the foot, *a priori* knowledge of the normal radiographic appearance is required (Linford 1987, Linford *et al.* 1993). In this respect, Colles (1983) and Butler *et al.* (1998) referred to a theoretical 'ideal radiographic conformation' for the equine foot. This 'ideal' was defined in the lateral radiograph by: -

- Vertical alignment of the centre of radius of curvature of the DIP midway along solar bearing surface of the foot.
- Parallelism between the dorsal aspect of the DP and the dorsal aspect of the hoof wall.
- Slight palmar inclination to the solear margin of the DP.
- Hoof wall of constant dorso-palmar depth and radiodensity.
- Dorsal aspect of the hoof wall being smooth and without ridges.
- Absence of radiolucent bodies within the hoof wall and dermis.
- Dorsal aspect of the DP exhibiting smooth linear profile distal of the extensor process and free of margination effects.
- Junction of the dorsal and solear margins of the DP forming a sharp acute angle.

Butler *et al.* (1998) concluded that the primary radiographic sign of degenerative change associated with the laminitic condition was related to the dislocation of the DP. Morgan (1972), Colles and Jeffcott (1977), Chandra *et al.* (1982) and (Stick *et al.* 1982) stated that angulation of

the DP relative to the dorsal aspect of the hoof wall confirmed the diagnosis of laminitis. However Morgan (1972) and Gillette *et al.* (1977) argued that capsular rotation in not recognised visually until an advanced stage of SADP separation.

Although marked changes within the foot are readily discernible, modest changes pose a diagnostic challenge by subjective assessment alone (O'Brien and Baker 1986, Hood *et al.* 1993b, Hood 1999a, and Collins and Reilly 2004a – Submitted). Indeed subjective radiographic assessment failed to detect this distal displacement in 75% of cases reviewed (Baxter 1986). O'Brien and Baker (1986) stated that an effective means of confirming a diagnosis in the absence of significant capsular rotation has not been well defined. This is of particular significance with regard to animals in which DP displacement predominates. In these instances parallelism between dorsal aspect of the hoof wall and the dorsal aspect of the DP is maintained (Baxter 1994, Butler *et al.*1998). This issue still remains largely unresolved, despite the suggested severity of this form of dislocation (Chapman and Platt 1984).

Hood *et al.* (1993b) and (Hood 1999a) also highlighted the significant variation that can occur in clinical presentation of affected foot, as a consequence of attendant digital pathology. This variation poses a particular diagnostic and prognostic challenge (Stick *et al.* 1982, Morgan *et al.* 1999).

1.11.5.2 Radiographic Morphometrics

Various studies, most notably Kameya (1973), Linford (1987), Eustace (1991,1992) Cripps and Eustace (1999a,b) and Hemker (2001), have sought to address the issues discussed in the previous section, by using objective measurements of key radiographic parameters that define the osseous and exosseous inter-relationships within the foot. These morphometric studies of the lateral radiograph have attempted to define the key anatomical characteristics of the normal equine foot. Linear and angular measurements have been used to arrive at a series of direct and derived radiographic parameters. These parameters represent objective baseline data for the characterisation of the normal foot. This information serves as a baseline and pathological divergence from it can then be effectively assessed. In this way, the nature and extent of pathological change can be accurately determined and quantified. However progress has been limited in the absence of a standardised approach to parameter selection, and through the adoption of inconsistent and confusing terminology (Collins and Reilly 2004b – Submitted). The selection criterion for the adoption of these parameters is poorly defined, and warrants a detailed review. This is covered in Chapter 3 of this thesis. Table 1.5 summarises the key radiographic parameters adopted in these studies.

Table 1.5 Summary of the Radiographic Parameters variably used to quantify the anatomical organisation of the equid foot.

Parameter	Description	Author				
		Kameya (1973)	**Stick *et al.* (1982)**	**Linford (1987)**	**Eustace (1991 1992)**	**Hemker (2001)**
Dorsal Hoof Wall Angle	Internal angle subtended between the dorsal aspect of the hoof wall and the Ground Line	✓ Parameter A	✗	✓ Parameter HFAX	✓ Parameter Angle S	✓ Parameter A
Angle of the Dorsal Aspect of the DP	Internal Angle subtended between the dorsal aspect of the hoof wall and the Ground Line	✓ Parameter B	✗	✓ Parameter DPAX	✓ Parameter Angle T	✓ Parameter B
Integument Depth at the Dorsal Aspect of the Foot	Perpendicular Linear distance from dorsal aspect of hoof wall to dorsal aspect of DP, perpendicular to the hoof wall	✓ Parameter **a** - Proximal **b** - Distal	✗	✓ Parameter STT **P** - Proximal **M** - Middle **D** - Distal	✓ Parameter **WT**	✓ Parameter **a** - Proximal **b** - Distal
Angle of Pastern Axis	Internal angle subtended between the PP-MP axis and the Ground Line	✓ Parameter **C**	✗	✗	✓ Parameter **Angle U**	✗
Angle of the Hoof Pastern Axis	Angular difference between the Dorsal hoof Wall Angle and Pastern Axis	✓ Parameter **C-A**	✗	✗	✗	✓ Parameter **C-A**
Measure of Capsular Rotation	Angular difference between Dorsal Hoof Wall Angle and Angle of the Dorsal Aspect of the DP	✓ Parameter **B-A**	✓ Parameter **Pedal Bone Rotation**	✓ Parameter **ROTA**	✓ Parameter **Angle H**	✓ Parameter **Angle H**
Measure of Phalangeal Rotation	Angular difference between Angle of the Dorsal Aspect of the DP and Angle of Pastern Axis	✓ Parameter **B-C**	✗	✗	✓ Parameter **Angle R**	✗
Measure of Distal Displacement of DP	Vertical linear difference between the proximal margin of the hoof wall and the proximal limit of the extensor process of the DP	✗	✗	✗	✓ Parameter **D**	✓ Parameter **D**

Key: ✓ Radiographic Parameter used by the Author. ✗ Radiographic parameter not used by the Author. **DP** distal phalanx. **MP** middle phalanx. **PP** proximal phalanx

Kameya (1973) conducted the first reported radiographic morphometric study in the horse. He objectively characterised the normal anatomical organisation of the foot, and also evaluated the nature and extent of DP rotation associated with laminitic condition. This author defined the anatomical organisation of the osseous and exosseous structures of the foot using 7 parameters. This study measured the HPA and quantified both the degree of capsular and phalangeal rotation present in the normal foot. In addition, the integument depth was established at the dorsal limit of the extensor process and at the apex of the DP, and the corresponding proximal to distal integument depth ratio. However no specific reference was made to the degree of DP displacement evident with the foot. The findings of this study indicated that the dorsal aspect of the DP in the normal horse was in near parallel alignment with the hoof wall, with a mean capsular rotation angle of 0.48° ± 1.4, integument depth ratio of 0.92 ±0.06, and mean phalangeal rotation angle of 2.94° ±3.6. The anatomical organisation of the distal limb displayed a straight HPA with a mean angle of 1.5°.

Subsequent studies have sought to build upon the pioneering work of Kameya (1973), not only by refining the ability to determine information regarding the nature and extent of DP rotation, but also to detect and quantify DP displacement. This has proved to be an area of conjecture with different researchers proposing different measurement parameters.

With regard to the laminitic condition, attention has been variably directed towards relating radiographic morphometry to: -

- Diagnosis of the condition (Linford 1987, Linford *et al.* 1993, Glöckner 2002)
- Prognosis of the condition (Stick *et al.*1982, Cripps and Eustace 1999a,b)
- Treatment outcome (Glöckner 2002)
- Recovery outcome (Stick *et al.*1982, Hemker 2001, Hemker and Hertsch 2002)
- Lameness severity (Cripps and Eustace 1999b)

This process of refinement and enhancement of Kameya's original study has inevitably increased the number of measurement parameters. Indeed the work of Linford (1987) and Linford *et al.* (1993) detailed over 25 morphometric parameters. This trend has resulted in the emergence of a complex multi-factorial matrix of measurement data. This combined with the varied nature of the anatomical change and attendant secondary pathology associated with the laminitic condition makes clinical interpretation and assessment difficult. Consequently there has been a tendency to focus upon individual components of the anatomical reorganisation, for example Stick *et al.* (1982), rather than assessing the combined effect of total anatomical change evident within the foot.

The recent work of Cripps and Eustace (1999b) has made progress in this direction through the use of step-wise regression analysis techniques. However even this approach has been used to identify single parameters of perceived critical diagnostic and prognostic importance.

As the foot represents a 3-dimensional organ (Reilly 1995) it is unlikely that any single anatomical parameter can effectively capture the key defining characteristics of the foot, or indeed accurately reflect the complexity of anatomical change associated with digital collapse (Collins *et al.* 2002). Hence there is a need to seek a means of encapsulating the combined information derived from key descriptors of the anatomy of the foot. Only then will it be possible to evaluate the full impact of the condition upon the foot (Collins *et al.* 2002).

1.11.5.3 Radiography of the Donkey Foot

In common with the general paucity of baseline veterinary information relating to the donkey there is little information regarding the normal radiographic anatomy of the foot (Bordalai and Nigam 1977). Hence fundamental issues such as the alignment of the HPA still remain largely unresolved (Reilly 1997). This situation poses a particular challenge specifically with regards to the laminitic condition. Not only is departure from normality central to diagnostic and prognostic evaluation of degenerative change (Colles and Jeffcott 1977, Colles 1983, Butler *et al.* 1998), but also it is instrumental in determining appropriate treatment modalities.

In the absence of species specific information, there has been a tendency to apply an equine model to the donkey. This however has proved to be unsatisfactory. For example, the recent emergence of information regarding anatomical differences between the two species has shown that the use of heart bar shoes as a therapeutic rationale for the laminitic condition is contraindicated in the donkey (Reilly 1997).

Commenting upon these issues, Walker *et al.* (1995) and Reilly (1997) stated there was an imperative need to address this situation, and establish baseline radiographic information for this species. In this way it will be possible to accurately degenerative change.

However progress has been limited and restricted in the main to anecdotal comment and empirical observation. Nevertheless, a picture is emerging that suggests the presence of fundamental differences between the two species. This information not only questions the validity of applying an equine model, but also raises important issues of diagnostic and prognostic consequence relating to the laminitic condition in the donkey.

Eley (2000) drew attention to the fundamental difference between the two species in the interrelationship that between osseous and exosseous structures in the normal foot. This author stated that the proximal limit of the extensor process of the DP is distad to the proximal margin of the dorsal aspect of the hoof wall, although this has not been objectively confirmed. This

apparent anatomical relationship is in marked contrast to horse, where they are in horizontal alignment. This apparent 'between species' difference is of particular significance with regard to the laminitic condition. This is because the relative position of these anatomical reference points is in the horse used as a diagnostic indicator of digital collapse within the foot.

Lateral radiographs of the laminitic donkey foot have been published previously by Walker *et al.* (1995), Reilly (1997) and Eley (1998). These have been used to illustrate the specific nature of the DP dislocation that can occur following digital collapse in this species. In particular, Eley (1998) published three lateral radiographs that where stated as illustrating the occurrence of DP Displacement, DP Rotation, and combined rotation and displacement events as a *sequelae* of digital collapse in the donkey foot.

Eley (1998) also presented visual information regarding the shape and radiographic morphology of the DP, describing it as being of "*normal appearance*". The shape of the DP was similar to that previously described by Walker *et al.* (1995) as being "*blunted*". This blunted appearance differs from the theoretical 'ideal radiographic appearance' of the equine DP detailed in 1.11.5.1 1.11.5.1. In fact, the profile of the donkey DP was similar to that illustrated, and described, by Linford *et al.* (1993) as displaying roentogenic change specifically associated with the onset of chronic laminitis in the horse. Walker *et al.* (1995) was unable to confirm whether this 'blunted' appearance represented a true anatomical difference between the two species, or if it was likewise, indicative of roentgenic change associated with laminitis.

Commenting upon the prognostic significance of radiographic evidence in the donkey, Eley and French (1993a) and Eley (1998) stated that the degree of DP rotation, and DP degeneration and remodelling was of greater prognostic value than the extent of DP Displacement. Empirical evidence (Crane 1999 – Pers Com., Bell 2000 – Pers Com.) would appear to support the assertions of these authors. These accounts further question the appropriateness of applying the equine model of the laminitic condition, in which DP displacement is of primary prognostic significance (Baxter 1986, Eustace 1991, Cripps and Eustace 1999b), to the donkey.

There is a clear need to resolve the issues regarding the normal radiographic anatomy of the donkey foot, and also to further elucidate the effect of laminitic condition in the donkey. Indeed, Walker *et al.* (1995) concluded that additional radiographic studies need to be conducted and related both to "*gross anatomical and histological*" findings in order to address these issues.

1.12 THESIS RATIONAL

The review of the literature detailed within this chapter of the thesis has highlighted the fact that the laminitic condition threatens all *Equidae* (Åkerblom 1934) but poses a particular risk to the domestic donkey living in temperate climates (Trawford 1998 – Pers Com.). The progression of the condition may ultimately lead to the humane destruction of the afflicted animal on the grounds of unremitting lameness. Despite these facts, there is a lack of information regarding the effects of this condition in the donkey (Mostafa 1986). This has led to the unsatisfactory adoption of an equine model for the diagnosis, prognosis and treatment modalities, irrespective of significant anatomical and physiological differences that exist between these two distinct equid species (Collins *et al.* 2002).

Laminitis is a condition of multifactorial origin that becomes manifest at the level of the foot. It results in acute and/or chronic digital lameness (Hunt 1993, Reilly *et al.* 1998b). The condition induces vascular disturbances (Hood 1997a), ischaemia, reperfusion injury, and/or tissue damage (Pollit 1998a, 2001, 2002). The stoical nature of the donkey and the absence of overt signs of pain compound this situation further. Consequently the laminitic condition is often not detected until an advanced stage of degenerative change (Trawford 1999 – Pers Com.).

Given these 'species specific' differences, and also the significant threat posed by the condition to the UK donkey population, there is a specific need to further investigate the impact of the laminitic condition in the donkey. The specific welfare issues related to this debilitating condition provides the *raison d'être* for this thesis.

Degenerative changes associated with the progression of the condition threaten the structural integrity of the SADP (Pollitt 1990a,b, 2001) that serves to unite the integument and the DP into an integrated functional unit (Pellmann 1995). Failure of this structure leads to irreversible, degenerative anatomical change within the foot. This event precipitates secondary, attendant digital pathologies (Herthel and Hood 1999). These changes further contribute to the pain and lameness associated with the condition. In fact, the chronic pain associated with the condition is linked to the degenerative changes induced within the foot. However there is a wide range of clinical presentations in the afflicted animal (Morgan *et al.* 1999), ranging from intermittent low-grade digital lameness to persistent severe lameness that necessitates euthanasia. It has been suggested that the degree of lameness and the severity of the condition is related to the specific nature and extent of these digital pathologies.

Effective management of the afflicted animal is therefore dependent upon early diagnosis of modest degenerative change (Collins and Reilly 2004b – Submitted), and an implicit understanding of the prognostic significance of these changes.

The early detection of degenerative change is reliant upon the *a priori* knowledge of normality (Cripps and Eustace 1999a). This knowledge is however lacking for the donkey, as indeed is information relating to the nature of the degenerative changes associated with the laminitic condition. The lateral radiograph represents the gold standard for the assessment of the anatomy of the equid foot (Tachio *et al.* 2002, Collins and Reilly 2004b – Submitted). Chapter 3 of this thesis specifically aims to address these issues, and achieve objective baseline data for the radiographic anatomy of the donkey foot. In addition the nature and extent of the degenerative associated with the laminitic condition will be objectively evaluated.

In spite of the functional significance of the hoof capsule, relatively little is known as to the precise effects of the condition upon the epidermal tissues of the foot. Historically, research into equine laminitis has focussed predominantly upon the pronounced pathophysiologic effects within the dermal tissues of the foot, and the digital circulation (Reilly *et al.* 1998b). These have been extensively reported including Coffman *et al.* (1970b), Ackerman *et al.* (1975), Hood (1984), Hood *et al.* (1994), Pollitt (1990b, 1998b), Weiss *et al.* (1994. 1996, 1997), Weiss (1997), Hinckley *et al.* (1996), Bailey (1998), and Bailey and Elliott (1998). More recently, important changes within the BM, that separates the dermis from the epidermis, have also been documented (Pollitt 1996, 1998b, 2001, Johnson *et al.* 1998, 2000).

An intimate relationship exists within the tissues comprising the integument. Indeed the avascular hoof capsule is totally reliant upon the dermis and its associated blood supply to support hoof horn production. Controlled and co-ordinated hoof horn growth is mediated by the basement membrane (Pollitt 2002 – Pers Com.). In addition, the structural organisation of the hoof horn material is dependent both upon the topographical modification of the dermis (Pellmann *et al.* 1993, Bragulla 2003), and the integrity of the BM (Pollitt 2002 – Pers Com.). Hence the pathophysiologic events detailed in the dermis, the digital circulation and the BM have the potential to impact upon the epidermal tissues of the foot. Although pathological changes in gross anatomical of capsular shape are well documented in associated with the laminitic condition, little is known as to the effects elsewhere within the design hierarchy (Collins *et al.* 2002). Indeed the effects upon the hoof horn material and its structural organisation at either the macroscopic and microscopic level have not been fully investigated (Reilly *et al.* 1998b).

Disruption to the digital blood supply may also results in the dermis no longer being able to support 'normal' horn production, leading to 'abnormal' horn formation (Obel 1948, Hendry *et al.* 1997, 1998). Changes to anatomical configuration of the dermis, and the loss of functional integrity within the BM may also adversely affect the structural organisation of the hoof at the macroscopic and microscopic level of the design hierarchy. Isolated descriptive accounts by

Mostafa (1986), Said *et al.* (1992) and Nakada *et al.* (1992) have made reference to 'structural irregularities' within the *SM* of the laminitic equine hoof. More recently, Collins *et al.* (2002) (2003) have provided evidence of changes in structure, within the *SM* of laminitic donkey hoof horn. However these changes have not been objectively assessed. Chapter 4 of this thesis seeks to achieve a morphometric characterisation of the structural organisation of the *SM* of the laminitic donkey hoof wall.

Given the intimate structure-function relationship that exists with biology, changes to the hoof horn material and its structural organisation, and hydration levels, will directly lead to changes in the material properties of the hoof. Whilst it generally accepted that laminitis results in the production of poor quality hoof horn, the effect of the condition upon the material properties of the hoof has not been evaluated. Chapter 5 of this thesis addresses this issue. Changes to the hydration status of the hoof wall in association with the laminitic condition have been inferred (Goetz 1987). However hydration levels with laminitic equid hoof horn have not been reported. Consequently little is known as to the effects of pathological change on the hydration status of the hoof (Collins *et al.* 1998, Hopegood 2002). However, it is widely documented that pathological conditions of human *Stratum corneum* are associated with changes in hydration levels (Takenouchi *et al.* 1986, Imokawa *et al.* 1991, Gniadecka *et al.* 1998). Chapter 5 of this thesis also focussed upon the issue of hydration levels within laminitic donkey hoof horn.

The collective changes that occur within the foot are considered to impair the normal biomechanical functioning (Reilly *et al.* 1998b) and prevent the integument and the DP acting as an integrated functional unit. This is of particular significance given the importance of this locomotor organ (Herthel and Hood 1999). Changes in the hoof's material properties, which are investigated in Chapter 6, coupled with changes in gross anatomical shape, may adversely affect normal hoof function, and its response to loading in particular. This may prevent the hoof from achieving smooth and painless force transfer within the foot and hence lead to the development of digital lameness within the afflicted animal. In order to evaluate the potential biomechanical effects of laminitic change within the hoof, an effective means of modelling is required. The penultimate chapter of this thesis focuses on the use of computer modelling to assess hoof wall function. These issues are of particular practical significance. This is because the development of effective treatment modalities can only be successfully achieved through a thorough knowledge of the likely functional consequences of degenerative change.

The precise effects of laminitis upon the design hierarchy of the hoof wall and its hydration status are not fully understood, nor indeed are the functional consequences of degenerative changes. The final chapter of the thesis examines the interactions between degenerative anatomical change, hoof structure, hydration levels, and material properties.

Given the functional significance of the hoof in the unguligrade stance, the hoof provides a valuable means of further investigating the debilitating effects of the condition. This represents an important new area of hoof research. Hoof research has however suffered as a consequence of adopting a less than scientific approach (May 1989, Reilly 1995), Traditionally hoof research has relied upon subjective and crude methods of assessment (Reilly 1995). These have lacked appropriate *rigor* and *gravitas*, and have not adhered to the guiding principles of the scientific method (Slater *et al.* 1995, Slater and Hood 1997).

In order to advance our current knowledge and understanding of the laminitic condition, there is a need to effectively elucidate the structure-function relationships within the hoof. This requires a new approach to the subject (Reilly 1995). This necessitates the application of objective methods of assessment. New measurement protocols must therefore be established that enables an objective materials characterisation of laminitic hoof horn. Achieving this aim however poses a particular intellectual challenge (Reilly 1995).

As hoof function is determined by a complex interaction of structural and material parameters (Bragulla *et al.* 1992, Reilly *et al.* 1996), the use of material testing and hoof modelling techniques are required, to provide new insight, and understanding, of the structure-function relationships in the hoof (Newlyn *et al.* 1998).

In this way, fundamental issues relating to the laminitic condition in the donkey can be addressed (Reilly *et al.* 1998b, Collins *et al.* 2002). These include: -

- Identification and measurement of the specific hoof horn parameters affected by laminitis
- Improved knowledge of the progression of the condition at the level of the hoof
- Enhanced awareness of the functional consequences of these changes
- Developed understanding of individual variation in response to the nature and/or extent of the digital collapse

Progress in these areas will ultimately lead to the emergence of an appropriate model for this debilitating condition that is specific to this unique and often neglected equid species.

This can lead to developments in: -

- Diagnostic markers for the laminitic condition
- Rapid screening methods as an adjunct to clinical radiography
- Cost effective laminitic monitoring of large donkey populations
- Reliable prognostic assessment
- Prediction and prevention of serious lameness
- Identification of condition predisposition

Indeed by developing an accurate understanding of the functional consequences of this condition, better management regimes and therapeutic strategies can be designed, and objectively evaluated, to the benefit of donkey welfare (Collins *et al.* 2002).

1.13 AIMS

The principle aim of this project was to investigate the effects of the laminitic condition on donkey hoof wall through the adoption of a novel multidisciplinary, material science approach.

The specific aims of this approach were: -

- To determine, radiographically, the nature and extent of the anatomical change within the foot associated with the laminitic condition
- To objectively characterise the structural organisation of laminitic donkey hoof horn within the hoof wall
- To evaluate the hydration characteristics of laminitic donkey hoof horn
- To establish the material properties of laminitic hoof wall horn in terms of resistance to deformation, and energy absorption.
- To assess the structure-function relationships acting at the gross anatomical, macroscopic and microscopic levels of the design hierarchy of the hoof wall
- To relate these findings to the anatomical organisation of the laminitic donkey foot

In this way to conduct a comprehensive:

"materials characterisation of laminitic donkey hoof horn"

The guiding principles of this approach were presented at the 3rd International Colloquium of the Working Equid, and are summarised in Trawford (1998) – see Appendix VII.

In the manner outlined above, this project aimed to explore differences, and associations, related to the laminitic condition, and confirm these relationships by departure from the null hypothesis. In particular, to statistically assess: -

- Differences between the radiographic morphometry of the normal and laminitic donkey foot.
- Differences in the nature of the anatomical changes within the foot of the laminitic donkey.
- Relationships between the morphometric characteristics of the hoof wall, and the radiographic anatomy of the laminitic foot.
- Relationships between the hydration characteristics of the hoof wall and the radiographic anatomy of the laminitic foot.
- Relationships between material properties of the hoof wall and radiographic anatomy of the laminitic foot.

- Relationships between either the morphometric or hydration characteristics of the hoof wall and its material properties.
- Differences between modelled function of the laminitic and normal donkey hoof wall.

2. GENERAL MATERIALS AND METHODS

2.1 PROJECT OVERVIEW

The preparatory phase of project sought to devise, develop, and optimise appropriate experimental techniques that would allow accurate and reliable means of objective assessment. The specific aims of this critical phase of the project were: -

- To establish effective methods for material sampling and specimen preparation from this highly friable and pathologically altered material
- To commission a computer based image analysis system capable of measuring defined 'feature' and 'field' specific hoof horn parameters
- To establish computer modelling techniques capable of assessing structure-function interactions

With the preparatory phase of the project completed the experimental phase could be planned. The specific aims of the phase of the project were: -

To identify animals of known laminitic history for preliminary hoof wall assessment

- To establish, on the basis of detailed medical histories, a trial donkey population, comprising trials groups of clinically normal and laminitic donkeys, maintained under standardised environmental, housing, management and farriery regimes
- To identify key radiographic and hoof horn parameters for subsequent evaluation
- To formulate a standardised methodology for the production of lateral radiographs of the foot
- To devise modified methods to enable hoof wall morphometry, mechanical testing, and moisture sample blocks to be derived from the same hoof capsule
- To devise appropriate operating procedures for the quantification of these defined parameters to include:
  - The morphological and morphometric characteristics of structure
  - The material properties of the laminitic donkey hoof wall

The experimental phase of this project involved two distinct stages, the preliminary, and the main experimental stage. In the preliminary experimental stage, an initial morphological and morphometric assessments, and material property analyses of the laminitic donkey hoof wall was conducted. The data from the preliminary stage of the experimental phase of the project was used to develop a computer-based model of the donkey hoof wall. With this successfully achieved the main experimental stage of the project could be initiated.

In the final analytical stage of the project results derived in this investigation were compared with previously published data for normal donkey and horse hoof horn. In addition, potential structure-function relationships within the laminitic hoof wall were investigated with the aid of computer modelling techniques.

2.2 INTRODUCTION

In order to achieve a materials characterisation of laminitic donkey hoof horn, there is a need to develop new methods of assessing the structure-function relationships of hoof horn (Reilly *et al.* 1998b). This however requires the prior characterisation of structure, and the assessment of functional capabilities.

The assessment of structure at the microscopic level, by histological appraisal, forms an important part in the study of tissue structure (Reid 1980). In addition this author argued that quantitative morphology was essential for the elucidation of structural and functional changes produced by disease. However histology is one of the last branches of scientific study to consistently adopt quantitative assessment methods. Effective protocols therefore need to be established which enable the objective characterisation of structure (Reilly *et al.* 1998b).

The application of stereometric techniques to biological materials can provide the opportunity to define structure in quantitative terms, at various levels within the hierarchy of cellular organisation (Weibel 1979). Hence sterometric techniques enable the assessment of pathological structural change to be placed on an appropriate quantitative basis (Reid 1980).

The successful application of stereometric techniques is reliant upon the development of effective sampling techniques (Reid 1980) and measurement procedures (Weibel 1979). Achieving these prerequisites in respect of laminitic hoof horn poses a particular challenge. Firstly, laminitic hoof horn is highly friable and inherently difficult to work (Budras *et al.* 1989, Frohnes and Budras 2001, Budras *et al.* 2002). Hence specific methods are required that enable specimen blocks and histology sections to be successfully prepared from this pathologically altered hoof horn material. Secondly, to be able to objectively characterise the structural organisation of hoof horn material, effective imaging methods need to be established. Finally, effective measurement itself is dependent upon the *a priori* identification of appropriate hoof horn parameters of functional significance.

This chapter deals specifically with the development of methodologies relating to the key objectives of the preparatory stage of this project, that is: -

- Material sampling, specimen block production, and preparation of histology sections
- Establishment of a computer based image analysis system (IAS)
- Formulation of procedures for reliable measurement of hoof horn parameters

In addition, general methodologies relating to the sampling protocols employed during the experimental phase of the project are detailed. The specific issues relating to radiographic and morphometric parameter selection are considered in Chapter 3 and 4 respectively, whilst the detailed methods relating to material testing are presented in Chapter 5, and computer modelling techniques in Chapter 6.

2.3 MATERIAL SAMPLING

The structural organisation of the hoof wall is dependent upon anatomical location within hoof capsule (Tscherne 1910, Nickel 1938a, 1949, Douglas 1998). Hence it is essential that sampling is standardised at a consistent, and accurately defined, anatomical location within the hoof capsule. In this way, differences in structural organisation arising from sample location can be controlled.

2.3.1 HOOF HORN SAMPLING

Hoof horn assessment has been variably performed upon hoof clippings (e.g. Hofstetter 1985, Zenker *et al.* 1995, Ley *et al.* 1998 and Hopegood 2002), hoof biopsies (e.g. Mostafa 1986, Linford 1987, and Ott and Johnson 2001) and morbid hoof samples (e.g. Tscherne 1910, Kasapi 1997 and Reilly 2001).

Distal hoof clippings, obtained as part of the normal management of the equid, provide a readily available, non-invasive and continuous source of hoof horn material. Their use in hoof horn research is, however, highly questionable. This is because material at the BB may be mechanically compromised, as a direct consequence of environmental degradation (Albarano 1993, Budras *et al.* 1998a).

This may occur either as part of a normal process in which wear and growth are kept in optimal balance (Budras and Schiel 1996), or as direct consequences of environmental contamination (Küng *et al.* 1991, 1993) and/or microbial degradation (Budras *et al.* 1998a) associated with husbandry practices.

The effects of these processes are not fully understood, however Bragulla (1993 - Pers Com.) refers to the process of "verdammern" or 'tubule fade out', in which degradation of the hoof horn results in the loss of cortical cell adhesion. This process leads to the progressive loss of structural organisation at the BB. In addition, Bertram and Gosline (1986), Geyer and Schultz (1994) and Hinterhoffer *et al.* (1998) have reported significant differences in the mechanical properties of distal clippings compared with material obtained from proximal sites.

Hopegood (2002) also commented upon the fact that capsular 'roll over', which occurs during the break over phase of the locomotor stride, can result in localised abrasion at the dorso-distal

margin of hoof wall. This can result in the loss of outer hoof wall material. Thus distal clipping material may only represent partial hoof wall depth. The normal process of controlled elimination of hoof wall material from the BB (Reilly *et al.* 1996, Budras and Schiel 1996) may also prevent the collection of full HWD samples.

Doubts therefore exist as to the representative nature of hoof horn material obtained from distal clippings. In addition, it is inherently difficult to discriminate between the effects of pathological change and environmental degradation on hoof horn material obtained in this manner. Finally the amount of material that can be obtained from distal clippings is limited, and therefore places restrictions upon subsequent methods of hoof assessment. Hence it was decided to use material in this project that was obtained from proximally located sampling sites, in which the effects of environmental degradation upon structure and material properties, are expected to be more limited.

Mostafa (1986), Linford (1987) and Ott and Johnson (2001) have used hoof biopsy techniques to overcome the inherent problems associated with distal clipping material.

However, these techniques may cause inducement of pain in the animal, and therefore can not be condoned on ethical and welfare grounds. In addition, the functional consequences to the animal resulting from the removal of hoof horn material are not understood.

The use of morbid hoof specimens obtained from either from those animals euthanased on medical grounds, or from slaughterhouse populations provide ethically acceptable sources from which non-environmentally degraded material can be readily obtained from proximally located sampling sites. Whilst samples from these animals tend to be biased in terms of their age and disease status, these issues are of minor consideration to this thesis, given the specific objective of performing a materials characterisation of laminitic hoof horn. In fact, these populations represent an invaluable and unrivalled source of laminitic hoof horn material.

Hence it was decided to base this study upon material obtained from morbid hoof capsules from animals euthanased on medical grounds, from the donkey population managed by The Donkey Sanctuary. Sourcing material in this way also assisted in the control of potential environmental factors, as animals at The Donkey Sanctuary are maintained under standardised management conditions. In addition, the medical histories of all animals are well documented, and thereby provide valuable information regarding concurrent disease status, and previous disorders of the feet.

2.3.2 THE MIDLINE DEAD CENTRE SAMPLING SITE

The sampling site chosen for assessment in this thesis was the midline dead centre site (MDC) described by Reilly *et al.* (1996).

Figure 2.1 Diagrammatic representation of the solear aspect of the donkey hoof to show the reference points used to determine the plane of the Midline Dead Centre (MDC).

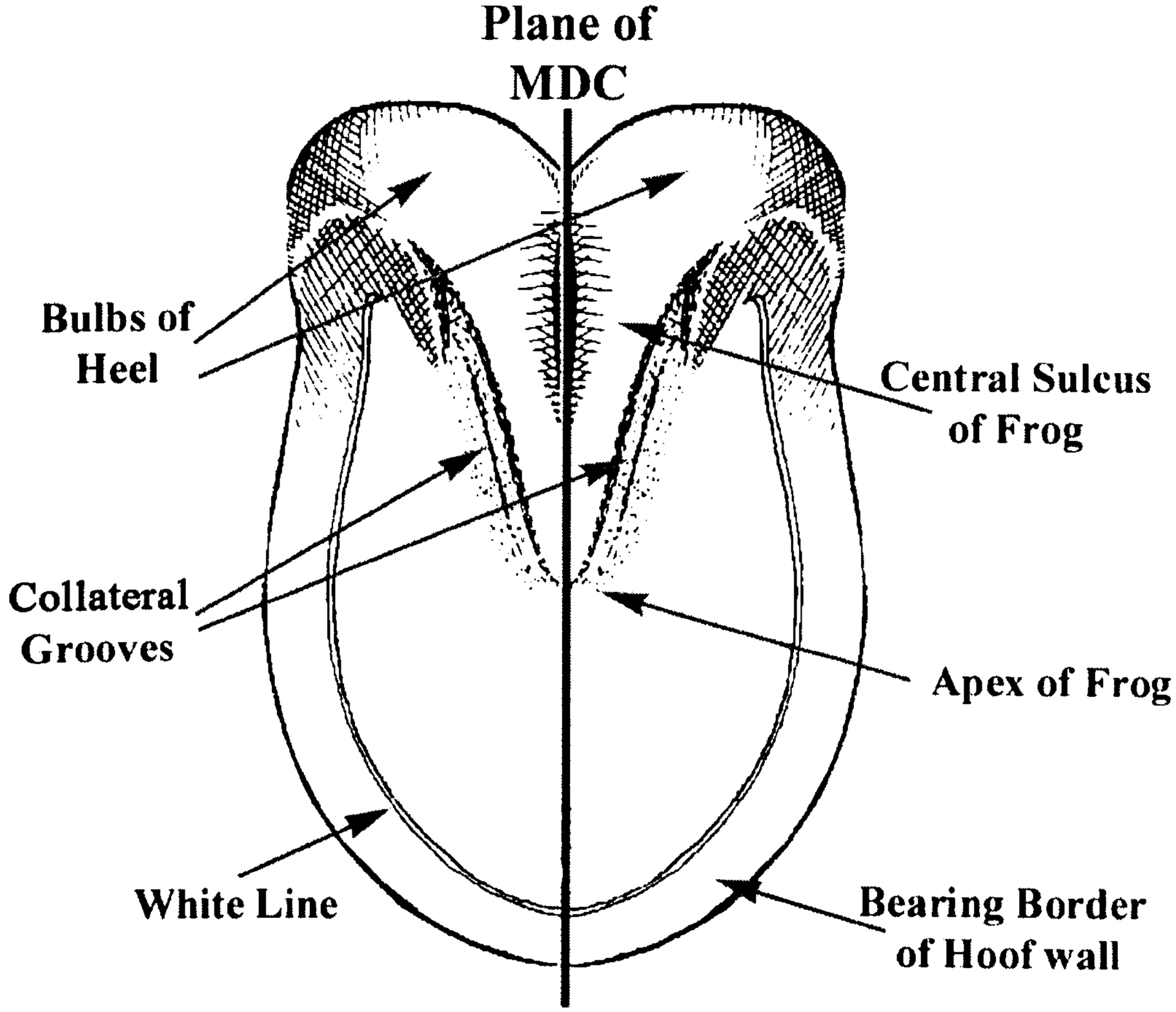

The MDC was selected because it offers several distinct advantages over other potential sampling locations within the hoof capsule. Primarily, it is one of the few sites that can be defined with accuracy, and is relatively easy to locate. It is therefore readily reproduced 'between individual samples'. Thus it ensures desired 'within sampling' consistency. In addition, the site affords the opportunity to achieve repeatability between studies. Hence the MDC site represents the ideal basis for future comparison.

The MDC site also offers the means by which the structural organisation of the hoof wall and white line can be accurately assessed. Accurate and consistent sample orientation is essential for effective morphometric analysis (Weibel 1979). With respect to the hoof wall, it is assumed that the tubules at the MDC are in a parallel array, and aligned in a proximo-distal direction (Greenough *et al.* 1981) perpendicular to the CB (Thomason *et al.* 1992). This particular structural arrangement enables accurate tubule sectioning, orthogonal to the longitudinal axis of the horn tubule. Orthogonal sectioning of the horn tubules facilitates determination of the transverse profile, and also the measurement of absolute linear and area parameters. In this regard, departure from the orthogonal sectioning plane would result in the production of 'false' cross sectional profiles of the horn tubules (Hofstetter 1985), and an over estimation of major axes and area measurements.

With regard to the laminitic condition, the MDC is also of particular relevance. Goetz (1987, 1989) stated that the effects of the laminitic condition were focused upon the dorsal aspect of the hoof capsule, and that the impact upon integumentary organisation was most pronounced at this site. In addition, Hood *et al.* (1994) and Pollitt (1995) demonstrated that vascular disruption to the dermal microcirculation was most notable at the dorsal coronary band, laminar and solear regions of the hoof, along the line of the MDC.

2.3.3 DEFINING THE PLANE OF THE MIDLINE DEAD CENTRE (MDC) WITHIN THE HOOF CAPSULE

All morbid feet were disarticulated at the metacarpo-phalangeal fetlock joint. The position of the MDC (see Figure 2.1) was determined in accordance with the protocol described by (Hopegood 2001). This was achieved by extending the long axis of the frog, defined as the line of best fit that bisects the heel bulbs, frog sulcus and the collateral grooves (sulci), forward to the dorsal margin of the hoof capsule at the BB. This point was marked with an indelible marker. A line drawn at right angles to the dorsal CB that united with this marker at the BB thus delimited the plane of the MDC.

2.3.4 PREPARATION OF THE MDC SAMPLING BLOCK

This methodology serves to produce a complete sample block (see Figure 2.2A-D) that encompassed the entire dorsal aspect of the hoof, complete with the wall sole junction. This sample block is referred to as the MDC Sampling Block.

The MDC was located and marked on the dorsal aspect of the hoof wall as outlined above. Two parallel control lines were drawn on either side of the MDC (see Figure 2.2A), each 13mm from the line of the MDC. Thereby a 26mm wide specimen block, symmetrical about the plane of the MDC was delimited. Two proximo-distal cuts (Cut 1 and 2) were made with an oscillating bone saw fitted with a 50mm mushroom blade, from the CB to the BB along these control lines. These cuts were made parallel to the plane of the MDC to the depth of the DP. The DP was readily detected by an increase in resistance to blade rotation. A final cut (Cut 3) was made on the solear aspect of the hoof, likewise to the depth of the DP, uniting Cuts 1 and 2 (See Figure 2.2B). A long-bladed scalpel was used to separate the connective tissue from the dorsal aspect of the DP. An incision was made a few mm proximal to the CB and progressively worked down the dorsal aspect of the DP towards the BB. In this way it was then possible to excise the intact MDC Sampling Block from the hoof (see Figure 1.22C).

2.3.5 OPTIMISED METHODOLOGY FOR MDC SAMPLING BLOCK PREPARATION

With the subsequent acquisition of a bench-mounted bandsaw, the MDC Sampling Block protocol was modified as follows: Instead of using the three-cut approach as detailed above, parasagittal cuts were made, along each of the two respective control lines, through the entire dorso-palmar extent of the foot. This produced a sagittal section of the foot along the plane of the MDC. This methodology, the sagittal approach, represented a significant timesaving optimisation over the previous three-cut approach.

2.3.6 HOOF WALL SPECIMEN BLOCK PREPARATION FROM THE MDC SAMPLING BLOCK

In order to account for between individual differences in absolute MDC Sampling Block heights, Hoof Wall Specimen Block preparation was conducted in terms of percentage Hoof Wall Height (%HWH). The inner aspect of the Hoof wall at the BB was defined as 0% HWH with the palmar aspect of the hoof wall at the CB defined as 100% HWH.

Figure 2.2 Diagrammatic representation of MDC Sampling Block Preparation.

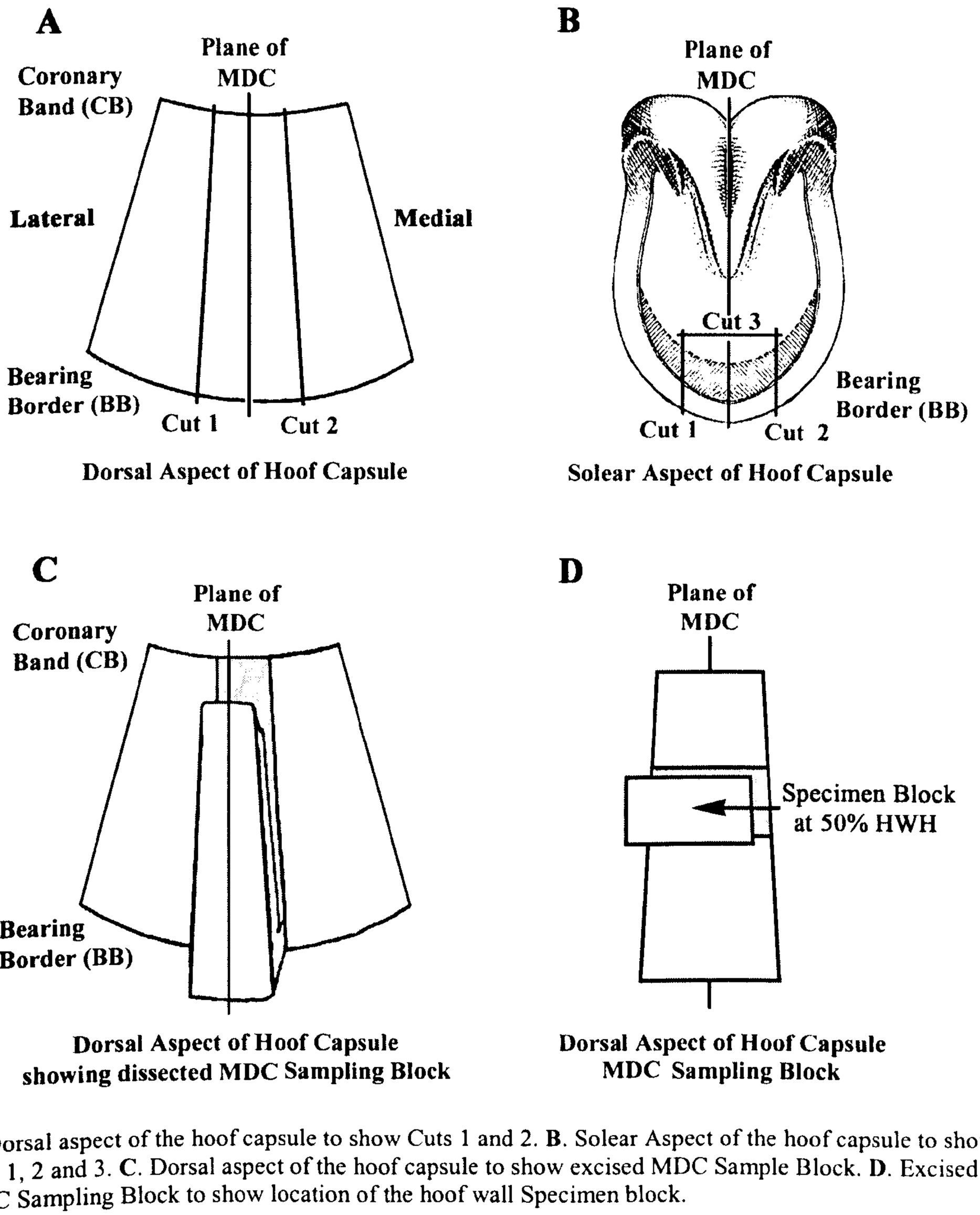

A. Dorsal aspect of the hoof capsule to show Cuts 1 and 2. **B**. Solear Aspect of the hoof capsule to show Cuts 1, 2 and 3. **C**. Dorsal aspect of the hoof capsule to show excised MDC Sample Block. **D**. Excised MDC Sampling Block to show location of the hoof wall Specimen block.

Hoof wall sampling was standardised at 50% HWH (see Figure 2.2D, Figure 2.3). This site was selected in order to minimise the effects of environmental degradation distally, whilst also ensuring sampling was performed distad to the keratagenous zone of the CB. In this way, sampling would be free of anatomical interference from the dermal papilla, and the material obtained would be composed of mature hoof horn material. The height of the MDC Sampling Block was measured in the sagittal plane from the palmar aspect of the BB to the CB. The midpoint marked on the palmar margin of the MDC Sampling Block. With the aid of a protractor, the position of the 50% HWH site was established (perpendicular to the tubule axes), and a dorso-palmar reference line marked across the entire HWD of the MDC Sampling Block. With the 50% HWH site established, all specimen block requirements could be accurately defined in a repeatable manner between individuals.

A 10mm high specimen block was prepared from the MDC Sampling Block with the aid of a hacksaw fitted with a fine toothed blade. Parallel cuts were made 3mm proximal and 7mm distal of the 50% HWH control line, to produce the Hoof wall Specimen Block.

This provided a Hoof Wall Specimen Block which had sufficient material, distad to the 50% HWH sampling site, to allow effective clamping within the microtome used to prepare sections for histology. There was also sufficient material proximad to the sectioning site, to provide protection against possible damage associated with the preparation of the specimen block.

2.3.7 PREPARATION OF HOOF WALL HISTOLOGY SECTIONS

Histological appraisal of the hoof wall was conducted on Hoof Wall Specimen Blocks obtained from the MDC Sampling Block at the 50% HWH site. Stereometric techniques aim to provide meaningful data on the quantitative balance, or relative fraction, of different cellular components within organs. These issues are discussed in detail in Chapter 4. It is therefore essential that the fine structure be preserved with as little change as possible arising from the tissue preparation processes (Budras *et al.* 2002). Tissue shrinkage due to fixation and embedding is a potential source of error (Reid 1980) that must be minimised. Commenting upon these issues, Budras *et al.* (2002) stated that effective methods of processing untreated ('fresh') hoof horn samples were desirable. Hence methodologies were developed that enabled hoof wall sections to be produced from untreated hoof horn material, without the need for tissue embedding and/or fixation.

The untreated specimen blocks were sectioned using a sledge microtome fitted with a D-profile steel blade at a cutting angle of 10°. The specimen block was orientated such that sections were cut from the external hoof wall (0% HWD) diagonally towards the internal aspect of the hoof

wall (100% HWD). The specimen block was initially trimmed at 20μm to produce a flat sectioning surface, devoid of any surface artefacts (e.g. saw blade marks). Subsequent sections were cut at 10μm. Sections for histological assessment were collected from the 50% HWH site of the specimen block. The sections were placed in distilled water, prior to staining, to prevent shrinkage and cellular damage resulting from ambient water loss.

Sections were stained with Alcian Blue, Periodic Acid, Schiff Reagent (AB-PAS). The staining protocol is summarised below:

<u>AB-PAS Staining Protocol</u>

- 2% Alcian Blue in 3% Acetic acid (w/v) – 5 min
  - Rinse with distilled water.
- 1% Periodic Acid (w/v) – 2 min
  - Rinse with distilled water.
- Schiff Solution – 10 min
  - Rinse with distilled water.

The AB-PAS technique preferentially stains muco-polysaccarides associated with the cell margin of the corneocyte and the ICC (Bolliger 1991). Thereby enhancing the appearance of the structural organisation of the cellular components within the stained sections. This makes this staining technique ideal for preparing sections for the morphometric analysis of structure (Hofstetter 1985). The gylcosaminoglycans (GAGs), that comprise the muco-polysaccarides, are a diverse series of sulfanated and non-sulfanated mucins (Ball 1999 – Pers Com.). Hence a 2% Alcian Blue in 3% Acetic acid Alcian Blue formulation (pH of 2.5) was employed, as this represents a non-specific stain formulation for all GAGs. This provided optimal cellular definition over that obtained by other potential Alcian Blue formulations, which are GAG specific (Collins – Pers Obs.).

Following staining, all sections were processed through a serial dehydration protocol, prior mounting with DPX. Specimens were not processed through normal cleansing and de-waxing procedures. This avoided aggressive dehydration and embrittlement of the hoof horn that can lead to specimen damage during the final stage of slide preparation (Collins – Per Obs.). In this way, it was assumed that the histology technique was optimised, with sample shrinkage, and artefact production, minimised.

Figure 2.3 Sagittal section of donkey foot to show hoof wall Sample Block reference points

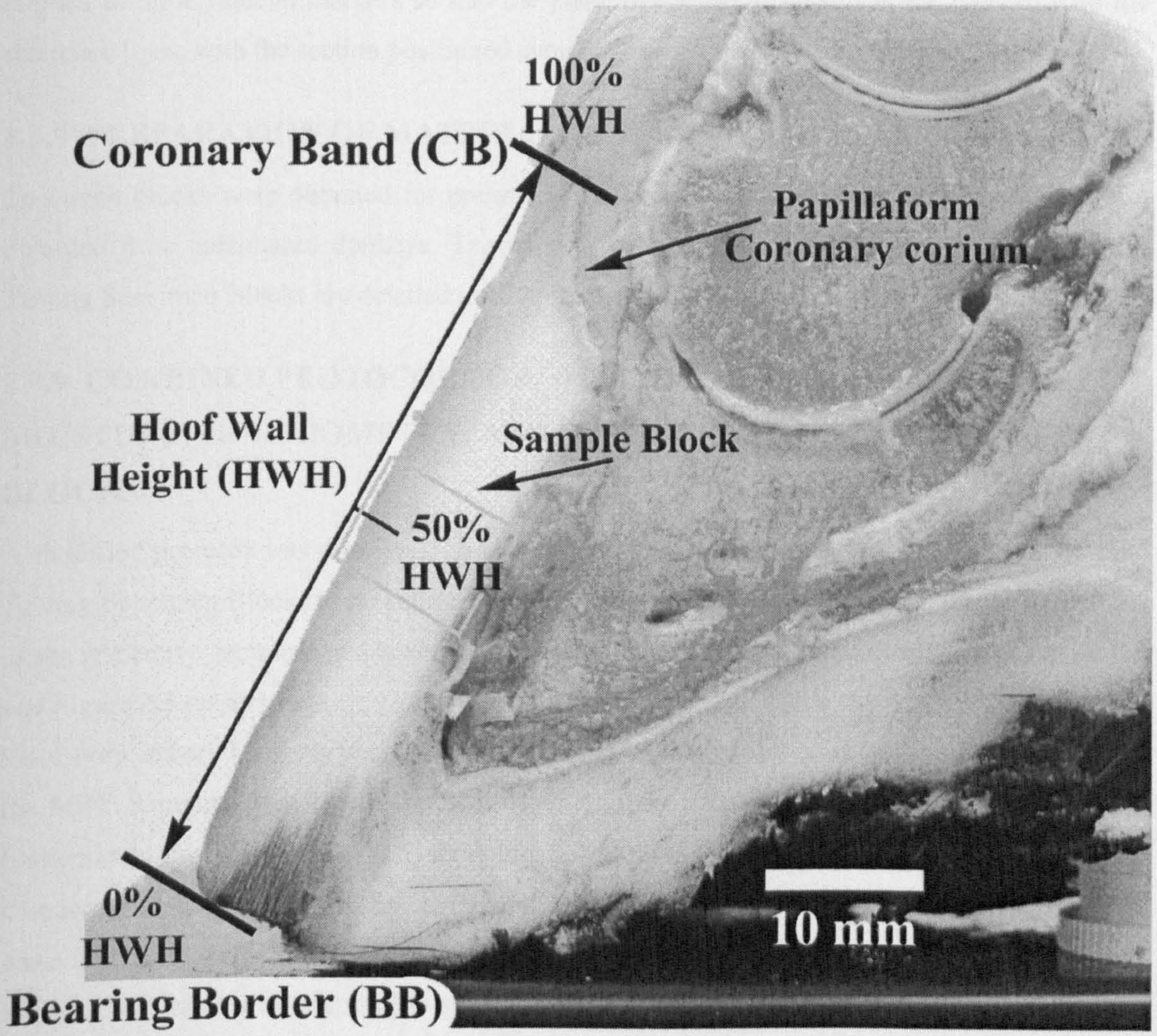

As movement of the microscope stage is restricted to either of two orthogonal directions, accurate mounting was essential in order to ensure histological assessment is performed along the plane of the MDC. To achieve this, the microscope slide was prepared with two, 5mm reference lines marked perpendicular to the midpoint of the long sides. The stained section was aligned to these fiducial markers so that the plane of the MDC was in linear register with the reference lines, with the section positioned symmetrically about these markers

2.3.8 PREPARATION OF MATERIAL TESING SPECIMEN BLOCKS

Specimen blocks were obtained for preliminary material testing from MDC Sampling Blocks obtained from euthanased donkeys. The specific protocols employed to prepare the Material Testing Specimen Blocks are detailed in Chapter 5.

2.3.9 COMBINED PROTOCOL FOR THE PREPARATION OF HOOF WALL MOISTURE, MORPHOMETRY, AND MATERIAL TESTING SPECIMEN BLOCKS

A modified protocol was developed to enable hoof wall Moisture, Morphometry and Material Testing Specimen Blocks to be sourced from a single disarticulated hoof capsule. The locations of the respective sampling and specimen blocks are summarised diagrammatically in Figure 2.4 and Figure 2.5 respectively.

Hoof horn material for morphometric and material testing of the hoof wall was obtained from the MDC Sampling Block, whilst a Moisture Sampling Block was sourced from hoof material immediately subjacent to the MDC Sampling Block. The Moisture Sampling Block was used in a concurrent study performed by this author to provide material for the investigation of hoof-water interactions, including the assessment of *'in vivo'* hydration status (see Chapter 5). It was therefore essential to obtain the Moisture Sampling Block immediately following euthanasia of the animal. Hence it was imperative that the sampling protocol could be successfully conducted under field condition, and that the excised Moisture Sampling Block could be effectively protected against ambient moisture loss prior to assessment.

The modified protocol involved a three-stage process: -

1. <u>Delimiting the MDC Sampling Block</u>

The MDC Sampling block was delimited in the manner described in Section 2.3.3and 2.3.4. In summary, the plane of the MDC was initialy determined from the solear aspect of the hoof capsule and its orientation marked on the dorsal aspect of the hoof wall. Two parallel control lines (1 and 2) were constructed on the dorsal aspect of the hoof wall respectively 13mm lateral

and 13mm medial of the MDC marker. In this way, the MDC Sampling Block was delimited on the dorsal aspect of the hoof capsule.

2. Delimiting the Moisture Sampling Block

With the MDC Sampling block delimited, a third parallel control line (3) was marked on the outer surface of the hoof wall 10mm medial of control line 2. Control lines 2 and 3 delimited the Moisture Sampling Block.

3. Removal and hermitic sealing of the Moisture Sampling Block

With the aid of an oscillating bonesaw, cuts were made along these respective control lines delimiting this sample block, to the depth of the DP. In a similar manner to that described in the three-cut approach for the removal of the MDC Sampling block (See Section 2.3.4), a final cut was made on the solear aspect of the hoof to unite these control lines 2 and 3.

Finally, with the aid of a scalpel, working down along the dorsal aspect of the DP from the CB to the BB, the Moisture Sample Block was removed from the hoof capsule. The excised Moisture Sampling Block was immediately wrapped in three overlapping layers of Parafilm in accordance with the methodology advocated by Collins *et al.* (1998) and Hopegood (2002), to produce an airtight seal that minimised moisture loss.

In this way, excised and sealed Moisture Sample Blocks were obtained within 20 minutes of euthanasia. The disarticulated foot was similarly wrapped in Parafilm and stored at 4^0C prior to further sample processing. With the production of the sealed Moisture Sampling Block, full HWD and Zonal Moisture Specimen Blocks could be prepared – see Figure 2.4.

4. Preparation of Hoof Wall Material Testing and Morphometry Sampling Blocks

The MDC Sampling Block was obtained from the disarticulated foot using the optimised sagittal approach (Figure 2.5) as described in section 2.2.5. The 50% HWH sampling site was established on both sagittal aspects of the MDC sampling block in accordance with Section 2.3.4, and the White Line removed (Figure 2.5, Cut 3).

The remaining portion of the MDC sample block was bisected along the plane of the MDC (Figure 2.5 Cut 4) and Material Testing and Morphometry Specimen Blocks ultimately prepared about the 50% HWH sampling site.

Figure 2.4 Diagrammatic representation of Moisture Specimen Block preparation.

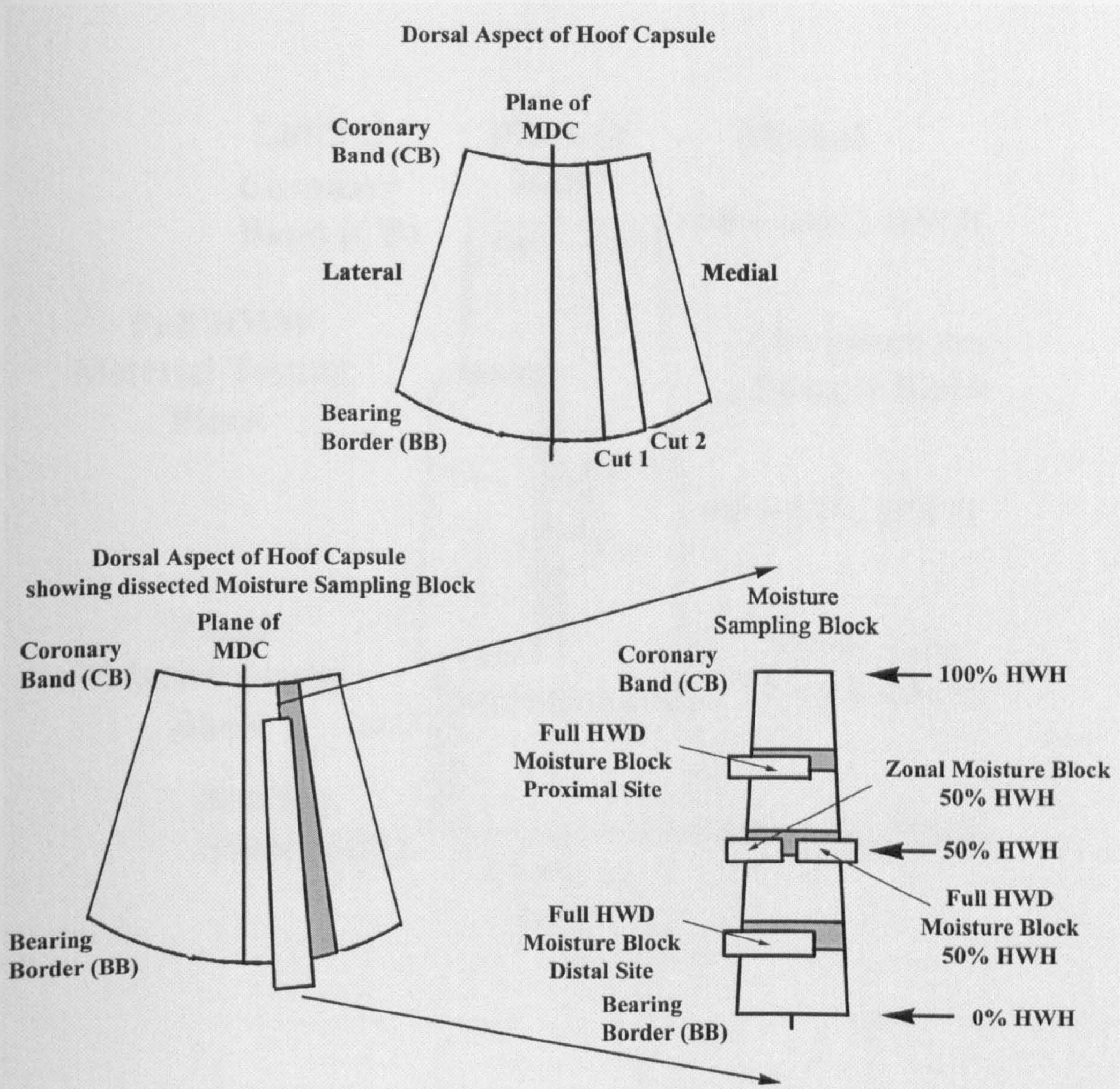

Figure 2.5 Diagrammatic representation of Material Testing and Morphometry Sample Blocks preparation.

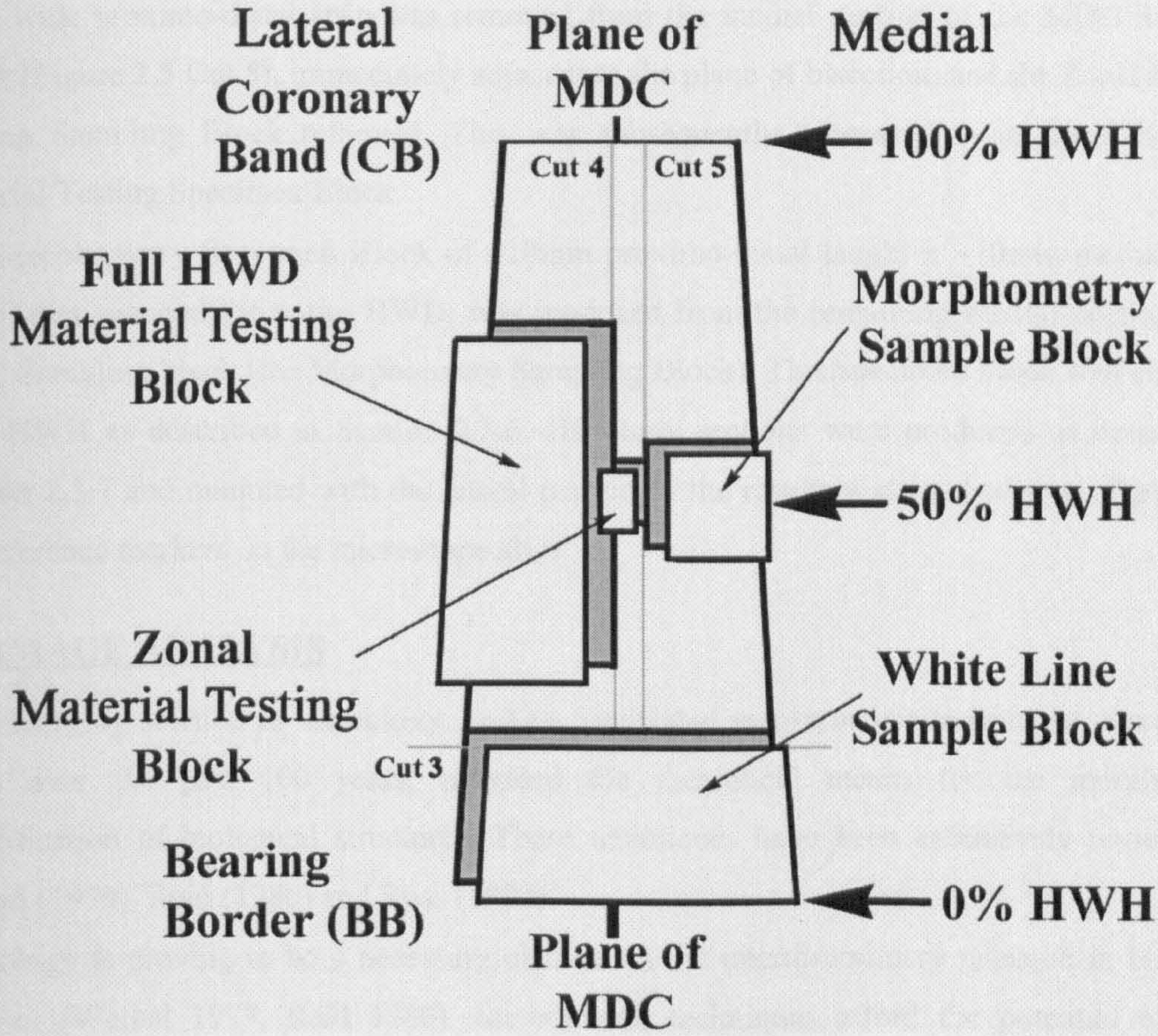

The specific procedures for the protocols for the production of the Full HWD and Zonal Material Testing Sample Blocks are detailed in Section 5.9.1.6. The Full HWD Material Testing Specimen Block was produced from the lateral portion of the bisected MDC Sampling Block, which constituted the Full HWD Material Testing Sampling Block. The Zonal Material Testing Specimen Block was prepared from the medial portion of the bisected MDC Sampling Block. A 3mm wide proximo-distal strip was removed from the medial portion of the MDC Sampling Block (Figure 2.5 Cut 5), immediately adjacent to the plane of bisection, and the Zonal Material Testing Sampling Block removed. This was subsequently processed to produce the Zonal Material Testing Specimen Block.

The Morphometry Specimen Block of ~10mm proximo-distal height x ~10mm medial lateral width, that spanned the entire HWD, was produced from the remaining medial portion of the MDC Sampling block (the Morphometry Sampling Block). This specimen block was centred at 50% HWH as described in Section 2.3.6. Histology sections were produced as described in Section 2.3.7 and mounted with the lateral margin of the resultant stained section aligned with the reference markers on the microscope slide.

2.4 IMAGE ANALYSIS

The emerging science of stereology, and its associated measurement techniques, stereometry have, over the past 100 years, provided the theoretical means for the morphometric quantification of biological structures. These techniques have been extensively reviewed by Wiebel (1979), Reid (1980) and Russ (1992).

Stereology is proving to be a necessary element in the interdisciplinary research in biological material (Weibel 1979, Reid 1980). Stereometric techniques afford the potential to detect pathological change where subjective evaluation can detect nothing, and provide the means by which the degree of change imposed on tissues by pathological change may be quantified (Reid 1980). Thus these techniques are of extreme value in elucidating structure-function relationships, and the assessment of functional impairment.

The practical application of stereometry to studies involving the large-scale assessments of histology sections have, however, been limited (Reid 1980). Traditionally such studies have relied upon manual measurements taken from either projected images or photomicrographs, with measurements being restricted to ratio quantification derived from point counting operations. Such work is very time-consuming, painstaking and laborious, requiring the services of several observers. In addition to the inherent costs involved in the studies, reliability issues, relating to repeatability and reproducibility of results, have emerged as major operational concerns (Wiebel 1979). The advent of computer and video technology has however made

quantification a realistic and practical option. Recent developments now provide a cost-effective alternative to manual based measurements systems.

Computer based imaging has the potential to significantly improve the reliability of these studies (Moore 1988), and also significantly reduce procedural time in situations where photomicrographs were needed (Gatlin *et al.* 1993). These advances also make it possible to obtain absolute linear and area measurements.

In addition, computer programming affords the opportunity to: -

- Automate many procedural operations (Wiebel 1979)
- Minimise observer 'sampling bias' (Leach 1996)
- Enhance images prior to object discrimination and measurement (Russ 1992)

In light of these distinct advantages, a highly flexible computer based IAS with the capabilities of delivering automated, or semi-automated, methods for the quantification of hoof horn parameters, was established. An overview of the system requirements, design theory, and the IAS established for this project is given in Appendix IV.

2.5 MEASUREMENT PROTOCOLS

With the availability of the dedicated IAS, standardised methodologies for the quantification of hoof horn parameters at the microscopic level could be developed. These are described in Chapters 4.

2.6 PRELIMINARY STAGE OF THE EXPERIMENTAL PHASE OF THESIS

With the sampling, sectioning and measurement techniques optimised, the preliminary experimental stage of the thesis could be initiated. The preliminary assessments were conducted on morbid hoof capsules harvested from donkeys that had been euthanased on medical grounds, with hoof horn material sourced from the left forefoot.

An animal was considered to be suitable for inclusion in these preliminary studies if the individual's medical history indicated a long-standing laminitic condition in the left forefoot (>12 months). In this way, it was assumed that the entire hoof capsule was composed of laminitic hoof horn material. A diagnosis of laminitis was accepted if the individual had a history of recurrent bouts acute phase laminitis and/or radiographic evidence of DP dislocation

The preliminary assessments of morphologic, morphometric and material properties are discussed in detail in Chapters 4 and 5. In addition, the preliminary work associated with development of the computer based hoof wall model is given in Chapter 6.

With the preliminary elements of the experimental phase completed, the main experimental stage was instigated.

2.7 MAIN EXPERIMENTAL STAGE OF PROJECT

The main experimental stage of the project was conducted on a trial population of 26[1] laminitic donkeys. These were selected from a population of donkeys who were due to be euthanased of medical grounds.

The selection process was based upon detailed medical and farriery records

The diagnosis of a laminitic condition was assumed if an individual had a long-standing history of recurrent bout of acute phase laminitis, and farriery records indicating degenerative problems of the foot. A single forefoot was randomly allocated for assessment, whilst assessment of the other foot was incorporated into a separate, concurrent study.

Pertinent details of the medical history/farriery comments for the laminitic group are summarised in Table 2.1. Specific details of the foot have only been included, if they relate to the forefoot used in this study.

Lateral radiographs of the allocated forefeet were obtained from both the laminitic and normal group. This aspect of the thesis is covered in Chapter 3. The lateral radiographs of the laminitic group were obtained 24 hours prior to euthanasia. In addition bodyweights were also determined immediately prior to euthanasia, in accordance with the nomogram published by Eley and French (1993b).

Bodyweight determination was based upon wither height and heart girth measurements where:

$$\text{Bodyweight (Kg)} = \text{wither height}^{0.24} \times \text{heart girth}^{2.576} \times 0.000252$$

$$\text{Corrected } R^2 = 0.923$$

Immediately following euthanasia, the allocated forefoot was disarticulated at the metacarpophalangeal joint, and the Moisture Sampling Block removed as described in Section 2.3.9.

---

[1] 26 animals were originally identified, and subsequently X-rayed prior to scheduled euthanasia. The decision to proceed with euthanasia was, however, rescinded in respect of three individuals. Hence all other experimental data were collected from the 23 donkeys that were euthanased

Table 2.1 Summary table of Age Weights and Medical Histories / Farriery Comments for the laminitic donkey group

Donkey	Age	Weight	Summary of Medical History / Farriery Comments
LD1	21	157	Overgrown Feet (85) Laminitis (85) Laminae abcesation (85) Laminitis (89) Laminitis (97) Seedy Toe (97) Chronic Founder (98) Laminitis (4/8 99) Solear weight bearing (E) Divergent growth rings (E) Perioplic hyperplasia (E) Dorso-concavity (E) Sunken CB (E)
LD2	26	178	Poor Feet (98) Dorsal Hoof wall Defect (98) Chronic Founder (98) Solear weight bearing (E) Sunken CB (E)
LD3	13	176	Laminitis (97) Solear Weight Bearing (E) Broken forward HPA (E)
LD4	29	242	Seedy toe (95) Foot Lameness (95) Laminitis (98) Solear weight bearing (E)
LD5	26	177	Overgrown feet (88) Laminitis (1/12 92) Laminitis (93) Laminitis (96) Laminitis (97) Laminitis (98) Laminitis (99) Chronic Founder (99) Solear weight bearing (E) Divergent Growth Rings (E) Dorso-concavity (E)
LD6	29	201	Lame (85) Laminitis (91) Seedy Toe (91) Laminitis (92) Laminitis (96) Solear weight bearing (E) Divergent growth rings (E) Perioplic hyperplasia (E) Dorso-concavity (E) Sunken CB (E)
LD7	19	215	Seedy Toe (92) laminitis (92) Overgrown feet (92) Laminitis (97) Solear weight bearing (E) Sunken CB (E)
LD8	24	117	Chronic Founder (93) Seedy toe (94) White Line disease (94) laminitis (98) Chronic DP Degeneration (98) Laminitis (99) Solear weight bearing (E) Divergent Growth Rings (E)
LD9	32	169	Overweight (82) Laminitis (85) Laminar abscessation (85) Laminitis (2/10 86) Chronic Founder (87) Laminitis (89) Laminitis (90) Laminitis (91) Laminitis (93) Laminitis (94) Laminitis (96) Laminitis (97) Laminitis (98) Laminitis (99) Solear weight bearing (E) Divergent growth rings (E) Dorso-concavity (E) Sunken CB (E)
LD10	22	118	Chronic Founder (93) W Line disease (94) Dorsal hoof wall defect (94) Laminitis (96) Laminitis (98) Laminitis (99) Divergent Growth Rings (E) Dorso-concavity (E)
LD11	31	147	Seedy Toe (97) Laminitis (97) Chronic Founder (97) Laminitis (98) Laminitis (4/5/6/8/10 99) Laminar Abscessation (00) Laminitis (00) Solear weight bearing (E) Divergent growth rings (E) Perioplic hyperplasia (E) Dorso-concavity (E) Sunken CB (E) Seedy Toe (E)
LD12	31	139	Laminitis (81) Chronic lameness (84) Lame (87) Seedy toe (87) Laminitis (93) Laminitis (94) Laminitis (96) Laminitis (99) Chronic lameness (00) Solear weight bearing (E)
LD13	32	180	Hyperlipaemia (99) Laminitis (99)
LD14	26	165	Chronic Founder (98) Laminitis (98) Laminitis (9/10/12 99) Solear weight bearing (E) Divergent growth rings (E) Perioplic hyperplasia (E) Dorso-concavity (E) Sunken CB (E)
LD15	11	174	Unresolved Lameness (98) Chronic Degenerative foot problems (98) Laminitis (99) Chronic Founder (99) Laminitis (00) Sunken CB (E) Divergent growth rings (E) Perioplic hyperplasia (E) Dorso-concavity (E)
LD16	38	202	Poor Hooves (98) Laminitis (99) Solear weight bearing (E) Sunken CB (E)
LD17	31	175	Overgrown feet (82) Overgrown feet (94) Dorsal Hoof wall defect (94) Chronic Founder / Sunken CB (94) Laminitis (95) Laminitis (97) Laminitis (98) Solear weight bearing (E) Divergent growth rings (E) Perioplic hyperplasia (E) Dorso-concavity (E)
LD18	25	215	Overgrown feet (99) Chronic founder (99) Laminitis (99) Laminitis (00) Solear weight bearing (E) Divergent growth rings (E) Dorso-concavity (E)
LD19	27	214	Hyperlipaemia (93) Laminitis (98) Laminitis (99) Solear weight bearing (E) Sunken CB (E)
LD20	32	150	Laminitis (98) Seedy Toe (E) Solear weight bearing (E)
LD21	22	174	Seedy Toe (92) Laminitis (94) WL abscessation (94, 95) Chronic Founder (96) Laminitis (98) Laminitis (1/99, 12/99) Solear weight bearing (E) Dorso-concavity (E)
LD22	27	159	Overgrown Feet (91) Chronic Founder (96) Solear weight bearing (E)

Donkey	Age	Weight	Summary of Medical History / Farriery Comments
LD23	**22**	**163**	Overgrown feet (93) White Line Separation (93) Laminitis (93) Overgrown feet (97) White line Separation (97) Laminitis (98) White line Abscessation (98) Laminitis (3/5/8/10 99) Laminitis (00) Solear weight bearing (E) Seedy Toe (E)
LD30*	**29**	**185**	Chronic Founder (96) Laminitis (97) Laminitis (98) Laminitis (99)
LD31*	**18**	**163**	Poor Hooves (98) Laminitis (98) Laminitis (99) Solear weight bearing (E) Sunken CB (E)
LD33*	**21**	**129**	Laminitis (94) Laminitis (96) Laminitis (97) Laminitis (98) Laminitis (99) Solear weight bearing (E) Divergent growth rings (E) Dorso-concavity (E) Sunken CB (E)

Key: (**XX**) Year, (**X/XX**) Month/Year, (**E**) At time of Euthanasia, * Animal not Euthanased – X-ray Data Only.

Of the 26 laminitic donkeys, two individuals, LD 9 and 14 displayed overgrown feet at the time of euthanasia. Thus they both displayed marked hoof wall overgrowth at the MDC, despite having previously received corrective distal hoof wall resection.

2.8 CONCLUSIONS

The methods described here together with those detailed within Chapters 4 and 5 enabled a comprehensive materials characterisation of laminitic donkey hoof horn to be undertaken. In addition, with the use of radiographic data, the relationships between anatomical change associated with the laminitic condition, the structural organisation of the hoof horn material at the microscopic level, and the mechanical properties of laminitic hoof horn could be evaluated. Finally through the development of computer modelling techniques, structure-function relationships within the laminitic donkey hoof wall could be investigated.

3. RADIOGRAPHIC ANATOMY OF THE NORMAL AND LAMINITIC DONKEY FOOT

3.1 INTRODUCTION

3.1.1 OVERVIEW

Eustace (1998) stated that in order to treat and prognose the laminitic condition one must first diagnose. Effective diagnosis is however dependent on prior knowledge of normality, such that pathological change can be detected and severity assessed (Linford 1987). This presents a particular problem with regard to the donkey as there is little information concerning the normal radiographic appearance of the foot (Walker *et al.* 1995, Bordalai and Nigam 1977). Hence there has been a tendency to employ radiographic guidelines for the pony or horse when assessing the radiographic anatomy of the donkey foot (Collins and Reilly 2004a – Submitted)

Diagnosis of degenerative change to the anatomical organisation of the laminitic equine foot has traditionally been based upon the subjective interpretation of radiographs (Cripps and Eustace 1999a). Whilst extreme degenerative change can be diagnosed with confidence by this subjective approach, modest changes, or changes of a less visually apparent nature, present a particular challenge to the clinician (Herthel and Hood 1999). Baxter (1996) reported that over 75% of DP displacement cases (Sinkers), where parallelism is maintained between the hoof wall and the DP, went undetected by subjective radiographic assessment. Hence an objective means of radiographic assessment is required to ensure early diagnosis of pathological change. This is of particular relevance to the donkey as clinical signs of pain associated with laminitis are often absent until an advanced stage of degenerative change. Thus presentation of the afflicted animal often does not take place until extensive damage has occurred within the foot. Prognostic evaluation is dependent upon the accurate assessment of the severity of pathological change (Butler *et al.* 1998). It is widely accepted that this is directly related to both the nature and extent of the degenerative anatomical change (Kameya 1973, Stick *et al.* 1982, Eustace 1991, Cripps and Eustace 1999b, Hemker 2001, Glöckner 2002). Hence, there is a need to both characterise the nature, and quantify the extent of these degenerative changes to the radiographic anatomy of the foot. This requires the careful selection of an appropriate series of measurement parameters. These must characterise and define the key elements of the radiographic anatomy, and also detect the specific pathological events associated with the laminitic condition (Collins and Reilly 2004b – Submitted.).

This chapter details work associated with this radiographic parameter selection process. It also reports on the objective characterisation of the radiographic anatomy of the normal donkey foot. In addition it reports the quantification and classification of degenerative changes associated with the laminitic condition within this equid species.

3.1.2 MORPHOMETRIC QUANTIFICATION OF THE RADIOGRAPHIC ANATOMY OF THE EQUINE FOOT

Collins and Reilly (2004b – Submitted) highlighted inconsistencies in approach and confusing terminology that had been employed in detailing the radiographic anatomy of the equid foot. These authors commented upon the difficulties this caused in the interpretation of digital radiographs.

A summary of the different morphometric methods previously used to determine the nature of the DP dislocation associated with laminitis is given in Table 3.1. Figure 3.0 illustrates the different morphometric approaches of A. Kameya (1973), B. Linford (1987), C. Eustace (1991), and D. Hemker (2001).

Kameya (1973) conducted the first reported morphometric study in the horse. Utilising lateral radiographs of the distal limb, this author objectively characterised the normal anatomical organisation of the foot. He also evaluated the nature and extent of DP rotation associated with laminitic condition. This author used a series of linear and angular measurement parameters to define the anatomical inter-relationship between the osseous and exosseous structures of the foot.

These parameters were: -

- The dorsal hoof wall angle (A) - defined as the angle subtended between the dorsal aspect of the hoof wall and the ground line.
- The dorsal angle of the DP (B) - defined as the angle subtended between the dorsal aspect of the DP and the ground line.
- The angle of the middle phalanx (C) - defined as the angle subtended between the dorsal aspect of the middle phalanx and the ground line.
- Integument Depth at the proximal limit of the DP (a) - defined as the perpendicular linear distance between the dorsal hoof wall and the dorsal aspect of the DP immediately distal to the extensor process of the DP.
- Integument Depth at the distal limit of the DP (b) - defined as the perpendicular linear distance between the dorsal hoof wall and the dorsal aspect of the DP at the apex of the DP.

Figure 3.0 Diagrammatic representation of radiographic parameters assessed in the work of Kameya (1973), Linford (1987), Eustace (1991) and Hemker (2001).

A. Kameya (1973).

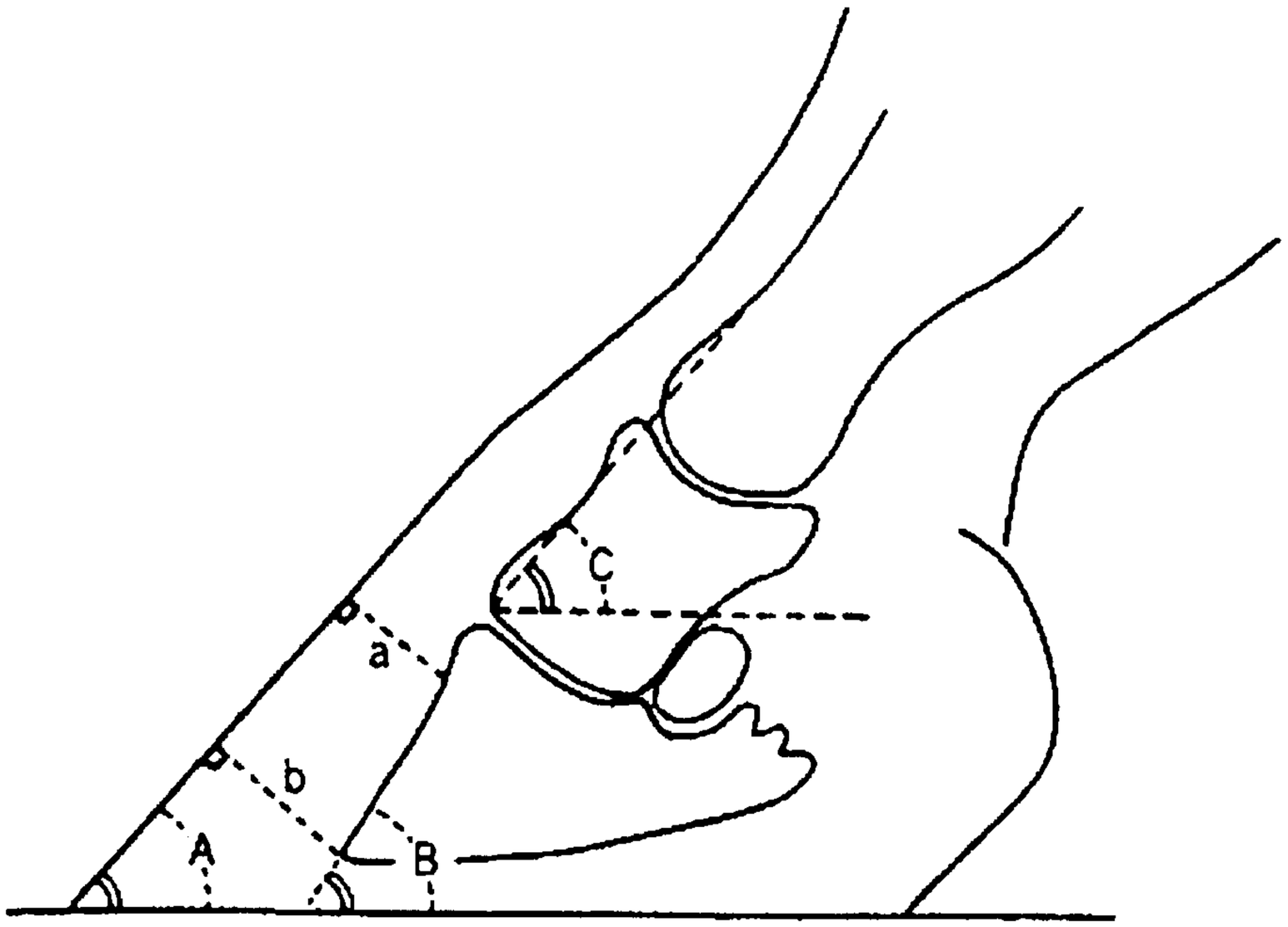

B. Linford (1987).

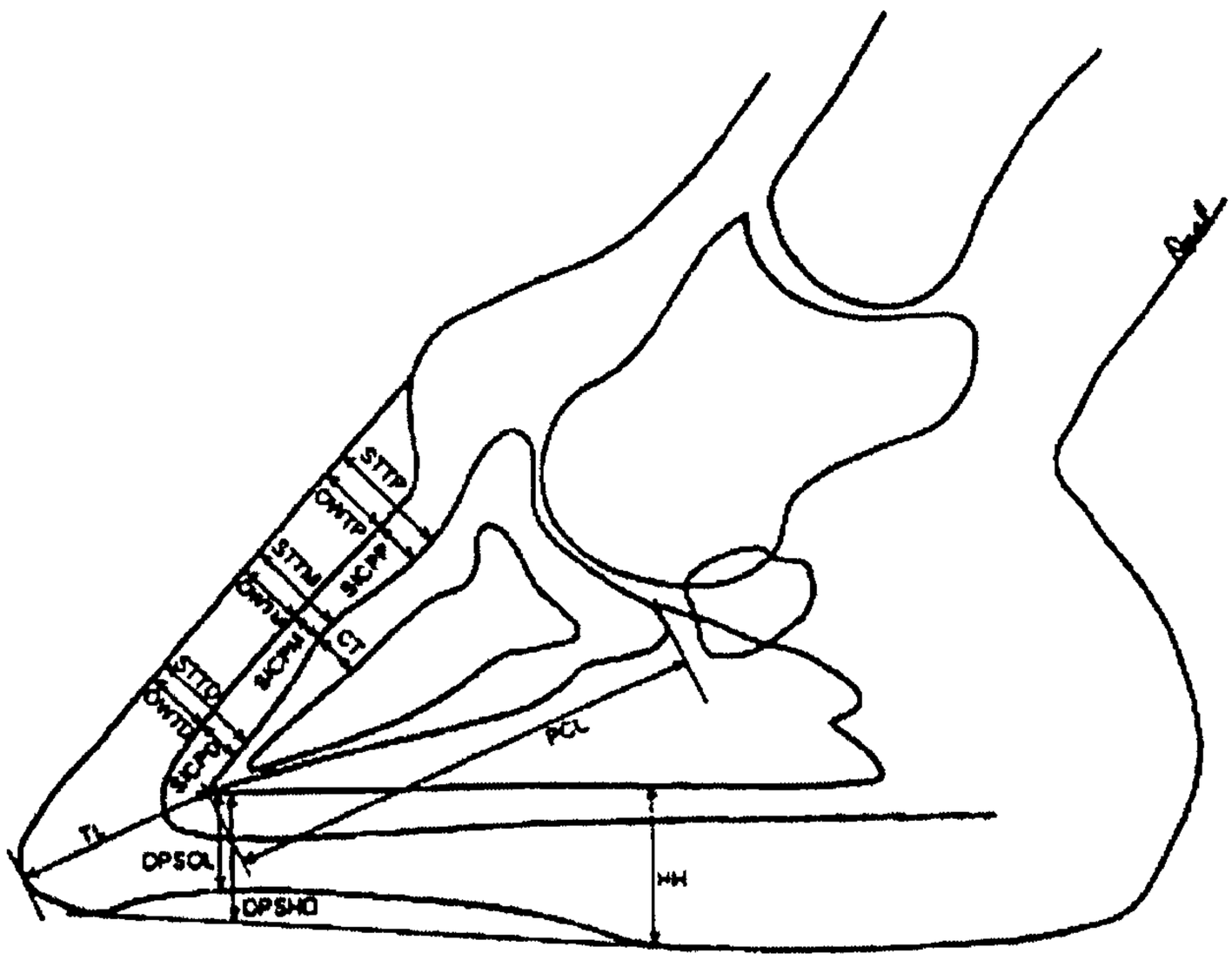

C. Eustace (1991).

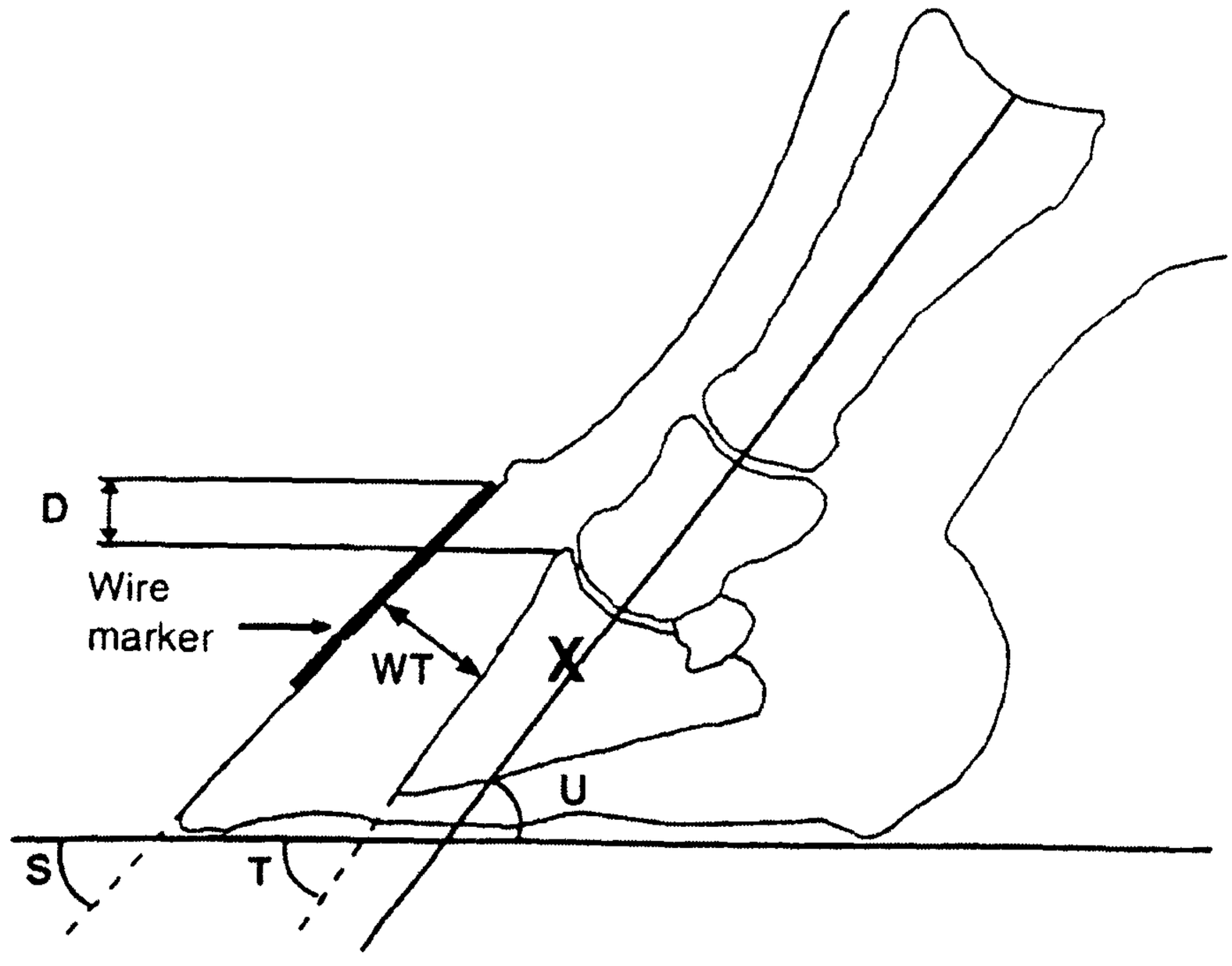

D. Hemker (2001).

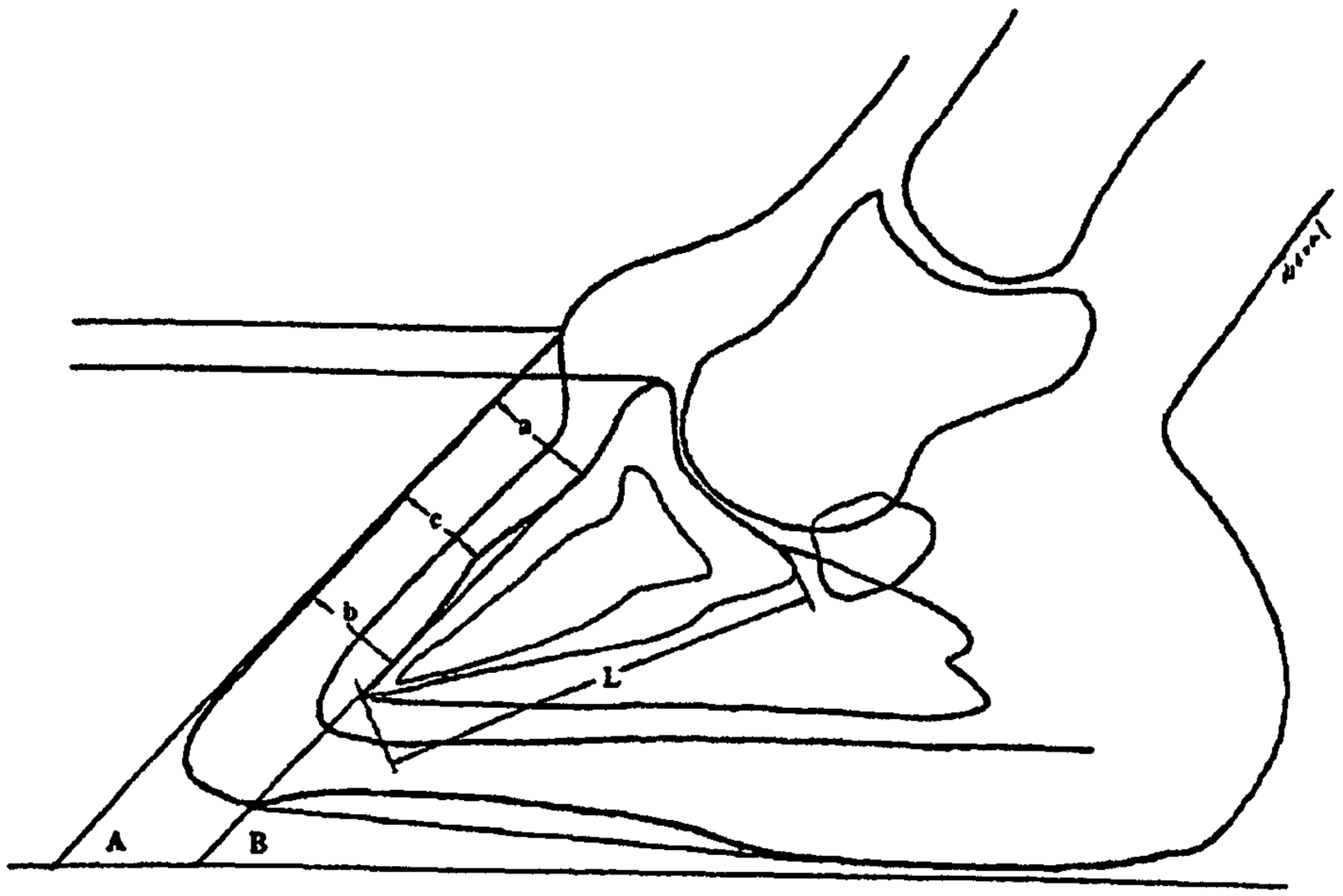

Table 3.1 Summary overview of the different methods used to determine the nature of the DP dislocation associated with the laminitic condition

Capsular Rotation			
Measurement Option	**Author**	**Advantages**	**Disadvantages**
Angular difference b/n the dorsal aspect of the hoof wall and the dorsal aspect of the DP	Kameya (1973), Stick *et al.* (1982), Linford (1987), Eustace (1991) Cripps and Eustace (1999a), Hemker (2001), Glöckner (2002)	• Widely accepted and reported • Related to Treatment and Recovery Outcome	Affected by: • Rasping/resection • Dorso-concavity and angulation Can not control for phalangeal rotation effects
Phalangeal Rotation			
Measurement Option	**Author**	**Advantages**	**Disadvantages**
Angular difference b/n the dorsal aspect of the hoof wall and the central axis of the PP	Kameya (1973), Eustace (1991) Cripps and Eustace (1999a), Hemker (2001), Glöckner (2002)	• Widely accepted and reported	Affected by: • Weight bearing • DP Remodelling • Farriery
DP Displacement			
Measurement Option	**Author**	**Advantages**	**Disadvantages**
Integument Depth at Mid Dorsal site Perpendicular linear distance b/n the dorsal aspect of the DP and the dorsal aspect of the hoof wall, midway b/n distal and proximal sites	Linford (1987), Hemker (2001), Glöckner (2002)	• Direct measurement parameter	Affected by: • Capsular rotation • Breed Type • Rasping/resection
Integument Depth at Midpoint site Normalised with respect to Palmar cortical DP Length (PCL)	Linford (1987), Hemker (2001), Glöckner (2002)	• Controlled for breed type/bodyweight variations	Affected by: • Size variation in DP • DP Remodelling
Perpendicular linear distance b/n the ground line and the apex of the DP	Redden (1998)	• Direct measurement parameter	Affected by: • Capsular rotation • Breed type • DP Remodelling • Bwt within breed
Perpendicular linear distance b/n the proximal limit of the dorsal hoof wall and the proximal margin of the extensor process	Eustace (1991), Cripps and Eustace (1999a), Hemker (2001), Glöckner (2002)	• Not affected by DP remodelling/farriery factors • Important prognostic indicator	Affected by: • Breed type? • Body weight within breed?
Combined DP Rotation and Displacement			
Linear difference between Integument Depth of the dorsal aspect of the foot measured at the distal and proximal sites	Hemker (2001), Hemker and Hertsch (2002)	• Summarises effect of rotational and displacement events	Affected by: • Farriery Can not discriminate between dislocation events

From these 5 basic radiographic measurements, a further series of derived parameters were established. These were: -

- Degree of Capsular Rotation (A minus B)
- HPA (A minus C)
- Degree of Phalangeal Rotation (B minus C)
- Integument Depth ratio (b divided by a)

Kameya (1973) utilised 7 parameters: (A), (B), (C), (A-B), (A-C), (B-C) and (b/a) to provide objective baseline information regarding the normal anatomical organisation of the equine foot. In this way Kameya (1973) was able to quantify key defining characteristics including the HPA, and the degree of capsular and phalangeal rotation present within the normal foot.

The principles of this author's approach have been widely accepted and incorporated into subsequent studies by Linford (1987) Eustace (1991), Cripps and Eustace (1999a) Hemker (2001) and Glöckner (2002).

The findings of Kameya (1973) supported the theoretically 'ideal' radiographic conformation of the equid foot described by Colles (1983) and Butler *et al.* (1998) – see Section 1.11.5.1, and also the theoretically ideal HPA, with minimal phalangeal rotation – see Section 1.8 and 1.8.1. Specifically, the dorsal aspect of the DP was in near parallel alignment with the hoof wall, with a mean capsular rotation angle of 0.48 ± 1.4 degrees. Integument Depth was of uniform dorso-palmar extent, with an Integument Depth ratio of 0.92 ±0.06. Phalangeal rotation was limited with a mean angle of 2.94 ±3.6 degrees.

Kameya's retrospective analysis of the radiographic anatomy laminitic foot highlighted the diagnostic potential of this approach. This analysis revealed that the morphometric characteristics of the laminitic foot differed from those of the normal foot. The laminitic foot was characterised by the presence of a 'Broken Forward' HPA, and was accompanied by an increase in the dorsal angle of the DP, and, a decrease in dorsal hoof wall angle.

The degree of capsular and phalangeal rotation also exceeded mean baseline values, as did the Integument Depth ratio. However Kameya (1973) did not evaluate these differences statistically to give the diagnostic nor predictive capabilities of this baseline data.

Kameya (1973), Stick *et al.* (1982), Hemker (2001) and Glöckner (2002) have all, retrospectively evaluated the association between morphometric characteristics of the laminitic foot and the recovery outcome of the afflicted animal.

Cases were variably classified into groups on different ordinal scales for increasing lameness post recovery.

These groups were: -

- Group 1 - Became sound
- Group 2 - Remained slightly or intermittently lame
- Group 3 - Persistent lameness
- Group 4 - Euthanased on medical grounds of severe lameness

These studies have all concluded that the degree of capsular rotation was related to the level of return to athletic performance (Kameya 1973, Stick *et al.* 1982, Hemker 2001, Glöckner 2002). However these different studies have reported different absolute group values. Conversely, the degree of phalangeal rotation reported by Kameya (1973) was independent of the post recovery lameness grade. The relationship between the degree of capsular rotation and recovery outcome within these respective studies are summarised in Table 3.2.

All authors have confirmed that an inverse relationship exists between the extent of capsular rotation and recovery outcome. Stick *et al.* (1982) and Glöckner (2002) concluded that capsular rotation in excess of 5.5 and 6.7 degrees respectively represented a guarded prognosis of treatment outcome. In fact, Cripps and Eustace (1999b) reported that capsular rotation was related to a binomial treatment outcome of success or failure to return to 'former athletic performance levels', with mean values of capsular rotation angles significantly higher in failure outcomes compared to successes ($P<0.01$).

These findings collectively suggest that both the nature and the extent of the DP rotation reflect condition severity and represent important prognostic determinants of recovery. In this regard, phalangeal rotation appears to be clinically less serious than capsular rotation (Kameya 1973). However, these assertions, and indeed, the predictive ability of these prognostic associations have yet to be confirmed experimentally.

Table 3.2 Relationship between the degree of capsular rotation and recovery outcome

Author	**Lameness group with mean capsular rotation angles**				
	Normal	Group 1 Became Sound No Lameness	Group 2 Intermittent Lameness	Group 3 Persistent Lameness	Group 4 Euthanased Severe Lameness
Kameya (1973)	-0.48+/-1.4	3.7+/-4.7	19.3+/-6.1	22.4+/-10.7	16.8+/-8.1
Stick *et al.* (1982)	N/A	~ 5	~9	~14	~15
Hemker (2001)	N/A	3.34	9.60	11.93	8.82
Glöckner (2002)	N/A	3.6 +/-4.55	6.9 +/-5.98	7.9 +/-6.70	8.17 +/-6.43

The experimental approach devised by Kameya (1973) does not however provide a means of diagnosing or quantifying the degree of DP displacement within the foot. Given the perceived severity of this form of DP dislocation (Baxter 1986), the inability of Kameya's method to detect and quantify this event is a major flaw. Linford (1990, 1996) highlighted the diagnostic importance of being able to detect DP displacement, stating that distal displacement was an

obligatory response to SADP compromise during the developmental phase of the laminitic condition. This author stated that DP displacement occurred within the first 72 hours of the condition, irrespective of the subsequent nature of DP dislocation.

Despite these facts, a unified approach in the diagnosis of DP displacement has not yet been achieved. Chapman and Platt (1984) and Hood (1999a) have commenting upon this issue, stating that DP displacement was difficult to assess radiographically. Various approaches in the assessment of DP displacement have been advocated most notably O'Brien and Baker (1986), Linford (1987), Redden (1998, 2002) and Cripps and Eustace (1999a).

Linford *et al.* (1993) summarising the earlier work of O'Brien and Baker (1986) and Linford (1987) argued that Integument Depth at the dorsal aspect of the foot could be used as an objective means of assessing DP displacement. This approach has been subsequently adopted by various researchers, however, critical diagnostic values of Integument Depth vary between authors. For example, O'Brien and Baker (1986) stated that a linear distance ≥20mm confirmed that DP Displacement had occurred within the foot, whereas Linford (1987) reported a value ≥15mm as confirming such a diagnosis. Eustace (1992) and Cripps and Eustace (1999b) commenting upon this issue, and reported significant 'between breed' differences in this parameter within the normal foot, and also, 'within breed' differences related both to bodyweight and hoof size.

Linford *et al.* (1993) recognised these potential confounding factors and argued that Integument Depth should be expressed as a percentage of the palmar cortical length of the DP (%PCL). This would control for bodyweight variations between breeds. In this way, Linford (1987, 1990, 1996) concluded that %PCL values >30% were diagnostic of digital collapse. Hemker (2001) and Hemker and Hertsch (2002) also reported a direct relation between %PCL and Recovery Outcome in a retrospective radiographic study. The mean %PCL values for the 4 lameness classes were ~34%, 44%, 49% and 44%. These authors concluded %PCL >37% represented a guarded prognosis of recovery outcome. However it is important to note that these results were based upon cases studies in which capsular rotation was evident. The ability of parameters based upon Integument Depth to discriminate and accurately quantify DP displacement is negated if capsular rotation is present within the foot. In addition, Roentogenic change in the form of bone resorption may reduce the absolute palmar cortical length of the DP, and hence result in an overestimation of the true extent of DP displacement within the capsule.

Redden (1997, 1998) suggested that the vertical linear distance between the apex of the DP and the ground line may serve as a preferred alternative to Integument Depth. However the absolute value of this parameter is not only similarly compromised by rotational events, but may also be

dependent upon breed differences and variation in foot size, and is also subject to the effects of farriery differences between individuals.

Conversely Eustace (1991), and more recently Cripps and Eustace (1999a,b), have quantified the degree of DP displacement, which they refer to as 'founder distance' (D). This parameter is defined as the linear vertical distance between the proximal boundary of the extensor process of the DP, and the proximal limit of the dorsal hoof wall. Establishing DP Displacement in this manner is independent of the effects of combined rotation events, roentogenic change and farriery effects. Hence it affords distinct advantages over alternative measurement parameters.

Cripps and Eustace (1999a) concluded that this parameter was of particular diagnostic relevance, as it was uncommon to find laminitic cases with D values within normal baseline limits.

Cripps and Eustace (1999b) provided statistical evidence, derived from stepwise logistic regression analysis, which indicated that the D parameter was also of prognostic significance of treatment outcome. Individuals with a D value >14mm had a 'probability of success', that is, the probability of recovery and 'return to former performance levels', of less that 50%. Whereas Hemker (2001) reported that D values >8 mm. represented a guarded prognosis of Recovery Outcome in which the animal would return to its former performance level. It is unclear as to what accounts for the difference in D value between studies, however the significant breed differences in this parameter within the normal foot reported by Cripps and Eustace (1999a) may contribute towards this discrepancy. If this is the case, then a means of controlling for variation in either bodyweight or hoof size may represent a logical refinement to this morphometric parameter. Hemker and Hertsch (2002) also reported a direct relationship between D values and the level of post recovery lameness. The greater the D value, the greater the degree of lameness, with mean class values of approx. 6, 7, 8, and 9mm respectively.

3.1.3 MORPHOMETRIC QUANTIFICATION OF ROENTOGENIC CHANGE IN THE EQUINE FOOT

Various studies including most notably Linford (1987), Linford *et al.* (1993), Hemker and Hertsch (2002) and Glöckner (2002) have investigated roentogenic change associated with the laminitic condition. These studies have attempted to identify the specific features of roentgenic change associated with the laminitic condition, and also to assess their diagnostic and prognostic significance for the condition.

Linford (1987) stated that new bone formation on the dorsal aspect of the DP was a pathognomonic *sequela* of the developmental stage of the laminitic condition. This feature, which later researchers have colloquially referred to as a 'dorsal hump', was defined by Linford

(1987) as dorsal bone presence midway along a line constructed along the dorsal aspect of the DP from immediately distal to the extensor process to 2mm proximal to the apex of the DP. Linford (1987) and Linford *et al.* (1993) interpreted this feature as representing active bone formation in response to localised increased forces acting within the dorsal aspect of the SADP associated with laminar compromise.

Linford (1987) also reported bone remodelling at the apex of the DP to produce a 'blunted appearance' to this structure associated with laminitis. Hemker (2001), Hemker and Hertsch (2002) and Glöckner (2002) refer to this particular morphological feature as DP atrophy. This feature is marked either by non parallel alignment of the dorsal aspect of the DP with a line forming a continuation of the previous control line to its intersection with the ground, or by new bone formation dorsal to this line. These respective roentogenic features were both associated with a curved intersection between the dorsal and palmar aspects of the DP. This was in marked contrast with the characteristic angular intersection evident in the normal foot.

Various authors included (Kameya 1973, Eustace 1995 and Hood 1999a) have variably reported the presence of degenerative bone resorption and/or remodelling of the DP associated with the chronic phase of the laminitic condition. These pathological events result in the development of a degenerative morphology marked by a variable loss of normal bone structure and/or the presence of spur formation at the apex of the DP.

Hemker (2001) and Glöckner (2002) have retrospectively evaluated the prognostic significance of these roentogenic changes. These authors concluded that resorption of the DP, and 'spur' formation at the apex of the DP were statistically significant factors in associated with recovery outcome. These finding are supportive of the guarded prognosis suggested by Eustace (1995) in Type 2 chronic founder cases.

3.1.4 MORPHOMETRIC AND RROENTOGENIC CHARACTERISTICS OF THE RADIOGRAPHIC ANATOMY OF THE DONKEY FOOT, AND THE EFFECTS OF THE LAMINITIC CONDITION

Whilst baseline radiographic data is available for the horse, there is little equivalent information for the donkey foot (Bordalai and Nigam 1977, Walker *et al.* 1995). Many fundamental anatomical issues relating to the anatomy of the donkey foot still remain unresolved (Reilly 1997), and there has been a tendency to apply an equine model to the donkey (Collins *et al.* 2002). Empirical descriptive accounts however suggest that important differences in the anatomical organisation of the foot may exist between the two species (Eley 2000, Crane 2000 – Pers Com., Bell 2001 – Pers Com.), although these remain to be objectively assessed.

The work of Walker *et al.* (1995) represents the only objective study of the radiographic anatomy of the donkey foot. This preliminary study, conducted on the mammoth donkey breed (N=10), documented the radiographic anatomy of the clinically normal foot, provided a limited number of baseline measurements, and described the roentogenic character of the DP.

The lateral radiographs confirmed the following morphometric findings and features of roentogenic change: -

1. <u>In the normal foot:</u>

- The dorsal aspect of the DP was in parallel alignment with the dorsal aspect of the hoof wall.
- Integument Depth, measured at the midpoint of the dorsal aspect of the DP, was greater in the forefeet than the hind in 85% of cases.
- Integument Depth ranged from 20 – 28mm, with a mean value of ~22.5 +/- 2mm.
- The apex of the DP had a 'blunt' appearance.
- Smooth to irregularly marginated bone formation was present in the mid-dorsal aspect of the DP in 6 out of 10 cases.
- Statistically significant associations existed between Integument Depth and the occurrence of mid-dorsal new bone formation.
- New bone formation occurred in forefeet having a mean STT value of 24mm compared with a mean value of 21mm in those forefeet without bone formation.

It is not known however, whether these baseline data can be directly applied to the smaller European donkey breeds. Indeed Cripps and Eustace (1999a) have reported significant 'between breed' difference, related to bodyweight, in radiographic data for the horse.

Walker *et al.* (1995) also evaluated the radiographic anatomy of 5 laminitic cases. However these authors were unable to detect significant differences in the radiographic anatomy of the normal and laminitic foot.

2. <u>In the laminitic foot:</u>

- The apex of the DP exhibited a 'blunt' appearance.
- Mid-dorsal bone formation occurred in 9 of the 10 forefeet.
- Integument Depth for the forefeet ranged from 21 - 25mm with a mean of 23 +/-2mm.
- Bone formation occurred in 9 of 13 feet in which Integument Depth values exceeded >22mm.
- DP Rotation occurred in only one foot.

Walker *et al.* (1995) commented upon the relatively large Integument Depth value observed within this study, compared to the values previously reported for the horse by Linford (1987) and Linford *et al.* (1993). Walker *et al.* (1995) stated that this might indicate that anatomical differences exist between the two species, or alternatively, that subclinical laminitis occurs in the donkey. The occurrence of mid-dorsal bone proliferation in the donkey DP is similar to that reported by Linford (1987) for the laminitic horse. This further supports the possibility of subclinical laminitic changes within the donkey foot. In fact, Walker *et al.* (1995) stated that new bone formation was absent in both fore and hind feet with an Integument Depth value <20mm, irrespective of group allocation. Walker *et al.* (1995) concluded that additional studies were required in order to confirm these preliminary findings, and stated that these studies should be conducted in association with a gross anatomical and histological evaluation of the donkey foot.

3.1.5 INVESTIGATING THE RELATIONSHIP BETWEEN RADIOGRAPHIC ANATOMY AND BIOMECHANICAL FUNCTION

Cripps and Eustace (1999b) reported a significant association between treatment outcome and lameness grade ($P<0.001$), with the proportion of treatment failures increasing with increased lameness grade. In addition these authors reported statistically significant associations between treatment outcome and the absolute value of specific radiographic parameters. These findings indirectly support the argument that the degree of biomechanical impairment is related both to the nature, and extent of the DP dislocation.

Hence a means of quantifying the nature and extent of the pathological change is essential for accurate prognostic assessment.

It is not known however, whether the nature and extent of the anatomical change within the foot is itself the causal factor of biomechanical impairment, or whether attendant, secondary pathological events, associated with DP dislocation, are responsible.

The question therefore remains as to what specific factors are responsible for the variation in condition severity and recovery outcome. In fact Hunt (1993) commented upon these issues, and raised concerns as to the value of prognostic radiographic evaluation considered in isolation.

If DP dislocation events are indirectly related to the biomechanical impairment of the afflicted foot, then the statistical association reported by Cripps and Eustace (1999b) would suggest that DP dislocation may be related to other secondary digital pathologies that are directly responsible for the biomechanical impairment. For example, to changes within the design hierarchy of the hoof wall itself. Important inter-relationships may therefore exist between

epidermal changes, the nature and extent of changes to the radiographic anatomy of the foot, and the biomechanical capabilities of the hoof (Reilly *et al.* 1998b).

In order to investigate these hypotheses, there is a need for accurate and objective measurements that fully characterise the effects of the laminitic condition upon the radiographic anatomy of the foot. However due to the increasing number of recognised events that can occur within the laminitic foot, an escalating number of radiographic parameters have been used to document these events. This has resulted in the emergence of a complex multifactorial data matrix that makes clinical interpretation difficult (Collins and Reilly 2004b – Submitted).

Previous radiographic studies have been limited by the fact that data analysis has been based upon evaluating different anatomical *sequelae* in isolation. Although the recent application of stepwise regression analysis by Cripps and Eustace (1999b) represents progress in this direction, comprehensive data analysis has still yet to be achieved.

A means of summarising and analysing the combined effects of the distinct anatomical *sequelae* is therefore required. Multivariate statistical analysis techniques provide a means by which this requirement can be attained.

3.1.5.1 Multivariate Statistical Analysis Techniques

These powerful techniques utilise the information contained within all measured variables (Alt 1990). These techniques afford the opportunity to conduct both variable and object directed analyses. In this way, variable interaction can be investigated, and object classification and discrimination analyses performed.

An overview of the theoretical basis underpinning the multivariate testing methods employed in this chapter is given in Appendix III.

The effectiveness of these techniques are however totally dependent upon the specific measurement parameters selected (Alt 1990). Hence the initial, and critical, stage in the multivariate analysis process is the application of *a priori* knowledge to arrive at an appropriate series of variables.

3.1.5.2 Measurement Parameter Selection

On the basis of the literature review associated with this thesis, a series of linear and angular, direct and derived, measurement parameters were selected for both bivariate and multivariate statistical analysis. It is this author's assertion that these parameters serve as an appropriate basis by which the radiographic anatomy of the normal donkey foot can be characterised. In addition, these parameters enable the nature and extent of the fundamental anatomical events associated with DP dislocation to be objectively assessed, namely capsular rotation, phalangeal

rotation, DP Displacement, and combined rotation and displacement events. These variables also afford partial control against the effects of both extreme roentogenic change, and individual bodyweight variation.

The variables selected are given below. In addition, a comprehensive summary of all direct angular and linear parameters and the resultant derived parameters are summarised in Table 3.3and Table 3.4, along with their respective selection criteria.

The selected morphometric parameters of the lateral radiograph were: -

Direct Angular Parameters (See Figure 3.1)

- Angle of the Dorsal Hoof Wall - Parameter S:
  - Angle subtended b/n the dorsal aspect of the hoof wall and the ground line
- Angle of the dorsal aspect of the DP - Parameter T:
  - Angle subtended b/n the dorsal aspect of the DP and the ground line
- Angle of the central axis of the PP – Parameter U:
  - Angle subtended b/n the central axis of the PP and the ground line
- Degree of angulation of Solear aspect of DP – Parameter Sole Ang:
  - Angle subtended b/n the solear margin of the DP and the ground line

Derived Angular Parameters

- Degree of Capsular Rotation - Parameter Ang H:
  - Angular difference b/n the dorsal aspect of the hoof wall and the dorsal aspect of the DP
- Degree of Phalangeal Rotation - Parameter Ang R:
  - Angular difference b/n the dorsal aspect of the hoof wall and the central axis of the PP
- Angulation of HPA - Parameter PAxis:
  - Angular difference b/n the central axis of the PP and the dorsal aspect of the hoof wall

Direct Linear Measurement Parameters (See Figure 3.1)

- Integument Depth of the dorsal aspect of the foot at the proximal site - Parameter A:
  - Perpendicular linear distance b/n the dorsal aspect of the DP and the dorsal aspect of the hoof wall, immediately distal of the extensor process
- Integument Depth of the dorsal aspect of the foot at the proximal site - Parameter B:
  - Perpendicular linear distance b/n the dorsal aspect of the DP and the dorsal aspect of the hoof wall, immediately proximal to the DP apex

Figure 3.1 Diagrammatic Representation of the lateral radiograph to show the Direct Angular (Top) and Linear (Bottom) radiographic parameters for the donkey foot.

Parameter S:
Dorsal Hoof Wall Angle

Parameter T:
Angle of the Dorsal Aspect of the DP

Parameter U:
Angle of the Pastern Axis

Parameter Sole Angle:
Angle of Solear Aspect of the DP

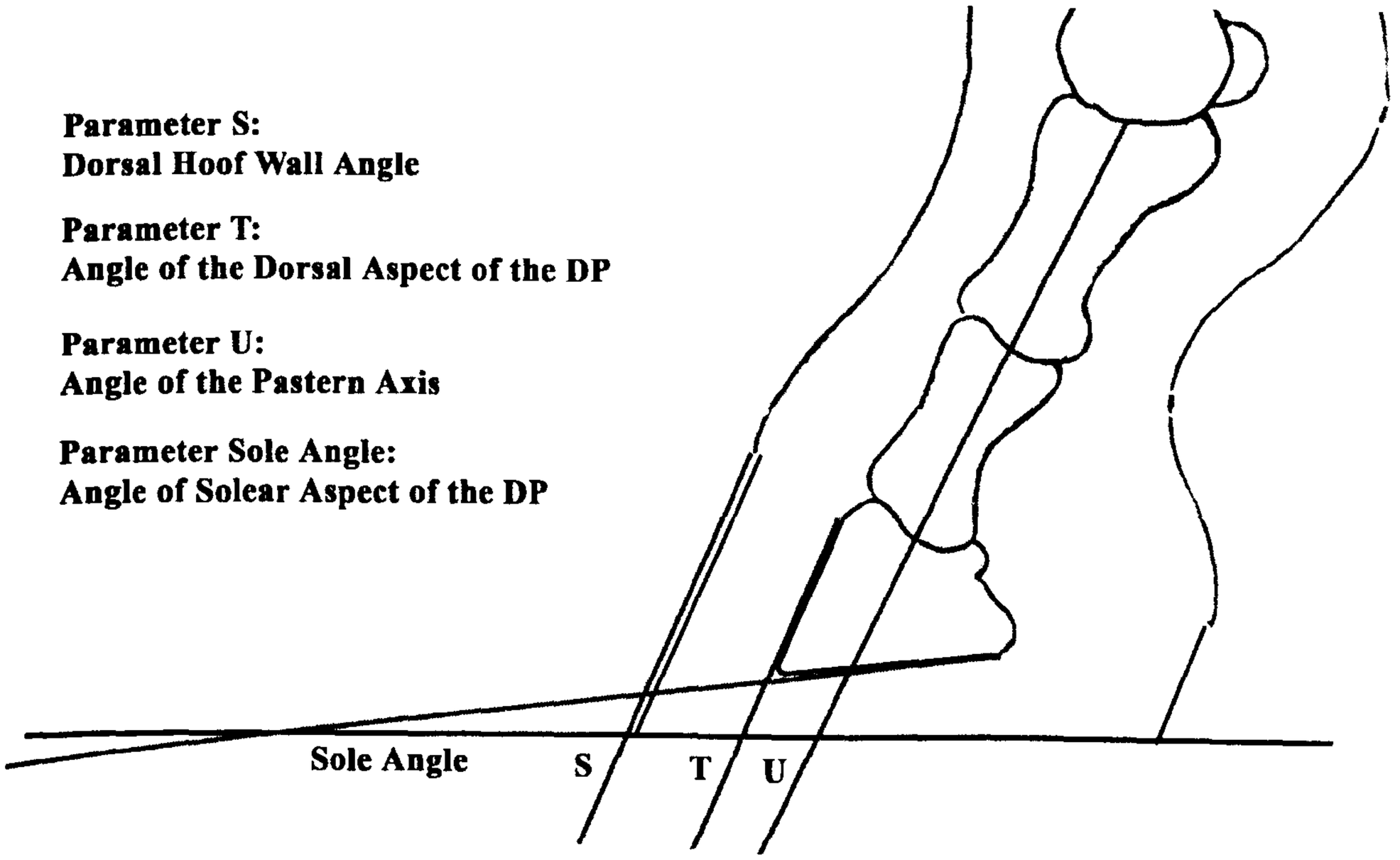

Parameter D:
Absolute Measure of DP Displacement

Parameter A:
Integument Depth Proximal Site

Parameter B:
Integument Depth Distal Site

Parameter P3:
Length of Dorsal Aspect of DP

Parameter CH:
Capsular Height

Parameter STTM:
Integument Depth Mid Dorsal Site

Parameter SD:
Sole Depth

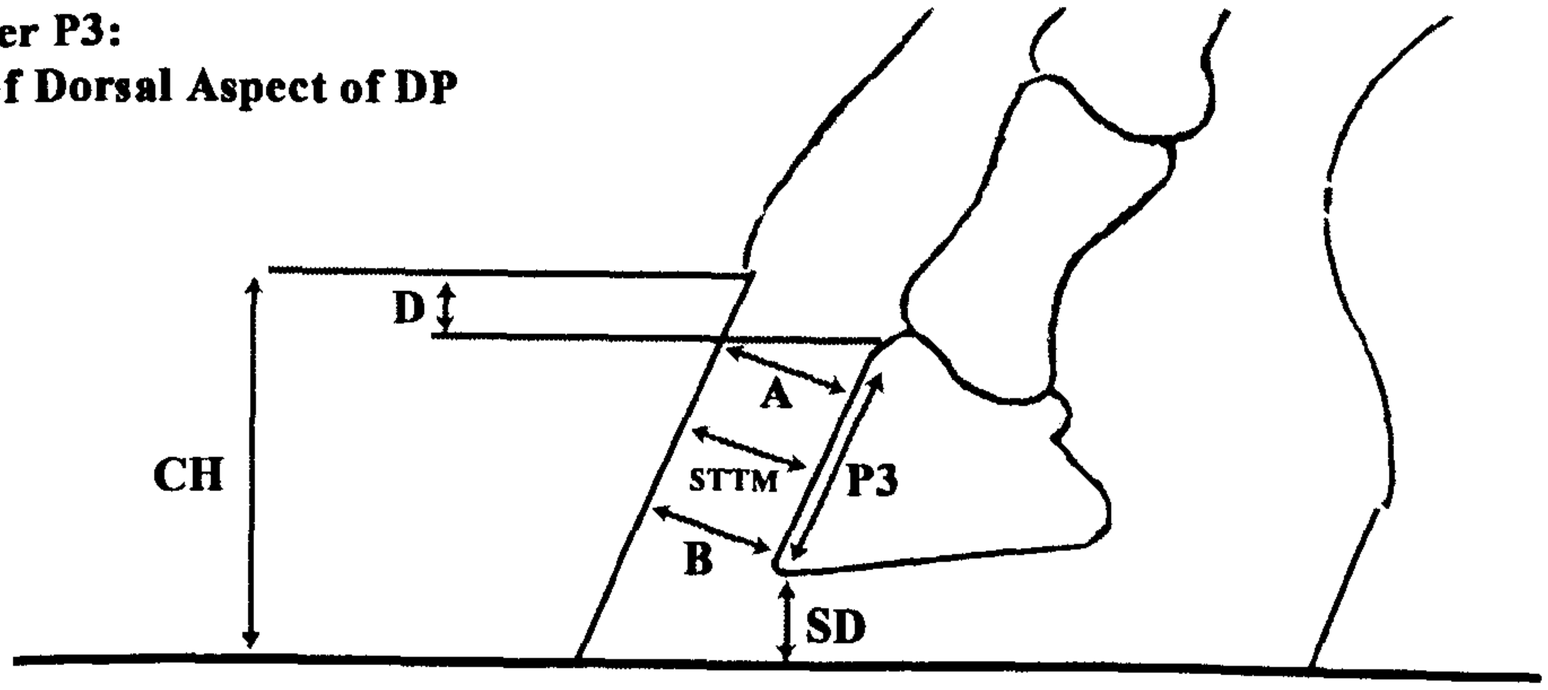

- Integument Depth of the dorsal aspect of the foot at the Mid Dorsal site - Parameter STTM:
  - Perpendicular linear distance b/n the dorsal aspect of the DP and the dorsal aspect of the hoof wall, midway between the proximal and distal measurement sites
- Absolute linear measurement of DP Displacement - Parameter D:
  - Perpendicular linear distance b/n the proximal limit of the dorsal hoof wall and the proximal margin of the extensor process

Derived Linear Measurement Parameters

- Integument Depth Ratio - Parameter A:B:
  - Ratio of the linear distances B and A
- DP Displacement as quotient of Normalised Capsular Height - Parameter D Ratio:
  - The vertical linear founder distance expressed as a quotient of normalised capsular height

3.2 RATIONAL

There is a need for additional radiographic studies in the donkey to expand our knowledge base of what represents the normal radiographic anatomy of the foot of the European donkey, and also the pathological changes associated with laminitis. It is only through achieving this realistically that progress can be made towards improving our diagnostic and prognostic techniques.

By measuring clearly defined radiographic parameters it will be possible to characterise the radiographic appearance of the donkey foot and thereby establish baseline values that represent normality. With this baseline data in place, it will be possible to investigate the effect of the laminitic condition on the anatomical organisation of the donkey foot.

In this way, the ability to detect and accurately evaluate anatomical and roentogenic change associated with laminitis in the donkey will be enhanced. This will ultimately enable the objective diagnostic assessment of the presented animal.

Table 3.3 Direct and derived Angular radiographic parameters

Parameter	Definition	Selection Criteria
S Dorsal Hoof Wall Angle	Angle subtended b/n the dorsal aspect of the hoof wall and the ground line.	Required to determine Capsular Rotation and HPA. Changes to Dorsal Hoof Wall Angle associated with laminitis (Stick *et al.* 1982.)
T Angle of the Dorsal Aspect of the Distal Phalanx (DP)	Angle subtended b/n the dorsal aspect of the DP and the ground line.	Required to determine Capsular and Phalangeal Rotation. Changes to Dorsal angle of DP associated with laminitis (Stick *et al.* 1982).
U Angle of Pastern Axis	Angle subtended b/n the central axis of the Proximal phalanx (PP) and the ground line.	Required to Establish HPA and determine Phalangeal Rotation.
Sole Angle Angle of Solear aspect of DP	Angle subtended b/n the solear margin of the DP and the ground line.	Additional indicator of rotational events. Control against effects of DP remodelling/resorption.
Ang H Degree of Capsular Rotation	Angular difference b/n the dorsal aspect of the hoof wall and the dorsal aspect of the DP. Ang H = T-S.	Primary Dislocation event. Important diagnostic and prognostic indicator (Stick *et al.* 1982, Hemker 2001, Glöckner 2002)
Ang R Degree of Phalangeal Rotation	Angular difference b/n the central axis of the PP and the dorsal aspect of the DP. Ang R = T-U.	Primary Dislocation event
P Axis Angle of the Hoof Pastern Axis	Angular difference b/n the dorsal aspect of the hoof wall and the central axis of the PP. P Axis = U-S.	Essential baseline characteristic. Required to confirm Phalangeal Rotation.

Table 3.4 Direct and derived linear radiographic parameters, and their selection criteria

Parameter	Definition	Selection Criterion
A Integument Depth at the Dorsal Aspect of the Foot – Proximal site	Perpendicular linear distance b/n dorsal aspect of the DP and the dorsal aspect of the hoof wall, immediately distal to the extensor process.	Measures combined effects of Capsular Rotation and DP Displacement. Required to determine A:B ratio.
B Integument Depth at the Dorsal Aspect of the Foot – Distal Site	Perpendicular linear distance b/n the dorsal aspect of the DP and the dorsal aspect of the hoof wall, immediately proximal to the apex of the DP.	Measures combined effects of Capsular Rotation and DP Displacement. Required to determine A:B ratio.
STTM Integument Depth at the Dorsal Aspect of the Foot – Mid Dorsal Site	Perpendicular linear distance b/n the dorsal aspect of the DP and the dorsal aspect of the hoof wall, midway b/n distal and proximal sites.	Important Diagnostic indicator of early laminitic change (Linford 1987).
CH Capsular Height	Perpendicular linear distance b/n the ground line and the proximal limit of the dorsal hoof wall.	Required to determine D Ratio.
D Absolute Measure of DP Displacement	Perpendicular linear distance b/n the proximal limit of the dorsal hoof wall and the proximal margin of the extensor process.	Absolute measure of DP Displacement. Independent of degenerative effects to DP. Important prognostic indicator of treatment outcome (Cripps and Eustace 1999b).
SD Sole Depth	Perpendicular linear distance b/n the ground line and the apex of the DP.	Required to determine Normalised Capsular Height.
P3 Linear length of Dorsal Aspect of the DP	The linear length along the dorsal aspect of the DP, from immediately distal to the extensor process to the intersection with the solear aspect of the DP. Line of best fit via 2 control points on the dorsal aspect of the DP - respectively 5mm distal of the extensor process and 10 mm proximal of the solear intersect.	Controls for variation in DP size. Control line also serves to aid identification of signs of Roentogenic Change at Mid Dorsal and Distal DP sites (Linford 1987).
A:B Integument Depth Ratio	Ratio of the linear distances B to A.	Indicator of Capsular Rotation Indicator of laminar wedge formation (Kameya 1973).
CHN(0.5) Normalised Capsular Height	Perpendicular linear distance b/n the ground line and the proximal limit of the dorsal hoof wall, normalised at an arbitrary SD of 5mm.	Required to determine D Ratio.
D Ratio DP Displacement expressed as a ratio of Normalised Capsular Height	The vertical linear founder distance expressed as a ratio of Normalised Capsular Height. D Ratio = D/CHN(0.5)	Normalised measure of DP Displacement. Controls for variation in hoof size and sole depth.

3.3 AIMS

To elucidate and objectively characterise the radiographic appearance both of the normal donkey foot in the European Donkey breed type and that which is associated with the laminitic condition in this breed type. Specifically: -

- To establish quantitative baseline data for the radiographic anatomy of the normal donkey foot
- To objectively describe the nature of the HPA in the normal donkey foot
- To determine the linear and angular characteristics of the osseous and exosseous structures of the foot
- To quantify the anatomical inter-relationship that exists between the osseous and exosseous components of the foot
- To identify the occurrence, and quantify the incidence of roentogenic change to the DP in the normal foot
- To objectively assess the anatomical organisation associated with the laminitic condition
- To identify and detail the nature and extent of any associated dislocation of the DP indicative of digital collapse
- To objectively assess the incidence of roentogenic change to the DP associated with the laminitic condition
- To identify and investigate any associations and inter-relationships between the various morphometric parameters by univariate and multivariate analysis techniques

3.4 MATERIALS AND METHODS

An initial radiographic assessment was conducted to establish baseline radiographic data of the normal donkey foot. This assessment included both morphometric and roentogenic parameters. A trial population of 19 'normal' donkeys was identified, based upon their medical history, farriery records, and the gross anatomical appearance of the hoof capsules. Normality was assumed if an animal had no previous history of disorders of the foot, and if the hoof capsule was devoid of anatomical signs consistent with an undiagnosed laminitic condition. These anatomical signs were as follows: divergent hoof growth at the heels, dorso-concavity or angulation of the hoof wall, and/or, the presence of a sunken coronary band. Lateral radiographs were then obtained from the trial population of laminitic donkeys (n=26) 24 hours prior to their scheduled euthanasia.

True lateral radiographs were obtained in accordance with the method described by Stick *et al.* (1982). This procedure was chosen because it represents the standard procedure for radiographic assessment employed by the Veterinary Centre at the Donkey Sanctuary.

3.4.1 X-RAY PROTOCOL

The feet were cleaned prior to radiography, and the hooves 'picked out' to allow normal weight bearing. A soft wire dorsal hoof wall marker of known length, measured to 1 decimal point using vernier callipers, was attached to the dorsal aspect of the hoof wall. Where appropriate, perioplic horn was removed to allow correct alignment of the dorsal hoof wall marker with the *Stratum medium*. The marker was positioned at the level of the palpable proximal margin of the hoof wall and 'moulded' to the dorsal profile of the hoof wall. This procedure allowed radiographic calibration and discrimination of the dorsal aspect of the hoof wall.

The foot was positioned on a wooden block containing a wire ground line marker in accordance with Stick *et al.* (1982). Care was taken to ensure that the limb was in a full weightbearing position, with the long axis of the metacarpal bone in perpendicular alignment to the ground line. Parks *et al.* (1999) stated that failure to achieve full weightbearing exaggerates phalangeal rotation within the foot.

A standard operating procedure for radiography was adopted, with a beam intensity of 70KV at 25mA, a 0.04 seconds exposure, and a 80cm beam object distance, with beam focus centred upon the lateral aspect of hoof capsule. A t-square was used to achieve perpendicular alignment of the radiographic plate and the foot, with the x-ray beam, thereby minimising obliquity effects. Hence, experimental error due to beam obliquity (Koblik *et al.* 1988, Tachio *et al.* 2002) could be minimised.

The resultant radiographic plates were developed, and the radiographs dried prior to scanning to disk. The Radiographs were digitised on a flatbed x-ray scanner, at a resolution of 400dpi, using a despeckle scan option. The resultant processed images were imported into a Machitosh PPC and analysed using NIH Image, Public Domain Shareware[2] (Ver 1.62).

3.4.2 DETERMINATION OF MORPHOMETRIC PARAMETERS

The scanned image was initially adjusted using the rotation function of the software program to ensure that the wire ground line marker was aligned with the horizontal (x) axis of the computer screen. The images were calibrated with respect to the wire dorsal hoof wall marker. A pixel count of the linear distance of the wire marker was determined, and used to derive the pixel count per unit length as follows: -

---

[2] National Institute of Health, Maryland, USA.

(1/known length of wire marker) * pixel count of wire marker

With this calibration factor determined, all subsequent linear measurements were automatically expressed in mm to 1 decimal place.

A two-stage measurement process was conducted to obtain linear and angular morphometric parameters.

3.4.3 STAGE 1 ANGULAR MEASUREMENTS

A series of control lines were constructed intersecting the ground as illustrated in Figure 3.1A. These were: -

1. The dorsal aspect of the hoof wall
2. The dorsal aspect of the DP (the line of best fit from the distal limit of the extensors process to 5mm proximal of the apex)
3. The central axis of the proximal phalanx
4. The palmar aspect of the DP

In this way the following parameters could be obtained: -

- Angle S = angle subtended between 1 and the ground line
- Angle T = angle subtended between 2 and the ground line
- Angle U = angle subtended between 3 and the ground line
- Solear angle = angle subtended between 3 and the ground line 4
- Angle H = T-S
- Angle R =T-U
- HPA = U-S

3.4.4 STAGE 2 LINEAR MEASUREMENTS

A series of control lines were constructed as illustrated in Figure 3.1B. These were located as followed: -

1. The proximal limit of the DHW marker in the x-direction
2. The proximal limit of the extensor process in the x-direction
3. A orthogonal line from the dorsal aspect of the DP to its intersection with the dorsal aspect of the hoof wall at: -
   A. The distal limit of the extensor process
   B. The apex of the DP
   C. Midway between the above
4. An orthogonal line, in the y-direction, from the ground line to the apical tip of the DP

Figure 3.1 Lateral radiograph of the donkey foot to show reference lines for the determination of angular and linear radiographic parameters for the donkey foot

A. Control lines, extended to their intersection with the ground line, that were used to determine direct angular radiographic parameters.

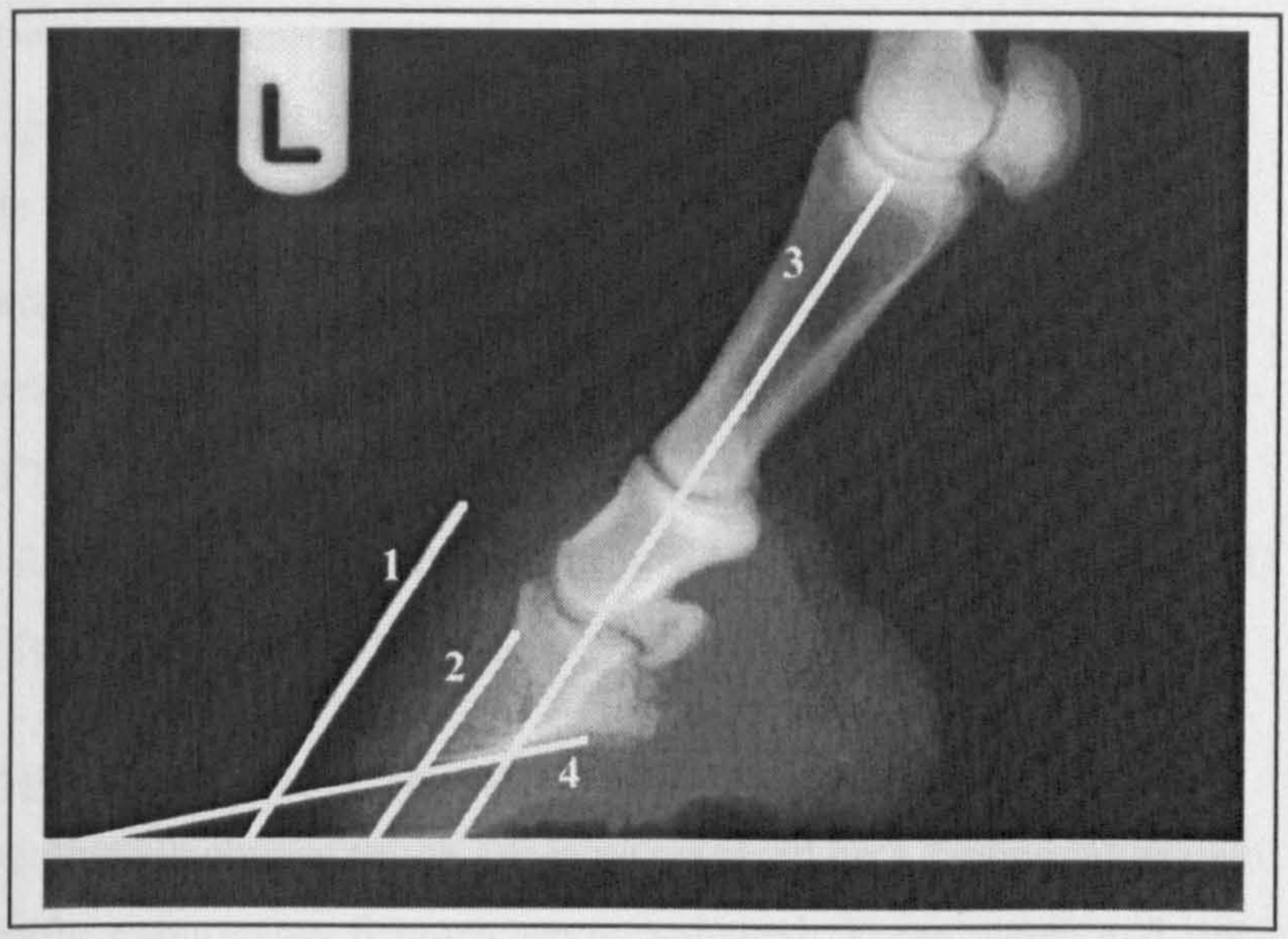

Key: **1** = Dorsal aspect of the hoof wall. **2** = Dorsal aspect of the distal phalanx (DP). **3** = central axis of the proximal phalanx (PP). **4** = Palmar aspect of the DP.

B. Control lines used to determine direct linear radiographic parameters

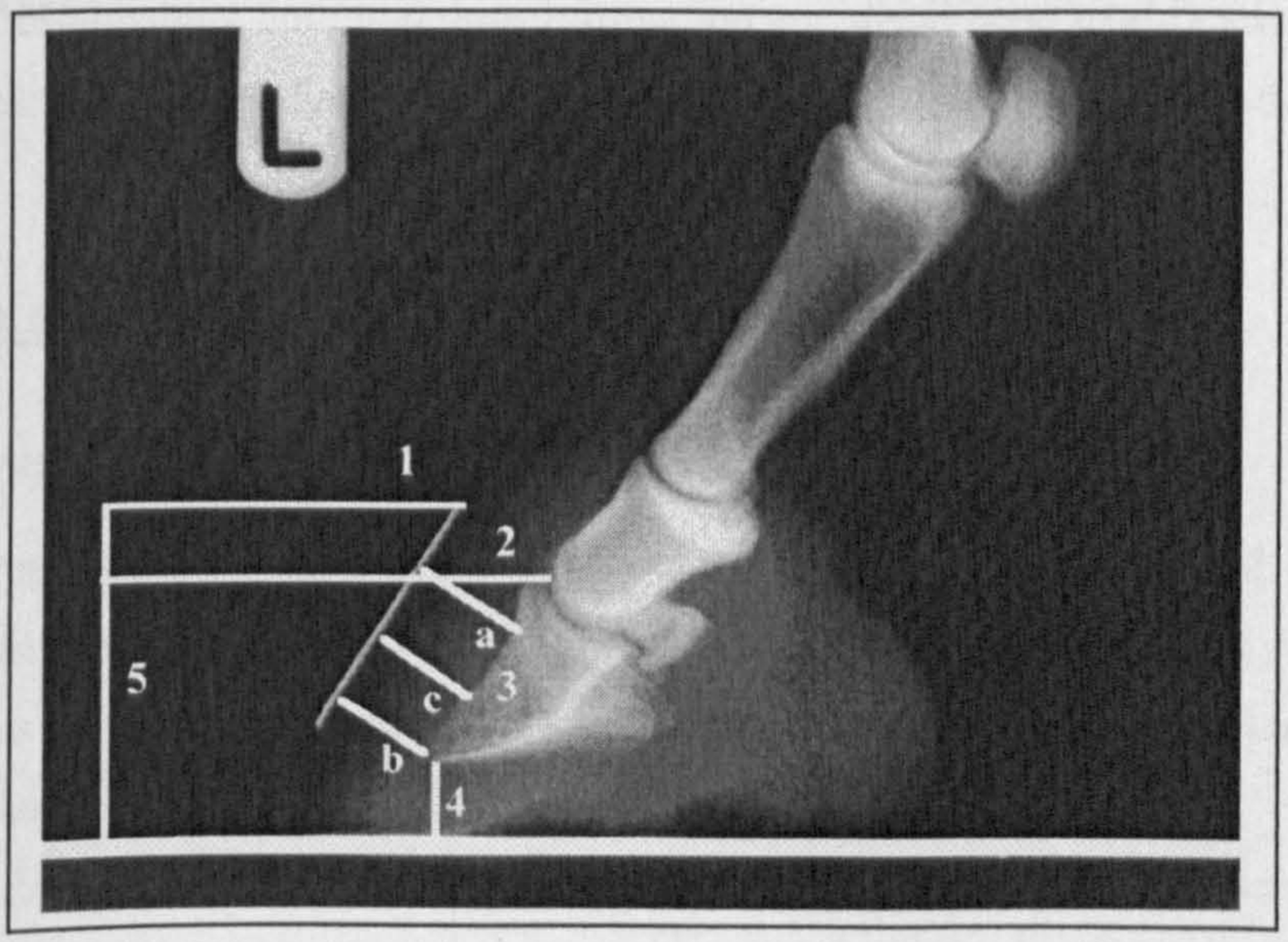

Key: **1** = Proximal limit of the DHW marker in the horizontal axis. **2** = Proximal limit of the extensor process in the horizontal axis. **3** = orthogonal line from the dorsal aspect of the DP to its intersection with the dorsal aspect of hoof wall at: **a**. The distal limit of the extensor process. **b**. The apex of the DP. **c**. Midway between a and b. **4** = Orthogonal line from the ground line to the apical tip of the DP. **5** = orthogonal line from the ground line to the proximal limit of the DHW marker.

5. A orthogonal line, in the y-direction, from the ground line to the proximal limit of the DHW marker

In this way the following parameters could be obtained: -

- D = Pixel calibrated linear distance in the y-direction from 1-2
- Capsular height = 5
- SD = Pixel calibrated linear distance 5
- Parameter A = Pixel calibrated linear distance 3A
- Parameter B = Pixel calibrated linear distance 3B
- STTM = Pixel calibrated linear distance 3C
- D Ratio = Ratio of Parameter D: Capsular height (normalised to a SD of 5mm)
- A:B Ratio = Ratio of Parameter 3A:3B

3.4.5 ROENTOGENIC CHANGE IN THE DISTAL PHALANX

Sign of roentogenic change to the DP were assessed on a binominal basis of present or absent. Three specific roentogenic features were evaluated. These were, mid dorsal bone formation, distal bone modification and distal spur formation and/or bone resorption. These roentogenic features are illustrated in Figure 3.2. The assessment approach was adapted after Linford (1987). The control line constructed along the dorsal aspect of the DP - see Section 3.4.3 served as a means of establishing both mid dorsal formation and distal bone modification. Distal resorption was based upon subjective visual assessment of degenerative change by the author in a blind fashion.

3.5 STATISTICAL ANALYSIS

3.5.1 UNIVARIATE STATISTICAL ANALYSIS

Nonparametric statistical testing was conducted on all restricted data and on continuous data that displayed a non-normal distribution. Parametric statistical testing was only used on continuous data that displayed normal distribution. Normality was assessed using the Anderson-Darling Normality test at an alpha level of 0.05.

Where data was both continuous and normally distributed, either parametric 2-sample t-tests were used, or in the case of multiple comparisons, one-way analysis of variance.

The significance of the respective group incidence of roentogenic change features was evaluated in respect of each roentogenic feature (class) by Chi 2x2 test of association.

In all cases 2 tailed test conditions were adopted, at a 5% significance level.

Hence the null hypotheses under these test conditions were:

H^o – There is no statistical difference between groups (A=B)

Set against the alternative hypotheses:

H^i – there is a statistical difference between groups (A≠B)

Wherever possible this thesis will restrict comment to the appropriate statistical descriptor. That is, to refer to mean values (+/- sd) in the case of continuous, and/or normally distributed data, and to report median values (IQ ranges) when data in either non-normal or restricted. Comparisons with previously reported data however, occasionally necessitate the use of inappropriate statistical descriptors as a matter of last resort. Hence summary tables may includes both parameter means (+/- sd), medians (with inter quartile range) and min-max ranges.

3.5.2 MULTIVARIATE STATISTICAL ANALYSIS

The data matrix was analysed using three different multivariate techniques. In order to take into account the different metrics of measurements evident in selected radiographic parameters, analysis was conducted using the correlation matrix. This in effect auto-scales each variable to produce a situation of unit variance. In this way, differences in measurement units would not influence the final statistical solution.

An initial analysis was performed using the variable-directed Principle Component Analysis technique (PCA). This variable-directed technique investigates the combined effect, and interactions, between all selected variables. This method seeks to simplify the data by producing new orthogonal axes or principle components (PCs) that maximise the variance within the data matrix. In addition, the respective contribution of each variable, to each of the resultant PCs is calculated. As the number of selected variables was relatively small in comparison with the number of objects (donkeys), the matrix was analysed using a single value decomposition algorithm.

A subsequent object–directed analysis was conducted in order to explore potential object grouping within the data, using the agglomerative classification technique of Hierarchical Clustering. This was performed using a Complete linkage rule, and a Squared Euclidean distance metric.

A final calibration and validation exercise was undertaken by Regularised Discriminative Analysis (RDA). This technique produces a mathematical classification rule, and also assesses the theoretical modelling capabilities of this classification rule. In this way, the recognition and prediction potential of the proposed model can be investigated.

Figure 3.2 Radiographs to illustrate roentogenic change to the distal phalanx.

A Mid dorsal bone formation

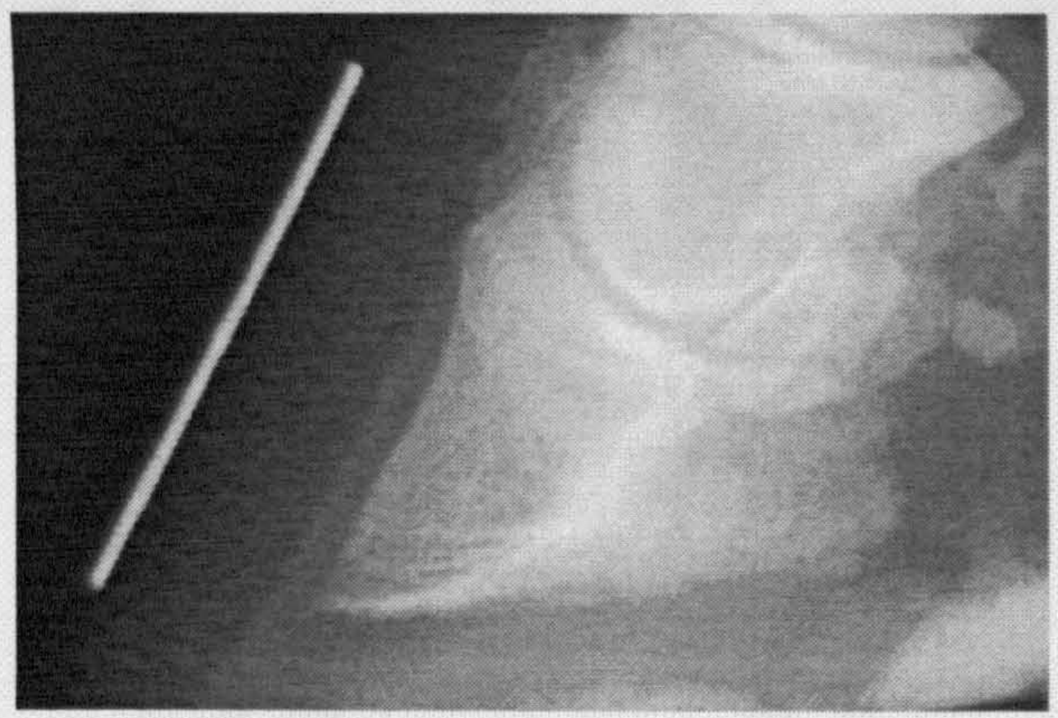

B Distal bone modification

C Spur bone formation

D Distal bone resorption

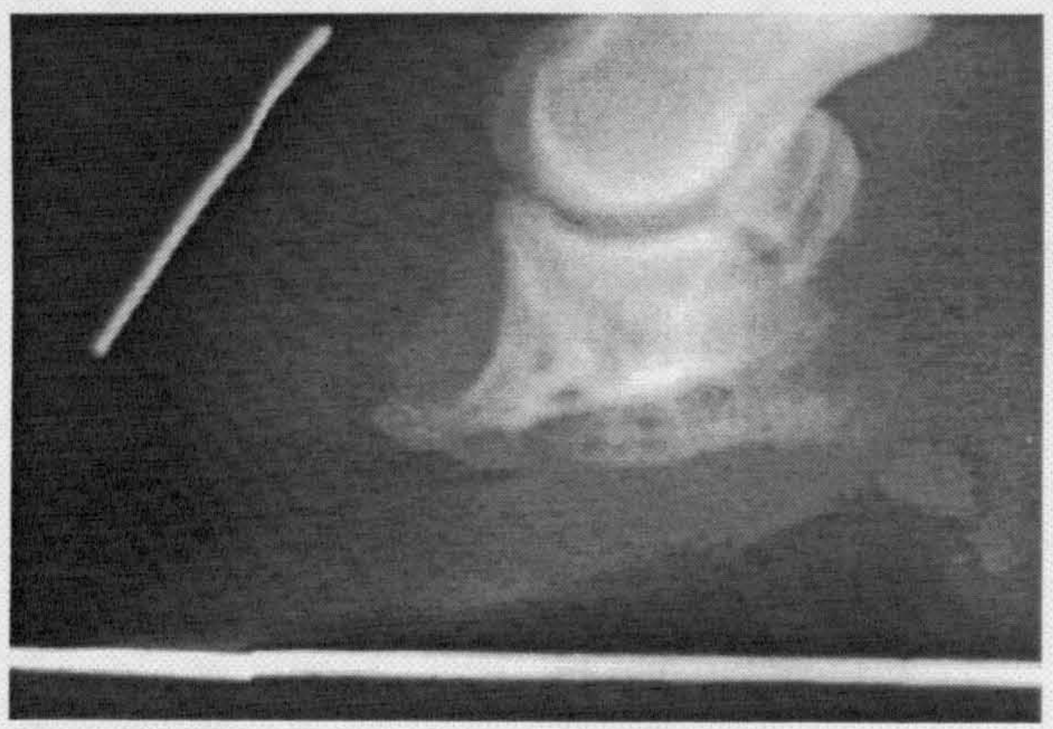

This analysis was performed in an unbiased and a 'weighted' modelling scenario, at unit loss function and an arbitrary loss function of 10 respectively. The 'weighted' modelling scenario guards against Type 2 statistical errors. This is of particular clinical significance in respect of the laminitic condition, where false 'positive' misclassifications are more favourable than false 'negatives'.

3.6 RESULTS

3.6.1 RADIOGRAPHIC ANATOMY OF THE NORMAL DONKEY FOOT

The radiographic anatomy of the foot of the normal donkey group is summarised in Table 3.5, along with corresponding data for the pony previously reported by Cripps and Eustace (1999a). Pony data has been included for comparative purposes as this equid approximates to the donkey both in its size and bodyweight.

The dorsal hoof wall angle (Parameter S) of the normal donkey group ranged from 40° to 74° with a median value of 60° (56.25 –63.75). The angle of the dorsal aspect of the DP (Parameter U) was in near parallel alignment with the hoof wall with a median of 62°.

The mean linear distances between the dorsal aspect of the DP and the dorsal hoof wall at the proximal, mid and distal measurement sites were 17.48 (+/-2.273), 17.28 (+/-3.157), and 17.48 (+/-2.649) mm respectively

The parallelism between these anatomical features was reflected in a median capsular rotation angle (Parameter Ang H) of 1.0° (-1.0 -1.8), and a median Integument Depth ratio (Parameter A:B) of unity (0.94-1.06). These values corresponded with a solear angle which ranged from 5.0 to 20.0 degrees, with a group median of 11.0 (10-16) degrees.

The phalangeal rotational angle (Parameter Ang R) ranged from –16 to 16 with a median value of 1.0 (-0.75-4.0) degree, and a corresponding HPA median of 1.0 (-275-5.0). The Degree of DP displacement within the capsule ranged from 5 to 21mm, with a mean of 12.3(+/-4.26), and a median D ratio value of 0.26 (0.1925-0.2975).

Comparison with the pony data revealed a broadly similar anatomical organisation. However distinct 'between species' differences were apparent in the finer anatomical detail. Mean values indicated that the donkey hoof was more upright by ~7°, as measured by the dorsal hoof wall angle (S). The angulation of the dorsal aspect of the DP (T), and the phalangeal axis (U) were also greater in the donkey. There was minimal phalangeal rotation (Ang R) within the donkey foot, unlike the pony. Integument depth, measured at the mid-point of the DP (STTM) was 4mm greater in the donkey, and represented a ~30% difference. The degree of DP displacement

differed considerably with a mean D value for the donkey at ~13mm compared with ~3mm for the pony.

Table 3.5 Summary table of the radiographic parameters of the normal donkey foot.

	Normal Donkey Group (n=19)			**Pony (n=7)** From Cripps and Eustace (1999a)
Angular Parameters (degrees)				
Parameter	**Mean (+/- sd)**	**Median (IQ Range)**	**Range Min-Max**	**Mean (+/- sd) Median Range Min-Max**
S	60.58 (5.621)	60.00 (56.25-63.75)	53.00-71.00	53.6 (7.92) 50.5 45-67
T	60.89 (5.141)	62.00 (56.75-65.50)	52.00-68.00	53.0 (7.13) 51.5 45-66
U	59.32 (6.237)	58.00 (55.50-62.75)	48.00-71.00	45.1 (4.98) 46.0 37-52
Solear Angle	11.11 (3.635)	11.00 (8.25-13.75)	5.00-20.00	N/A
Ang H	0.3158 (3.560)	-1.000 (-1.000-1.750)	-5.000-9.000	-0.6 (1.84) -0.1 -3-3
Ang R	1.579 (6.907)	1.000 (-0.75-4.00)	-16.00-16.00	7.9 (5.8) 8.5 0-18.0
P Axis	1.263 (8.61)	1.000 (-2.75-5.00)	-17.00-21.00	N/A
Linear Parameters (mm)				
Parameter	**Mean (+/- sd)**	**Median (IQ Range)**	**Range Min-Max**	**Mean (+/- sd) Median Range Min-Max**
A	17.48 (2.272)	16.60 (16.15-19.15)	13.40-22.60	N/A
B	17.48 (3.157)	16.60 (15.18-19.15)	13.40-24.50	N/A
STTM	17.28 (2.649)	16.60 (15.30-18.92)	13.40-22.60	13.2 (1.93) 12.3 11.1-16.1
D	12.32 (4.260)	12.70 (9.100-14.20)	5.700-21.00	3.1 (2.21) 2.9 0-6.3
P3	24.20 (2.33)	25.50 (23.23-25.80)	18.00-26.60	N/A
A:B*	0.995 (0.075)	1.000 (0.940-1.060)	0.880-1.100	N/A
D Ratio*	0.253 (0.074)	0.260 (0.194-0.298)	0.130-0.370	N/A

* Denotes Unit-less Parameter

Note: An explanation for each radiographic parameter is given in Table 3.3and Table 3.4.

3.6.2 THE RADIOGRAPHIC ANATOMY OF THE LAMINITIC DONKEY FOOT

Table 3.6 summarises the radiographic features of the Laminitic Group. Considerable variation was evident in all radiographic parameters, indicating differences in anatomical presentation. Dorsal hoof wall angles displayed a greater, min – max range than that recorded in the normal group ranging from 40 to 74 with a median of 65 (55-67) degrees. Whereas Parameter T values ranged from 55 to 91 degrees with a median of 70(66.0-76.0) degrees, the corresponding solear angles ranged from 7.0 to 27.0 with a median of 13.5 (10-16).

Table 3.6 Summary table of the direct and derived, angular and linear radiographic parameters of the laminitic donkey foot

Laminitic Donkey Group (n=26)			
Angular Parameters (degrees)			
Parameter	**Mean (+/- sd)**	**Median (IQ Range)**	**Range Min-Max**
S	61.69 (8.615)	65.00 (55.00-67.00)	40.00-74.00
T	71.58 (8.963)	70.00 (66.00-76.00)	55.00-91.00
U	58.23 (9.668)	56.50 (52.00-64.00)	40.00-84.00
Solear Angle	14.00 (5.614)	13.50 (10.00-16.00)	7.000-27.00
Ang H	9.885 (13.54)	4.50 (-1.000-20.00)	-6.000-39.00
Ang R	13.35 (11.22)	13.00 (6.000-19.00)	-14.00-38.00
P Axis	3.462 (16.32)	5.000 (-2.000-13.00)	-44.00-31.00
Linear Parameters (mm)			
Parameter	**Mean (+/- sd)**	**Median (IQ Range)**	**Range Min-Max**
A	18.70 (4.504)	17.75 (15.60-21.40)	12.70-29.20
B	21.28 (6.305)	19.45 (17.00-22.80)	13.60-35.00
STTM	19.83 (5.028)	17.95 (16.60-21.90)	12.90-31.20
D	12.45 (4.768)	11.45 (8.800-15.70)	4.900-24.40
P3	21.55 (3.975)	21.80 (23.23-25.80)	14.60-28.40
A:B*	1.132 (0.1384)	1.120 (1.030-1.210)	0.8900-1.440
D Ratio*	0.2623 (0.08487)	0.2450 (0.190-0.330)	0.1200-0.4300

* Denotes Unit-less Parameter
Note: An explanation for each radiographic parameter is given in Table 3.3 and Table 3.4.

The mean Integument Depth values at the proximal, mid and distal measurement sites were 18.7(+/-4.50), 19.83(+/-5.028), and 21.28 (+/-6.305) mm respectively, and the corresponding A:B ratio ranged from 0.89 to 1.440 with a median of 1.12 (1.030 –1.210) mm.

Median Ang H, and Ang R and P axis values, along with the mean A:B ratio confirmed the presence of combined capsular and phalangeal rotation events, and a 'broken' HPA. The median HPA within the laminitic group was 5 degrees. Capsular rotation values which ranged from –6.0 to 39.0 with a median of 4.50 (-1.0 - 20.0) degrees.

Phalangeal rotation angles also showed considerable variation ranging from –14.0 to 38.0 degrees with a group median of 13.0 (6.0-19.0) degrees. DP displacement within the group ranged from 4.9 to 24 mm with a mean of 12.45 (+/- 1) mm, and a corresponding median D ratio of 0.24.5 (0.19-0.43). Mean D and D ratio values were, however, similar to the Normal Group, indicating that DP displacement was not a predominant characteristic of laminitis.

3.6.3 BETWEEN GROUP COMPARISON OF THE RADIOGRAPHIC ANATOMY OF THE DONKEY FOOT

3.6.3.1 ANGULAR RADIOGRAPHIC PARAMETERS

Between group comparisons revealed significant differences ($P<0.05$) at a 95% confidence level between group medians in respect of the angular parameters T ($P=0.0000$), Ang H ($P=0.0139$), and Ang R ($P=0.0001$) – see Figure 3.3, Figure 3.4 and Figure 3.5 respectively. All other angular comparisons between group medians were not statistically significant ($P>0.05$).

3.6.3.2 LINEAR RADIOGRAPHIC PARAMETERS

Statistically significant between groups differences were established in parameter STTM ($P=0.034$), B ($P=0.012$), the A:B ratio ($P= 0.008$) see Figure 3.6 and Figure 3.7, and also P3 ($P=0.0107$). All other between group linear comparisons were not statistically significant ($P>0.05$).

3.6.4 ROENTOGENIC CHANGE IN THE DISTAL PHALANX OF THE DONKEY FOOT

The incidence of the three classes of roentogenic change in the DP are presented by group association in Table 3.7.

Figure 3.3 Box plot showing 'between group' comparisons in Parameter T

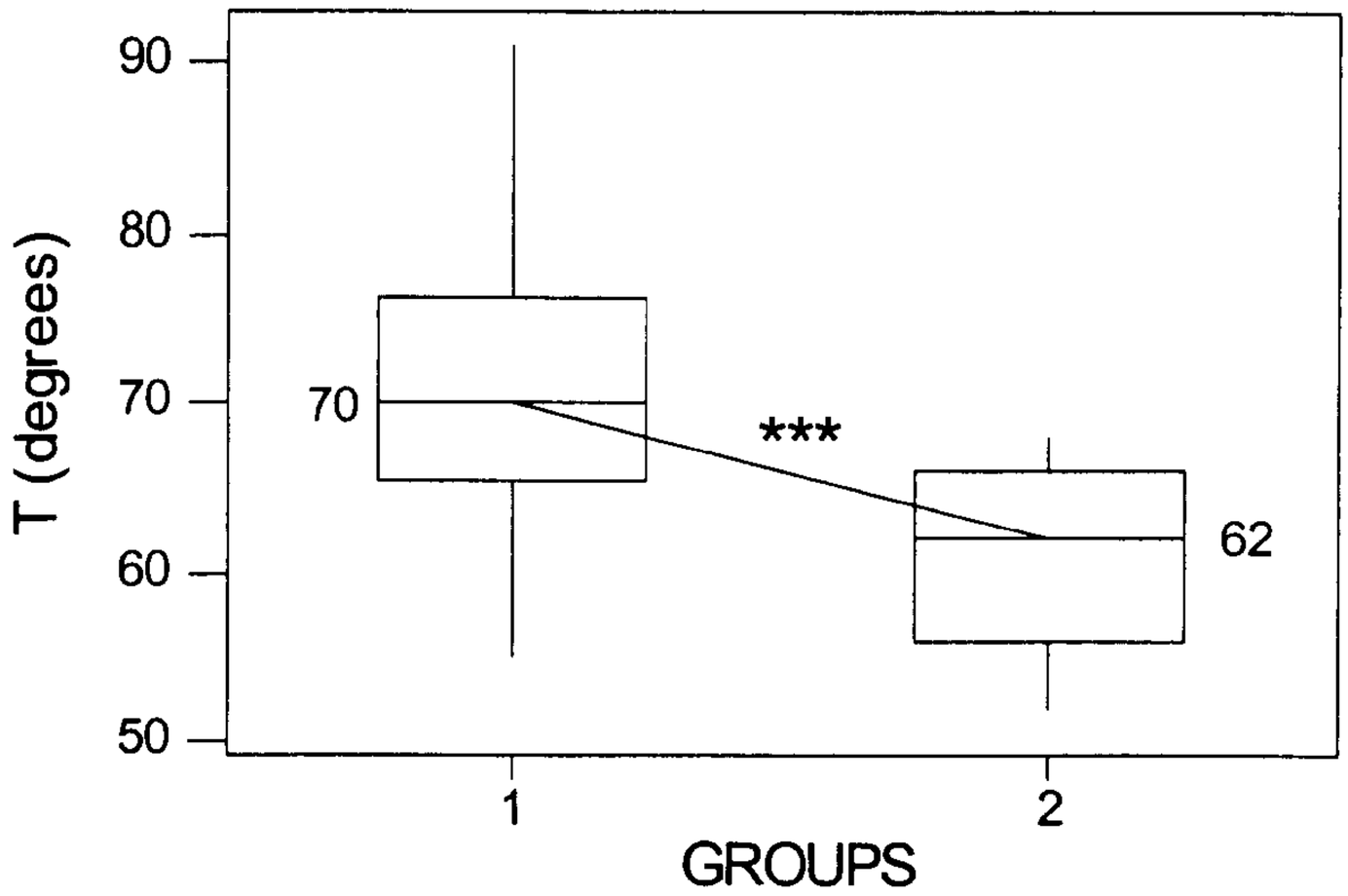

Key: Group 1 = Laminitic Group. Group 2 = Normal Group

Figure 3.4 Box plot showing 'between group' comparisons in Parameter Ang H

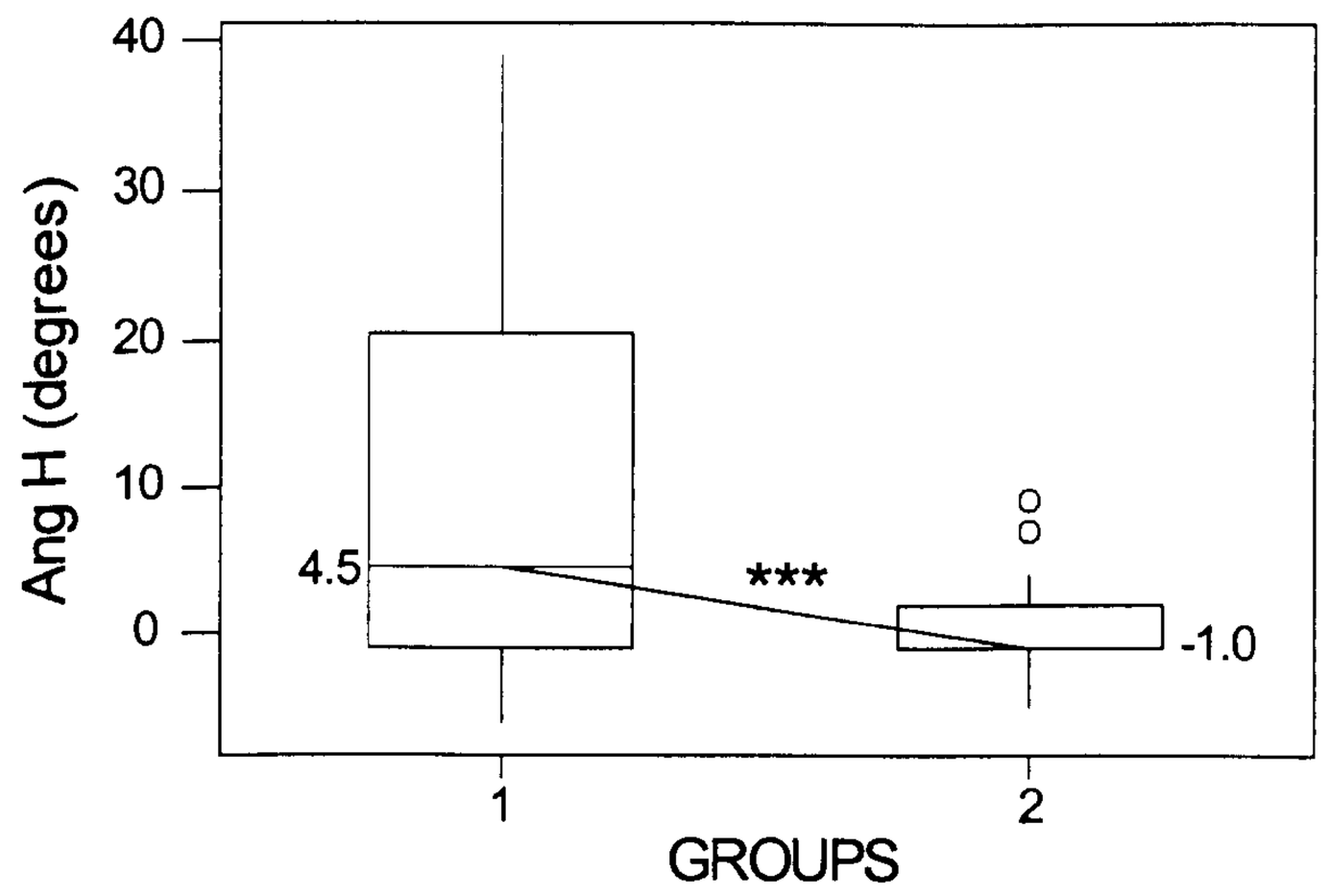

Key: Group 1 = Laminitic Group. Group 2 = Normal Group

Figure 3.5 Box plot showing 'between group' comparisons in Parameter Ang R

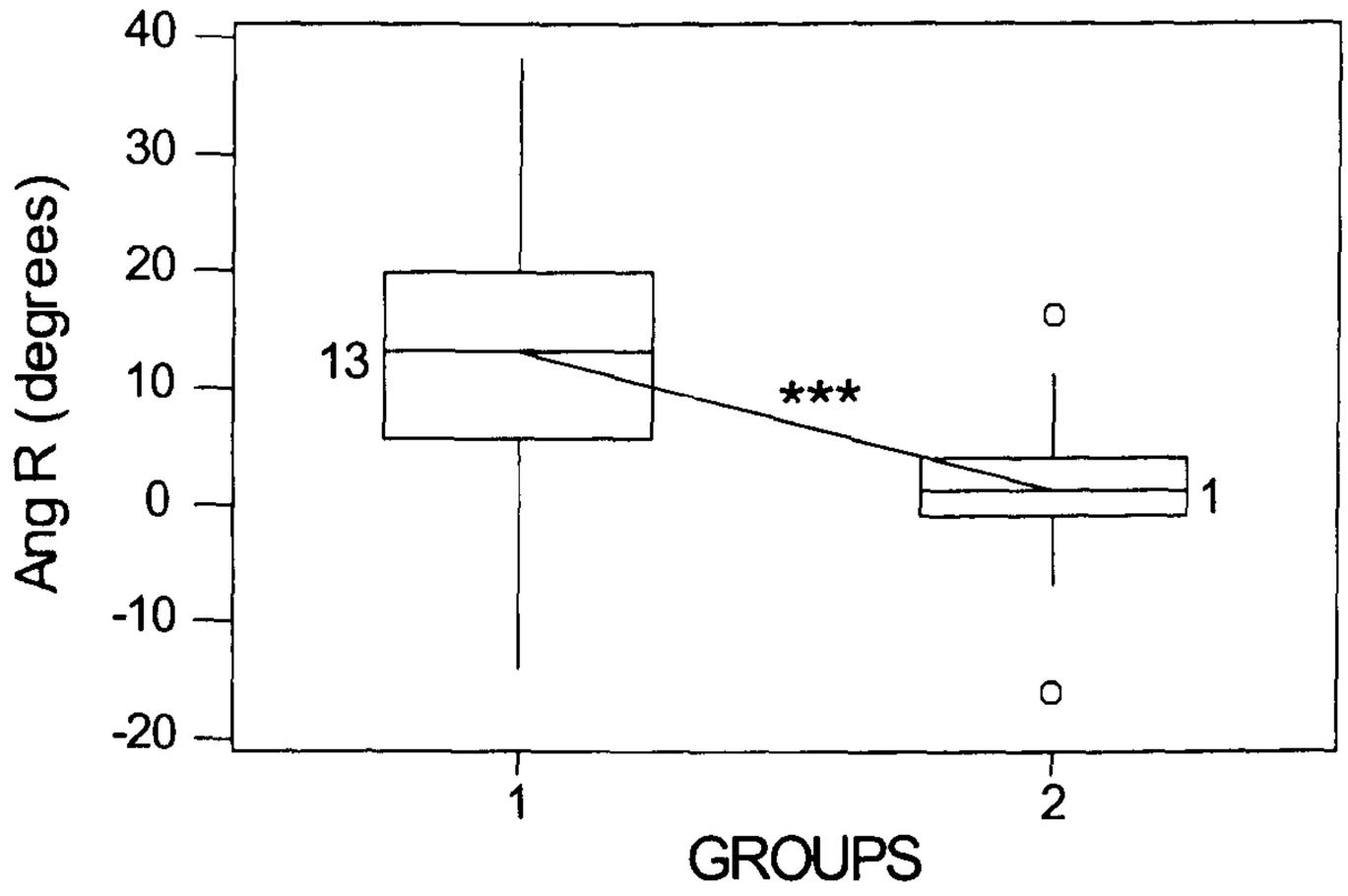

Key: Group 1 = Laminitic Group. Group 2 = Normal Group

Figure 3.6 Box plot showing 'between group' comparisons in Parameter A:B Ratio

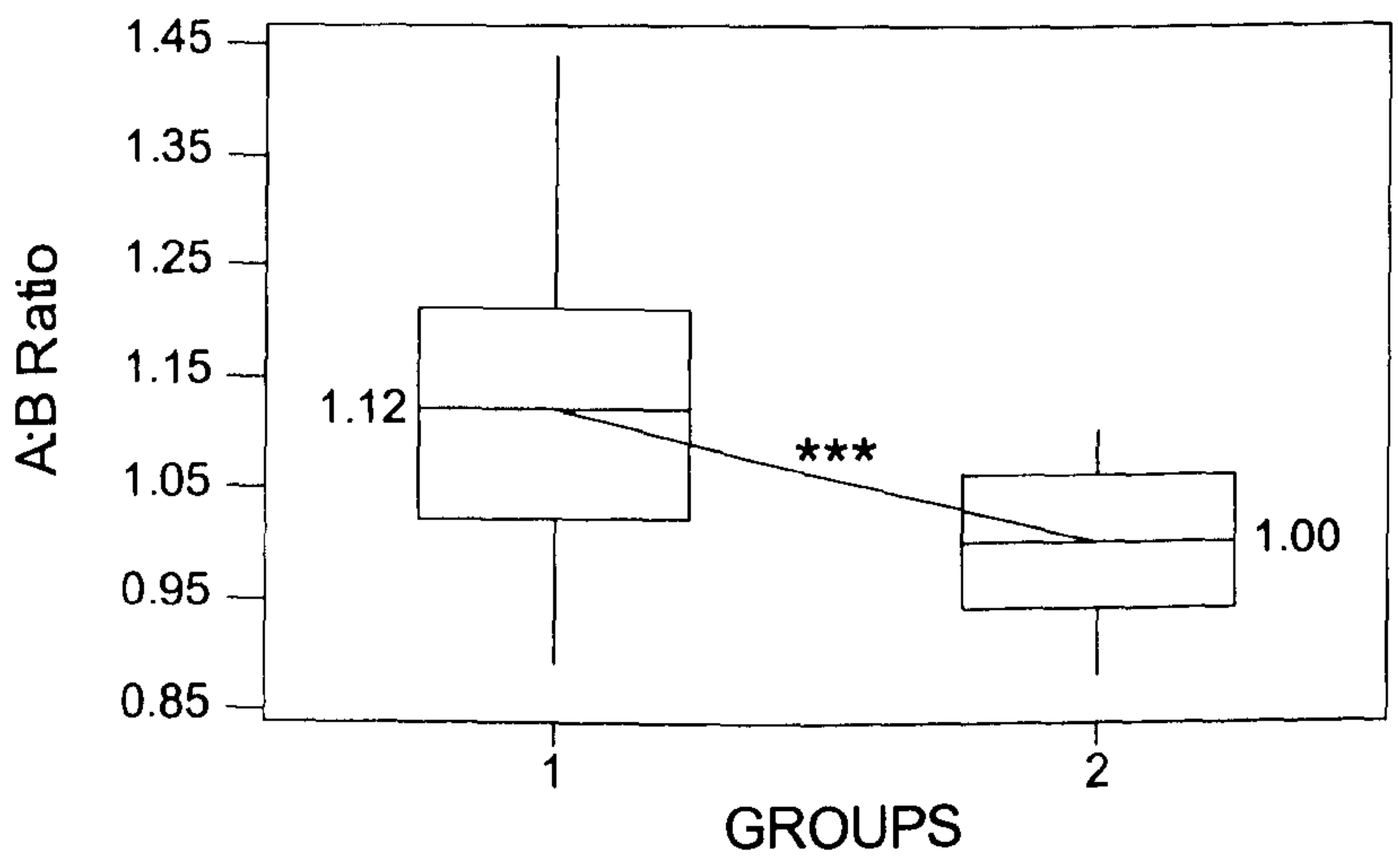

Key: Group 1 = Laminitic Group. Group 2 = Normal Group

Figure 3.7 Histogram showing 'between group' comparisons in Parameters A, STTM and B

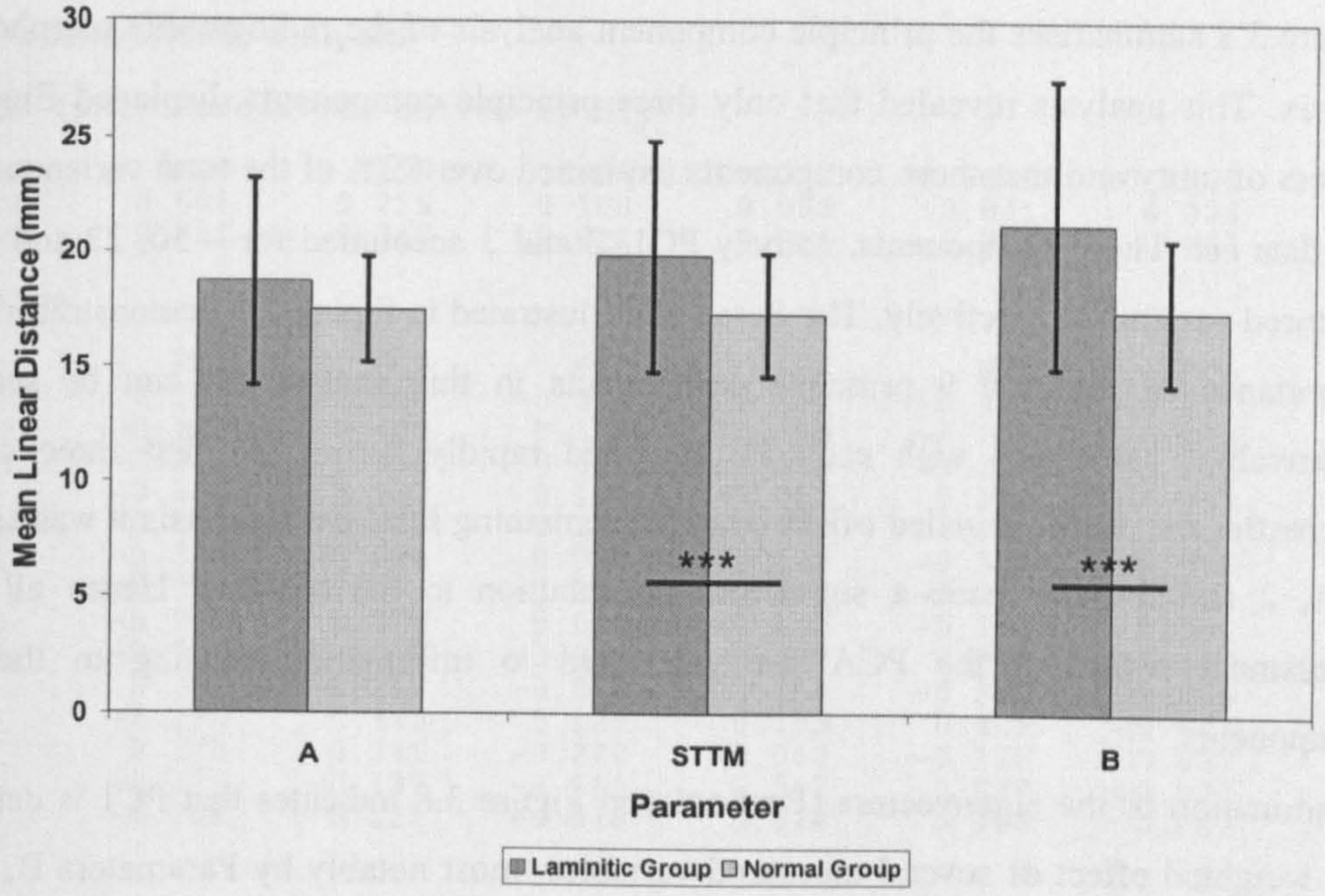

Table 3.7 Summary table of Roentogenic change

Roentogen Change	Laminitic Group (n=26)		Normal Group (n=19)	
	Present	Absent	Present	Absent
Mid dorsal bone formation	**9**	**17**	**5**	**14**
Distal bone formation	**5**	**21**	**11**	**8**
Distal resorption / spur formation	**14**	**12**	**0**	**19**

All three measured classes of roentogenic change were observed within the laminitic group. However only mid dorsal bone formation and distal bone modification were recorded in the normal group.

3.6.5 BETWEEN GROUP COMPARISONS OF THE INCIDENCE OF ROENTOGENIC CHANGE IN THE DISTAL PHALANX

There were significant differences ($P<0.05$) in the incidence of distal bone modification and distal spur formation and resorption between the normal and laminitic groups.

3.6.6 MULTIVRIATE ANALYSIS

3.6.6.1 PRINCIPLE COMPONENT ANALYSIS

Figure 3.8 summarises the principle component analysis of the radiographic morphometry data matrix. This analysis revealed that only three principle components displayed Eigenvalues in excess of unity and that these components explained over 82% of the total variance captured in the data set. These components, namely PC1, 2 and 3 accounted for ~ 50, 22 and 11% of the captured variance respectively. The Scree plot illustrated in Figure 3.9 demonstrates the relative importance of the first 9 principle components in this analysis. It can be seen that the Eigenvalues associated with each PC declined rapidly across the first three components. Thereafter the profile levelled off through the remaining PCs. On this basis it was assumed that PC1, 2 and 3 only made a significant contribution to the analysis. Hence all other data assessment regarding the PCA was restricted to information relating to these specific components.

Examination of the eigenvectors (PcaLoa's) in Figure 3.8 indicates that PC1 is determined by the weighted effect of several measured variables, most notably by Parameters B, Ang H and STTM and A (eigenvectors <- 3.5) balanced against the opposing effect of Parameters P3, P axis and Ang S (eigen vectors >2.5). Conversely, PC2 is dominated by the weighted average of Parameters Ang R and T (eigenvectors >4.0) balanced primarily by the influence of Parameter U. The final component, PC3, is significantly influenced by the weighted average of Parameters D and D Ratio (eigenvectors <-0.5) balanced against the effects of Parameters U and A:B (eigenvectors >0.2).

Figure 3.8 Summary of PCA analysis to show Eigenvalues and Eigenvectors for the first 6 principle components of variance

Principal Component Analysis

Calculated from Correlation Matrix by SVD

Eigenvalue	7.0208	3.0195	1.4675	0.8207	0.5681	0.4633
Proportion	0.501	0.216	0.105	0.059	0.041	0.033
Cumulative	0.501	0.717	0.822	0.881	0.921	0.954

Eigenvectors

Variable	PC1	PC2	PC3	PC4	PC5	PC6
S	0.253	0.300	-0.058	0.311	-0.490	-0.211
T amend	-0.233	0.409	0.127	0.168	-0.215	-0.104
U	-0.218	-0.286	0.386	0.378	-0.234	-0.248
Ang H AM	-0.350	0.133	0.139	-0.067	0.144	0.053
Ang R AM	-0.030	0.548	-0.183	-0.143	-0.003	0.099
STTM	-0.326	-0.034	-0.098	-0.190	-0.508	-0.000
A	-0.324	-0.079	-0.128	-0.413	-0.237	-0.229
B	-0.365	0.024	0.010	-0.142	-0.191	0.086
A:B	-0.252	0.202	0.219	0.397	0.000	0.659
P3	0.280	-0.162	-0.024	0.264	-0.285	-0.056
Sole Ang	-0.195	0.342	0.127	0.193	0.405	-0.604
P Axis	0.273	0.341	-0.270	-0.062	-0.125	0.037
D	-0.227	-0.139	-0.561	0.367	0.027	-0.073
D Ratio	-0.246	-0.121	-0.548	0.278	0.158	0.041

Figure 3.9 Scree plot showing Eigenvalues for the first 9 Principal Components

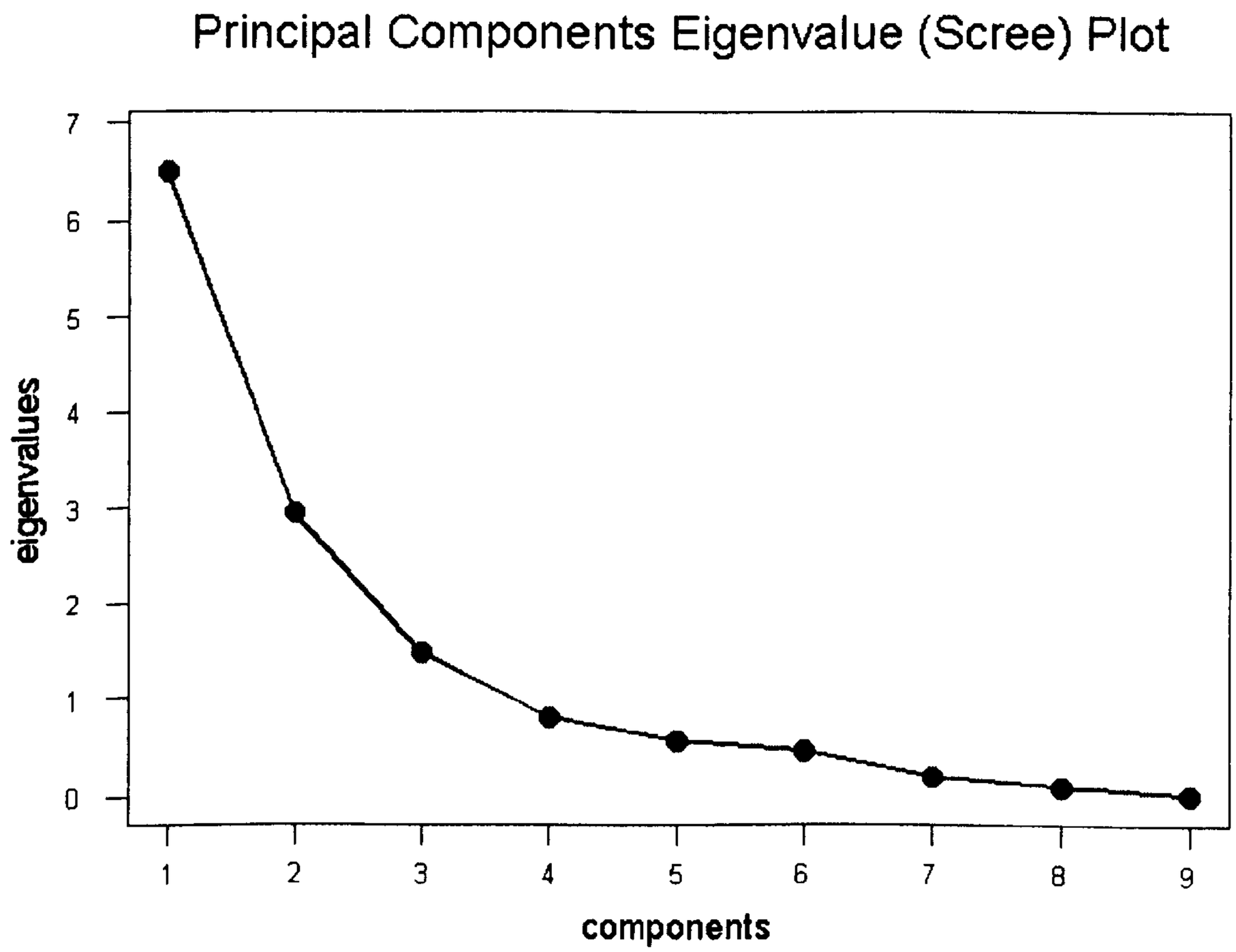

PCA Loading Plot

The loading plot for PC1 Vs PC2 (see Figure 3.10) graphically depicts the vectorial characteristics of the measured variables, and their respective interactions in the plane of maximum variance. The absolute size of each vector reflects its relative contribution, or importance, within the plane of variance, whilst its orientation reflects its relative contribution to each PC. Collectively, the size and orientation indicate both the direction and magnitude of its effect within the plane of variance. The spatial disposition of the vectors illustrates their weighted interaction, and hence demonstrates their combined effect with regard to object separation.

PCA Score Plot

The score plot of PC1 Vs PC2 illustrates the spatial distribution of the trial animals in respect of the plane of maximum variance (See Figure 3.11). The respective location of each individual reflects the combined vectorial effect of the measured parameters within that animal. It can be observed that the normal population appears in a relatively tightly bound cohesive group. This indicates a degree of similarity in the anatomic organisation of the normal foot, as defined by the selected parameters.

Conversely the distribution of the laminitic group is varied and more widespread. In this regard, the laminitic group is separated from the majority of the normal animals both in respect of PC1 and PC2. However certain laminitic individuals appear to be influenced predominantly by effects in the direction of PC1, whereas others appear to be separated from the normal group in the direction of PC2 only. This suggests not only that the radiographic appearance of the laminitic foot differs from that seen in the normal foot, but also that considerable variation exists in the nature and extent of these differences.

This apparent variation in the radiographic anatomy of the foot within the laminitic group suggests that further sub-division, based upon these anatomical differences, may be appropriate in order to investigate further the effects of the laminitic condition.

Figure 3.10 Parameter Loading Plot for the first two Principle Components of variance.

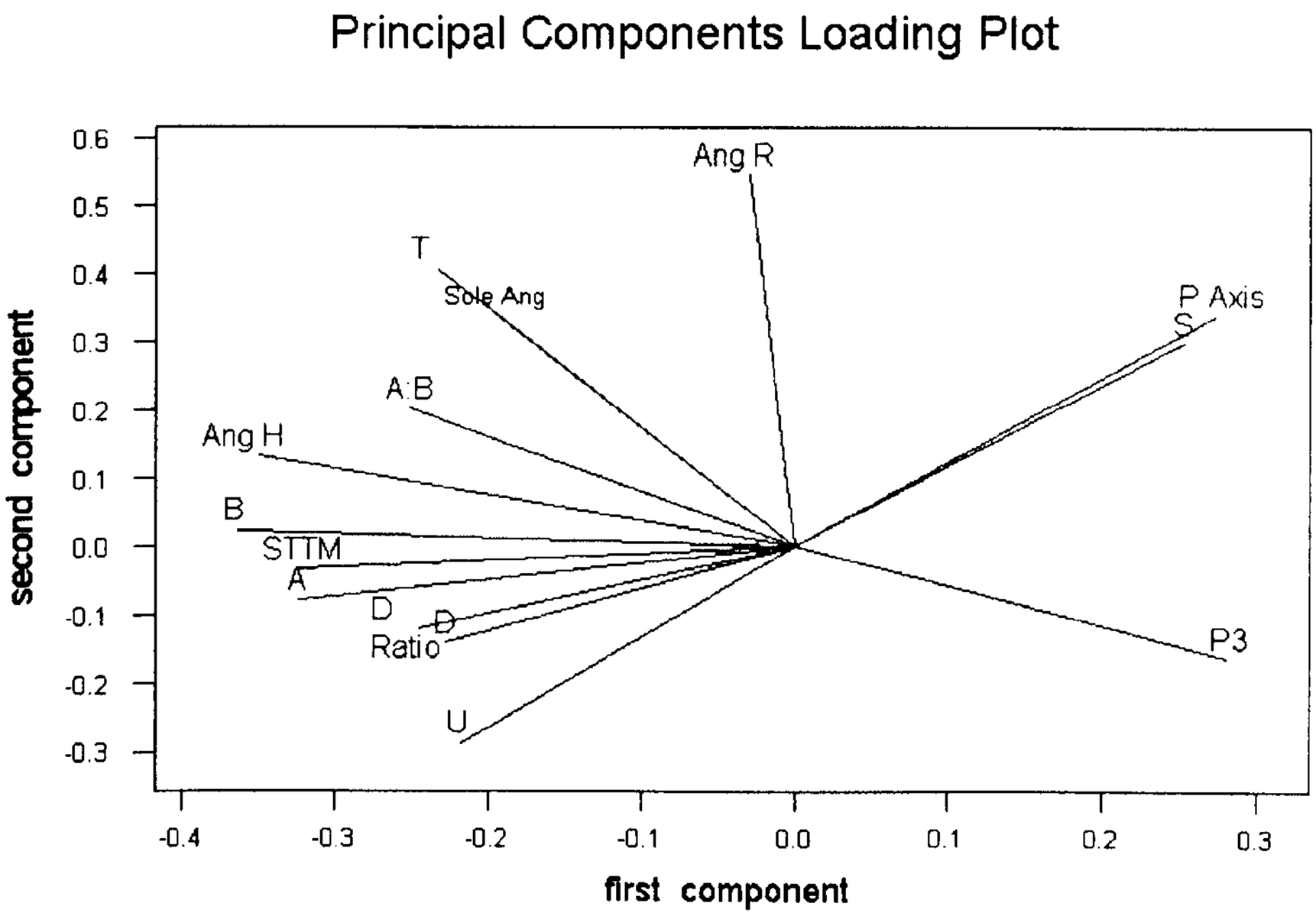

Figure 3.11 Scatter Plot of the Principle Component Scores by individual in respect of the first two Principle Components of variance.

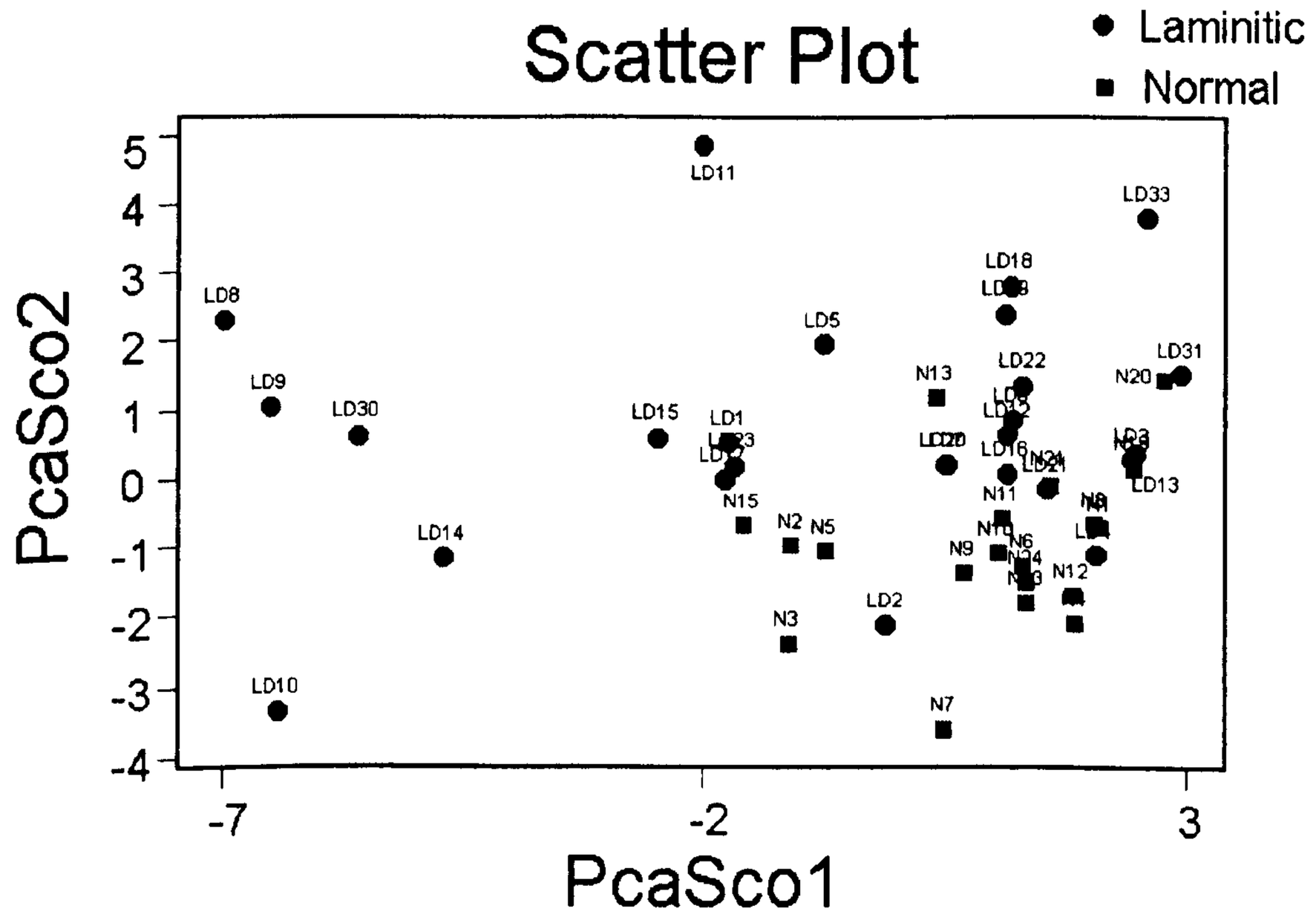

3.6.6.2 HIERARCHICAL CLUSTER ANALYSIS

The results of this analysis are summarised in the binary linkage dendrogram illustrated in Figure 3.12. The agglomeration dendrogram reveals the presence of two main branches that unite at a similarity level approaching zero. A relatively large threshold distance (similarity level) exists between the two respective branches and the final linkage step that unites their respective clusters into a single population. These distances are approximately 33% and 70% for the left and right branches respectively. This indicates that the two clusters are highly dissimilar, but that they respectively share a degree of anatomical similarity within each respective cluster. Difference existed however between the agglomeration characteristics within the two respective branches. In the right-hand branch, linkage occurred rapidly with little threshold distance between successive agglomeration steps, with all animals united into a single cluster at a 70% similarity level. This indicates that these individuals are highly similar in respect of the measured variable and share at least 70% similarity in radiographic anatomy.

The situation in the left-hand branch of the dendrogram was more varied both in terms of the similarity levels at which agglomeration occurred, and the threshold distance between them. This indicates a greater degree of dissimilarity between individuals. Nevertheless all individuals cluster into a single group that share a minimum of 33% similarity in radiographic anatomy between individuals.

The agglomeration characteristics described above suggest that a division of the dendrogram to produce a two-cluster partition may be appropriate. In order to investigate this further the laminitic trial population was subdivided into two classes or groups hereafter referred to as, Laminitic Group A and B respectively.

Laminitic Group A comprised trial animals LD 1,2,8,9,10,11,14,15,17,23 and 30 with the remaining donkeys (LD 3,4,5,6,7,12,13,16,18,19,20 21 and 22 allocated to Laminitic Group B.

Further analysis was conducted in order to evaluate the statistical basis of this proposed 2-fold classification.

Analysis of the object-cluster distance matrix plot based upon this two-cluster division (see Figure 3.13) illustrates both the distance of each object from its cluster centroid, and the relative separation of the respective clusters.

Figure 3.12 Dendogram showing agglomerative hierarchical clustering of the laminitic group

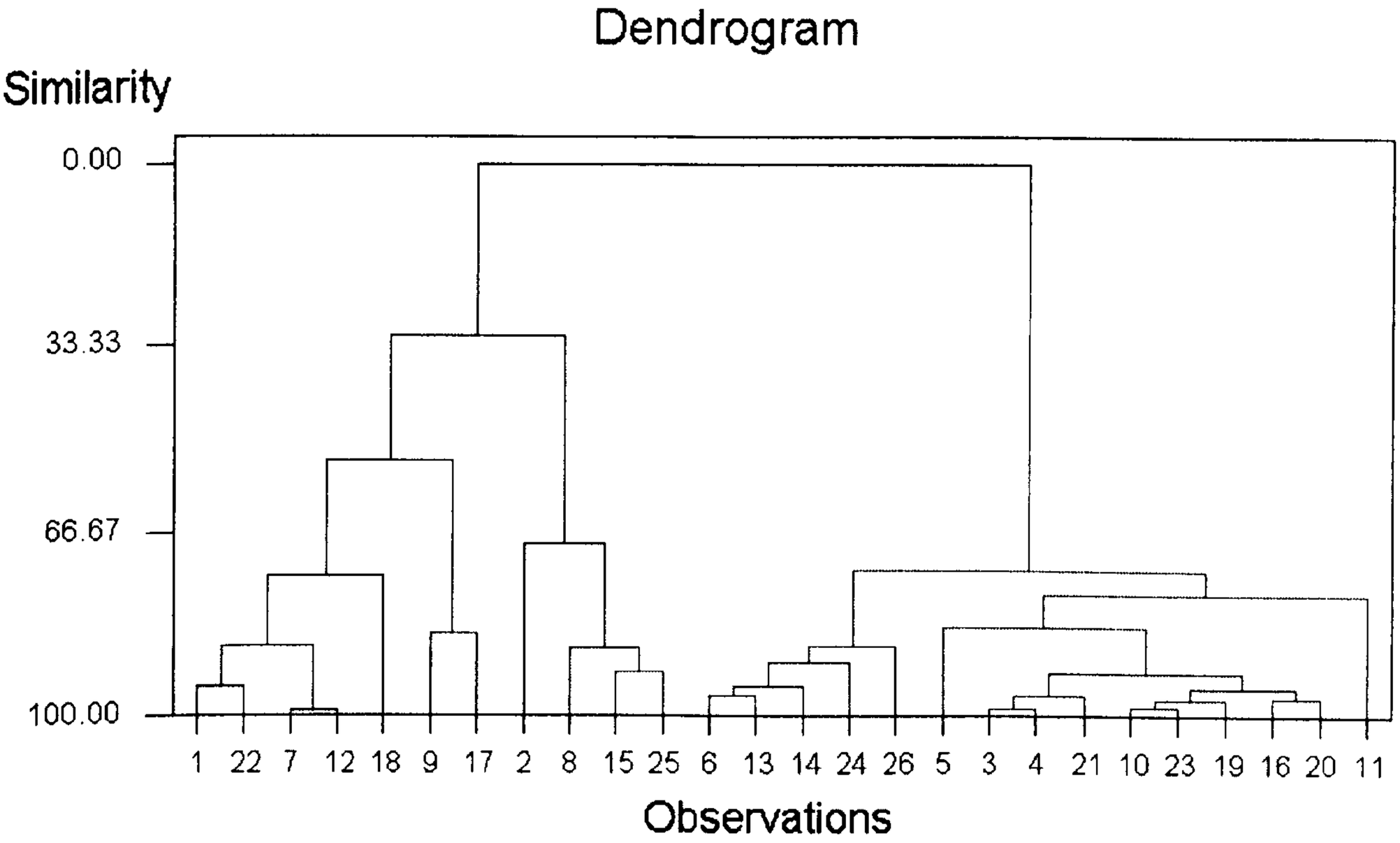

Figure 3.13 Cluster centroid plot showing cluster separation

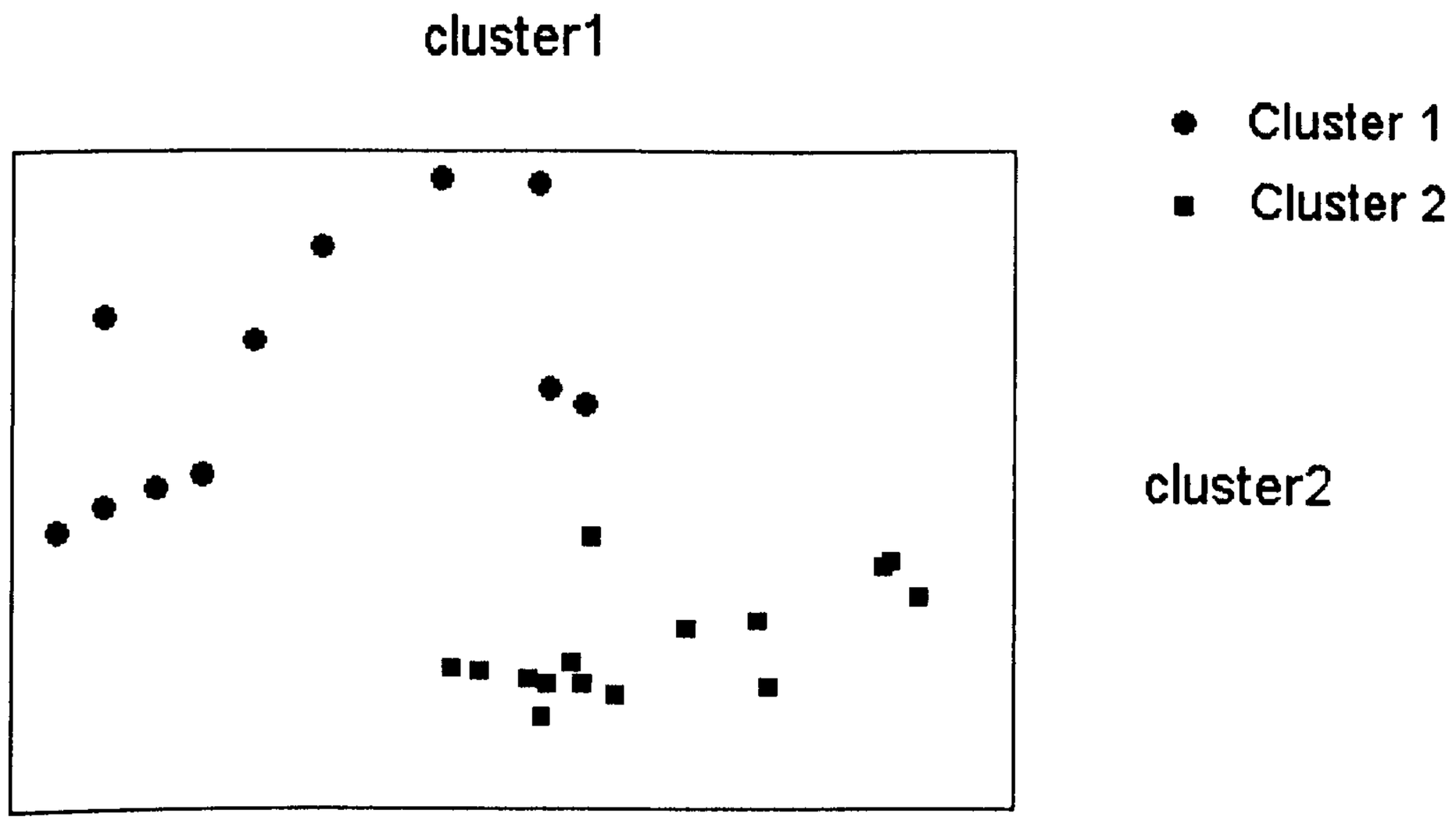

Figure 3.14 Scatter plot of Principle Component scores by group based on hierarchical class allocation

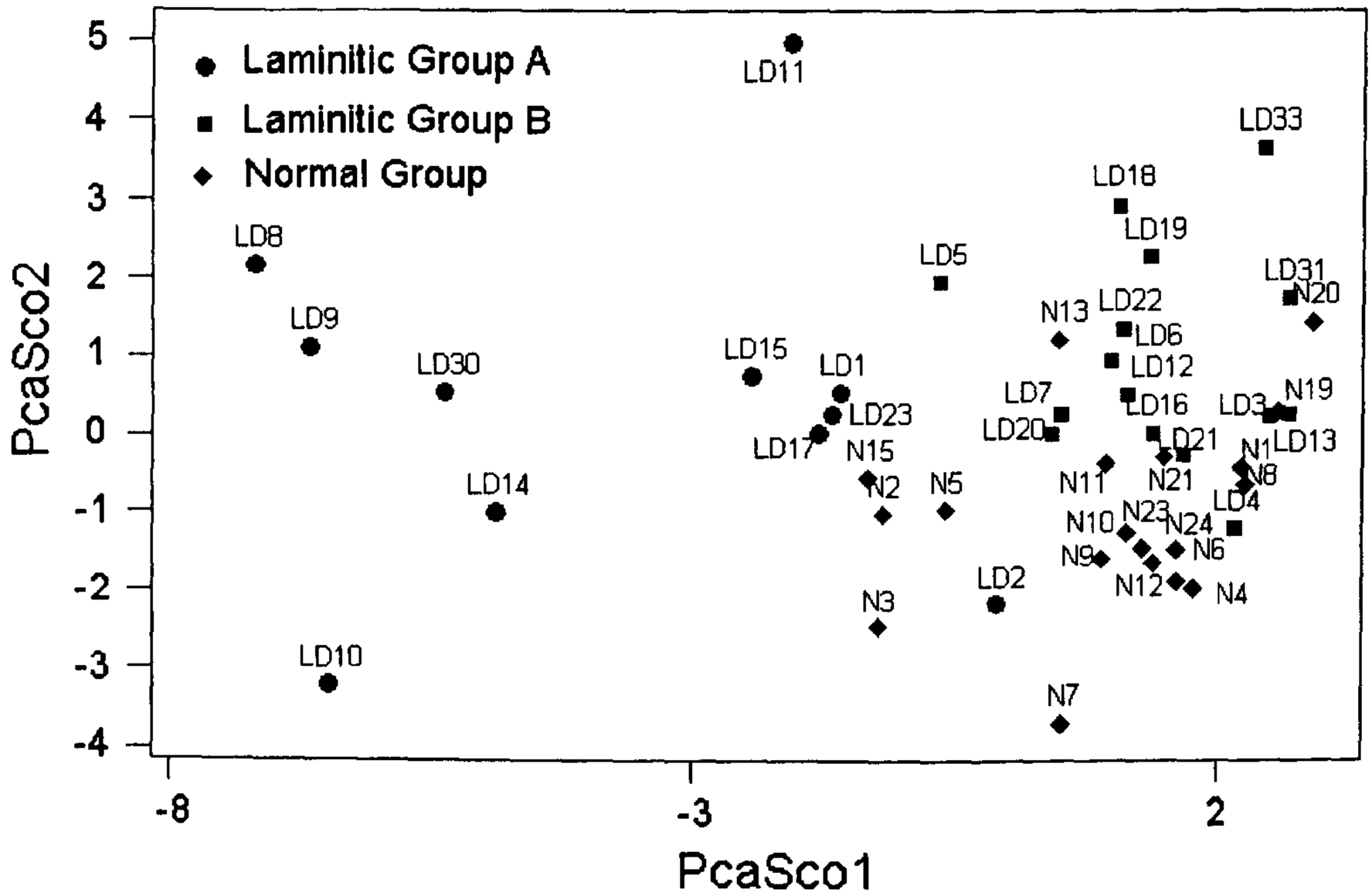

Figure 3.14 illustrates the laminitic group partitioning in respect of the previously presented PC Scores in the plane of maximum variance. Visual inspection of the resultant scatter plot suggests an acceptable fit, and therefore adds confidence to the adoption of this proposed cluster partitioning.

3.6.6.3 Regularised Discriminative Analysis

All analyses out performed the no model test statistics, that is, the classification error and recognition risk statistics of the optimum model was lower that the critical threshold of the no model statistics. This indicated that was a robust statistical basis to the proposed classification system, and that the models offer acceptable levels of goodness of recognition and prediction.

Unit loss function

The class assignment matrix at unit loss function (see Figure 3.15) revealed the modelled class assignment using the theoretical optimum classification rule. The classification matrix revealed that 10 of the 11 Laminitic Group A animals (Class 1) were assigned to their class. The remaining animal, LD2, was assigned to class 3 (Normal Group). Of the 15 animals comprising Laminitic Group B, 14 were assigned to their class. LD 4 was however assigned to the Normal Group. 15 of the normal animals were assigned to their corresponding class with N13, 19, 20 and 21 being assigned to Laminitic Group B (class 2).

The corresponding cross validation classification matrix indicated the potential predicitive capabilities of the optimum classification rule. This analysis assigned 9 Laminitic Group A animals to their corresponding class. LD2 was again assigned to the Normal Group, and LD11 to Laminitic Group B. 13 of the 15 Laminitic Group B animals were assigned to their respective class. LD4, 13 and 16 was however assigned to the Normal group. The cross validation assignment in class 3 was identical to that determined by the classification matrix.

Figure 3.15 Class assignment and cross-validated matrices at unit loss function

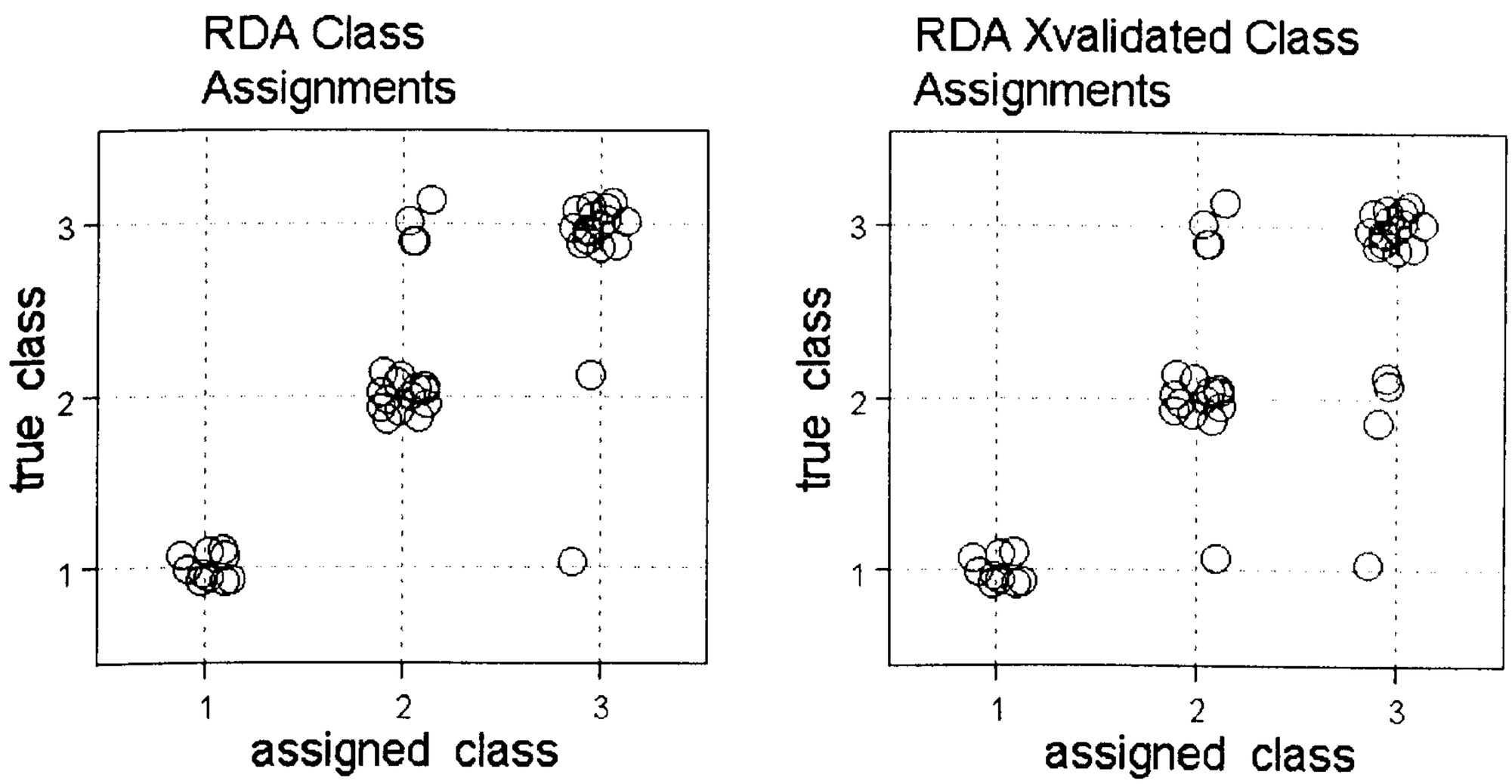

WEIGHTED LOSS FUNCTION

The optimum model selected at the weighting loss function of 10 differed from the unit loss function scenario. The effect of these changes in respect of the associated classification rule and class boundaries can be seen in the corresponding class assignment matrix illustrated in Figure 3.16. The assignment picture in respect of Lamintic Group A was in agreement with the previous model. All individuals were assigned to their corresponding group both in the classification and cross validation classification analyses, with the exception once more of LD2 that was assigned to the Normal group. All Laminitic Group B individuals were assigned to their group. The assignment situation with regard to the Normal Group was however more varied. 14 individuals were assigned to their corresponding class during classification. N1, 8, 13 and 19 were however assigned to Laminitic Group B. These individuals were also allocated to this group in the cross validation exercise, in addition to N9, 11, 20 and 21.

Figure 3.16 Class assignment and cross-validated matrices at weighted loss function of 10

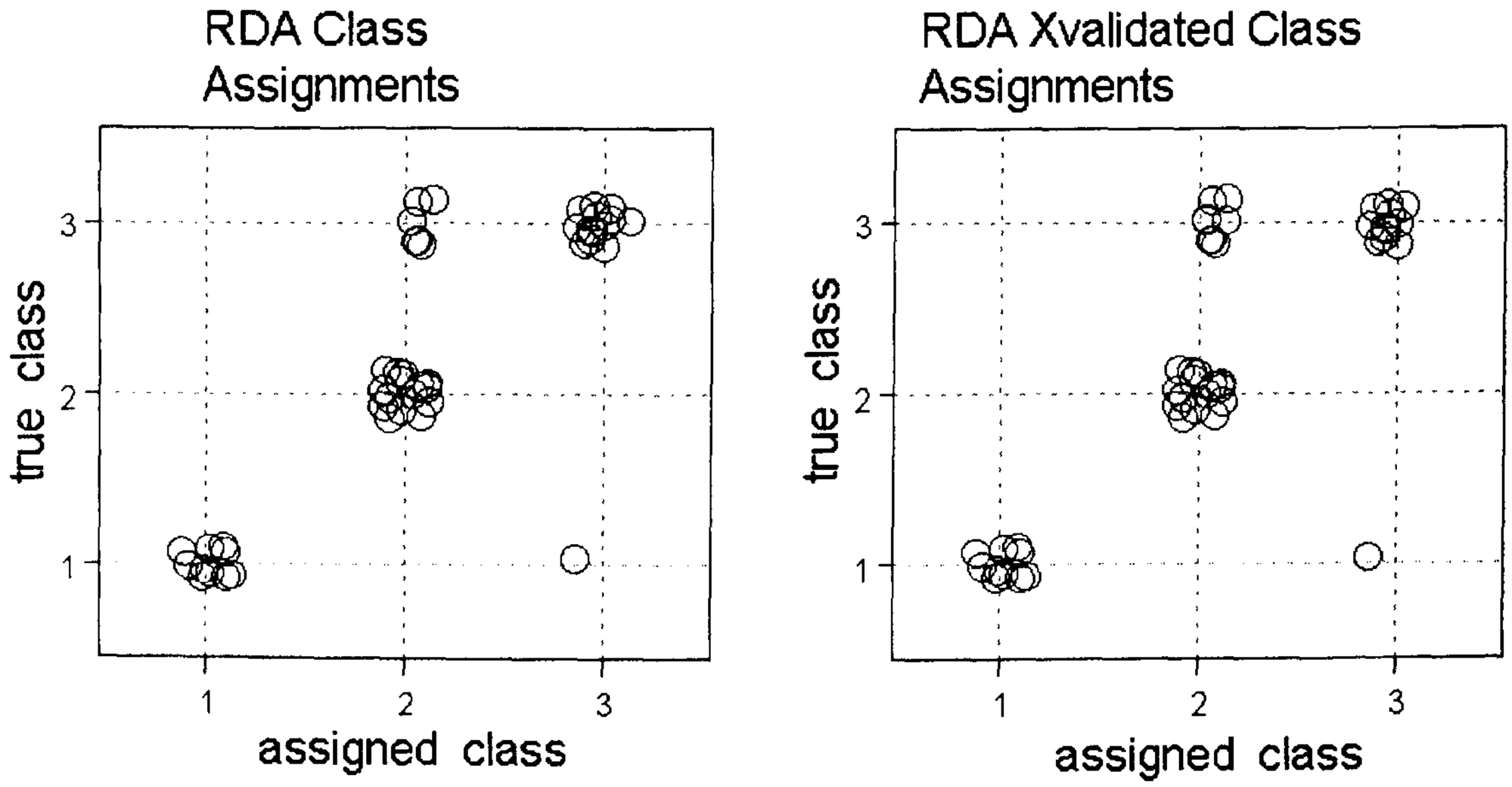

3.6.7 SECONDARY STATISTICAL ANALYSIS OF PARTITIONED DATA

A secondary statistical analysis was performed on the grouped data to further investigate the nature and significance of this derived partitioning. A descriptive summary of the Principle Component scores for the first three components and the radiographic parameters of Laminitic Group A and B are given in Table 3.8 and Table 3.9 respectively. 'Between group' analyses of the partitioned PC scores for PC1-3 for the Laminitic Group A, B and the Normal Group, using one-way analysis of variance (ANOVA) revealed significant 'between group' differences ($P<0.05$) in PC1 and PC2 at 95% confidence levels.

Table 3.8 Summary table of Principle Components Scores by group for the first three principle components of variance.

Parameter	Laminitic Group A			Laminitic Group B		
	Mean (+/- sd)	Median (IQ Range)	Range Min-Max	Mean (+/- sd)	Median (IQ Range)	Range Min-Max
PcaSco1	-2.582 (2.1220)	-1.492 (-4.814--0.9725)	-5.364 - 0.4160	1.893 (0.8383)	1.747 (1.620-2.543)	0.06353-3.34)
PcaSco2	-0.04721 (2.0710)	-0.1094 (-1.076-0.8278)	-3.234-4.093	0.03462 (1.2020)	-0.3483 (-0.7033-0.8855)	-1.966-2.619
PcaSco3	0.2237 (1.2140)	0.2452 (-0.9953-1.447)	-1.389-1.671	-0.1640 (0.9527)	-0.03664 (-0.7244-0.3384)	-1.908-1.874

The associated P values were P <0.0000 and P = 0.001 respectively. In respect of PC1, Tukey pairwise comparisons revealed SDs between Laminitic Group A and B, and also between Laminitic Group A, and the Normal group. Conversely, in the case of PC2, SDs occurred between Laminitic Group B and the Normal group only. These findings are summarised in Figure 3.17.

Table 3.9 Summary table of radiographic parameters by group.

Parameter	Laminitic Group A			Laminitic Group B		
	Mean (+/- sd)	Median (IQ Range)	Range Min-Max	Mean (+/- sd)	Median (IQ Range)	Range Min-Max
S	55.1 (8.97)	54.0 (52.3-63.8)	(40.0-67.0)	66.5 (3.96)	67 (65.0-68.0)	(59.0-74.0)
T	76.6 (3.96)	76 (70.0-87.3)	(55.0-91.0)	66.5 (4.42)	68.0 (62.3-71.0)	(62.0-77.0)
U	64.1 (10.0)	65.0 (56.8-70.0)	(51.0-84.0)	53.9 (6.98)	55.0 (52.0-57.8)	(40.0-64.0)
Ang H	21.6 (13.07)	22.0 (12.3-29.8)	(-5.0-39.0)	1.3 (4.47)	0.0 (-1.0-4.0)	(-6.0-12.0)
Ang R	12.6 (14.70)	16.0 (4.3-18.5)	(-14.0-38.0)	13.9 (8.35)	12.0 (7.3-21.0)	(1.0-30.0)
STTM	24.3 (4.51)	23.0 (20.8-28.5)	(17.6-28.5)	16.5 (1.80)	16.6 (15.6-17.8)	(12.9-19.6)
A	22.4 (4.41)	22.3 (19.0-25.8)	(15.7-29.2)	16.0 (1.86)	15.6 (15.2-17.8)	(12.7-18.6)
B	27.0 (5.46)	25.2 (22.4-32.9)	(20.4-35.0)	17.1 (2.37)	17.5 (15.6-18.0)	(13.6-22.4)
A:B	1.21 (0.111)	1.18 (1.13-1.29)	(1.05-1.40)	1.07 (0.133)	1.06 (1.0-1.13)	(0.89-1.44)
Solear Angle	16.4 (6.90)	15 (10.3-22.0)	(7.0-27.0)	12.3 (3.83)	12.0 (10.0-14.8)	(7.0-22.0)
P3	18.4 (3.27)	17.5 (15.7-20.9)	(14.6-24.0)	23.9 (2.62)	24.3 (21.6-25.3)	(20.0-25.3)
P Axis	-9.0 (16.13)	-6.0 (-18.0- -6.0)	(-44-16.0)	12.6 (8.85)	13.0 (6-18.5)	(2.0-31.0)
D	16.9 (3.37)	16.0 (15.4-18.4)	(11.6-24.0)	9.2 (2.07)	(7.7-11.8)	9.0 (4.9-11.8)
D Ratio	0.35 (0.05)	0.35 (0.31-0.39)	(0.27-0.43)	0.20 (0.04)	0.2 (0.17-0.23)	0.2 (0.12-0.26)

Figure 3.17 Histogram showing 'between group comparisons' of Principle Component Scores in respect of the first three Principle Components of Variance

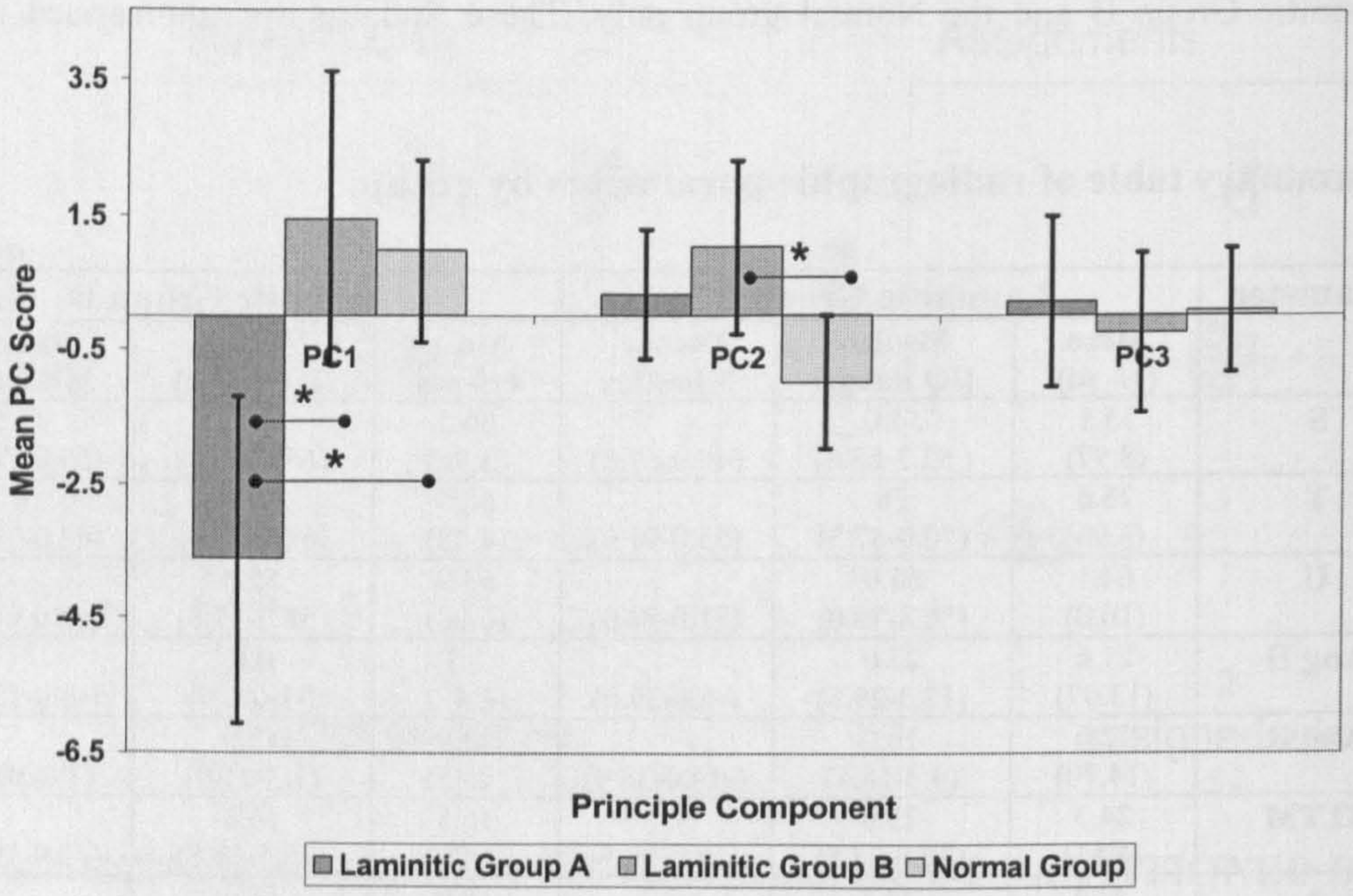

'Between group' comparisons of the angular parameters, conducted using Kruskal-Wallis testing (nonparametric equivalent of ANOVA), indicated significant 'between group' differences ($P<0.05$) in all parameters except Sole Angle. Pairwise comparisons using Mann-Whitney tests are summarised in Table 3.10.

The analysis of the linear measurement parameters using appropriate parametric or nonparametric testing methods, revealed significant 'between group' differences in all parameters. The results of the pairwise comparisons are presented in Table 3.11.

On the basis of this analysis it was decided to accept the partitioning of the laminitic animals into a 2-fold sub-group allocation. These sub-groups are hereafter referred to as Laminitic Group 1 and 2, with Group 1 and 2 corresponding respectively to the former Laminitic Groups A and B. The 3-Group categorisation of the radiographic anatomy of the donkey foot is illustrated in Figure 3.19, and their defining anatomical characteristics summarised.

Table 3.10 Summary table of between group comparisons of angular radiographic parameters

Parameter: S

	Lam Group A	Lam Group B	Normal Group
Lam Group A		SD P=0.0008	NSD
Lam Group B			SD P=0.0022
Normal Group			

Parameter: T

	Lam Group A	Lam Group B	Normal Group
Lam Group A		SD P=0.0168	SD P=0.0002
Lam Group B			SD P=0.0004
Normal Group			

Parameter: U

	Lam Group A	Lam Group B	Normal Group
Lam Group A		SD P=0.0146	NSD
Lam Group B			SD P=0.0386
Normal Group			

Parameter: Ang H

	Lam Group A	Lam Group B	Normal Group
Lam Group A		SD P=0.0005	SD P=0.002
Lam Group B			NSD
Normal Group			

Parameter: Ang R

	Lam Group A	Lam Group B	Normal Group
Lam Group A		NSD	SD P=0.0129
Lam Group B			SD P=0.0001
Normal Group			

Parameter: Paxis

	Lam Group A	Lam Group B	Normal Group
Lam Group A		SD P=0.0003	SD P=0.0450
Lam Group B			SD P=0.0006
Normal Group			

Table 3.11 Summary table of between group comparisons of linear radiographic parameters

Parameter: A

	Lam Group A	Lam Group B	Normal Group
Lam Group A		SD	SD
Lam Group B			NSD
Normal Group			

Parameter: STTM

	Lam Group A	Lam Group B	Normal Group
Lam Group A		SD	SD
Lam Group B			NSD
Normal Group			

Parameter: B

	Lam Group A	Lam Group B	Normal Group
Lam Group A		SD	SD
Lam Group B			NSD
Normal Group			

Parameter: A:B

	Lam Group A	Lam Group B	Normal Group
Lam Group A		SD P=0.0086	SD P<0.0000
Lam Group B			NSD
Normal Group			

Parameter: D

	Lam Group A	Lam Group B	Normal Group
Lam Group A		SD P<0.0000	SD P=0.0111
Lam Group B			SD P=0.0183
Normal Group			

Parameter: D Ratio

	Lam Group A	Lam Group B	Normal Group
Lam Group A		SD P<0.0000	SD P=0.0019
Lam Group B			SD P=0.018
Normal Group			

Parameter: P3

	Lam Group A	Lam Group B	Normal Group
Lam Group A		SD	SD
Lam Group B			NSD
Normal Group			

Figure 3.19 Diagrammatic summary of the categorization of the radiographic anatomy for the normal and laminitic donkey foot.

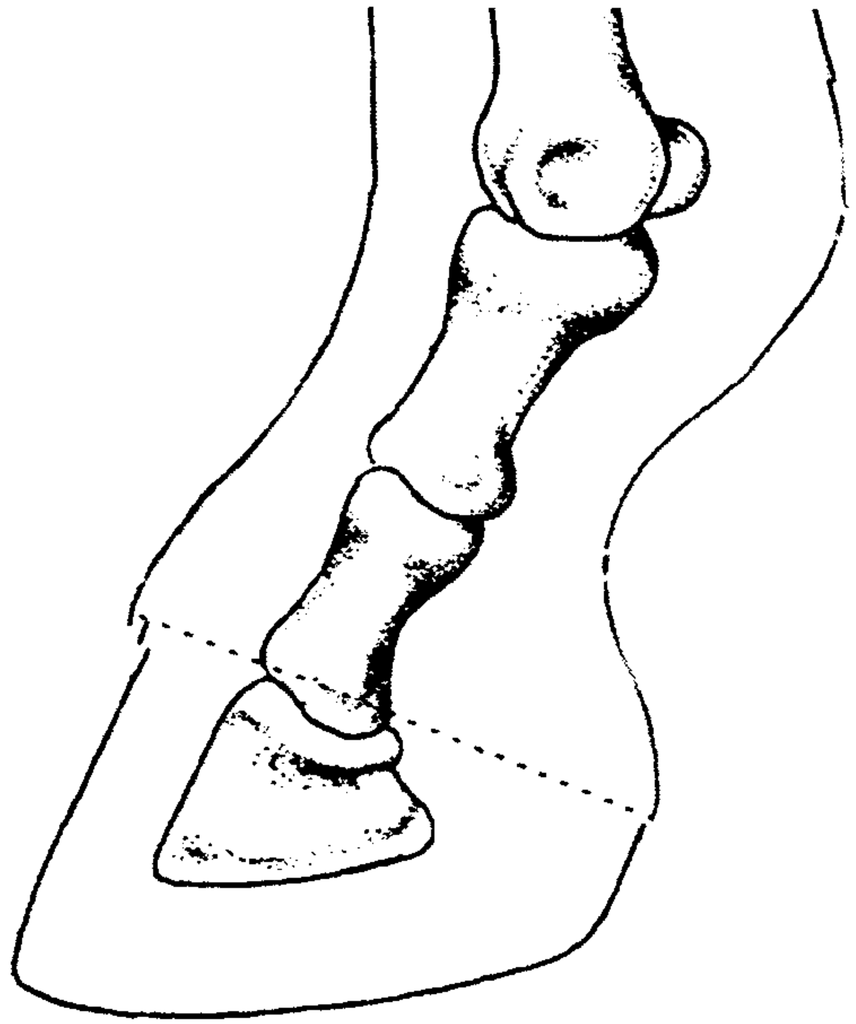

Normal Donkey
Characterised by: -
- Near parallelism b/n the dorsal aspect of the hoof wall and the DP
- Minimal Capsular and/or Phalangeal Rotation,
- Integument depth ratio ~1
- Mean D Ratio ~0.25
- 'Straight' HPA
DP 'blunted' appearance

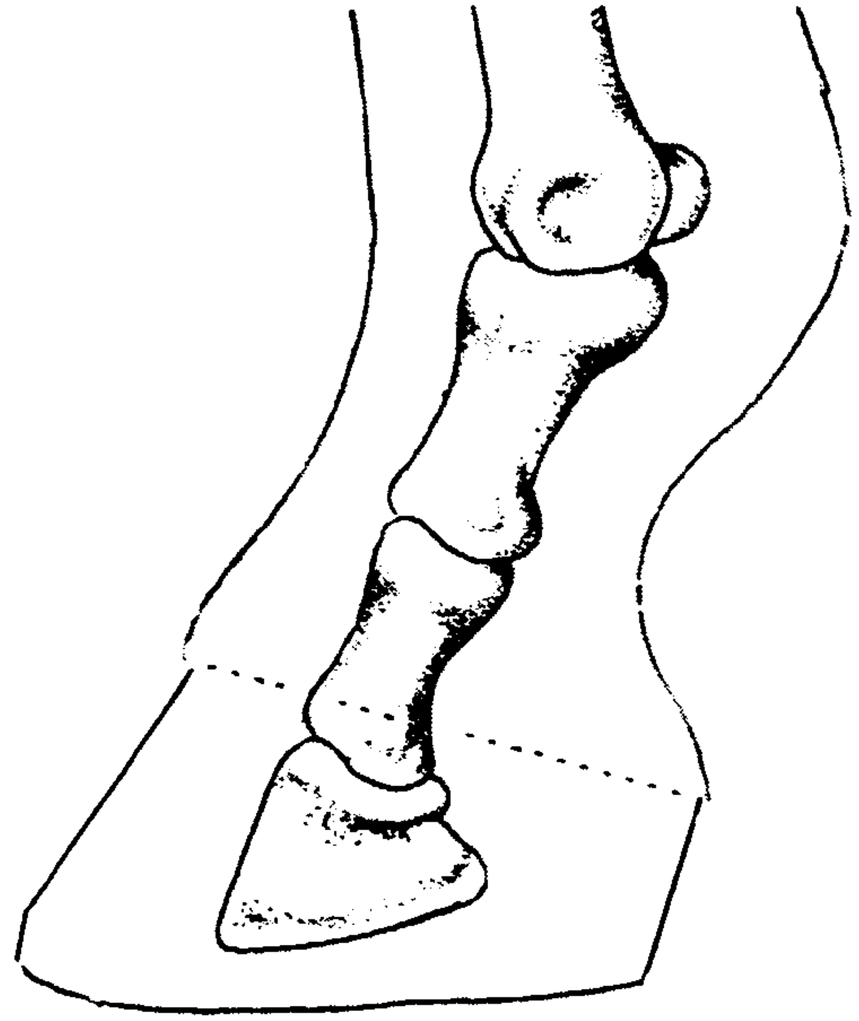

Laminitic Group 1
Characterised by: -
- Absence of parallelism b/n dorsal aspect of hoof wall and DP
- Capsular Rotation and DP Displacement, which may/may not be associated with concurrent Phalangeal Rotation
- Integument depth ratio A:B >1
- Mean D Ratio ~0.35
- 'Broken Back' HPA
DP Deterioration – resorption / bone spur

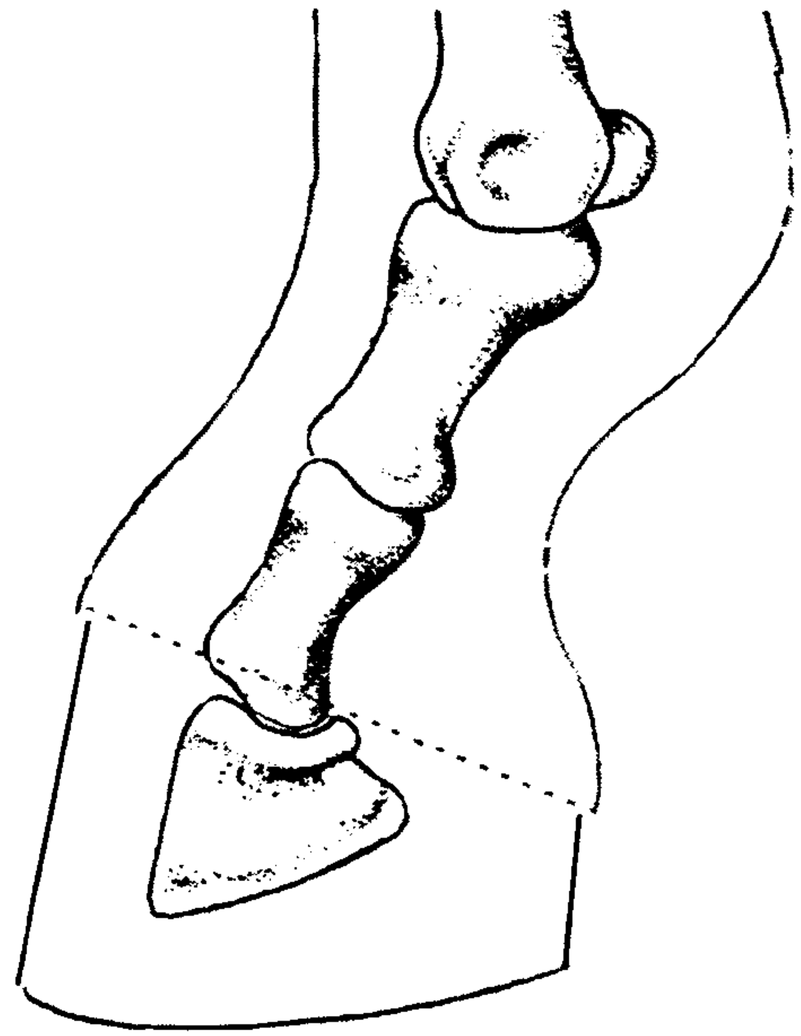

Laminitic Group 2
Characterised by: -
- Near parallelism between the dorsal aspect of the hoof wall and the DP
- Phalangeal Rotation with minimal Capsular Rotation
- Integument depth ratio A:B ~ 1
- Mean D Ratio ~0.20
-'Broken Forward' HPA
DP 'blunted' appearance

3.7 DISCUSSION

This study represents the first detailed evaluation of the radiographic anatomy of the distal limb of the European donkey breed. It compliments the preliminary findings reported for the Mammoth donkey by Walker *et al.* (1995).

This assessment provides baseline data for the lateral radiograph of the normal foot and defines the anatomical impact of laminitis. Specifically the nature and extent of the DP dislocation have been objectively characterised. Univariate analyses have been conducted using traditional analysis techniques previously used in the horse. In addition, a novel multi-parameter approach has been presented. This represents the first time that these techniques have been applied to measurements derived from equid foot radiographs. The use of these techniques represents a logical progression from former methods of radiographic assessment, and has enabled a comprehensive appraisal of anatomical change within the foot.

The use of a semi-automated computer-based imaging approach achieves considerable time saving over traditional manual quantitative assessment. Whilst control lines can be constructed readily, the positioning of the dorsal hoof wall marker (Eustace 1991), remodelling of the DP (Linford 1987) and alignment of the foot relative to the x-ray beam (Tachio *et al.* 2002) all represent potential sources of experimental error.

The use of standard operating procedures, for foot preparation and positioning, focal length, beam alignment and incidence, and a single operator minimises these sources of experimental error. The use of a set-square, to align the x-ray machine and foot, ensured that beam incidence was below the critical obliquity limit of 10° reported by Koblik *et al.* (1988) and Tachio *et al.* (2002). Potential errors in delimiting the dorsal aspect of the DP in cases where remodelling has occurred, were more difficult to control and quantify. The use of reference points immediately distal to the extensor process and 5mm proximal to the apex of the DP minimises this error (Linford 1987).

The radiographic anatomy of the European donkey foot displays broad similarities to the 'theoretical ideal' described by Colles (1983) and Butler *et al.* (1998). This study also supports the existence of a straight HPA in the normal donkey, based upon data for the P Axis parameter, although the axis is more upright than that reported for the horse.

Absolute values for key radiographic parameters within the donkey foot are markedly different from those reported in the horse. These suggest important species differences. In particular, the mean D value was greater in the donkey. This finding supports the empirical observation by Eley (1998, 2000) that the DP of the donkey is positioned more distally within the hoof capsule.Hence, the extensor process of DP in the donkey hoof is not in alignment with the CB,

as is the case in the horse. In addition, mean integument depth, measured at the mid-point of the dorsal aspect of the DP, was approximately 30% greater in the donkey than those recorded in the pony by Cripps and Eustace (1999a). In fact, the donkey value is comparable with that recorded in the larger thoroughbred and warmblood breed types by Linford *et al.* (1993), and Cripps and Eustace (1999a). These results suggest that some of the radiographic guidelines for the interpretation of donkey radiographs, which are based on results from the pony and horse, should not be used. Indeed, the results suggest that new guidelines should be adopted for the donkey.

These issues are of particular diagnostic and prognostic significance with regard to laminitis. Critical values have been proposed by O'Brien and Baker (1986), Linford (1987) and Cripps and Eustace (1999b), both with regard to the diagnosis of chronic degenerative change, and the 'likely' recovery outcome (Cripps and Eustace 1999b).

Cripps and Eustace (1999a,b) stated that D values in the normal equine foot vary with breed type by up to 6mm, with values >8mm in 'sinker' cases. These values fall below the mean value recorded in this study. Indeed Cripps and Eustace (1999b) stated that D values ≥14mm carried a guarded prognosis.

Linford *et al.* (1993) stated that Integument Depths >15mm were diagnostic of laminitis in thoroughbreds. However, these 'critical' values fall within the range for the normal donkey foot observed within this study. It is not known whether they reflect 'species differences' or subclinical laminitic change within the foot of the donkey. Given the prevalence of degenerative foot conditions in the UK, further and comparative radiographic assessment of the donkey in its native environment is required to resolve this issue. Although integument depth values in this study approached those reported by Walker *et al.* (1995), they were lower than the mean of 22.5mm observed in the mammoth donkey. This may indicate important breed difference in this parameter for the donkey.

Univariate analysis of the radiographic data for the laminitic foot indicates that the condition is associated with anatomical changes consistent with DP Dislocation in which capsular and phalangeal rotation events predominate.

The nature of the DP dislocation is considered to be of clinical importance. Eley (1998) and Bell (2001- Pers Com.) suggested that the donkey foot could withstand DP displacement events more readily than rotation. This is in marked contrast with the guarded equine prognosis (Baxter 1986) associated with DP Displacement events.

It is unclear whether Eley (1998), or Bell (2001 – Pers Com.), discriminated between capsular and phalangeal rotation. However degenerative remodelling of the DP predominated in those donkeys exhibiting capsular rotation (Collins – unpublished data). This may be significance as

DP remodelling is pathognomonic for equine Type II chronic founder (Eustace 1995). Coffman *et al.* (1972), Linford (1996) and Johnson *et al.* (2000) referred to this as refractory exacebative laminitis (REL). REL cases were characteristically unresponsive to treatment, and suffered from ongoing bouts of unremitting pain. Eley and French (1993a) have reported the prognostic importance of DP remodelling in the donkey. Eley (2000) stated that therapeutic strategies must be directed towards preventing further deterioration of the DP.

The incidence of a blunted appearance to the DP within the normal group suggests either the possibility of anatomical differences between the donkey and the horse, with the donkey displaying extensive morphological variability, or conversely the widespread occurrence of subclinical laminitic change to the DP.

The variability in the data for the laminitic donkey foot indicates considerable 'between animal' variation in the anatomy of the foot. This is consistent with the views expressed by Hunt (1993) and Parks *et al.* (1999) concerning the varied nature of degenerative change encountered within chronically affected laminitic horse feet. These findings suggest the need to establish a method of evaluating the combined effects of this variation.

The multivariate analysis techniques used in this study provide such a means of evaluation, both in terms of variable- and object-directed assessment. The PCA analysis demonstrated that the plane of maximum variance accounted for 70% of the total information contained within the measured parameters. Hence assessment in this plane affords a significant insight into the radiographic anatomy of the foot, individual variation, and degenerate anatomical change associated with laminitis.

Confidence in the three-group categorisation can be inferred as the two distinct multivariate techniques, each using different methods of calculation, provide results that are in broad agreement (James 2002 – Pers Com.). In addition, statistically significant 'between group' differences, in both PC scores, and variable profiles, further supports this partitioning. The RDA analyses however, not only lends support to this categorisation, but also it indicates that effective mathematical models can be trained to this categorisation, and that class discrimination, based upon these models, produce a high level of success.

This categorisation revealed additional information regarding degenerative anatomical change (see Table 3.10 and Table 3.11). For example, partitioned D and D ratio data indicated significant DP displacement events within Group 1, compared to the Normal Group. This event was otherwise undetected. In addition, the degree of DP displacement was significantly greater in the Normal Group than in Group 2. This may indicate that subclinical laminitis, of a Group 1 nature, was present within the Normal Group.

Both multivariate techniques highlight differences in cluster cohesion between the laminitic sub-groups. This may reflect the fact that Group 2 is characterised primarily by phalangeal rotation, whereas Group 1 is characterised by a more diverse series of anatomical change including both capsular rotation and DP Displacement. Varying degrees of DP remodelling also occurred within this group. DP remodelling may directly affect absolute radiographic parameters and/or increase measurement error associated with control line construction, and thus contribute to the variation recorded within this group.

The precise mechanisms that result in the development of anatomically distinct laminitic sub-groups are unknown. However Herthel and Hood (1999) have proposed models by which capsular and phalangeal rotation are generated within the foot, as a *sequelae* to laminitis. The functional consequences of these anatomical changes are poorly defined. Efficient locomotor function, devoid of pain, is likely to be dependent upon achieving optimal stress and strain distribution within the distal limb. The anatomical configuration of the 'ideal' HPA contributes towards this biomechanical objective (Balch *et al.* 1991, Tacchio *et al.* 2002). Although the precise biomechanical consequences have not been fully modelled, the development of a 'broken' axis may alter this optimal balance (Balch *et al.* 1991, Curtis 1999). Hence differences in the nature of the HPA, within the laminitic sub-groups, may contribute towards the apparent variation in the donkey's ability to withstand displacement and rotation events. Further work is required to elucidate the interactions between the HPA and laminitis.

Principle component analysis provides a visual method by which the radiographic anatomy of the presented foot can assessed readily, irrespective of the nature of the resultant degenerate change. Ongoing expansion of baseline data for both normal and laminitic feet will permit further refinement of our knowledge of the radiographic anatomy of the donkey foot, and the effects of laminitis. This will also enhance the accuracy of the mathematical models used to describe the different anatomical groupings, and may ultimately lead to a mathematical rule for diagnosis. By achieving this, together with an improved understanding of the biomechanical consequences of the associated anatomy, it will be possible to enhance diagnosis, assess severity, monitor progression, evaluate response to therapy, and thereby improve prognoses associated with laminitis, to the benefit of the donkey.

4. MORPHOLOGY AND MORPHOMETRY OF THE *STRATUM MEDIUM* OF THE LAMINITIC DONKEY HOOF WALL

4.1 OVERVIEW

The equid *SM* exhibits an ordered structural organisation comprising tubular and intertubular horn. This structural organisation is considered to be intimately associated with the biomechanical functioning of the hoof wall, although the precise nature of the relationship is not fully understood.

Morphologically distinct tubule types are recognised based upon differences in tubule size, shape, and cellular organisation. These different tubule types are organised into distinct regional populations that produce a zonal variation in structure across the HWD. These morphologically distinct zones are characterised by differences in macroscopic appearance, staining affinity, tubule type, and tubule numbers. Whilst the structural organisation of the equine *SM* is well documented, little is known of the corresponding organisation within the *SM* donkey.

The functional significance of this zonal organisation is poorly defined. However if there is a structure-function relationship operating at this level of the hierarchy, then zonal differences in structure are likely to be associated with differences in material properties. In order to investigate this relationship within the donkey, there is a need to establish the zonation pattern for this species, and objectively characterise the defining features of the structural organisation of the respective zones.

Isolated reports have detailed structural changes, at the microscopic level of the design hierarchy of the equine hoof wall, in association with the laminitic condition. Irregularities in structure have also been reported in the *SM* of laminitic donkey hoof wall.

The mechanisms that are responsible for the development of these structural irregularities within the hoof wall are unknown. It is unclear as to whether these irregularities in structure arise as consequence of formational or deformational changes within the hoof.

Pathological events associated with the progression of the laminitic condition may affect the normal process of controlled and co-ordinated hoof horn formation within the afflicted foot. This may directly lead to formational changes in structure within the *SM*, or alternatively, leave the *SM* susceptible to structural deformation during weightbearing. Changes in force distribution within the foot following digital collapse may also contribute to these structural changes within the *SM*.

This chapter covers work associated with characterising the structural organisation of *SM* at the microscopic level of the design hierarchy, in the laminitic donkey hoof.

4.2 INTRODUCTION

The formation of the *SM* and the intimate association that exists between the dermis and epidermis, and the BM that forms the dermo-epidermal junction, has been outlined in Chapter 1. The structural organisation of the *SM,* that comprises tubular (Tu) and intertubular (IT) horn fractions, is determined by the papillarform dermal modification of the coronary coria (Banks 1993). Hoof horn production is dependent upon the dermal circulation (Bruhnke 1931, Nickel 1938a,b 1939), and is controlled, mediated and co-ordinated by the BM (Pollitt 2002 – Pers Com., Bragulla 2003).

The size, thickness and apical shape of the papillary structures have been reported to vary both around and across the coronary corium of the horse. Whilst the precise effect upon horn tubule formation has not been fully elucidated, Pellmann *et al.* (1993) and Bragulla (2003) stated that these variations were responsible for the generation of distinct tubule types. Schummer *et al.* (1981) stated that variations in papilla morphology were related to the 'degree' of horn formation, whilst Hirschberg *et al.* (2001) stated that horn formation was also significantly affected by the status of the papillary microcirculation.

The early anatomists including Chauveau (1853), summarising the earlier work of Gurtl (1836), Delafond (1845) and Bouley (1851), Fleming (1871) and Mettam (1896), and have described that the structural organisation of the *SM* of the hoof wall varies both across and around the hoof wall.

The pioneering work of Kersting (1777) made specific reference to the ordered nature of the structural organisation of the *SM* and stated the tubular and intertubular horn was:

"...related to each other in a precise manner ..."

and commented as to the:

" ...individual nature of the horn tubules and their specific inter-relationship with each other..."

Kersting (1777) also noted that the tubules varied in their:

"...appearance, thickness (sic size) and density ... across and around the hoof wall".

4.3 MORPHOLOGY VERSES MORPHOMETRY

To explore the structure-function relationships that operate in the *SM* at the microscopic level of the design hierarchy, and the potential effects of the laminitic condition, there is a need to effectively characterise the structural organisation of the *SM*.

Two distinct approaches to characterisation of structure have emerged, namely morphology and morphometry. Morphology can be defined as the subjective study of form and shape, whereas morphometry can be defined as the objective science of form and shape.

Morphological characterisation has traditionally formed the basis by which this has been achieved. However there has been a tendency to be critical of the perceived subjectivity inherent in the field of morphology. Reilly (1995, 1998, 2001) argued that hoof science had suffered as a direct consequence of a reliance upon subjective modes of characterisation. This author stated that there was a need to adopt objective measures in order to make progress.

The emerging science of morphometry has enabled the study of form to be placed upon a quantitative basis. This has brought into question the validity of the morphological approach. However it is this author's assertion that morphology and morphometry applied together in an appropriate manner represent a powerful synergistic approach, and provide an effective means for the characterisation of structure. Indeed, Eisenmann (1986) concluded that the issue is not to choose on philosophical grounds between the two approaches, but to strike a balance between the two. To achieve this balance, it is appropriate to assess the respective merits of the morphological and morphometric approach. Table 4.1 summarised the fundamental tenets of the respective approaches, and details their potential strengths and inherent limitations. Commenting upon this subject, Eisenmann (1986) concluded that descriptive accounts, photographs drawings, contingency tables and measurements are equally useful to record, communicate and document conclusions.

Objective measurements represent a powerful enhancement to the traditional morphological approach. Numbers can highlight subtle differences that are not 'visually apparent', or conversely, reveal form and structure that is overshadowed by other, more 'visually apparent' features.

Objective measurements also provide the means by which structure-function relationships can be explored. In this regard Vincent (1992) argued that the science of material testing of biological materials represents an extension of morphology (*sic* the characterisation of shape and form), and stated that:

> ***"...as morphology becomes more numerate, through the use of engineering to describe shape, so shape can be related to function via material and structural properties."***

Vincent (1992) argued that the study of material properties of biomaterials (*sic* mechanical properties), to explore structure-function relationships, has the vigour of the interdisciplinary hybrid, and stated that it is transforming all areas of biology, particularly morphology.

4.4 STRUCTURAL ORGANISATION OF THE *STRATUM MEDIUM*

To investigate the structure-function relationships within the *SM* effectively, there is a need to objectively characterise the structural organisation of the *SM*.

4.5 MORPHOLOGICAL CHARACTERISTICS OF THE *STRATUM MEDIUM*

Histological examinations of the *SM* have revealed morphological differences in tubule form, the organisation of the IT horn fraction, and the inter-relationship between these two horn fractions within the *SM* both of the equine hoof (Tscherne 1910, Bruhnke 1931) and the donkey hoof (Hifny and Misk 1983).

4.6 TUBULE CATEGORISATION

Tscherne (1910), Bruhnke (1931), Nickel (1938a,b, 1939), Rössner (1940), Wilkens (1964), Stump (1967), Leach (1980), Bolliger (1991) and Kasapi and Gosline (1997) have variably described the presence of distinct tubule forms or types within the equine SM. However these studies have tended to adopt different morphological parameters and different classification terminology as the basis for tubule categorisation. This has led to considerable confusion in this aspect of structural characterisation. These tubule types have been variably characterised on the basis of tubule size, cross sectional shape, cellular organisation, and cellular orientation. Table 4.2 summarises the principle findings of these previous morphological studies. There has been little progress in attempting to compare different tubule types between studies, or indeed, between different equid species.

More recently Kasapi and Gosline (1997) have revisited the issue of tubule classification within the *SM*. These authors assessed the tubule morphology at the MDC of the *SM* in each of 6 sequential sampling regions (Ia,Ib, IIa,IIb, IIIa,IIIb), which spanned the entire HWD. They concluded that the horn tubules did indeed display a helical pattern of organisation. In addition these authors reported that the tubules within these sampling regions were morphologically distinct, and a continuous variation in tubule morphology occurred across the hoof wall depth. On the basis of this investigation, Kasapi and Gosline (1997) constructed diagrammatic representations of the 'average' structural organisation and tubule form in each of the respective sampling regions, that both attempted to reflect differences in cellular orientation, and also shape and size variation. As such, these schematics may be considered to represent a revision of Nickel's former tubule types. However, as photomicrographs of the different tubule types were not published, direct comparison with the work of Wilkens (1964) and Bolliger (1991), and Leach (1980) is not possible.

Table 4.3 summaries the morphological characteristics of the Donkey Tubule Types proposed by Collins *et al.* (2002).

Table 4.1 Summary table comparing the morphological and morphometric approaches of characterising biological structure

Approach	Definition	Mode of Reporting	Method of Reporting	Data	Advantages	Disadvantages
Morphology	Science of form and structure	Subjective Descriptive Quaitative	Descriptive accounts Photographs Drawings	Discontinuous only Nominal (categorical) Ordinal (relative)	• Readily conveys 'image' of form • Simplifies data into broad categorical units • Pattern recognition – inherent capability of the human eye • Discriminates between issues of allometry and isometry (Δ relative Form Vs Δ relative Size)	• Open to subjective bias • Conclusions based upon opinion • Lack of rigour • Every specimen can not be described in detail • Assimilation of large data-sets difficult • Comparisons difficult
Morphometry Including: (Histometry) (Biometry)	Measurement of form and structure Measurement of form and structure in histology Measurement of biological structure	Objective Definitive Quantitative	Numerical Absolute measurements Contingency Tables	Continuous and discontinuous Nominal Ordinal Interval Ratio	• Unbiased • Rigorous approach • Identification of subtle differences • Can handle large sample numbers • Reliability of conclusions improved by increased sample numbers • Numbers easy to store • Data manipulation possible • Open to Statistical analysis (univariate, bivariate and multivariate analysis) • Evaluation of closeness of morphological 'classes' • Conclusions based upon robust mathematical criteria • Inter-relationships can be evaluated • Variable assessment possible • Minimises speculative conclusion	• Can not readily convey the 'image' of form • Reliant upon appropriate variable selection • Data collection is time consuming • Difficult to discriminate between effects of allometry and isometry (ΔForm verses ΔSize) • Pattern recognition difficult

Table 4.2 Summary table of equine tubule characterisation

Author	Tubule Type	Cortical organisation			Cross sectional shape	Tubule Size (Relative)
Horse						
Tscherne (1910) Bruhnke (1931)	Outer Zone	Concentrically ordered cortex of variable thickness Tu/IT boundary distinct			Oval - wedge	Small - Large
	Middle Zone	Concentrically ordered cortex Cell size increase progressively from marrow Tu/IT boundary distinct			Oval - round	Small
	Inner Zone	Distinct cortical morphology Tu/IT boundary indistinct			Round	Very Large
Nickel (1938a,b, 1939)	VSG 'predominantly Steep' Tubule	Inner region 2 cell layers flat helical orientation	Middle region 6 cell layers steep helical orientation	Outer region 2 cell layers flat helical orientation	Round	N/A
	VFG 'Pedomonantly Flat' Tubule	Inner region 2 cell layers flat helical orientation	Middle region 2 cell layers steep helical orientation	Outer region 6 cell layers flat helical orientation	Oval -Wedge dependant upon prevailing forces	N/A
Bucher (1987)* Bolliger (1991)* König (2001)* Patan (2001)*	Type 1 Tubule	'Flat pancake' cells only			Oval	Large
	Type 2 Tubule	1-2 layers 'Flat pancake' cells	Several layers of 'Spindle cells' Parallel to tubule axis	Few layers of 'Spindle cells' Perpendicular to tubule axis	Round	Small
Stump (1967) Leach (1980)	Type I Tubule	N/A			Round	Small
	Type II Tubule				Round	Large
	Intermediate Tubule				Intermediate	Intermediate
	Type III Tubule				Oval	Small
Kasapi and Gosline (1997)	Type Ia Tubule	Inner region flat helical orientation		Outer region steep helical orientation	Round	Large
	Type Ib Tubule	Inner region flat helical orientation		Outer region steep helical orientation	Round	Large
	Type IIa, IIb, IIIc Tubules	Inner region flat helical orientation	Middle region steep helical orientation	Outer region flat helical orientation	Oval	Small
	Type IIIb Tubule	Inner region flat helical orientation	Middle region steep helical orientation	Outer region flat helical orientation	Oval	Large

Key: Tu - Tubular horn. **IT** - Intertubular horn. * After Wilkens (1964)

Table 4.3 Summary table of donkey tubule characterisation (After Collins *et al.* 2002).

Donkey						
Collins *et al.* (2002) Collins and Reilly (2004a - Submitted)	Type 1 Tubule	Concentrically ordered cortex of variable thickness, comprising lunate cortical cells Tu/IT boundary distinct			Oval	Small
	Type 2 Tubule	Concentrically ordered cortex comprising 2-4 layers of lunate cortical cells			Round	Very Small
	Type 3a Tubule	2-4 layers of lunate cortical cells Tu/IT boundary indistinct	Expansive region of polyhedral cortical cells	2-4 layers of lunate cortical cells	Oval	Large
	Type 3b Tubule	2-4 layers of lunate cortical cells Tu/IT boundary indistinct	Expansive region of polyhedral cortical cells	2-4 layers of lunate cortical cells	Round	Large

Key: **Tu** - Tubular horn. **IT** - Intertubular horn

4.7 ZONATION OF THE EQUINE *STRATUM MEDIUM*

The *SM* of the equid hoof wall has been variably subdivided into distinct regions or zones. This zonation has been conducted both at the macroscopic and microscopic level of the design hierarchy.

At the macroscopic level this has been based upon: -

- Visual appearance (Emery *et al.* 1977, Greenough 1982)
- Pigmentation (Nörner 1886, NAV. 1994, Dyce *et al.* 1987, Wagner *et al.* 2001)
- Staining characteristics (Tscherne 1910, Bruhnke 1931, Bucher 1987, Bolliger 1991)

At the macroscopic level zonation has been based upon: -

- Optical properties (Nickel 1938a,b)
- Birefringence (Wilkens 1955, 1964)
- Tubule type (Stump 1967, Leach 1980, Kasapi and Gosline 1997)
- Tubule density (Reilly *et al.* 1996, 1998a, Reilly 2001)

Table 4.4 summarises proposed schemes of zonation of the equine *SM*. In this regard, Kasapi and Gosline (1997) stated that variability in 'design' within the *SM* was best exemplified by differences in tubule morphology, with tubular morphology dependent upon specific location both around and across the *SM*. This may be of particular importance with regard to hoof wall function, if a structure-function relationship operates at this level of the hierarchy within the *SM*. Nickel (1938a,b) considered this regional distribution of tubule types to be of fundamental importance. He believed that the structural organisation of the horn tubule was intimately linked to the biomechanical functioning of the *SM*.

Indeed Kasapi and Gosline (1997) stated that although the changes in tubule morphology across the HWD were in general gradual, two abrupt morphological transitions were evident at their Ib/IIa and IIIa/IIIb junctions respectively. That is, transitions occurring respectively at 66.6% HWD and 12.5% HWD.

The first transition was characterised by changes in both tubule size and design, and was evident macroscopically in stained sections with the unaided eye. At the microscopic level, this transition was marked by a palmo-dorsal reduction in the number of 'steep orientated' cortical cell layers, the development of an outer cortical layer, a change in cross sectional shape from predominantly circular to elliptical profile, and a reduction in tubule size.

The second transition was marked at the microscopic level by an increase in the number of inner and outer cortical cell layers, an palmo-dorsal increase in the helical orientation of the middle cortical cell, and an increase in tubule size.

Bruhnke (1931) stated that this three-fold zonal pattern was common to other domestic equid species. However, considerable variation, most notably in the relative development of the middle zone was evident between species. This author did not however provide any evidence in support of this statement, nor indeed did he confirm the particular species studied. Bolliger (1991), Patan (2001) and König (2001) stated that these zones were of equal dorso-palmar depth within the equine *SM*.

With specific regard to the *Equidae*, Schummer *et al.* (1981) stated that the structural organisation and tubule morphology was fundamentally the same in both domestic and native equids. Kind (1961) however reported differences both in respect of relative tubule size, and the zonal arrangement of horn tubules between the equine and zebra *SM*.

The functional significance of this zonal organisation of different tubule types within the hoof wall is poorly defined. However if there is a structure-function relationship operating at this level of the hierarchy, then zonal differences are likely to be linked to the functional demands placed upon the hoof wall. Differences in structural organisation are likely to be related to different functional characteristics across and around the hoof wall.

Differences in the zonation characteristics between species may indicate differences in the biomechanical functioning of the hoof, the loading forces placed upon the hoof, the manner in which these forces loads are distributed within the hoof, or the deformational response of the structure to these loads. These issues are discussed in the Section 4.9.

4.8 THE MORPHOLOGICAL APPEARANCE OF THE DONKEY HOOF WALL

Knowledge of the structural organisation and tubular morphology of the *SM* in the donkey is extremely limited. Consequently there has been reliance upon a small number of dated publications most notably the work of Doguer (1943), Tohara (1948) and Hifny and Misk (1983).

Doguer (1943) commented upon the macroscopic appearance of the *SM*, stating that it was divided into an outer 'lighter' region and a 'darker' inner region. This macroscopic appearance differs from that given for the horse by ANON (1994). Tohara (1948) stated that the relative transverse size of the horn tubules of the donkey were larger *sic* 'thicker' than those seen in the horse.

Table 4.4 Zonation of the *Stratum medium* of the equine hoof wall

Author	Methodology Basis of zonation	0% HWD ⟷ 100% HWD		
Nörner (1886) ANON (1994)	Macroscopic Appearance Pigmentation	*Zona pigmentosa*		*Zona nonpigmentosa*
Tscherne (1910) Rössner (1940)	Light Microscopy Staining Characteristics	Outer Zone	Middle Zone	Inner Zone
Nickel (1938a,b, 1939)	Macroscopic Appearance Optical Properties Staining Characteristics	Dark zone	Light zone	Dark zone
		Incl. *SE*	Different refractive indices	Incl. *SI*
Nickel (1938a,b) Schroth (2000)	Light/ Polarised Microscopy Tubule Morphology	Outer Zone Oval ← Round tubules Mainly VFG Tubules	Transitional Region (not to scale) Transitional Morphology	Inner Zone Large round tubules Mainly VSG Tubules
		Pigment if present		Non pigmented
Leach (1980) After Stump (1967)	Light/ Polarised Microscopy Tubule Morphology	Outer Zone Type 3 tubules Oval ← Round	Intermediate zone (not to scale) Transitional tubule forms between Type 2 and 3	Inner Zone Round Tubules Type 2 Tubules Large / Type 1 Tubules Small
Emery *et al.* (1977) Greenough (1982)	Macroscopic Appearance	Outer Zone Small Oval Tubules Wilkens Type	Middle Zone Small Round Tubules Wilkens Type	Inner Zone Large Round Tubules Wilkens Type Zona nonpigmentosa
		Water Line		
Bolliger (1991) After Wilkens (1964)	Light/ Polarised Microscopy Tubule Morphology	Outer Zone Type I tubules - oval ← round IT horn at 45°to Tubule axis	Middle Zone Type I tubules small round	Inner Zone Type II tubules large round
Kasapi and Gosline (1997)	Light/ Polarised Microscopy Tubule Morphology	Region IIIb Large Oval Type III tubules	Region IIIa Small Oval Type III tubules	Region IIb Small Oval Type II tubules
		Region IIa Small Oval Type II tubules	Region Ib Large Round Type 1 tubules	Region Ia Large Round Type 1 tubules
		Variation in tubule morphology across HWD		
		Abrupt Morphology Transitions at Ib/IIa and IIIa/IIIb		

At the microscopic levels Hifny and Misk (1983) reported the presence of 2 distinct tubule forms that varied in respect of cross sectional profile, relative size, and cortical organisation. These were: -

- Large round tubules – characterised by a narrow medulla and a 2 zone cortex comprising an expansive light inner region, surrounded by a narrow dark outer region
- Small oval tubules – characterised by a narrow medulla surrounded by a light cortical region.

These authors concluded that the donkey *SM* could be divided into two distinct zones, based upon the regional distribution of these tubule types, and the relative proportion and visual appearance of the IT horn fraction. This two-fold zonal pattern was characterised by: -

- The Outer Zone – characterised by small oval tubules with a relatively large proportion of IT horn, of 'dark' appearance, with the cross sectional profile of the tubules becoming progressively more elliptical towards the outer aspect of the hoof wall.
- The Inner Zone – Characterised by large round tubules with relatively small proportion of IT horn. IT horn of 'light' appearance

However, the relative dorso-palmar extent of these respective zones was not stated, nor indeed was the location of the zonal boundary detailed.

Recent work including Reilly (1997), Collins *et al.* (1998, 2002), Hopegood (2002), Reilly *et al.* (2003 – Submitted) and Collins and Reilly (2004b – Submitted) have further characterised the organisation of the *SM* of the donkey hoof wall, and challenged the earlier findings of Doguer (1943) and Hifny and Misk (1983).

Collins *et al.* (2002) and Collins and Reilly (2004 – Submitted) have reported the presence of three distinct tubule types in the Donkey *SM*. These were referred to respectively as Donkey Tubule Types 1, 2 and 3 respectively. This three-fold categorisation was based upon cortical cell morphology, with a further sub-division of the Type 3 tubule based upon the cross sectional profile of the tubule. The Type 3a tubule was characterised by an oval cross sectional profile, whilst the Type 3b tubule displayed a circular cross sectional profile (see Figure 4.1).

The Donkey Type 1 Tubule resembled that of the Type III described for the horse by Kasapi and Gosline (1997), whilst the Tubule Types 3a and 3b resembled Kasapi and Gosline's Type I and Type II tubules respectively. The donkey Type 2 Tubule has not been previously reported for the horse.

Figure 4.1 Photomicrographs of Donkey Tubule Types 1, 2, 3A and 3B of the *Stratum medium* of the hoof wall (After Collins *et al.* 2002).

A. Type 1 Tubule.

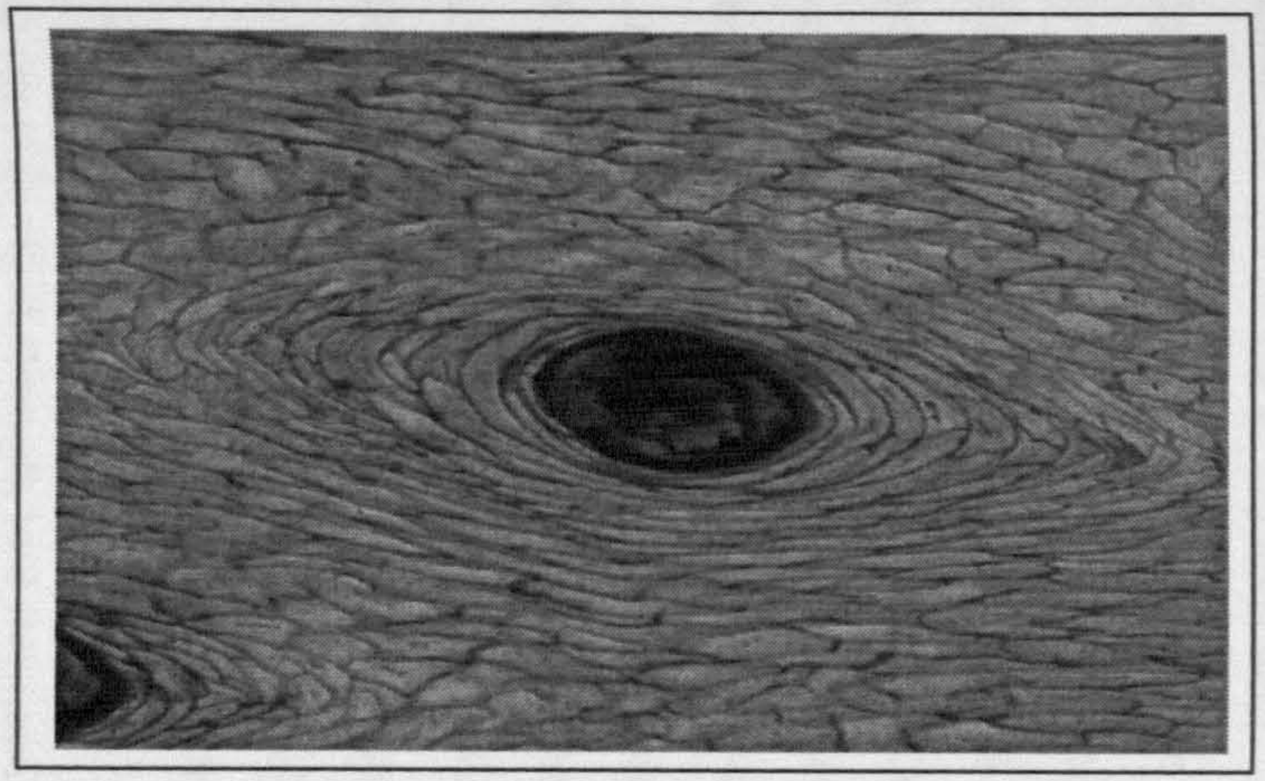

B. Type 2 Tubule

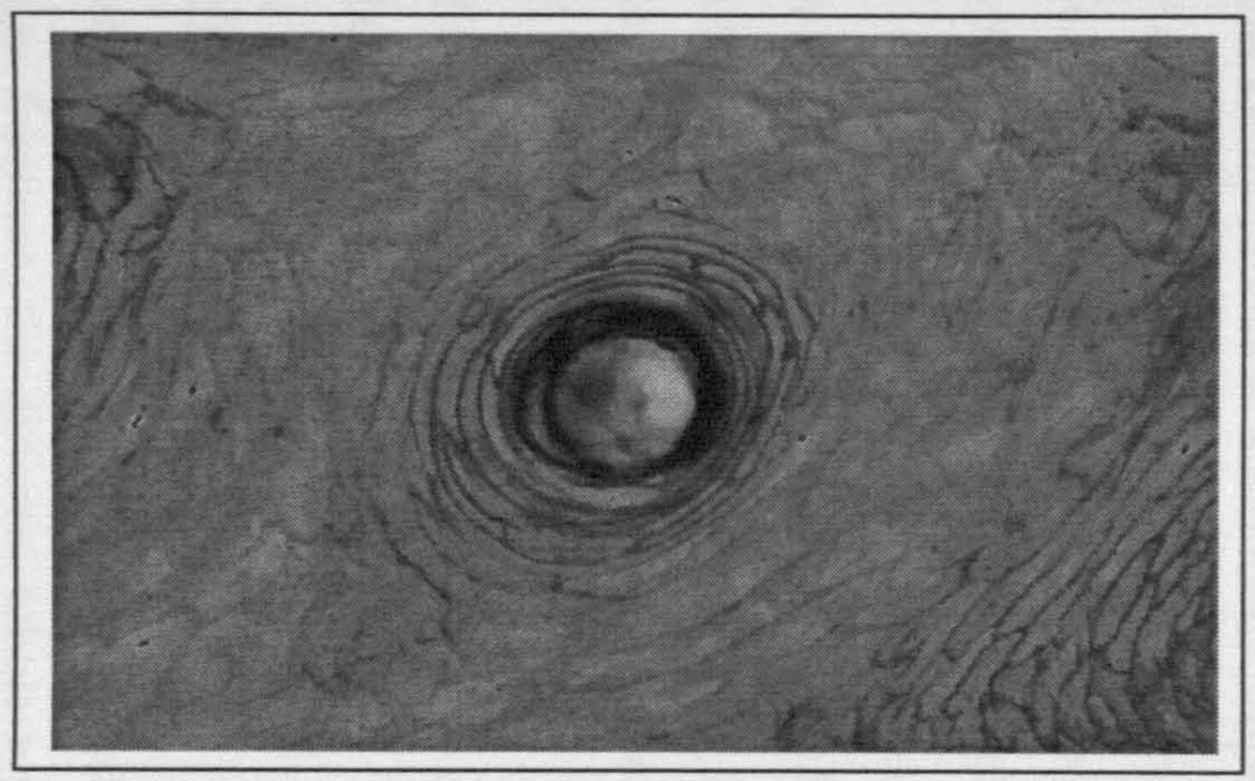

C. Type 3a Tubule.

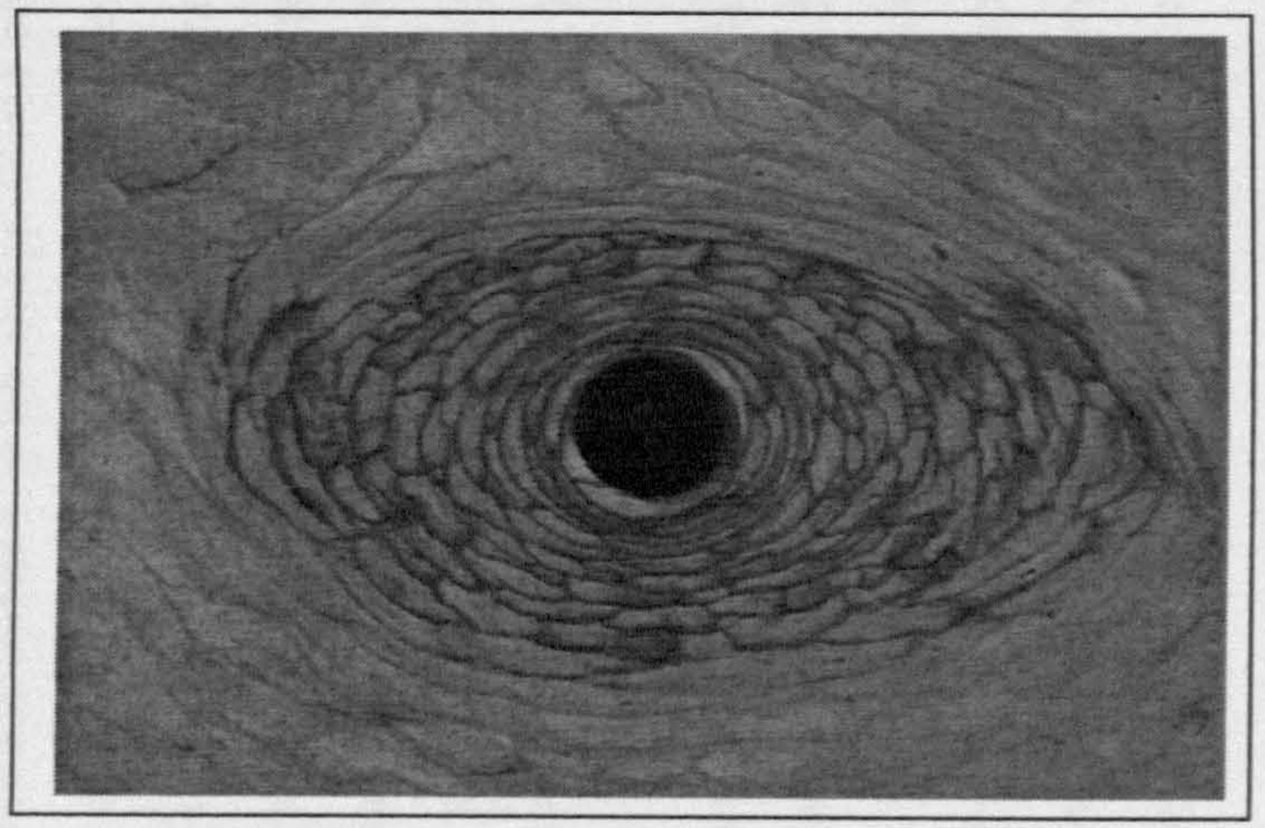

D. Type 3b Tubule.

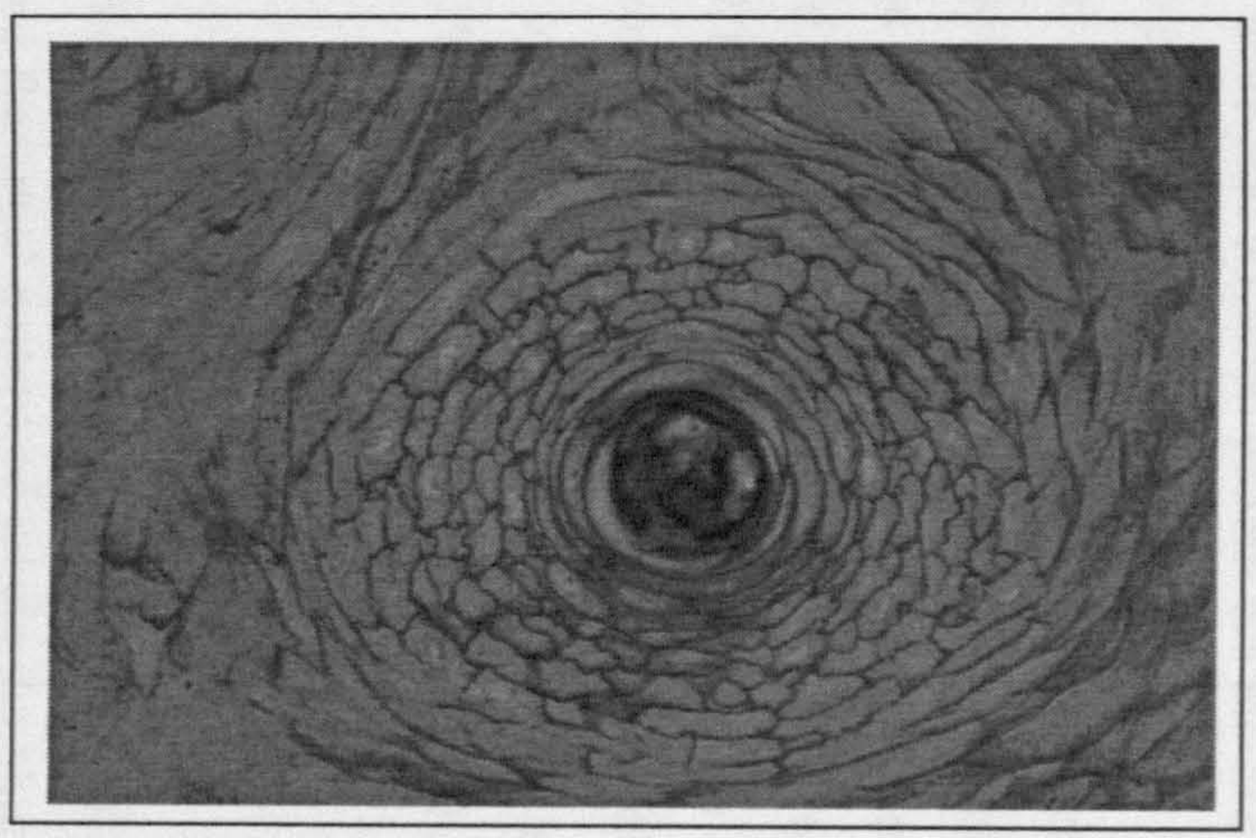

The Donkey Type 1 Tubule resembled that of the Type III described for the horse by Kasapi and Gosline (1997), whilst the Donkey Tubule Types 3a and 3b, resembled Kasapi and Gosline's Type I and Type II tubules respectively. The Donkey Type 2 Tubule has not been previously reported for the horse.

Collins and Reilly (2004a – Submitted) proposed a three-fold zonation pattern for the donkey *SM* based upon the regional distribution of these tubule types across the HWD (see Figure 1.17). This represents a further refinement to that proposed by Hifny and Misk (1983). Collins *et al.* (2002) concluded that these findings highlighted 'species specific' differences in the design hierarchy of the hoof wall between the donkey and the horse. These differences were most evident in the macroscopic appearance of the *SM*, and reflected 'between species' differences in the zonal distribution of tubule types across the HWD. Preliminary work associated with this thesis, Collins (1999 – Unpublished data) indicated zonal boundaries at the MDC of the donkey hoof wall occurred at ~25 and 40% HWD. These zonal boundaries were different to those reported for the horse either by Kasapi and Gosline (1997), or Bolliger (1991), Patan (2001) and König (2001).

4.9 FUNCTIONAL MORPHOLOGY

Considerable debate exists as to the functional significance of the structural organisation of Tu and IT horn fractions, the different tubule types, and the zonal pattern of tubule distribution evident within the *SM* of the equid hoof wall.

Two fundamentally different approaches have been adopted in order to interpret the functional mechanics of the hoof wall. The 'Anatomical approach' has interpreted function in terms of anatomy at the level of the tubule (e.g. Nickel 1938a,b, 1939). This approach has focused upon the micromechanics of hoof wall function. Conversely the 'Materials Science approach', has sought to elucidate the macromechanical functioning of the hoof wall, by attempting to relate anatomy to function at the level of the hoof capsule (e.g. Betram and Gosline 1987). The latter approach is covered within Chapter 5 of this thesis.

Nickel (1938a,b, 1939) stated that the arrangement of Tu and IT horn was of primary functional importance in stress transfer and resilience within the hoof. This author hypothesised that the horn tubules acted as struts, offering axial resistance to vertical compressive forces generated during weightbearing. In this regard, Leach (1980) stated that the horn tubules augmented the rigidity of IT horn, whilst the IT horn fraction maintained mechanical stability within the *SM* (Klema 1937). Leach (1980) argued that this arrangement represented a compromise between the need to provide rigid strength and the need to store energy. However, this author concluded

that the relative importance of the two components, in determining the mechanical properties of the equine hoof wall, remained unknown.

Nickel (1938a,b) argued that differences in the structural morphology of the different tubule types resulted in different micromechanical properties. These functional interpretations however remain an area of considerable scientific debate (Reilly 1995). Indeed, Kasapi and Gosline (1997) stated that the coupling of morphological form and function at micromechanical level has been largely conjectural. In fact Wilkens (1964) argued that it was inappropriate to extrapolate morphology to function in the absence of supportive empirical data.

More recently however, Newlyn *et al.* (1999) and Kasapi and Gosline (1999) have provided objective data that lends support to the Nickel's theory of tubular micromechanics. Newlyn *et al.* (1999) published a theoretical mathematical model of the outer region of the *SM*, which indicated that the structural organisation of the hoof horn material into horn tubules produced a 30% increase in axial resistance to applied load compared to a 'no structure' model – See Chapter 6. This modelled evaluation was subsequently supported by the experimental work of Kasapi and Gosline (1999). These authors reported significant differences in the modulus of elasticity, a measure of axial resistance, between Tu and IT horn fractions, and also between different tubule types across the HWD in the equine hoof.

Bertram and Gosline (1986), Reilly *et al.* (1996, 1998a) and Kasapi and Gosline (1997) have suggested that the structural organisation of the *SM* may also serve to prevent crack propagation. Bertram and Gosline (1986) reported that the fracture behaviour of the *SM* was dominated by crack progression through the IT horn fraction. Hence de-bonding along the Tu/IT interface would act as an effective crack stopping mechanism.

There is little detailed information as the functional significance of zonation within the hoof wall. However, if the structural organisation of Tu and IT horn fraction does indeed determine the biomechanical functioning of the hoof wall, then zonal variations in structural organisation are likely to exhibit different functional characteristics (Reilly *et al.* 1996 1998a, Newlyn *et al.* 1999, 2004 – Submitted).

Ottaway (1955), summarising the earlier work of Nickel (1938a, 1939), argued that the dorso-palmar variations in structural organisation affects the ability of the hoof wall to accommodate 'thrust'. Indeed Rooney (1978, 1980) stated that the zonal organisation within the *SM* was directly related to differences in the nature of the loading forces generated within the hoof wall during weight bearing. Reilly *et al.* (1996) also suggested that this zonal variation determined the manner in which these loading forces were accommodated within the hoof wall, and was responsible for achieving smooth and painless force transfer between the ground and the skeleton.

Kasapi and Gosline (1996) and Reilly *et al.* (1996) have suggested that the *SM* might operate in a manner similar to a multi-laminar ply, with the transition between zones marked by decreased cohesion. Delamination at these zonal interfaces would also serve to absorb energy, and thus provide an additional crack stopping mechanism within the hoof wall.

4.10 POTENTIAL EFFECTS OF THE LAMINITIC CONDITION UPON THE STRUCTURAL ORGANISATION OF THE *STRATUM MEDIUM*

Reilly *et al.* (1998b) argued that structural changes might occur within the *SM* of the equid hoof wall associated with the laminitic condition. The acute phase of the condition is marked by the disruption of the normal blood supply to the foot. This can lead to vascular compromise, tissue damage and degenerative changes within the dermal tissues of the foot. As the metabolic processes associated with hoof horn formation have to be supported by diffusion from the dermis (Leach 1980, Bragulla *et al.* 1992), hoof horn formation may be adversely affected. In fact Hirschberg *et al.* (2001) stated that even minor changes to the dermal microcirculation lead to reactive changes within the overlying epidermis.

The progression of the condition within the laminar region of the foot is also associated with the disruption of the dermo-epidermal junction (Pollitt 1995), and degeneration of the BM (Pollitt 1996, 1998b, Pollitt and Daradka 1998, Johnson *et al.* 1998, 2000). This can lead to the total separation of the epidermis from the dermis. It is not known whether this event occurs within the coronary corium. However Johnson *et al.* (1998) doubted whether BM degradation would be solely restricted to the laminar coria. Indeed papillae separation within the coronary coria has been reported in association with the laminitic condition by Eustace (1992) and Hood (1999a). Degenerative changes within the dermo-epidermal junction of the coronary corium may also adversely affect control and co-ordination hoof horn formation within the *SM*.

The chronic phase of the laminitic condition is marked by the anatomical dislocation of the DP, which initiates the development of secondary pathologies within the foot. These changes, described in detail in Chapter 1, variably include compression of the coronary corium, dorso-palmar stretching of the corium, and reorientation of the dermal papillae. The consequences of these pathological changes upon subsequent horn production, and the structural organisation of the laminitic hoof horn material, are yet to be fully investigated (Reilly *et al.* 1998b). However changes to the gross anatomical appearance of the laminitic hoof capsule indicate alterations to the normal process of hoof horn formation.

Laminitis is widely accepted to result in the production of 'inferior quality' horn, which is incapable of achieving normal hoof function (Bragulla *et al.* 1992, Reilly and Kempson 1992). If hoof wall function is determined by the structural organisation within the design hierarchy,

then structural changes at the microscopic level are to be anticipated in the laminitic hoof wall (Reilly *et al.* 1998b, Collins *et al.* 2002). Similarly changes in normal hoof horn formation and/or force distribution within the laminitic may leave the hoof wall susceptible to deformation changes in structure during weightbearing.

Empirical evidence lends support to this assertion of structural change within the *SM*. For example, Mostafa (1986), Nakade *et al.* (1992) and Said *et al.* (1992) have referred to 'irregularities' in the horn tubules of laminitic equine hoof horn. However details were not given.

Commenting upon the subject of pathological change, Ruldolf Virchow (cited by Ranther 1966) stated that quantitative changes of existing structures are more likely to occur rather than the formation of completely new structures. Hence there is a need to adopt a morphometric approach to ensure an effective characterisation of structural change. This is dependent upon devising appropriate measurements strategies. Given the fact that pathological events are inextricably linked to alterations in normal function, it is appropriate to focus upon those parameters where change is likely to result in functional alteration. These issues are discussed in Section 4.14.

The alteration in hoof horn production associated with the laminitic condition is also marked by changes in the macroscopic structure of the hoof wall. These changes include a dorso-palmar thickening of the hoof wall. This increase in HWD is widely accepted to result from the dorso-palmar elongation of the coronary corium following DP dislocation. This macroscopic change in structure may represent a useful pathognomonic marker for the condition. However this increase in HWD, associated with the laminitic condition has not been objectively assessed.

Variations in HWD may be an important contributor to the structure-function relationships that govern hoof function. This is because the response of a loaded body is dependent not only upon its material properties, but also on the amount of material present. Vincent (1995 – Unpublished data) recorded a linear relationship between equid bodyweight (Bwt) and dorso-palmar HWD, whilst Hopegood (2002) presented an algorithm for the normal donkey that described 85% of variation between HWD at the MDC, and Bwt, where:

$$HWD(mm) = 0.73 + 0.0328Bwt(kg)$$

Thus with prior knowledge of donkey Bwt, the effects of the laminitic condition upon HWD at the MDC can be objectively assessed.

4.11 MORPHOMETRIC CHARACTERISTICS OF THE EQUINE *STRATUM MEDIUM*

It is widely accepted that the *SM* displays an ordered structural organisation at the microscopic level of the design hierarchy, and that the size and shape of the horn tubules vary both around and across the hoof wall. However knowledge of the precise morphometric characteristics of the equine *SM* is limited.

Chauveau (1853) published the first morphometric data relating to the equine hoof wall. This author stated that the cross sectional diameter of the horn tubules ranged in a dorso-palmar direction from 0.02 – 0.4mm. Peuche and Lesbre (1855) reported tubule diameter values ranging from 0.15 – 0.5mm, and marrow diameter values of 0.02 – 0.05mm (Cited by Tscherne 1910).

Whilst the early work of Chauveau (1853) and Peuche and Lesbre (1855) objectively recorded the variation in tubule diameters, it was not until the later work of Tscherne (1910) and Rössner (1940) that a detailed understanding of the morphometric characteristics of the equine *SM* across the HWD was achieved.

These studies measured a series of clearly defined morphometric parameters. These included both linear and area 'feature' specific measurements and 'field' specific characteristics. However the selection criteria for these parameters appeared to have been arbitrary. Similarly Tscherne (1910) and Rössner (1940) detailed the structural organisation of the *SM* at the inner, middle and outer zones, for the dorsal aspect of the hoof wall (MDC), and the quarters and heels respectively. However results were restricted to small sample fields, and to a small number of individuals.

It is only with the recent advent of computer technology that the limitations of these earlier studies have been overcome, and progress made towards achieving a comprehensive morphometric characterisation of the *SM*. Although the recent work of Pellmann *et al.* (1993), Kasapi and Gosline (1997), Mostafa and El-Ghoul (1999), Schroth (2000), Patan (2001), König (2001) and Reilly (2001) have added greatly to the knowledge base, the morphometric characterisation of the equid *SM* is still in its infancy.

There has however been a lack of a unified approach, with different researchers adopting different methods and measurement criteria (See Table 4.5). This has resulted in the emergence of confusing and/or contradictory terminology and modes of reporting data. Consequently direct comparisons 'between studies' are difficult and must be viewed with caution. A standardised methodology and reporting system must therefore be adopted if further progress is to be achieved.

Table 4.5 Summary table of 'feature' and 'field' specific morphometric parameters used to detail the structural organisation of the hoof horn

'Feature' Specific Parameters		
Parameter	**Definition**	**Authors**
Diameter of Tubule or Marrow	The diameter of the specified feature	1, 2, 5, 6
Cortical Thickness	The linear difference between the tubule and marrow diameters. Defined as the linear distance from the marrow cortical boundary to the tubular intertubular boundary measured along the diameter	1, 2, 5
Major axis of Tubule or Marrow	The linear distance of the major axis of the ellipse of the specified feature	1, 2, 4, 7
Minor axis of Tubule or Marrow	The linear distance of the minor axis of an ellipse of the specified feature. Orthogonal to the major axis	4, 7
Max:Min Tubule axes ratio	The ratio of the Maximum to Minimum tubule axes	4, 7
Circumfential axis of Tubule or Marrow	The linear distance of the axis of the ellipse in the medio-lateral plane	4
Radial axis of Tubule or Marrow	The linear distance of the axis of the ellipse in the sagittal plane	4
Tubule Area	Area enclosed by the outer perimeter of the cortex – the tubular intertubular boundary	3, 4*, 5*, 7*, 8*, 9, 10
Marrow Area	Area enclosed by the inner perimeter of the cortex – the marrow cortical boundary	4*, 5*, 7*, 8*, 9, 10
Cortical area	Area enclosed between the marrow cortical boundary and the tubular intertubular boundary	4*, 5*, 7*, 8*, 9, 10
Thickness of Tubule Cortical Lamellae Type	Thickness of the respective Cortical cell subregions in the direction of the max Tubule axis	4
'Field' Specific Parameters		
Parameter	**Definition**	**Author**
Tubule Density	The number of tubules per unit area	1, 2, 3, 6, 7, 9
Quotient of Marrow to Tubule area	Marrow area as a fraction of the total tubule area	5, 9, 10
Marrow to Tubule area ratio/quotient	The ratio of the tubule to marrow area	4, 9, 10
Marrow to Cortex area ratio	The ratio of the tubule to marrow area	7, 8
Quotient of Marrow to Tubule diameter	Marrow diameter as a fraction of the tubule diameter	5
Tubule to Marrow diameter ratio	The ratio of the tubule to marrow diameters	6
Max Marrow axis to Thickness of Cortex	The Max Marrow axis expressed as a quotient of the thickness of the cortex	5
Thickness of Cortex to Max Tubule Axis	The thickness of the cortex expressed as a quotient of the max Tubule axis	5
Tubule Area fraction	The total tubule area as a fraction of the total field area – often expressed in percentage terms	2, 3, 6, 7, 9, 10
IT Area Fraction	The total IT horn area as a fraction of the total field area – often expressed in percentage terms	2, 3, 6, 7, 9, 10
Marrow Area fraction	The total marrow area as a fraction of the total field area – often expressed in percentage terms	6, 9, 10
Cortical Area Fraction	The total cortical area as a fraction of the total field area – often expressed in percentage terms	4 *[1], 6, 9, 10
Surface Density (After Leuenberger and Martig 1979)	The product of the mean tubule area and the number of tubules per unit area (TD)	5

Key: 1. Tscherne (1910) 2. Rössner (1940) 3. Pellmann *et al.* (1993) 4. Kasapi and Gosline (1997) 5. Mostafa and El-Ghoul (1999) 6. Schroth (2000) 7. Patan (2001) 8. König (2001) 9. Reilly (2001) 10. Collins 1997, 1998 – unpublished data
* Derived from first principles *[1] Total Field area – Total Marrow Area

Table 4.6, 4.7 and 4.8 summarises previously reported zonal morphometric characteristics for the equine *SM* at the MDC. A common reporting system has been adopted in order to facilitate a guarded comparison between the respective studies. However no comparative information exists for the donkey despite the apparent 'between species' differences in morphological appearance and zonal organisation described in Chapter1 of this thesis.

Table 4.6 Summary table of the morphometric characteristics of the inner zone of the *Stratum medium* of the equine hoof wall.

Author Method	Breed / Group Site	Tubule (Tu)					Marrow (Ma)			Cortex (Co)		Ma:Tu ratio / quotient	Co:Ma ratio
		Maj axis (μm)	Min axis (μm)	CS Area (μm^2)	Min:Maj Axis ratio	Area Fraction	Maj axis (μm)	CS Area (μm^2)	Area Fraction	Thickness (μm)	Area Fraction		
Tscherne (1910) OM	WB	**385** R: 70-665					**35**			**105**			
Rössner (1940) OM	WB Base Narrow					**47.7**	**60**			R: 60 - 180			
	WB Base Wide					**39.6**	**60**			R: 60 - 180			
Kasapi and Gosline (1997) DT	NS Region Ia	**199**	**193**	**34000**	**1.15:1**		**37.1**						
	NS Region Ib	**240**	**218**	**46000**	**1.19:1**		**38.2**						
Schroth (2000) IAS	CP	**266.5**					**43.3**		**1.8**		**41.1**	**6.2:1**	
	IH	**272.7**					**44.1**		**1.6**		**42.3**	**6.3:1**	
	TB	**272.5**					**43.2**		**1.8**		**41.3**	**6.3:1**	
König (2001) DT	WB	**353** 356.1 R: 112.7-648.4	**269.5** 251.7 R: 95.0-463.2	**79559.5** 66411.0 R: 8228.4-191339.0		**54.0** 57.0 R: 45.0-60.0	**55.2** 53.4 R: 33.7 – 84.5	**1826** 1712 R: 873.9-4817.1					**43.1:1** 46.1:1 R: 30.1 :1 - 47.1 :1
Patan (2001) DT	EP	**283.2**	**187.0**	**35655.4**	**1.3:1**	**51.6**	**45.8**	**1198.0**					**30.3:1**
	WB	**271.3**	**194.11**	**43235.2**	**1.4:1**	**42.7**	**46.7**	**1269.7**					**36.1:1**
Reilly (2001) IAS	P Zone 4			**21920**		**25**		**1634**	**1.5**		**23.5**	1:15.9 6.3%	
Collins* (1998) IAS	SH Zone 1			**39752**		**35.1**		**1272**	**1.15**		**33.9**	1:30.5 3.2%	
	IH Zone 1			**53190**		**31.7**		**1862**	**1.09**		**30.6**	1:28.9 3.5%	

Key: Breed/ Group - WB. Warmblood TB. Thoroughbred EP. *Equus przewalskii* P. Pony CP Connemara Pony. IH. Irish Hunter SH. Slaughter House - mixed breed types Method: OM. Ocular Micrometer DT. Digitising Tablet IAS. Image Analysis System. Figures: NS. Not stated **Bold** = Mean Value. Lower case = Median. R: = Min – Max Range * Unpublished Data. CS cross sectional. *1 Zone 1 material unavailable from distal clippings at MDC sampling site.

Table 4.7. Summary table of the morphometric characteristics of the middle zone of the *Stratum medium* of the equine hoof wall.

Author Method	Breed / Group Site	Tubule (Tu)					Marrow (Ma)			Cortex (Co)		Ma:Tu ratio / quotient	Ma:Co ratio
		Maj axis (µm)	Min axis (µm)	CS Area (µm²)	Min;Maj Axis ratio	Area Fraction	Maj axis (µm)	CS Area (µm²)	Area Fraction	Thickness (µm)	Area Fraction		
Tscherne (1910) OM	WB	**140** R: 70-210					**35**			**70**			
Rössner (1940) OM	WB Base Narrow					**32.7**	**80**			R: 40-120			
	WB Base Wide					**34.0**	**80**			R: 20-80			
Kasapi and Gosline (1997) DT	NS Region IIa	**181**	**121**	**18000**	**1.50:1**		**45.1**						
	NS Region IIb	**204**	**125**	**21000**	**1.62:1**		**47.3**						
König (2001) DT	WB	**256.9** 281.7 R: 99.9-441.9	**158.0** 167.3 R: 66.8-283.2	**34617.2** 38910.8 R: 5927.5-93484.6		**43.0** 40.0 R: 32.0-51.0	**62.9** 63.1 R: 42.9-98.3	**NS** 2232.3 R: 920.4-4846.7					**14.7:1** 15.4:1 R: 8.8-23.4
Patan (2001) DT	EP	**165.5**	**122.1**	**16448.9**	**1.36:1**	**33.53**	**53.8**	**1658.0**					**9.7:1**
	WB	**173.9**	**118.0**	**16818.6**	**1.47:1**	**32.5**	**52.6**	**1457.9**					**10.3:1**
Reilly (2001) IAS	P Zone 3			**13034**		**22**			**3.0**		**19**	1:7.8 13.4%	
	P Zone 2			**10691**		**22**			**4.7**		**17**	1:4.6 21.7%	
Collins* (1998) IAS	SH Zone 3			**25814**		**27.8**		**1856**	**2.0**		**25.8**	1:13.9 7.19%	
	IH Zone 3			**32394**		**30.1**		**1652**	**1.5**		**28.6**	1:19.6 5.1%	
	SH Zone 2			**18666**		**24.1**		**2240**	**2.9**		**21.2**	1:8.31 12.0%	
	IH Zone 2			**27604**		**27.9**		**2898**	**3.3**		**27.9**	1:9.5 10.5%	

Table 4.8. Summary table of the morphometric characteristics of the outer zone of the *Stratum medium* of the equine hoof wall.

Author Method	Breed / Group Site	Tubule (Tu)					Marrow (Ma)			Cortex (Co)		Ma:Tu ratio / quotient	Ma:Co ratio
		Max axis (µm)	Min axis (µm)	CS Area (µm²)	Min;Maj Axis ratio	Area Fraction	Maj axis (µm)	CS Area (µm²)	Area Fraction	Thickness (µm)	Area Fraction		
Tscherne (1910) OM	WB	**210** R: 175-280					N/A R: 35-70			R: 70-105			
Rössner (1940) OM	WB Base Narrow					**51.4**				**60** R: 30-180			
	WB Base Wide					**45.2**				**90** R: 45-135			
Kasapi and Gosline (1997) DT	NS Region IIIa	**237**	**160**	**31000**	**1.50:1**		**54.3**						
	NS Region IIIb	**249**	**125**	**33000**	**1.57:1**		**69.0**						
Schroth (2000) IAS	CP	**156.8**					**47.7**		**3.4**		**27.0**	**3.3:1**	
	IH	**173.9**					**48.5**		**3.5**		**28.9**	**3.6:1**	
	CB	**170.3**					**50.4**		**3.9**		**29.1**	**3.4:1**	
König (2001) DT	WB	**235.0** 242.2 R: 78.2-463.3	**121.5** 125.6 R: 48.6-227.1	**24024.3** 23456.7 R: 3103.1-7857.2		**45.0** 49.0 R: 31.0-54.0	**64.9** 66.2 R: 32.4-116.0	**2118** 1919.9 R: 278.6-7093.2					**10.7:1** 10.2:1 R: 4.8- 14.3
Patan (2001) DT	EP	**147.5**	**80.6**	**10063.7**	**1.9:1**	**33.53**	**62.15**	**1746.5**					**5.1:1**
	WB	**166.0**	**81.2**	**11213.7**	**2.0:1**	**32.5**	**71.6**	**2101.8**					**5.5:1**
Reilly (2001) IAS	P Zone 1			**8976**		**28**		**2088**	**6.4**		**21.6**	1:4.2 23.8%	
Collins* (1998) IAS	IH Zone 1*1												
	SH Zone 1			**15149**		**27.2**		**1833**	**3.3**		**23.9**	1:8.21 12.1%	

Key: Breed/ Group - WB. Warmblood TB. Thoroughbred EP. *Equus przewalskii* P. Pony CP Connemara Pony. IH. Irish Hunter SH. Slaughter House - mixed breed types Method: OM. Ocular Micrometer DT. Digitising Tablet IAS. Image Analysis System. Figures: NS. Not stated **Bold** = Mean Value. Lower case = Median. R: = Min – Max Range * Unpublished Data. CS cross sectional. *1 Zone 1 material unavailable from distal clippings at MDC sampling site

4.12 FACTORS AFFECTING THE MORPHOMETRIC CHARACTERISTICS OF THE EQUINE *STRATUM MEDIUM*

The precise factors that control the morphometric characteristics remain an area of scientific conjecture. A number of specific factors have been variably reported these are summarised in Table 4.9.

4.13 THE EFFECTS OF LAMINITIS ON THE MORPHOMETRIC CHARACTERISTICS OF THE EQUID *STRATUM MEDIUM*

The pathophysiology and anatomical changes that can occur within the foot in association with the development and progression of the laminitic condition have the potential to affect the morphometric characteristics of the *SM* (Reilly *et al.* 1998b, Collins *et al.* 2002).

Changes to these morphometric characteristics are likely to affect the material properties of the hoof wall, and thereby alter the functional capabilities of the hoof capsule (Reilly *et al.* 1998b, Newlyn *et al.* 1999, Collins *et al.* 2002).

If specific structure-function relationships exist, then the degree of functional impairment may be commensurate with the degree of morphometric change. This may also relate directly to the nature and extent of the degenerative changes evident within the afflicted foot, and the severity of the condition. Despite these issues, there is little knowledge of the precise effect of the laminitic condition upon the morphometric characterisation of the equine *SM*.

Hence there is a need to develop an understanding of the interaction between the morphometric characteristics of the SM and the nature and severity of the laminitic insult.

This approach offers several distinct advantages: -

- An unbiased objective means of structural assessment
- A dataset which lends itself to statistical analysis - hence subtle changes can be detected
- The degree of change can be related to the extent of the anatomical change
- The potential to investigate the effect of structural changes upon the material properties of the hoof wall
- The potential to model and predict effects upon the functionality of the hoof and the foot

The work of Mostafa and El-Ghoul (1999) represents the only detailed morphometric assessment of laminitic hoof horn. These authors investigated the effect of grain induced laminitis on the morphometric characteristics of the SM in a controlled trial during the first 75 days of the condition.

Table 4.9 Summary table of reported determinants of the morphometric characteristics of the equine *Stratum medium*

Factor	Summary
Organogenesis and the Morphology of the dermal papilla	Schummer *et al.* (1981) stated • Size and shape of papilla affects degree of horn production and tubule size • Variation in papillae size and shape around and across the coronary corium • Shape of apical tip of papillae varies across / around the coronary corium • Precise control mechanism of supra- and peripapillary horn production unknown.
Location	Tscherne (1910) reported • Variation in morphometric characteristics of the *SM* around / across the hoof wall. • Variations in morphometric characteristics 'within' and 'between' zones.
Species and Breed	Fleming (1871) stated • Warmbloods had larger tubules, and fewer tubules per unit area, c.f. Coldbloods Between species and breed differences noted in the zonal morphometric characteristics previously reported for • *Equus caballus* (König 2001) • *Equus przewalskii* (Patan 2001) • Native Pony (Reilly 2001)
Age	Schummer *et al.* (1981) stated • Tubule size increases with age, and tubule numbers decrease Schoth (2001) reported • Cortical size increases with age, and IT percentage decreases
Body weight (bwt)	Reilly (2001) reported • Significant correlation between bwt and Zone 3 tubule area measurements
Hoof shape	Rössner (1940) reported • Differences in 'field' and 'feature' morphometric characteristics between 'base wide' and 'base narrow' hooves
Depth of Hoof Wall	Rössner (1940) suggested • Potential relationship between morphometric characteristics and HWD. Potential significance to laminitic condition given increase in dorso-palmar wall depth as *sequela* to DP Dislocation
Hoof Quality	Tscherne (1910) reported • 'Poor quality' hoof horn associated with large marrow area • 'Good quality' hoof displays greater cortical thickness Potential significance to laminitis given association of condition with the production of 'poor quality' hoof horn
Nutrition	Speculative presence of nutrition – hoof horn axis (Geyer and Leu 1988, Geyer and Schultze 1994). Dittrich *et al.* (1994) and Reilly (2001) reported • SDs in morphometric parameters following biotin supplementation
Disease Status	Isolated accounts suggest potential link between disease status and morphometric characteristics. Pollitt (1995) reported: • Absence of normal tubular structure associated with digital abscessation Collins (1997) noted: • SD in tubular area sizes and tubular area fraction in laminitic pony horn compared with normal baseline pony data
Season	Patan (2001) and Budras *et al.* (2003a) reported a Seasonal effect on hoof wall morphometric characteristics
Other Potential Factors	Beko (1967), Pflug (1978), Waltz (1979), Pflug *et al.* (1980) and Distl *et al.* (1982) have variably reported that Environment, Housing, and Heredity also influence the morphometric characteristics of bovine hoof wall. Waltz (1979), Pflug *et al.* (1980) and Distl *et al.* (1982) also reported differences between the morphometric characteristics of the hoof wall in the fore and hind limb

These authors reported statistically significant differences in morphometric characteristics between laminitic horses (n = 10) and a control group of 'normal' horses (n=10). The findings of this study indicated significantly lower values ($P<0.05$) in maximum tubule diameter, cortical thickness and the quotient of cortical thickness to maximum tubule diameter for the laminitic group. In addition, significantly greater values ($P<0.05$) were recorded within this group in maximum marrow diameter, quotient of marrow diameter to cortical thickness, quotient of marrow diameter to maximum tubule diameter, marrow area, and quotient of marrow area to tubule area.

No significant difference were recorded in tubule area or surface density between the laminitic and control groups, however there was an apparent trend towards lower values within the laminitic group. Collins (1997) however, recorded significantly lower tubule area measurements and tubule area fraction data in laminitic pony hoof horn compared to normal baseline data for the pony.Mostafa and El-Ghoul (1999) also assessed the variation in morphometric characteristics of the laminitic group over time. Morphometric assessments were performed at Day 1, 2, 6, 10, 20, 30, 40 and 75. However specific details relating to the precise sample site, and the sampling technique employed, were not described.

These authors reported statistically significant findings at Day 2 and 6 including decreases in surface density and cortical thickness, and corresponding increases in marrow and tubule areas, and in the marrow to tubule area quotient. Thereafter these authors described the variation in morphometric characteristics over time was described as:

"……inconstant significant changes ……from 10 to 75 days."

There are however, a number of critical concerns relating to this study. It is unclear whether the analysis represented the full HWD, or a specific dorso-palmar location within the *SM*. One may assume that as these authors compare TD values with those reported by Tscherne (1910) and Rössner (1940) for the inner zone, that their study relates to this region. If this is the case, then the reported mean tubule area measurements of ~3500μm^2 appears to be an order of magnitude lower than other reported values for this zone.

It is also unclear as to why baseline normal data was not obtained from the laminitic group prior to the inducement of the condition. In this way, the respective horses would serve as their own internal controls. Hence this would have removed the need for a separate 'normal' group and would have controlled for potential covariate effects highlighted in Section 4.12 and given in Table 4.9.

With specific regard to the statistical analyses used in this study, it was noted that parametric testing techniques were employed throughout, even for the assessment of restricted data. It is also unclear how accurate sampling of this material over time was achieved, and indeed how it

was possible to accurately discriminate horn production separated by as little as 24 hours. In addition, 'feature' specific morphometry is dependent upon orthogonal sectioning relative to the tubular axis. Conversely contemporaneous growth intuitively follows the curvilinear dorso-palmar profile of the coronary corium. Hence it is unexplained how material prepared in an orthogonal plane can represent a definitive and contemporaneous time frame.

4.14 A MECHANICAL CONSIDERATION OF STRUCTURE AND PARAMETER SELECTION CRITERIA

Effective morphometric characterisation of structure can only be achieved if measurements are performed upon an appropriate series of clearly defined parameters that are of functional significance. Achieving this end represents a key challenge. Section 4.9 emphasised the fact that a considered mechanical approach to parameter selection was required. Only in this way will it be possible to elucidate the structure-function relationships evident within the *SM*. By adopting this approach, morphometric differences associated with specific digital pathologies will potentially be of biomechanical relevance.

Hence there is a need to identify those parameters that are likely to be of biomechanical significance. The structural organisation evident within the microscopic level of the design hierarchy of the *SM* can be assumed to act both at a macro- and micromechanical level. The application of basic engineering principles can, by first approximation, suggest several key measurement parameters that are likely to be of functional significance at the macro- and micromechanical level (Newlyn *et al.* 1999).

It can be argued that the key functional role of the *SM* is that of accommodating and ultimately resisting the forces associated with static and dynamic weight bearing. Hence the ability of the structure to offer axial resistance without excessive deformation or catastrophic failure is of paramount functional importance. In this regard, Newlyn *et al.* (1999) suggested that composite material theory might offer the opportunity to further elucidate the structure-function relationships within the *SM*.

If the *SM* act as a unidirectional fibre composite at the macromechanical level, then its resistance to axial loading will be determined by the modulus of elasticity, and volume fractions, of the respective fibre and matrix phases (see Appendix I). Thus the 'field specific' parameters of the volume fractions of the tubular and intertubular horn represent important structural characteristics at the macromechanical level.

In addition laminate composite theory dictates that difference in axial resistance between laminates will affect the manner in which loading forces are accommodated within the structure. Hence it is essential that volume fraction quantification be performed for each structurally

distinct sub-region. Thus the zonal characterisation of structure across the HWD is vital in order to assess fully the macromechanics of the *SM*.

At the micromechanical level, the functional capabilities of a composite material are affected by 'feature' specific structural characteristics, as opposed to 'field' specific characteristics. These 'feature' specific characteristics govern the precise manner in which loading forces are accommodated within the structure, and significantly affect potential modes of failure of the structure.

As the hoof wall is subject to compressive forces, its ability to resist buckling is of primary importance with regards to 'likely mode of failure' (see Appendix I). Resistance to buckling is dependent upon the amount of material resisting the axial load. The critical Euler buckling load in a strut of given length is proportional to the square of the minimum cross sectional dimension. Hence the absolute value of the minimum cross sectional tubule axis will be of critical functional importance within the *SM*. If however, the horn tubules posses a medullary cavity, then resistance to Euler buckling will be dependent both upon the thickness of the cortex, and also the distribution of the cortical material with respect to the central axis of the tubule. Thus the marrow and tubule diameters constitute important measurement parameters, as these collectively define the limits from which the second moment of area (I) of the cortical material is calculated. The second moment of area represents the 'effective' distribution of the material within a hollow tube (Vincent 1992).

Failure by local buckling however is independent of I, and is solely dependent upon the thickness of the cortex.

Buckling theory also suggest that the size and shape of the tubules are of importance in terms of stress concentration within the structure. Hence the major to minor axis ratio, and the cross sectional area of the respective horn tubules may also be of functional significance

The presence of voids within a material leads to the development of stress concentration at the material/void interface during loading. This is of particular relevance with regards to crack initiation and propagation. A measure of the void space within the structure therefore represents another potentially important morphometric characteristic. Indeed the fundamental engineering issues raised by the presence of medullary cavities may account for the apparent relationship described by Geyer and Leu (1988), Geyer and Schulz (1994) and Zenker et al. (1995), that 'poor quality' hoof horn is characterised by the presence of enlarged marrows.

4.15 DETERMINATION OF VOLUME FRACTION DATA FROM TWO-DIMENSIONAL PLANIMETRY OF HISTOLOGY SECTIONS

Morphometric evaluation of the *SM* by planimetry can only provide area fraction data of specific morphological features. However the Delesse principle states:

Σ Area of Feature / Total Sampling Area = Σ Volume of Feature / Total Sampling Volume

Hence area fraction data obtained in this way, will equate to the corresponding volume fraction of the measured feature. Thus it is possible to compute the volume fraction of a specific feature within a body from the two-dimensional assessment of histology sections.

4.16 SELECTED PARAMETERS OF STRUCTURE WITHIN THE *STRATUM MEDIUM*

Based upon the biomechanical considerations discussed in Section 4.9 and 4.14, and the stereological considerations outlined in Section 4.15, a series of direct and derived area and linear morphometric parameters were adopted. These parameters, which are detailed in Table 4.10 and Table 4.11 along with their selection criteria, were considered to be of primary importance for the elucidation of the structure-function relationships within the *SM*. The 'field' and 'feature' specific parameters formed the basis for a comprehensive characterisation of structure in transverse section. In summary these parameters were: -

- Area fraction of the Tu and IT horn
- Area fraction of the cortical and marrow horn components
- Absolute cross-sectional area measurements of the horn tubules and their respective cortical and marrow horn components (referred to as the absolute area of the specified morphological feature)
- Major and minor axes of the horn tubules
- Ratio of the major: minor tubule axes
- Marrow axes
- Quotient of marrow to tubule area

4.17 RATIONAL

In order to evaluate the structure-function relationships at the microscopic levels of the design hierarchy in the *SM* of the Donkey hoof wall there is a need to conduct a comprehensive morphological appraisal of the *SM*. There is specifically a need to: -

- Objectively characterise the different tubule types
- Detail their respective distribution within the *SM*
- Assess the appropriateness of zonation based upon morphological variation

With this in place, it will be possible to: -

- Establish similarities/differences in the structural organisation of the *SM* between the donkey and other equids
- Objectively assess the association between the nature and extent of the DP dislocation and the structural organisation of the *SM*
- Investigate the associations between specific morphological characteristics and material properties, and moisture levels
- Identify an appropriate basis for further investigating dorso-palmar variations in these material properties and moisture levels
- Provide baseline data so that the macro- and micromechanical functioning of the *SM* can be further investigated through computer modelling techniques

Table 4.10 Direct and derived area morphometric parameters of the structural organisation of the *Stratum medium* in transverse section.

'Field' Specific Parameters		
Parameter	**Definition**	**Selection Criterion**
Sampling Area	Total area of sampling field corrected for 'edge' effects	Prerequisite for the calculation of all area fraction data
TuAF Tubular Horn Area fraction	Sum total of tubular horn cross sectional area expressed as a fraction of the total area of the sampling field	Provides axial resistance during weightbearing (Nickel 1939, Rooney 1978, 1980) Important determinant of hoof function Required to determine volume fraction of fibre phase of the *SM* Required for macromechanical modelling of material performance
ITAF Intertubular Horn Area fraction	Total area of intertubular horn expressed as a fraction of the total area of the sampling field	Provides mechanical stability within the hoof wall (Klema 1937, Schummer *et al.* 1981) Required to determine volume fraction of matrix phase of the *SM*
MaAF Marrow Area Fraction	Sum total of medullary cross sectional area expressed as a fraction of the total area of the sampling field	Provides measure of %voidage within the *SM* Required to determine volume fraction of load bearing component of the fibre phase Required for micromechanical modelling of *SM* as voids with a material act as a potential 'stress raiser' (Wainwright *et al.* 1976)
CoAF Cortical Area Fraction	Sum total of cortical horn cross sectional expressed as a fraction of the total area of the sampling field	Believed to be an important determinant of hoof function (Geyer 1980, Pellmann *et al.*1993) Measure of the load bearing component of the fibre phase Required for macromechanical modelling of material performance
'Feature' Specific Parameters		
Parameter	**Definition**	**Selection Criterion**
TuArea Absolute Cross Sectional Area Measurement of the Horn Tubule	Cross sectional area of the horn tubule	Essential baseline characteristic (Hofstetter 1985) Defines the size of the individual horn tubules Important contributor to hoof wall function (Bragulla *et al.* 1992, Pellmann *et al.* 1993) Important determinant of micromechanical performance (Newlyn *et al.* 1999)
MaArea Absolute Cross Sectional Area Measurement of the Marrow of the Horn Tubule	Cross sectional area of cortical component of the horn tubule	Essential baseline characteristic (Hofstetter 1985) Defines size of void within the horn tubule Important determinant of micromechanical performance due to 'stress raiser' effects (Leach 1980)
CoArea Absolute Cross Sectional Area Measurement of the Cortex of the horn tubule	Cross sectional area of the marrow component of the horn tubule	Essential baseline characteristic (Hofstetter 1985) Defines area of loadbearing component of the horn tubule Important determinant of micromechanical performance (Newlyn *et al.* 1999)
Ma:Tu(%) Marrow to Tubule Area Quotient	Absolute marrow area expressed as a percentage of the horn tubule	Intuitive descriptor detailing the marrow to tubule relationship (Collins 1997, Reilly 2001) Measure of marrow size relative to horn tubule size Enlarged marrows associated with 'poor quality' hoof horn (Geyer 1980, Geyer and Schulze 1994)

Table 4.11 Direct and derived linear morphometric parameters for the transverse profile of the horn tubule.

'Feature' Specific Parameters		
Parameter	**Definition**	**Selection Criterion**
Tu(MA) Major Axis of the horn tubule	Absolute linear measurement of the major axis of the horn tubule	Baseline characteristic of the horn tubule Important descriptor of cross sectional size
Tu(MI) Minor Axis of the horn tubule	Absolute linear measurement of the minor axis of the horn tubule	Baseline characteristic of the horn tubule Important descriptor of cross sectional size
Tu(MA:MI) Major to Minor Tubule Axis Ratio	Ratio of the major to minor axes of the horn tubule	Baseline characteristic of the horn tubule Key descriptor of cross sectional shape Important for micromechanical modelling of the *SM*
Ma(MA) Major Axis of the Marrow	Absolute linear measurement of the major axis of the marrow component of the horn tubule	Required to determine cortical thickness Important descriptor for defining the distribution of cortical material relative to tubular axis in the direction of the minor tubule axis. Parameter affects *I* (Second moment of Area) of a column. Important for Euler 'buckling effects' (Vogel 1988)
Ma(MI) Major Axis of the Marrow	Absolute linear measurement of the major axis of the marrow component of the horn tubule	Required to determine cortical thickness Important descriptor for defining the distribution of cortical material relative to tubular axis in the direction of the minor tubule axis. Parameter affects *I* (Second moment of Area) of a column. Important for Euler 'buckling effects' (Vogel 1988)
Tu:Ma(MA) Tubule to Marrow Major Axis Ratio	Ratio of the major tubule to marrow axes of the horn tubule	Important determinant of hoof wall function
Tu:Ma(MI) Tubule to Marrow Minor Axis Ratio	Ratio of the minor tubule to marrow axes of the horn tubule	Important determinant of hoof wall function
Co (MAT) Cortical thickness (Major Axis)	Cortical thickness in the direction of the major axis of the horn tubule Half the linear difference between the major axis of the horn tubule and the marrow	Descriptor of wall thickness of the horn tubule Important for Euler and local 'buckling effects' (Wainwright *et al.* 1976, Vogel 1988)
Co (MIT) Cortical Thickness (Minor Axis)	Cortical thickness in the direction of the major axis of the horn tubule Half the linear difference between the minor axis of the horn tubule and the marrow	Descriptor of wall thickness of the horn tubule Important for Euler and local 'buckling effects'

4.18 AIMS

The aims of this chapter were to: -

- Assess the morphological characteristics of structure within the *SM* of laminitic donkey hoof horn at a precisely defined anatomical location within the MDC sampling site
- Determine the morphometric characteristics of the structural organisation of the *SM* of laminitic donkey hoof horn.

  Specifically to measure by direct means: -

  – Area fraction of the Tu and IT horn, and the marrow and cortical components
  – Absolute area of the horn tubules, and the marrow and cortical components
  – Major and minor axes of the horn tubules
  – Major and minor marrow axes

  To Derive, by indirect means: -

  – Area fraction of the cortical horn components
  – Absolute area of the cortical horn components
  – Cortical thickness in the direction of the major and minor tubule axes
- Define the zonal morphometric characteristics of structure of laminitic donkey hoof horn at this site
- Explore the empirical relationship between nature and extent of DP dislocation and morphometry by investigating the effect of 'group' upon zonal morphometric characteristics
- Explore the effect of Age and bodyweight upon these characteristics
- Obtain baseline data to further explore the functional morphology of laminitic donkey hoof horn

4.19 MATERIALS AND METHODS

4.19.1 HOOF WALL MORPHOLOGY

An initial morphological appraisal was conducted, as part of the preliminary stage of the experimental phase of thesis, to establish the dorso-palmar variation in the morphological appearance of the *SM* of the laminitic donkey hoof wall. This was performed on histology sections prepared from the MDC sampling site at 50% HWH, as described in Chapter 2. In particular, this assessment documented the morphological appearance of the horn tubules of the

SM, the regional distribution of different tubule types, and described irregularities in structure within the *SM* of the hoof wall. Irregularities in structure were defined as a structural organisation that did not conform to the recognised or 'accepted' organisation of tubular and intertubular horn as described by Collins and Reilly (2004a – Submitted). This preliminary appraisal was conducted on histology sections obtained from the left forefoot of 9 randomly selected laminitic donkeys, which had been euthanased on medical grounds.

4.19.2 HOOF WALL MORPHOMETRY

With the preliminary morphological appraisal completed, the tubule types established and the zonal pattern of the *SM* established, the morphometric characterisation of structure could be initiated.

A three stage semi-automated method was developed that provides both 'feature' specific and 'field' specific data for the *SM* of hoof wall. This included absolute dimensional measurements of marrow, cortex and tubule, and area fraction information for the tubular and intertubular components and marrow to tubule ratio.

Images of AB-PAS stained sections were captured in 8-bit greyscale to produce images in 256 grey scale. Preliminary trials revealed that, in common with many biological materials, there was insufficient grey scale contrast between the structural features to permit automated object discrimination. Consequently a manual segmentation approach was employed to overcome this limitation.

However, there was an inherent problem with such an approach. In order to be able to define accurately the structural features of the hoof wall high power magnification was required. The decision to use powerful objectives meant that the number of features within a given field of view was reduced. A compromise therefore has to be reached between magnification levels required to permit feature discrimination and feature numbers required for the sample to be considered representative of the structure. Initial image acquisition was performed with a 4 x objective and a 3.3 x photo-eyepiece. This combined with a 1.25 x gain arising from the configuration of the trinoccular microscope head, resulted in a total magnification of ~20 x.

4.19.2.1 PIXEL CALIBRATION OF THE IMAGE ANALYSIS SYSTEM

The image analysis system was calibrated with respect to the total magnification using the captured image of a stage micrometer. A pixel count of a known micrometer distance was made both in the horizontal (x) and vertical (y) direction. This enabled two important calibration calculations to be carried out. These were firstly the pixel count per unit length and secondly,

the aspect ratio. The aspect ratio is the ratio between the pixel count per length in the x-direction compared to that in the y-direction.

4.19.2.2 CORRECTION PROCEDURE FOR VARIATION IN LIGHT INTENSITY

As uniform illumination is recognised to be an important determinant in accurate boundary definition, a 'blank field' capture was performed. The resultant image was considered to represent uniform white light. All subsequent images are then displayed in 256 grey scale relative to this baseline level of illumination. In this way it was possible to control for any inherent variation in light intensity within the microscope, and also the effects of ambient lighting.

4.19.2.3 REPRESENTATIVE SAMPLING

An inherent problem exists with regards to morphometric characterisation. In order to be able to accurately define the tubule boundary, high power magnification is required. However, by using high power objectives, it is not possible to capture the full HWD of each zone within the field of observation.

Therefore, an effective method of representative sampling was sought that would provide an accurate defined and repeatable sampling location within each respective zone. It was decided to sample at the midpoint of each respective zone as determined by tubule type at a total image magnification of x 20.

ESTABLISHING THE POSITION OF 0% HWD AT THE MDC

The MDC marker at the dorsal margin of the hoof wall section was aligned with the cross hair of the ocular graticule. Thereby centring the section within the field of view, with the plane of the MDC registered in the y-direction of the microscope stage. This position was regarded as 0 %HWD, and marked the dorsal boundary of Zone 1. The position of the slide in the y-direction was recorded directly from the vernier scale of the microscope stage.

DETERMINATION OF THE ZONE 1 SAMPLING SITE

The section was moved in the y-direction until the cross hair of the graticule was aligned with the first Type 3b Tubule. This was regarded as marking the boundary between Zones 1 and 2. The corresponding position of the microscope stage was recorded from the vernier scale. The midpoint of Zone 1 was therefore calculated as 50% of the total distance travelled by the microscope stage in the y-direction.

DETERMINATION OF THE ZONE 2 SAMPLING SITE

The section was moved in the y-direction until the cross hairs of the ocular graticule were aligned with the first Type 2a Tubule. This position was considered to mark the Zone 2/3 boundary. The position of the microscope stage was once more recorded and the mid-zonal sampling site determined as 50% of the y-directional travel from the Zone 1/2 boundary.

DETERMINATION OF THE ZONE 3 SAMPLING SITE

The slide was moved in the y-direction until the cross hairs of the ocular graticule were aligned with the apical tip of the dermal lamellae. This position was regarded as 100 %HWD, and marked the palmar boundary of Zone 3. The zonal mid-point was determined as 50% of the distance travelled from the Zone 2/3 boundary to the 100 %HWD boundary.

In this manner described above the midpoint sampling sites for Zones 1, 2 and 3 were established. This procedure enabled accurate and repeatable mid-zonal sampling between individuals. The stage was moved in tern to each of these three respective sampling sites, by direct reference to the vernier scale of the microscope stage prior to image capture.

DETERMINATION OF THE DORSO-PALMAR DEPTH OF THE *STRATUM MEDIUM*

The total distance traved by the microscope slide in the y-direction from the 0% HWD reference point to 100 % HWD reference point was recorded from the vernier scale of the microscope stage. This linear distance, which represented the dorso-palmar depth of the *SM,* was referred to as the HWD of the sample.

4.19.2.4 IMAGE CAPTURE WITHIN EACH ZONE

A similar balance has to be struck between the ability to accurately define the morphological boundaries of the tubular horn components and attaining an acceptable number of horn tubule measurements. Two distinct approaches are possible. These are: -

- Low magnification image capture with subsequent boundary enhancement through image processing (as adopted by Reilly 2001)
- High magnification image capture with subsequent image tiling and minimal image processing

The latter option was adopted in this thesis. The specific protocol for each respective zone reflected the significant variation in absolute tubule size evident between zones.

In this regard, 2 sequential images in the x-direction were obtained in respect of both Zones 1 and 2. However in Zone 3, a 2 x-direction by 2 y-direction series of sequential fields were produced, with the y-directional images attained palmar of the mid-zonal site. The resultant

images were captured and 'stitched' to produce a 2x1 image montage for Zones 1 and 2 respectively and a 2x2 Image montage for Zone 3.

4.19.2.5 MORPHOMETRIC ANALYSIS

The captured images were imported into the NIH-Image program and subsequently analysed through the computer interface. Images were processed and enhanced prior to analysis in order to improve edge detection, thereby aiding manual discrimination. A standardised procedure of image processing was adopted to ensure consistency of operation. Such consistency is a vital prerequisite for accurate 'between sample' comparisons (Weibel 1979, Russ 1992). The image processing procedure involved passing the captured image through a 'Smoothing' operation once, and then a single 'Sharpening'. Having completed this process a three-stage analysis was initiated (see Figure 4.2A-D).

STAGE 1 MARROW DISCRIMINATION

The internal margin of the tubule was used to delimit the tubule marrow/medullary cavity. Discrimination of the marrow was achieved by outlined this margin using the free hand drawing tool. The enclosed area was then 'shaded' by allocating an arbitrary grey value (see Figure 4.2 B). The resultant image was segmented, using the 'Density Slice' processing function, to leave only areas possessing the grey scale value selected in the shading process for further analysis and measurement. The resultant image contained not only the desired 'true particles' *i.e.* the medullary features, but also other false particles of the same grey value. Two methods of image editing were employed in order to remove these 'false particles' and achieve successful segmentation prior to measurement. Firstly, particle discrimination limits were set such that only objects measuring between 99-9999 pixel units were selected. The 'true particles' were then numbered using the labelling option in preparation for measurement and a copy of this image was stored on hard disc, prior to measurement.

STAGE 2 TUBULE DISCRIMINATION

The outlining procedure was repeated for the external tubule margin but in this case the cortico-intertubular interface was not readily discernible. Those cells whose margin arched around the tubule were considered to be cortical, whereas those cells whose margins arched away from the tubule were adjudged to be intertubular horn. On this basis, the tubules were delimited. Once this had been completed for each tubule, the object was shaded as for the marrow. Similar segmentation and discrimination procedures to Stage 1 were adopted to separate 'true' from 'false particles' prior to labelling (see Figure 4.2C).

STAGE 3 TOTAL AREA DETERMINATION

The total area of the image was calculated by outlining the perimeter of the image taking into account edge effects. Only those tubules that completely fell within the image were considered as 'true particles'. Part tubules at the edge of the field of view were excluded from the measurement process, being considered as 'false particles'. The enclosed area was shaded and labelled as described previously (See Figure 4.2D). It is important to note that these edge effects result in an over estimation of the intertubular horn area fraction, as it is not possible to quantify the area of intertubular horn associated with the part tubules.

MEASUREMENT

Measurement criteria were selected to include area measurements, and lengths of the major and minor axes, of the discriminated/labelled features. Having previously established pixel calibration criteria, all measurements were automatically converted to μm^2 and μm respectively for the axes and area. Having established the marrow and corresponding tubule measurements, the cortical values were obtained by difference. The resultant data were stored for subsequent analysis. In this way, a 'field' specific, and 'feature' specific objective assessment of hoof horn structure was possible to provide a macroscopic and microscopic structural characterisation of the *SM*.

Figure 4.3 summarises the procedure for 'field' specific, area fraction determination of the hoof horn components within the *SM* of the hoof wall, based upon this image analysis technique. Conversely Figure 4.4 gives a diagrammatic representation of the direct 'feature' specific area and linear measurement parameters of horn tubule structure.

SEMI-AUTOMATION

Following the successful development of this technique a 'macro' program was designed to automate the image editing and measurement procedures, after the initial manual discrimination of the structural components.

Figure 4.2 Summary of the three-stage image analysis process for the determination of marrow, tubular area measurements and marrow tubular and intertubular horn Area Fraction data.

Sample Field Montage (A)

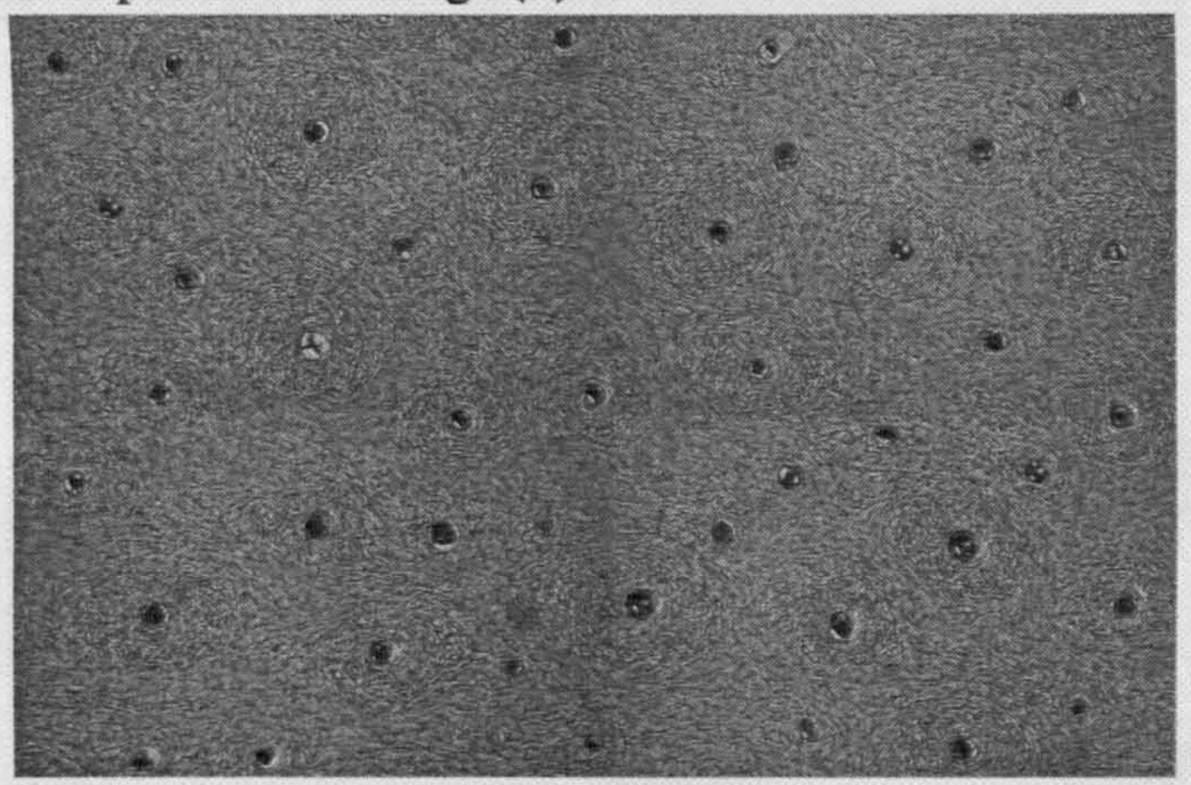

Stage 1 Marrow Discrimination (B)

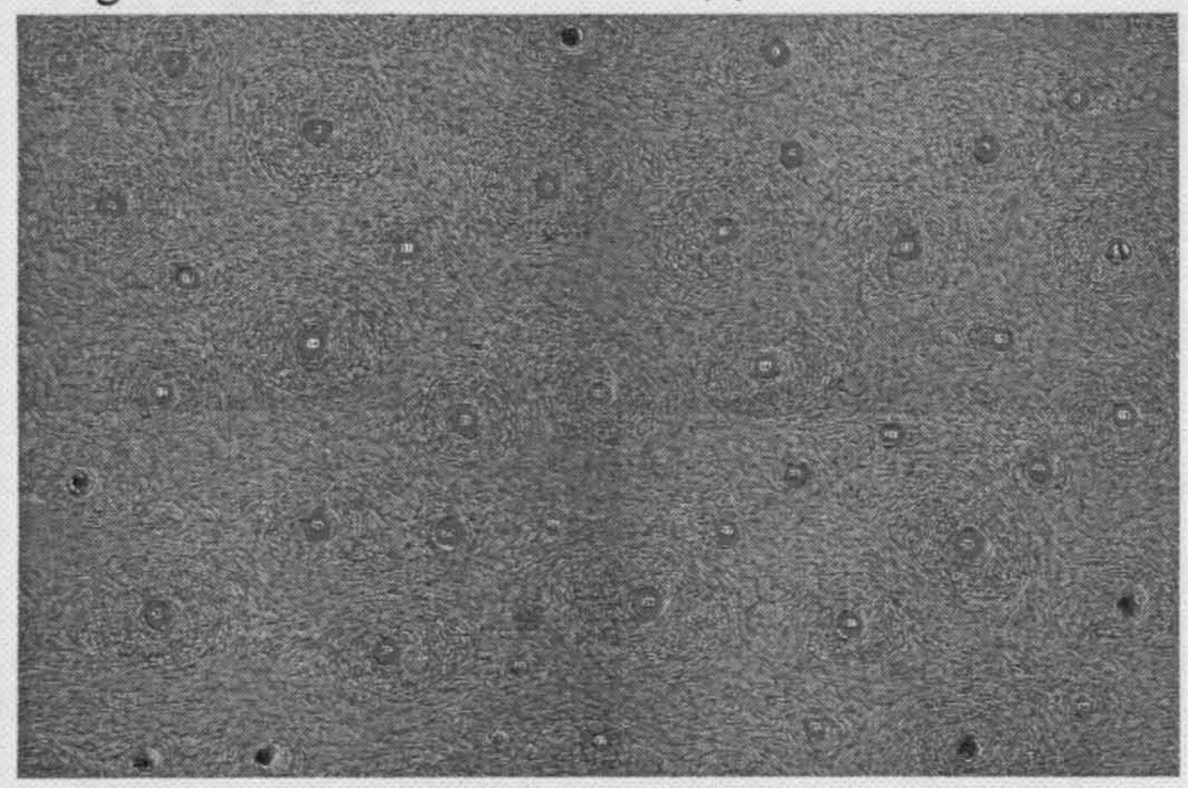

Stage 2 Tubule Discrimination (C)

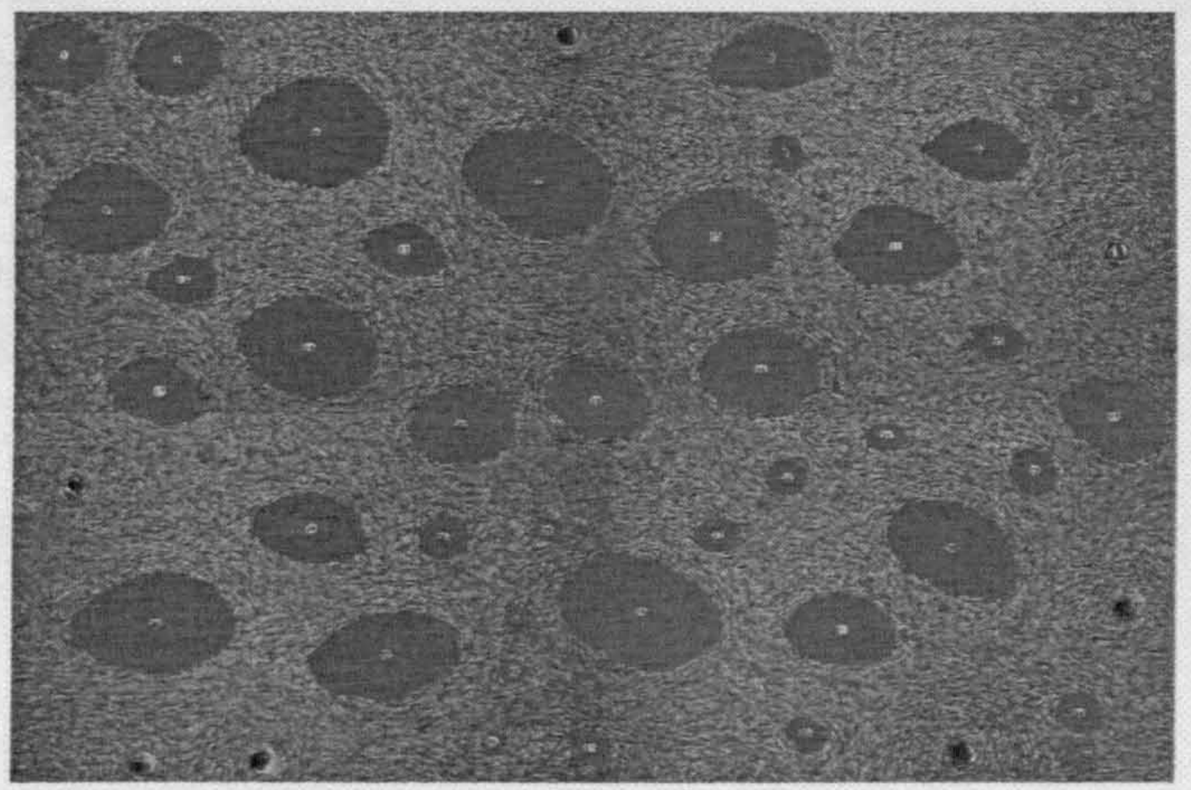

Stage 3 Total Area Determination (D)

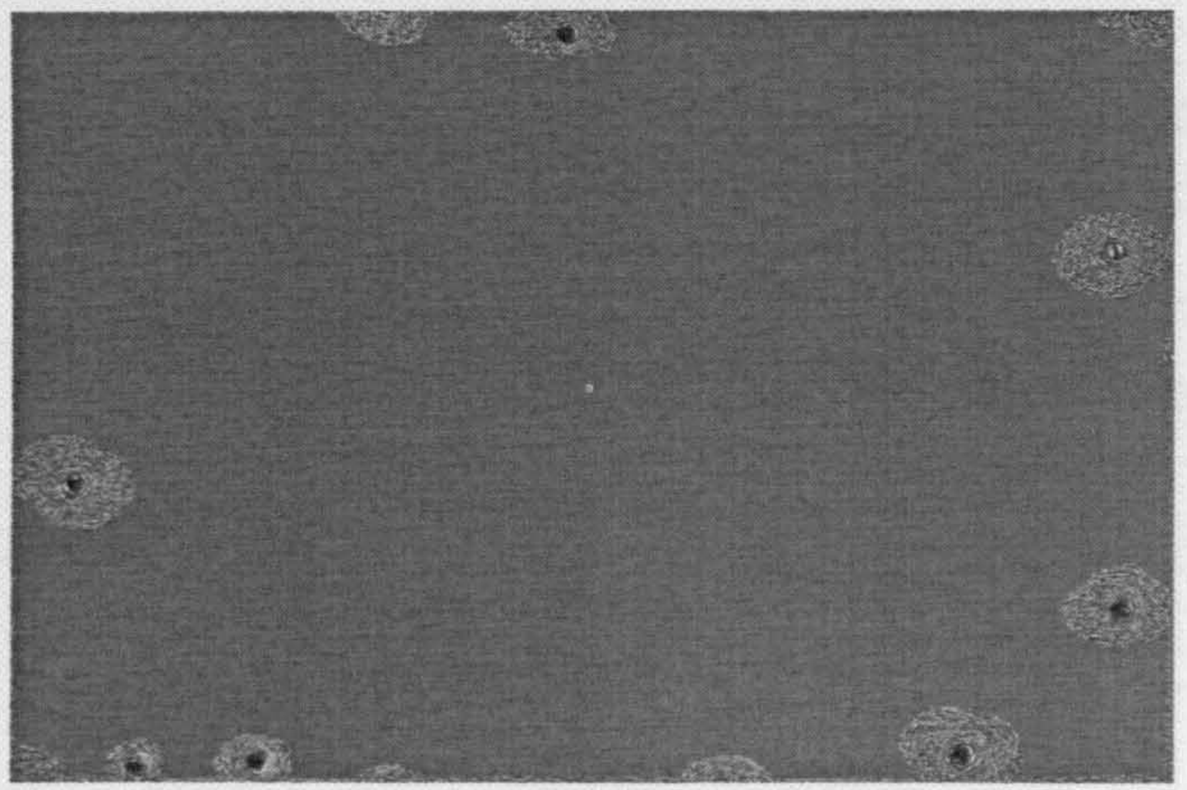

Figure 4.3 Diagrammatic representation of direct and derived 'feature' specific area measurements (modified after Reilly 2001).

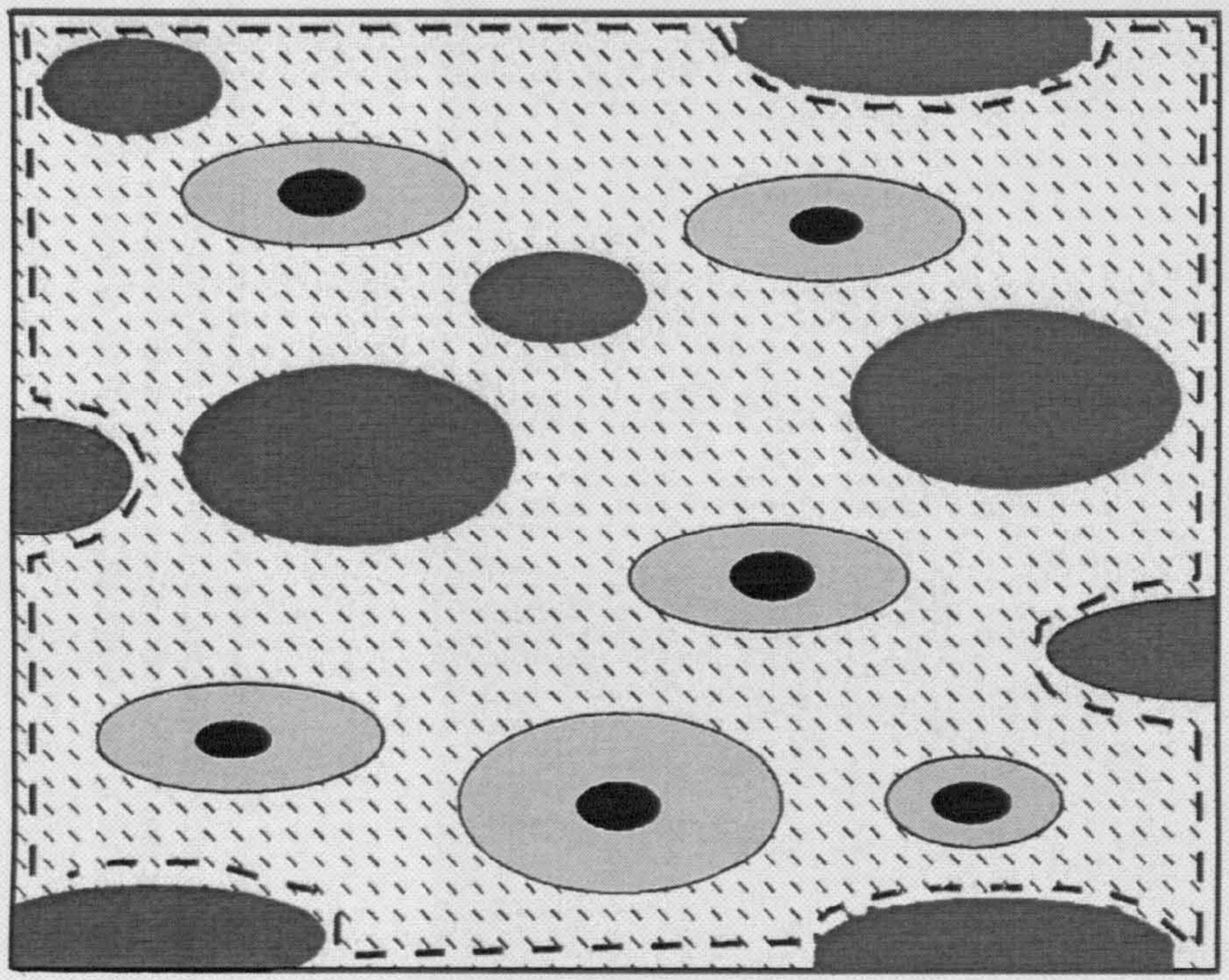

For zone .....

Σ ● Within Boundary = Marrow Area Measurement

Σ ● Within Boundary = Tubule Area Measurement

Σ ● Within Boundary = Cortical Area Measurement

$$\frac{\Sigma \bullet \text{ within boundary}}{\text{Total area within boundary}} = \text{Marrow Area Fraction}$$

$$\frac{\Sigma \bullet \text{ within boundary}}{\text{Total area within boundary}} = \text{Tubular Horn Area Fraction}$$

$$\frac{\Sigma \bullet \text{ within boundary}}{\text{Total area within boundary}} = \text{Cortical Area Fraction}$$

$$\frac{\Sigma \bullet \text{ within boundary}}{\text{Total area within boundary}} = \text{Intertubular Horn Area Fraction}$$

Marrow Cortex Tubular Horn Intertubular Horn

Figure 4.4 Direct area and linear 'feature' specific parameters of horn tubule structure

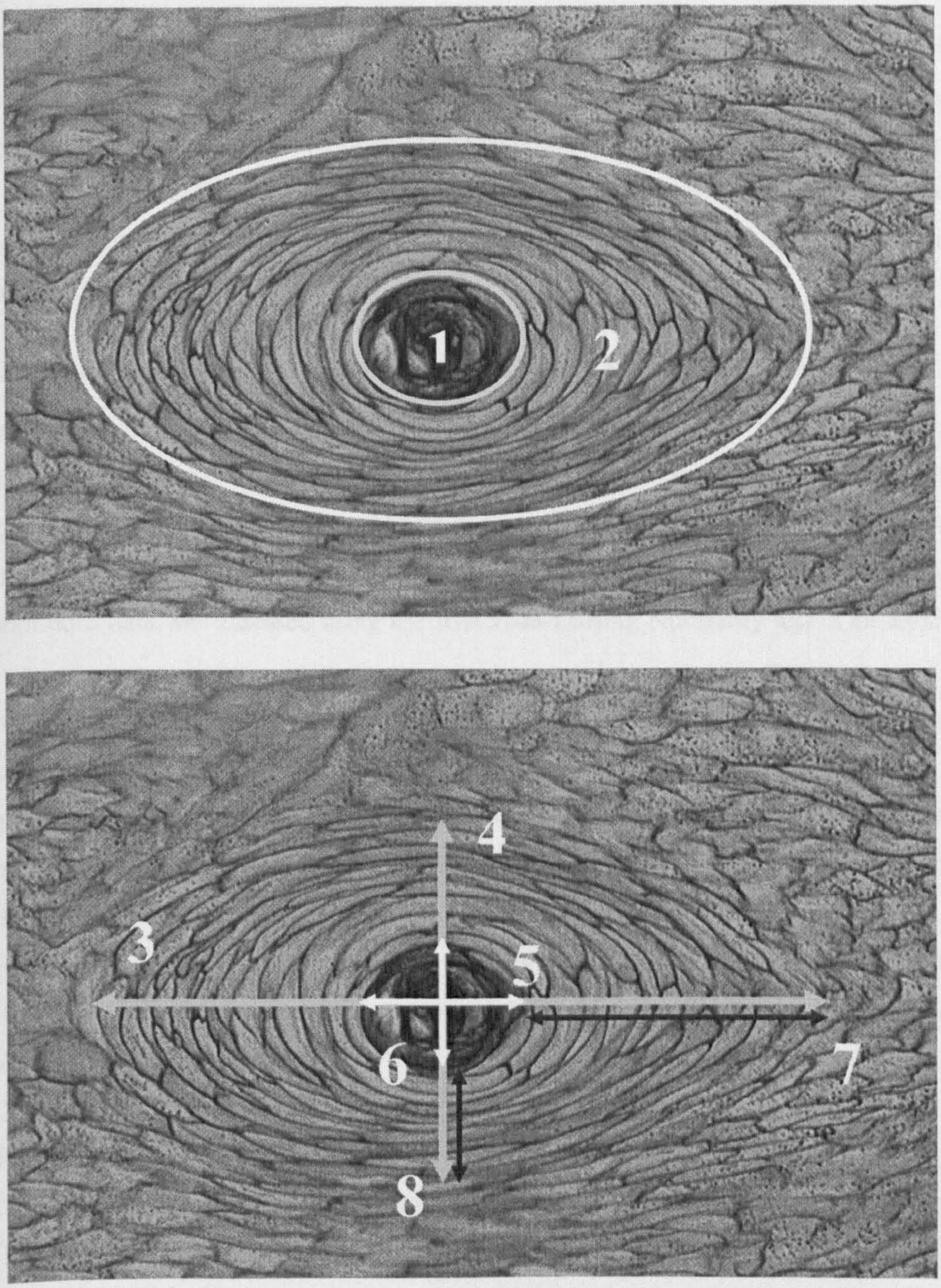

Key: 1, Marrow Area measurement. **2**, Tubule Area Measurement. **3**, Major axis of the horn tubule, Tu(MA). **4**, Minor axis of the horn tubule, Tu(MA). **5**, Major axis of the marrow, Ma(MA). **6**, Minor axis of the marrow, Ma(MI). **7**, Cortical thickness in the direction of the major axis of the horn tubule, Co(MAT). **8**, Cortical thickness in the direction of the major axis of the horn tubule, Co(MIT).

4.19.3 MORPHOMETRIC CHARACTERISATION OF MATERIAL DERIVED FROM THE MAIN EXPERIMENTAL PHASE OF THE PROJECT

A morphometric characterisation was performed on the samples originating from the main experimental stage of the experimental phase of thesis. This was conducted at the MDC site using histology sections prepared from the Morphometry Sample Block as detailed in Section 2.3.7 and 2.3.9 (see Figure 2.5). Morphometric characterisation was conducted at the zonal midpoints of the three respective zones in accordance with the methodology detailed throughout Sections 4.19.2.

4.19.4 STATISTICAL METHODS AND ANALYSES

Statistical methods followed the convention given in Section 3.5.1. Descriptive statistics are presented in accordance with the appropriate statistical descriptors. Hence mean values (+/- sd) are given for normally distributed continuous data, whilst median values (IQ ranges) and min-max ranges are given for either non-normal distributed continuous or restricted data. Normality of continuous data was assessed using the Anderson-Darling Normality test at an alpha level of 0.05.

Nonparametric statistical testing was conducted on all restricted data and on continuous data that displayed a non-normal distribution. Nonparametric pairwise comparisons were assessed using Mann-Whitney testing. Multiple comparisons were conducted using Kruskal-Wallis testing, the non-parametric equivalent of ANOVA, with 'between class' comparisons by Mann-Whitney testing with a Bonferroni correction for multiple 'between class' comparisons.

Parametric statistical testing was only used on continuous data that displayed normal distribution. Where data were both continuous and normally distributed, either parametric 2 sample T-tests were used, or in the case of multiple comparisons, one-way analysis of variance (ANOVA), with pairwise comparisons by Tukey testing.

In all cases 2 tailed test conditions were adopted, at a 5% significance level.

Hence the null hypotheses under these test conditions were:

H^o – There is no statistical difference between classes (A=B)

Set against the alternative hypotheses:

H^i – there is a statistical difference between groups (A≠B).

In addition, age and bodyweight interactions were assessed by correlation and regression analyses.

4.20 RESULTS

4.20.1 MORPHOLOGICAL APPRAISAL OF THE *STRATUM MEDIUM*

The structural organisation of the *SM* was consistent with the 3-zoned donkey pattern proposed by Collins *et al.* (2002), based upon the regional distribution of morphologically distinct tubule types across the dorso-palmar HWD. Donkey Type 1, 2, 3a and 3b Tubules were evident in all sections. Zone I (Z1) was characterised by presence of Type 1 Tubules, and Zone 3 (Z3) by Type 3b Tubules. A relatively narrow region, Zone 2 (Z2), that contained Type 2 and Type 3a Tubules, separated these two morphologically distinct zones.

4.20.1.1 STRUCTURAL IRREGULARITIES WITHIN THE *STRATUM MEDIUM*

Although the general structural organisation of the *SM* in laminitic cases conformed to that proposed by Collins *et al.* (2002), examples of unconventional tubular forms were observed in all cases. These structural irregularities, which are illustrated in Figure 4.5, included the following: -

1. Multi–Marrowed Type 1 Tubule (MMT1)

These structures consist of 2 medullae contained within a common cellular cortex to form a single, unified, morphological unit (see Figure 4.5A). The cortical organisation is consistent with the Type 1 Tubule.

2. Multi–Marrowed Type 3 Tubule (MMT3)

These structures comprised of 2 or more medullae contained within a common cellular cortex (see Figure 4.5B). Each medulla was however surrounded by 2-3 cortical cell layers, contained within this common cortex. The common cortex displayed a cellular organisation consistent with the Type 3 Tubule.

3. Multi–Type 3 Tubule complex (MT3C)

These structures consisted of 2 or more horn tubules linked together to form a single complex (see Figure 4.5C). These structures differed from the MMT in that an extensive cellular cortex surrounded each respective medulla, and the common cellular cortex observed in the MMT was absent. The cortical organisation is consistent with the Type 3 Tubule.

Figure 4.5 Structural irregularities of the *Stratum medium* in laminitic donkey hoof horn.

A. Multi-Marrowed Type 1 Tubule (MMT1).

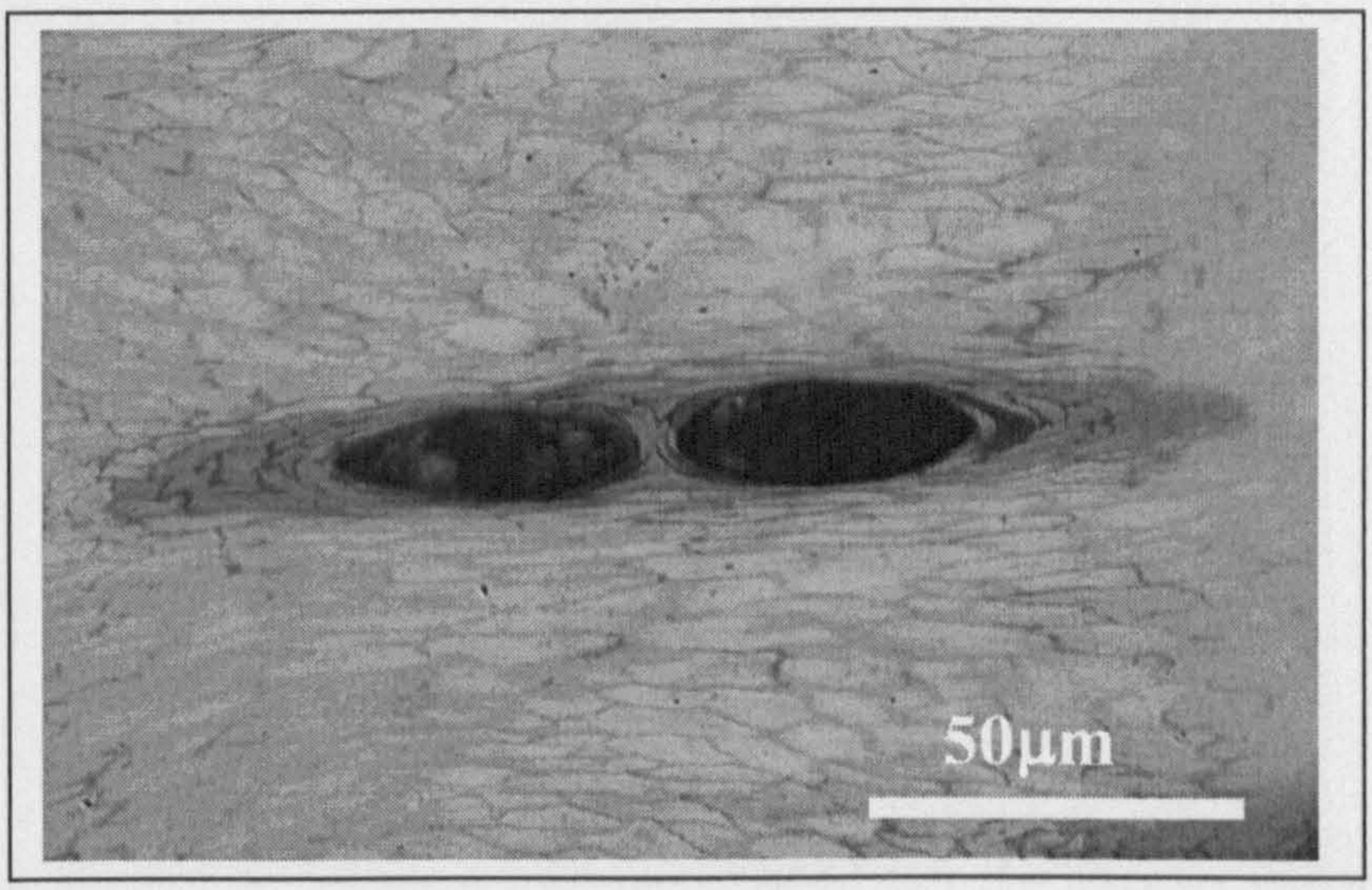

B. Multi-Marrowed Type 3 Tubule (MMT3)

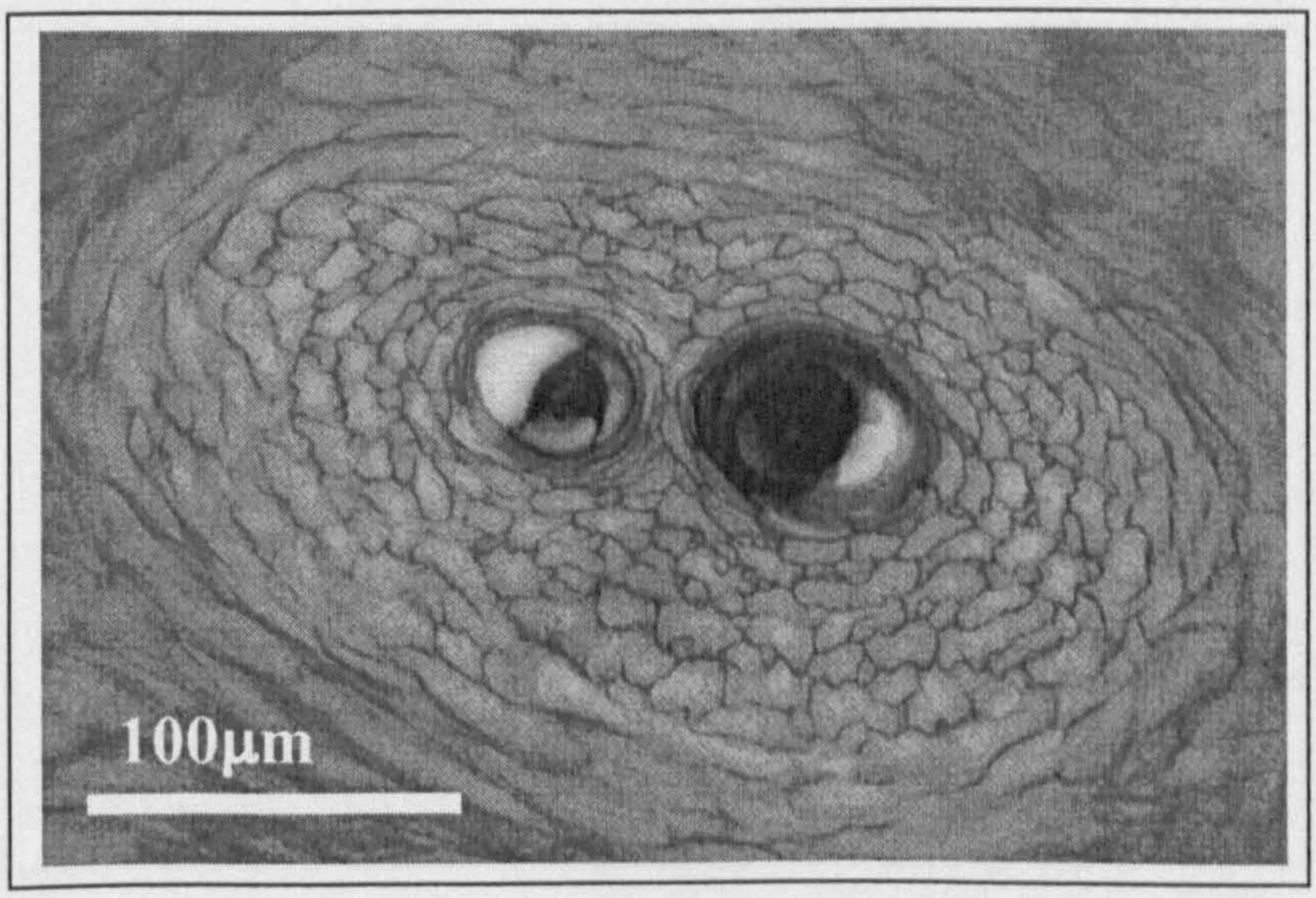

C. Multi-Type 3 Tubule Complex (MT3C)

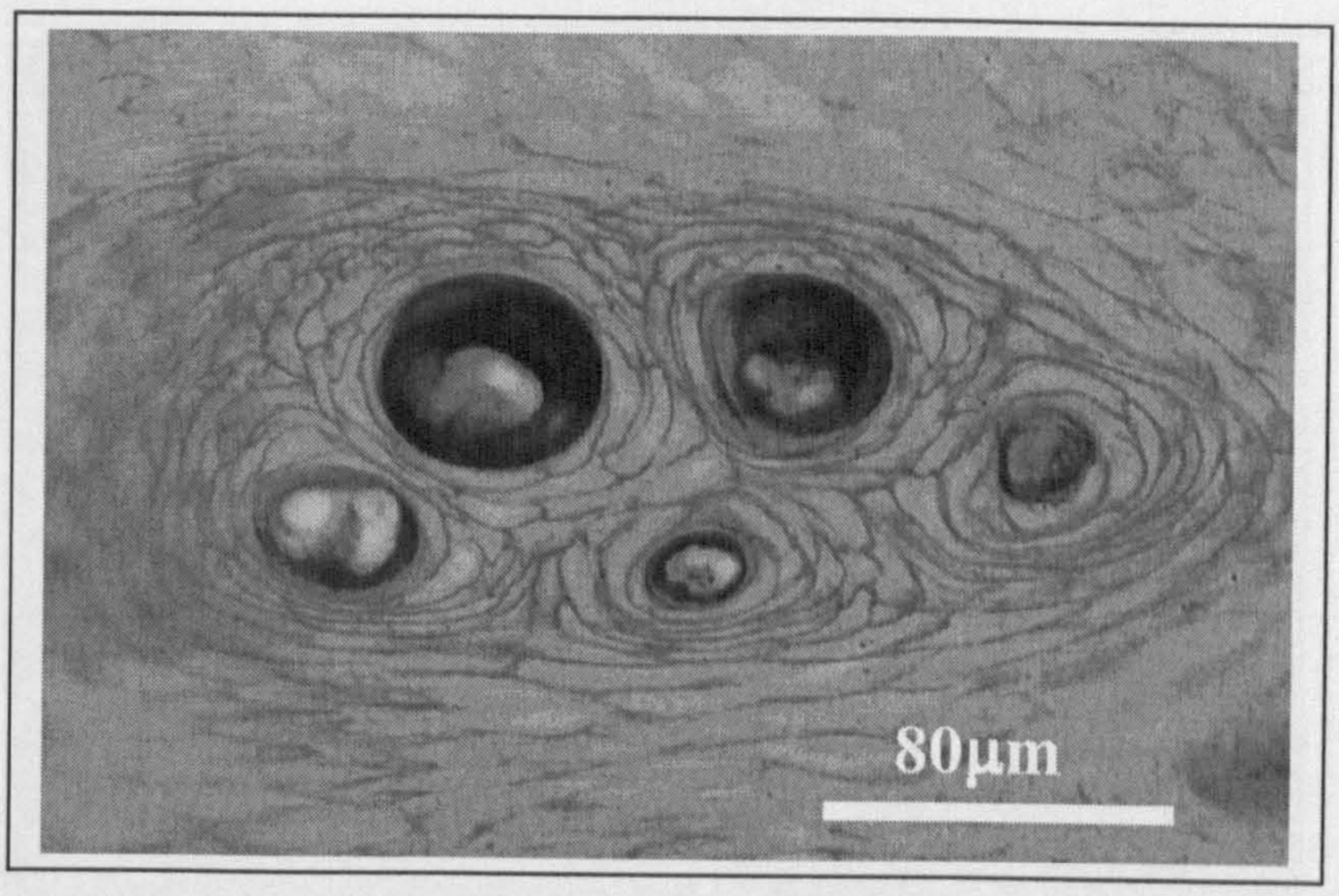

D. Wavy Tubule (WT).

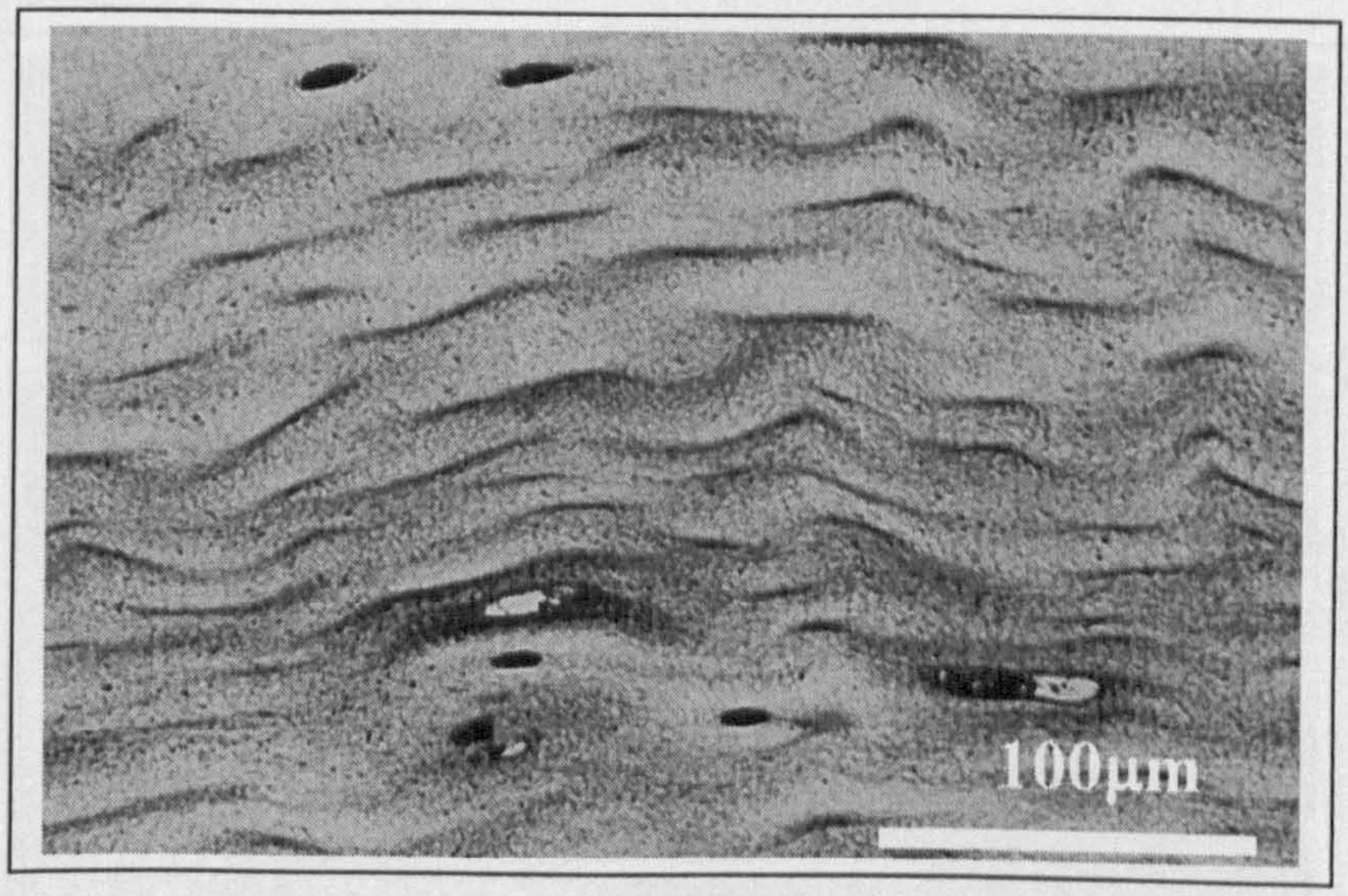

E. Tubule Void (TV) - Note degradation of the tubule cortex.

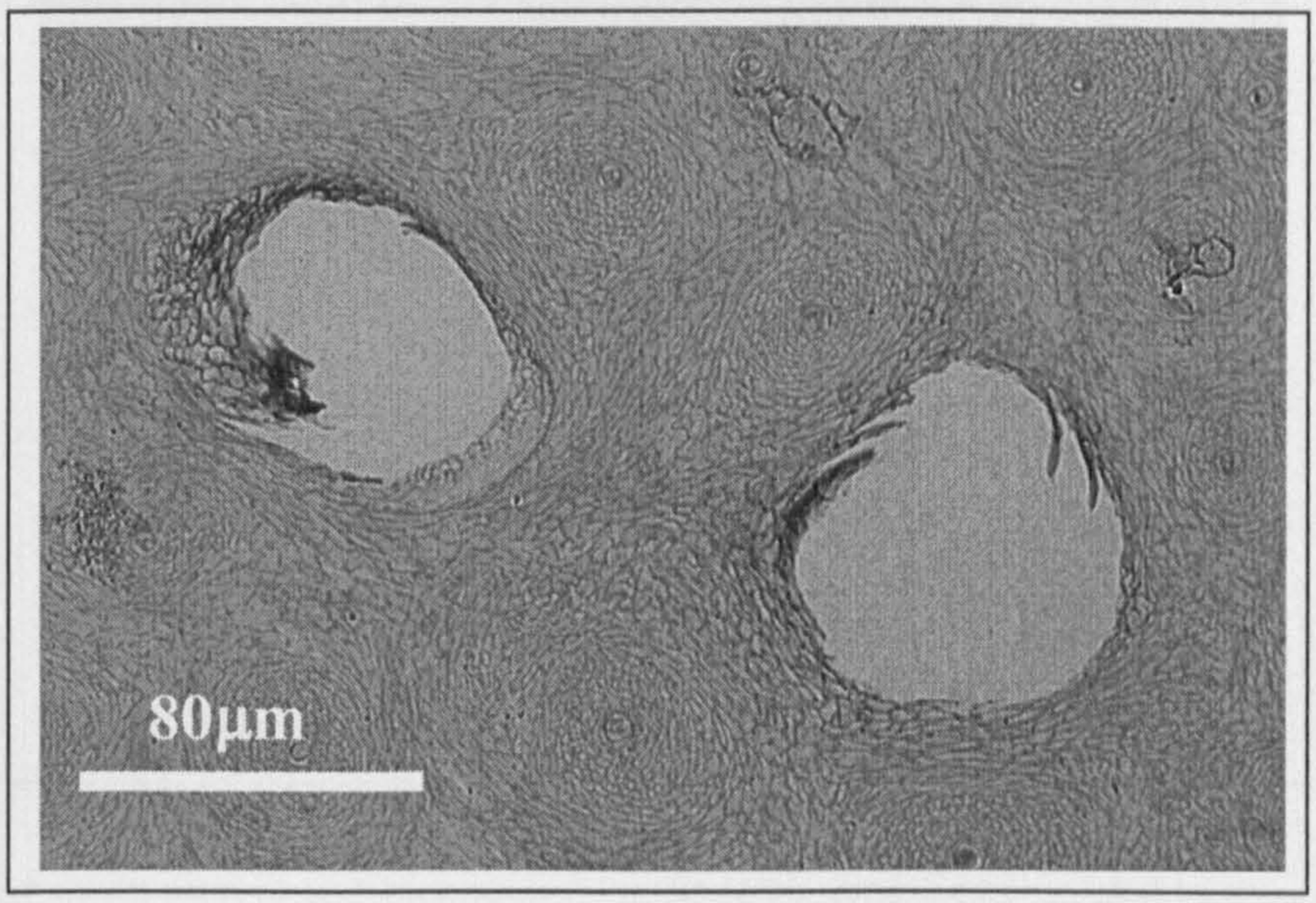

F. Mis-shapped or Misaligned Tubule (MT).

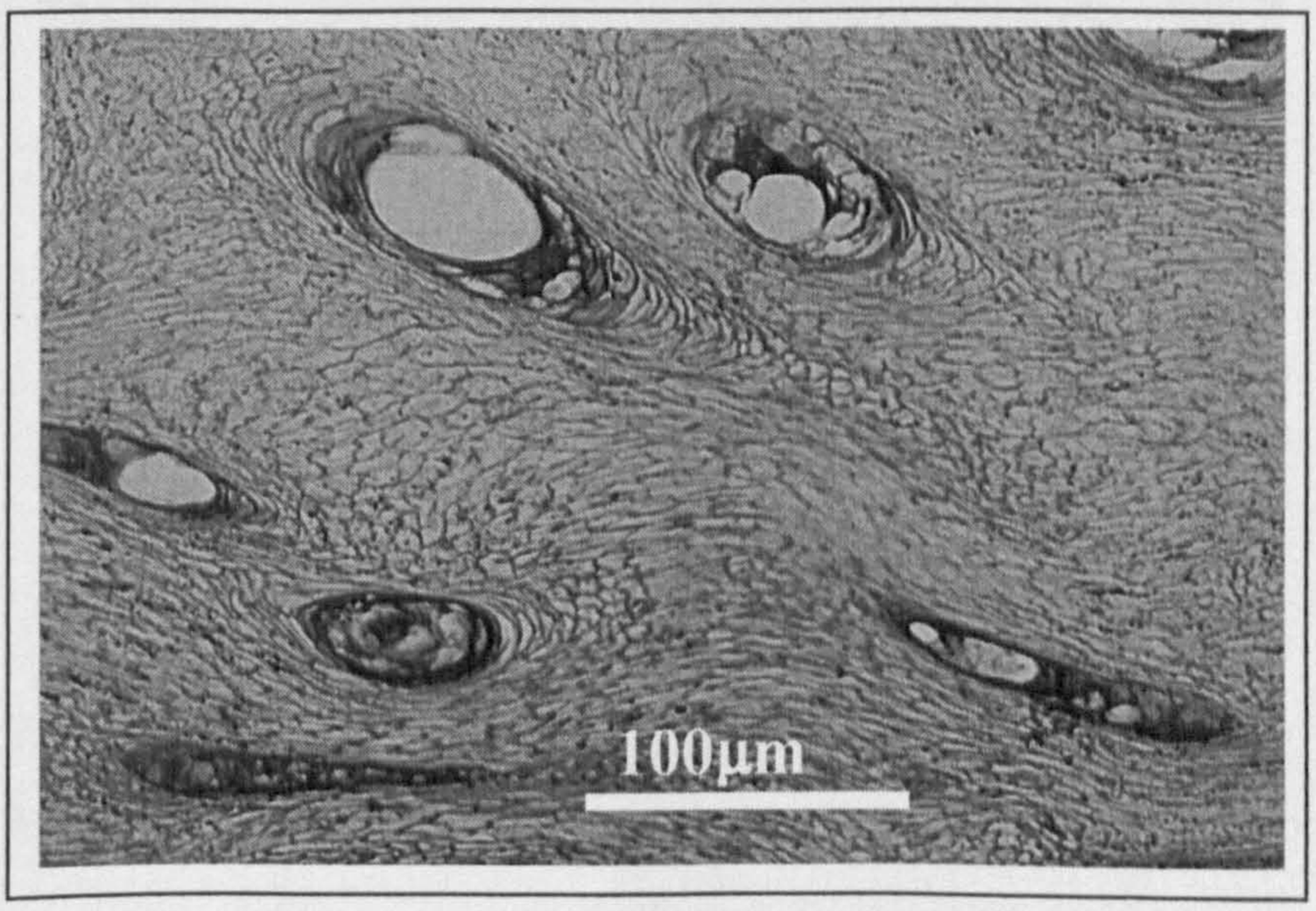

G. Enlarged Marrow (EM).

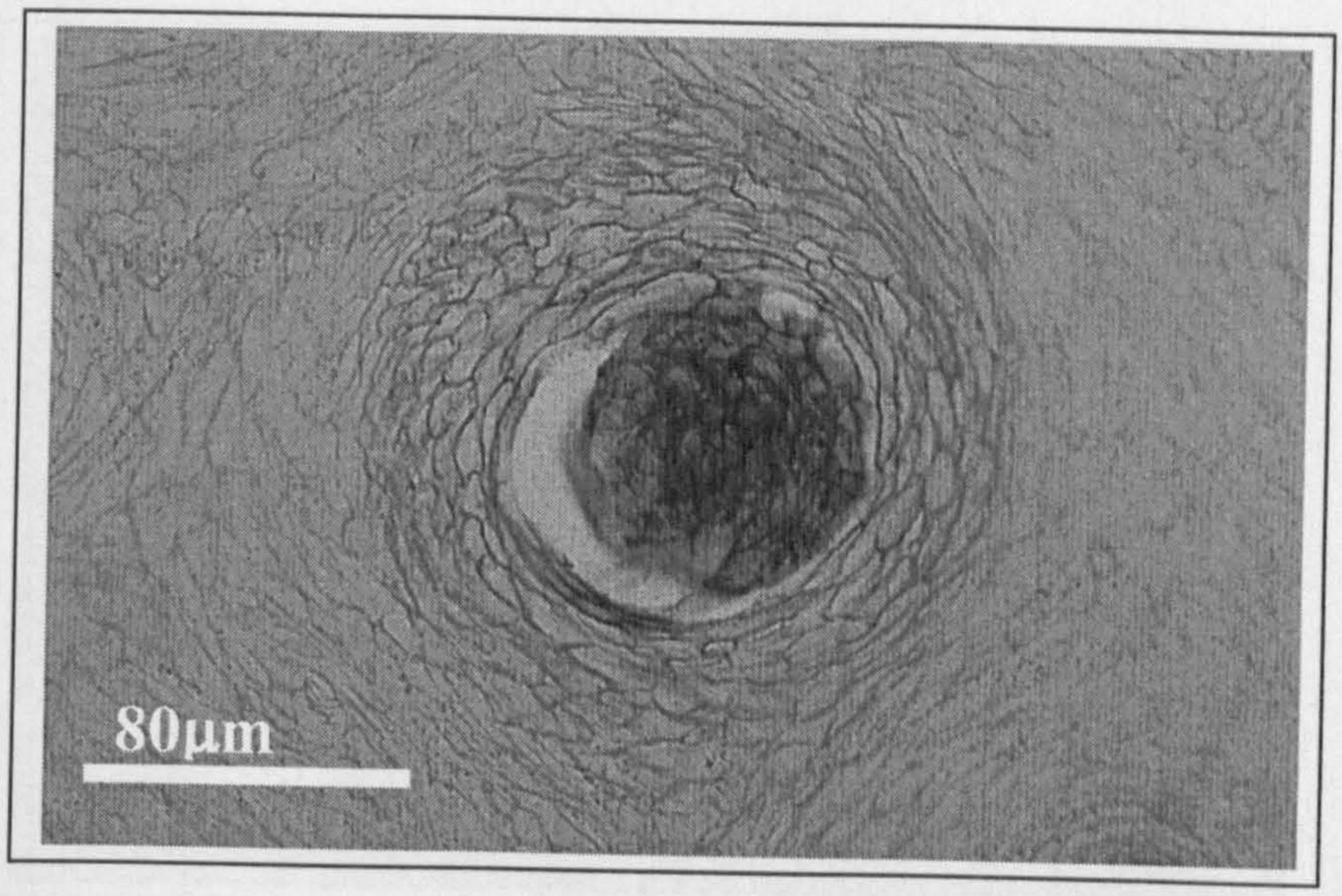

H. Enlarged Type 3 Tubule (ET) with loss of normal cortical organisation.

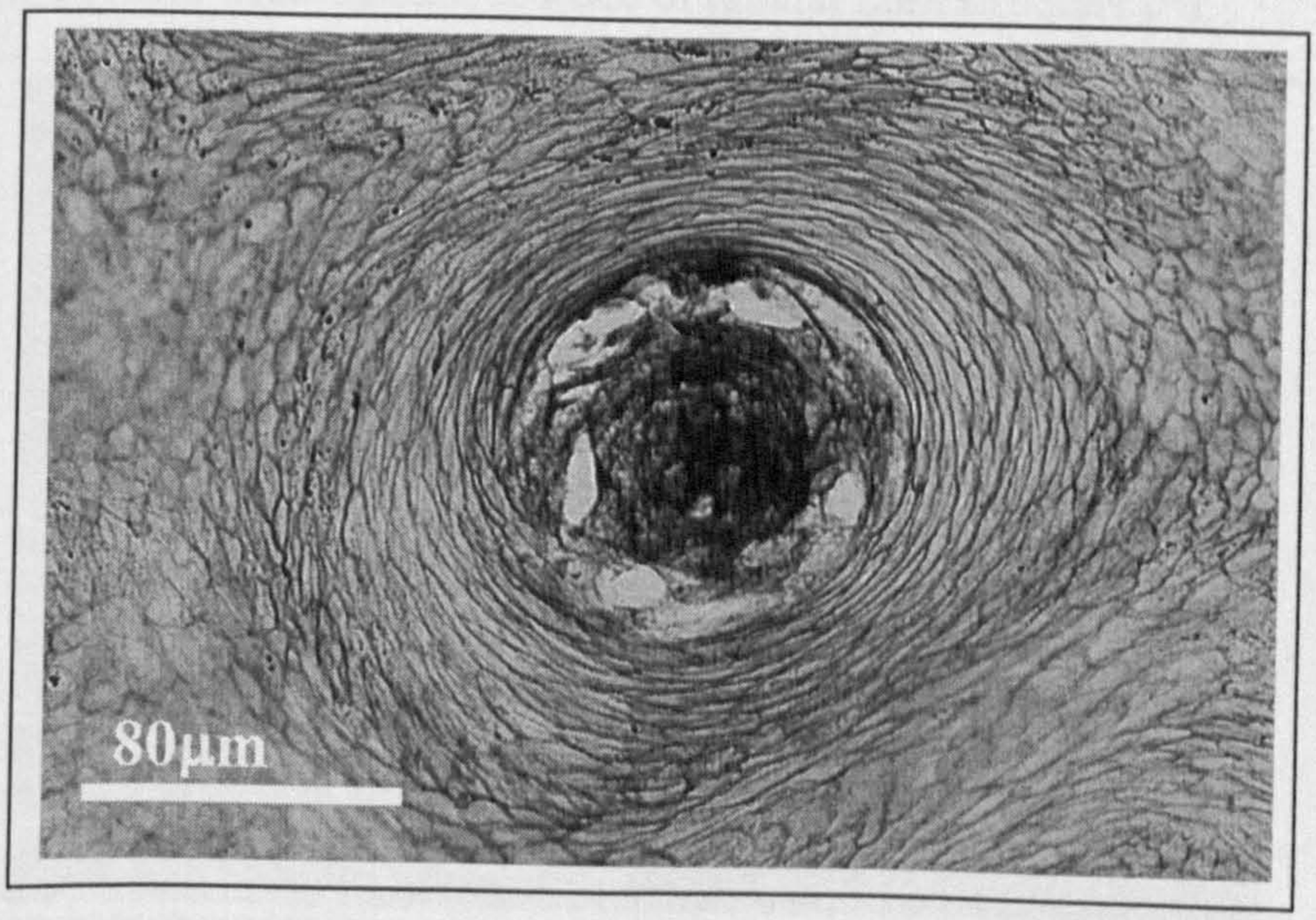

I. Aberrant Tubule (AT).

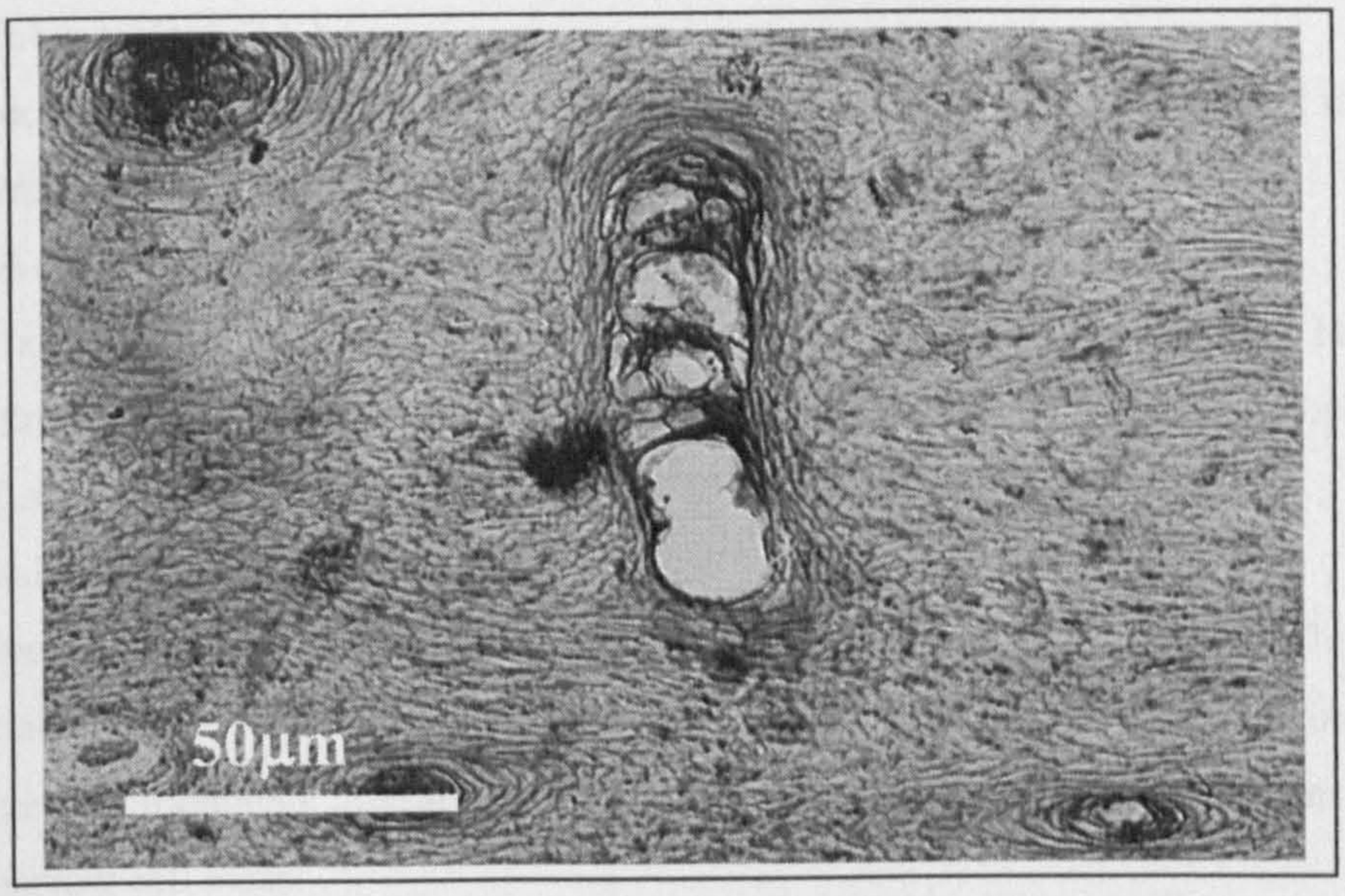

J. Aberrant Tubules with regional absence of tubular horn structure (*).

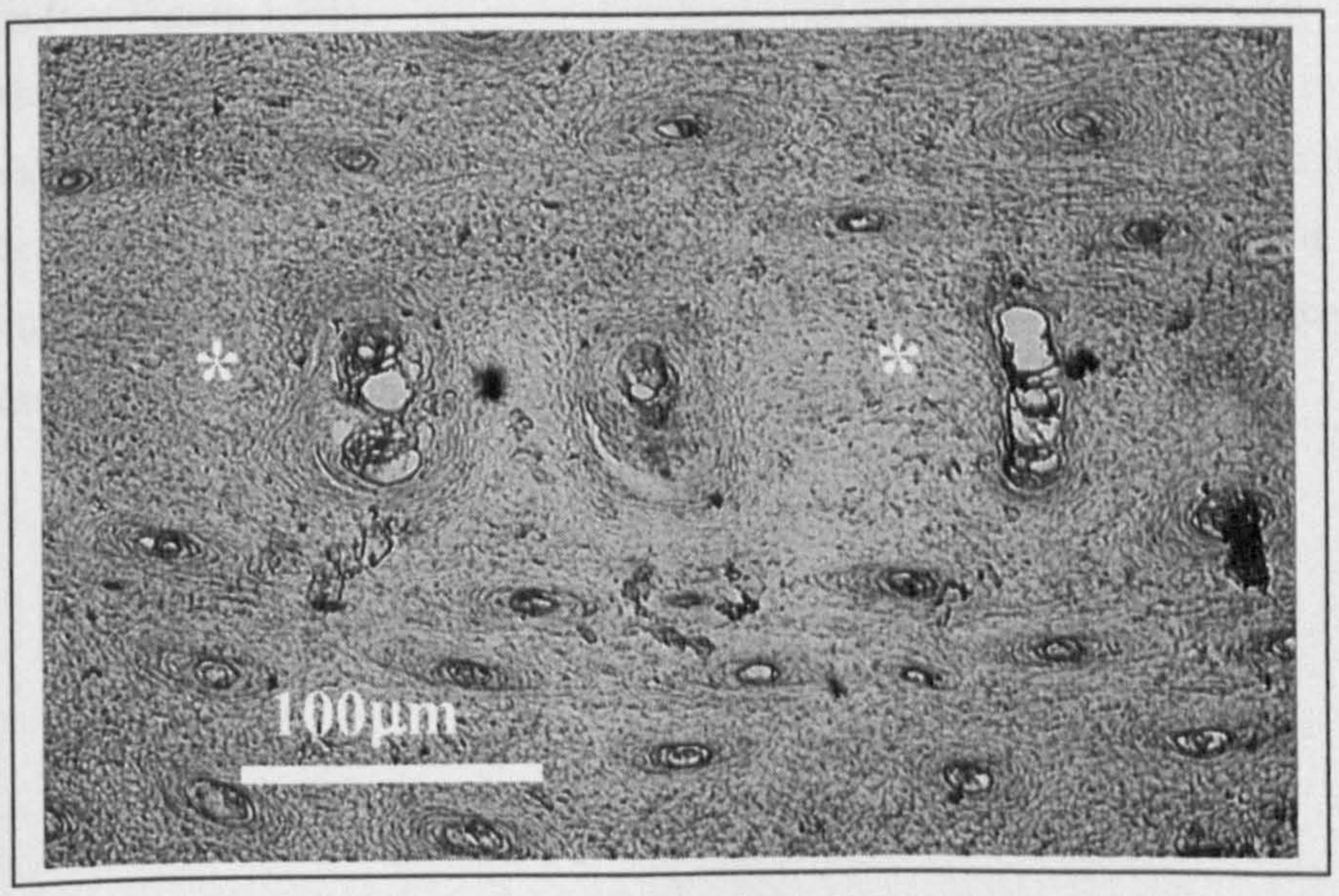

4. Wavy Tubule (WT)

These structures were characterised by a 'wavy' form that appeared as elongated positively stained elements within the *SM* (See Figure 4.5D). The cortical and medullary components of these structures were not readily discernible.

5. Tubular Void (TV)

These structures appeared as 'voids' within the *SM* (see Figure 4.5E). The voids were bounded by an intensely stained cortical remnant.

6. Mis-shapped or Misaligned Tubules (MT)

These structures were consistent with the 'accepted' form of the horn tubule. However their cross sectional profiles displayed an atypical shape, or a preferred alignment or orientation that differed from that previously reported for the *SM* (see Figure 4.5F).

7. Enlarged Marrow (EM)

These enlargements occurred within Type 1 and 3 Tubules (see Figure 4.5G). These structures were characterised by a markedly large marrow, compared with that typically observed in that tubule type. Enlargements appeared either as an expanded medullary cavity or as an intensely stained marrow cell mass.

8. Enlarged Tubule (ET)

These structures displayed a structural organisation consistent with that of the Type 1 Tubules, except that they were markedly larger in size. These structures differed from the EM irregularities in that both the cortex and the marrow were enlarged. Marrow enlargement within Type 3 Tubules was often associated with disruption to the normal cortical organisation of this tubule type (see Figure 4.5H).

9. Aberrant Tubules (AT)

The AT appeared as an intense positively stained, rod-shaped medullary cell mass that lacked an obvious cellular cortex (see Figure 4.5I). These structures were aligned within the *SM* in a dorso-palmar direction. This irregularity was associated with the regional absence of a normal tubular horn structure, referred to as ATH (see Figure 4.5J).

LOCATION AND INCIDENCE OF STRUCTURAL IRREGULARITIES

The occurrence, location and associations between the different structural irregularities observed within and between the *SM* of the sample group individuals are summarised in Table 4.12. Structural irregularities differed between individuals, and consistent patterns of location were not evident. Table 4.12 highlights the non-specific nature of the incidence of the different structural irregularities, both 'within' and 'between' individuals.

Multi-marrow tubules were observed within all zones, although MMT1 and MMT3 did not always occur concurrently. The, MTC and TV irregularities were only recorded within Z3 of the *SM*. These were irregularly distributed throughout Z3. Conversely the MMT3 irregularities were primarily restricted to a narrow region located either within and adjacent to the Z2, and/or to the inner aspect of the Z3.

The WT and AT irregularities were only observed within the Z1. These structures were present either as isolated elements surrounded by normal horn tubules or they formed a thin band situated within the Z1. The AT form however were observed only as disparate and isolated structures situated within regions of the Z1 that were otherwise devoid of a normal tubular horn structure (ATH).

The MS irregularity was observed both in Z1 and 3 of the *SM*. In Z1 of the *SM* the alignment of the major axis of these structures was at variance with the 'accepted' medio-lateral orientation. Whereas within Z3 of the *SM* these structures displayed an oval cross sectional profile that was in marked contrast with the normal round cross section found in this zone.

Table 4.12 Occurrence, location and associations between structural irregularities within the *Stratum medium (SM)* of the hoof wall at the Mid-line Dead Centre (MDC) of laminitic donkey hoof horn

Donkey	Type of Structural Irregularity								
	MMT1	MMT3	MT3C	WT	TV	MT	EM	ET	AT/ ATH
1	X^{1}	X^{3}	$X^{2,3}$	X^{1}					
2					X^{3}			X^{3}	
3			$X^{2,3}$			X^{2}	$X^{1,3}$		
4							X^{3}		X^{2}
5	X^{1}	X^{3}			X^{3}				
6								X^{1}	X^{2}
7		X^{3}				$X^{1,2,3}$			
8			X^{2}	X^{1}					
9		X^{3}		X^{1}					

Key: **MMT1** = Type 1 Multi–Marrowed Tubule. **MMT3** = Type 3 Multi–Marrowed Tubule. **MT3C** = Multi-Type 3 Tubule Complex. **WT** = Wavy Tubule. **MT** = Mis-shapped or Misaligned Tubule. **EM** = Enlarged Marrow. **ET** = Enlarged Tubule. **AT** = Aberrant Tubule with regional absence of normal tubular horn structure of the *SM* (**ATH***)*.
X = Irregularity present within the *SM* at the MDC. Superscript **1** = Zone 1 - Outer region of *SM*. **2** = Zone 2 - Middle region of *SM*. **3** = Zone 3 - Inner region of *SM*.

4.20.2 MORPHOMETRIC CHARACTERISTICS OF MATERIAL DERIVED FROM THE MAIN EXPERIMENTAL PHASE OF PROJECT

4.20.2.1 DORSO-PALMAR HOOF WALL DEPTH OF THE *STRATUM MEDIUM*

The dorso-palmar hoof wall depth of the *Stratum medium* (HWD) ranged from 5.27 to 13.34mm with a mean of a median of 8.85mm (IQ 7.83–10.27). 21 of the 23 animals displayed HWD values in excess of those predicted by the algorithm of Hopegood (2002). One individual displayed a HWD value that corresponded with the predicted value, and one individual displayed a lower HWD value that predicted. The HWD values exhibited an inhomogenous distribution that contrasted with the normal distribution of the predicted HWD values. The median difference between actual and predicted values was 2.1mm (IQ 1.8-4.4) with values ranging from –1.0 to 11.1mm.

4.20.2.2 'FIELD' AND 'FEATURE' SPECIFIC AREA MEASUREMENTS

MARROW AREA MEASUREMENTS

ZONE 1

Z1 marrow area (Ma Area) measurements ranged from 133.6-4245μm^2. The Ma Area displayed a non-normal distribution with positive skew (skewness value = 0.6) i.e. mean > median, and a kurtosis of 0.5. Assessment of the normal probability plot indicated that there was a tendency for the distribution of the Ma Area to be 'lighter' (less numerous) at lower area values, and 'heavier' (more numerous) at high Ma Area sizes, than would be expected in a normal distribution. The median Z1 Ma Area was 1158.1μm^2 with an IQ range 702-1642μm^2. An evaluation of the box plot representation of the Z1 Ma Area revealed a number of outliers that display large area values (see Figure 4.6).

ZONE 2

The Z2 Ma Area displayed a non-normal distribution, with a positive skew. However the nature of the distribution was more extreme than that observed in Z1. The skewness value in Z2 was 2.8, with a corresponding kurtosis of 16.34. The normal probability plot indicated a greater tendency for Ma Area values to be 'lighter' at low area values and more numerous at higher area values. Ma Area values ranged from 131-8901μm2 with a median Ma Area measurement of 1219μm2. The IQ range in Z2 was 837 -1700μm2. Outliers at high Ma Area values were also evident within this zone (see Figure 4.6).

ZONE 3

The Ma Area distribution in Z3 also displayed a non-normal distribution with a positive skew. The skewness and kurtosis values at 1.5 and 2.3 respectively, were intermediate between those recorded in Z1 and Z2. The spread of Ma Area sizes ranged from 200-6143μm^2, with a median of 1219μm^2 and an IQ range of 906-2205μm^2. The normal probability plot for this zone also indicated that the distribution was lighter at the extreme lower area values and 'heavier' at the higher values. Outliers at high area values were evident within Z3 (see Figure 4.6).

Figure 4.6 Boxplot comparison of median Marrow Area measurements (μm^2) by zone

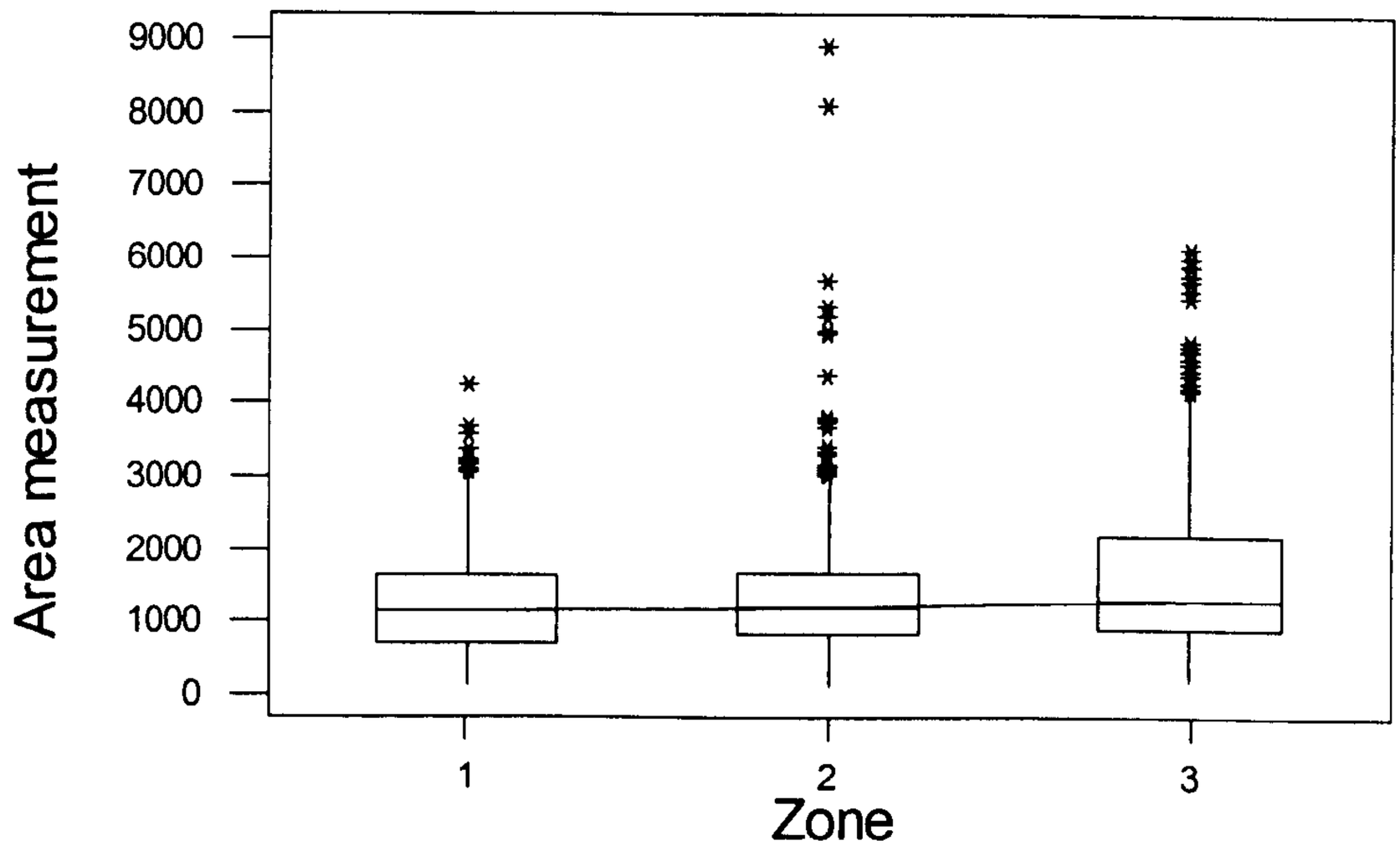

ZONAL MARROW AREA COMPARISONS

The zonal variation in Ma Area measurements is given in Figure 4.11. 'Between zone' comparisons by Kruskal-Wallis testing revealed a significant difference in median zonal Ma Area measurements ($P<0.005$). Pairwise comparisons by Mann-Whitney testing revealed significant differences in median Ma Area measurements between all zones ($P<0.05$) – see Figure 4.6.

TUBULE AREA MEASUREMENTS

ZONE 1

Z1 tubule area (Tu Area) measurements ranged from 306-34237μm^2. The Tu Area measurements displayed a non-normal distribution with a positive skew and kurtosis of 1.1 and 1.2 respectively. There was a tendency for the distribution to be 'lighter' at lower area values.

The median Z1 Tu Area measurement was 6197μm^2, with an IQ range of 3005-10135μm^2. The boxplot distribution reveals a number of outliers at larger area values (see Figure 4.7).

ZONE 2

Z2 Tu Area measurements displayed a non-normal distribution with a modest positive skew of 0.5. The normal probability plot revealed the tail to be 'lighter' at the lower tubule values. The median Tu Area recorded in this zone was 16187μm^2 with an associated IQ range of 5740-27269μm^2. The spread of the data was greater than that observed in Z1, with Tu Area sizes ranging from 547-62833μm^2.

ZONE 3

Z3 tubules ranged from 737 - 141745μm^2. Once more, the Tu Area measurements displayed a non-normal distribution with a modest positive skew at 0.6. The normal probability plot also indicated that the distribution was 'lighter' at the lower area values. The median Tu Area value within this zone was 40065 μm^2, with an IQ range of 25307- 57177μm^2.

ZONAL TUBULE AREA COMPARISONS

Figure 4.12 illustrates the zonal variation in Tu Area measurements statistically significant 'between zone' differences were evident in median Tu Area measurements ($P<0.05$) – see Figure 4.12. Pairwise zonal comparisons revealed significant differences between the median Tu Area measurements of all zones ($P<0.05$).

Figure 4.7 Boxplot comparison of median Tubule Area measurements (μm^2) by zone

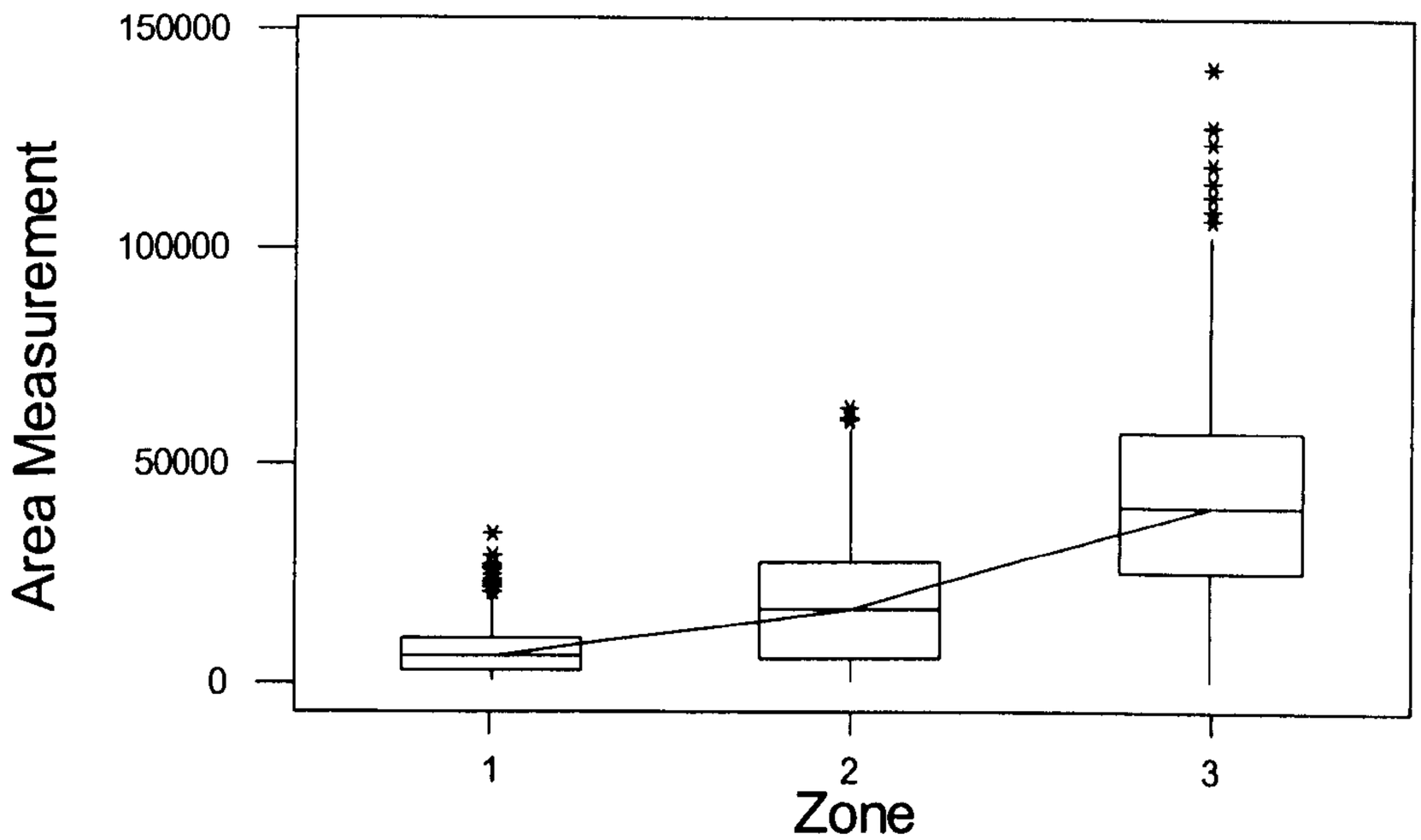

CORTICAL AREA MEASUREMENTS

ZONAL DESCRIPTIONS

Z1 Cortical area (Co Area) measurements ranged from 23-32917μm2 and displayed a non-normal distribution with a positive skew of 1.5. The median Co Area within this zone was 4918μm2 with an IQ range of 1956-8894μm2. The Co Area measurements within Z2 similarly displayed a non-normal distribution ranging from 15-61899μm2 with a median of 15848 μm2 and an IQ range of 5605-25220μm2. Co Area measurements in Z3 also displayed a non-normal distribution with area measurements that ranged from 157-141064μm2. The median Co Area measurement in Z3 was 39437μm2 and an IQ range of 157-141064μm2. Analyses of the respective normality plots revealed that the distribution in all zones were 'lighter' within the lower area range.

ZONAL CORTICAL AREA COMPARISONS

Figure 4.8 presents the zonal variation in Co Area measurements. Kruskal-Wallis testing revealed a statistically significant between zone difference in median cortical area measurements ($P<0.05$). Subsequent pairwise comparisons indicated that significant differences were present between all zones ($P<0.05$).

Figure 4.8 Boxplot comparison of median Cortical Area measurements (μm^2) by zone

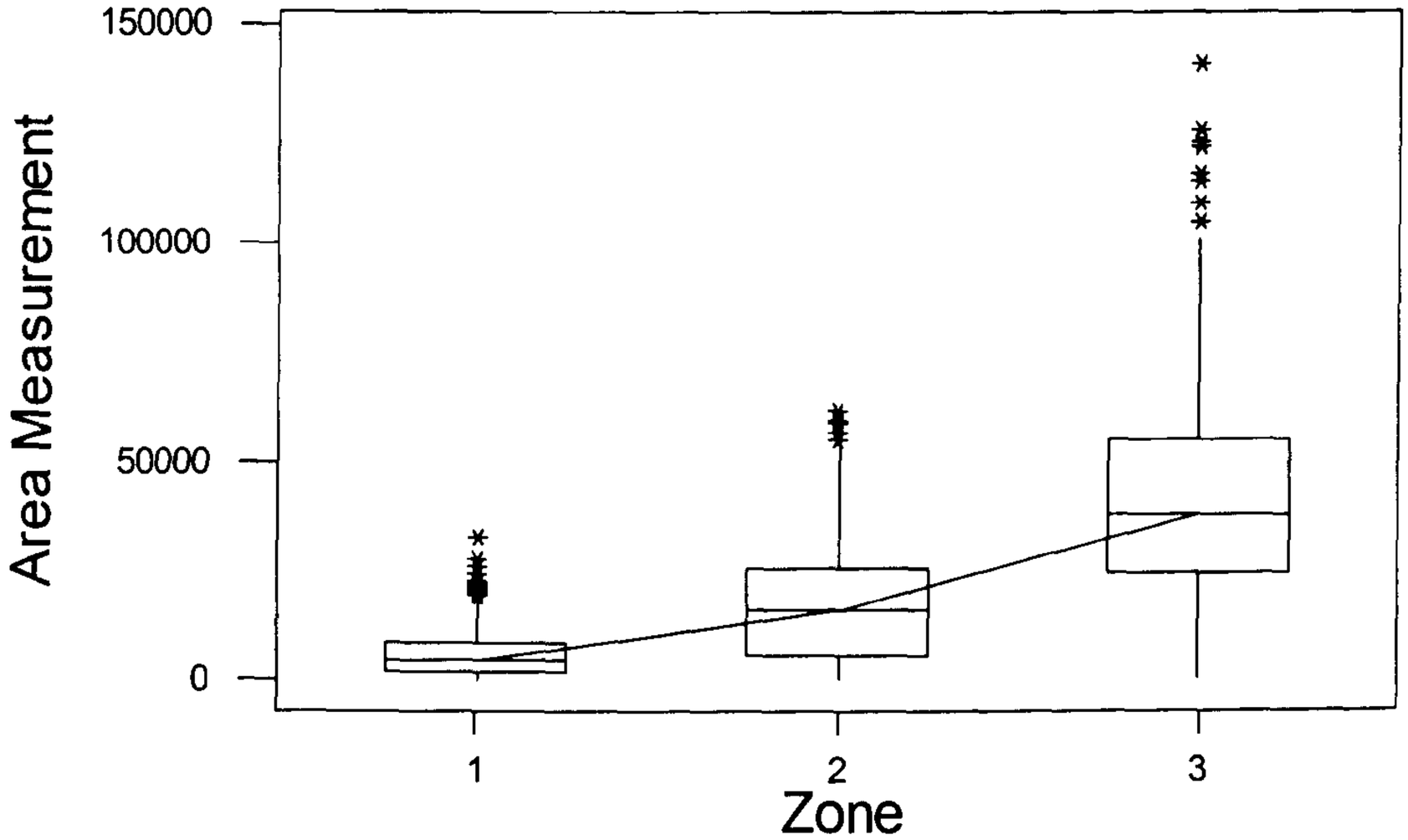

MARROW AREA FRACTION

The marrow area fraction (MaAF) within Z1 ranged from 0.012-0.050 with a median value of 0.033 and an IQ range of 0.023-0.044. This compared to a min-max range within Z2 of 0.011-0.040. The median marrow area fraction within this zone was 0.018 with a corresponding IQ range of 0.014-0.024. The zonal marrow area fraction within Z3 ranged from 0.005-0.027 with a median of 0.013 and an IQ range of 0.008-0.019.

Figure 4.9 presents the zonal variation in MaAF. The 'between zone' difference was statistically significant ($P<0.005$). Pairwise comparisons revealed statistically significant distances in median MaAF between all zones.

Figure 4.9 Boxplot comparison of Marrow Area Fraction by zone

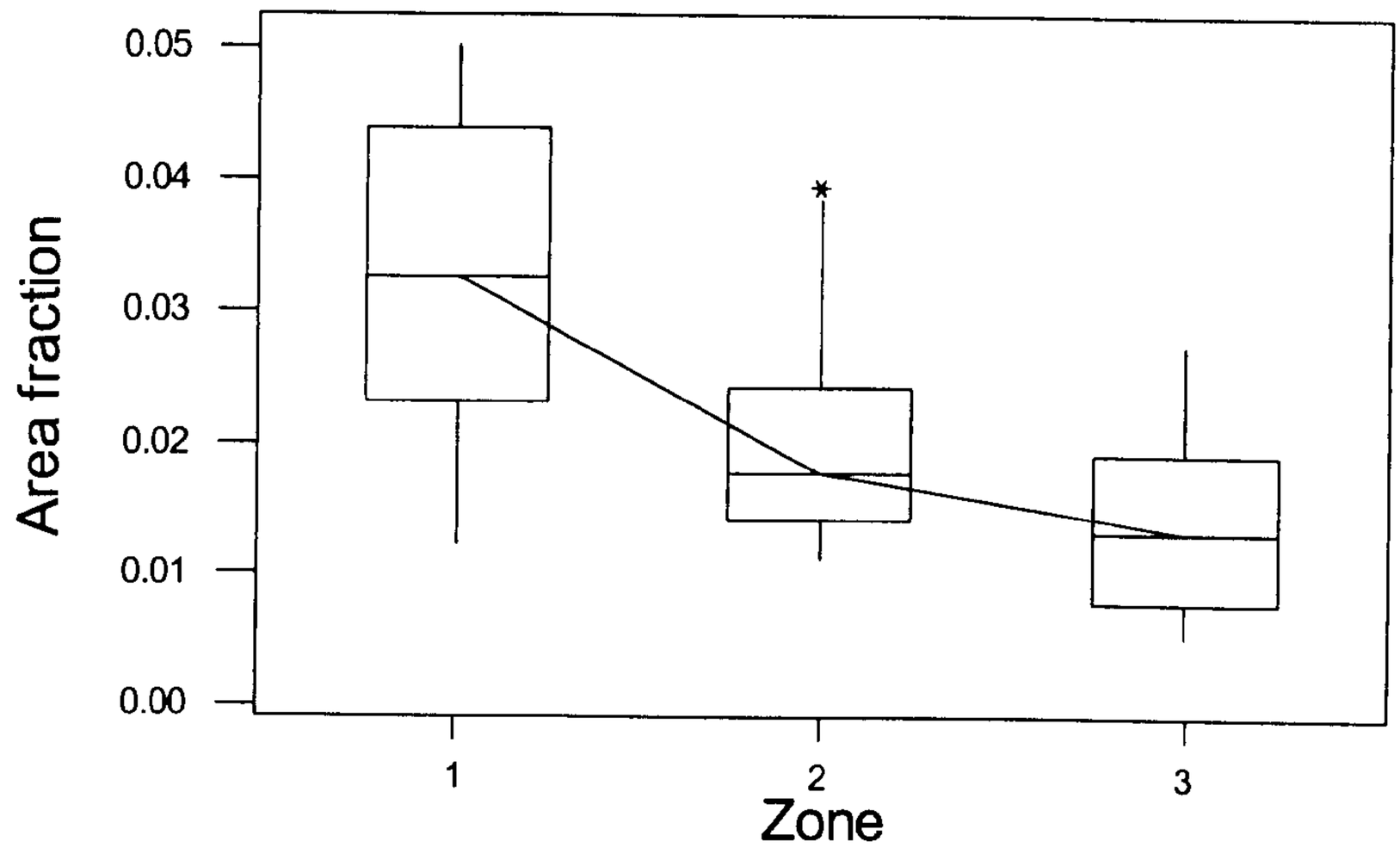

TUBULE AREA FRACTION

The median tubule area fraction (TuAF) measurements for Z1, 2 and 3 were 0.224, 0.256 and 0.340 respectively – see Figure 4.10. The corresponding zonal IQ ranges were 0.140-0.256, 0.237-0.293, and 0.316-0.369. Kruskal-Wallis testing indicated a statistically significant 'between zone' difference in the TuAF measurements ($P<0.05$).

Pairwise comparisons revealed that statistically significant differences were present between all zones ($P<0.05$).

CORTICAL AREA FRACTION

The median cortical area fraction (CoAF) measurements for the three zones were 0.173, 0.236 and 0.317 respectively with IQ ranges of 0.100-0.227, 0.215-0.269, and 0.356-0.297 (see Figure 4.11). A statistically significant 'between zone' difference was present ($P< 0.05$). Subsequent pairwise comparisons indicated statistically significant differences between all zones ($P<0.05$).

Figure 4.10 Boxplot comparison of Tubule Area Fraction by zone

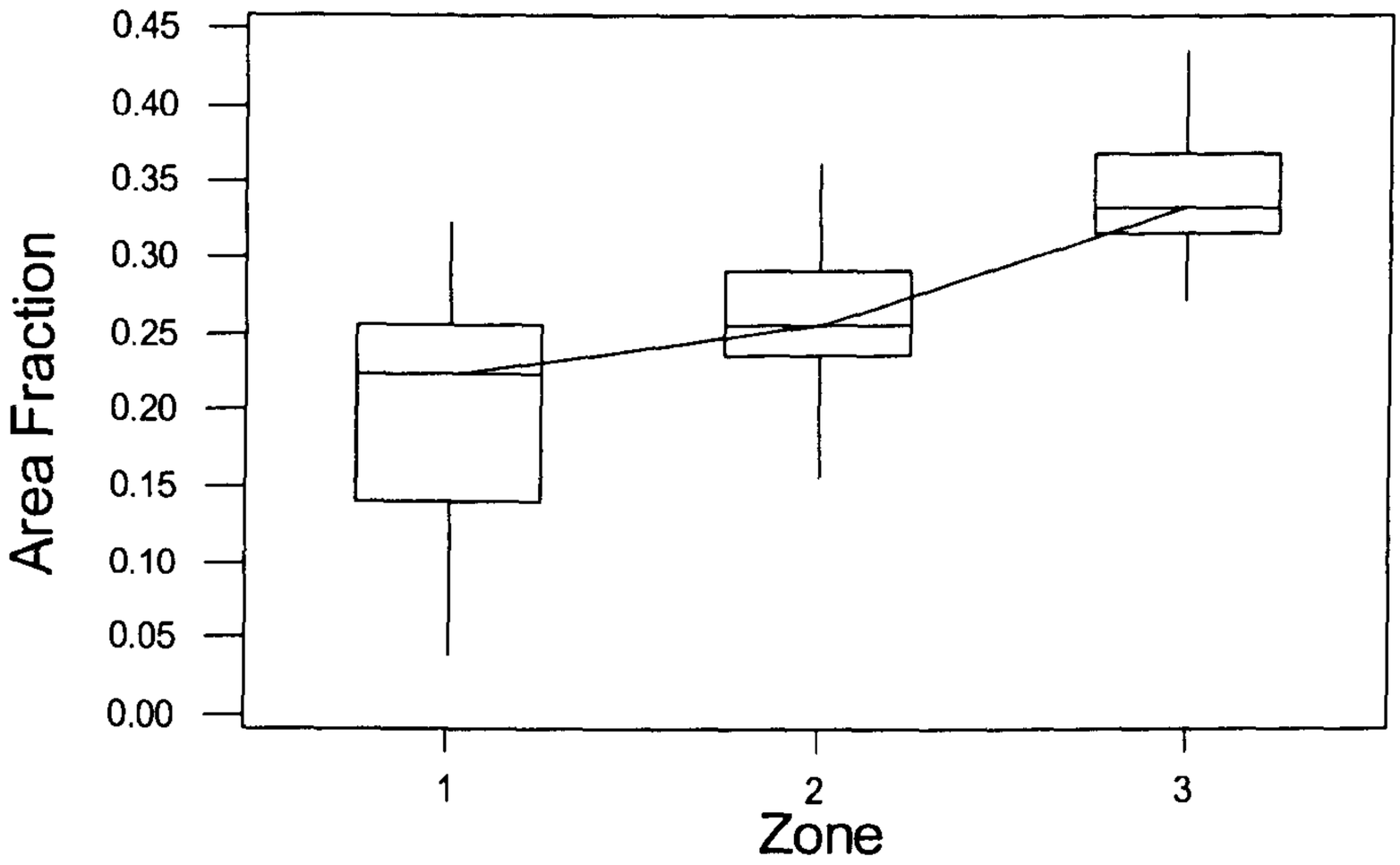

Figure 4.11 Boxplot comparison of Cortical Area Fraction by zone

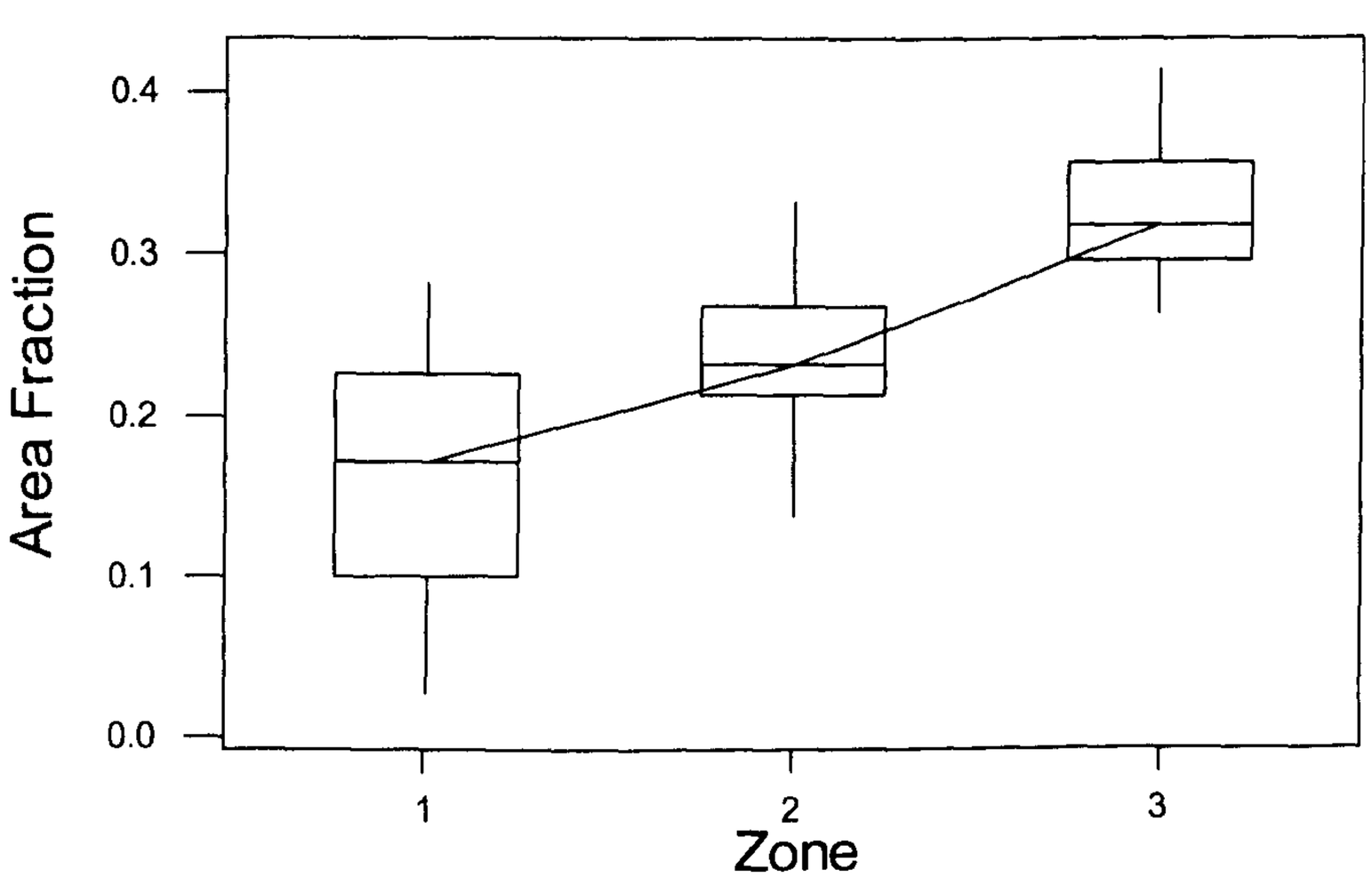

4.20.2.3 'FEATURE' SPECIFIC LINEAR AND AREA MEASUREMENTS

Comparison of the median linear and area 'feature' specific data given in Table 4.13 revealed the 'zone specific' nature of the morphometric characteristics of structure of the horn tubules. The Z1 tubules were relatively small in comparison to the horn tubules of the other zones. They were characterised by a relatively large marrow to tubule quotient, Ma:Tu(%) at ~17%, a

marked oval cross sectional profile with a major to minor tubule axis ratio, Tu(MA:MI) of ~3.0, and a tubule to marrow major axis ratio, Tu:Ma(MA), and minor axis ratio, Tu:Ma(MI), of ~3.0 and 2.0 respectively. Cortical thickness in the direction of the major and minor tubule axes, Co(MAT) and Co(MIT) respectively, were relatively small with median values of 50 and 13μm respectively. The ratio of the cortical thickness in the direction of the major and minor axes was ~4:1.

The Z2 tubules displayed a median size intermediate between the relatively small tubule of Z1 and the relatively large tubules of Z3. The Z2 tubules were characterised by a median Ma:Tu(%) at 7.17%, a modest oval cross sectional profile with Tu(MA:MI) at ~1.8:1. The cortical thickness was greater than the Z1 tubule, with median Co(MAT) and Co(MIT) values of ~ 75 and 35μm respectively. The ratio of the cortical thickness in the direction of the major and minor axes within this zone was ~2:1.

The Z3 tubules were relatively large with median Tu(MA) and Tu(MI) respectively at 106 and 80μm. They displayed a relatively small Ma:Tu(%) at ~4.0%, a circular cross sectional profile, with a Tu(MA:MI) ratio approaching unity (1.27:1), and a large cortical thickness, with values of 106 and 80 μm in the direction of the major and minor tubule axis respectively. The cortical thickness ratio for the Z3 tubule was 1.2:1.

Significant 'between zone' differences were confirmed in all feature specific variables defining the morphometric characteristics of horn tubule structure. ($P<0.05$), with the exception of the Ma(MA) parameter.

Further analyses of these significant 'between zone' differences revealed that significant differences were present in median values between all zones ($P<0.05$), apart from the Ma(MI) parameter where differences only occurred between Z1 and Z2, and Z1 and Z3. The median Ma(MI) values for Z1 were lower than those recorded in Z2 and Z3.

Table 4.13 Summary table of the area and linear 'feature' specific morphometric characteristics of horn tubule structure by zone

Parameter	Zone		
	Zone 1	Zone 2	Zone 3
Ma:Tu(%) Marrow to Tubule Quotient (%)	**17.10**[1] (13.24 - 21.25) 7.37 - 31.23	**7.17** [2] (5.60- 9.97) 4.40- 14.96	**3.77**[3] (2.19-5.47) 1.80- 8.51
Tu(MA) Tubule Major Axis (μm^2)	**158.4**[1] (137.38-185.01) 92.06- 209.17	**198.5**[2] (171.4-232.6) 136.5-14724.2	**262.8**[3] (229.7-284.7) 198.7-313.0
Tu(MI) Tubule Minor Axis (μm^2)	**52.98**[1] (45.02-66.70) 20.15-86.38	**99.4**[2] (86.1-124.0) 79.6-132.6	**208.1**[3] (186.3-222.2) 136.8-243.6
Tu (MA:MI) Major to Minor Tubule Axis Ratio	**2.93**[1] (2.41-3.30) 1.90-4.21	**1.78**[2] (1.70-2.07) 1.59-3.05	**1.27**[3] (1.19-1.38) 1.15-1.49
Ma(MA) Marrow Major Axis (μm^2)	**51.5**[1] (48.7-60.4) 38.4-65.5	**43.7**[1] (41.7-50.6) 34.1-92.4	**41.6**[1] (38.12-60.41) 33.05-67.42
Ma(MI) Marrow Minor Axis (μm^2)	**26.6**[1] (24.7-29.9) 12.1-35.9	**33.0**[2] (31.2-37.9) 26.5-56.8	**35.1**[2] (32.5-51.9) 27.9-61.2
Tu:Ma(MA) Tubule to Marrow Major Axis Ratio	**2.85**[1] (2.62-3.21) 2.01-4.39	**4.43**[2] (3.71-4.9) 3.28- 337.55	**5.33**[3] (4.53- 6.952) 3.65-7.93
Tu:Ma(MI) Tubule to Marrow Minor Axis Ratio	**1.98**[1] (1.67-2.20) 1.52-2.94	**2.81**[2] (2.59-3.45) 2.19-4.04	**4.72**[3] (3.89-6.54) 3.22-7.22
Co(MAT) Cortical Thickness Major Axis (μm)	**53.2**[1] (42.6-62.8) 25.3-80.7	**77.6**[2] (64.9-90.3) 47.9-7340.6	**106.2**[3] (92.3-118.1) 75.7-129.9
Co(MIT) Cortical Thickness Minor Axis (μm)	**13.0**[1] (9.6-17.7) 4.1-28.9	**34.2**[2] (26.9-40.6) 23.1-47.5	**80.6**[3] (67.3-91.7) 48.1-98.7

Key: Parameters are defined in Table 4.10and Table 4.11.
Data, **Bold** – Median. (AA-BB) – IQ Range. AA-BB – Min, Max Range.
Subscripts, different numbers denote significant difference between zones ($P<0.05$).

These results confirmed a dorso-palmar zonal increase in the Tu:Ma(%), Tu(MA), Tu(MI), Tu:Ma(MA), Tu:Ma(MI), Co(MAT) and Co(MIT) parameters of horn tubule structure. Conversely there was a dorso-palmar zonal decrease in Ma:Tu(%) and Tu(MA:MI) parameters of tubule structure.

4.20.2.4 Age and Bodyweight Effects on the Morphometric Characteristics of the *Stratum medium*

There was no relationship between age, and the morphometric characteristics that defined the structural organisation of the *SM*, however significant associations with bodyweight were recorded. These inter-relationships are considered further in Chapter 7.

4.20.2.5 DORSO-PALMAR HOOF WALL DEPTH OF THE *STRATUM MEDIUM* OF LAMINITIC GROUPS 1 AND 2

The dorso-palmar hoof wall depth of the *Stratum medium* (HWD) for each of the Laminitic Groups are given in Table 4.14, along with the corresponding predicted HWD values derived from Hopegood's algorithm. Both groups displayed median actual HWD values in excess of predicted values, with a median difference of 4.4 and 2.0mm respectively for Group1 and Group 2. 'Within group' comparisons indicated a significant difference ($P<0.05$) between actual and predicted values for both groups.

Table 4.14 Summary table of Predicted and Actual HWD of the *Stratum medium* for Laminitic Group 1 and 2

Laminitic Group					
Group 1			Group 2		
Actual HWD (mm)	Predicted HWD (mm)	Difference (mm)	Actual HWD (mm)	Predicted HWD (mm)	Difference (mm)
10.5[1]	**6.1**[2]	**4.4**	**8.7**[1]	**6.6**[2]	**2.0**
(7.7-13.4)	(5.3-6.5)	(1.9-7.6)	(7.9-9.2)	(6.2-7.8)	(0.1-2.4)
5.3-17.3	4.6-6.6	-1.00-11.1	7.7-9.5	5.3-8.6	0.0-3.5

Key: Data, **Bold** – Median. (AA-BB) – IQ Range. AA-BB – Min, Max Range.
Different numbers denote significant difference between actual and predicted values within group ($P<0.05$).

4.20.2.6 THE MORPHOMETRIC CHARACTERISTICS OF THE *STRATUM MEDIUM* OF LAMINITIC GROUPS 1 AND 2

Group descriptive statistics for the two respective laminitic groups are summarised below in Table 4.15. The median zonal Ma area measurements for Laminitic Group 1 were 1007, 1269 and 1649μm^2 respectively. These compared with zonal values of 1230, 1190 and 1068 μm^2 for Group 2.

Table 4.15 Summary table of zonal area measurements, and area fraction data, for the marrow tubular and cortical horn components for Laminitic Group 1 and 2

	Laminitic Group 1			Laminitic Group 2		
	Median	IQ Range	Min - Max	Median	IQ Range	Min - Max
Parameter	**Marrow Absolute Area Measurement**			**Marrow Absolute Area Measurement**		
Z1 (μm^2)	1007	476-1438	146 - 3077	1230	835-1754	134-4245
Z2 (μm^2)	1269	869-1773	131 - 8901	1190	828-1664	131 - 3688
Z3 (μm^2)	1649	1099-2450	200 - 6143	1068	841-1682	360 - 4777
Parameter	**Tubule Absolute Area Measurement**			**Tubule Absolute Area Measurement**		
Z1 (μm^2)	4962	1800-8651	465-34237	6780	3952-11398	306-28928
Z2 (μm^2)	14273	25391-4613	624-60399	18245	7353-28020	547-62883
Z3 (μm^2)	35321	55786-22091	737-141745	44573	30017-58523	2789-02710
Parameter	**Cortex Absolute Area Measurement**			**Cortex Absolute Area Measurement**		
Z1 (μm^2)	5159	1307-7511	33-32917	5481	2801-9971	23 - 27644
Z2 (μm^2)	15283	3373-23333	15-58874	18642	7645-26844	77 - 61899
Z3 (μm^2)	38057	19751-53161	157-141064	43220	28650-56709	1574-98250
Parameter	**Marrow Area Fraction**			**Marrow Area Fraction**		
Z1	0.028	0.012-0.033	0.012-0.047	0.038	0.029-0.049	0.019-0.050
Z2	0.021	0.015-0.024	0.012-0.040	0.020	0.014-0.028	0.011-0.039
Z3	0.017	0.015-0.024	0.006-0.027	0.011	0.007-0.018	0.005-0.021
Parameter	**Tubule Area Fraction**			**Tubule Area Fraction**		
Z1	0.160	0.077-0.184	0.039-0.322	0.242	0.220-0.264	0.120-0.297
Z2	0.236	0.188-0.268	0.016-0.314	0.280	0.246-0.322	0.238-0.362
Z3	0.324	0.321-0.386	0.034-0.391	0.339	0.288-0.368	0.272-0.436
Parameter	**Cortical Area Fraction**			**Cortical Area Fraction**		
Z1	0.113	0.064-0.156	0.028-0.283	0.205	0.170-0.235	0.087-0.259
Z2	0.214	0.169-0.252	0.139-0.275	0.241	0.227-0.287	0.220-0.332
Z3	0.315	0.300-0.368	0.285-0.375	0.331	0.284-0.345	0.263-0.414

Statistically significant 'between zones' differences were present in both groups. Pairwise comparisons revealed that Ma Area measurements were significantly different between all zones both in Laminitic Group 1 and 2.

Median Tu Area measurements for the three respective zones were 4692, 14273 and 35321 μm^2 in Laminitic Group 1. The corresponding values for Group 2 were 6780, 18245 and 44573 μm^2. Statistically significant differences ($P < 0.05$) were present between all zones in the two respective groups.

Median Co Area measurements also varied between zones. Group 1 values were 5159, 15283 and 38057 μm^2 respectively. These compared with median values of 5481, 18642 and 43220 μm^2 for Group 2. Statistically significant differences occurred between all zonal comparisons in both laminitic groups ($P < 0.05$).

Statistically significant 'between zone' differences were also evident in all zonal Ma, Tu, and Co AF comparisons ($P < 0.05$) in both laminitic groups.

'Between zone' Ma, Tu and IT Area Fractions comparisons for the respective laminitic groups are given in Table 4.16.

Table 4.16 Zonal Comparisons of Marrow, Tubular and Intertubular Horn Area Fractions for Laminitic Group 1 and 2

Zone	Laminitic Group 1			Laminitic Group 2		
	MaAF	TuAF	ITAF	MaAF	TuAF	ITAF
Zone 1	0.028^{1}	0.160^{1}	0.840^{1}	0.038^{1}	0.242^{1}	0.758^{1}
Zone 2	0.021^{2}	0.236^{2}	0.764^{2}	0.020^{2}	0.280^{2}	0.720^{2}
Zone 3	0.017^{3}	0.324^{3}	0.676^{3}	0.011^{3}	0.339^{3}	0.661^{3}

Key: MaAF-Marrow Area Fraction. **TuAF**-Tubular Area Fraction. **ITAF**- Intertubular horn Area Fraction. Different numerical Subscripts denote statistically significant 'between zone' differences - Mann-Whitney test ($P<0.05$).

Table 4.17 summarises the area and linear 'feature' specific morphometric parameters of tubule structure by laminitic group. Significant 'between zone' differences ($P<0.05$) were revealed within Group 1, for all parameters excluding Ma(MA). Significant differences were recorded in all zonal comparisons ($P<0.05$) for parameters Ma:Tu(%), Tu(MA), Tu(MI), Tu:Ma(MA), Co(MAT) and Co(MIT). There was a dorso-palmar zonal increase in median Tu(MA), Tu(MI), Tu:Ma(MA), Co(MAT) and Co(MIT), and a dorso-palmar zonal decrease in Ma:Tu(%). Significant differences only occurred between Z1 and Z2, and Z1 and Z3 for both the Ma(MA) and Tu:Ma(MI) parameters, with Z1 values lower than those recorded in Z2 and Z3.

Within Group 2 however, significant 'between zone' differences were recorded for all parameters, including Ma(MA). The trend in zonal comparisons were similar to those evident in Group 1, apart from that for parameter Tu:Ma(MI). In this group, significant differences were recorded in median Tu:Ma(MI) values for all zones. A dorso-palmar zonal increase was evident in parameters median Tu(MA), Tu(MI), Tu:Ma(MA), Tu:Ma(MI), Co(MAT) and Co(MIT), and a corresponding decrease in Ma:Tu(%).

Table 4.17 Summary table of area and linear 'field' specific morphometric characteristics of horn tubule structure for Laminitic Group 1 and 2

Parameter	Laminitic Group					
	Group1			Group 2		
	Zone 1	Zone 2	Zone 3	Zone 1	Zone 2	Zone 3
Ma:Tu(%) Marrow to Tubule Quotient (%)	**16.06[1]** (13.94-29.23) 10.14-31.23	**9.661[2]** (6.46-11.07) 4.95-12.60	**4.55[3]*** (3.78-6.35) 1.96- 8.51	**17.15[1]** 12.34-20.98 7.37- 24.62	**7.00[2]** 4.67-8.35 4.40-14.96	**2.52[3]*** 1.90-4.88 1.81- 6.01
Tu(MA) Tubule Major Axis (μm^2)	**136.2[1]** (100.8-177.9) 92.1-189.6	**170.2[2]** (161.6-235.7) 136.1-310.4	**261.2[3]** (200.8-289.2) 198.7-305.0	**170.1[1]** (148.7-186.7) 138.0-209.2	**204.1[2]** (180.2-233.4) 175-14724	**264.4[3]** (238.3-286.7) 223.2-313.0
Tu(MI) Tubule Minor Axis (μm^2)	**52.8[1]** (41.9-67.1) 20.2-80.2	**93.7[2]** (83.3-13.2) 79.6-132.7	**200.3[3]** (150.2-221.1) 136.9-243.6	**55.4[1]** (42.6- 66.6) 35.1-86.4	**103.8[2]** (87.3-126.2) 84.8-131.0	**211.5[3]** (201.9-223.2) 162.6-237.2
Tu (MA:MI) Tubule Major to Minor Axis Ratio	**2.40[1]** (2.06-3.95) 1.90-4.21	**1.77[2]** (1.67-2.40) 1.63-3.06	**1.31[2]** (1.23-1.40) 1.16-1.49	**2.96[1]** (2.84-3.25) 2.42-3.83	**1.79[2]** (1.73-2.05) 1.59-2.73	**1.26[3]** (1.18-1.36) 1.16-1.48
Ma(MA) Marrow Major Axis (μm^2)	**50.4[1]** 39.9-51.5 38.4-61.1	**45.4[1]** 42.4-53.8 39.1-92.4	**52.3[1]** 40.5-64.0 37.4-67.4	**55.6[1]** 47.4-62.2 46.4- 65.5	**43.6[2]** 39.7-50.7 34.1-63.1	**38.9[2]** 37.5-57.2 33.0-65.2
Ma(MI) Marrow Minor Axis (μm^2)	**26.3[1]** 24.2-26.7 12.1-30.4	**33.9[2]** 31.3-38.9 29.6-56.8	**46.2[2]** 34.5-54.8 32.0- 61.2	**28.4[1]** 25.3-33.2 23.1-35.9	**32.3[2]** 31.2-35.5 26.50-47.3	**32.9[2]** 31.5-49.5 27.97-56.2
Tu:Ma(MA) Tubule to Marrow Major Axis Ratio	**2.85[1]** 2.31-3.13 2.01-3.45	**3.69[2]*** 3.32-4.69 3.20-5.01	**4.78[3]*** 4.36- 5.43 3.65-7.08	**2.89[1]** 2.69-3.30 2.51-4.38	**4.57[2]*** 4.3-5.1 3.8-337.61	**6.39[3]*** 4.80-7.21 4.28-7.93
Tu:Ma(MI) Tubule to Marrow Minor Axis Ratio	**2.07[1]** 1.67-2.55 1.66-2.63	**2.63[2]** 2.40-2.95 2.19-3.89	**4.28[2]** 3.42-4.85 3.22- 7.13	**1.97[1]** 1.63- 2.07 1.516- 2.938	**3.14[2]** 2.73- 3.66 2.574- 4.036	**6.21[3]** 4.24--6.79 3.77-7.22
Co(MAT) Cortical Thickness Major Axis (μm)	**42.9[1]** 26.1-63.2 25.3-64.3	**63.3[2]** 55.8-92.3 48.5- 109.0	**104.0[3]** 80.3-116.2 75.2-143.9	**56.0[1]** 45.0- 75.4 42.5-80.8	**81.5.9[2]** 69.8-90.9 68.1-7340.6	**108.4[3]** 101.3-123.9 91.5-129.4
Co(MIT) Cortical Thickness Minor Axis (μm)	**13.1[1]** 8.4-20.4 4.1-24.9	**23.7[2]** 25.0-36.9 23.1- 44.9	**73.8[3]** 58.7-89.6 48.1-98.7	**12.4[1]** 8.1- 17.4 5.9-28.4	**35.9[2]** 28.7 -44.7 26.7-47.9	**87.2[3]** 78.0-92.0 65.1-97.1

Key: Parameters are defined in Table 4.7A and B. Data, **Bold** – Median. (AA-BB) – IQ Range. AA-BB – Min, Max Range. Subscripts, different numbers denote significant difference between zones ($P<0.05$).
* denote significant difference in zonal median values between groups ($P<0.05$).

4.20.2.7 Comparison of Area Data by Laminitic Group

Marrow Area Measurements

Statistically significant 'between group' differences in median Ma Area measurements were evident in Z1 and 3 ($P < 0.05$) In respect of Z1 (see Figure 4.12), the median Ma Area measurement in Group 1 was significantly smaller than that recorded in Group 2. There was NSD in respect of Zone 2 (see Figure 4.13). Conversely, the median Ma Area in Z3 was significantly larger for Group 1, compared with Group 2 (see Figure 4.14).

Figure 4.12 'Between group' comparison of Zone 1 median Marrow Area measurements (μm^2)

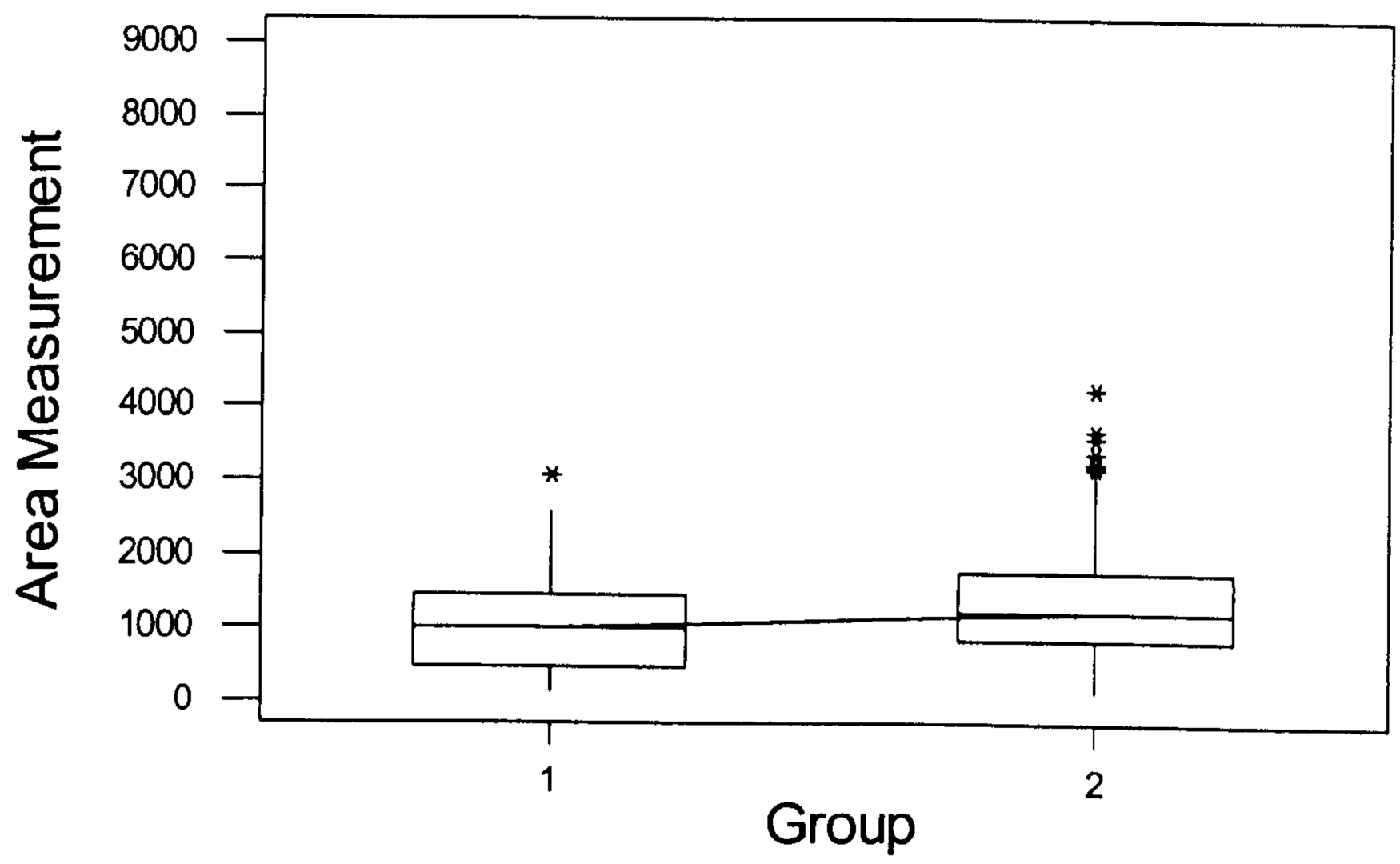

Key: Group 1 = Laminitic Group 1. Group 2 = Laminitic Group 2.

Figure 4.13 'Between group' comparison of Zone 2 median Marrow Area measurements (μm^2)

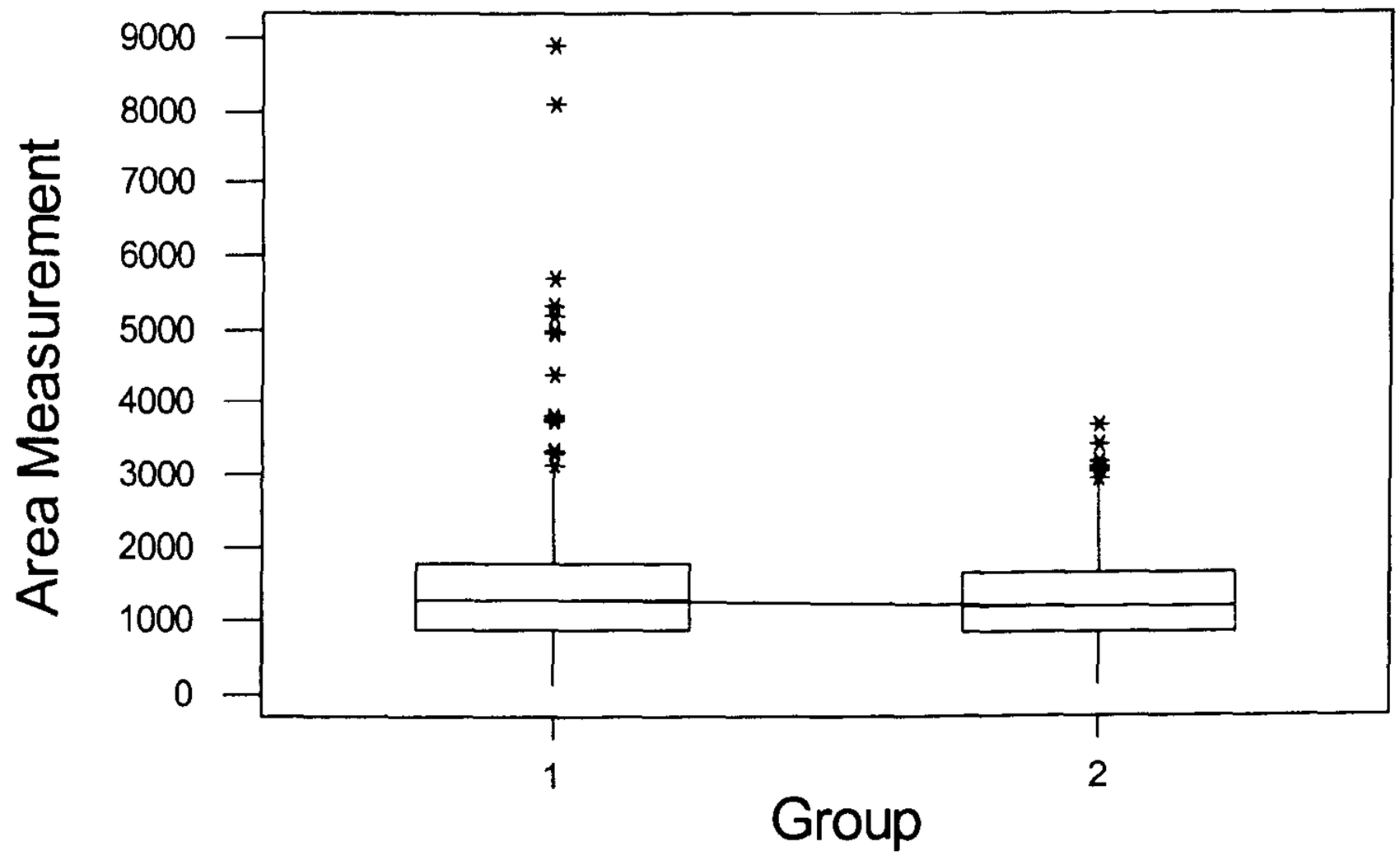

Key: Group 1 = Laminitic Group 1. Group 2 = Laminitic Group 2.

Figure 4.14 'Between group' comparison of Zone 3 median Marrow Area measurements (μm^2)

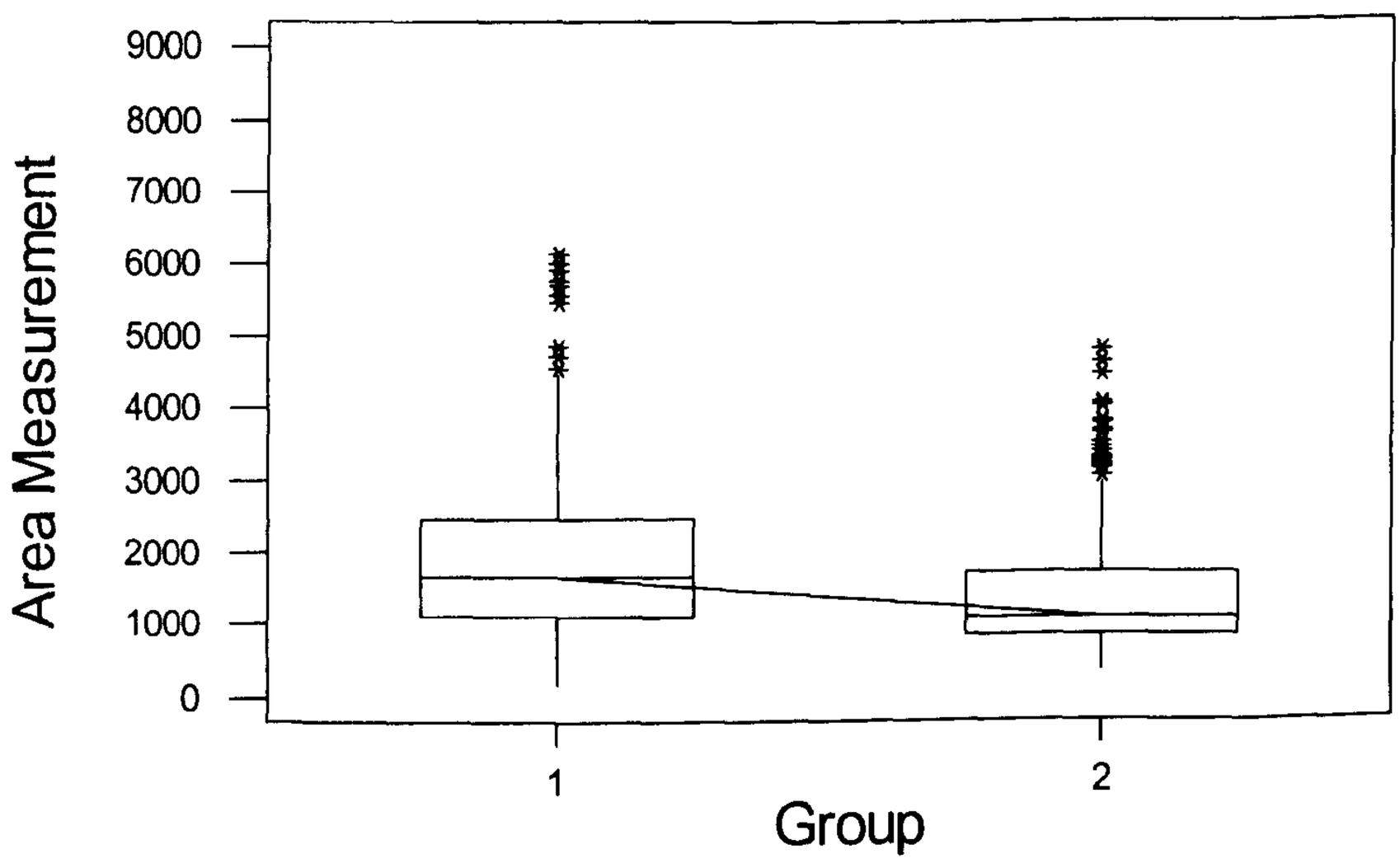

Key: Group 1 = Laminitic Group 1. Group 2 = Laminitic Group 2.

TUBULE AREA MEASUREMENTS

Tu Area measurements within Group 1 were significantly different in each respective zone compared with those values recorded for Group 2. In all 'between zone' comparisons the median Tu Area measurement in Group 1 were significantly smaller than Group 2 ($P<0.05$) – see Figure 4.15, Figure 4.16, and Figure 4.17 respectively.

Figure 4.15 'Between group' comparison of Zone 1 median Tubule Area measurements (μm^2)

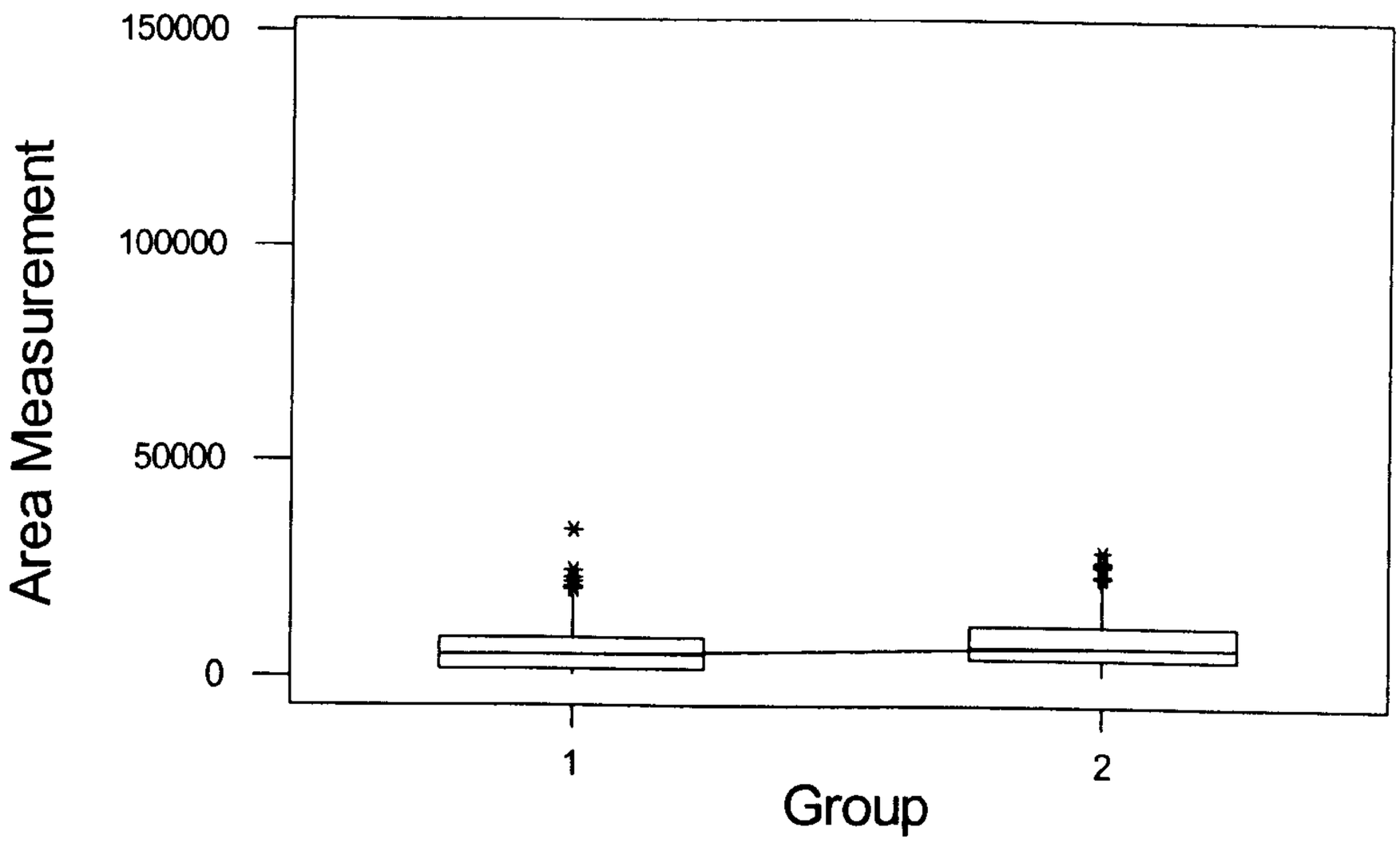

Key: Group 1 = Laminitic Group 1. Group 2 = Laminitic Group 2.

Figure 4.16 'Between group' comparison of Zone 2 median Tubule Area measurements (μm^2)

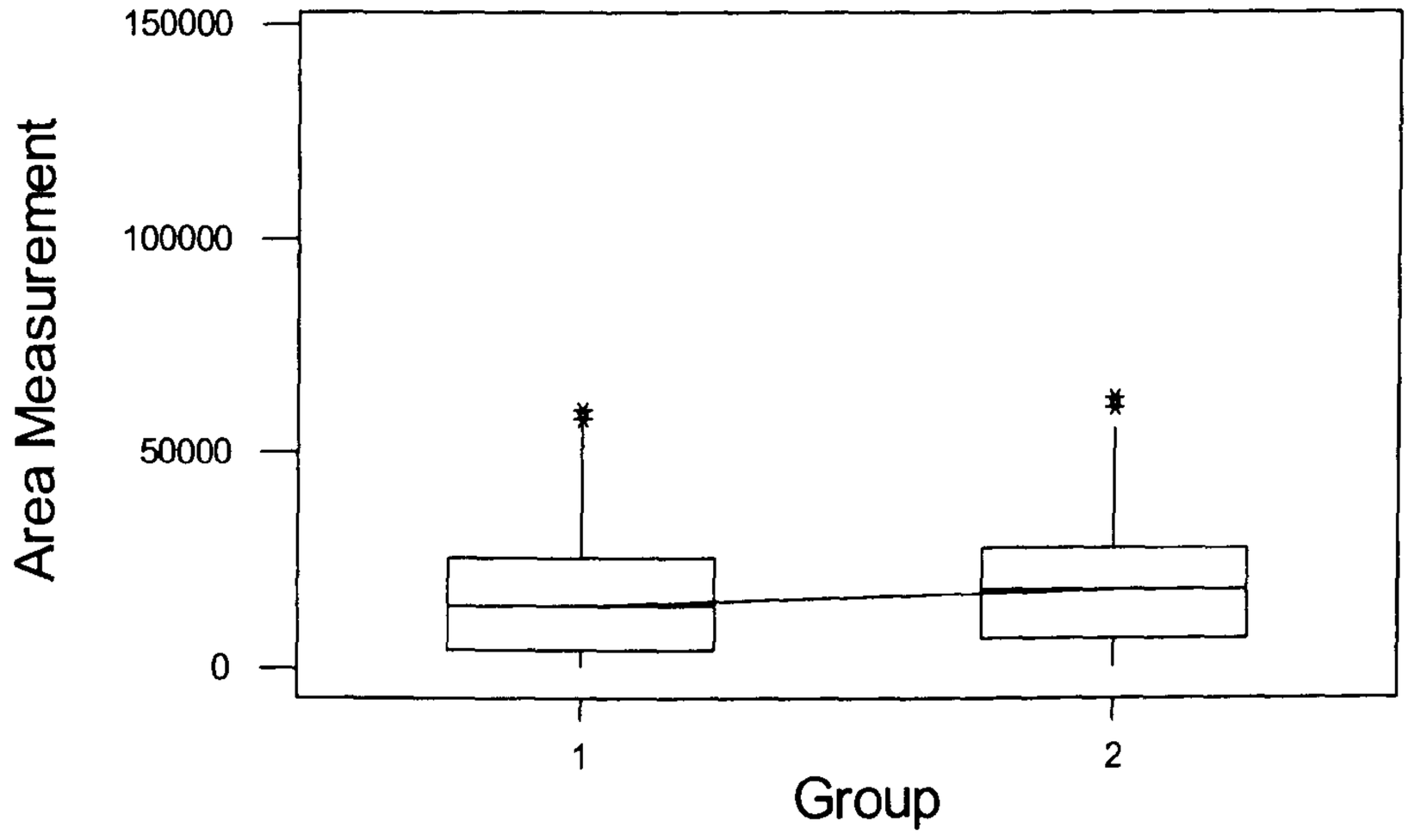

Figure 4.17 'Between group' comparison of Zone 3 median Tubule Area measurements (μm^2)

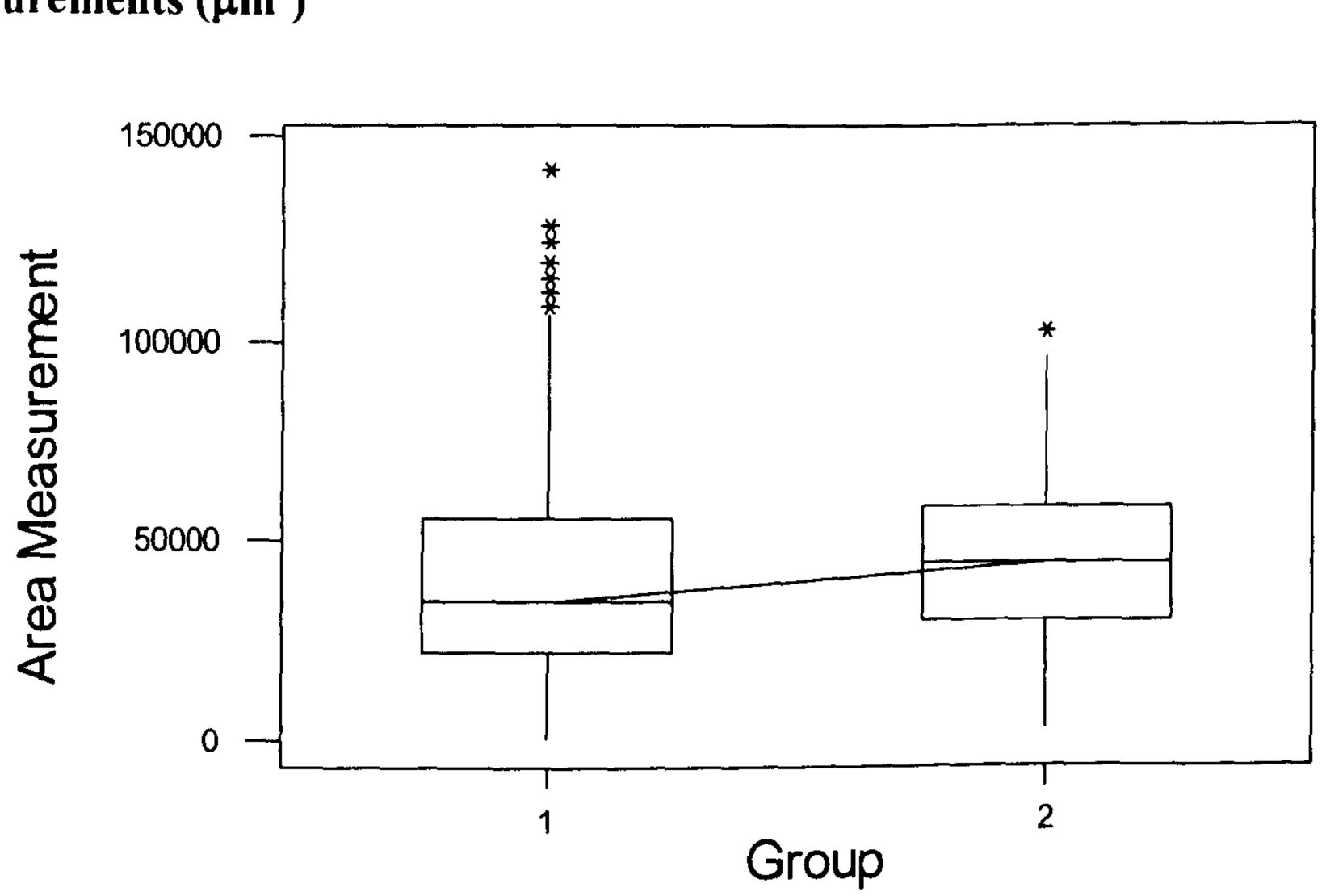

CORTICAL AREA MEASUREMENTS

Statistically significant 'between group' differences were present in each respect zone ($P< 0.05$). Co Area measurements within each zone for Group 1 were significantly smaller than the corresponding Group 2 values (see Figure 4.18, Figure 4.19 and Figure 4.20).

Figure 4.18 'Between group' comparison of Zone 1 median Cortical Area measurements (μm^2)

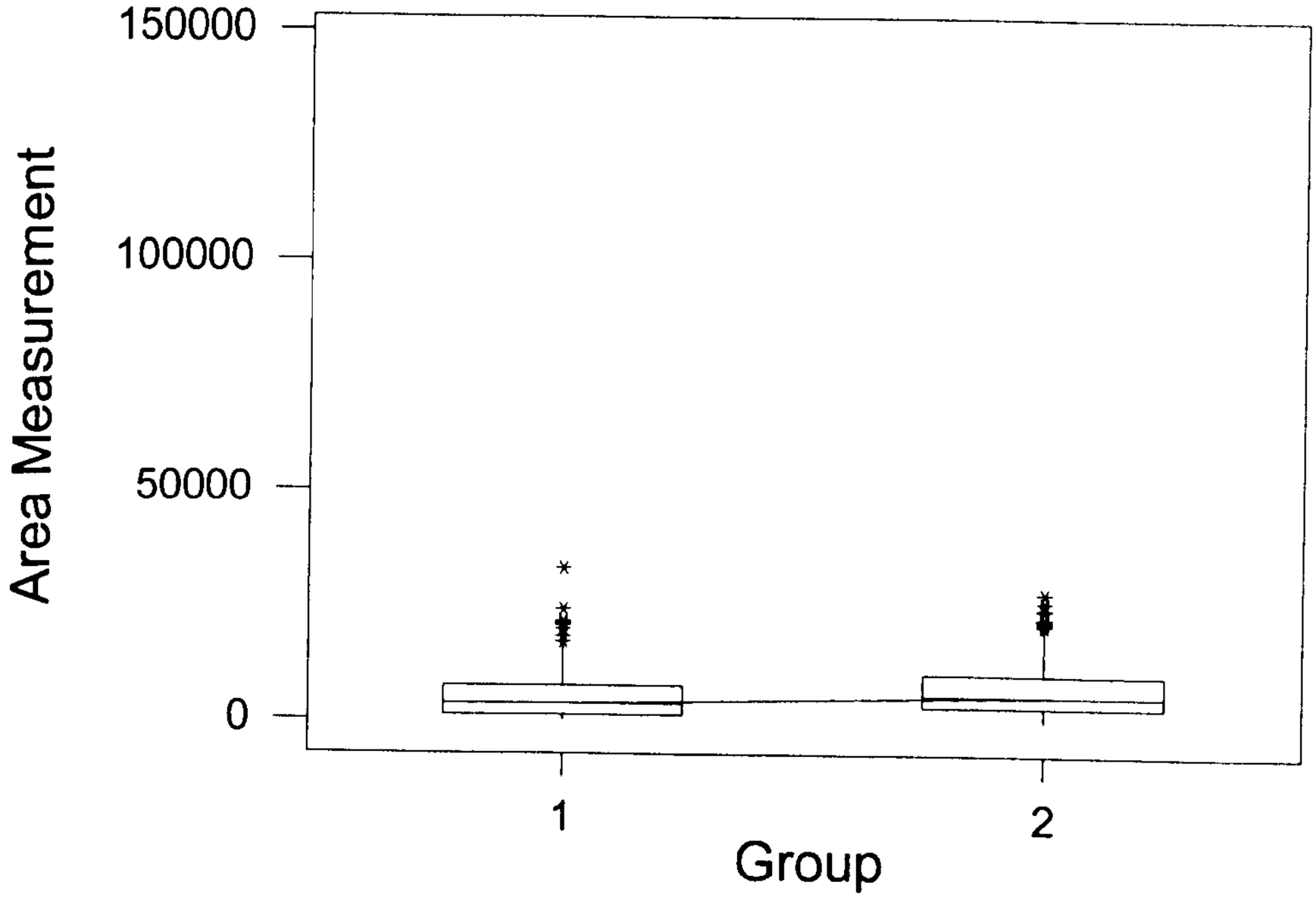

Figure 4.19 'Between group' comparison of Zone 2 median Cortical Area measurements (μm^2)

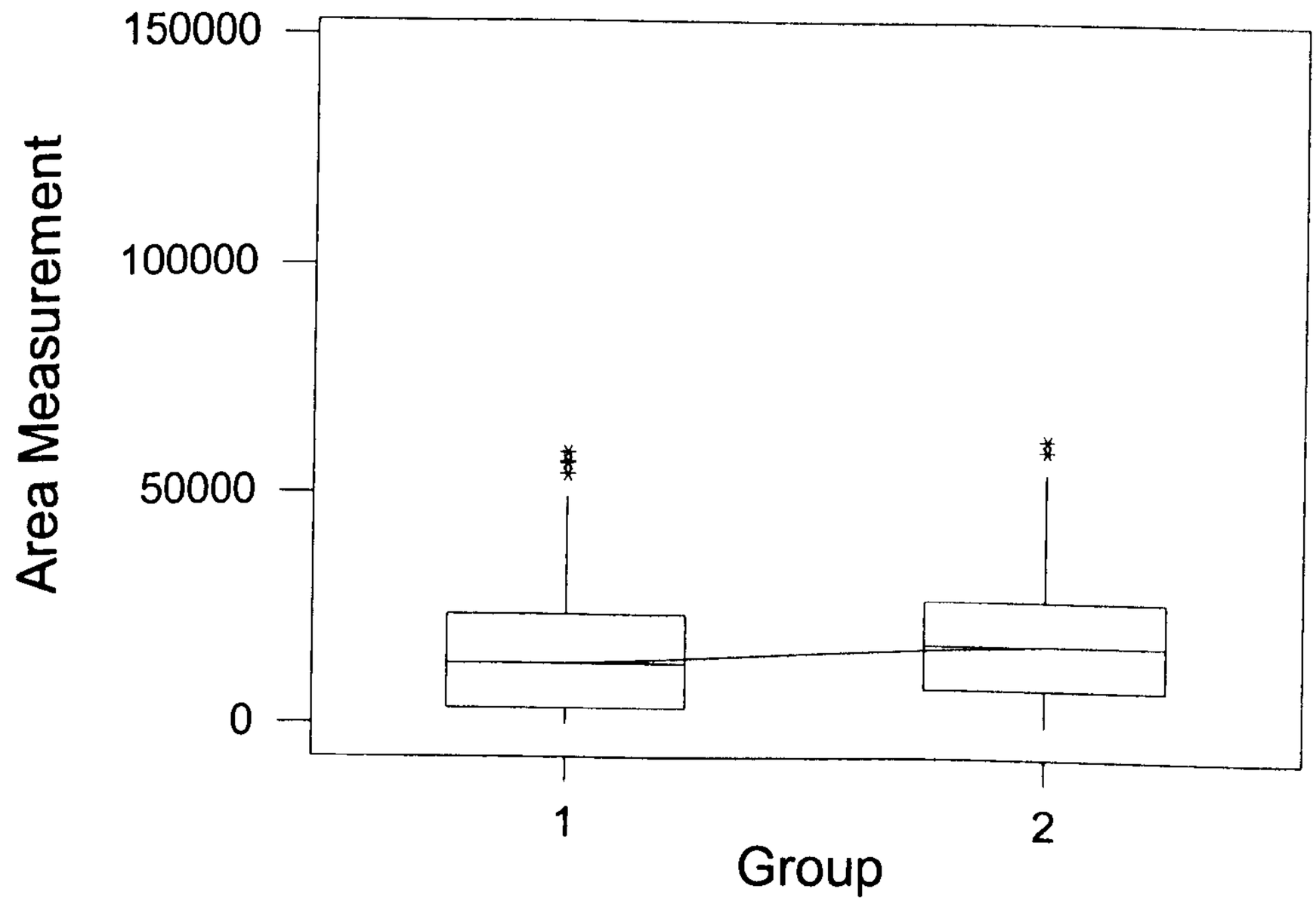

Figure 4.20 'Between group' comparison of Zone 3 median Cortical Area measurements (μm^2)

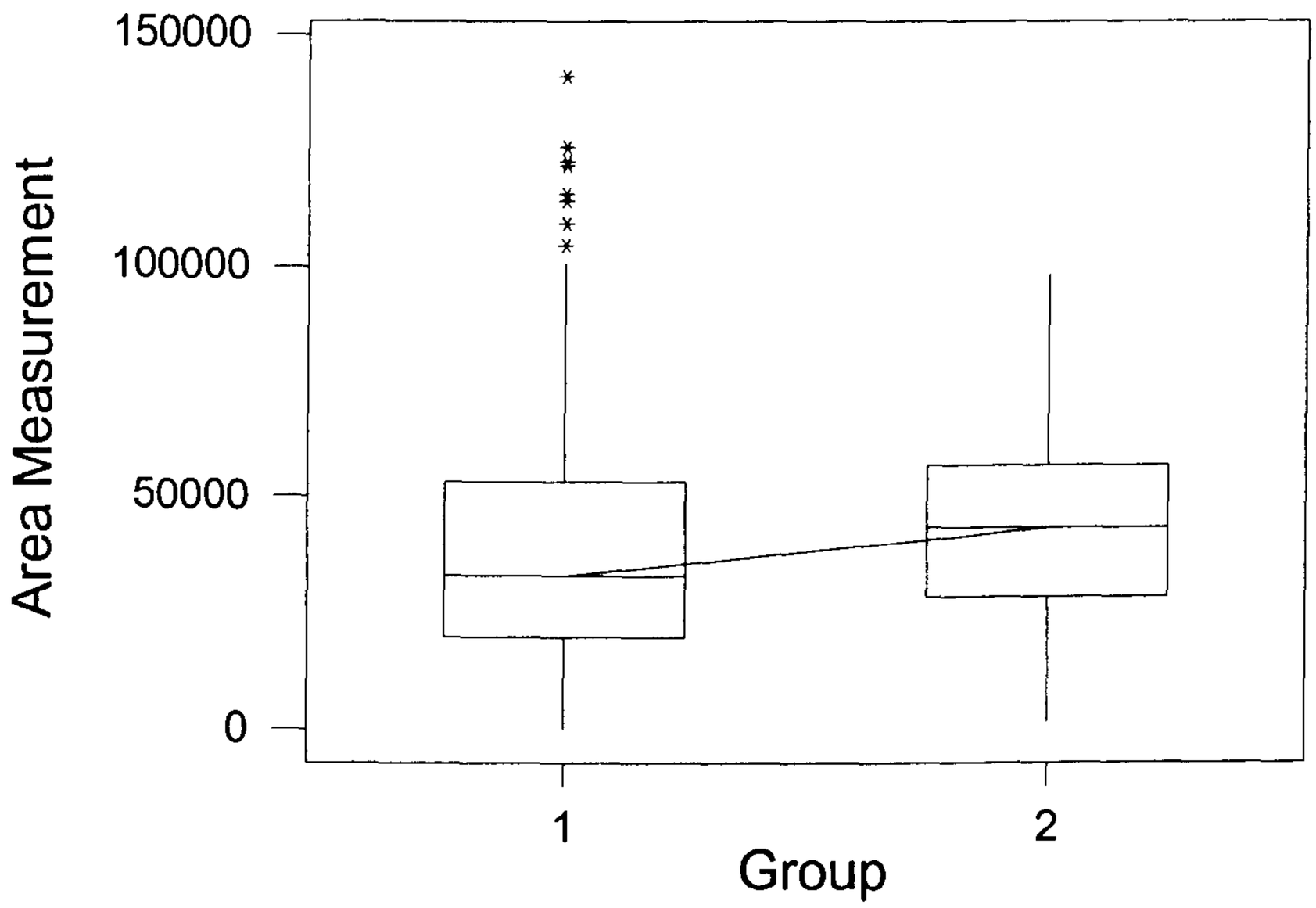

4.20.2.8 COMPARISON OF AREA FRACTION DATA BY LAMINITIC GROUP

MARROW AREA FRACTION

There was a tendency for Group 1 MaAF to be larger than that recorded for Group 2 (P=0.06), although this comparison was not significantly different at the 5% significance level. However 'between group' zonal comparisons revealed a significant difference in Z1 MaAF (P< 0.05), with Group 1 having a significantly lower area fraction than Group 2 – see Figure 4.21.

TUBULE AREA FRACTION

The median TuAF values in Z1 was significantly different between groups (P<0.05), with Group 1 displaying a smaller TuAF than Group 2 – see Figure 4.22.

CORTICAL AREA FRACTION

Similarly, Group 1 median CoAF data for Z1 was significantly lower in Group 1 compared with Group 2 (P<0.05) – see Figure 4.23.

Figure 4.21 'Between group' comparison of median Zone 1 Marrow Area Fraction

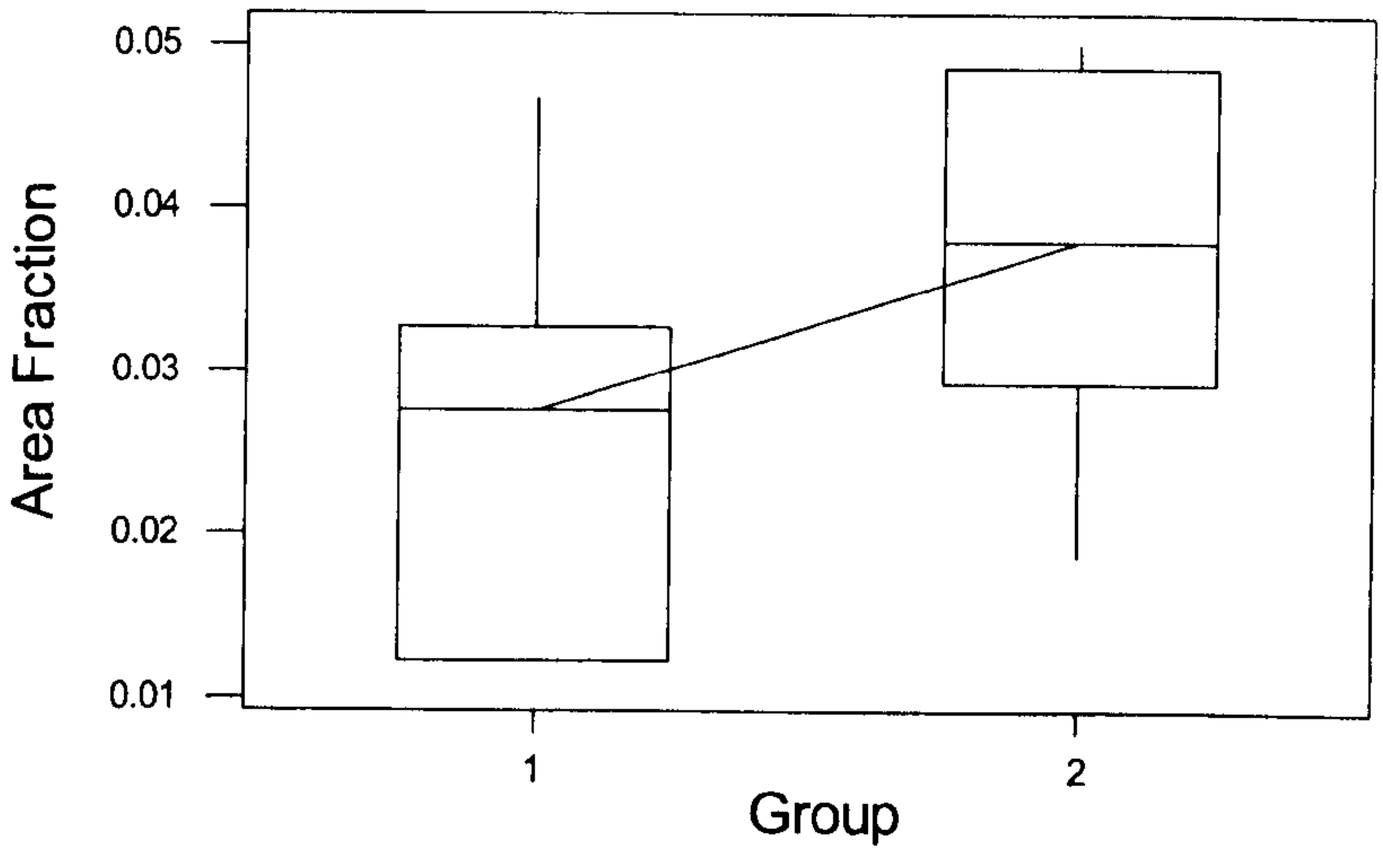

Figure 4.22 'Between group' comparison of median Zone 1 Tubule Area Fraction

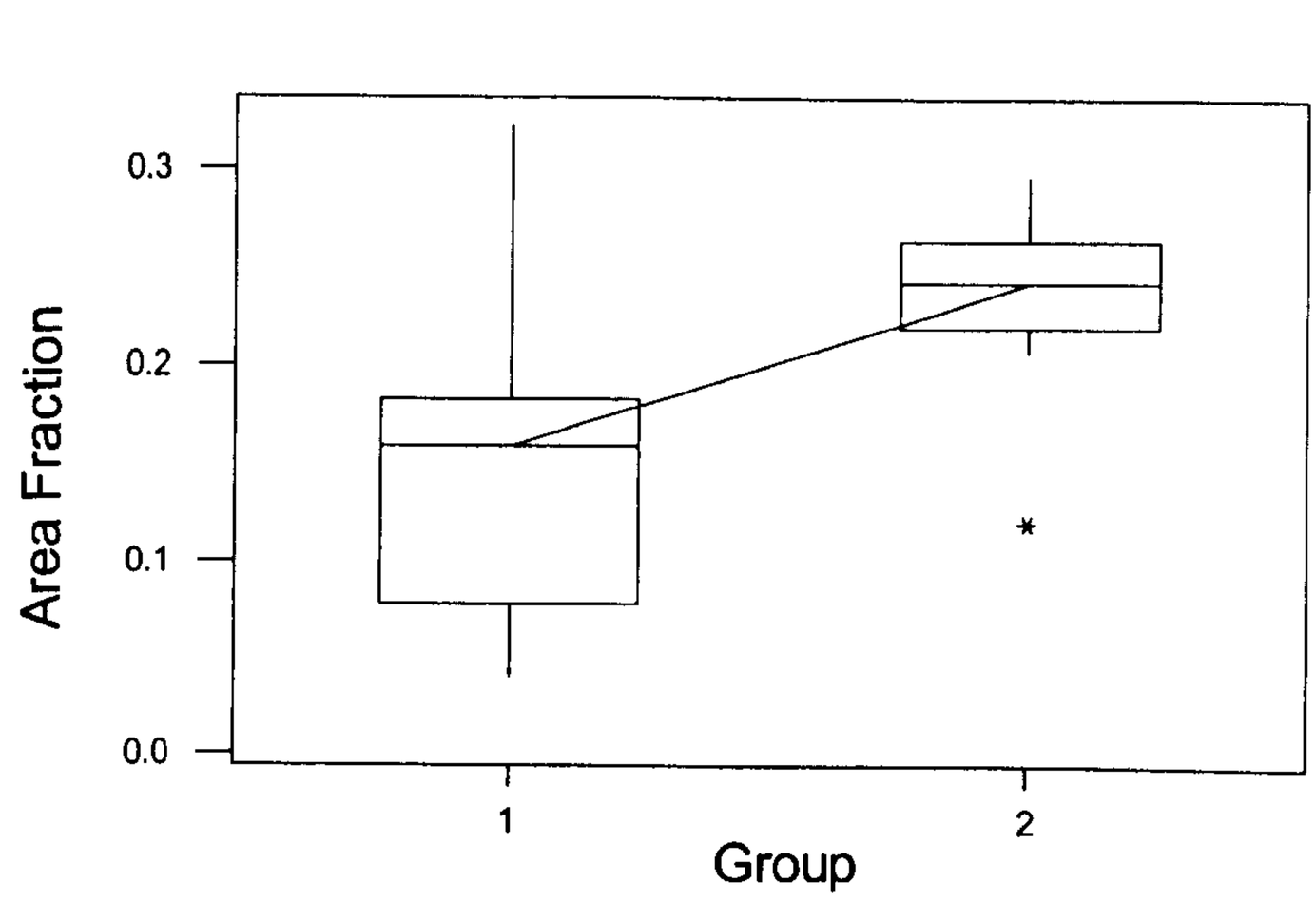

4.20.2.9 Comparisons of 'Feature' Specific Morphometric Parameters of Horn Tubule Structure

'Between group' comparisons revealed significant differences for parameters Tu:Ma(MA) in Z2 and Z3, with Group 1 displaying lower ratio values, and Ma:Tu(%) values in Z3, where Group 1 displayed higher percentage values. All other 'between group' comparisons were not significant

at the alpha level of 5%, however there was a trend for Tu(MA) and Ma(MA) to be lower in Group 1 (P=0.13).

Figure 4.23 'Between group' comparison of median Zone 1 Cortical Area Fraction

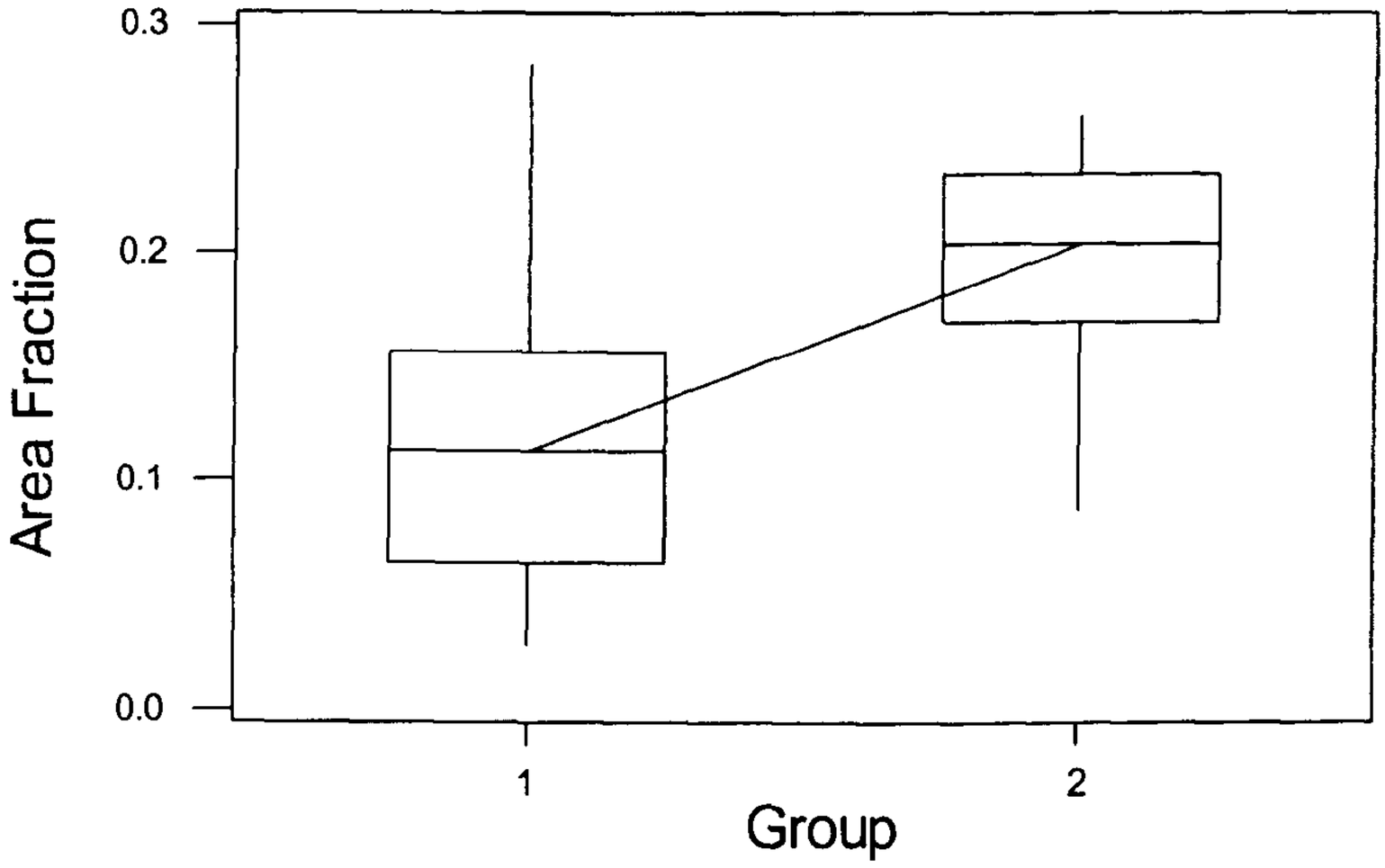

4.21 DISCUSSION

This study represents the first comprehensive characterisation of the structural organisation of the *SM* of the donkey hoof wall associated with the laminitic condition. It builds upon the former knowledge of this equid species reported by Doguer (1943) and Hifny and Misk (1983). This work differs from these former studies in that it has applied a synergistic approach combining morphology and morphometry. In this way, the structural organisation of the *SM* has been described and illustrated, and the key defining characteristics have been quantified. This approach has enabled the macroscopic and microscopic structure of the *SM* to be established. In addition, the effects of the laminitic condition upon structure have been investigated.

This study has adopted a unique materials science approach. It has specifically focused upon those structural features that are likely to affect the mechanical performance of the hoof wall. Hence this characterisation provides a basis from which the structure-function relationships can be further investigated.

In general, the structural organisation of the laminitic donkey *SM,* at the light microscopic level, conforms to the preliminary findings outlined by Collins *et al.* (2002). At this level of the design hierarchy, the *SM* was characterised by the presence of the three morphologically distinct tubule types, Donkey Tubule Types 1, 2 and 3, as described by Collins *et al.* (2002) and Collins and Reilly (2004b – Submitted). Both variants of the Type 3 Tubule, Type 3A and 3B, were present

within the *SM*. These tubule types all displayed a conventional or 'accepted' horn tubule structure, characterised by a relatively small marrow or medullary cavity, surrounded by a cellular cortex.

The regional distribution of these tubule types across the dorso-palmar depth of the *SM* conforms to the three-fold equid zonation pattern proposed by Kind (1961) and Schummer *et al.* (1981). However the finer detail of this zonation pattern differs from that described for the equine by Rössner (1940), Bucher (1987), Bolliger (1991) Schroth (2000), König (2001) and Patan (2001). Whilst the dorso-palmar depth of the three zones was described by these authors as being of 'equal dorso-palmar depth', the respective dorso-palmar zonal depths vary in the donkey.

Preliminary morphometric analysis of structure across the full HWD, by sequential image field, revealed the complex nature of the tubule size and shape changes that underlies the dorso-palmar change in zonal structure (Collins 1999 – Unpublished data). A broadly consistent pattern of changing structure across the HWD was evident between individuals, with zonal boundaries marked by statistically significant structural differences occurring at ~25% and ~40% HWD.

Confidence in this zonal division is supported both by empirical and experimental observation. These zonal boundaries are in broad agreement with the marked changes in macroscopic structural appearance evident within the *SM* of the donkey hoof wall (see Figure 1.15). There is also good agreement between the zonal boundaries established here, based upon regional difference in tubule morphology, and those reported by Hopegood (2002) and Reilly *et al.* (2003) which were based upon the dorso-palmar variation in tubule density (Figure 1.16).

The zonal boundaries for the donkey *SM* differ from those reported for the horse by Kasapi and Gosline (1997). This author reported major changes in tubule morphology occurring at 12.5 and 67%HWD This 'species specific' difference is consistent with the emerging picture of structural differences between other equid species (e.g. Kind 1961), and between other ungulate species (e.g. Reilly *et al.* 2002a).

The functional significance of the 'species specific' difference in zonation is unknown. This may indicate important differences in the biomechanical functioning of the hoof between the donkey, the horse, and other equid species, and therefore warrants further investigation.

Morphometric characterisation of the respective zones has resulted in an objective characterisation of macroscopic ('field' specific) and microscopic ('feature' specific) structure. On this basis the structural organisation of the tubular, cortical, and marrow and intertubular horn components has been elucidated, and horn tubule structure enumerated. However the effective morphometric characterisation of structure is dependent on experimental accuracy.

The image analysis protocol documented in this chapter provides the basis by which the morphometric assessment of hoof horn structure can be standardised and experimental accuracy optimised. It forms the means by which objective measures of structure can be ascertained, and pathologic structural change evaluated. This methodology has built upon the work of Reilly (2001). The use of image tiling has reduced the need to compromise image resolution in order to increase the size of the sampling area. Both of these factors are key considerations in striking the optimal balance between achieving measurement accuracy whilst ensuring that the resultant measurements are truly representative of the structure under examination.

In addition, measurement errors arising from image processing are minimised. As image resolution is maintained, there is no need for aggressive image processing to ensure satisfactory detection of feature boundaries. Aggressive image processing can results in image distortion, and thereby increases the potential risk of measurement error.

Accurate Area measurement, and Area Fraction determination is dependent upon effective discrimination of feature boundaries. The Ma-Co interface was readily detected across the entire dorso-palmar depth of the *SM*. Whilst the Tu-IT interface was similarly, established readily in Z1 and Z2, difficulties were encountered in delimiting this interface within Z3. Geyer (1980) also commented upon this fact within the inner zone of the equine *SM*. The inability to define this boundary with confidence may result in measurement error within this particular region of the *SM*.

Direct area measurement represents a logical progression from former methods (e.g. Kasapi and Gosline 1997, König 2001 and Patan 2001) of indirect determination of area. These were based upon the application of formula for simple geometric form to direct axis measurements. Direct measurement therefore improves measurement accuracy. It also offers the opportunity to accurately quantify irregular shapes. This is of particular significance when either deformational structural change has occurred or when the pattern of force distribution within the *SM* results in the generation of irregular, non-uniform cross-sectional tubule profiles. Both of these events are potential *sequela* to the laminitic condition.

The dorso-palmar zonal variation in the morphological appearance of structure is associated with a complex pattern of morphometric change. In summary, this was characterised by statistically significant dorso-palmar zonal increase in TuAF, CoAF, Ma, Tu and Co Area measurements, and cortical thickness, Co(MAT), Co(MIT). This zonal variation was also marked by a corresponding statistically significant dorso-palmar decrease in Area Fraction of both the Intertubular and Marrow horn components, and also the Ma:Tu(%).

The structural characteristics evident within the *SM* must reflect the functional demands placed upon this capsular component. Hence the structural characteristics detailed in this chapter must

relate to the hoof wall's ability to accommodate and ultimately resist the loading forces associated with weightbearing (Leach 1980), and its ability to achieve this without incurring excessive deformation or catastrophic failure.

The precise functional significance of these trends remains to be fully investigated. However, each of these different morphometric patterns are likely to exert distinct functional and mechanical effects upon the hoof wall. These effects will alter across the dorso-palmar HWD in line with its' zonal variation in structure. Thus the mechanical properties of the wall will result from the complex interaction of the different zonal structural effects.

The statistically significant differences in 'field' specific structural organisation and 'feature' specific horn tubule structure evident between zones are likely to affect the material properties of the respective zones, and thus influence the manner in which loading forces are distributed within the *SM* during weightbearing. Hence the structural changes across the HWD are therefore likely to contribute to the mechanical performance of the hoof wall, and influence the way in which force transfer is achieved between the ground and the skeleton.

Wainwright *et al.* (1976) concluded that energy absorption was as important as static strength in similar biological lead bearing structures. These authors stated that energy absorption is related to the amount of void space. This is because voids focus stress within a material and lead to crack generation and propagation (Griffith 1921).

The dorso-palmar zonal decease in zonal MaAF will tend to concentrate stress within the outer region of the *SM*. This may serve as an effective mechanism by which the sensitive structure of the foot are protected for aggressive stress concentration occurring at the laminar interface. In addition, by concentrating the loading forces within the outer region of the *SM*, stress can be focus within this region, microdamage can be accumulated within this superficial region, and damaged material eliminated in a controlled fashion, thus affording further protection to the deep structures of the foot.

The absolute shape and size of the Ma will also affect this process. This is because the degree of stress concentration is inversely related to the radius of curvature of the void (Gordon 1976). Hence under identical loading conditions, the stress raising effect of an ellipsoid is significantly greater than a circular void of similar area (Wainwright et al. 1976). Hence the oval shaped Ma of Z1 will concentrate stress at the Ma-Co boundary along the major axis of the Ma, where the radius of curvature is smallest.

The preferred orientation of the oval marrows in Z1, with their major axis aligned circumferentially around the hoof wall, may also be of functional significance. This orientation would encourage circumferential elimination of material, as crack propagation would tend to

course between regions of the high stress concentration focussed upon the major axis of the marrow. This mechanism would further discourage inward crack propagation.

The regional distribution of the relatively small Donkey Type 1 Tubule within this zone may also contribute to the process of energy absorption and also the controlled elimination of damaged material. De-bonding at the tubular-intertubular interface may serve to absorb energy within the hoof, in a similar manner to that which has been reported for composite materials by Cook and Gordon (1964). Hence the significant surface area to volume advantage of the relatively small Type 1 Tubules would significantly enhance the process of energy absorption within this region prior to failure. In addition, the preferred orientation of the tubule observed within this zone, with their major axis arranged circumferentially around the hoof wall, ensures that maximal surface area is presented to prevent inward crack propagation.

Controlled elimination of material from Z1 may also explain the 'simple' morphological appearance of the cortical cell organisation evident within the Type 1 Tubule (see Table 4.3 and Figure 4.1). It is has been argued by Kasapi and Gosline (1997), that the development of cortical complexity, in which different cell types and /or cortical cell orientation occur within the horn tubule, is directly linked to the development of crack deviation and mechanisms within the hoof. Thus the presence of a simple cortical organisation within Z1 would aid circumferential elimination of material.

The progressive reduction in marrow area fraction across the hoof wall, combined with the dorso-palmar zonal size reduction may minimise the risk of crack initiation at depth.

The axial rigidity of a column, its' resistance to loading deformation, is dependent upon the amount of material resisting the applied load (Biewener 1992, Vogel 1988). Hence, the skew in the distribution of absolute tubule and cortical area measurements within the respective zones potentially indicates that a minimum functional tubule size exists that prevents critical levels of deformation occurring during weightbearing.

The cortex serves to prevent stress transfer to the marrow (Leach 1980). Hence the cortex limits the stress raising effects of the medullary cavity, and thus may also be important in preventing crack initiation.

Failure in axial columns most commonly results from buckling (Wainwright *et al.* 1976). The thickness of the tube wall is the critical factor in the initiation of local buckling events (Biewener 1992). Conversely Euler buckling effect is inversely related to I (Biewener 1992). I increases the further the material is located from the neutral axis (Tubular axis), by the square of the distance from the axis (Wainwright *et al.* 1976). Thus the variation in cortical thickness and the marrow size will be critical factors limiting zonal buckling effects.

The pattern of increasing tubule size across the wall may produce a structure that progressively accommodates the mechanical demands, with each zone being more tolerant of the effects of deformation, without incurring failure. Thereby this structural organisation affords protection to the laminar interface, whilst also providing an effective method of energy absorption. In this way the structural organisation of the *SM* may represent an 'optimal design' in the manner described by Okamoto (1994).

The relatively thin cortical wall of the Type 1 Tubule potentially predisposes this tubule type to Local buckling effects. The oval cross sectional profile and the cortical streamlining evident within this tubule type, further compounds the situation. Thus the Ma(MI) and Tu(MI) values represents the determining factor governing Euler buckling effects in this tubule type. Whilst the Type 3A Tubules of Z2 similarly display a similar oval cross sectional profile, the relative size of the tubules, and the greater cortical thickness, represent significant theoretical mechanical advantages over the Type 1 Tubule. The presence of large diameter tubules, with large cortical thickness and small round marrows within Z3 may serve to optimise axial rigidity, limit Local and Euler buckling effects, and minimise crack initiation within this sensitive region of the *SM* that is adjacent to the laminar interface.

Leach (1980) however stated that hydration effects further mediate zonal rigidity across the HWD. This author stated that these hydration effects resulted in the inner hoof wall being more susceptible to compressive deformation than the outer wall. However, Nickel (1938a,b, 1939) suggested that the tensile forces generated within the intertubular horn during weightbearing were translated to the tubules, resulting in the generation of axial tension that resist the direct effect of axial compression.

Direct comparisons between the morphometric characteristics of the donkey and horse are difficult given the absence of a standardised assessment protocol. Whilst the morphological characteristics of Z1 bears certainly similarities to the equine, the morphometric characteristics highlight differences in structure.

With regard to 'field' specific characteristics, Z1 in the donkey displays a lower TuAF, and therefore a higher ITAF, than the majority of the corresponding data given for the horse by the European anatomists, e.g. Schroth (2000), König (2001) and Patan (2001). However the donkey value approaches that recorded by Collins (1998 – Unpublished data) for a slaughterhouse population of horses, and by Reilly (2001) for the pony. MaAF data for the donkey is comparable with the lower range of the corresponding equine data, and markedly lower than the pony value reported by Reilly (2001). 'Feature' specific data highlight other key differences. The cross sectional profile of the donkey Type 1 Tubule was more elliptical than that recorded for the horse in Z1, tubule and marrow area measurements were lower, as was the Tu:Ma(%). It

is therefore not possible to state categorically whether the Donkey Tubule Type 1 represents a similar structure to that described for this zone of the *SM* in the horse. Similarly it is not known whether these morphometric differences in structure represent 'species specific' differences, or the effects of differences in bodyweight and/or pathological change associated with the laminitic condition. Future work is required to resolve this issue.

With regard to Z2, The morphometric characteristics of structure showed a closer affinity with the horse. Donkey TuAF, CoAF and MaAF were consistent with the majority of data previously presented for the equine. Tu, Co, and Ma Area measurements were also comparable with the corresponding horse data (see Table 4.8).

However, the morphological characteristic of this zone highlight differences in structure. Specifically, the Donkey Type 3A Tubule, with its complex cortical cell organisation, does not resemble the horn tubule structure described within this zone for the equine by either Bolliger (1991) or Kasapi and Gosline (1997). In addition, the Type 2 Tubule, present within this zone of the donkey *SM*, has not been reported for the equine.

There is however a large degree of agreement in both the morphological and morphometric characteristics for Z3. Similarities are evident in both 'field' and 'feature' specific data. This suggests that the structural organisation of the *SM*, and also the horn tubule structure are common between these two equid species, within this zone.

In no zone of the *SM* were the tubule area measurements larger than those reported for the horse or pony. This challenges the assertion of Tohara (1948) that the donkey tubules are larger than the horse. What is evident however is a difference in the relatively dorso-palmar development of Z3 between species. In the donkey this accounts for ~60% of the HWD. This compares with ~25-33 % of the HWD in the horse. This difference may create the illusion of larger tubule sizes upon the macroscopic comparison of the respective *SM*.

In the absence of a concurrent control population of normal donkeys, it is not possible to assess the extent to which the structural characteristics are detailed above are affected by pathological change associated with the laminitic condition. This represents a key area for future work.

However indirect morphometric evidence of potential structural change was evident at the macroscopic level of the design hierarchy within the laminitic material obtained during the main experimental phase of thesis. The finding that 21 of the 23 trial animals displayed a dorso-palmar HWD greater than the predicted depth, derived in accordance with the algorithm of Hopegood (2002), is consistent with coronal elongation, linked to DP dislocation, resulting in alterations to subsequent hoof horn formation. Disruption to normal hoof horn production was further supported by the incidence of structural irregularities within the *SM* of material obtained during the preliminary stage of the experimental phase of this project.

This preliminary study represents the first occasion in which departures from the conventional structural organisation of hoof horn have been described in the donkey. Several of the structural irregularities appear to be comparable with those previously described for horse hoof by Tscherne (1910), Brunhke (1931), Rössner (1940) and Bucher (1987). Similar irregularities were found in this study to those reported to be associated with equine laminitis in controlled trials by Mostafa (1986), Nakada *et al.* (1992) and Said *et al.* (1992). This suggests that a similar mechanism may be involved in the development of these structural irregularities in both the donkey and the horse. In addition, several previously unreported irregularities were recorded. Whether these structural irregularities are directly linked to the laminitic condition, or whether they are secondary to pathologies occurring within the foot following digital collapse, remain to be fully investigated.

The incidence of structural irregularities with the *SM* suggests that the hoof may provide us with valuable sources of evidence of laminitic change. If this indeed is the case, then careful hoof wall assessment would permit us to investigate the effects of the condition still further. It is not possible at this stage to infer any direct association between the occurrence of these irregularities and the laminitic condition. However, as localised irregularities were observed in all cases, the possibility of an association with the laminitic condition can not be discounted. Further controlled objective trials are required to resolve this issue. Establishing appropriate control measures within the UK donkey population however, poses a particular challenge. Crane (2002) stated that all donkeys maintained within temperate grasslands are subject to a continuum of degenerative foot conditions. Hence study of material obtained from donkeys in their native environment may be an appropriate means of answering these questions in a controlled manner.

The presence of different irregularities suggests that different processes may be involved in their pathogenesis. These irregularities might either be of a formational or deformational origin. Formational changes may arise from vascular compromise, inflammatory response, papillary damage within the coronary corium, and/or degradation of the BM. Alternatively, they may reflect regenerative processes associated with wound healing response mechanisms.

Deformational events may result as a consequence of alterations in force distribution within the *SM*, degenerative anatomical changes with the foot, or as a *sequela* of 'poor quality' horn production, that is not able to sustain normal hoof function.

Knowledge of the biomechanical consequences of digital collapse associated with laminitis is limited. However Oliver (1987) and Hood (1999a) stated that compromise to the SADP prevents normal force transfer across the laminar interface. This increases the forces acting both within the *SM*, and upon the coronary corium. As the mechanical and functional properties of

the *SM* are influenced by the structural organisation of tubular horn and intertubular horn, changes to the accepted structural organisation may have profound effect upon hoof function. These structural changes probably alter the material properties of laminitic hoof horn, and hence directly affect stress and strain distribution across the HWD. Conversely, changes in structure may themselves be indicative of functional compromise. This may result as a consequence of the production of 'poor quality' hoof horn material or from changes in force distribution within the *SM*, and altered force transfer across the laminar interface due to SADP compromise.

Insights into changes in force transfer across the hoof wall, and laminar interface, and elsewhere within the donkey hoof capsule, in normality and disease, will be possible with the further development of the finite element analyses previously reported by Newlyn *et al.* (1998, 1999).

The non-specific nature of the structural irregularities between individuals may indicate that different individuals may be affected by laminitis differently. In this regard, Hunt (1993) stated that laminitis results in a diverse series of digital pathologies, and that the progression of the condition varies considerably between individuals. Thus differences may reflect the severity and duration of the acute phase, the nature and extent of the DP dislocation, attendant secondary pathologies, and/or the effectiveness of the wound healing responses. Conversely these differences may reflect individual distinctiveness in response to the condition, or different stages in a continuous series of common events linked to the progression of the condition.

Different structures occurring in different regions across the HWD may suggest zonal differences in response to the condition. This may relate to the presence of different papillar types, or conversely it could imply that the effects of the condition differ across the dorso-palmar depth of either the coronary corium and/or the *SM*.

Although the precise effects of laminitis upon the dermal papillae are unknown, there are isolated reports of anatomical changes to papillary bodies within the coria of the foot. For example, papillar branching has been recorded in the bovine solear corium in association with overgrown feet (Singh *et al.* 1992), Rusterholtz sole ulcers (Mauske 1972), and laminitis (Maclean 1971b).

The occurrence of the MMT irregularity suggests papillar branching, with several apical tips within a single dermal papillary body. The MTC irregularity could arise either as a result from a more extensive division of a single papillary body to that which gives rise to the MMT irregularity, or from the presence of adjoining papillary bodies, with no intervening interpapillary dermis.

Maclean (1971b) also reported that the solear papillae in laminitic cattle were broader than normal. This may reflect a similar inflammatory response to the oedematous broadening of the dermal lamellae associated with laminitis. Similar broadening within the coronary corium may

account for the presence of ET irregularities. The loss of normal cortical organisation within the ET irregularity may indicate BM degradation within the coronary region leading to a disruption in the normal co-ordinated pattern of horn formation.

Singh *et al.* (1992) also reported the loss of normal dermal topography within the solear corium in laminitic cattle. Dermal papillae were either completely absent or when present, were flattened. Similar regional changes to the coronary papillae may account for the presence of the AT irregularity, and may explain their association with regions characterised by the absence of tubular horn structure. Alternatively, sectioning of 'kinked' or 'crimped tubules' may account for either the AT irregularity and its association with regional ATH, and/or the MT irregularity. Conversely changes in the force distribution within *SM* might provide a deformational origin for the MT and AT irregularities.

The occurrence of the WT irregularity may result from either formational or deformational events. This irregularity may directly reflect localised papillar compression in the outer region of the coronary corium. The association of the WT irregularity with hoof wall splitting (Collins – Pers Obs.) lends supports to a deformational origin.

The specific mechanism by which the effective marrow size is determined is unknown. Marrow enlargement may arise as a direct consequence of primary changes in the size or shape of the papillar tip, mitotic activity within the suprapapillary region, or diffusion deficiencies following disruption to the papillary blood supply. These events are likely *sequelae* of the vasoconstriction, oedema, infarction and/or BM degradation associated with laminitis. However, Geyer (1980) suggested that marrow enlargement occurred in 'poor quality' hoof as a consequence of cortical degradation. Aberrant keratinisation and cornification results in reduced cellular cohesion within the cortex, and produces a tubular structure that is less resistant to cortical degradation in response to biomechanical forces acting upon the *SM*.

The EM irregularities are characterised by an expansive cortex, hence there is no morphological evidence to suggest Co degradation. The TV irregularity however suggests extensive degradation of the Co. In addition, the atypical cortical staining observed in this irregularity resembles that typically seen within the partially keratinised marrow horn fraction of the horn tubule.

The presence of different structural irregularities within the respective zones of the *SM* suggests that laminitis affects the different regions of the *SM* and/or coronary corium differently, or at different times. In addition, between-case variation in their occurrences may suggest individual differences in response to the condition. This may reflect variations in the nature and extent of the DP dislocation, the severity of dermal tissue damage and circulatory compromise, and/or the degree to which regenerative processes restore normal hoof wall function. However, individual

variation in bodyweight, hoof shape, and hoof size are also likely to contribute to this variation. These factors will contribute to the nature and extent of force distribution within the foot and also influence the functional capabilities of the hoof capsule.

Between group comparisons of both 'field' and 'feature' specific parameters reveal a complex picture of difference in structure. Whilst the precise mechanisms responsible for this difference in structure are unknown, these structural differences were associated with a significant difference in the degree of anatomical coronal disruption, assessed by the dorso-palmar difference in predicted and actual HWD, between the two groups. The degree of coronal disruption was greater within Group 1, compared with Group 2. With regard to 'field' specific characteristics of structure, Group 1 displayed significantly lower Z1 TuAF, CoAF and MaAF values, lower Z1 Ma Area measurements, lower zonal Tu and Co Area values and greater Z3 Ma Area measurements. Significant 'between group' differences in feature specific characteristics of horn tubule structure were also recorded, with Group 1 having a lower Z3 Tu:Ma(%) and Z2 and Z3 Tu:Ma(MA) values.

These findings suggest that the effects of this difference in the degree of coronal disruption occur across the entire dorso-palmar extent of *SM*. However the precise nature of the structural change that the coronal disruption causes varies between zones. These findings indicate that morphometric characteristics of structure are related to the degree of anatomical change associated with DP Dislocation.

It is not known whether these changes represent formation changes of deformation events occurring within the *SM*.

Anatomical disruption to the coronary corium associated with DP dislocation results in disruption to the coronal circulation that is commensurate with the extent of dislocation (Hood *et al.* 1993b, 1994). This leads to reactive changes in the degree of horn production (Hirschberg *et al.* 2001). This disruption is particularly marked within the papillary microcirculation (Hood *et al.* 1993b), and hence could explain the reductions noted in absolute area measurements for the horn tubule.

Reductions in TuAF and CoAF values may also reflect the physical process of dorso-palmar elongation of the coronary corium. If the number of papillae remains constant during this process, then the TuAF and CoAF must decrease an automatic *sequela* of the physical increase in area of the coronary corium.

Conversely the reductions in tubule may reflect the effects of deformation changes to structure within the *SM*. The incidence of the WT tubule irregularity and also zonal delaminition provides indirect evidence of deformational structural change occurring within the *SM* of the donkey in associated with laminitic condition. Feature specific data of tubule structure also suggest that

deformational change may be present. The trend towards a 'between group' difference in median Z1 Tu(MA) values (P=0.13), whilst between group median Tu(MI) values remain similar (P=0.97) is difficult to explain in terms of reactive hoof horn formation. In this regard, deformation of structure in the direction of the major tubule axis, seem a more logical explanation.

These 'between group' structural differences are likely to result in differences in the material properties, and thereby lead to differences in the finer functioning of the *SM*. This may ultimately affect the manner of force distribution and transfer within the *SM*, and could have an important bearing upon the level of biomechanical impairment within the laminitic foot. For example, the lower cortical area recorded in Group 1 is likely to result in a lower axial resistance for a given load, and result in a greater deformation compared to Group 2. Subtle functional consequences are also suggested in the absence of direct statistical differences. For example median Co(MIT) values are similar between groups, hence the propensity for Local buckling are likely to be similar, however as Ma Area measurements are significantly smaller in Group 2, the *I* for Z3 tubules in this group will be lower than that for Group1. Thus the critical Euler buckling load within Group 2 will be anticipated to lower than that for Group 1. This may be of particular relevance with regard to the laminitic condition. This is because tubule crimping, which is a common macroscopic observation in laminitic hoof horn, may be evidence of buckling failure occurring within the *SM*.

Structural changes associated with anatomical disruption could account for the reported relationship between condition severity, the degree of biomechanical impairment, and the extent of anatomical change evident within the afflicted foot.

Although it is not possible at this stage to confirm whether changes in structure occur in association with laminitic condition in the donkey, morphometric changes have been reported for the horse by Mostafa and El-Ghoul (1999). Reductions in zonal Tu and Co Area measurements and Area Fraction data were recorded by Collins (1997 – unpublished data) in a blinded assessment of laminitic pony *SM* compared with control normal pony material.

It is not possible at this stage to confirm what specific morphometric characteristics of the donkey *SM*, documented within this chapter of the thesis are affected by the laminitic condition? Whether the nature and/or extent of the DP dislocation event do indeed directly affect the structural characteristics? What formational and/or deformational events are involved? How does the progression of the condition alter the structural organisation of the *SM*? These are all critical questions arising from this study that need to be investigated further. The answers to these questions will only come from controlled trials involving normal donkey material to provide essential baseline structural data. Concurrent radiographic evaluation is required to

further investigate the potential relationship between morphometric characteristics of structure, and DP dislocation. In addition, careful hoof horn assessment, including serial sectioning and three-dimensional image reconstruction techniques, is needed to assess structural changes over time. This however is totally reliant upon sourcing material from animals in which an accurate time line for the condition is known. Hoof horn assessment conducted in this way would also serve to provide information regarding potential structural change of formational origin. Histometric and/or morphometric evaluation of the dermo-epidermal junction at the CB would also provide evidence as to dermal changes that may affect hoof horn formation e.g. BM degradation, changes in papillary morphology, papillary branching, or loss of papillary structure.

Finally morphological assessment of material previously loaded at stress levels in excess of bioyield, coupled with non-linear computer modelling techniques, may provide a means of simulating structural change of deformation origin.

5. MATERIAL TESTING OF LAMINITIC DONKEY HOOF HORN

5.1 OVERVIEW

The objective assessment of hoof quality in respect of function poses a particular challenge (Reilly 1995). Resolving these issues represents an important step towards unravelling the structure-function relationships that exist within the hoof, and also in understanding the functional effects of pathological change.

The ability of the hoof wall to achieve its functional objectives of force modulation and energy absorption is ultimately governed by its defining material properties. Hence the assessment of material properties represents an essential element of a comprehensive materials characterisation of laminitic hoof horn.

The ability of the hoof wall to accommodate and resist imposed forces is determined by its modulus of elasticity, whilst energy absorption, prior to permanent deformation, is determined by the resilience of the 'material'. The objective assessment of these specific material properties is therefore of paramount importance in elucidating the biomechanical function of the hoof, and assessing the effect of pathological change.

Whilst the modulus of elasticity has been widely reported within normal equine hoof horn, and more recently in the donkey by Collins *et al.* (1998) and Hopegood (2002), little is known of the energy absorption capabilities of equid hoof horn. In addition, despite the debilitating biomechanical consequences of the laminitic condition, its effects upon these key material properties have not been previously reported in the equid. These issues represent major shortcomings within the present knowledge base.

This chapter seeks to address these outstanding issues, and details work associated with the objective assessment of both the modulus of elasticity and resilience of laminitic donkey hoof horn under controlled testing conditions.

5.2 INTRODUCTION

The biomechanical capabilities of a biological system are dependent upon the material properties of its constituent elements (Wainwright *et al.* 1976, Vogel 1988, Vincent 1992, Biewener 1992). However the specific loading response of a 'material' is also affected by the nature, magnitude, and direction of the applied load (Gordon 1976).

Hence Vincent (1992) stated that mechanical testing of biological materials must appropriately reflect the conditions under which the material functions. Thus this author stated that the tensile

testing of a biomaterial that is predominantly subjected to compressive forces '*in vivo*' is inappropriate when endeavouring to elucidate the materials functional capabilities.

Due attention must therefore be given to the nature and extent of the loading condition to which the material is subjected '*in vivo*' (Vincent 1992). This information must form the basis by which relevant mechanical properties are identified, and also, in establishing appropriate testing protocol by which to investigate these mechanical properties.

5.3 MATERIAL PROPERTIES OF EQUID HOOF HORN

Various studies dating back over the past 100 years have attempted to characterise the material properties of equid hoof horn. However these studies have variably used a range of different material testing techniques, in an apparent *ad hoc* manner, to define a number of different material properties. In fact, until the recent work of Leach (1980), Kasapi and Gosline (1996, 1997), Collins *et al.* (1998), Hinterhofer *et al.* (1998), Reilly (2001) and Hopegood (2002), there has been little detailed debate as to scientific rational behind their selection criteria. Direct comparisons between these historical studies have been limited further by the fact that standard testing protocols have not been adopted. Hence progress to date in establishing the structure-function relationships within the hoof wall has been limited. As a consequence of these facts, our knowledge of the impact of pathological change is poorly understood, and the biomechanical consequences of these changes are unknown.

If effective progress is to be achieved, there is need to review this situation and ensure that relevant material properties are identified, appropriate testing techniques employed, and standard testing protocols adopted. This must take into account knowledge both of the biomechanical functioning of the hoof wall, and the structural organisation and material properties of the hoof horn. In addition, the practical limitation of conducting mechanical testing within the laboratory environment must be considered in arriving at appropriate testing regimes. In this way it will be possible to objectively assess the key defining material characteristics of the material in a controlled and repeatable manner. This will ensure a common basis of reporting. In addition, this approach will provide a basis by which structure-function relationships can be further investigated, and effects of pathologic change effectively evaluated. Section 1.9, highlighted that fact that the hoof wall deforms in a consistent and repeatable manner during loading. This deformation generates internal forces that counter these loading forces. This deformation however must not be excessive, so as to maintain protection to the sensitive structures of the foot and prevent catastrophic failure. This deformational response is central to the process of force modulation and energy absorption within the hoof, and also the cyclic force transfer between the skeleton and the ground.

The modulus of elasticity (E) that dictates the degree to which a linear elastic material deforms for a given load, whilst the resilience of the material determines the amount of elastic energy absorbed during this deformation (Wainwright *et al.* 1976). As such, these parameters represent fundamental defining characteristics which have specific functional importance to the hoof (Collins *et al.* 2002). An intimate relationship exists between E and resilience (See Appendix I). That is: -

Resilience = $\sigma_Y^2 / 2E$

Where:

E = Modulus of Elasticity

σ_Y = Yield Stress – the stress level that marks the proportional limit of the stress-strain relationship of the 'material'.

5.3.1 THE MODULUS OF ELASTICITY OF EQUID HOOF HORN

The E of equine hoof horn has been widely reported – see Table 5.1. However determination of this parameter has been conducted under a range of different testing and loading conditions. E has been determined under uniaxial conditions, including both tensile and compressive loading forces, and also under flexural loading (bending). It is important to note however, that absolute values are strongly influenced by the nature of the loading conditions. In this regard, flexural E only approximates to E derived under uniaxial conditions (BSEN 2746 1998). In fact E values obtained under uniaxial conditions may themselves differ, dependent upon whether the material is tested under tensile or compressive loading conditions. Hence in order to arrive at E values that are of functional relevance, testing must be performed under conditions that appropriately reflect '*in vivo*' loading conditions.

Considerable debate exists however as to the precise nature of the '*in vivo*' forces to which the hoof wall is subjected (Newlyn *et al.* 1998). Leach (1980) summarising the earlier theoretical work of Mair (1974) and Bartel (1978) relating to hoof function stated that the hoof wall was likely predominated by the influence of compressive forces. More recently, '*in vivo*' surface strain gauge studies by Thomason *et al.* (1992), Chang *et al.* (1993) and Thomason (1998) have reported that the hoof wall was indeed subject to biaxial compression at the MDC anatomical site during weight bearing.

Table 5.1 Summary table of modulus of elasticity values for the Full HWD equid hoof horn

Author	Area of Hoof Wall Tested	Modulus of Elasticity (MPa)	Hydration Status	Strain Rate $\mu\varepsilon s^{-1}$
Tensile Testing				
Bertram (1984)				
Bertram and Gosline (1986)	Dorsal wall	410-485 2630 3360 14600	MR_M MR_{RH75} MR_{RH53} MR_0	3333
Kasapi and Gosline (1996)	Dorsal wall	280 320 470 850	MR_M	1600 32000 330000 70000000
Compression Testing				
Butler (1976)	Dorsal wall	372	MR_M	4233
Zoerb and Leach (1978)	Dorsal wall	215	MR_F	850
Landeau *et al.* (1983)	Dorsal wall	216-402	MR_M	1730 - 2870
Flexural Testing				
May (1924)	Dorsal Aspect	500	MR_M	Not Stated
Garnhaft (1925)	Dorsal Aspect	471-491	MR_M	Not Stated
Kasapi and Gosline (1996), Kasapi (1997)	Dorsal wall	410	MR_M	32000
Reilly (2001)	MDC - PNHG	1347 457 345	MR_0 MR_F MR_M	694

Key: MR, Moisture Regain. Subscript, **M** for Maximal Hydration Level, F for Fresh, 'in vivo' Hydration Level. **0**, Dehydrated. **RHXX**, equilibrated at specified relative humidity.

However Hood *et al.* (1991) utilising force transducers capable of discriminating between compressive and bending forces stated that pure compression alone was not recorded in the hoof wall. These authors stated that the hoof wall was subject to either pure bending or, a combination of compressive and bending forces. Indeed computer modelling of the donkey hoof wall by Newlyn *et al.* (1998) also predicted a similar combination of compression and bending forces occurring at the MDC anatomical site. These findings have been used both by Reilly (2001), in respect of the horse, and Hopegood (2002), with the donkey, as a justification for the adoption of flexural testing protocols.

However the relative proportion of these two forces has not been determined in either equid. What can however be deduced from first principles is that, the steeper the DHWA, the greater the compressive component will be. This may be of particular relevance with regard to the donkey, given the relative upright nature of the hoof wall. Hence the relative compressive component is likely to be greater than that experienced within the horse. This remains a pivotal

issue with regard to establishing an optimal testing protocol for the assessment of donkey hoof horn.

Several researchers including most recently Kasapi and Gosline (1996, 1997), Douglas *et al.* (1996, 1997) and Douglas (1998) have determined the E in response to tensile loading conditions. There is however little evidence to support the '*in vivo*' predominance of tensile forces within the capsule. Whilst it is accepted that the occurrence of tensile forces are an essential prerequisite for crack formation, there distribution within the hoof capsule is likely to localised, or occur in association with compressive forces due to flexure within the hoof capsule.

It is not known whether the uniaxial modulus of elasticity is independent of nature of the loading force. Douglas *et al.* (1996) reported significant differences between the E obtained by tensile and compression testing. The tensile modulus (E_T – Subscript T for tensile) was significantly lower than the corresponding value obtained by compressive loading (E_C – Subscript C for compressive) However these authors could not discount the potential effects of experimental error, due to sample slippage within the retaining clamps. Hence they were unable to confirm an actual difference in uniaxial moduli. Until this issue is resolved direct comparisons of data obtained under tensile and compressive loading must be viewed with due caution. This issue is also of particular relevance with regard to the determination of the flexural modulus (E_F – Subscript F for flexural). This is because one of the guiding tenets of bending theory is that the both the compressive and tensile moduli of the material are assumed to be the same.

5.3.1.1 Intrinsic Factors Affecting the Modulus of Elasticity of Hoof Horn

Nature has a tendency to rely upon pliant materials that exhibit visco-elastic material properties. In addition the organisation of these materials is such that a distinct directional component often occurs within the structure. These factors combine to produce a biomaterial in which material properties are also highly dependent upon: -

- Sample orientation
- Loading rate
- Hydration level

MECHANICAL ANISOTROPY

The structural organisation evident within many biological materials results in the generation of anisotropic mechanical behaviour (Wainwright *et al.* 1976), where the E is dependent upon the

direction of loading. The anisotropic nature of equid hoof horn has been reported by several researchers including, Leach (1980), Bertram and Gosline (1987) and Kasapi and Gosline (1997).

It is not known what elements within the design hierarchy of the hoof that is responsible for the development of this anisotropic behaviour (Kasapi and Gosline 1997). However it has been suggested by Schummer *et al.* (1981), Cope *et al.* (1998) and Newlyn *et al.* (1998, 1999) that the structural organisation of the equid hoof at the microscopic level may act as a unidirectional fibre composite. In this regard, the horn tubules serve as reinforcing fibres dispersed within a matrix of intertubular horn. It was suggested by Newlyn *et al.* (1998) that this structural organisation exists to afford the hoof with the mechanical advantage inherent within composite material (see Section 1.9.2). If this indeed is the case, it is reasonable to expect that there would be a relationship between the structural organisation and the principle loading forces evident within the hoof wall.

Surface strain gauges have been used to attempt to elucidate this potential relationship in both the horse (Thomason *et al.* 1992, Chang *et al.* 1993) and the donkey (Chang *et al.* 1993). The results of these experiments are equivocal. Whilst Thomason *et al.* (1992) reported that no such relationship could be discerned, Chang *et al.* (1993) stated that a direct relationship existed between the tubular axis and the direction of principle loading strain in both horses and donkeys.

HYDRATION EFFECTS

The effect of hydration upon the E of horn material has been well documented. This has been investigated in Gemsbok head horn (Kitchener 1987, Kitchener and Vincent 1987), Bovine claw horn (Baillie *et al.* 2000), equine hoof horn (Bertram and Gosline 1986, Reilly 2001) and donkey hoof horn (Collins *et al.* 1998, Hopegood 2002, Hopegood *et al.* 2003a). These studies have variably investigated E values across a range of moisture levels ranging from dehydrated to maximal hydration. The results of these studies are broadly consistent in two important respects. Firstly there is an inverse relationship between the level of hydration and E. It is important to note however, that the detailed work of Baillie *et al.* (2000) suggests that this relationship is not linear. The sigmoidal relationship reported by these authors is consistent with that expected from a viscoelastic material passing through glass transition. Secondly, specimen hydration, from dehydrated to maximal hydration, results in an order of magnitude decrease in E, a gigapascal to megapascal shift. The results of the work of Hopegood (2002) are given in Table 5.2. In addition Latham (2001 – Pers Com.) recorded a mean E_F for full HWD of 205MPa at maximal hydration.

Collins *et al.* (1998), Reilly (2001) and Hopegood (2002) commenting upon the effects of hydration upon *E*, stated that in order to effectively compare *E*, specimens must be controlled with respect to their moisture levels.

In order to arrive at appropriate control measures for the effects of moisture a concurrent analysis of the hydration characteristics of laminitic donkey hoof horn was undertaken. This study was conducted on material obtained from the laminitic trial population (Collins 2003 – Unpublished data).

This assessment used gravimetric techniques to characterise gross moisture levels within the hoof horn material. Percentage Moisture Content, %MC (Von Bergen 1963) and Moisture Regain, MR (ASTM D1576-90) data were determined, both at 'in vivo' (subscript F for fresh) and maximal (subscript M for maximal) hydration levels. This was performed in accordance with the desiccant drying technique advocated by Collins *et al.* (1998) and Hopegood (2002). Percentage Saturation (%S) data were also determined at '*in vivo*' hydration levels, based upon Moisture Regain (subscript R for regain).

In addition, the technique of differential scanning calorimetry (DSC) was used to further investigate the nature of the water-hoof interaction. This inferential technique enabled the objective assessment of the partitioning of water within the material into distinct 'bound' and 'free' water fractions. This is of particular importance because it is water that binds directly to the material (the 'bound' water fraction) which is responsible for the modulation of material properties, through the process of 'plasticisation' (Marks 1981).

The data obtained from this hydration characterisation study are summarised in Appendix VII. These analyses highlighted the following: -

- A statistically significant dorso-palmar increase in zonal moisture content (MC) and moisture regain (MR) values across the HWD ($P<0.05$), at both '*in vivo*' and maximal hydration levels.
- $\%S_R$ data indicated that at 'in vivo' hydration levels, the full HWD was at ~90% of the material's capacity to hold water
- Zonal differences were present in the absolute amounts of 'bound' and 'free' water, and also in the partitioning ratio of 'bound' to 'free' water fractions within each respective zone
- At 'in vivo' hydration levels predicted data indicated that Z2 and Z3 were at moisture levels which exceeded their respective bound water capacity, whilst Z1 was 1.6gH_2O/100gDM below its bound water capacity
- There were no 'between Laminitic Group' differences in MC_F, MR_F, MR_F, MR_M, or $\%S_R$ values

- There was NSD in full HWD and zonal MC_F, MR_F, MR_F, MR_M values, between laminitic donkey hoof horn obtained in this study, and corresponding data previously reported for normal donkey hoof horn by Hopegood (2002), at either '*in vivo*' or maximal hydration levels
- There was NSD in either full HWD or zonal $\%S_R$ values between laminitic donkey hoof horn calculated in this study, and data derived by this author, from MR data reported for normal donkey hoof horn by Hopegood (2002)

In conclusion, there appears to be no laminitic effect upon the gross moisture levels within donkey hoof horn. In addition, the '*in vivo*' hydration levels suggest that the donkey hoof horn material is in a state approaching full plasticisation. The specific implications of these findings in respect of material testing are discussed in Section 5.6.4.

Table 5.2 Full HWD moduli values for donkey hoof horn at three different hydration levels (after Hopegood 2002) Adapted to meet the convention of this thesis

Hydration Level	Mean	SD	*CV*
Dehydration (0%MC)	2168 MPa	+/- 510 MPa	**0.23**
'In Vivo' Hydration (MC_F)	194 MPa	+/- 64MPa	**0.33**
Maximal Hydration (MR_M)	135 MPa	+/- 42 MPa	**0.28**

Key: MR, Moisture Regain. Subscript **F** for 'fresh'. Subscript **M** for Maximal.

STRAIN RATE DEPENDENCY

The work of Kasapi and Gosline (1996) is the only study that has attempted to assess the effect of strain rate upon *E* within equine hoof horn. These authors investigated tensile *E* of fully hydrated hoof horn over a range of strain rates that were considered to span the likely '*in vivo*' levels encountered by the hoof wall. The results of this study revealed that the tensile *E* of equine hoof horn was strain rate dependent. A four order of magnitude increase in strain rate (ranging from $1.6x10^{-3}$ – $70x10^{6}\mu\varepsilon s^{-1}$) resulted in a three-fold increase in tensile *E*. It is important to note that the higher strain rate used in this study reflects the initial, and transient, high velocity ground impact spike, that these authors considered was responsible for crack initiation. The effect of strain rate upon the *E* in donkey hoof horn has not been previously investigated. However if this material does indeed display a similar characteristic to that of equine hoof horn, then a clear understanding of its precise effects needs to be established.

5.3.2 DORSO-PALMAR VARIATION IN MODULUS OF ELASTICITY

The dorso-palmar variation in *E* across the equine hoof wall has been widely reported (Leach 1980, Douglas *et al.* 1996, Kasapi and Gosline 1997, Hinterhofer *et al.* 1998, Wagner *et al.* 2001). These studies have indicated the presence of a dorso-palmar decrease in *E* across the

HWD. However, the nature and extent of the variation in *E* remains uncertain, as indeed are the mechanisms that account for its presence within the hoof wall, and the functional significance of this variation within the hoof wall.

Reilly *et al.* (1996) suggested that the dorso-palmar variation in structural organisation and hydration levels (previously detailed in Chapter 4) might provide a mechanism for modulating material properties across the hoof wall depth.

Progress towards elucidating these issues has been hampered in the absence of standardised testing protocols with adequate controls of confounding variable effects. Consequently different studies have adopted different testing methods, performed at different hydration levels, and divided the hoof wall differently.

Whilst earlier studies by Leach (1980) divided the hoof wall on an arbitrary basis into an 'inner' and 'outer' region, the latter work of Kasapi and Gosline (1996, 1997) and Wagner *et al.* (2001) have used variation in macroscopic tubular morphology as a basis for division. More recently, Latham (2001 – Pers Com.) and Hopegood (2002) have reported a similar dorso-palmar trend of decreasing *E* within the hoof wall of the donkey. These studies recorded the regional variation in flexural *E* across the hoof wall depth, at the MDC sampling site. Whilst the work of Latham (2001 – Pers Com.) was conducted at maximal hydration, Hopegood (2002) established *E* values at three different hydration levels. The results of these studies are summarised in Table 5.3 and Table 5.4 respectively.

Hopegood (2002) concluded that dorso-palmar variations in MC alone accounted for the variation in *E* evident across the HWD. This study did not however fully investigate the potential effects of structural organisation, nor indeed consider the issue of water partitioning within the hoof.

In this regard, regional anisotropy has been recorded across the dorso-palmar depth of the hoof in equine hoof horn. Indeed Douglas *et al.* (1996) and Kasapi and Gosline (1997) reported significant differences between axial and lateral *E*. These findings are inconsistent with the assertion of Hopegood (2002) that moisture content alone accounts for the variation in *E*. The findings of Douglas *et al.* (1996) and Kasapi and Gosline 1997) suggest that the structural organisation of the hoof horn material also affects this relationship.

The functional significance of this dorso-palmar variation is not known and remains a matter of debate. Leach (1980) and Reilly *et al.* (1996) suggested that these variations might be of fundamental importance in achieving the smooth and painless stress transfer to the dermal tissues of the foot. Conversely zonal variation in *E* may also serve to concentrate stress within the outer regions of the hoof wall and hence protect the sensitive structures of the foot (Reilly et al. 1996, 1998a and Kasapi and Gosline 1997). The zonal variations in E may result in the hoof

wall acting in a similar manner to a laminar ply. Bolliger (1991) stated that these zonal differences might result in decreased cohesion in the transitional region between zones. Indeed it is to be expected that stress would be concentrated within such transitional regions, leading to zonal delamination.

Table 5.3 Zonal moduli values for donkey hoof horn at maximal hydration (after Latham 2001 – Pers Com.). Adapted to meet the convention of this thesis.

	Zone 1	Zone 2	Zone 3
Mean	**355 MPa**	**168 MPa**	115 MPa

Table 5.4 Zonal moduli values for donkey hoof horn at different hydration levels (after Hopegood 2002) Adapted to meet the convention of this thesis.

	Zone 1	Zone 2	Zone 3
Dehydrated (0%MC)			
Median	1754 MPa	1993 MPa	1547 MPa
IQ Range	1413-2918 MPa	1147-2230 MPa	1151-2016 MPa
Min - Max	1390-3600 MPa	882-2371 MPa	933-2210 MPa
'In vivo' Hydration (MR_F)			
Median	996 MPa	360 MPa	411 MPa
IQ Range	707-1852 MPa	215-1098 MPa	313-476 MPa
Min - Max	602-2122 MPa	91-1172MPa	259-515 MPa
Maximal Hydration (MR_M)			
Median	279 MPa	100 MPa	79 MPa
IQ Range	203-574 MPa	73-298 MPa	68-125 MPa
Min - Max	162-642 MPa	60-311 MPa	66-136 MPa
38gH_2O/10gDM Hydration (MR_{38})			
Median	279 MPa*	252 MPa	244 MPa
IQ Range	203-574 MPa	154-713 MPa	154-713 MPa
Min - Max	162-642 MPa	119-765 MPa	127-614 MPa

Key: MR, Moisture Regain. Subscript **F** for 'in vivo' Hydration level. Subscript **M** for Maximal Hydration level. *Zone 1 $MR_{38} = MR_M$.

5.3.3 ENERGY ABSORPTION IN THE HOOF

The ability of the equine hoof to absorb energy has not been evaluated in detail. In fact, the work of Kasapi of Gosline (1997) represents the only detailed study to have reported energy absorption within the hoof wall. These authors reported total energy absorbed to failure in fully hydrated hoof horn for the outer, middle and inner hoof wall zones at 7.5, 5.9 and 8.0 MJm^{-3}. However, based upon the reported yield stress values for the respective zones at 9.5, 7.5 and 6.5MPa, the corresponding resilience values for the respective zones can be derived from first principles (see Appendix 1). The derived resilience values recorded in this study were ~0.080, 0.065 and 0.070 MJm^{-3} respectively, to give a 'weighted' average for the full HWD of 0.072MJm^{-3}. Zoerb and Leach (1978) cited resilience values for full HWD samples obtained from one individual. These authors recorded energy absorption at 0.23 MJm^{-3}

5.4 THE EFFECT OF LAMINITIS UPON THE MECHANICAL PROPERTIES OF HOOF HORN

Despite the debilitating effects of hoof horn defects, there is little objective information regarding the effect of pathologic change upon the mechanical properties of the equid hoof horn. Indeed the work of Garnhaft (1925) is the only published study to have reported *E* values for laminitic hoof horn.

This study however commented upon the inherent difficulty in obtaining consistent and repeatable values from this pathologically altered material. Indeed the study was therefore restricted to the assessment of only two individuals. In this regard, Garnhaft (1925) stated that the published values must be viewed as a guarded estimate of the 'true' *E*. Drawing definitive conclusions from this early study is therefore inappropriate.

5.5 MODE OF TESTING

The objective assessment of the *E* is dependent both upon the mode of testing and the practical limitations inherent within the respective testing techniques. Hence the suitability of these respective techniques must be assessed in context of the functional relevance and accuracy of the data obtained.

5.5.1.1 TENSILE TESTING

Although tensile testing has been widely adopted including Douglas 1998, Kasapi and Gosline (1997), and Ley *et al.* (1998), tensile forces do not predominate during *'in vivo'* capsular loading (Leach 1980, Thomason *et al.* 1992). Hence the value of the derived *E* is of doubt with specific regard to locomotor function.

In addition, sample slippage represents a particular concern when assessing the accuracy of published data, especially when displacement readings taken from the testing machine has been used to calculate the resultant *E*. Sample slippage results in an overestimation of actual sample displacement, and hence results in an underestimation of true *E*. Kasapi and Gosline (1996, 1997) realised this fact, and countered the slippage effect by obtaining displacement values direct from the sample specimen. This was achieved by the use of an extensometer attached to the specimen. This procedure, however, not only necessitates the added complication of accurately calibrating, and effectively securing the extensometer to the specimen, but it also requires the accurate fashioning of necked test samples. These issues pose particular practical problems with regard to sample preparation.

5.5.1.2 Flexural Testing

In order to obtain functionally relevant data, testing must be approximate to 'in vivo' conditions, both in respect to the nature and direction of the loading forces. In this regard, flexural and/or compressive testing of the hoof horn would appear to be more appropriate mode of testing in comparison to tensile testing. In fact, Flexural testing of equid hoof horn has been widely reported in the horse (Hinterhofer *et al.* 1998, Wagner *et al.* 2001), the pony (Reilly 2001), and the Donkey (Collins *et al.* 1998, Hopegood 2002, Hopegood *et al.* 2003a).

There are however, inherent issues relating to flexural testing that affects the suitability of this specific testing mode for obtaining functionally relevant data. These issues have not received due consideration. These issues arise due to a combination of intrinsic factors, relating to bending theory, and extrinsic factors regarding the geometry of the hoof capsule.

Bending theory dictates that the effects of inter-laminar shear must be negligible within the test specimen. Inter-laminar shear results in the underestimation of the true E_F. A minimum span to depth ratio of 10:1 is required within the test sample so as to control against inter-laminar shear effects during testing (Jackson 1992).

This has a profound effect upon the sample size and sample orientation that can be successfully used for testing. This is particularly the case, when assessing Full HWD E_F. Indeed given the biological constraints of capsule geometry, it is only possible to manufacture, and appropriately test, Full HWD samples in the circumferential y-z plane, i.e. perpendicular to the tubular axis. This plane of loading is contraindicated by '*in vivo*' hoof capsule deformation, and hence this questions the functional relevance of testing in this plane.

In fact it is not readily possible to even attain partial HWD samples, fashioned in a direction which allows appropriate '*in vivo*' loading directions, that conform to the 10:1 depth to span requirement. Hence serious doubts must be expressed with regard to the recent work of Hinterhofer *et al.* (1998) and Wagner *et al.* (2001) as to whether the test samples used in these studies conformed to this minimum depth to span requirement.

Hopegood (2002) tested zonal samples, which meet the 10:1 depth to span requirement, in the y-z plane. Not only was the testing conducted in a loading direction of questionable function relevance, but also the test samples were only of 1mm proximo-distal height. This raises two additional concerns regarding the suitability of this testing protocol.

Firstly, there is the question as to how representative of the hoof wall is a sample of only 1mm proximo-distal height. Secondly, Hallab *et al.* (1991) and Vincent (1992) stated that there was a need to consider whether it was the structure, or the material, which was being evaluated during testing. In this regard, Hallab *et al.* (1991) stated that sample size must be sufficiently large to reflect the structural organisation of the material. There is clearly uncertainty as to whether the

macroscopic structural organisation is effectively being assessed in such relatively small test samples. Further work is required to address these concerns and provide definitive answers.

The practical limitations detailed above need to be successfully addressed in order to obtain accurate values of E that are of functional relevance, and which reflect the structural organisation of the hoof wall. Compression testing affords this opportunity.

5.5.1.3 COMPRESSION TESTING

Compression testing offers several distinct advantages over flexural or tensile testing modes. These include: -

- Samples can be readily tested in accordance with the nature and direction of *'in vivo'* loading forces
- Relatively large samples can be used - hence the effect of structural organisation can be investigated
- Structural anisotrophy can be investigated
- Minimal test sample preparation
- No specimen clamping required
- Specimen displacement can be readily measured direct from the testing machine

The E_C of equid hoof horn has been evaluated by several researches most notably Butler (1976), Zoerb and Leach (1978), Leach (1980), Leach and Zoerb (1983) Landeau *et al.* (1983) and Douglas *et al.* (1996). However standardised testing protocols have not been adopted between studies, hence direct comparisons between the resultant data is inappropriate without careful consideration. This is further complicated by the fact that the rational and detail relating to the specific testing protocols adopted in these studies is poorly defined. This is of particular relevance, as effective compressive testing of biomaterials represents a particular challenge (Wainwright 1998 – Pers Com.), and requires careful evaluation of experimental design (Vogel 1998 – Pers Com., Bertram 1998 – Pers Com.).

5.6 THEORETICAL CONSIDERATIONS

The accurate determination of E_C assumes: -

- Equal stress distribution within specimen
- Conditions of plain strain
- Absence of 'End effects' – uninhibited response to loading at the platen-specimen interface
- Absence of buckling phenomena

There are however, a number of inherent practical problems in attaining these ideal test conditions associated with compression testing techniques (Wainwright 1998 – Pers Com., Vogel 1998 – Pers Com.). These potential sources of experimental error can significantly affect the accuracy of the E_C determination. These are discussed in detail in ASTM D 695 – 96 and E9 – 89A$^{\varepsilon 1}$. It is therefore imperative that these issues are both fully evaluated, and also that measures are introduced in the testing protocol that either eliminate, or at least minimise, their effect upon E_C determination.

These sources of potential error relate to: -

- Specimen preparation
- Specimen geometry
- Mode of force application
- Measurement of specimen displacement

The accurate determination of E_C assumes conditions of uniform load distribution, and also uninhibited specimen displacement in response to this load. In respect of load application, this necessitates that the platens are in parallel alignment. In addition, the loading surfaces of the specimen must be not only parallel, but also orthogonal to the direction of the applied load. Failure to achieve this will result in uneven loading, leading to stress concentration and the generation of shear forces within the specimen. This leads to an underestimation of E_C. Therefore ensuring that specimen preparation and force application results in uniform force distribution is of paramount importance

Friction at the platen specimen interface is a limiting factor in attaining conditions of plain strain. In this respect, the orthogonal expansion of the specimen is restricted at each platen interface. This leads to the development of what ASTM E9 – 89A$^{\varepsilon 1}$ refers to as 'barrelling' behaviour, in which the specimen assumes the shape of a barrel during loading. This behaviour results in an overestimation of E_C. Hence reducing the frictional coefficient evident at the platen-specimen interface, and also minimising this barrelling behaviour, is of primary importance.

The greater the cross sectional area of the loading surface, the greater is the frictional resistance to lateral expansion. The extent of this barrelling behaviour is also affected by specimen size, in particular, by the aspect ratio of the specimen, i.e. the ratio between the height, or gauge length of the specimen, and its width, and depth. The smaller the aspect ratio the greater the barrelling effect for a given load. In this regard, increasing gauge length will minimise specimen barrelling.

However, increasing gauge length also increases the likelihood of initiating specimen buckling. Specimen buckling results in an underestimation of E_C as apparent displacement for a given

load is increased. The buckling load is inversely proportional to the square of the length to minimum cross sectional dimension. Hence, the extent of buckling within a sample is related to the aspect ratio of the test sample. A compromise therefore has to be struck between 'barrelling' and 'buckling' effects. In this regard, Linde *et al.* (1992), and Linde (1994) recommends that E_C determination should be conducted at an aspect ratio of 2:1.

It is important to note that this critical ratio allows both full HWD and zonal samples to be manufactured and tested in functionally significant loading directions, i.e. in the axial and lateral direction. In addition, the limiting ratio is such that test samples of relatively large proximo-distal height can be produced. In this way, there can be confidence in the fact that the structural organisation of the hoof wall is being assessed during tested.

Linde *et al.* (1992) and Linde (1994) commented upon another form of 'end effect' that presents itself when testing cellular solids. Cellular solids have unsupported 'free ends' at the platen specimen interface. The lack of transverse resistance to deformation results in specimen splaying at the platen specimen interface, as the cellular components bend and slide in the transverse direction. This deformation results in an overestimation of specimen strain for a given load, and thereby contributes to an underestimation of E_C. The greater the proportion of the gauge length occupied by these unsupported free ends the greater the underestimation of E_C.

The mode of assessing specimen displacement represents a key factor in the accurate determination of E_C. Displacement can be determined either by direct or indirect means. The difficulties associated with direct determination of sample displacement have been discussed previously in Section 5.5.1.1. Indirect determination of sample displacement, in which the machine displacement is recorded, also represents a potential source of experimental error. This results as a consequence of inherent compliance within the testing machine.

5.6.1 MACHINE COMPLIANCE

Machine compliance is the 'give' inherent within the 'load string' of the testing machine. The load string comprises the platens, their couplings, the test rig and the load cell. Each component with the 'load string' is displaced during sample testing, dependent upon the stiffness of the respective components within the 'load string'. This results in an underestimation of the actual stiffness of the sample, and thereby leads to a corresponding underestimation of 'true' E_C. Hence there is a need to correct these data in respect of machine compliance in order to achieve an accurate value of E_C.

5.6.1.1 CALCULATION OF COMPLIANCE CORRECTED E_C

Stiffness (F/X) = force per unit displacement

- Apparent stiffness of sample (F/X_{APP}) = slope of the force displacement plot in the initial linear region
- Machine stiffness (F/X_{MAC}) = 1/Machine compliance

Where:

- F/X_{MAC} = slope of the force displacement plot of the compliance test sample

Hence:

- Compliance corrected stiffness of sample (F/X_{COR}) = Apparent stiffness/(1-(Apparent stiffness/Machine stiffness))

Thus:

- Compliance corrected stiffness $(F/X_{COR}) = (F/X_{APP})/(1-((F/X_{APP})/ (F/X_{MAC}))$.....**(1)**

Compressive modulus of elasticity E_C = stress/strain

Where:

- Stress = F/Area
- Strain = ΔLength/Original Length

Hence:

- E_C = (F/(Width x Depth))/(X/Gauge Length) .....**(2)**

Thus by rearranging equation **(2)**:

- Apparent $E_C = (F/X_{APP}$ x Gauge Length)/(Width x Depth)

Compliance corrected E_C = compliance corrected sample stiffness normalised for specimen dimension.

Thus:

- Compliance corrected $E_C = (F/X_{COR}$ x Gauge Length)/(Width x Depth) .....**(3)**

5.6.1.2 WORKED EXAMPLE OF COMPLIANCE CORRECTION

Let:

- Gauge Length = 20mm, Width = 10mm, Depth = 10mm
- F/X_{APP} = 725 N/mm
- F/X_{MAC} = 5643 N/mm

Hence:

Compliance corrected stiffness $F/X_{COR} = F/X_{APP} / (1- (F/X_{APP} / F/X_{MAC}))$

= 725 / (1-(725 / 5643))

= ~ 832 N/mm

Apparent $E_C = (F/X_{APP}$ x Gauge Length)/(Width x Depth)

= (725 x 20) / (10 x 10)

= 145 MPa

Compliance corrected E_C = (F/X_{COR} x gauge length)/(width x depth)

= (832 x 20) / (10 x 10)

= 166.4 N/mm^2

= 166.4 MPa

Thus failure to correct calculations in respect of machine compliance results in a 13% underestimation of actual E_C.

5.6.2 VISCOELASTIC MATERIAL BEHAVIOUR

If donkey hoof does indeed display viscoelastic material behaviour, then rheological principles dictate that E_C will be both dependent upon strain rate and moisture levels. Hence strain rates and moisture levels must be controlled. This has important practical implications with regards to testing protocol.

5.6.3 STRAIN RATE

Strain rate ($\mu\varepsilon s^{-1}$) = Crosshead speed (mm $s^{-1)}$)/gauge length (mm).

Where crosshead speed is the distance moved by the platen per unit time.

Specimen gauge length must be such that the resultant aspect ratio approaches the optimal 2:1 recommended by Linde *et al.* (1992). However, as sample depth vary, due to the biological variation evident in HWD gauge length must be adjusted accordingly. Hence, in order to control for strain rate, the crosshead speeds must be adjusted in line with this gauge length variation.

5.6.4 MOISTURE LEVELS

Whilst testing at MC_F provides information regarding *'in vivo'* mechanical properties of hoof horn, the dorso–palmar variation in moisture levels prevents further investigation of structure-function relationships within the hoof wall. In order to make progress in this area, it is necessary to control for water effects within the structure. However, the effective and appropriate control of moisture levels requires careful consideration.

Mechanical testing of hoof horn has previously been conducted at: -

1. 0%MC
2. Specific %MC (equilibrated at a specific relative humidity)
3. MC_M

However there has been little debate regarding the justification of these different experimental approaches.

1. 0%MC

Material testing at 0%MC may appear to be an obvious approach, however it is important to consider the effect of sample desiccation. This may result in gross distortion of the sample and/or disruption of the structural organisation of the hoof horn. In addition, the total removal of water from the sample will result in phase transition and material embrittlement. Hence the associated material properties are likely to be fundamentally different to their '*in vivo*' characteristics.

2. Specific %MC

Equilibrating samples to a specific %MC offers the opportunity of testing material above its phase transition. Hence material properties are more likely to approach '*in vivo*' characteristics. However, little is known as to the degree of plasticisation that occurs at a given %MC in either full HWD or zonal samples, nor indeed the critical %MC value that marks the glass transition. Normalising different zones to a constant %MC would result in notable 'between zone' differences in $\%S_R$. It is therefore likely that zonal differences will occur, both in the degree of plasticisation and the actual Free Water levels.

3. MC_H

Although 'between sample' differences in the absolute amount of water will occur at MC_H, all samples will be acting at maximal $\%S_R$. Therefore samples will be normalised in respect of their water holding capacity, and will be in a fully plasticised state, and at their maximal Free Water level. In addition, Hopegood (2002) reported no significant difference between the E_F of donkey horn at this hydration level, and that recorded at *'in vivo'* hydration levels.

Indeed it is the opinion of the author of this thesis that testing at MC_H represents the most effective means of controlling for moisture effects. By adopting this approach, it is possible to investigate the specific inter-relationship between structure and the material properties of the hoof wall.

5.6.5 THE COMPRESSIVE RESPONSE OF EQUID HOOF HORN

A summary overview of previous reported studies specifically relating to the compressive response of equid hoof horn is detailed in Table 5.5. These have been appraised with particular attention to the critical issues of experimental design outlined within the preceding sections.

Table 5.5 Summary table of compressive testing of equid hoof horn

Author	Site	Element of hoof wall	Specimen Geometry	Aspect Ratio	Loading Direction	Hydration Status	Strain Rate $\mu\varepsilon s^{-1}$	Test Parameter	Compliance Correction	Values
Butler (1976) Butler and Hintz (1977)	MDC	Full HWD	'Cubic'	~1:1	Axial (y)	MG_H	Not stated	E_C σ_Y	No correction	E_C Axial (y) – 3.72 MPa*[1] σ_Y Axial (y) – 146 MPa
Zoerb and Leach (1978)*[2]	MDC	Full HWD	Cubic	~1:1	Axial (y)	Not stated	Mean 8500 Range not stated	E_C σ_Y Resilience	No correction	E_C Axial (y) –215 MPa σ_Y Axial (y) – 11.1 MPa Resilience 0.230 MJm^{-3}
Leach and Zoerb (1983)	MDC	Inner Region Outer Region	Cubic	1:1	Axial (y) Lateral (x) Lateral (z)	MC_F	Mean 3870 Range not stated	E_C	No correction	**Outer wall** Axial (y) – 355 MPa Lateral (x) – 499 MPa Lateral (z) – 309 MPa **Inner wall** Axial (y) – 237 MPa Lateral (x) – 283MPa Lateral (z) – 172 MPa
Landeau *et al.* (1983)	MDC	Full HWD	Cylindrical	2:1	Axial (y)	MC_H	Range 1730 - 2870	E_C	No correction	Axial (y) – 240-460 MPa
Douglas *et al.* (1996) Douglas (1998)	MDC	Inner Region Outer Region	Rectlinear Axial / Lateral samples	6:1	Axial (y) Axial (y)	MC_F Outer - 27.9% Inner – 35.5%	Mean 1060 Range not stated	E_C	Displacement measured by direct means	**Outer wall** Axial (y) – 1049 MPa Lateral (x) – 963 MPa **Inner wall** Axial (y) – 560 MPa Axial (y) – 487 MPa

*[1] Cited by Leach and Zoerb (1983) at 377 MPa. *[2] Study conducted on one individual only

5.7 CONCLUSIONS

The E_C and resilience represent key defining material characteristics of fundamental importance to hoof function. However, these characteristics have not been previously investigated in laminitic hoof horn in either equid species. Nor indeed has the relationship between these characteristics and either the structural organisation of the laminitic hoof wall, or the nature and extent of degenerative changes within the laminitic foot, been investigated.

These relationships may be of particular significance with regard to the biomechanical functioning of the laminitic foot, and the severity of the condition within the afflicted animal.

To further elucidate these potential relationships within the hoof wall, standard material testing techniques need to be established that can quantify these key material properties. The mode of testing must approximate to '*in vivo*' loading conditions, and also offer the opportunity to explore relationships both at the full HWD and zonal level. In addition, the testing mode must provide the opportunity to investigate the effects of structure and specimen orientation. In this regard it is the author's assertion that compression testing is the most suited testing mode.

Specific operating protocols are however required to effectively control for the effects of those confounding variables which are known to modulate material properties. It is only in this way that structure-function relationships of the hoof wall can be effectively assessed, and the materials characterisation further elucidated.

Testing protocols must also minimise potential sources of experimental error inherent within the selected mode of testing. These issues have been fully appraised in previous sections within this chapter.

5.8 AIMS

The aim of this chapter of the thesis was to complete a characterisation of the material properties of laminitic donkey hoof horn obtained from the MDC sampling site. In particular, to determine the compliance corrected E_C and the resilience of the donkey hoof horn material.

The specific aims of this chapter were: -

In the preliminary phase of project

- To devise a standard methodology for the optimised determination of the E_C of elasticity and resilience of hoof horn, corrected for machine compliance and controlled for hydration effects

In the preliminary stage of the experimental phase of project

- To obtain consistent force displacement data from this compromised hoof horn material
- To establish the stress strain relationship in laminitic hoof horn

- To devise a means of generating compliance corrected, baseline E_C and resilience data for laminitic hoof horn
- To investigate the strain rate dependency of E_C determination in laminitic hoof horn
- To explore mechanical non-isotropy - Establish the axial to lateral E_C ratio within the donkey hoof wall
- Establish the stress and strain levels at 'bioyield' in laminitic donkey hoof horn

In the main experimental phase of project

- To evaluate full HWD and zonal variation in E_C
- To establish the resilience of the full HWD
- To investigate the effect of 'group' upon mechanical parameters of E_C and resilience
- To compare these results with previously published data for 'normal' donkey hoof horn
- To provide data for the subsequent computer modelling of the hoof wall, and the theoretical modelling of the effect of the laminitic condition upon hoof wall function

5.9 MATERIALS AND METHOD

5.9.1 COMPRESSIVE MODULUS, RESILIENCE, AND YIELD STRESS AND STRAIN DETERMINATION

5.9.1.1 OVERVIEW OF MATERIAL TESTING EQUIPMENT AND TEST THEORY

Mechanical testing was conducted on an Instron 4032 material testing machine using series IX software[3].

The E_C and Resilience were calculated from experimentally derived force displacement data. The test sample was displaced at a given rate, determined by the crosshead speed of the testing machine so as to achieve a constant strain rate between samples. Sample displacement was obtained by indirect means of internally monitored platen movement. The corresponding reaction force from the specimen was measured directly from a calibrated load cell.

The apparent stiffness of the sample was determined from the slope of the initial linear section of the resultant force displacement relationship. The apparent stiffness of the specimen was corrected in respect of 'machine stiffness', to provide the actual stiffness value of the sample. The correction process was performed from first principles in accordance with Section. Machine stiffness was determined by a standardised method.

[3] Instron Corp. Massachusetts, USA.

Finally, sample stiffness was normalised with respect of test sample geometry to provide the compliance corrected E_C for the material.

The area under the linear region of the derived force displacement plot represented the work done by the specimen, that is, the elastic strain energy absorbed by the sample during loading. This was quantified from first principles as follows, to derive the resilience of the sample.

Yield stress (σ_Y) was established by normalising the force recorded at the upper limit of the linear, or proportional, section of the force displacement plot (i.e. the point of bioyield) in respect of specimen geometry. With σ_Y established, the elastic strain energy capacity per unit volume of material (resilience) was calculated from the compliance corrected E_C, where resilience = $(\sigma_Y^2)/2E$.

5.9.1.2 EXPERIMENT 1 MACHINE COMPLIANCE DETERMINATION

The compliance of the Instron 4032 testing machine was determined prior to sample testing. This was performed in accordance with recommended guidelines (Instron Corp. USA), using a rigid material with a stiffness value significantly greater than the 'load string' of the testing machine. The compliance procedure was conducted using either a 20x10x10mm or 6x3x3mm (height x width x depth) steel block with milled parallel plane faces. These two blocks replicated the approximate specimen geometry of the full HWD and Zonal samples respectively. The parallel faces ensured uniform uniaxial loading and hence minimised potential end effects.

Compliance determination was performed in respect of each testing protocol, at the same cross head speed that was to be employed. In this way, machine stiffness was determined at the same rate of strain as the actual test samples. The resultant force displacement data represented the 'give' of the load string in response to the specific rate of strain for each testing protocol. This machine stiffness data was subsequently used to determine the appropriate correction to the force displacement data generated from the individual test samples.

On the basis of preliminary experiments, it was decided to conduct this correction manually, based upon first principles, as opposed to using the automatic correction facility of the software program. This was due to the fact that the arbitrary nature, by which automatic compliance correction was performed, resulted in E values that were both inconsistent and difficult to rationalise (Collins - Pers Obs.).

5.9.1.3 EXPERIMENT 2 STRAIN RATE DEPENDENCY

The evaluation of the strain rate dependency of E_C was conducted on material obtained from the MDC sampling site of seven laminitic donkeys. A 20mm wide MDC sampling block was

removed from the hoof capsule in accordance with Section 2.3.4. This was stored in distilled water for 7 days to ensure maximal hydration

The HWD of the MDC sampling blocks were ~10mm. Hence in order to achieve an optimal aspect ratio of 2:1 in the finished testing sample, a 22mm proximo-distal specimen block, that symmetrically spanned 50%HWH site, was obtained in the following manner. The position of the 50%HWH site was established on the sagittal aspect of the MDC sampling block (see Section 2.3.6). The proximo-distal limits of the testing block were established, respectively 11mm proximal and distal of the location of 50%HWH site. Care was taken to ensure that these reference lines were constructed perpendicular to the tubular axis. The medio-lateral extent of the specimen block was marked on the dorsal aspect of the MDC sampling block parallel to the tubular axis, 6mm medial and lateral of the plane of the MDC. A bandsaw was used to cut the MDC sampling block along the proximal, distal, medial and lateral reference lines. In this way, a specimen block of approx. 22mm proximo-distal height x 12mm medio-lateral width x ~10mm HWD was achieved, with an aspect ratio that approached 2:1. The medial lateral and proximal and distal faces were milled to produce parallel planar faces in the finished test specimen. The finished test samples were approximately 20mm x10mm x10mm.

The samples were returned to distilled water storage for a further 7 days to ensure maximal hydration. Finally, in order to both safeguard against any effect of differential expansion during this storage, and also to minimise friction at the specimen platen interface, the proximal and distal loading surfaces were 'planned' using a sledge microtome.

The blocks were removed from storage immediately prior to testing and blotted to remove excess water. Removal of excess water will reduce frictional effects at the specimen platen interface. The specimen dimensions were recorded using a micrometer. Three measurements were made respectively of the specimen height (gauge length), width and depth, with the average of each, used for all subsequent calculations.

E_C determination was conducted at three different strain rates that spanned a three order of magnitude variation in strain rate. These rates fell within the range that Kasapi and Gosline (1997) suggested were typically encountered by the equid hoof capsule during static and dynamic loading. The strain rates were 667, 1667 and 10000$\mu\varepsilon$ s^{-1}. Mechanical testing protocols were established to produce the desired strain rates.

Strain rate is dependent upon both the crosshead speed of the test, and the gauge length of the test specimen, where strain rate = (crosshead speed/gauge length).

Hence appropriate crosshead speeds were calculated, assuming a gauge length (specimen height) of 20mm, to produce the desired rate of strain. In this respect, crosshead speeds of 0.8mm min^{-1}, 2.0mm min^{-1} and 12mm min^{-1} would result in strain rates of 667, 1667 and

$10000\mu\varepsilon s^{-1}$ respectively in a test sample of 20mm gauge length. Crosshead speeds were adjusted in line with slight individual variation in gauge length so as to maintain the desired strain rate. Samples were tested to a maximun load of 200N, and three consecutive determinations of E_C were conducted at each respective strain rate. As the test samples were subjected to multiple loading cycles, it was essential to guard against exceeding bioyield. Hence an 'end test' strain limit of 0.5% strain was incorporated into the testing protocol. This measure ensured that if sample strain reached 0.5%, the test would terminate irrespective of the force level. This level of strain represented ~66% of the bioyield value previously reported for equine hoof horn (Leach 1980), and also fell below the bioyield of laminitic donkey hoof horn (Collins - Pers Obs.).

A standard operating procedure was adopted to minimise experimental error and hence improve the accuracy of E_C determination. This focused upon the primary sources of error discussed in Section 5.6. This procedure involved: -

- Platen alignment
- Machine compliance
- Sample positioning
- Pre-loading
- Stress relaxation
- Maintenance of specimen hydration level

PLATEN ALIGNMENT

In order to ensure that that the platens were in parallel alignment, the test protocol was performed in the absence of a test specimen, with the loading surfaces of the platens in direct contact. In 'settling' the platens in this way, conditions of true axial loading are assumed.

MACHINE COMPLIANCE

Machine compliance was determined as described in Section 5.6.1, prior to initiation of each testing protocol.

SAMPLE POSITIONING

To achieve condition of even axial loading, the test sample was carefully located in the centre of the base platen.

PRE-LOADING

In order to settle the sample within the test rig, and prevent the occurrence of sample backlash during testing, the sample was preloaded to 5N prior to initiating the testing protocol. In this way, conditions of axial loading could be maintained throughout the testing cycle.

STRESS RELAXATION

A defining characteristic of viscoelastic behaviour is that stress relaxation after the removal of load, is not instantaneous as in true 'Hookean' material, but is time dependent. This residual stress can adversely affect the accuracy of *Ec* determination. Hence samples were monitored to ensure that they had returned to the initial preload of 5N prior to re testing. Hence each consecutive E_C determination was were performed under similar pre-load test conditions.

MAINTENANCE OF SPECIMEN HYDRATION LEVEL

In order to minimise the loss of moisture to the atmosphere, testing was performed in an environmentally controlled testing laboratory. Ambient conditions were maintained at 70%RH. In addition, specimens were returned to distilled water storage for 30 minutes after the completion of the third determination at each strain rate. The three consecutive determinations were completed in less than 3 minutes. In this way, moisture loss to the environment was considered to be minimal, and that E_C determination at each respective strain rate was performed at MC_M conditions.

5.9.1.4 EXPERIMENT 2 AXIAL TO LATERAL MODULI RATIO

The axial to lateral E_C ratio was determined at the MDC sampling site of six laminitic donkeys. 10mm x 10mm x ~10mm cubic samples were prepared at 50%HWH site in a similar manner to that previously described. However in this case, the proximo–distal extent of the test blocks were established 5mm proximal and distal of 50%HWH.

Samples were stored at 4°c in distilled water for seven days to achieve MC_M. The samples were removed from storage and blotted prior to testing, and sample dimensions recorded

The standard testing procedure detailed in Section 5.9.1.3 was adopted. Samples were tested in compression, at a crosshead speed of 1mm min^{-1} to a maximum load of 100N in both the axial and lateral direction. Three consecutive E_C determinations were performed in each loading direction. Samples were returned to distilled water storage for 30 minutes after the third determination in the former direction so to maintain MC_M conditions during testing. The resultant compliance corrected E_C values were used to calculate the axial to lateral E_C ratio for laminitic hoof horn.

It is appreciated that these test samples did not correspond to the optimal 2:1 aspect ratio necessary to minimise end effects. Hence absolute E_C values will reflect the sub optimal test conditions. However as the aspect ratio in both test directions were the same at 1:1, 'end effects' were likely to be the same in both test directions. Therefore the resultant E_C ratio can be assumed to be insensitive to their effects, and thereby represents an accurate measure of the directional E_C ratio.

5.9.1.5 Experiment 3 Evaluation of the Compressive Stress-Stain Behavior of Laminitic Hoof Horn

A preliminary assessment of the stress strain behaviour of laminitic hoof horn was conducted using MDC sampling blocks of unknown origin. Specimen blocks of ~ 20x10x10mm were prepared and rehydrated in distilled water for 7 days prior material testing to ensure maximal hydration. These blocks were tested to failure, at an arbitrary crosshead speed of 2mm minute^{-1}.

5.9.1.6 Experiment 1 Determination of Full HWD and Zonal Moduli

Test Sample Preparation

Full HWD and zonal material testing samples from the MDC sampling block obtained from the trial population of laminitic donkeys. The MDC sampling block was divided in two along the plane of the MDC using a bandsaw see Section 2.3.9.

Full HWD mechanical testing blocks of 20mm x 10mm x ~10mm that spanned 50%HWH were prepared and finished from the medial portion of the bisected MDC sampling block.

Zonal blocks were prepared from the medial portion of the MDC block. A 3mm wide proximo-distal strip, immediately adjacent to the plane of the MDC, was removed from this block using a bandsaw. From which, a full HWD strip of 5mm proximo-distal height that symmetrically spanned the 50%HWH site was removed with the aid of a craft knife. Cuts were made perpendicular to the tubular axis 3mm proximal and distal of 50%HWH.

In this way, a 6x3x full HWD specimen block was produced.

This block was divided into zonal testing blocks based upon variation in the macroscopic tubular morphology evident in the dorso-palmar aspect of this block. This division produced zonal testing blocks for Z1, 2 and 3 respectively of ~3mm, 2.5mm and 4.5mm HWD. A final proximo-distal cut was made on the inner aspect of the Z3 block, to produce a final test block size of ~3mm HWD.

The zonal test samples were 'finished' in a similar manner to that described for full HWD samples. In this way, planar zonal samples approx. ~5x 2.5x 2.5 were produced, with an optimal 2:1 aspect ratio.

HYDRATION AND MEASUREMENT PROTOCOL

Full HWD and zonal samples were placed in distilled water storage for 7 days prior to testing. After rehydration, the load bearing faces planned by microtome as in Section 5.9.1.3, and final specimen dimensions determined by micrometer.

DETERMINATION OF FULL HWD COMPRESSIVE MODULI

E_C determination of full HWD samples was conducted as described previously at a strain rate of 1667 $\mu\varepsilon s^{-1}$. Standard operating procedures detailed in Section 5.9.1.3 were adopted.

DETERMINATION OF ZONAL COMPRESSIVE MODULI

In order to ensure that the determination of zonal E_C was performed at a similar strain rate to that of full HWD samples, the crosshead speed of the test was reduced to 0.5mm min^{-1}. Standard operating procedures detailed in Section 5.9.1.3 were observed, with a preload of 1N. Samples were compressed to a maximum load of 14N with an end strain limit of 4%. Three consecutive E_C determinations were made.

5.9.1.7 RESILIENCE DETERMINATION OF FULL HWD SAMPLES

A final mechanical test was performed to establish the resilience of the sample block. The test samples were compressed to a maximum load of 200N without an 'end strain' limit. Bioyield was assessed as the point of departure from the initial linear section of the resultant stress strain curve. The corresponding area under the stress strain plot up to bioyield was determined. This was considered to represent the resilience of the material. Resilience was calculated in accordance with Section 5.3.

5.10 RESULTS

5.10.1 MATERIAL TESTING

Figure 5.1 illustrates the typical stress strain behaviour of full HWD tested to ultimate failure. The stress strain plot revealed the nature of the stress strain relationship with increasing strain. Three distinct regions were evident. Between 0 and ~0.75% strain, the stress strain behaviour displays a linear, 'Hookean' relationship, in which stress is proportional to strain.

Figure 5.1 Stress strain plot of full HWD sample tested to ultimate failure.

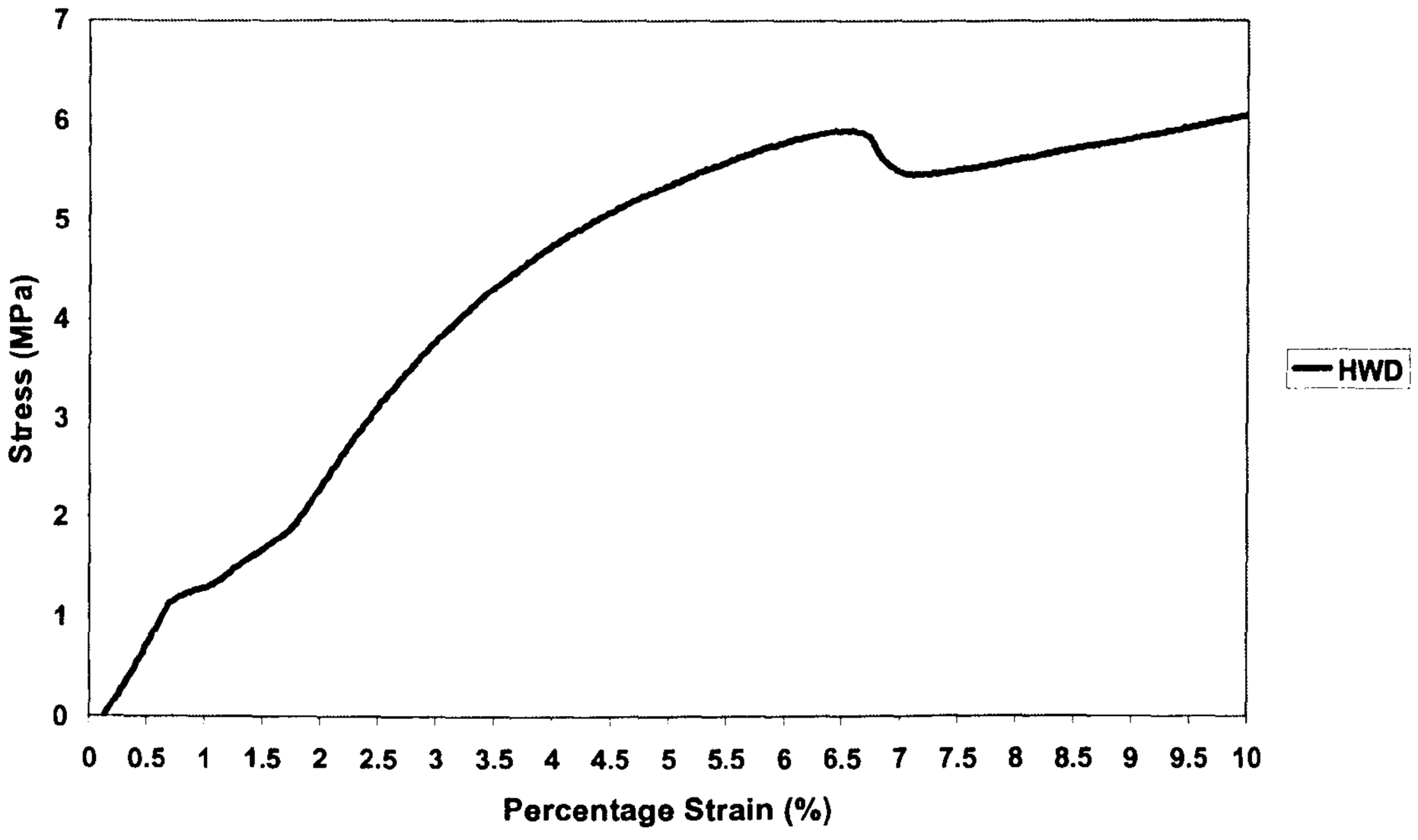

At approximately 0.7% strain there was a marked departure from this linear relationship. This departure was associated with appearance of proximo-distal cracking between the 'outer' and 'inner' regions of the hoof. The second region extended from ~0.8-6.5% strain. In this region the stress strain relationship was sigmoidal. Initially, the tangent of the curve was lower than the gradient within the initial linear region. However with increasing strain the tangent of the curve approached that of the slope within the linear region. From 3.5-6.5% strain the tangent decreased progressively. At ~6.5% strain a second abrupt transition occurred. This was associated with the proximo-distal delamination (separation) of the 'outer' and 'inner' regions of the wall. Thereafter a final linear region was observed of modest slope. Figure 5.2 illustrates the typical stress strain behaviour of zonal samples to failure. Marked differences in the stress strain behaviour are evident between zones. Never the less, all zones display an initial linear region where stress is proportional to strain. The corresponding gradients within this region of the stress strain plots differ between zones, with Z1>Z2>Z3. Departure from this linear relationship occurs respectively at ~7, 6.5 and 5% strain. This is in marked contrast with the bioyield of 0.75% strain noted in the full HWD. The stress strain response evident within Z1 following bioyield differed markedly from that observed within Z2 and 3. In the case of these latter zones, the response was characterised by the presence of a second linear region. Albeit that the transition into this region was more pronounced in Z3 than in Z2. The gradient of this

second linear region was similar between zones, and was modest in comparison with that recorded for the initial linear region. There was no evidence of gross failure within either zone.

Figure 5.2 Typical stress strain behaviour of zonal samples to tested to failure.

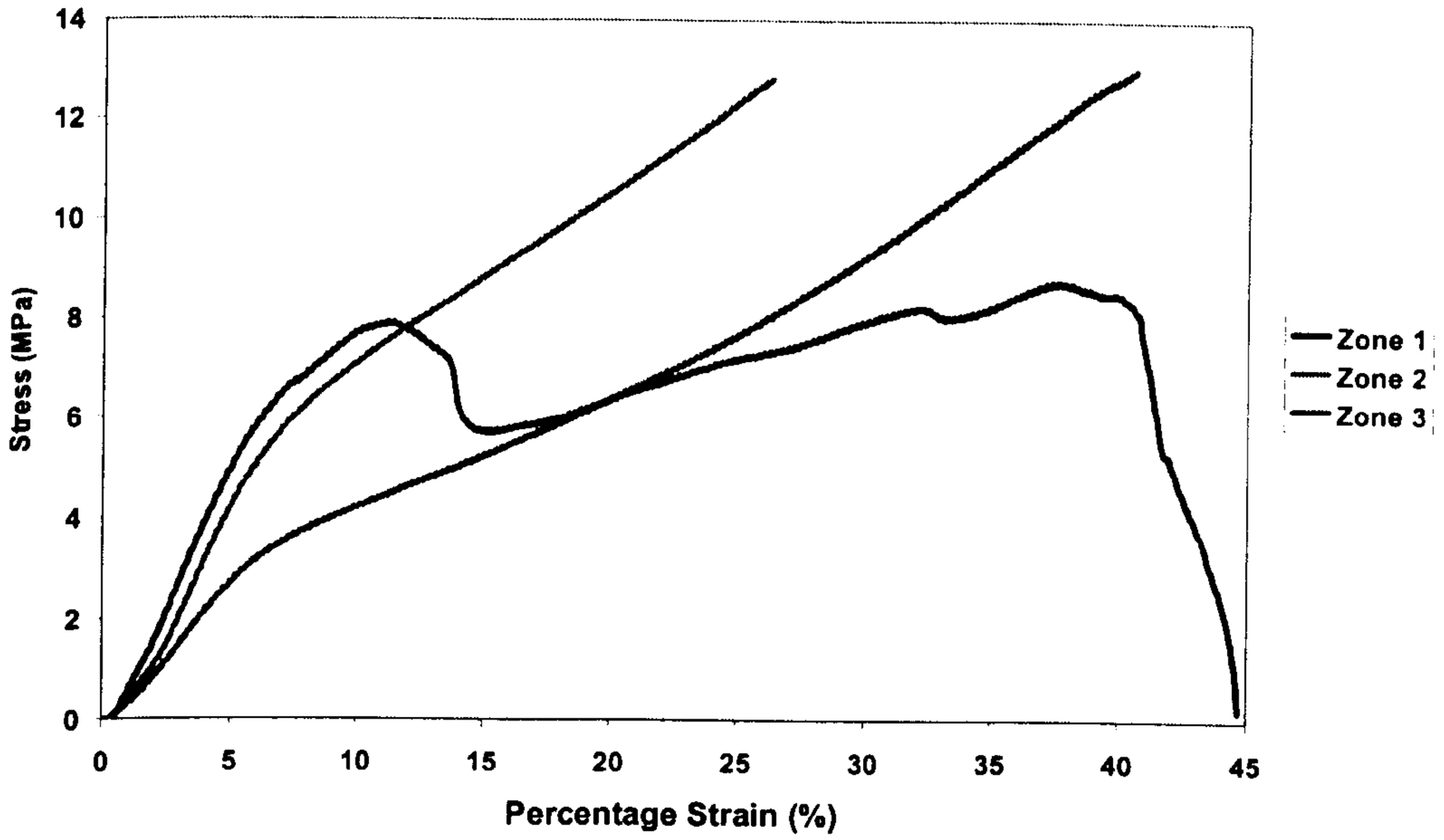

The stress strain behaviour in Z1 was more complex. Following bioyield, the stress strain plot displays a marked transition into a second linear region. This was associated with the appearance of gross signs of proximo-distal cracking. This second linear region was of very modest slope compared to that observed in Z2 and 3. This region of the stress strain relationship was marked by progressive crack formation, which ultimately resulted in catastrophic specimen failure at ~40% strain.

5.10.1.1 Compressive Modulus

Compliance

Compliance correction in respect of the different testing protocols underestimated the true E_C by 14-18%

Strain rate dependency

E_C in HWD samples increased with increasing strain rate. The mean E_C at the 3 experimental strain rates were 191, 221 and 246MPa respectively. Between rate comparisons by paired t-test indicated statistically significant differences in the mean E_C recorded at each strain rate (P<

0.05). A 2 order of magnitude increase in strain rate resulted in a 29% increase in E_C. Figure 5.3 illustrates the effect of strain rate upon E_C for full HWD donkey samples at maximum hydration levels, compared to that reported for the horse by Kasapi and Gosline (1997). A similar power law relationship between mean E and strain rate as reported by these authors for the horse, was also evident in full HWD donkey hoof horn samples. The R^2 for the fitted trend line ~ 0.92.

Figure 5.3 Comparison of the strain rate dependency of compressive moduli for full HWD laminitic donkey samples with moduli data for equine hoof horn samples previously reported by Kasapi and Gosline (1996).

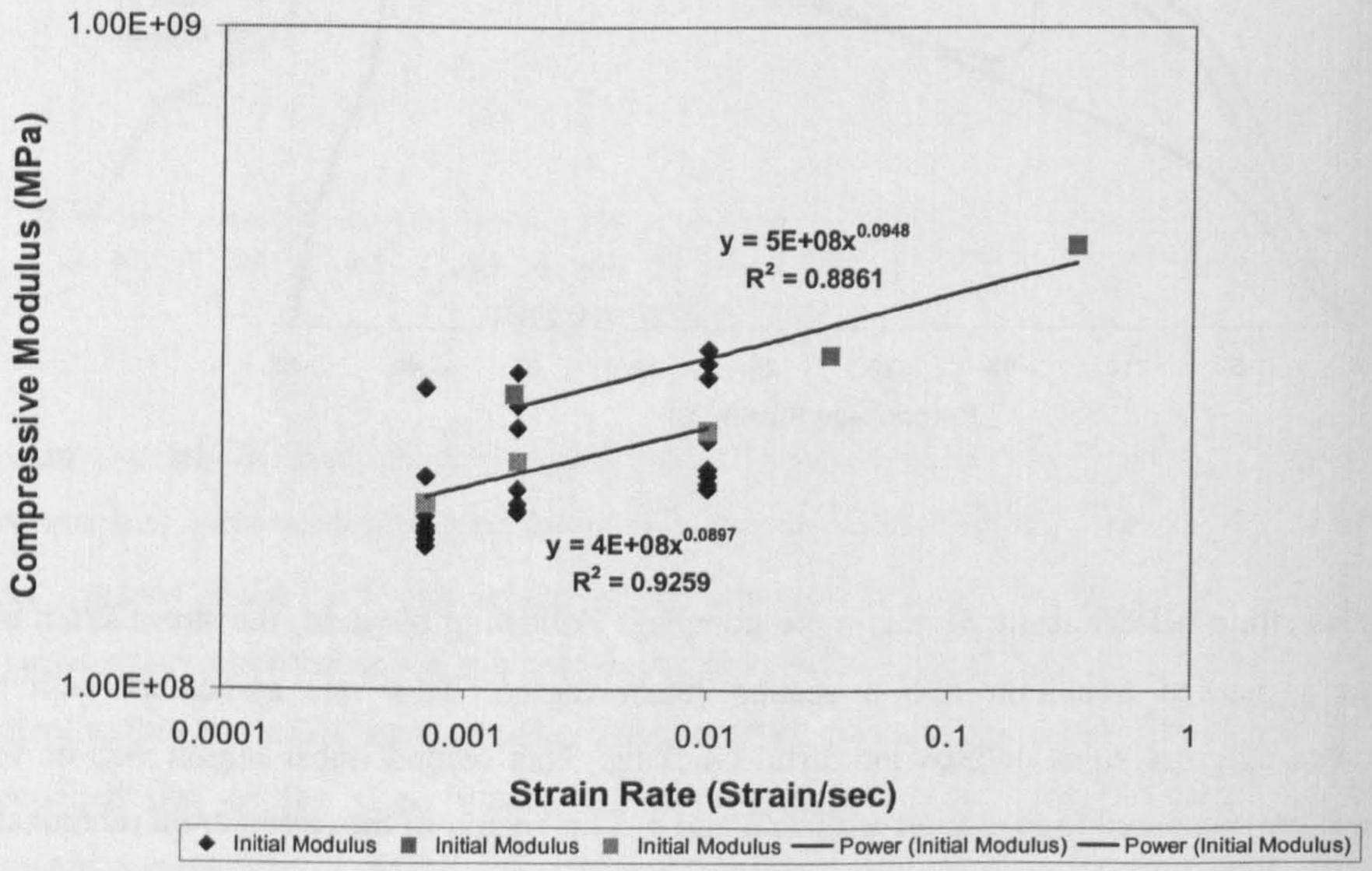

Key: Blue, Donkey individual moduli. **Green**, Donkey Mean moduli. **Pink**, Horse Mean moduli

AXIAL TO LATERAL COMPRESSIVE MODULI RATIO COMPARISONS

The axial to lateral E_C ratio ranged form 1.2:1 to 1.7:1 with a median value of ~1.5:1.

MAXIMAL HYDRATED COMPRESSIVE MODULI FOR LAMINITIC HOOF HORN

Anderson – Darling Normality testing confirmed that the E_C within both full HWD and zonal samples displayed a normal distribution ($P>0.05$). Comparison between the three separate E_C determinations for each sample confirmed that there was no significant difference between tests ($P<0.05$). However there was a tendency for the initial determination to be lower for each sample than the values recorded in subsequent determinations.

It was therefore decided that all reported results and analyses were to be based upon data arising from the second E_C determination. Compliance corrected E_C for full HWD samples ranged from 143 to 253MPa with a mean of 187MPa (+/- 32.3 SD). The coefficient of variation (*CV*) for full HWD E_C was 0.17. Mean E_C values for the three respective zones were 211, 167 and 103MPa respectively. A detailed summary of the zonal E_C is given in Table 5.6.

Table 5.6 Summary table of the compliance corrected zonal compressive moduli

Zone	Mean E_C	Standard Deviation	Min – Max Range	*CV*
Zone 1	211MPa	+/- 28.9MPa	152 – 253MPa	0.137
Zone 2	167MPa	+/- 40.4MPa	93 – 272MPa	0.241
Zone 3	104MPa	+/- 23.1MPa	66 – 152MPa	0.221

Key: E_C, Compressive modulus. ***CV***, Coefficient of variation.

Analysis of variance indicated significant 'between sample site' differences in E_C ($P<0.05$). Tukey pairwise comparisons revealed significant difference between Z1 and Z2 and Z3, Z2 and Z3, and also Z3 and full HWD (see Figure 5.4).

Figure 5.4 Histogram showing 'between sample site' comparison of compliance corrected compressive moduli.

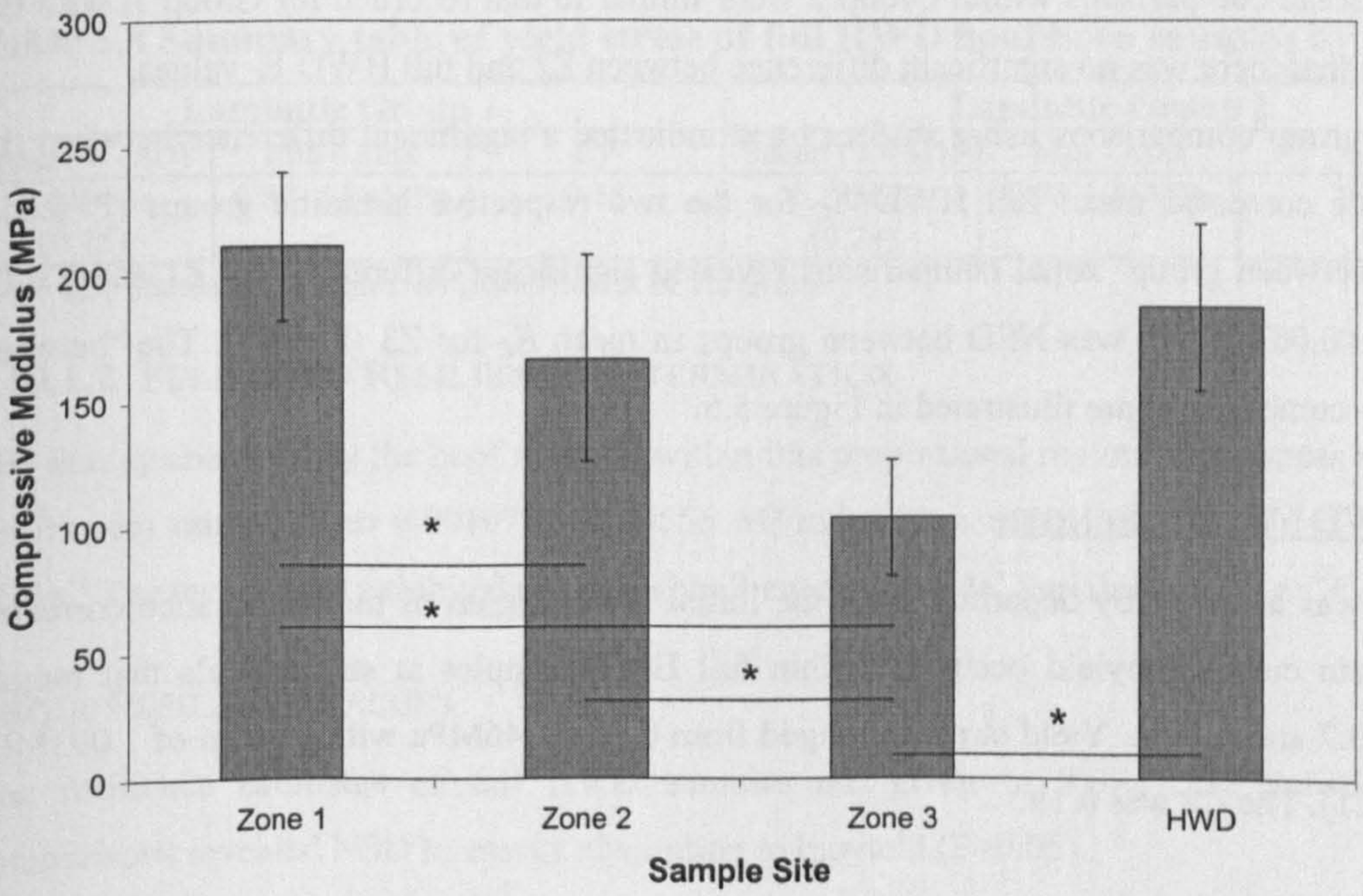

GROUP COMPARISONS

The E_C of the full HWD samples in Laminitic Group 1 ranged from 152 to 225MPa with a mean of 171MPa (+/- 21.5). The *CV* for the full HWD samples was 0.125. This compared with a mean

E_C for Group 2 of 196MPa (+/- 34.8), and a *CV* of 0.178. The E_C for Group 2 ranged from 143 – 253MPa.

Maximum Hydrated Resilience of laminitic hoof horn.

The compliance corrected zonal E_C data for the two respective laminitic groups is summarised below in Table 5.7. Comparison of compliance corrected E_C within the two respective laminitic groups by ANOVA revealed significant 'between sample site' differences ($P<0.05$). In the case of Group 1, Tukey pairwise comparisons confirmed significant differences between Z1 and Z2 and Z3, Z2 and Z3, and full HWD and Z2 and Z3.

Table 5.7 Summary table of the compliance corrected zonal compressive moduli by group

Parameter	Laminitic Group 1			Laminitic Group2		
	Zone 1	Zone 2	Zone 3	Zone 1	Zone 2	Zone 3
Mean E_C	184MPa	146MPa	102 MPa	226MPa	181MPa	105MPa
SD	23.4 MPa	26.0 MPa	24.7 MPa	19.5MPa	42.7MPa	22.6MPa
Min – Max	152–225MPa	93–167MPa	66–147 MPa	186–253MPa	129–272MPa	72–152MPa
CV	0.127	0.178	0.242	0.086	0.236	0.215

Key: E_C, Compressive modulus. **SD** Standard deviation. ***CV***, Coefficient of variation

Pairwise zonal comparisons within Group 2 were similar to that recorded for Group 1, with the exception that there was no significant difference between Z2 and full HWD E_C values.

Between group comparisons using student t-test indicated a significant difference between the compliance corrected mean full HWD E_C for the two respective laminitic groups ($P=0.05$). Similar 'between group' zonal comparisons revealed significant differences for Z1 and Z2 E_C values ($P<0.05$). There was NSD between groups in mean E_C for Z3 ($P>0.05$). The 'between group' E_C comparisons are illustrated in Figure 5.5.

FULL HWD YIELD STRENGTH

Bioyield was assessed by departure from the initial linear region of the compliance corrected stress strain curve. Bioyield occurred within full HWD samples at strain levels that ranged between 0.7 and 0.89%. Yield strength ranged from 0.73 - 1.46MPa with a mean of 1.093MPa (+/- 0.2121). The *CV* was 0.19.

Group Yield Strength values

The yield strength of the two respective laminitic groups is summarised in Table 5.8. There was NSD between groups in yield strength values ($P>0.05$).

Figure 5.5 Histogram showing 'between group' comparisons of compliance corrected compressive moduli

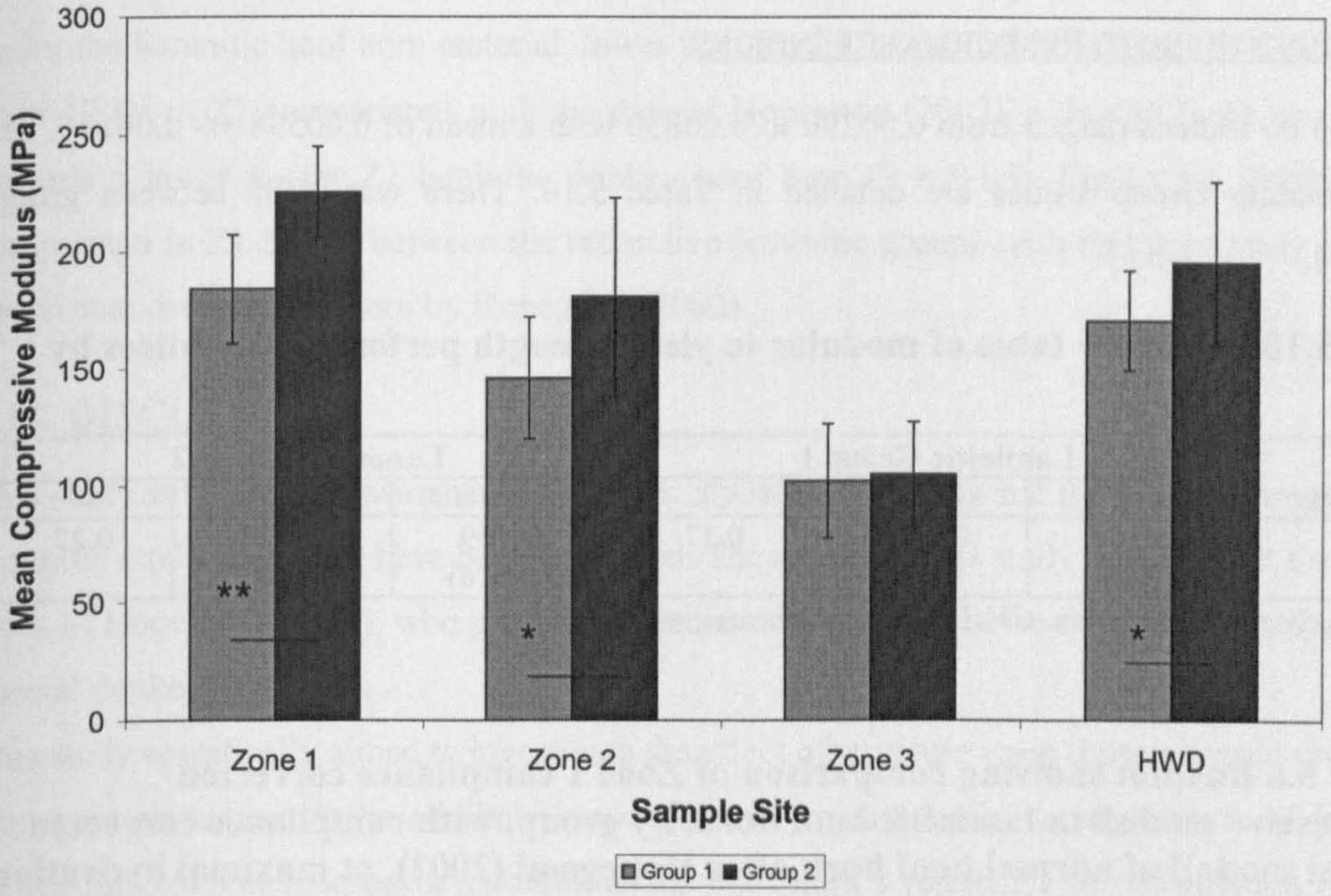

Table 5.8 Summary table of yield stress of full HWD hoof horn samples by group

Laminitic Group 1			Laminitic Group 2		
Mean (+/- SD)	Min - Max	*CV*	Mean (+/- SD)	Min - Max	*CV*
1.04MPa (0.15)	0.85- 1.34MPa	0.15	1.13MPa (0.24)	0.73-1.46MPa	0.22

Key: SD, Standard deviation. ***CV***, Coefficient of variation.

5.10.1.2 Full HWD Resilience Determination

The energy absorbed by the hoof material within this proportional region of the stress strain plot (resilience) ranged from 0.00107 to 0.00556 MJ/m^{-3} with a mean of 0.00337 (+/- 0.00129) MJ/m^{-3} The test sample exhibited considerable 'between sample' variability with a *CV* of 0.38.

Group Resilience values

The resilience estimates of full HWD samples are given in Table 5.9. Between group comparisons revealed NSD in energy absorption to bioyield (P>0.05).

Table 5.9 Summary table of full HWD resilience values by group

Laminitic Group 1			Laminitic Group 2		
Mean (+/- SD)	Min - Max	*CV*	Mean (+/- SD)	Min - Max	*CV*
0.00323 MJ/m^{-3} (0.00104)	0.00226 - 0.00556 MJ/m^{-3}	0.322	0.00345 MJ/m^{-3} (0.00146)	0.00107 - 0.00553 MJ/m^{-3}	0.423

Key: SD, Standard deviation. ***CV***, Coefficient of variation.

MODULUS STRENGTH PERFORMANCE INDICES

The E to σ_Y indices ranged from 0.00290 to 0.00830 with a mean of 0.00598 +/- 0.00138. The corresponding Group values are detailed in Table 5.10. There was NSD between groups ($P>0.05$).

Table 5.10 Summary table of modulus to yield strength performance indices by group

Parameter	Laminitic Group 1			Laminitic Group 2		
	Mean (+/-sd)	Min - Max	*CV*	Mean (+/-SD)	Min - Max	*CV*
σ_Y/E	0.0061 (0.0010)	0.0048-0.0084	0.17	0.0059 (0.0016)	0.0029-0.0082	0.27

Key: sd, Standard deviation. ***CV***, Coefficient of variation.

Figure 5.6 Boxplot showing comparison of Zone 1 compliance corrected compressive moduli in laminitic hoof horn, by group, with compliance corrected flexural moduli of normal hoof horn after Hopegood (2002), at maximal hydration levels.

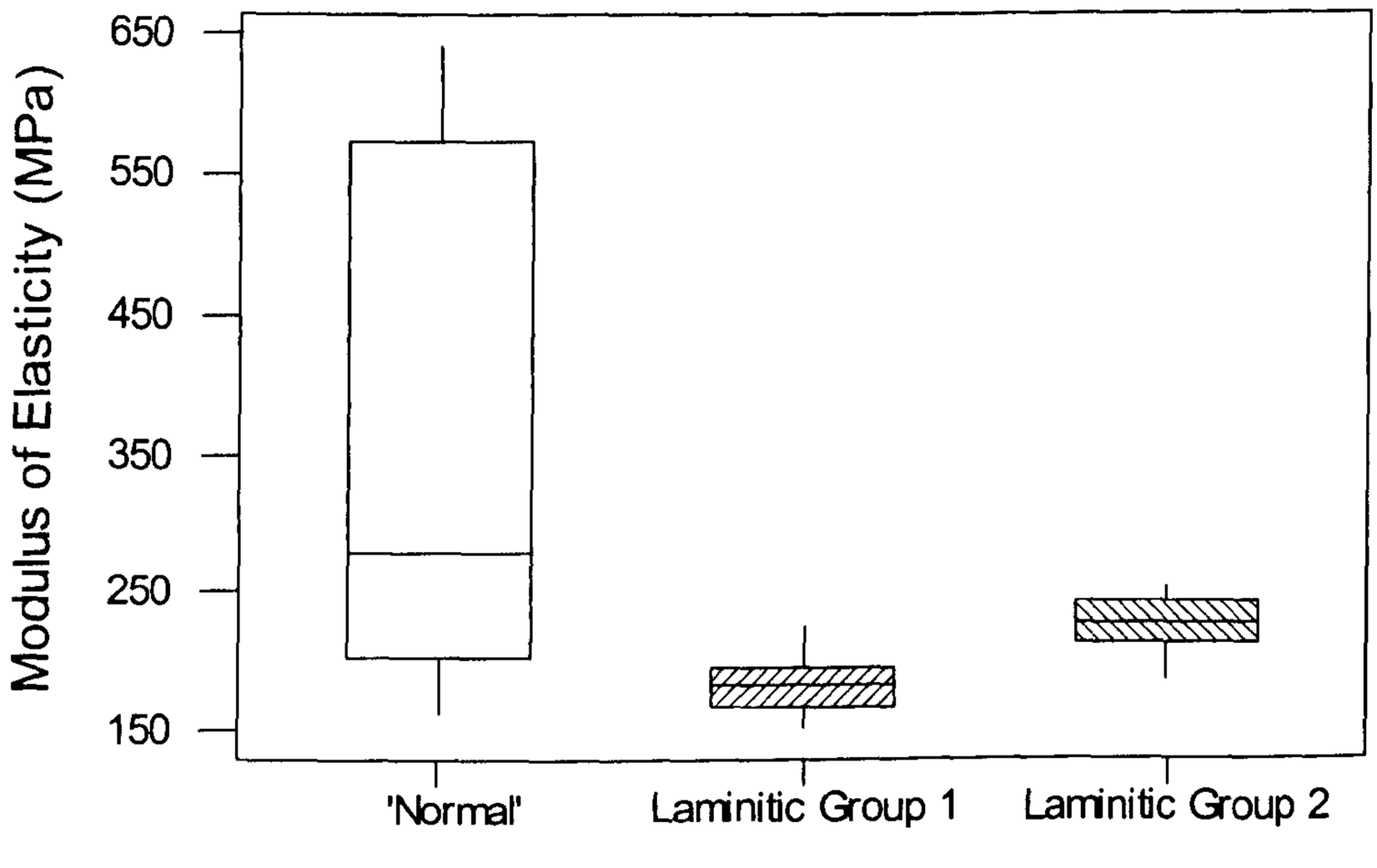

COMPARISON OF LAMINITIC VS NORMAL MODULI OF ELASTICITY

Comparison of full HWD E_C with E_F data previously recorded at MR_M by Latham (2001 – Pers Com.) and Hopegood (2002) were equivocal. Although significant differences between laminitic and normal donkey hoof horn E were indicated in both comparison, full HWD E_C was significantly lower than the Latham's study but were significantly higher than Hopegood's

study (P< 0.05). Zonal comparisons were similarly varied in their findings. Comparisons with the data of Latham (2001 – Pers Com.) revealed significant differences between E for Z1, with E_C for the laminitic hoof horn material, lower than the E_F for normal hoof horn (P< 0.05). There were NSDs in Z1 comparisons with the data of Hopegood (2002), although there was a trend towards a lower E_C for Z1 laminitic donkey hoof horn (P = 0.06). Figure 5.6 illustrates the comparison in Z1 E data between the respective laminitic groups with that previously reported for normal donkey hoof horn by Hopegood (2002).

5.11 DISCUSSION

This study is the first occasion since the work of Garnhaft (1925) that the material properties of laminitic equid hoof horn have been evaluated. The results of this study complement the former work of Hopegood (2002), who provided baseline data to characterise the material properties of normal donkey hoof horn.

This study specifically aimed to investigate the effect of structure upon those material properties that were considered to be of likely biomechanical importance in determining hoof function. Hence this chapter focused upon defining the hoof horn's resistance to deformation (E), and also its ability to absorb energy (Resilience). Whilst E values have been widely reported for the equine hoof, there is little information regarding the resilience of hoof horn. This represents a notable gap in the current knowledge base, which is of particular functional significance. This is because energy absorption within the hoof is considered to be important in attenuating concussive forces associated with dynamic weightbearing (Dyhre-Poulsen *et al.* 1994). This attenuation process serves to protect the sensitive structures of the distal limb from concussive damage, and hence is vital in ensuring efficient locomotor function.

In order to investigate the effect of structure upon these defining characteristics, material was controlled in respect of moisture levels. This is because water is known to be a modulator of material properties of donkey hoof horn (Collins *et al.* 1998, Hopegood 2002).

All material was therefore tested at maximal hydration level. In this way the material was fully plasticised, and the resultant material properties assumed to be a function of the structural organisation of the material within the hoof wall. This is not the case at other levels of hydration that have typically been used to assess the material properties of hoof horn. This is because the hoof horn material is not in a state of full plasticisation at these hydration levels.

Concurrent studies performed by this author demonstrated the complexity of the water-hoof interaction across the HWD, and the difference levels of plasticisation that occur at given levels of hydration. For example, predicted water partitioning at 'in vivo' hydration levels (see Appendix VII) indicated sub-maximal bound water levels with Z1. Hence the material

properties of the hoof wall at this level of hydration are likely to be further modulated by moisture.

Material properties were established by compression testing. This differed from the approach of Hopegood (2002), who conducted three-point bending tests to derive estimates of E_F. The compressive testing technique offered several distinct advantages over other potential modes of testing. Most notably, this technique enabled relatively large sample sizes to be used. Hence confidence can be expressed in the fact that the resultant data reflected the effects of the structural organisation of the hoof horn material. In addition, this testing technique was not limited by the biological constraints of capsular shape, thus it was possible to test samples in a manner that likely mimicked 'in vivo' loading conditions. Both of these issues are of fundamental importance in the effective characterisation of biomaterials (Wainwright *et al.* 1976, Vogel 1988, Vincent 1990).

The force displacement plot of both full HWD and zonal samples revealed an initial region that displayed a Hookean relationship of linear elasticity. This was in agreement with testing observations made by Leach (1980) and Kasapi and Gosline (1997) for the horse, Reilly (2001) for the pony, and Collins *et al.* (1998) and Hopegood (2001) for the donkey.

Data obtained for successive tests of the same sample showed no significant difference in the derived E between tests. Whilst this is in agreement with results previously reported for normal equid hoof horn by Zoerb and Leach (1978), Leach (1980), Reilly (2001) and Hopegood (2002), this was in marked contrast to the findings of Garnhaft (1925) for laminitic equine hoof horn. This author was unable to achieve repeatability 'between tests' by cantilever testing methods, either for full HWD or partial HWD samples, nor indeed was he able to obtain 'within test' linearity in the force displacement data. In fact, Garnhaft (1925) was forced to abandon his evaluation of laminitic equine hoof horn because of this.

The techniques developed within this project have successfully addressed the experimental difficulties of working with this pathologically altered material. In addition these techniques and the sampling methodology enabled concurrent full HWD and zonal material testing. Consequently this present study represents the first occasion in which the comprehensive characterisation of laminitic hoof horn has been effectively achieved.

Direct comparisons with previously reported E data must be viewed with caution. This is because testing methodologies have not been standardised. Consequently different modes of testing have been employed, with samples tested in different orientations, at different levels of hydration, and at different strain rates. All of these factors are known to affect the resultant data. The initial assessment of machine compliance reinforced the need to ensure that all published data is corrected with respect to machine compliance of the testing equipment used. Whilst the

machine compliance in this study revealed an underestimation of E_C by 14%, corresponding values for single column testing machines can be as high as 48% (Collins – unpublished data). This important potential source of experimental error has largely been overlooked in previous studies.

It is acknowledged that testing biomaterials, in either mode of testing raise questions concerning the validity of explicit assumptions inherent within compression, tensile and bending test theory. However the specific assumptions that have to be made in respect of flexural testing are most difficult to substantiate. Hence particular care must be taken when assessing flexural data. In addition, the flexural E represents an only approximation of the true E (BSEN 2746 1998).

The analysis of the effect of strain rate upon E_C indicated that a two order of magnitude increase in strain rate resulted in a 29% increase in E_C. This is in broad agreement with the findings of Kasapi and Gosline (1997) for the horse. These authors recorded an 18% increase in E_T over the corresponding range of strain rate. This indicates that a similar visco-elastic response occurs within the donkey hoof wall to that evident in the horse. In this way, the degree of capsular deformation is inversely proportional to the rate of loading. This response may serve to further protect the sensitive structures of the foot from excessive deformation associated with high velocity impacts during conditions of 'extreme' loading. This would further aid the maintenance of smooth and painless stress transfer across the laminar interface.

This strain rate dependent response further reinforces the need to standardise testing conditions between studies. In addition, this must be appropriately standardised at a level that approximates to 'in vivo' loading conditions.

In this regard, the strain rate selected for this present study fell within the physiological strain rate range for the horse cited by Kasapi and Gosline (1997). In order to simulate static weightbearing, the strain rates selected were lower than the range of surface strain rates reported for the dorsal aspect of the pony hoof capsule, during walk and trot, by Thomason *et al.* (1992) and Chang *et al.* (1993). Hence the resultant material property data presented in this chapter can be considered as representing, by first approximation, the true effects of structure upon laminitic donkey hoof horn. Hence this forms a reliable basis for the characterisation of the material properties of laminitic donkey hoof horn.

The force displacement data for the full HWD and the three respective zones, normalised in respect of specimen geometry to give the stress-strain relationship, provides a valuable insight into the response of laminitic donkey hoof horn to direct load. This gives an understanding of how the material accommodates and resists load. In addition defining material characteristics such as E_C, σ_Y and ε_Y can be established. These are essential if horn horn assessment is to be placed upon an objective basis.

The stress-strain relationships highlight zonal differences in E_C, σ_Y and ε_Y, and their respective post-yield characteristics. Similarly the stress-strain relationship for the full HWD indicated that this zonal interaction results in a distinct loading response to ultimate failure. All samples are assumed to be fully plasticised, hence the responses reflect the effect of structural organisation of the hoof horn material within the respective zones and, in the case of full HWD samples, the combined interaction of these structurally distinct zones.

The compressive stress-strain relationship to failure for full HWD laminitic donkey hoof horn was similar to that presented for the horse by Butler and Hintz (1977) and Landeau *et al.* (1983). Similarly, zonal stress-strain relationships recorded for the donkey were in broad agreement with that reported by Kasapi and Gosline (1997) for the horse. This suggests similar mechanistic responses to applied load and/or similar modes of failure. However the absolute values which define these mechanical responses, and characterise the nature of the material, tended to be lower for laminitic donkey hoof horn compared to corresponding values for the horse. Due to the paucity of information relating to the normal donkey, it is not possible to conclude whether these differences arise as a direct consequence of the laminitic condition or result from species differences.

Bioyield occurred in full HWD donkey samples at stress levels ranging from 0.73-1.46MPa, at strain levels between 0.7 and 0.9%. This compares with typical values reported for the horse by Landeau *et al.* (1983) of ~2-3MPa and ~2-3 % strain.

The zonal pattern in bioyield across the HWD was in broad agreement with that previously reported for the horse by Kasapi and Gosline (1997).

This was characterised by a dorso-palmar decrease in yield strain and strength. Although the yield strains for Z1, 2 and 3 were similar to those for the horse at 7, 6 and 5% respectively, the corresponding yield strengths were markedly lower in the donkey.

This is the first study to have defined the energy absorption characteristics of donkey hoof horn. Resilience data reported in this chapter provides an estimate of the capacity of the laminitic donkey hoof horn to absorb elastic strain energy, with a mean full HWD resilience value of $0.003MJ/m^3$.

Direct comparisons with experimentally derived data for full HWD equid hoof horn at maximal hydration are not possible. However weighted average data, derived by this author from zonal stress strain data reported for equine hoof horn at maximal hydration by Kasapi and Gosline (1997), suggests an equine resilience value for the full HWD that is approximately 23 times greater than the donkey.

However it is important to note that this derived estimate was based upon zonal data reported by Kasapi and Gosline (1997). Hence this did not take into account 'between zone' interaction

within the full HWD. This interaction resulted in an order of magnitude decrease in σ_Y within this present study. A similar decrease in yield strength for the horse would result in similar resilience values between species.

Consequently, difference in hoof size between the donkey and the horse may represent a significant 'between species' difference in the hoof's capacity to absorb elastic strain energy during weightbearing. This may reflect a scaling effect related to differences in bodyweight. Conversely this may suggest 'species specific' differences in hoof function, or indicate that different absorbing methods are present within the foot, involving other tissues. It is also important to note that differences in hoof shape are likely to affect the degree of deformation for a given load. This will also affect the degree of energy absorption within the hoof horn material. The mean full HWD axial to lateral E_C ratio of 1.5:1 confirmed that the directional component of tubular structure was associated with an increased resistance to compression, and indicated the presence of mechanical anisotropy within laminitic donkey hoof horn.

This finding supports the results of Douglas *et al.* (1996) and Kasapi and Gosline (1997) who recorded axial reinforcement within the inner and outer regions of the equid hoof wall, at 'in vivo' and maximal hydration condition respectively. However, Leach (1980) reported mechanical isotropy in the inner region of the hoof wall, and an axial to lateral E ratio of <1 for the outer region, which suggested mechanical anisotropy with lateral reinforcement in this region. Bertram and Gosline (1986) also reported lateral reinforcement within the equine hoof wall.

A satisfactory explanation for these contradictory findings can not be given. Future work is therefore required to address this key structure-function issue.

The absolute E_C values for full HWD laminitic donkey hoof horn were markedly lower than E data previously reported for the horse at maximal hydration (see Table 5.1).

Comparison of data recorded in this present study, with those previously recorded for 'normal' donkey hoof horn were equivocal. Mean full HWD E_C recorded in this present study (185MPa) was significantly higher than the mean E_F of 135MPa reported by Hopegood (2002), but were significantly lower than the mean E_F of 205MPa recorded by Latham (2001 – Pers Com.).

A satisfactory explanation for these contradictory findings can not be given. This may suggest that factors other than laminitis and moisture, such as age, bodyweight season, nutrition, degree of environmental and mechanical degradation, which were not controlled between these respective studies, also have a significant effect upon E.

It is also appreciated that different modes of testing were employed between studies, on material obtained from different sites, and at different rates of strain, all of which are likely to make direct comparison more difficult.

The precise effects of these differences are likewise difficult to assess retrospectively. However differences in the strain rate alone, between these studies, can not account for differences in *E*. It is also important to note that material tested by Hopegood (2002) was not clinically diagnosed as normal. Hence the health status of this material can not be confirmed.

The data obtained in this present study exhibited a relatively low *cv* at 0.14, this compared with value of 0.29 in the study of Hopegood (2002). This difference may reflect a true difference in *cv* of *E* between normal and laminitic donkey hoof horn. Conversely, this increased level of variation within the study of Hopegood (2002) may reflect the presence undiagnosed laminitic hoof horn material, the effects of variable mechanical and environmental degradation of the distal clipping material between samples, and/or inherent issues relating to the assumptions made in flexural testing.

The dorso-palmar decrease in E_C across the HWD corresponds with previously recorded data for the horse (Kasapi and Gosline 1997) and donkey (Hopegood 2002).

The absolute values recorded for the donkey in this present study were lower than the corresponding zonal values for the horse. These findings were consistent with those of Latham (2001 – Pers Com.) and Hopegood (2002) for 'normal' donkey hoof horn, and suggests a 'between species' difference in the material properties. The functional significance of this 'between species' difference is unknown, however this finding is consistent with the assertion that the donkey is a unique equid. Consequently the critical evaluation of the material property data reported in this chapter has predominantly focused upon a 'within species' assessment.

The mean E_C of 185MPa for full HWD laminitic donkey hoof horn at maximal hydration, was in broad agreement with the weighted average of ~145MPa derived from the respective zonal E_C data, assuming a 'rule of mixtures' contribution to the full HWD E_C. In this respect, the volume fraction contribution of Z1, 2 and 3 were assumed to be 25,15 and 60% respectively, which is in line with the relative dorso-palmar contribution of the respective zones to the HWD. The underestimation of the actual full HWD E_C may indicate that the actual *E* is further modulated by zonal interaction, and that structural organisation of the hoof wall does not result in conditions of uniform strain (isostrain) assumed in the 'rule of mixture' estimate. Alternatively, this underestimation may reflect 'between individual' variation in the actual volume fraction contribution of the respective zones.

Hopegood (2002) similarly provided an estimate of full HWD E_F. This figure (188MPa) was based upon a zonal average of the respective E_F data. This estimate resulted in an overestimation of actual E_F. However the zonal E_F data used for this estimate was not derived from material concurrent with that used to establish the full HWD E_F.

The statistically significant differences recorded in E_C between the respective structurally distinct zones, suggests that the structural organisation of the hoof horn material is a primary determinant of the material properties of laminitic donkey hoof horn. The final chapter of this thesis will explore further the potential structure-function relationship indicated by these results.

In this present study, significant differences were recorded in E_C between all zones, whereas Hopegood (2002) reported significant differences only between Z1 and Z3.

This may indicate a specific laminitic effect in which the Z1 E is decreased as a consequence of the condition. This assertion is further supported by the significantly lower Z1 E value recorded in this present study compared to data provided by Latham (2001 – Pers Com.) and the trend towards a lower Z1 E (P=0.06) in comparison with the data of Hopegood (2002). These findings suggest the possibility of a zone-specific structural response to the laminitic condition, with changes to the structural organisation of the hoof horn material occurring within Z1.

The zonal difference further questions the robustness of the 'normal' donkey data provided by Hopegood (2002). This is because it is difficult to reconcile the situation in which there are NSDs between zonal normal and laminitic hoof horn yet normal full HWD E is significantly lower than that of laminitic donkey hoof horn. Two issues are worthy of further comment. Firstly the material used to arrive at full HWD and zonal data was not concurrent. Seasonal effects have been previously reported for equine hoof horn both in respect of structure (Patan 2001) and material properties (Zenker 1991, Ley *et al.* 1998, Patan 2001). This may in part account for the discrepancy between the estimated full HWD E_F value and the actual HWD value reported by Hopegood (2002).

In addition, the *cv* evident within Z1 data reported by Hopegood (2002) was extremely high at >0.7 in comparison with that obtained in this study. This may indicate the presence of variable zonal degradation of the material tested by Hopegood (2002). In this respect, it is possible that mechanical and environmental degradation is focused within this region of the hoof wall. Indeed Hopegood (2002) commented upon the fact that degradation was particularly evident within the dorsal 10% of the HWD. This may arise simply as a consequence that this region is on the outside of the hoof capsule. Alternatively, the zonal variation in E may serve to focus stress within this region, as part as a optimised and controlled mechanism that protects structures deep to the dorsal aspect of the hoof.

Conversely Z1 *cv* levels may reflect the presence of undiagnosed laminitic hoof horn. Hence it is considered that the data of Latham 2001 – Pers Com.) represents a more appropriate E baseline for the normal donkey hoof horn. Consequently these values have been adopted within Chapter 8 of this thesis.

It is important to note that, in addition to the issues raised regarding the potential effects of 'between study' differences in the testing protocols, the Z1 and Z2 data of Latham (2001 – Pers Com.) and Hopegood (2002) were based upon samples taken from within the two zones. This is in contrast to this present study, where the entire dorso-palmar extent of each of the two respective zones was tested.

The analysis of the material properties by laminitic group revealed that this 'response' belied a more complex and variable association, in which E_C was related to the nature of the degenerative anatomical change evident within the foot.

These differences were marked by the fact that mean full HWD E_C values for Group 1 were significantly lower than Group 2. Although both laminitic groups exhibited a dorso-palmar zonal decrease in E_C across the HWD, there were differences in absolute values for Z1 and Z2 between groups. Group 1 values were significantly lower than those recorded for Group 2. This suggests that degenerative anatomical change, associated with the laminitic condition, may lead to a region-specific response within the donkey hoof wall, which affects the outer region (Z1 and Z2). The specific changes in E_C result in a distinct pattern of zonal material characteristics across the HWD in the two respective groups.

The evaluation of the E_C data suggests a possible scenario in which anatomical changes occurring within Group 1 are associated with a marked decrease in Z1 E_C, leading to a corresponding marked reduction in full HWD E_C.

Anatomical changes within Group 2 also lead to a reduction Z1 E_C, however the magnitude of this decrease is less than that evident in Group1. In addition, a corresponding increase in Z2 E_C occurs. The net effect of these opposing 'responses', is a modest decrease in full HWD E_C.

The functional significances of either the regional change in E_C, or the different zonal pattern of E_C across the HWD are not known. These 'responses' are however likely to affect force distribution within the hoof wall. Changes in force distribution may be important in terms of hoof wall function. These issues will also be examined further in Chapter 6.

Between group differences also suggest that the E_C of laminitic donkey hoof horn is related to the specific nature of the anatomical change that occurs within the afflicted foot. Radiographic analysis given in Chapter 3 highlighted that Group 1 was characterised predominantly by capsular rotation, whereas Group 2 was marked by phalangeal rotation.

This would suggest that capsular rotation affects hoof horn formation, within that region of the coronary corium that supports Z1, to a greater extent than is the case in phalangeal rotation. This may have a direct bearing upon biomechnical compromise within the laminitic foot.

The increase in Z2 E_C is not readily explained. However it is expected that axial compression is increased as a consequence of phalangeal rotation. In this regard, the increase in E_C may reflect

a positive feedback to counter axial compression, in a similar manner to that evident within stressed bone.

Further work is required to confirm these potential laminitic effects. This must be conducted under standardised experimental conditions, with appropriate experimental controls including clinically diagnosed normal donkey hoof horn material.

If laminitis does indeed result in measurable differences in *E*, then careful hoof wall sampling of the outer aspect of the hoof wall may provide an additional method both for laminitic screening, and the assessment of material property response to therapeutic intervention.

Hopegood (2002) stated that the 'best' method to normalise zonal donkey hoof horn material for the effects of water, prior to material testing, was to equilibrate samples to $38gH_2O/100gDM$. However Z3 E_F values recorded by Hopegood (2002), at this level of hydration, were significantly higher than those recorded at maximal hydration. This would indicate that material testing was performed on zonal samples that were not fully plasticised. This suggests that the bound water capacity for this zone exceeded $38gH_2O/100gDM$.

Although Hopegood (2002) found that there was NSD between E_F at $38gH_2O/100gDM$ and maximal hydration, for either Z1, or Z2, there was a tendency for Z2 E_F values to be higher at $38gH_2O/100gDM$.

Hopegood (2002) that equilibrating samples to $38gH_2O/100gDM$ normalises the material in respect of the effects of moisture. The actual zonal bound water capacities for normal donkey hoof horn are unknown. However predicted data for laminitic donkey hoof horn, established from concurrent hydration studies performed during this project (see Appendix VII), did not support the assertion of Hopegood (2002). These predicted results suggest that at a hydration level of $38gH_2O/100gDM$, Z1, 2 and 3 are on average at 7.7, 6.3 and $-0.1gH_2O/100gDM$ of their respective bound water capacity. Thus Z3 will be at a critical hydration point with regard to plasticisation. 'Between sample' variation in bound water capacity, combined with ambient dehydration of the sample during testing are likely to have a pronounced affect upon E_F values at this particular level of hydration.

These factors may in part account for the differences in zonal E_F values between $38gH_2O/100gDM$ and maximal hydration reported by Hopegood (2002), with Z3 material at a sub-maximal bound water level when equilibrated at a hydration level of $38gH_2O/100gDM$. Similarly, the tendency for Z2 E_F to be higher at $38gH_2O/100gDM$ than at maximal hydration suggests the possibility that Z2 material was also at a sub-maximal bound water level when tested at $38gH_2O/100gDM$ hydration.

In fact pathological conditions of the *Stratum corneum* are associated with a decreased bound water capacity (Takenouchi *et al.* 1986). Hence the zonal bound water capacities given in this

thesis may represent an underestimation of their corresponding values within normal donkey hoof horn. Hence it is the recommendation of this thesis that in order to control for the effects of water, future material testing should be standardised and performed at maximal hydration levels. This is because it is only at this hydration level that hoof horn material is fully plasticised.

Hopegood (2002) conducted zonal material testing to establish 'in vivo' E_F for the respective zones of 'normal' donkey hoof wall. The resultant zonal average reported by this author was 3.5 times greater than the actual full HWD E_F data recorded at this level of hydration. Hopegood (2002) suggested that this difference might indicate that the testing of full HWD samples masks the finer zonal detail. However it is unlikely that zonal interactions alone could account for such a level of difference. It is more likely that the issue of specimen dehydration during the preparation and testing of zonal samples, which Hopegood (2002) referred to, was a major contributing factor to this difference.

This study has endeavoured to investigate the effect of structure on the material properties of laminitic hoof horn by the appropriate control of moisture within the material. It is appreciated that by controlling the material in this respect, moisture levels were outside of the normal physiological range. This would potentially lead to an alteration in material properties. However the water-partitioning data indicated that this effect is likely to be restricted to Z1 only. In addition, the 'in vivo' gross moisture level data for this zone further suggests that the material is approaching a fully plasticised state, and can thus be considered to be at a moisture level above its 'critical point of plasticity'. Hence the likely effects of controlling for moisture, in the manner adopted here, are likely to induce a modest change in material properties within this zone.

It can therefore be argued that the material property data represent a reasonable first approximation of '*in vivo*' material properties. Hence this data can be used to model potential structure-function relationships within the hoof wall, and aid the further investigation of the effects of the laminitic condition. In addition, the results generated within these models can be assumed to be of 'in vivo' functional relevance. These issues are developed further in the following chapter.

6. COMPUTER MODELLING OF THE DONKEY HOOF WALL

6.1 OVERVIEW

The previous chapters of this thesis have dealt specifically with a detailed characterisation of the structural and material properties of donkey hoof horn associated with the laminitic condition. However management concerns regarding the afflicted animal are directed towards the impact upon the biomechanical functionality of the hoof and the foot.

There exists an important distinction between properties and functions (Marks 1981). Properties represent measured physical characteristics, whilst functions reflect the application and response of that material to a specific set of conditions. Clearly an intimate relationship exists between properties and functions. Indeed functions are largely dependent upon material and structural properties and modulated by the effects of geometric form.

Despite these facts, Hoof research has, historically, focused primarily upon defining properties. Hence the precise effect of properties upon hoof function is poorly understood at either the gross, macro- or micromechanical level. Reilly (1995) recognised this fact, and stated that there was an urgent need to develop our understanding of the structure-function relationships of the hoof.

However achieving this end poses a particular intellectual challenge (Newlyn *et al.* 1998). This is because difficulties exist in establishing a credible means by which 'functions' can be accurately recorded, measured and assessed (Newlyn *et al.* 1998, 1999, Davies 2002), and the functional effects of changes in 'properties' evaluated (Newlyn *et al.* 1998). Hence progress to date in this important field of research has been limited (Davies 2002). There is clearly a need to further explore the application of specific techniques that can investigate the effect of material and structural 'properties' upon biomechanical function (Newlyn *et al.* 1999). Indeed it is only through such an approach that progress can be achieved (Davies 2002)

One such technique that may be of potential value is that of Finite Element analysis (FEA). The Finite element (FE) technique provides a sophisticated method of simulating or modelling the theoretical response of an object to applied load, based upon information specifically relating to the material and structural properties of the object. Thus it has the potential to further elucidate hoof function, and also provide a basis by which structure function relationships within the hoof can be investigated.

This chapter details work associated with the application of the FE technique to the theoretical modelling of the donkey hoof wall at the gross anatomical, macro and microscopic levels of the design hierarchy. In addition, the chapter has sought to elucidate the structure function

relationships within the hoof wall, and also assess the potential effects of the laminitic condition, using material and structural 'properties' data established within the previous chapters of this thesis.

6.2 THE FINITE ELEMENT (FE) TECHNIQUE

FEA is a computer based modelling technique that is used widely in the engineering industry to determine how a body reacts theoretically to applied forces in both static and dynamic situations. The FE technique has been widely used by to model the theoretical relationship between properties and mechanical function.

This technique offers the ability to model function not only at the gross anatomical level but also at the macroscopic and microscopic level. Indeed this technique provides a means by which the various structure function relationships that operate within the design hierarchy of the hoof wall can be assessed. In this way, key issues of hoof function can be investigated further. For example, the issue as to whether the structural organisation of Tu and IT horn does act as a fibre composite can be addressed.

6.3 THE FE METHOD

The FE method is a mathematical technique that determines the displacements, strains and force intensities that occurs within a body object in response to specific loading and restraint conditions.

When an object is loaded it responds in a manner such that internal forces are generated to counter the applied forces, thereby re- establishing the equilibrium state within the body. According to the theory of elasticity, this equilibrium state may be represented by an infinite number of partial differential equations. In general, it is not possible to solve these equations except in the simplest of geometric forms.

The FE method replaces this infinite series of differential equations with a finite number of simpler algebraic equations at specific locations within the body object. In this way, approximate solutions can be obtained to complex problems.

This approach can be summarised thus: -

Structure divided into a finite number of discrete sub-regions or Finite Elements

Method develops mathematical equations that relate the displacements created to the forces applied specifically to these Finite Elements in the manner that:

$$\{F\} = [K]\ \{u\}$$

where:

$\{F\}$ = vector of nodal force

$[K]$ = element stiffness

$\{u\}$ = vector of nodal displacement

Nodal intersections between adjoining elements allow equations to be assembled to throughout the entire structure in response to the loading conditions

Derived displacements are used to calculate stress and strain levels

Given specific boundary conditions in the form of nodal forces and/or displacements the resultant set of equations can be resolved in respect of all nodal positions. Hence the theoretical response of the entire object can be modelled, and the associated stress levels and strain distribution within the object predicted.

The theoretical stress and strain values can be displayed in various forms. The magnitude of the Maximum Principal stress can be plotted as can the Minimum Principal stress, or, a combination of these related to various failure theories.

Two stress states may be of interest, these are: -

1. The Maximum shear stress (Tresca)
2. The Von Mises Stress (Shear strain energy theory)

The von mises stress value is a theoretically derived stress value. It represents the equivalent uniaxial stress that would have to be applied in order to generate a strain energy level equivalent to the total strain energy recorded in each of the three orthogonal x, y, and z-axes

Both of these stress states are usually related, in engineering applications, to failure in ductile materials. Such a mode of failure may be appropriate to hoof wall modelling, due to the potential plasticising effect of the material's inherent moisture content described by Cope *et al.* (1998).

6.4 THE FEA PROCESS

The finite element analysis of an object involves a three-stage process. This is: -

1. Model creation
2. Solution
3. Result validation and interpretation

6.4.1 MODEL CREATION

In order to generate a computer-based model of the object the key defining characteristics need to be established both in respect of the geometric shape or form of the object, and its 'material properties'.

The form of an object can be defined as: -

" The spatial disposition of the respective elements that constitute the body object".

At the gross anatomical level of the design hierarchy of the hoof, form is concerned with the geometry of the capsule, and the spatial disposition of the respective hoof horn component within the hoof capsule.

Conversely at the microscopic level, the form of the hoof wall relates to the size and shape of the respective horn tubules and their distribution within the IT horn component. In this regard, it is the structural organisation of the hoof horn material that is of interest.

With this information the actual process of model creation within the computer can commence. This process involves a three-stage approach: -

1. Generation of finite elements
2. Definition of the material properties of the model
3. Creation of the loading and interfacial conditions, and the denotation of boundary constraints

Newlyn *et al.* (1998) provides a detailed account of process of computer-based model generation (see Appendix VII).

6.4.1.1 Constructing the FE Model – Generation of Finite Elements and Nodal Intersects

This process can be summarised thus: -

1. A series of control points are defined in space
2. Mathematical curves or 'splines' are constructed that unite these control points to delimit the boundaries of the object and thereby define its surfaces
3. The resultant object is sub-divided or meshed into discrete finite elements
4. In the case of a three-dimensional model, the volume contained within this surface mesh is itself divided into discrete elements
5. The resultant finite element mesh is validated to ensure continuity of nodal intersections throughout the entire system

It is important to note that the precision of the resultant analysis is determined both by the type and number of the finite elements, and by the number of nodes between finite elements. These ultimately determine the total number of equations that have to be solved.

6.4.1.2 Defining the Material Constraints of the Model

With this in place, the material properties of the model are stipulated with respect to the finite elements. This process is dependent upon the nature of the analysis to be conducted.

In the case of an isotropic material model, the material properties can be defined by two material properties, namely the E and the poisson ratio (ν), the ratio of transverse to axial strain.

More complex material models require these constraints to be defined in directional terms, and also require the shear modulus of the material to be specified.

6.4.1.3 Loading and Interfacial Conditions, and Boundary Constraints

LOADING CONDITIONS

Loading conditions are specified both in respect of the point/s of application and the magnitude and direction of the applied loads.

INTERFACIAL CONDITIONS

Interfacial conditions, between components of differing material properties, can greatly affect the modelled response, especially with regard to stress and strain concentration at locations of abrupt transition. Where appropriate, the specification of progressive transition in material properties across these interfaces can minimise these effects.

BOUNDARY CONSTRAINTS

Boundary constraints are required to prevent free or rigid body movement in response to the applied loads. Particular attention must be given to ensure that the object is not constrained in an inappropriate manner to the functionality of the object.

6.4.1.4 Model Solution

With the model created and the loading conditions and boundary constraint specified the analysis can be performed. The solution time for the FEA is dependent both upon the computer processing speed and the total number of equations which have to be solved. The analysis is validated by a number of back-checks to ensure that the model has been correctly 'defined'. The analysis is completed when the nodal displacement and desired derived quantities of stress and strain levels have been calculated.

6.4.1.5 Result Validation and interpretation

VALIDATION

Validation of results represents a crucial stage in the analysis process. Validation involves two distinct issues (Huiskes and Choa 1983). These are: -

1. Model validation
2. Model accuracy

MODEL VALIDATION

This relates to the degree to which the model represents the real object. This is influenced by the assumptions and approximations made during the modelling process, with specific regard to: -

- Geometric form
- Material 'properties'
- Loading and interfacial conditions and boundary constraints
- Errors in respect of the above will result in the production of a deficient model.

MODEL ACCURACY

The assessment of model accuracy can be determined by both intrinsic and extrinsic means.

1. Intrinsic Accuracy Determination

Many FE programs employ convergence tests to further refine the accuracy of the analysis. These convergence tests seek to enhance the accuracy of the solution by increasing, in a step by step manner, the number of elements and nodes in critical areas of the model. This process is continued until a point is reached where the value of a given variable, for example, principal strain does not alter significantly from one refinement to the next. At this point in the refinement process the model is described as having reached convergence. The validation process should also include, wherever possible, direct comparisons with existing experimental data.

2. Extrinsic Accuracy evaluation

The validation of the accuracy of the modelled response must also take into account extrinsic sources of information including: -

- Empirical observations of '*in vivo*' and '*in vitro*' function
- Information from other analytical techniques for example:
  - Surface strain and photoelastic shear stress data
  - Data from load-sensing implants
- Traditional macro- and micromechanical analysis techniques, theory of elasticity and composite material theory
- Observations regarding the morphological and structural organisation present within the modelled object

6.5 THE APPLICATION OF THE FE TECHNIQUE TO THE EQUID HOOF

This mathematically based modelling technique has been used to investigate internal deformations and stress distribution in several biological structures. These have variable included: bone (Hogan 1992, Dalstra *et al.* 1995), ligament (Hirokawa and Tsuruno 2000, Weiss

and Gardiner 2001), tendon (Zhang and Roberts 2000), cartilage (Beek *et al.* 2000), skin (Bischoff *et al.* 2000), and tooth (Zhoa *et al.* 1989). In addition, FE analyses have been performed both for the fingertip (Wu *et al.* 2003), and the tiger claw (Mattheck and Reuss 1991), however the application of this technique to the hoof has been limited.

The pioneering work reported by Wichtmann *et al.* (1990) and Hogan *et al.* 1991, Hood and Wichtmann (1991) represented the initial application of the FE technique to the equid foot. These authors used this technique to evaluate the theoretical force distribution within the various structures of the foot in response to static loading. This assessment was based upon a 2-dimensional model of the sagittal plane of the equine foot, loaded via the middle phalanx.

However this study was limited considerably by the computer technology of the time. Hence the number of nodes within the model was relatively low in comparison with today's standards. In fact this model of the entire foot consisted of only 457 elements and 964 nodes. This compares for example, with the ~18000 elements, and 11608 nodes in the model of the donkey hoof wall reported by Newlyn *et al.* (1998). Therefore the work of Wichtmann *et al.* (1990) and Hogan *et al.* 1991, Hood and Wichtmann (1991) did not afford the modelling detail that is presently achievable.

With the rapid growth of computer processing capacity the application of this technique to the equid hoof has gained momentum. Indeed the work of the hoof research group at De Montfort University (Newlyn *et al.* 1998, 1999, 2004 – Submitted) has been in the vanguard of this movement.

Most notable amongst the work of other research groups, has been that of Hinterhofer (1996), Hinterhofer *et al.* (1997, 2000, 2001), McClinchey (2000), McGlinchey *et al.* (2001 – Submitted) and Thomason *et al.* (2002). However these studies have tended to focus upon the effect of farriery and remedial therapy on the hoof, as opposed to investigating the structure-function relationships within the hoof and/or the effect of pathology upon hoof function. Only the most recent work of Thomason *et al.* (2002) has evaluated the effect of geometric form upon hoof function.

It is also important to note that all these studies have been based upon the hoof capsule of the horse. The geometric form of the donkey differs markedly from that of the horse (Doguer 1943, Hifny and Misk 1983). This is of particular significance, as it is accepted that variations in geometric form directly affect functional response to loading (Collins *et al.* 2002).

The preliminary work associated with this thesis represents the only work specifically relating to donkey and the structure function relationships evident within the equid species. In addition, these studies have specifically sought to investigate the nature of the structure function relationships evident with the primary load-bearing component, namely the hoof wall. This

investigation has been conducted both at the gross anatomical level (Newlyn *et al.* 1998), and the macro- and micromechanical level (Newlyn *et al.* 1999).

6.6 DONKEY HOOF WALL MODEL DEVELOPMENT

The successful development of these models has been reliant upon the detailed characterisation of the material properties, structural organisation and geometric form of the donkey hoof wall at various levels within its design hierarchy.

The model has been optimised and refined with data established in Chapters 3, 4 and 5 of this thesis, and also by reference to baseline data reported by Hopegood (2002). Use of this data has facilitated the definition of structural and material characteristics both at the macroscopic and microscopic level.

Although this thesis is not concerned with the effects of shape associated with the laminitic condition, capsular geometry remains an important determinant of function – see Section 1.9.2. Hence an effective means of shape determination represents an essential prerequisite if the functional consequences of the materials characterisation reported within this thesis can be modelled with confidence.

Therefore the characterisation of the geometric form of the hoof wall at the gross anatomical level warrants further comment and discussion.

6.6.1 CHARACTERISING THE GROSS ANATOMICAL FORM OF THE DONKEY HOOF WALL

As object function is determined partly by the geometric form of the body, then it is essential to be able to objectively define the geometry of the object with accuracy.

However, the equid hoof capsule displays a highly complex three-dimensional geometric form. Hence establishing an effective means by which the key defining aspects of this complex structure can be measured represents yet another demanding challenge.

The shape of hoof capsule has been variably described by first approximation as representing an inclined and obliquely truncated, conical (Leach 1980, 1990b, Hood and Jacobson 1997), or cylindrical form (Clark 1817, 1820).

If this assertion is correct and the geometry of the capsule can indeed be approximated to this frustrum or cylinder form, then it is possible, by first principals, to characterise the geometry of the capsule with a relatively small number of critical measurements or 'descriptors'.

Indeed the geometry of the hoof wall can be divided intuitively into a number of defining elements that can be measured independently. These elements, when combined together, collectively summarise the underlying nature of the geometric form of the hoof wall. This

approach formed the basis for the development of the donkey hoof wall model previously reported by Newlyn *et al.* (1998).

In summary a four-stage process of shape description was hypothesised to characterise the geometry of the donkey hoof wall. That is: -

1. Establishment of the basal template of the object
2. Determination of the degree of object inclination
3. Evaluation of the degree of object truncation
4. Discrimination between conical or cylindrical object geometry

6.6.2 SHAPE DESCRIPTION THEORY

The basal template of the object was defined as the profile of the solear aspect of the hoof wall. This basal template represents a transverse profile of the object geometry parallel to the ground surface. The spatial disposition of this basal template can be accurately defined in relation to the plane of the MDC. From this baseline it is possible to describe all other aspects of object geometry as follows.

Firstly, the dorsal hoof wall angle, the respective heel angles, and the angle of the tubular axis (recorded at a specified number of measurement sites) in the sagittal plane collectively would define object inclination.

The respective lengths, from the BB to the CB measured along the tubular axis, at each of the measurement sites would describe the degree of object truncation. Finally the angles, in the medio-lateral plane, of the medial and lateral hoof wall, recorded at the widest point of the hoof wall would discriminate between conical and cylindrical object geometry.

In this way the key defining aspects of hoof geometry could be established through the measurement of specific parameters. These descriptors established in the manner described above could form the necessary control points for FE model creation. Once this has been successfully achieved, and a reliable representation of the geometric form of the donkey hoof wall established, this could be standardised throughout the subsequent modelling analyses. Thus the specific functional effects of the structural organisation and material properties of laminitic donkey hoof horn could be investigated.

6.7 AIMS

The aims of this chapter were to: -

- Establish a shape measurement protocol to characterise the key defining aspects of donkey hoof wall geometry

- Construct a FE model of the donkey hoof wall both at the gross anatomical and microscopic level
- Assess the ability of the shape determination and model creation protocols to effective replicate hoof wall geometry
- Model the macro- and micromechanical function of the hoof wall. Specifically to investigate displacements and stress and strain distribution in response to static loading
- Explore the 'through depth' stress and strain distribution at the MDC
- Determine the effects of dorso-palmar variation in *Ec* on stress and strain distribution at the MDC
- Examine the assertion that the hoof wall acts as a unidirectional fibre composite
- Investigate the effects of laminitis upon the macromechanical functioning of the hoof wall at the MDC. Specifically to evaluate both the nature and magnitude of surface and 'through depth' stress and strain distribution

6.8 MATERIALS AND METHOD

6.8.1 SHAPE DETERMINATION OF THE DONKEY HOOF WALL

The initial hoof wall model was based upon measurements of a hoof capsule obtained from the left forefoot of a donkey, which had no apparent signs of disorders related to the feet. The animal had been humanely destroyed on medical grounds. Immediately after destruction, the foot was disarticulated and sealed in Parafilm1 to prevent shrinkage of the capsule resulting from moisture loss. The foot was stored at 4°c until autolytic degradation of the dermal/epidermal junction allowed removal of the intact hoof capsule. Measurements were taken immediately after capsular removal to minimise the effect of moisture loss.

The plane of the MDC was established in accordance with Section 2.3.3. The position of this plane was marked both on the dorsal and solear aspect of the capsule. The hoof capsule was positioned on graph paper so that the plane of the MDC was aligned with a central axis previously established on the graph paper. This axis is referred to as the z-direction. The outer aspect of the BB was accurately traced from the MDC to the most palmar aspect of weightbearing surface on both the lateral and medial aspects of the hoof wall. The hoof capsule was removed from the graph paper and a series of linear measurements were determined as follows.

An initial control line was drawn to connect the palmar weight-bearing aspect of the medial and lateral wall. The linear distance along the central axis from the dorsal aspect of the hoof wall (0% Capsular Depth) to the intercept with the palmar weightbearing control line (100%

Capsular Depth) was measured. This linear distance defined the capsular depth. A series of reference measurements were then made, orthogonal to the central axis (x-direction), at specified locations along the axis, defined in terms of percentage Capsular Depth (%CD). The linear distance was recorded from the central axis to the outer aspect of the hoof wall at each of eight additional reference sites, both medially and laterally.

The reference sites were 0, 2.5, 7.5, 20, 35, 50, 62.5, 75, 87.5 and 100%CD on both the medial and lateral aspect of the hoof wall. Reference sites were intentionally weighted, medially and laterally between 0-20%CD. This is because the solear aspect of the donkey hoof exhibits maximum curvature in this region, and therefore displays the greatest rate of change in medio-lateral width. In this way, it was anticipated that the selected reference sites were optimised to capture shape information.

The hoof capsule was repositioned on the graph paper and the intercepts of these reference sites marked on the dorsal aspect of the hoof wall at the level of the BB. Subsequently, the through-depth thickness of the hoof wall was established in the y-z plane at each reference site around the BB, with the aid of callipers. In the case of the MDC site (0%CD) the through-depth thickness was determined in the z-direction (i.e. along the plane of the MDC), whilst the through-depth thickness at all other sites were recorded orthogonal to the plane of the MDC (i.e. in the y-direction). In the manner described above, the basal template of the hoof wall geometry was defined, and the outer and inner boundaries of the hoof wall delimited.

Control lines were then engraved on the dorsal aspect of the hoof wall along the line of the tubular axis from BB to the CB at each reference sites. Calibrated photomicrographs were obtained of the dorsal medial and lateral aspects of the hoof wall, using a standardised technique of focal length, object camera distance and object centring.

From the resultant photomicrographs the inclination of the capsule was defined by measuring the DHWA (i.e. the angle subtended between the dorsal aspect of the hoof wall and the BB, and the respective medial and lateral heel angles (i.e. the angle subtended between the hell and the BB). The degree of object truncation was established from the medial and lateral photographs by measuring both the angle, and the magnification corrected length from the BB to the CB, of each of the control lines. Finally to discriminate between cylindrical and conical hoof wall geometry, the angles subtended between the medial, and lateral, aspect of the hoof wall and the BB, were established in the x-y plane using the dorsal photograph.

These baseline data were mapped into a computer assisted drawing package, to form two series of control points that described the BB and the CB of the hoof wall respectively. From these control points the gross anatomical FE model of the donkey hoof wall was constructed, in

accordance with the methodology detailed by Newlyn *et al.* (1998). The key steps in the model generation are summarised below.

6.8.2 DEVELOPMENT OF A GROSS ANATOMICAL MODEL OF THE DONKEY HOOF WALL

The finite element model of donkey hoof wall was constructed from the control points established in the shape measurement protocol, using a finite element software program[4]. With the aid of a surface modeller, the bounding curves and splines were established and the bounding surfaces created. The model was produced with a 2mm mesh to arrive at a completed three-dimensional model, consisting of ~18000 elements, and 11608 nodes. The selection of mesh size represents a balance between modelling detail and computer processing time. A 2mm mesh gives respectable modelling detail at an acceptable generation time.

A linear elastic analysis was conducted assuming isotropic material properties in response to a simulated static loading. The hoof wall was initially modelled assuming isotropic material properties, with an E of 500MPa (Wichtmann *et al.* 1990), and a Poisson's ratio of 0.4 (Chang *et al.* 1993).

A vertical static load of 375 N was used for the model. This represents a static loading force equivalent to a 150kg bodyweight animal, distributed equally between the four hooves. 150 kg is a typical bodyweight for a donkey (Chang *et al.* 1993). This force was applied uniformly around the wall in a manner designed to simulate the suspension of the DP within the hoof capsule (Pellmann 1995), via 400 lamellae (Hifny and Misk 1983). The bearing border of the hoof wall was restrained vertically to simulate '*in vivo*' ground contact conditions. In addition the BB at the MDC was fully restrained preventing displacement at this anatomical site in any direction. These boundary conditions were consistent with the observations of Lungwitz (1883, 1891) and video footage published by Pollitt (1993) for the horse.

A general arrangement, light shaded view, of the 2mm mesh models is shown in Figure 6.2A, with arrows indicating the loading surfaces and red circles indicating the boundary restraints. Displacement, stress concentration, principal strain, and force distribution across the hoof wall were evaluated. This analysis required the solution to 34,261 equations.

6.8.3 VALIDATION OF THE GROSS ANATOMICAL MODEL

In order to assess the effectiveness of the shape determination theory to capture the key defining aspects of the geometry of the hoof wall a 'reverse engineering approach was adopted. The

---

[4] Algor Inc., Pittsburgh Pennnsylvannia, USA.

computer file generated in the model creation process was used to reverse engineer the build of a replica of the hoof wall by rapid manufacture.

The replica build was constructed to scale via a Stratasys FDM machine. The effectiveness of shape determination was based upon direct visual comparison with the actual hoof capsule used to construct the model.

6.8.4 ASSESSING THE EFFECT OF DORSO-PALMAR VARIATION IN MODULUS OF ELASTICITY

The effect of the dorso-palmar variation in modulus across the hoof wall depth was investigated at the MDC. Two separate analyses were performed on the hoof wall model. The first analysis assumed a constant value of *E* across the entire HWD at 250MPa, whilst the second analysis was performed with a variable modulus. An arbitrary dorso-palmar variation in modulus was used to reflect the dorso-palmar decrease in rigidity previously reported in the horse (Leach 1980, Douglas *et al.* 1996, Kasapi and Gosline 1996, Hinterhofer *et al.* 1998) and the donkey (Hopegood 2002, Collins *et al.* 2002). The hoof wall was divided into 4 arbitrary layers or laminates of equal percentage HWD. The weighted-average of the moduli of the 4 respective laminates equalled that of the bulk modulus of 250MPa used in the previous analysis.

The dorso-palmar variation in *E* was: -

- 0-25% HWD – *E* of 400MPa
- 25-50% HWD – *E* of 300MPa
- 50-75% HWD – *E* of 200MPa
- 75-100% HWD – *E* of 100MPa

Von Mises, and maximum and minimum principal stress values were calculated respectively at 0, 25, 50, 75 and 100% HWD at 50% HWH at the MDC, in both modelled scenarios.

6.8.5 DEVELOPMENT OF FE MODEL AT THE MICROSCOPIC LEVEL

The morphometric analysis conducted in this thesis provided the data to construct FE models of the structural and geometric arrangement of the hoof wall at the microscopic level for Z1 and 3 of the *SM* of the donkey hoof wall. Z1 and 3 were selected because they represent extremes in structure evident within the *SM*. The structural organisation of the respective zones differs markedly in terms of tubule size, shape, TuAF (see Chapter 4) and TD (Hopegood 2002).

In developing these models, the microstructure of the hoof wall was considered as a 2 component (phase) hollow fibre reinforced composite. Each phase was treated as an isotropic linearly elastic component, with perfect bonding assumed at the interface between the horn tubules and the IT horn.

The geometric structure was simplified by assuming a hexagonal array of repeating horn tubule units. The tubule transverse profiles were constructed in line with the mean Tu(MA:MI) Axis ratio data established for each respective zone. The absolute transverse area measurements of the horn tubules, cortices and medullary cavities were similarly based on mean recorded values. Table 6.1 summarises the morphometric parameters used to construct the zonal micro-models for Z1 and Z3.

Table 6.1 Summary table of the morphometric characteristics of the Zone 1 and 3

Site	Tubule Area Fraction	Mean Tubule Area measurement (μm^2)	Major to Minor Tubule Axis ratio	'Derived' Tubule Density (Tubules mm^{-2})
Zone 1	0.17	6899	3.07:1	24.9
Zone 3	0.23	32000	1.13:1	7.28

The horn tubule spacing (inter-fibre spacing) combined with the absolute tubule dimensions, was used to generate a fibre density (referred to as 'Derived' TD in Table 6.1) consistent with the mean zonal TuAF data. The resultant 2 phase micro-structural models for Z1 and 3 are illustrated in Figure 6.1.

6.8.5.1 Theoretical Determination of Potential Moduli

The E for the composite was approximated using the 'simplified' equations for unidirectional laminae (Hull 1981). There are however, difficulties in applying these equations directly to the hoof wall. This is because neither the E for the Tu, or IT fractions are known. Hence a theoretical derivation had to be performed.

Figure 6.1 2 phase micro-structural models for Zone 1 (left) and 3 (right) of the donkey hoof wall to show the structural and geometric organisation of tubular and intertubular horn in transverse section.

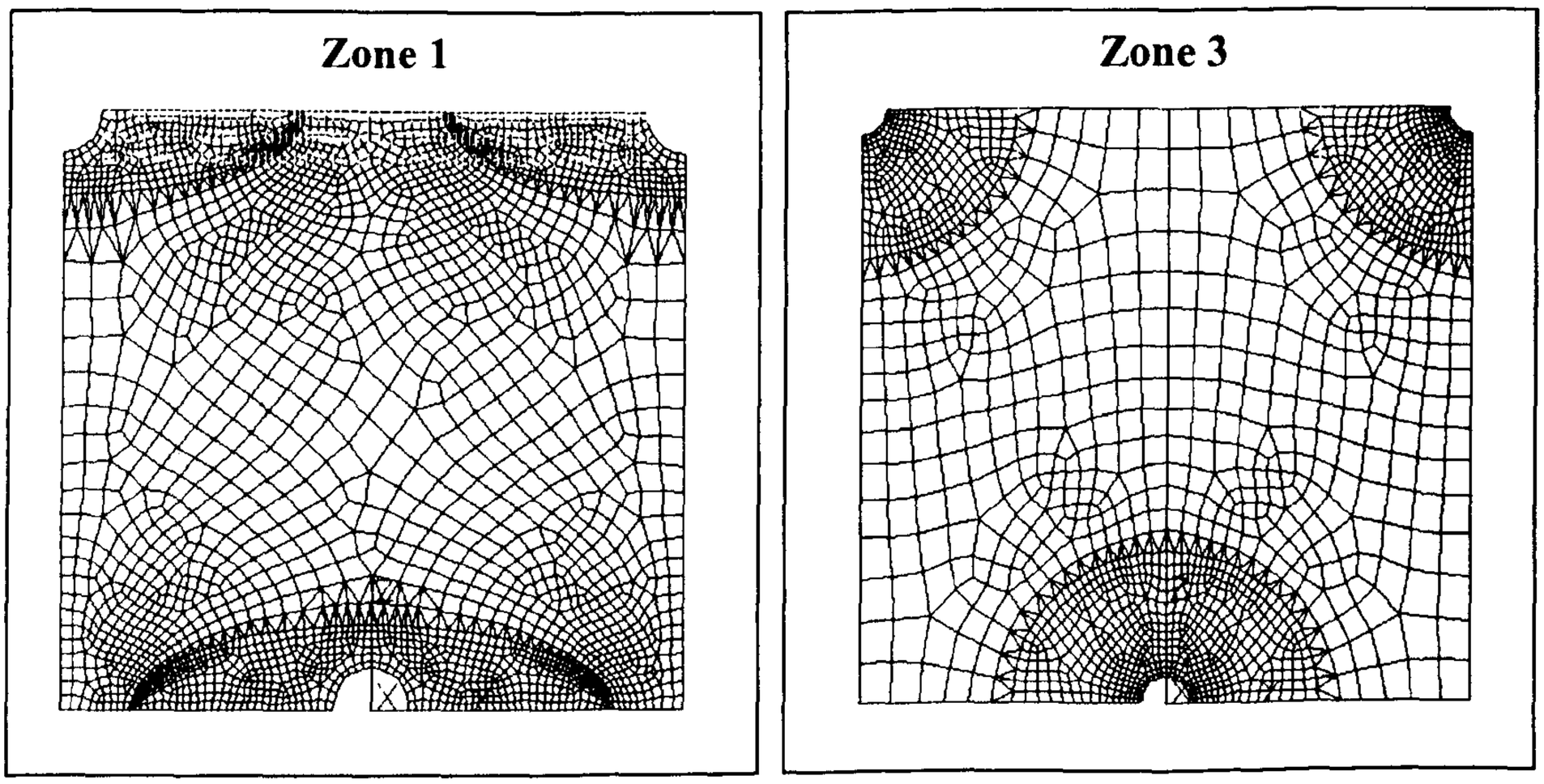

This was achieved by introducing a moduli ratio (K) of E tubule to E matrix, *Et/Em* (Subscript *t* for tubule, *m* for matrix). In this way, it was possible to assess the variation in E, for a range of *Et/Em* ratios.

'Rule of Mixtures' equations for unidirectional composites (Hull 1981)

1. Axial Modulis (Ex) parallel to fibre orientation

$$Ex = EfVf + EmVm$$

Where:

Ef = Modulus of Elasticity of the fibre phase

Vf = Volume fraction of the fibre phase

Em = Modulus of Elasticity of the matrix phase

Vm = Volume fraction of the martrix phase

Hence in a two phase composite system

$$Ex = EfVf + Em(1 - Vf)$$

Therefore

$$\frac{Ex}{Em} = KVf + (1 - Vf)$$

Where

$$K = \frac{Ef}{Em}$$

2. Lateral Modulus (Ey) orthogonal to fibre orientation

$$Ey = \frac{EmEf}{Ef(1 - Vf) + EmVf}$$

$$= \frac{Ef}{K(1 - Vf) + Vf}$$

Hence

$$\frac{Ey}{Em} = \frac{K}{K(1 - Vf) + Vf}$$

Modified equations for unidirectional laminae (after Hull 1981) were used to take account of contraction affects due to poison ratio (v):

$$Ey = \frac{Em'Ef}{Ef(1 - Vf) + Em'Vf}$$

Where

$$Em' = \frac{Em}{1 - v^2}$$

Hence

$$\frac{Ey}{Em} = \frac{K}{K\left(1-\nu^2\right)\left(1-Vf\right)+Vf}$$

The resultant modulus is hereafter referred to in this chapter as *E*, expressed in directional terms, that is y- and/or z-direction

This approach was used to investigate experimentally determined values of modulus, with a view to extracting a tubule and matrix modulus. A range of values of *K* were selected based upon previously reported material testing data (see Table 6.2).

Table 6.2 Summary table of axial to lateral hoof wall moduli for equid hoof horn

Source	Hoof Wall Region	Axial modulus (*E*x) MPa	Lateral modulus (*E*y) MPa	Axial to lateral moduli ratio	Hydration state
Leach (1980)	Outer	171	220	0.78:1	MC_F
	Inner	93	118	0.79:1	
Douglas *et al.* (1996)	Outer	998	912	1.09:1	MC_F
	Inner	544	460	1.18:1	
Kasapi and Gosline (1997)	Outer	560	310	1.81:1	MC_M
	Inner	300	180	1.66:1	
Collins (2003)	Full HWD	N/A	N/A	1.5:1 (1.2:1-1.7:1)	MC_M

It can be seen however from the table that the ratio of axial modulus (*E*x) to medio-lateral lateral modulus (*E*y) is not well defined. If the equations for axial and lateral modulus are used, at a given tubular volume fraction, for example, of 0.2, then it can be demonstrated that values of *K* from 0.2 to 3.5 span the range of experimental data.

Based upon these values and the area fraction data obtained from the morphometric analysis, the axial and lateral moduli were determined using the 'rule of mixture' and modified Hull equations. In this way, theoretical *E* values were determined for both Z1 and Z3. By expressing the predicted axial and lateral *E*, by convention as a ratio to the matrix modulus *Em*, then the reinforcing effect of the structural organisation on the matrix material can be evaluated for different values of *K*. It is anticipated that a fibre composite structure, reinforced in a given direction would display a modulus in that direction > *Em*.

6.8.5.2 Macromechanical FE Modelling of the Donkey Hoof Wall

FEA was used to determine the lateral *E* by a fixed displacement approach using two-dimensional plain strain elements. This was achieved by applying a unit displacement on one edge, and restraining the opposite edge with 'stiff' boundary elements of a known stiffness

constant. The mid-point of the restrained edge was fully restrained such that no displacement was possible in any directional plane. All other nodes were free to move.

The *E* was determined by assessing the force in the boundary elements and the overall displacement in the chosen direction. This analysis was repeated over a range of ratios of *Et/Em* from ~0.28 to 3.5. It is appreciated that by using plane strain elements that the resultant values would be greater than that predicted by the modified Hull equation, due to poisson effects in the x -direction. Hence all FE outputs were corrected in this respect, and factored to pass through unity at *K*=1.

This procedure was conducted both in the medio-lateral (y) and dorso-palmar (z) direction. In this way *E* values were obtained in each lateral direction, that is *E*y and *E*z. This approach was applied to both zonal sites. In addition, maximum stress and strain concentration factors were calculated over the range of *K* for both the Tu and IT horn fractions. Concentration factors were based respectively upon the ratio of maximum to mean stress, and strain, within each horn fraction over the range of *K* values.

6.8.5.3 MICROMECHANICAL FE MODELLING OF THE DONKEY HOOF WALL

Further interpretation of the FEA was conducted to investigate the micro stress/strain concentration developed as a consequence of the structural organisation of Tu and IT horn. In this way, the effects of tubular shape upon the mechanical properties of the hoof could be further elucidated. Whilst it is appreciated that this approach cannot be used directly to assess possible failure, given that the Tu and IT components are likely to possess differing material properties, it may indicate areas of potential weakness. Such weaknesses may be of significance in crack initiation and crack stopping phenomena.

6.8.6 INVESTIGATION OF THE EFFECTS OF THE LAMINITIC CONDITION ON HOOF WALL FUNCTION

A final modelling experiment was performed to investigate the functional significance of the differences in zonal *E* associated with the laminitic condition that were reported in Chapter 5 of this thesis.

An initial analyses were conducted at the MDC of the hoof wall based upon the baseline zonal *E* data detailed by Latham (2001 – Pers Com.). This data was adjusted to conform to the convention of the donkey hoof wall zonation adopted in this thesis. This analysis was subsequently repeated using both the mean laminitic zonal *E* detailed in Chapter 5, and also the mean zonal *E* for Laminitic Group 1 and 2. The 'through depth' material properties of the hoof wall were defined in each respective analysis as detailed in Table 6.3 below.

Table 6.3 Summary table of the zonal moduli used in the four respective modelling scenario

	Zone 1	Zone 2	Zone 3
	0-25 %HWD	25-40 %HWD	40-100 %HWD
Model 1 Baseline Data*	365 MPa	170 MPa	105 MPa
Model 2 Laminitic Data	210 MPa	165 MPa	105 MPa
Model 3 Laminitic Group 1	185 MPa	145 MPa	100 MPa
Model 4 Laminitic Group 2	225 MPa	180 MPa	105 MPa

* Latham (2001 - Pers Com.)

A linear elastic analysis was performed assuming isotropic material properties, with a ν of 0.4. The analyses were performed using the same model geometry, with identical loading conditions and boundary constraints. Von Mises stress values and maximum and minimum principal stress and strain data were established across the hoof wall depth at 5, 50 and 95% HWH.

6.9 RESULTS

6.9.1 DEVELOPMENT OF A GROSS ANATOMICAL MODEL OF THE DONKEY HOOF WALL

The general arrangement, light shaded view of the resultant 2mm mesh model is shown in Figure 6.2A with arrows indicating the loading surfaces and red circles indicating the boundary restraints. Figure 6.2B, C and D illustrate the deformation of the hoof wall model in response to loading and boundary restraints. A comparison of the displaced shape with the original unloaded structure revealed an outward displacement at the heels (Figure 6.2B). This displacement increased progressively towards the palmar aspect attaining a maximum value of 2.36mm. A dorso-concave deformation of the dorsal aspect of the MDC was indicated, with the proximal region experiencing an inward deflection of 0.3 mm. The 'total deflection' at any point around the hoof wall model in the loaded state is shown in Figure 6.2C, whilst deflections in the mediolateral y-direction are presented in Figure 6.2D (sign denotes direction of displacement relative to central axis).

The maximum principal strain in the outer aspect varied around the hoof wall. In general, strain values increased from the heels towards the MDC, attaining a maximum value in the order of 2500με at the proximal region of the MDC. The direction of the principal strains indicates that the maximum principal strain at the MDC was aligned along the x-axis both proximally and distally, and that the hoof wall at this site was subjected to biaxial compression. The magnitude of biaxial compression was greater proximally than distally (see Figure 6.2E).

Figure 6.2 Finite element modelling of the hoof wall at the gross anatomic level (After Newlyn *et al.* 1998).

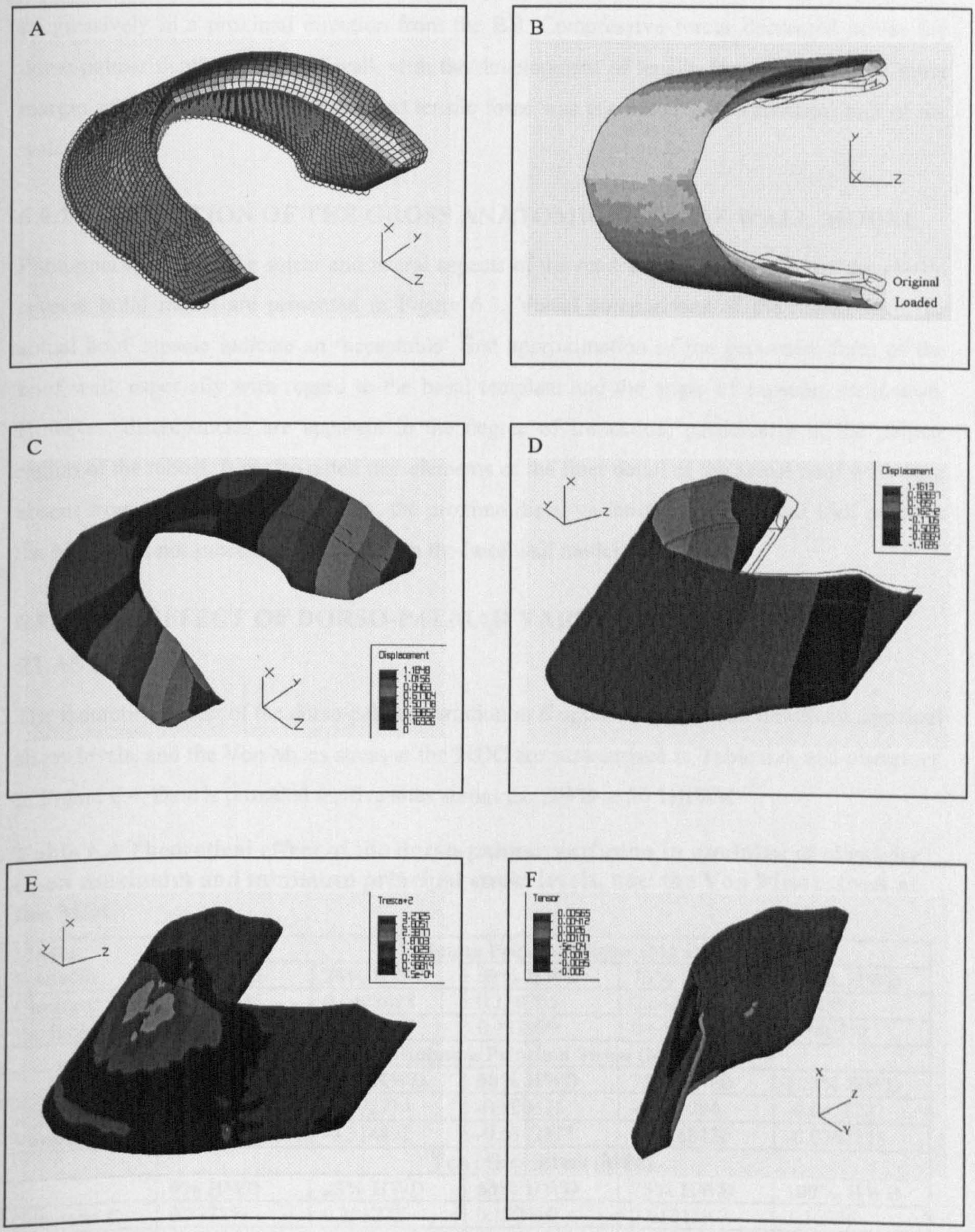

A modelled sagittal section taken along the plane of the MDC (illustrated in Figure 6.2F) revealed the pattern of 'through depth' stress distribution. This indicated that the dorsal aspect of the hoof wall was subjected to compressive forces. The magnitude of these forces increased progressively in a proximal direction from the BB. Compressive forces decreased across the dorso-palmar depth of the hoof wall, with the development of tensile forces towards the inner margin of the wall section. The greatest tensile force was generated in the proximal half of the wall.

6.9.2 VALIDATION OF THE GROSS ANATOMICAL HOOF WALL MODEL

Photomicrographs of the solear and lateral aspects of the modelled hoof capsule and the plastic reverse build model are presented in Figure 6.3. Visual comparisons of the model with the actual hoof capsule indicate an 'acceptable' first approximation of the geometric form of the hoof wall, especially with regard to the basal template and the angle of capsular inclination. However, discrepancies are apparent in the degree of truncation, particularly in the palmar region of the model. It is also noted that elements of the finer detail of the actual hoof wall were absent from the model. For example, the proximo-distal variation in dorsal hoof wall angle at the MDC was not successfully captured in the hoof wall model.

6.9.3 THE EFFECT OF DORSO-PALMAR VARIATION IN MODULUS OF ELASTICITY

The theoretical effect of the dorso-palmar variation in *E* upon maximum and minimum principal stress levels, and the Von Mises stress at the MDC are summarised in Table 6.4, and illustrated in Figure 6.4. Data is provided for five sites across the HWD at 50 %HWH.

Table 6.4 Theoretical effect of the dorso-palmar variation in modulus of elasticity upon maximum and minimum principal stress levels, and the Von Mises stress at the MDC

Model Scenario	Maximum Principal Stress (MPa)				
	0% HWD	25% HWD	50% HWD	75% HWD	100% HWD
Constant *E*	0.0465035	0.0428688	0.110705	0.64209	1.24891
Variable *E*	0.0444129	0.0309479	0.422999	0.663681	0.740572
	Minimum Principal Stress (MPa)				
	0% HWD	25% HWD	50% HWD	75% HWD	100% HWD
Constant *E*	-0.848336	-0.392774	-0.100415	-0.021294	-0.0478781
Variable *E*	-1.24897	-0.314492	-0.0192817	-0.0168136	-0.0267858
	Von Mises Stress (MPa)				
	0% HWD	25% HWD	50% HWD	75% HWD	100% HWD
Constant *E*	0.777151	0.391775	0.187710	0.618139	1.16986
Variable *E*	1.12852	0.332675	0.411551	0.611304	0.68143

6.9.3.1 CONSTANT 'THROUGH DEPTH' MODULUS MODEL

MAXIMUM AND MINIMUM PRINCIPAL STRESS

In the constant 'through depth' modulus (Constant *E*) model there was a dorso-palmar increase in maximum principal stress levels across the HWD. This increase was not however progressive. Stress levels remained constant across the initial 50% HWD at ~0MPa, before rising progressively, in a linear fashion, across the remaining dorso-palmar HWD to reach a maxima of 1.24 MPa at the laminar interface (100% HWD).

The highest level of minimum principal stress (-0.8MPa) occurred at 0% HWD. Minimum principal stress levels decreased progressively in a dorso-palmar direction, and approached 0MPa at 70% HWD. Minimum principal stress levels remained at this level across the remainder of the dorso-palmar HWD.

These results indicate that in the constant *E* model the outer aspect of the hoof wall is subject to uniaxial compression. The magnitude of the uniaxial compression decreases across the HWD until, at ~50% HWD, the hoof wall is in an unstressed state. Thereafter the hoof wall is subjected to a progressively increasing uniaxial tensile stress which reaches its maximal value at 100% HWD.

VON MISES STRESS

Von Misses stress levels decreased in a linear manner, from a level of ~0.8MPa, at the outer hoof wall, to reach a minima of ~0MPa at 50% HWD. Thereafter, stress levels rose in a linear manner across the remaining HWD, with peak Von Mises stress levels of 1.17MPa predicted at the laminar interface (100% HWD).

Figure 6.3 Photographic comparison of the solear (top row) and lateral (bottom row) aspect of the actual modelled hoof capsule (left), and a reverse engineered model (right) constructed from data obtained by the shape characterisation methodology.

Solear Aspect

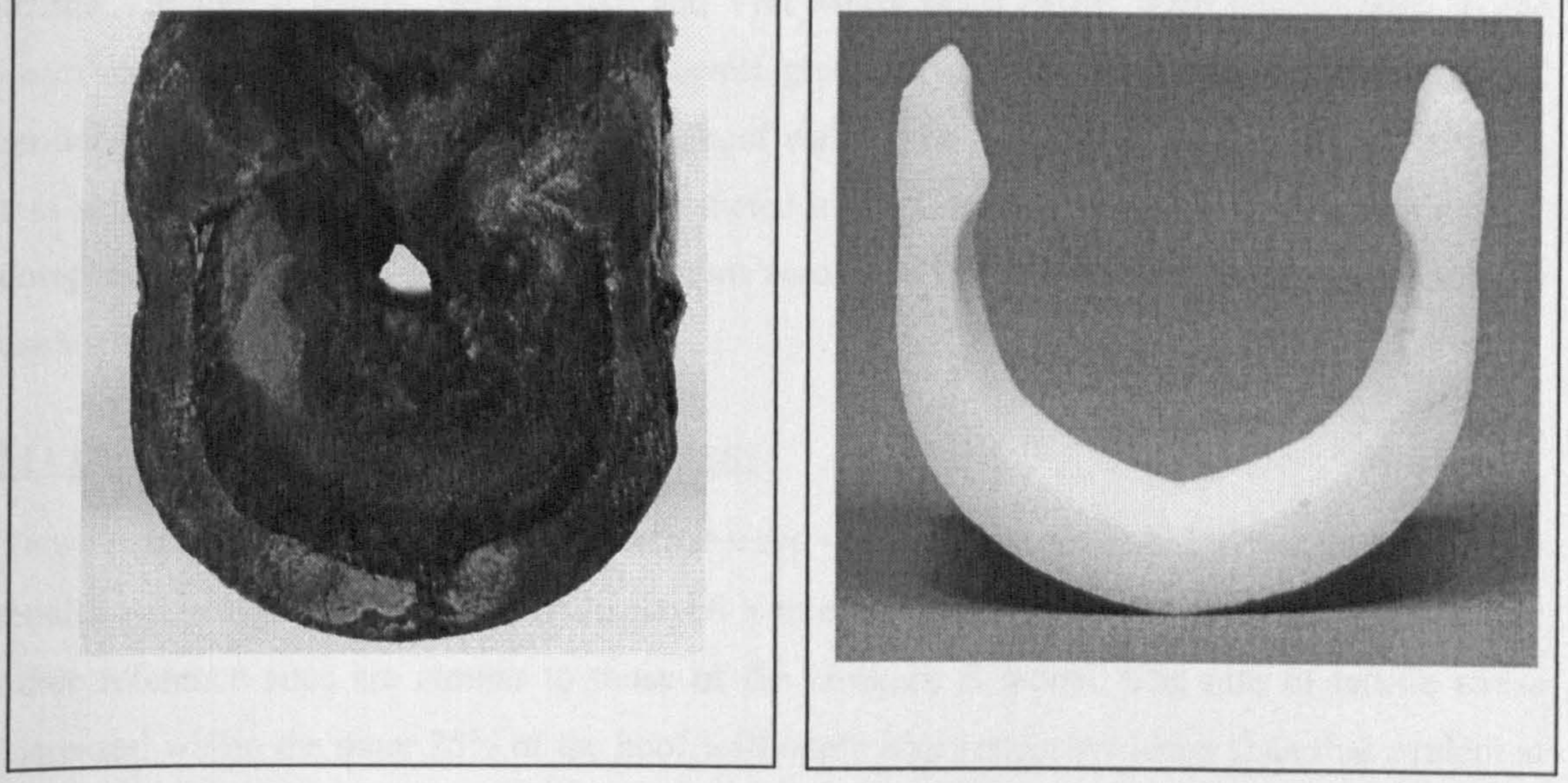

Lateral Aspect

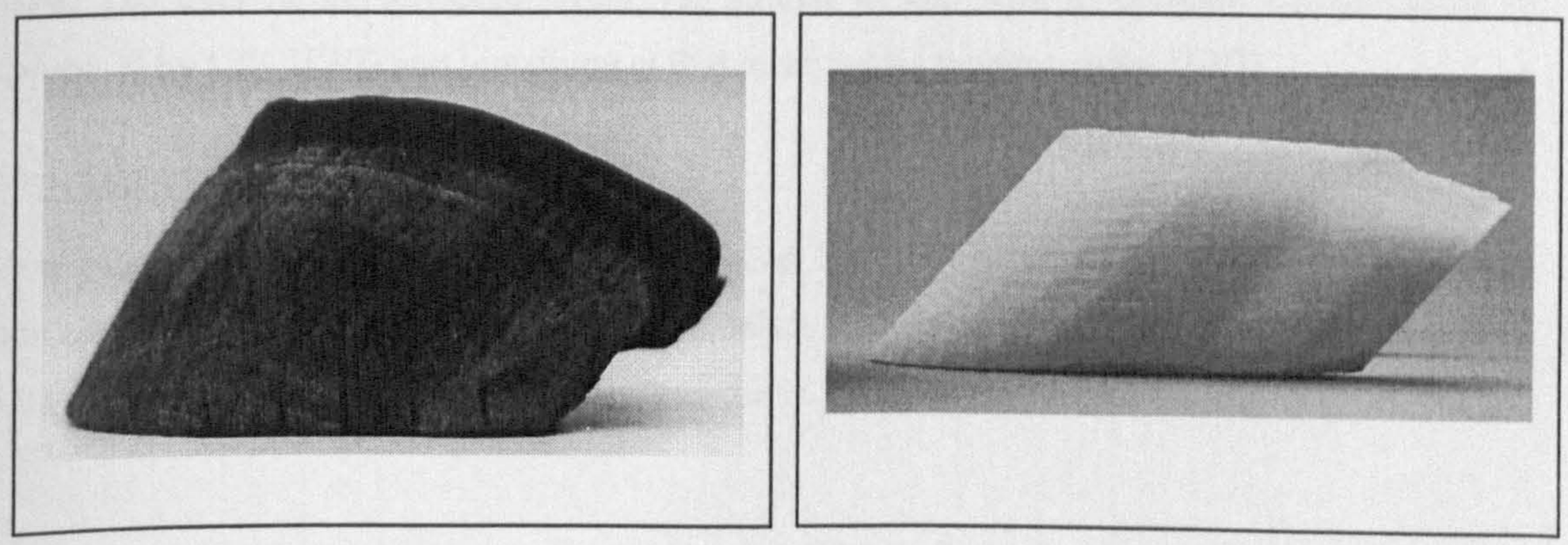

Note: Data used to construct the reverse engineered model was that used in the FE modelling of the donkey hoof wall.

6.9.3.2 VARIABLE 'THROUGH DEPTH' MODULUS MODEL

Although the dorso-palmar stress patterns across the hoof wall depth in the variable modulus (Variable *E*) model displayed a broadly similar pattern to that predicted in the constant *E* model it differed in its finer detail. The differences in finer detail reflected the modulating effect of *E* upon stress distribution within the hoof wall.

In the Variable *E* model, compressive and Von Mises stress levels were concentrated in the outer region of the hoof wall, attaining levels greater than those recorded in the Constant *E* model. Conversely the inner aspect of the hoof wall in the Variable *E* model was subjected to less severe stress conditions than those predicted in the Constant *E* model. A 'between model' comparison of the dorso-palmar stress patterns across the HWD are presented in Figure 6.4, for each respective stress parameter.

MAXIMUM AND MINIMUM PRINCIPAL STRESS

Tensile stress levels at the laminar interface were ~62% of that predicted at constant *E*, whilst tensile stress levels at 50% HWD displayed a three-fold increase. Tensile stress levels at the other reference sites are similar to those of the constant *E* model. The rate of tensile stress increased within the inner 25% of the hoof wall depth was noticeably lower than that evident at constant *E*.

Compressive stress values displayed a 47% increase at 0% HWD, reaching a maxima of -1.25 MPa. The trend in compressive levels was similar to that seen at constant *E*, decreasing to approx. 0 by 50% HWD and remaining at that level across the remaining HWD.

VON MISES STRESS

Von Mises stress levels were increased at 0 and 50% HWD, and markedly decreased at the laminar interface. The rate of change of Von Mises stress within the inner 25% of the hoof wall was reduced in a similar manner to that observed in maximum principal stress.

Figure 6.4 Comparison of modelled stress patterns across the hoof wall depth at the MDC in the constant and variable modulus scenarios.

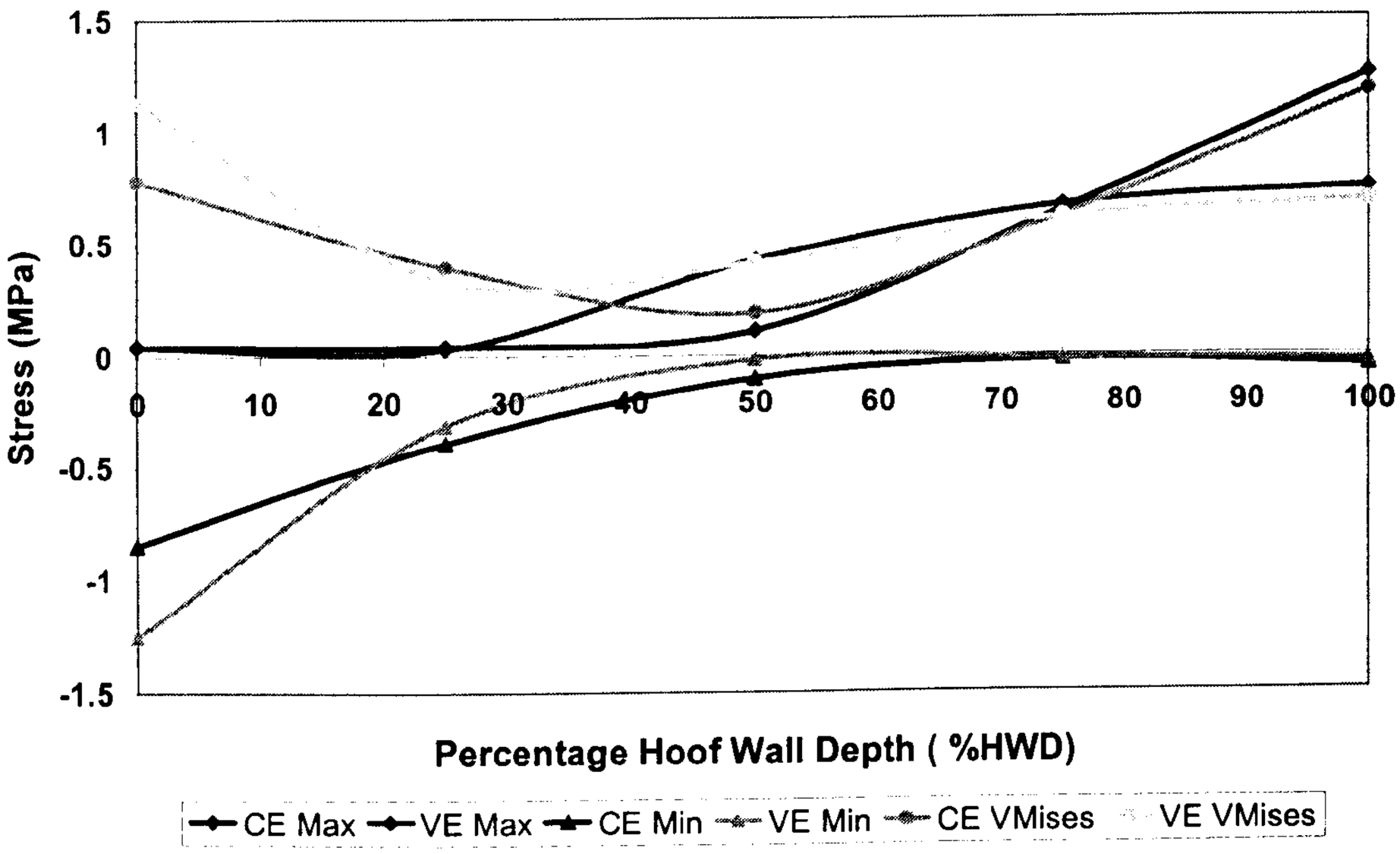

Key: CE Max - Maximum Principal Stress Constant Modulus model. **VE Max** - Maximum Principal Stress Variable Modulus model. **CE Min** - Minimum Principal Stress Constant Modulus model. **VE Min** - Minimum Principal Stress Variable Modulus model. **CE V Mises** - Von Mises Stress Constant Modulus model. **VE V Mises** - Von Mises Stress Variable Modulus model.

6.9.4 DEVELOPMENT OF THE FINITE ELEMENT MODEL AT THE MICROSCOPIC LEVEL

6.9.4.1 THEORETICAL DETERMINATION OF POTENTIAL MODULI

Figure 6.5 illustrates the variation in theoretical E ratio, both in the x- and y-direction, with increasing K. This figure shows that if the equations for axial and lateral E are used at a fibre to matrix volume fraction of 0.2 (20%), then K values between 0.28 and 3.5 will provide data that lie in the approximate range of mechanical data reported for equid hoof.

Figure 6.5 Theoretical determination of potential moduli with increasing *K*

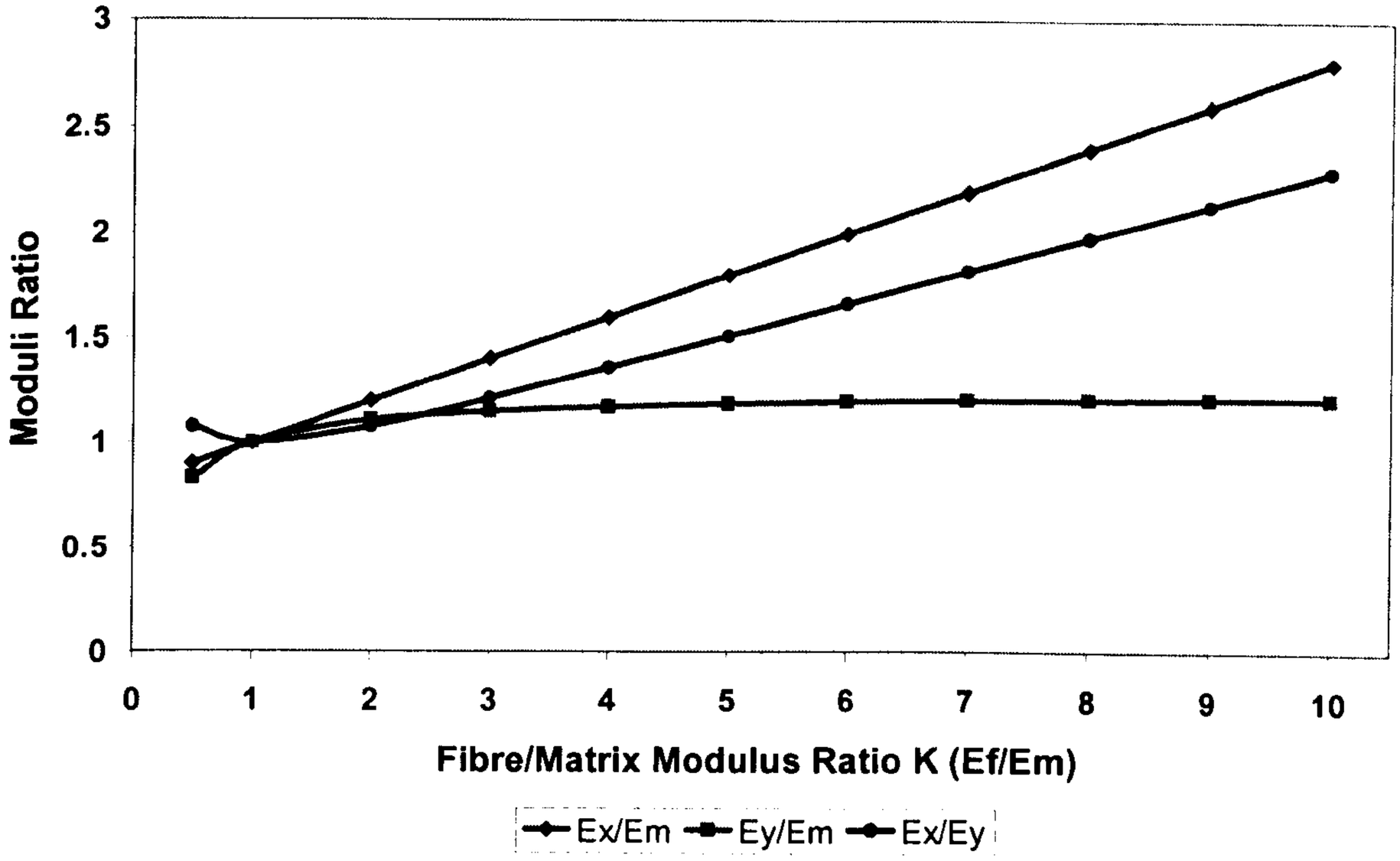

6.9.4.2 MACROMECHANICAL FE MODELLING OF THE DONKEY HOOF WALL

Figures 6.6 and 6.7 illustrate moduli ratios obtained from FE analysis for a *K* range of tubule (t) to matrix (m) moduli ratios (Et/Em) from 0.285 to 3.5. These are given in the y- and z-direction in respect of both zonal models, and are shown as a ratio relative to the probable axial moduli (*E*x), derived from the 'rule of mixtures' relationship. It can be seen that the lateral to axial moduli ratios are close to unity in both models, over the range of *K* values tested. However as *K* increases from 1, the lateral to axial moduli ratio reduced consistently as the reinforcing in the axial direction becomes more dominant.

Figures 6.8 – 6.11 present detailed plots showing the modelled lateral moduli ratios compared with those calculated using the modified Hull equations. These comparisons are given both in the y- and z-direction for each zonal site. These are expressed in ratio the axial moduli (*E*x), derived from the 'rule of mixtures' relationship.

It can be seen that the lateral to matrix modulus ratio determined from the FEA analysis corresponds closely to the values obtained from the modified Hull equations, in both the y- and z-directions. However it is noteworthy that whilst Z3 ratios appear to broadly similar over the range of *K* values tested, the moduli ratios in Z1 diverge in the y-direction with increasing *K*.

Figure 6.6 Moduli ratios obtained from FE analysis for a *K* range of tubule (t) to matrix (m) moduli ratios (*E*t/*E*m) from 0.285 to 3.5 in the y- and z-direction in Zone 1.

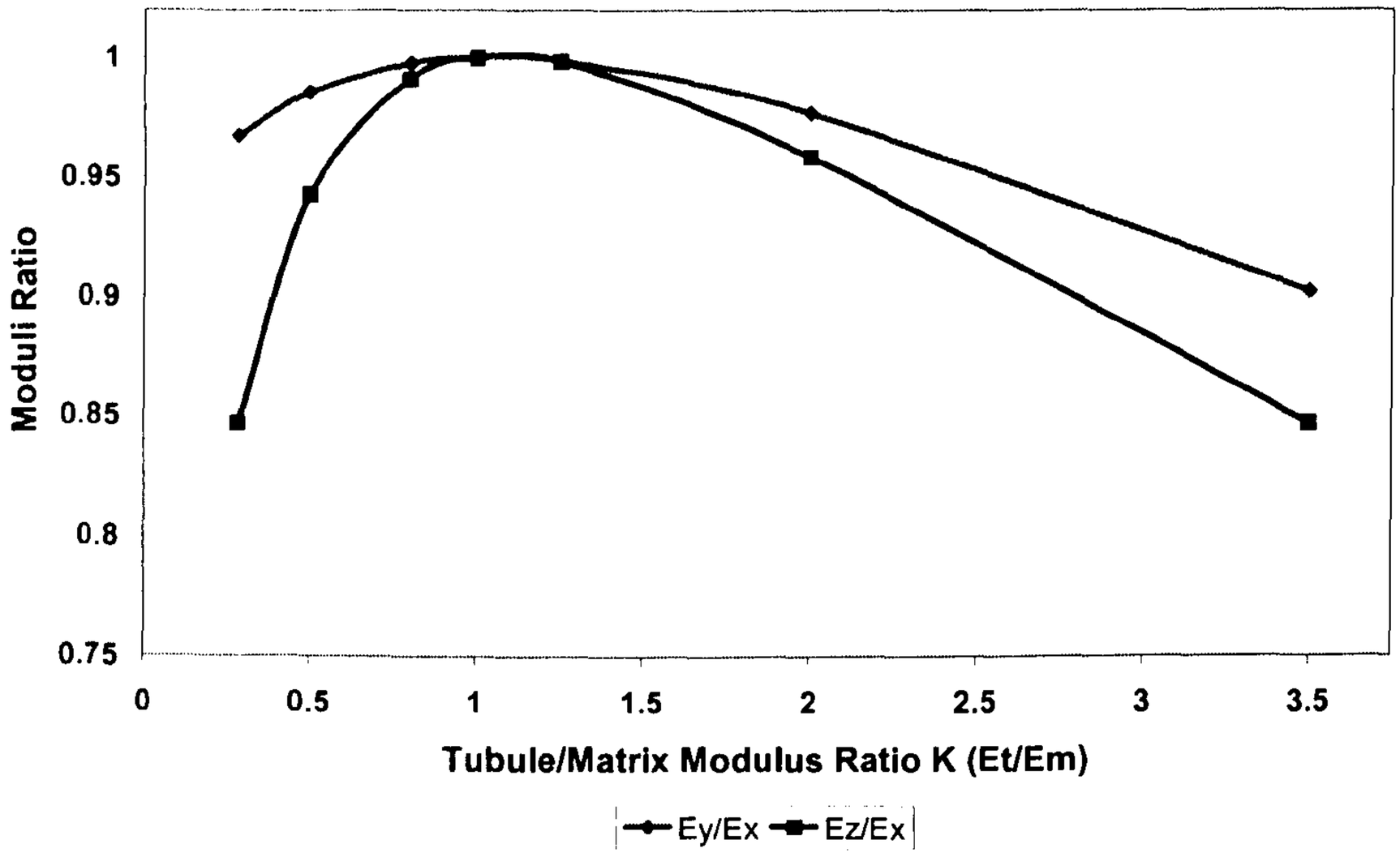

Figure 6.7 Moduli ratios obtained from FE analysis for a *K* range of tubule (t) to matrix (m) moduli ratios (*E*t/*E*m) from 0.285 to 3.5 in the y- direction and z-direction in Zone 3.

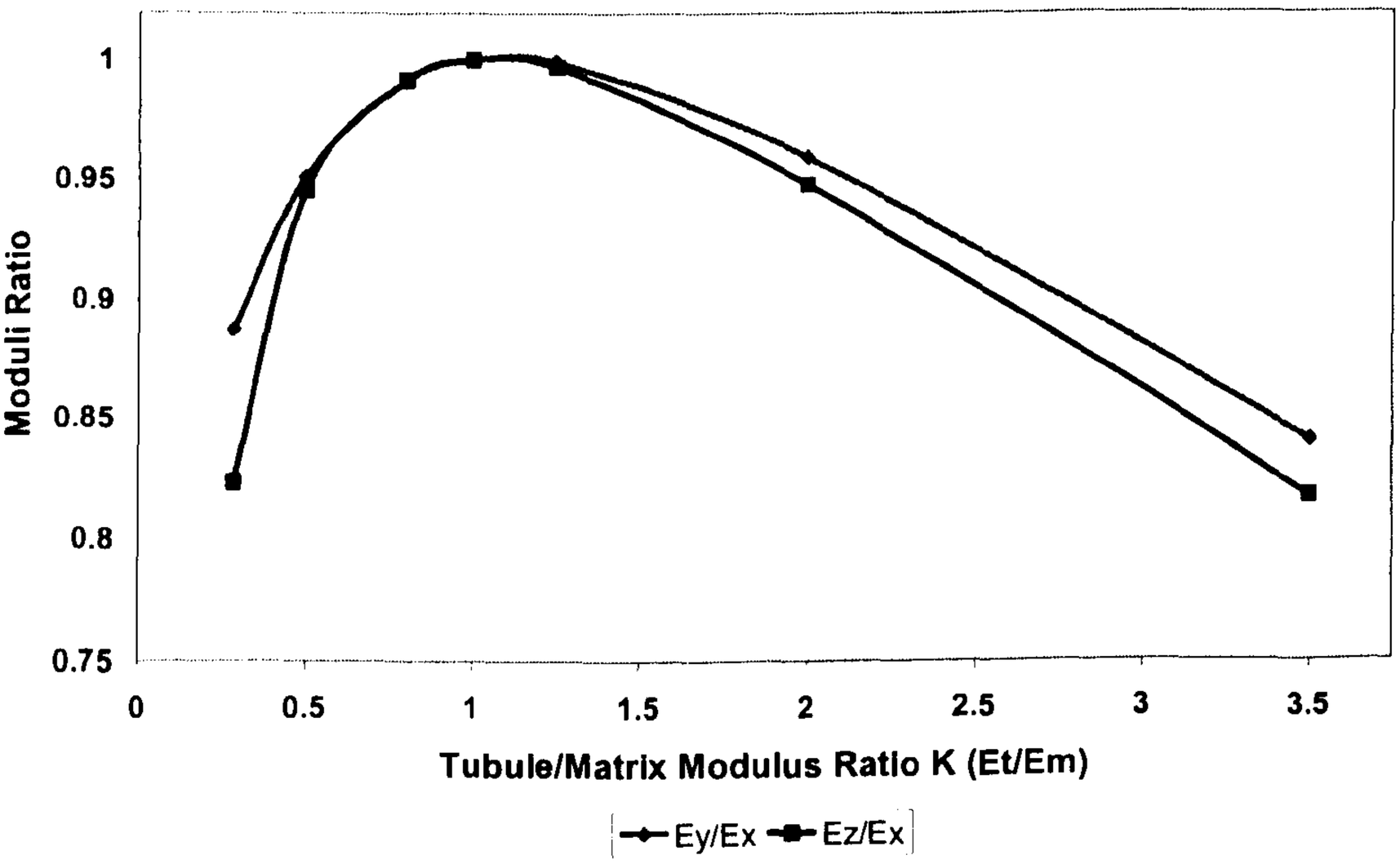

Figure 6.8 Modelled lateral moduli ratios compared with those calculated using the modified Hull equations with increasing *K* for Zone 1 in the y-direction.

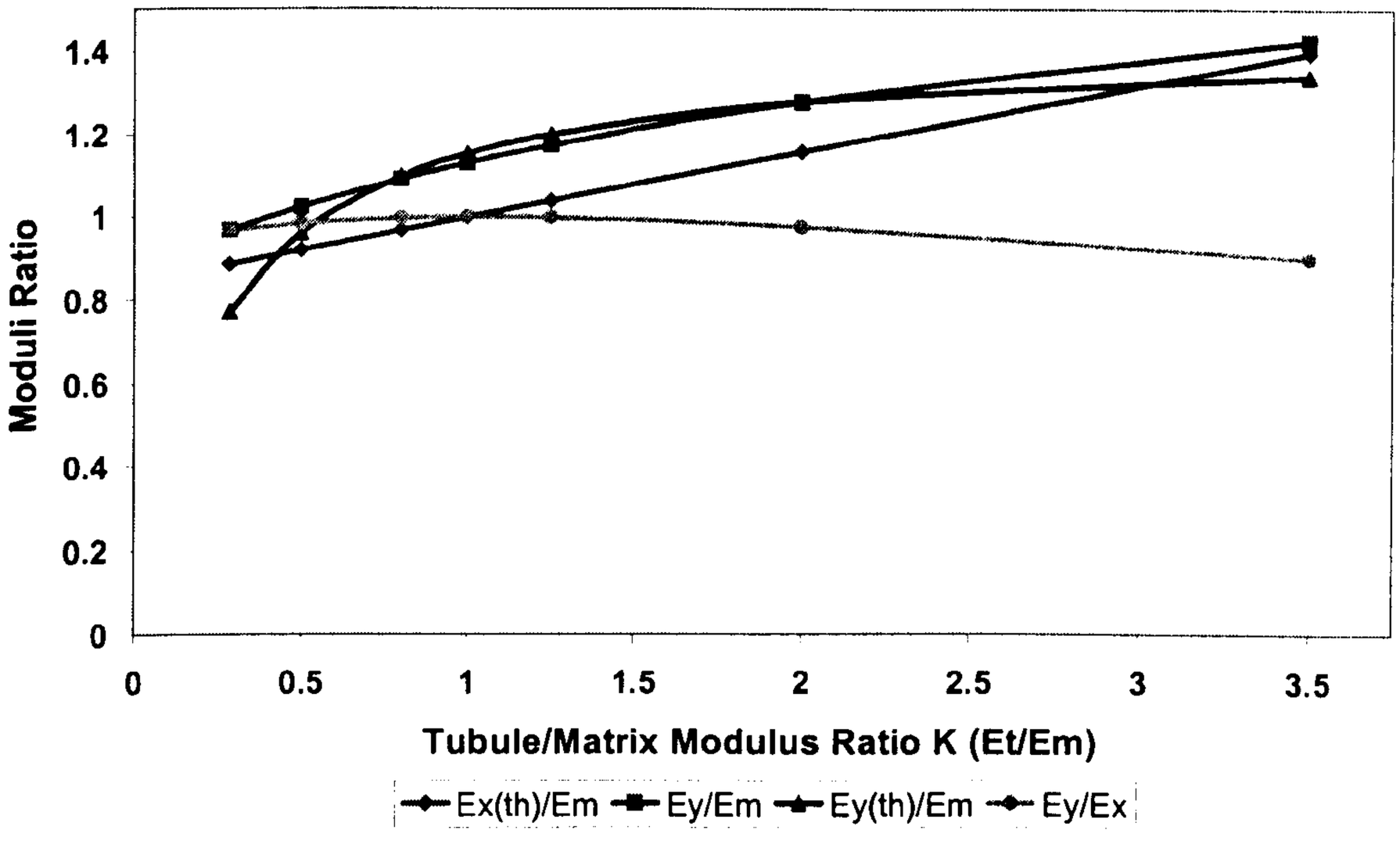

Figure 6.9 Modelled lateral moduli ratios compared with those calculated using the modified Hull equations with increasing *K* for Zone 1 in the z-direction.

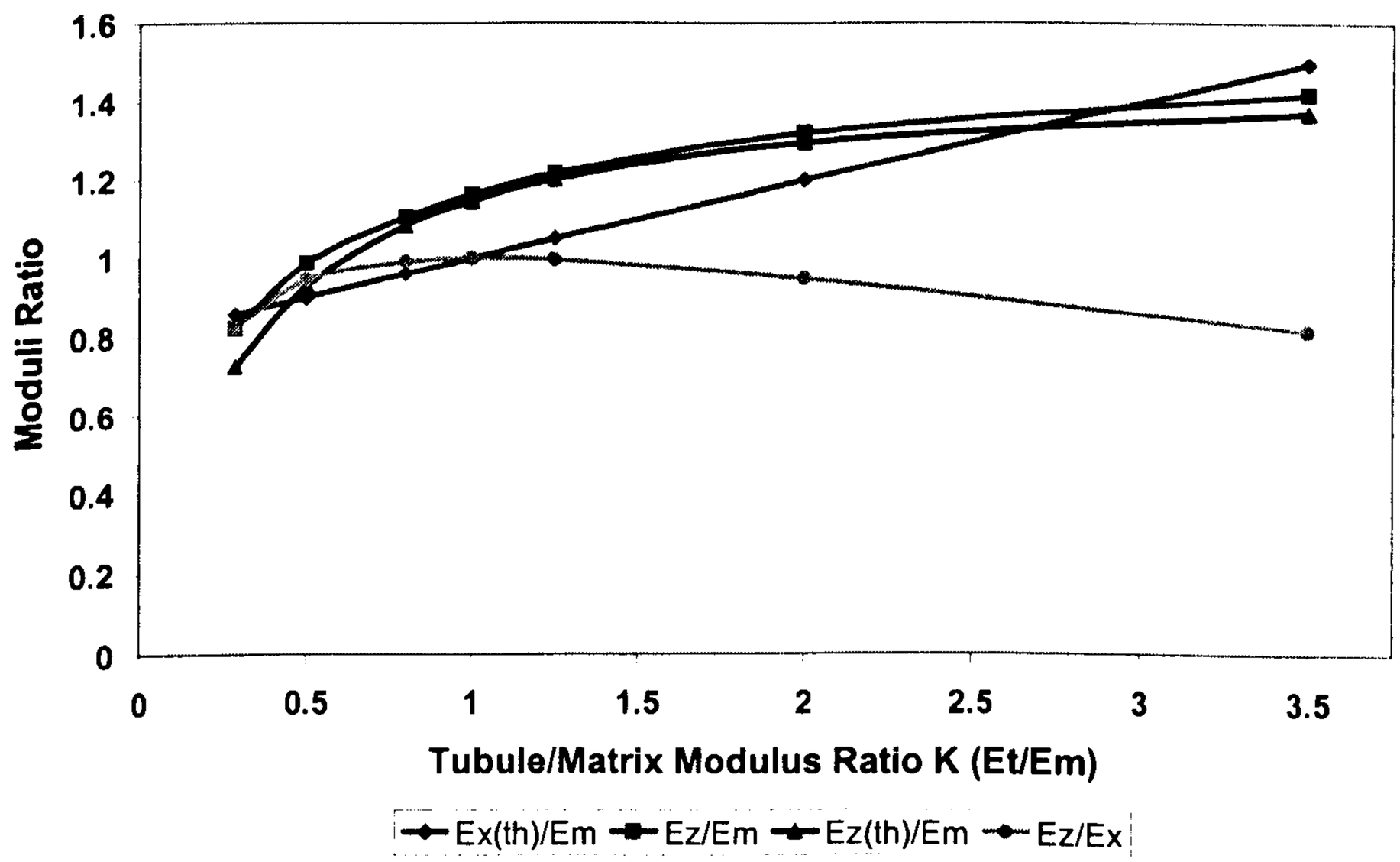

Figure 6.10 Modelled lateral moduli ratios compared with those calculated using the modified Hull equations with increasing *K* for Zone 3 in the y-direction.

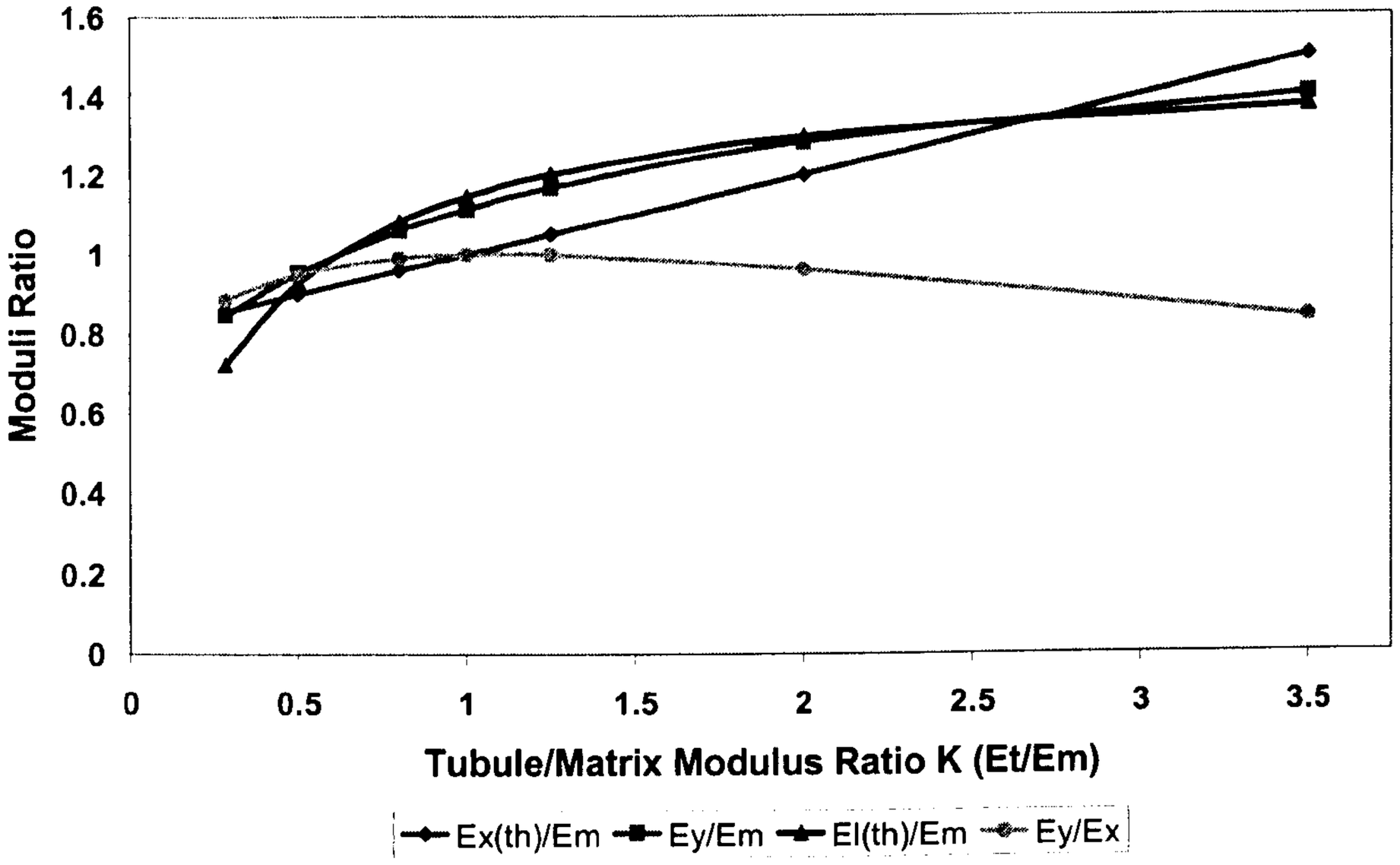

Figure 6.11 Modelled lateral moduli ratios compared with those calculated using the modified Hull equations with increasing *K* for Zone 3 in the z-direction.

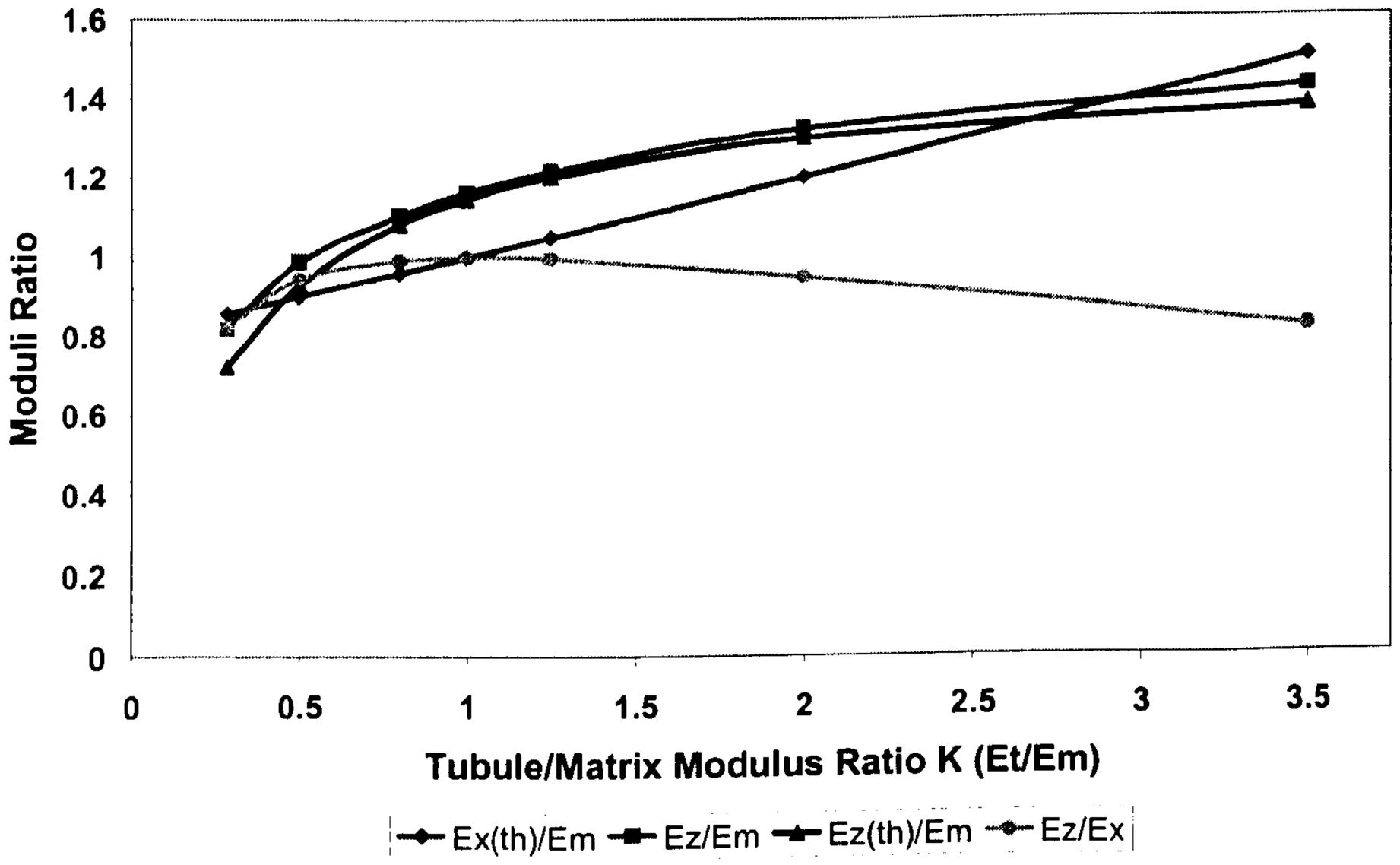

MODELLED MODULI RATIOS IN ZONE 1

At an Et/Em ratio of 3.5 the lateral to axial moduli ratios are 0.9 and 0.85 in the y- and z-direction respectively. This indicates that there are relative differences (of these specific orders) in the E between the keratinous material in the two respective phases. At this K value the axial modulus is ~42 and 34% greater than the matrix material in the y- and z-direction respectively.

MODELLED MODULI RATIOS IN ZONE 3

The corresponding modelled lateral to axial ratios for Z3 are 0.84 and 0.82. This equates to an axial *E* 40 and 42% greater than the matrix material in the y- and z-direction respectively.

6.9.4.3 STRESS AND STRAIN CONCENTRATION FACTORS

Figures 6.12 – 6.15 illustrate the stress and strain concentration factors within the respective hoof horn fractions over the range of *K* values tested. These values are presented in respect of loading both in the y- and z-direction for each zonal site.

ZONE 1 STRESS STRAIN CONCENTRATION FACTORS

The maximum stress and strain concentration factor plots displayed a similar trend in both the y- and z-direction (See Figures 6.12 and 6.13). However the exact values were dependent upon the direction of loading. In general terms, the stress concentration factor within the tubular horn fraction increased with increasing *K*. Maximum strain concentration factors in the tubular component reached three times the mean at *Et*/*E*m of 1. This trend was accompanied by a corresponding reduction in tubule strain concentration factor. The rate of change decreased progressively with increasing *K*. The absolute values predicted in the y-direction were greater than those in the z-direction for a given value of *K*.

The rate of change of stress and strain concentration factor within the tubule horn fraction was similar in the z-direction. However in the y-direction, the rate of change in tubule stress concentration factor was greater than the rate of change in tubule strain concentration.

Figure 6.12 Maximum stress and strain concentration factor plots in the y-direction for Zone 1.

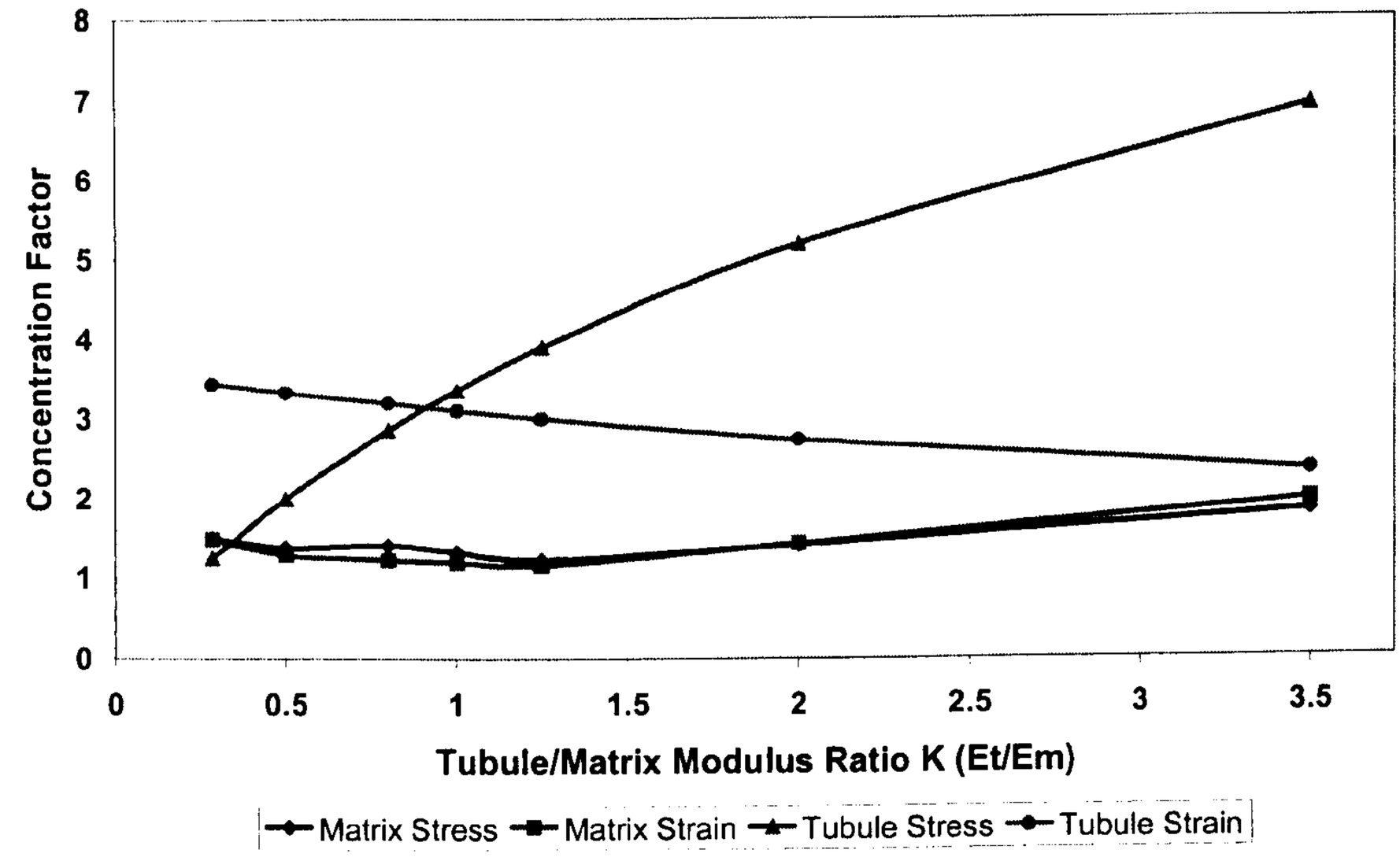

Figure 6.13 Maximum stress and strain concentration factor plots in the z-direction for Zone1.

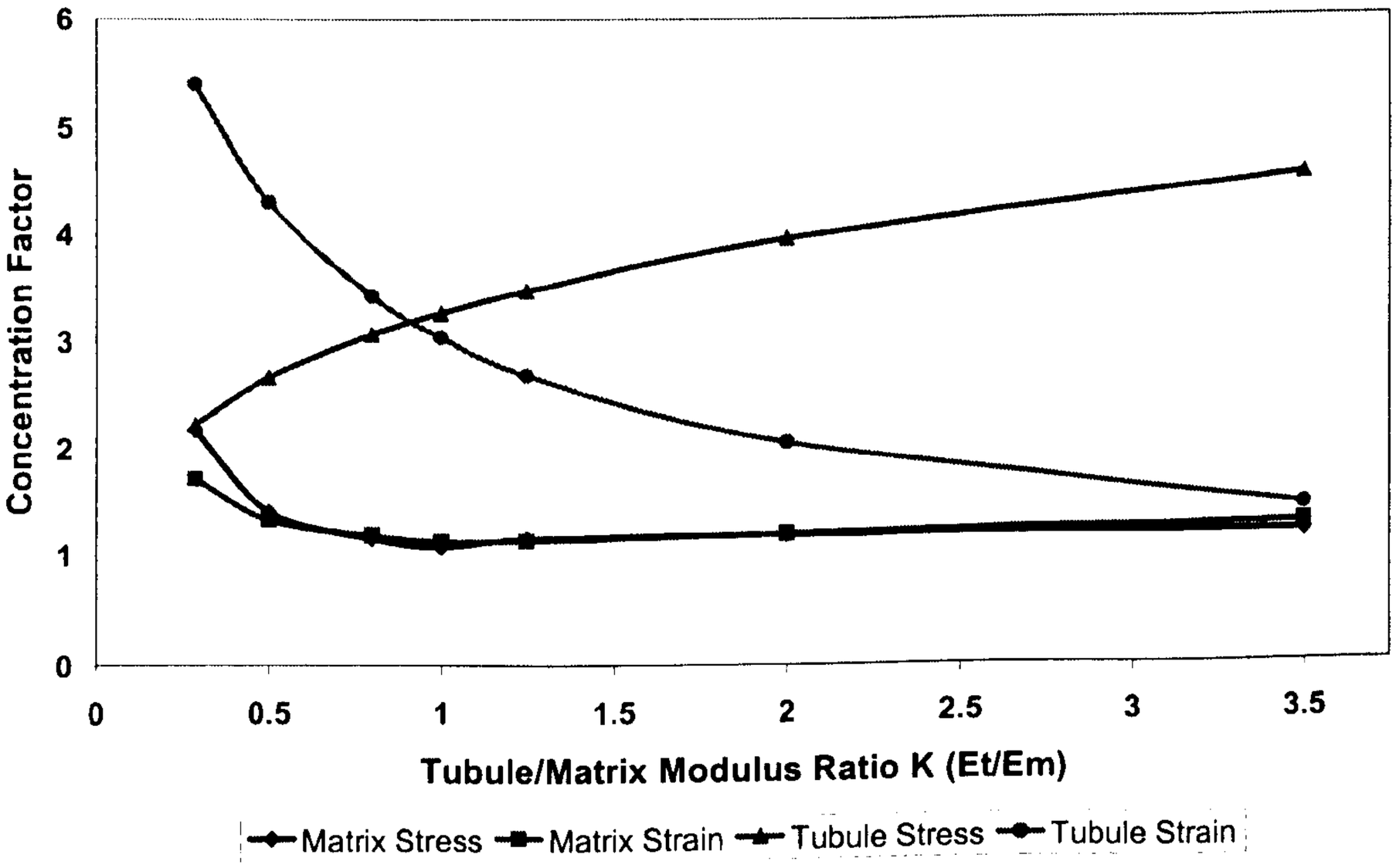

Figure 6.14 Maximum stress and strain concentration factor plots in the y-direction for Zone 3.

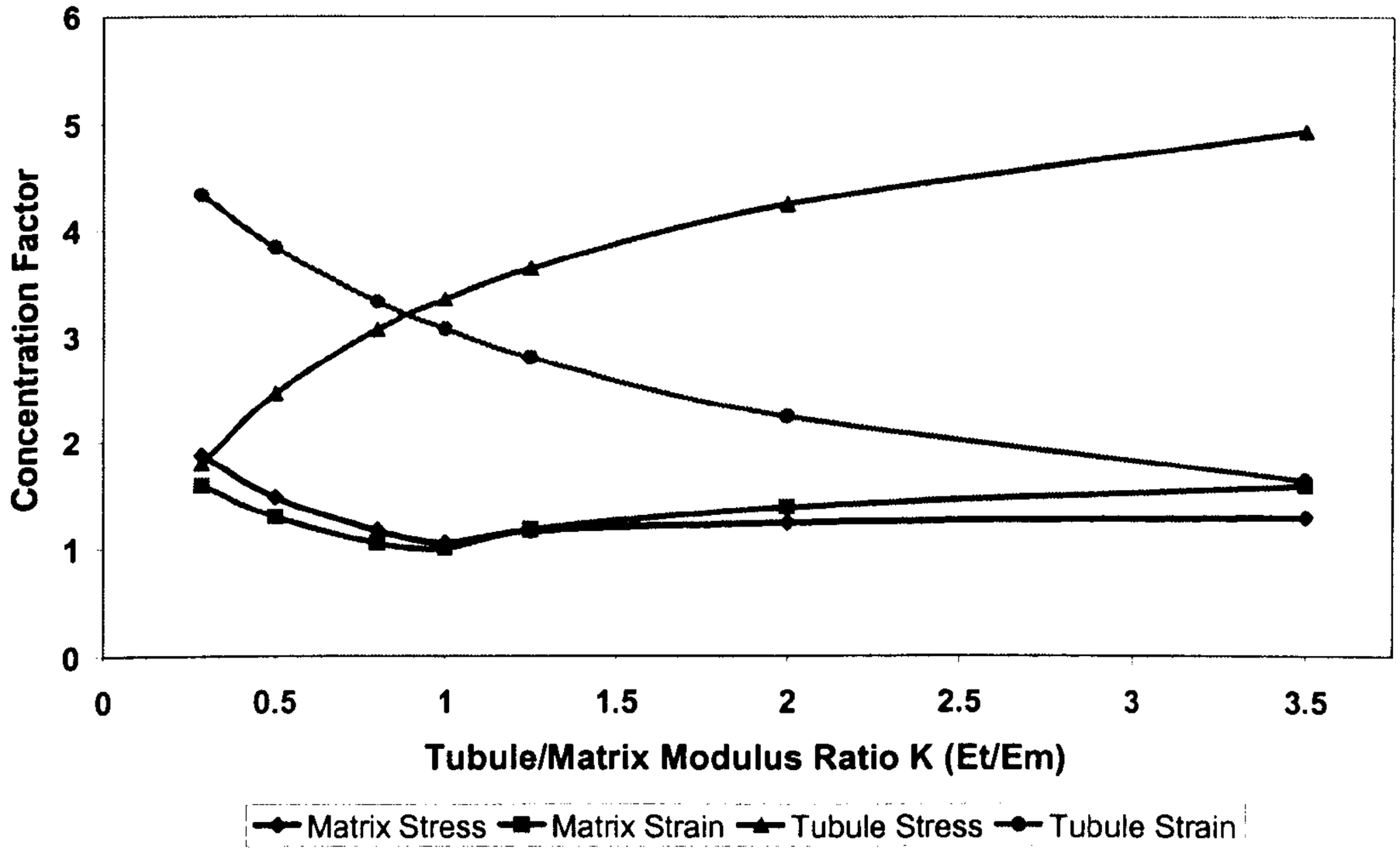

Figure 6.15 Maximum stress and strain concentration factor plots in the z-direction for Zone 3.

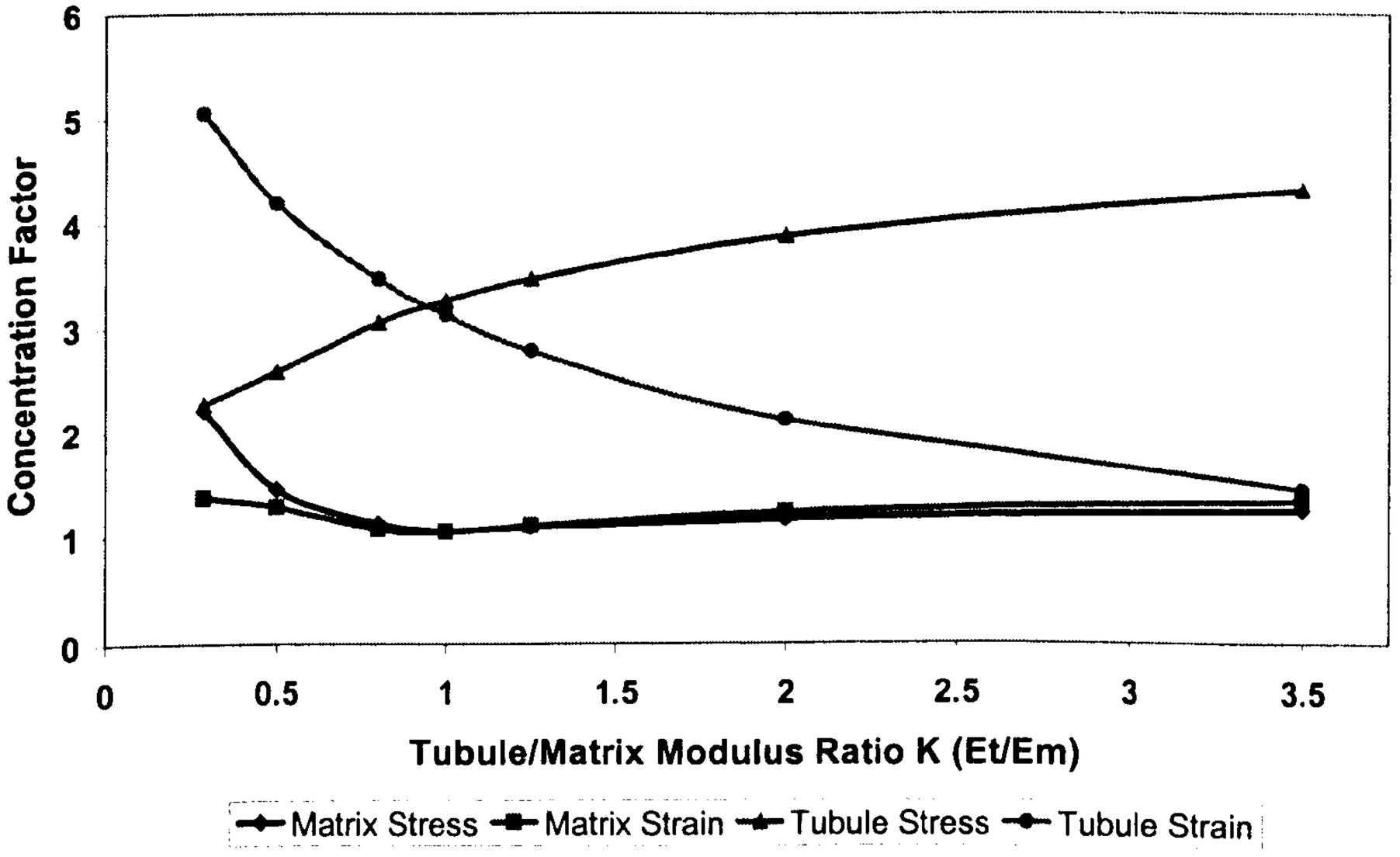

Stress and strain concentration factors within the matrix increased progressively with increasing *K* above unity. However the rate of change was modest in comparison with the tubular horn fraction. Absolute values of stress and strain concentration factors were approximately equal for any given value of *K*. However, there was an indication that these values diverged at *K*>2.5. This apparent trend was more pronounced within the y-direction. Maximum stress and strain concentration factors within the matrix did not exceed twice the mean values either in the y or z direction across the range of *K* values. By extrapolating the results beyond *K* of 3.5, suggest that strain concentration factors within the respective horn fractions reach parity at a *K* value of ~ 4 - 4.5. The ratio of maximum to mean strain at this K value is ~ 2.25.

ZONE 3 STRESS STRAIN CONCENTRATION FACTORS

The stress strain concentration factors in response to y- and z-directional loading for Z3 are given in Figures 6.14-6.15. These plots display a similar trend to those reported for Z1. However the absolute values are consistently lower. Tubule and matrix strain concentration factors reach parity in the y and z loading direction at a *K* of ~3.5. The ratio of maximum to mean strain at this *K* value is ~1.5 and 1.8 in the y- and z-direction respectively.

6.9.4.4 MICROMECHANICAL FE MODELLING OF THE DONKEY HOOF WALL

The distribution of the region of maximum strain was dependent upon *K* value, loading direction, and Zone.

In the Z1 model loaded in the y-direction, the point of maximum strain moved as *K* increased from unity to 3.5. At unity this was located at the tubular-matrix interface adjacent to the apex of the tubule minor axis. As *K* values increased, the loci of maximum strain concentration moved progressively towards the interface at the apex of the tubule major axis. At *K* of 3.5 the position of maximum strain concentration was located at the interface adjacent to the tubule major axis.

In the case of z-direction loading at $K = 1$, the strain concentration was centred upon the apex of the major axes. With increasing *K*, strain concentration moved towards the minor axis. However, the degree of movement was less pronounced than in y-direction loading. At *K* of 3.5 the location of maximum strain was centred on the tubular-matrix interface at a point equidistant between the major and minor axis. Figure 6.16 illustrates the resultant Von Mises stress distribution within the Z1 model loaded in the z-direction, at $K = 1$.

In the Z3 model, strain concentration was similarly centred at the tubular-matrix interface orthogonal to the respective direction of loading, at *K* values of 1, both in respect of y- and z-direction loading. As *K* increased, the centre of strain concentration moved towards the

direction of loading. The degree of this movement in response to z-direction loading was similar to that observed in the Z1 model. However the degree of movement recorded in y-direction loading was less pronounced than in the Z1 analysis. With regards to strain distribution within the horn tubules, the position of maximum strain in both zonal models was located at the boundary with the medullary cavity, normal to the direction of loading, over the range of K values analysed.

Figure 6.16 Von Mises stress distribution within the Zone 1 model loaded in the z-direction, at $K = 1$.

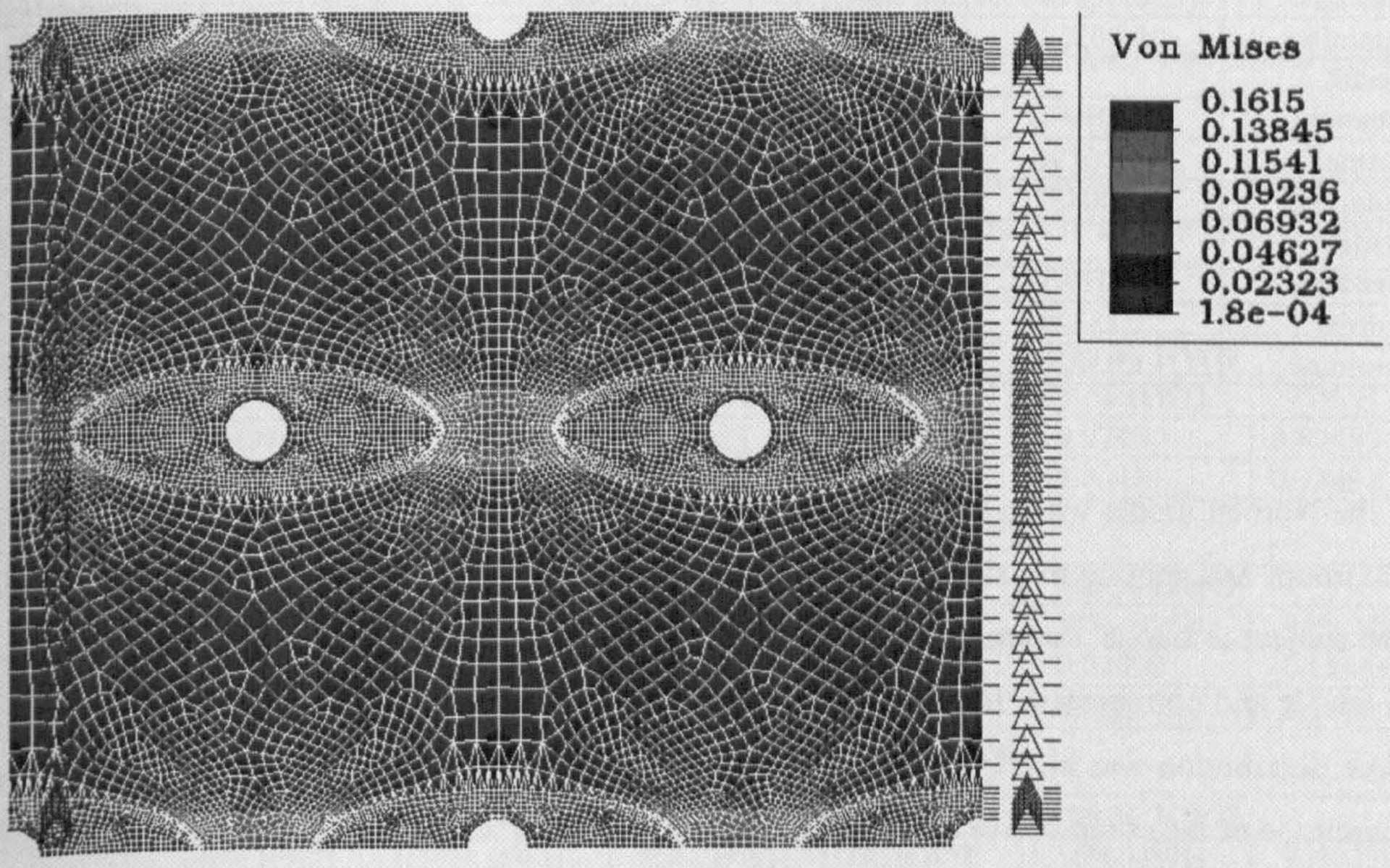

6.9.5 INVESTIGATION OF THE EFFECTS OF THE LAMINITIC CONDITION ON HOOF WALL FUNCTION

The theoretical mechanical responses at the MDC to differences in zonal E associated with the laminitic condition are detailed below. Results are presented both in respect of dorso-palmar effects at 50%HWH, and disto-proximal effects at 0 and 100% HWD.

6.9.5.1 DORSO-PALMAR EFFECTS

Modelled mechanical responses at the MDC are summarised in Table 6.5. Predicted dorso-palmar stress and strain values are given 0, 25, 40 70 and 100% HWD at 50% HWH in respect of both the normal and laminitic modelling scenario.

Table 6.5 Summary comparison of modelled dorso-palmar stress and strain levels in normal and laminitic hoof horn at the MDC site at 50% HWH.

Model Scenario	**Maximum Principal Stress**				
	0% HWD	25% HWD	40% HWD	70% HWD	100% HWD
Normal	-0.02409	0.00547	0.08486	0.45771	0.97484
Laminitic	-0.01265	0.00692	0.05151	0.43108	1.04481
Model Scenario	**Minimum Principal Stress**				
	0% HWD	25% HWD	40% HWD	70% HWD	100% HWD
Normal	-1.43275	-0.46986	-0.15692	-0.01778	0.02095
Laminitic	-1.19700	-0.51625	-0.24976	-0.05293	0.02025
Model Scenario	**Maximum Principal Strain**				
	0% HWD	25% HWD	40% HWD	70% HWD	100% HWD
Normal	0.00244	0.00132	0.00097	0.00414	0.00842
Laminitic	0.00353	0.00216	0.00136	0.00406	0.00910
Model Scenario	**Minimum Principal Strain**				
	0% HWD	25% HWD	40% HWD	70% HWD	100% HWD
Normal	-0.00296	-0.00122	-0.00150	-0.00220	-0.00430
Laminitic	-0.00437	-0.00176	-0.00178	-0.00240	-0.00456
Model Scenario	**Von Mises Stress**				
	0% HWD	25% HWD	40% HWD	70% HWD	100% HWD
Normal	1.23129	0.43525	0.22369	0.43754	0.87682
Laminitic	1.03220	0.50401	0.26248	0.43746	0.94687

In the Normal model which was based upon the moduli data of Latham (2001 – Pers com.), the maximum and minimum principal stress data indicated that the outer aspect of the hoof wall was subject to biaxial compression. At 25 % HWD, the hoof wall was subject to a combination of tensile and compressive forces, with compressive forces predominating. A Similar pattern of force distribution was also evident at 40% HWD, however tensile forces had increased and the magnitude of the compressive force had decreased. The hoof wall at 70%HWD was also subject to a combination of tensile and compressive forces, however tensile forces predominated. At the laminar interface (100% HWD) the wall was subject to biaxial tensile forces.

Although the pattern of force distribution was similar in the laminitic model, there were marked differences in the magnitude of the maximum and minimum principal stress, and also in the Von Mises stress and the associated maximum and minimum strain levels acting at the corresponding HWD sites. In particular, Von Mises stress levels were greater at all sites, as were both the maximum and minimum strain levels. These differences were associated at 50%HWH with the outer aspect of the hoof wall being subjected to elevated levels of strain (a 40% increase in maximum principal strain), whilst the laminar interface experienced higher levels of tensile stress (an 8% increase in both Von Mises stress, and Maximum Principal stress).

6.9.5.2 DISTO-PROXIMAL EFFECTS

Modelled mechanical responses at the MDC are summarised in Table 6.6. Predicted stress and strain values are given at 5, 50 and 95% HWH in respect of both the normal and laminitic modelling scenario. In both models the outer aspect of the hoof wall is predominantly subject to compressive forces that increase from the 5% to the 95% HWH sites, this is also associated with a disto-proximal increase in Von Mises stress. However at the laminar interface, the 5% HWH site was subject to a combination of tensile and compressive forces, at 50%HWH, biaxial tension, and biaxial compression at 95% HWH. Comparison between the two models indicated that in the laminitic model, the hoof wall in the vicinity of the coronary corium is subject to altered levels of maximum and minimum principal stress, and strain, and also Von Mises stress.

Table 6.6 Summary comparison of modelled disto-proximo stress and strain levels in normal and laminitic donkey hoof horn at 0 and 100% HWD at the MDC site.

	Maximum Principal Stress					
Model	**0 % HWD**			**100 % HWD**		
	7% HWH	50% HWH	95% HWH	7% HWH	50% HWH	95% HWH
Normal	0.497659	-0.02409	-0.46053	0.13872	0.97480	0.80095
Laminitic	0.14712	-0.01265	-0.27486	0.29095	1.04481	0.75492
	Minimum Principal Stress					
Model	**0 % HWD**			**100 % HWD**		
	7% HWH	50% HWH	95% HWH	7% HWH	50% HWH	95% HWH
Normal	-0.64909	-1.43275	-2.97290	-0.22353	0.02090	-0.11446
Laminitic	-0.90175	-1.19697	-2.24310	-0.70551	0.020247	-0.16950
	Maximum Principal Strain					
Model	**0 % HWD**			**100 % HWD**		
	7% HWH	50% HWH	95% HWH	7% HWH	50% HWH	95% HWH
Normal	0.002954	0.00244	0.002884	0.004404	0.008420	0.007566
Laminitic	0.003515	0.00353	0.003790	0.005610	0.009098	0.007549
	Minimum Principal Strain					
Model	**0 % HWD**			**100 % HWD**		
	7% HWH	50% HWH	95% HWH	7% HWH	50% HWH	95% HWH
Normal	-0.00235	-0.00296	-0.00675	-0.00777	-0.00430	-0.00464
Laminitic	-0.00348	-0.00437	-0.00909	-0.00768	-0.00456	-0.00477
	Von Mises Stress					
Model	**0 % HWD**			**100 % HWD**		
	7% HWH	50% HWH	95% HWH	7% HWH	50% HWH	95% HWH
Normal	1.27412	1.23129	2.37017	0.84672	0.87682	0.82183
Laminitic	0.94881	1.03220	1.84081	0.88331	0.94687	0.83038

6.9.6 INVESTIGATION OF LAMINITIC GROUP EFFECT ON HOOF WALL FUNCTION

The theoretical mechanical responses at the MDC to laminitic group differences in zonal E_C are detailed above in Table 6.7 and Table 6.8. Results are presented in respect of dorso-palmar effects across the HWD at 50%HWH. Comparison between the two respective laminitic groups revealed a similar pattern of Maximum and Minimum Principal stress and strain distribution and also Von Mises stress distribution across the dorso-palmar HWD.

Table 6.7 Summary of 'between group' comparison of modelled dorso-palmar stress and strain levels in laminitic hoof horn at the MDC site at 50% HWH.

Model Scenario	**Maximum Principal Stress**				
	0% HWD	25% HWD	40% HWD	70% HWD	100% HWD
Group 1	-0.01110	0.00839	0.05104	0.42378	1.05454
Group 2	-0.01426	0.00512	0.05185	0.43760	1.03692
Model Scenario	**Minimum Principal Stress**				
	0% HWD	25% HWD	40% HWD	70% HWD	100% HWD
Group 1	-1.17044	-0.51827	-0.25578	-0.06153	0.01980
Group 2	-1.22053	-0.51938	-0.24598	-0.04478	0.02075
Model Scenario	**Maximum Principal Strain**				
	0% HWD	25% HWD	40% HWD	70% HWD	100% HWD
Group 1	0.00392	0.00245	0.00158	0.00423	0.00966
Group 2	0.00335	0.00201	0.00124	0.00408	0.00901
Model Scenario	**Minimum Principal Strain**				
	0% HWD	25% HWD	40% HWD	70% HWD	100% HWD
Group 1	-0.00486	-0.00203	-0.00194	-0.00257	-0.00483
Group 2	-0.00415	-0.00163	-0.00171	-0.00235	-0.00454
Model Scenario	**Von Mises Stress**				
	0% HWD	25% HWD	40% HWD	70% HWD	100% HWD
Group 1	1.01022	0.50340	0.26606	0.43675	0.95751
Group 2	1.05146	0.50628	0.26177	0.43783	0.93778

Table 6.8 Summary of 'between group' comparison of modelled disto-proximo stress and strain levels in laminitic hoof horn at 0 and 100% HWD at the MDC site.

	Maximum Principal Stress					
Model	**0 % HWD**			**100 % HWD**		
	7 %HWH	50 %HWH	95 %HWH	5 %HWH	50 %HWH	95 %HWH
Group 1	0.31912	-0.01110	-0.29445	0.24460	1.05454	0.82023
Group 2	0.34870	-0.01426	-0.32515	0.21475	1.03692	0.81922
	Minimum Principal Stress					
Model	**0 % HWD**			**100 % HWD**		
	7 %HWH	50 %HWH	95 %HWH	5 %HWH	50 %HWH	95 %HWH
Group 1	-0.70791	-1.17044	-2.16500	-0.76153	0.01980	-0.14070
Group 2	-0.75520	-1.22053	-2.31226	-0.76149	0.02075	-0.13332
	Maximum Principal Strain					
Model	**0 % HWD**			**100 % HWD**		
	7 %HWH	50 %HWH	95 %HWH	5 %HWH	50 %HWH	95 %HWH
Group 1	0.004218	0.003915	0.004355	0.005639	0.009661	0.008256
Group 2	0.00374	0.00335	0.00378	0.00509	0.00901	0.00782
	Minimum Principal Strain					
Model	**0 % HWD**			**100 % HWD**		
	7 %HWH	50 %HWH	95 %HWH	5 %HWH	50 %HWH	95 %HWH
Group 1	-0.00355	-0.00486	-0.00980	-0.00845	-0.00483	-0.00520
Group 2	-0.00313	-0.00415	-0.00858	-0.00792	-0.00454	-0.00488
	Von Mises Stress					
Model	**0 % HWD**			**100 % HWD**		
	7 %HWH	50 %HWH	95 %HWH	5 %HWH	50 %HWH	95 %HWH
Group 1	0.94100	1.01022	1.75380	0.90669	0.95751	0.86031
Group 2	1.01146	1.05146	1.86548	0.88501	0.93778	0.85347

6.10 DISCUSSION

This study represents one of the first applications of this powerful modelling technique to equid hoof wall function. There are many advantages in applying FEA to this type of mechanical problem. Firstly it is possible to generate a general understanding of the structure and analyse how it performs under various loading conditions. In particular it is possible to determine with reasonable confidence, conditions in regions of the hoof wall where experimental results are difficult to achieve. Secondly it is possible to work at different levels within the design hierarchy of the hoof wall, so that a more detailed analysis of the structural complexity of the hoof wall, and its performance, can be achieved. Finally, FEA provides an ideal focus for bringing together information derived from a multidisciplinary materials characterisation of properties so that they can be critically assessed in terms of hoof wall function.

This study differs from other work within this field, most notably by Hinterhoffer 1996, Hinterhoffer *et al.* 1997, McClinchy 2000, McClinhy *et al.* (2001 – Submitted) and Thomason *et al.* (2002) in that the modelling exercise has not been restricted to the gross anatomical level. This study has also evaluated the macro- and micromechanical performance of the donkey hoof wall. In addition this study has investigated the potential effect of pathological change against baseline performance criteria for the donkey hoof wall. In this way, this investigation represents a logical development of former FEA analyses of equid hoof wall function. It has provided new insight into the structure-function relationships that exist at various levels within the design hierarchy of the donkey hoof wall.

Various authors including Zenker (1991), Douglas (1998) and McClinchy (2000) and Thomason *et al.* (2000) have adopted elements of the approach detailed in Section 6.6.1 and Section 6.6.2 to describe the shape of the hoof capsule. However this represents the first occasion in which the rationale behind parameter selection has been elucidated fully.

The use of a reverse engineering approach to generate a physical model of the hoof wall, based upon measurements taken from the hoof wall enabled a subjective assessment of the model development protocol. The validation of the model development phase of the FE process represents an essential prerequisite for effective FEA. This assessment indicated that the shape description protocol, detailed in Section 6.8.1 and Section 6.8.2, provided an acceptable first approximation of the gross anatomical shape of the donkey hoof wall. This is the first occasion in which a means of shape validation has been employed.

The initial analysis of the donkey hoof wall model at the gross anatomical level gave a predicted pattern of deformation, in response to static loading, which is in broad agreement with '*in vivo*' observations given for the horse by Lungwitz (1889, 1891) and Pollitt (1993). This was characterised by outward expansion of the heels, dorsoconcavity of the proximal MDC, and a proximo-dirtal reduction in capsular height at the MDC. This was in marked contrast with the work of Hinterhofer *et al.* (1997), who were not able to achieve deformation consistent with 'in vivo' observations when modelling this capsular component in isolation.

The similarity of the predicted deformation pattern to '*in vivo*' observations for the horse suggests that the mode of mechanical functioning of the donkey hoof wall may be similar to that of the horse. However differences were noted in the finer detail of the deformation pattern. The displacement diagram illustrates that in the region of the quarters and heel the displacement value is greater proximally than distally. This contradicts '*in vivo*' observations in the horse where lateral expansion is greatest at the BB reported by Thomason *et al.* (1992). However it is important to note that the displacement values are nominal, that is they give absolute displacement values only, and are not vector quantities giving directional information. The

corresponding displaced space plot in the lateral (y) direction indicates a uniform outward expansion in the donkey. Therefore, the predicted values given for total displacement suggest that the proximal region of the quarters may be subjected to a combination of different compressive, tensile, bending, and torsion forces.

Thomason *et al.* (1992) suggested that the proximal region of the heels in the horse were subjected to an inwardly directed tensile force that results in an outward and upward movement of the heel distally. However the displacement plot in the y-direction for the donkey predicts uniform outward expansion proximally and distally. Hence this suggests in the case of the donkey that axial compressive forces contribute to total displacement predicted at this site. These differences may reflect the sophistication of the model, and the assumptions made in this respect, or may represent a genuine difference in hoof wall function between donkey and horse.

Reilly (1997) and Collins *et al.* (2002) have commented upon the anatomical differences between horse and donkey hoof capsule, and suggested that there may be different amounts of movements within the two capsules during loading. It can be argued in term of mechanical principles, that geometrical differences in the hoof capsule are likely to affect displacement under loading. In this case, heel expansion resulting from rotation and/or bending is likely to be less in the more upright donkey capsule due to increased axial resistance. In addition, tapering of the hoof wall depth in the heel region of the horse (Reilly 1997, Collins *et al.* 2002), combined with an inclined geometry, presents less material to resist displacement, and increases the tendency to accommodate such movement.

The theoretical distribution of principle strain around the outer surface of the hoof wall indicates the occurrence of maximum principle strain centred upon the proximal region of the MDC. This is consistent with experimental observations using surface strain gauges for the horse (Thomason *et al.* 1992, Chang *et al.* 1993) and for the donkey (Chang *et al.* 1993), and suggests that this FEA model is reproducing '*in vivo*' conditions. In addition, the principal strain distribution in the hoof wall model was comparable with that reported in the donkey hoof by Chang *et al.* (1993).

Focusing strain levels in the proximal part of the hoof wall may represent an important means of biofeedback that enables hoof horn production to be modulated to produce an optimal structure to meet the functional requirements of the hoof wall.

The stress distribution at the surface of the capsule, that is derived from the strains using the stated E and ν, can be displayed in various forms. The magnitude of the Maximum Principal stress can be plotted as can the Minimum Principal stress, or, a combination of these related to various failure theories. However given the complexity of the structural hierarchy evident in the hoof wall (Reilly *et al.* 1996, Kasapi and Gosline 1997), and our limited knowledge of the

material properties of hoof horn (Reilly 1995), it is difficult to say which failure mode is applicable. However two stress states may be of interest, the Maximum shear stress (Tresca), and the Von Mises Stress (Shear strain energy theory). Both of these are usually related, in engineering applications, to failure in ductile materials. Such a mode of failure may be applicable to hoof wall modelling due to the potential plasticising effect of the material's inherent moisture content (Cope *et al.* 1998). However, as the material is non-isotropic and possibly behaves in a non-linear fashion when loaded at high speed, these values can only give an indication of the resultant conditions. The accuracy of the results can only be as accurate as that of the assumptions made in developing and resolving the model.

The Shear stress plot is also interesting in that it relates to the isochromatic fringes produced in photoelastic analysis. A plot of two times the Tresca stress is used to simulate photoelastic surface strain and is used as a comparison. This analysis provided a modelled response that was in broad agreement with 'in vitro' Photoelastic shear stress data reported for the equine hoof by Dejardin *et al.* (1999, 2001).

The accuracy of a FEA is dependent upon contributions from the geometrical modelling of the structure, the selected mesh size, the specified material properties, the defined boundary conditions, and the chosen load and means of loading. Whilst confidence can be expressed in terms of the geometric modelling and the boundary restraints, several important assumptions and compromises have had to be made with respect to the other factors.

The accuracy of the solution is related to the mesh size. The software used in these simulations can provide an indication of accuracy by calculating a precision value. It takes the values of the quantity of interest, for example, stress, and compares the values derived at a node from all the elements connected at that node. These will differ depending on the mesh size and the local stress/strain gradients. The precision is defined as the maximum difference between these values divided by the maximum stress in the body.

Although the force generated by an average donkey bodyweight during static loading can be calculated with relative ease, there is a lack of scientific evidence as to how this force is distributed between the four hoof capsules. Stashak *et al.* (2002) stated that the forefeet support 60% of the body weight of the horse. If a similar situation exists in the donkey then the results of this preliminary study, based upon an even force distribution acting through each hoof, under-represents the effect of static loading upon the deformation and stress distribution in the forelimb donkey hoof wall. In addition, there is limited information regarding the means by which the force is transferred from the axial skeleton to the ground via the hoof capsule. It is not known if the load is transferred equally via the 400 lamellae or whether more weight is taken at the MDC as suggested by Douglas *et al.* (1996) in the horse. Foot balance has also been

reported to affect the loading characteristics of the hoof (Chang *et al.* 1993). This study assumes mediolateral foot balance, although there is limited information regarding natural foot balance in the donkey. Williams (1993) suggested that the donkey naturally takes more weight on the medial aspect of the BB in the hindfoot, however, it is not known whether the same is true for the forefoot.

This study is also based upon the assertion that the hoof wall constitutes the load-bearing element of the equine hoof capsule (Nickel 1938a, 1939), but there is debate as to whether the sole in the donkey should be load-bearing (Reilly 1997). For example, Whitehead *et al.* (1991) and Fowler (1995) stated that the anterior third of the sole plays an important role in weightbearing. Reilly (1997) referred to the present lack of knowledge concerning the extent to which the sole bears weight or whether in fact, the sole naturally should be concave and hence bear no load.

The application of FEA to hoof mechanics has been limited. The different modelling techniques employed, and the working assumptions made, make direct comparison difficult. Wichtmann *et al.* (1990) and, Hood and Wichtmann (1991) modelled a two-dimensional sagittal section at the MDC of the equine foot, loaded via the second phalyanx. This model of the foot consisted of only 964 nodes and 457 elements and therefore did not afford modelling detail.

Compression bending and rotation of the wall were described resulting in dosoconcavity of the proximo dorsal aspect of the hoof wall, consistent with the results of this study. However such a two-dimensional representation cannot model the effect of compressive forces generated at the MDC by heel expansion, nor the tensile forces generated orthogonal to the tubular axis as described by Leach (1980) and Thomason *et al.* (1992). Consistency of dorsoconcavity between this present study and Wichtmann *et al.* (1990) supports the assumption that it is possible to model the hoof wall in isolation and still generate accurate '*in vivo*' simulation. Comparison of displaced shape and stress concentration plots reveal similarity between this study and the work of Hinterhoffer 1996, Hinterhofer *et al.* (1997, 2000, 2001), McClinchy (2000), McClinchy *et al.* (2001 – Submitted), and Thomason *et al.* (2002).

As the gross deformation of the model is consistent with in vivo observations, confidence can be expressed in predicted stress and strain distribution within the hoof wall structure.

The assessment of stress and strain distribution across the dorso-palmar HWD highlighted the functional effects of zonal variation in E across the HWD.

Under conditions of material homogenisity, the modelled sagittal section taken along the plane of the MDC revealed that the dorsal aspect of the hoof wall was subjected to compressive forces which increased progressively in a proximal direction from the BB. These compressive forces decreased across the dorso-palmar extent of the HWD, with the development of tensile forces

towards the inner aspect of the hoof wall in the region of the laminar interface. The greatest tensile force was generated in the proximal half of the wall.

These findings are consistent with the hypothesis of Nickel (1938a) that the equid hoof wall is subject to a combination of axial compression and radial tension, and also the theoretical force distribution pattern across the HWD stated by Reilly (2001).

The variation in the predicted pattern of stress and strain distribution across the HWD, in response to a progressive dorso-palmar decrease in E, suggests that a situation of variable E may be particular functional importance. Material inhomogenisity resulted in stress concentration within the outer aspect of the hoof wall, a reduction in the stress and strain gradient within the inner region of the hoof wall, and decreased tensile forces at the laminar interface. These findings are consistent with a means of affording protecting to the sensitive structures of the foot, by focusing stress at a distance from the laminar interface, preventing excessive deformation at this site, and achieving smooth stress transfer across the laminar interface.

The macro- and micromechanical modelling of the hoof wall extends the preliminary evaluation of gross hoof wall function, to the consideration of the composite nature of hoof horn structure. It is the first study to use this technique to investigate the macro-and micromechanical behaviour of the equine hoof wall, at the microscopic level of the design hierarchy, during loading.

Confidence in such modelling techniques should always be tested by comparison of the theoretical predictions with results from experimental work. In this respect, it has been previously demonstrated that the results from these theoretical techniques are within 1-2% of experimental values for synthetic composite materials (Hull 1991). In addition, the theoretical outputs obtained by both 'rule of mixtures' and the modified Hull equation closely correspond with experimental testing data reported by Douglas *et al.* (1996) and Kasapi and Gosline (1997) for the horse and full HWD data for the donkey generated in Chapter 5 of this thesis.

Although agreement between results from these models and experimental data does not necessarily confirm that hoof horn is a natural composite material, these findings support the suggestion that the hoof may operate in a manner similar to a unidirectional fibre composite.

Whilst the macromechanical value of the ratio of axial to lateral E of ~2 may appear to be very small in comparison with values encountered for synthetic composites, it is not unexpected as both the Tu and IT horn fractions are essentially different structural arrangements of the same cellular material. As such the E for the fibres (i.e. the horn tubules) and the matrix (i.e. the IT horn) are not likely to be greatly different and consequently the E(f):E(m) ratios are typically low when compared with those for synthetic composites; this is typical of many natural

composite materials. For example, cortical bone values for E(f):E(m) have been estimated in the range from 1:1 to 10:1 (Hogan 1992). Although no previously published values exist for donkey hoof horn, Kasapi and Gosline (1999) have recently provided experimental data for the horse. These authors recorded Tu:IT E ratios of 2.1:1 and 5.9:1 for the Z2 and Z3 respectively at maximal hydration.

Although the Tu volume fraction (VF) values may be considered to be relatively low when compared to synthetic composite materials, it has been noted that natural composites are optimum structures best suited to an organism in its natural environment (Saliba 1991). In this respect, the structural organisation of the hoof wall may have been optimised by natural processes to achieve a balance between the accommodation of, and resistance to, loading forces. In this way the structure would provide dampening of concussive forces without material failure. In addition, the MDC site of the hoof wall is subjected to biaxial compression during static weightbearing (Leach 1980, Thomason *et al.*1992), hence a material that exhibits a modest Ex:Ey ratio may be adaptive to ensure adequate resistance to lateral as well as axial loading forces.

Curiskis and Feughelam (1983), reporting data for synthetic composites, stated that the greatest rate of change in the value of Ey:Ex, for a given increase in fibre VF, occurred in the VF range of 0-25%. Thus, it is possible that the TuVF of the hoof wall may have been optimised to achieve the greatest potential modulation of material properties.

Conversely this functional range leaves the animal susceptible to the effects of pathological change in circumstances where pathology affects Tu and/or IT VF levels. Indeed the modest 'between Laminitic Group' differences recorded within Chapter 4 of this thesis are likely to exert a maximal effect upon performance.

The results of this study demonstrate that the use of FEA applied to models based on the experimental morphometric analysis of the donkey hoof wall can predict E values that are consistent with experimental results. On this basis, FEA represents a valuable modelling technique that can be further employed to the development of an understanding of the structure-function relationships at the microscopic level of the design hierarchy of the hoof wall.

Given that the FEA modelling technique provides results consistent with those from the modified Hull equation at the macromechanical level, it is reasonable to expect that the theoretical predictions at the micromechanical level will also provide good agreement. This assertion is supported further by the work of Hull (1981) and Saliba (1991) who recorded stress concentration factors in synthetic composite materials which are similar to those predicted for the hoof wall models. For example, using a TuVF of 0.25 taken from the morphometry studies, the FEA model produces stress concentration values of ~2.

The stress concentration factors predicted within the Tu components are significantly affected by the presence of the Ma. These voids act as stress concentrators within the structure, during loading, and their presence results in the generation of stress normal to the direction of loading. The stiffer the Co, the lower the stress concentration at these sites due to the reinforcing effect of the Co. This structural arrangement may be necessary to protect the Ma from strain and thereby protect the capsule from failure. If the Co had very similar properties to the IT, then crack propagation would result in catastrophic failure. The results predicted by the model indicate that, at an E(t):E(m) value > 4.0 - 4.5, the strain is transferred from the Tu to the IT, *i.e.* away from the Ma. At this point the IT is taking the majority of the deformation; this may represent a means of increasing and preserving the integrity of the structure. This may be of particular relevance within Z3 if donkey Tu:IT E ratios for the donkey are similar to the 5.8:1 ratio recorded by Kasapi and Gosline (1999) in the horse. This may represent an additional mechanism that serves to protect the sensitive structure deep to the hoof wall.

The pattern of strain gradient predicted may be useful in determining the susceptibility of the hoof wall to crack production and diversion. However, it is noted that perfect bonding of the material at the TuIT interface has been assumed in the models used in this study. If the structural organisation of this boundary is such that a more compliant or viscoelastic interface is formed, then the resultant stress concentration would be significantly reduced. The exact nature of this TuIT interface remains has yet to be determined experimentally.

The relatively high TD evident within Z1 of the hoof wall might significantly increase the work of fracture. The high number of tubules per unit area may create an obstructed pathway to inward crack propagation (Kasapi and Gsline 1997). The TuIT interface may provide an effective crack stopping site, with energy absorbed in the separation of the two different material phases (Gordon 1976). Conversely it may be argued that localised stress concentrations jeopardise the material by reducing the total energy required to cause fracture. Thus the high TD observed within Z1 may add to the stress concentration within this part of the hoof wall, and lead to the controlled elimination of damaged hoof wall, thereby protecting the hoof capsule from catastrophic failure.

The validity of the modelling outcome is dependent on the assumptions made in developing and resolving the model. The predictions from the 'rule of mixtures' calculations are dependent upon the E of the respective material phases and their respective VF, whereas the modified Hull equation relies also on ν. In the absence of ν for the donkey a representative ν for equine material was selected for this analysis. Further work is required to establish an appropriate ν value for donkey hoof.

FEA, however, is further dependent upon contributions from the geometrical modelling of the structure, the selected mesh size, the specified material properties, the defined boundary conditions, and the means of loading.

Specific assumptions have been made with respect to the adoption of the hexagonal array, the isotropic nature of the components, linear elasticity, and ignoring the effects of other levels within the design hierarchy.

There appears to be modest morphometric difference between the Z1 and Z3 hoof wall models at the microscopic level. This would suggests that a considerable difference in the relative E(t):E(m) ratio exists between the respective zones. Whilst the E(t):E(m) has been reported for Z3 in the horse there is no corresponding data for Z1. Similarly there is no information regarding zonal Tu and IT E for the donkey. Kasapi and Gosline (1999) provided theoretical estimates of zonal VF and E for the IF and IFAP elements of hoof wall ultrastructure. These authors reported marked zonal differences in IF E between Z2 and Z3. These differences were related to corresponding zonal differences in macroscopic E. However, corresponding estimates for Z1 were not given. These zonal differences suggest the possibility that material properties at the macroscopic level may reflect the combined effect of factors acting at both the microscopic and ultrastructural level of the design hierarchy in a manner suggested by Bragulla *et al.* (1992), Pellmann *et al.* (1993) and Reilly (1995).

The FE analysis of performance has been conducted assuming linear elastic properties and uniaxial loading. Given the plasticising effect of water within hoof horn material (Collins *et al.* 1998, Hopegood 2002), the 'in vivo' moisture levels recorded within donkey hoof horn, and the strain rate dependency of E (see Chapter 5) it is likely that hoof wall performance reflects viscoelastic material properties. Further work is therefore required to characterise the viscoelastic nature of the donkey hoof wall such that future refinement of these models can be achieved.

It has been suggested that during static weightbearing, the MDC site is subjected to bending as well as compression. Consequently the effect of bending and compression on the tubules is an issue which also needs to be explored. Such an analysis is likely to be difficult. This is because the approach used here assumes that the tubules and the matrix both behave as isotropic, linearly elastic components, and that their properties are constant across the hoof wall. It may be appropriate to consider the tubules as anisotropic components, stiffer in the longitudinal direction due to the Co cell alignment and the preferred IF orientation within the Co cells. The precise effect of this structural arrangement has yet to be fully investigated. In addition further work needs to be undertaken to assess the possibility of non-isotropy within the IT.

It is also important to note that the hoof capsule has to perform not only under static but also under dynamic loading conditions. The precise nature of the forces acting on the structure and those generated within it are not fully understood under dynamic loading conditions. It is however likely that the hoof wall will be subjected to a complex pattern of multidirectional forces. In addition, the material will probably behave in a non-linear fashion when loaded at high locomotor speed (Newlyn *et al.* 1999). All of these factors are likely to further modulate hoof wall performance.

The modelled analysis of hoof wall performance at the MDC in response to material properties changes associated with the laminitic condition provides a unique and previously unobtainable insight as to the potential effects of the condition upon hoof wall function. The use of a constant hoof wall model throughout the respective analyses ensured that the predicted results were controlled against potential confounding shape effects. Thus the results reflect the effects of material property changes only.

The predicted results indicate that the laminitic condition is likely associated with marked changes in hoof wall performance at the MDC site. These changes are characterised by increased stress and strain levels both within the outer aspect of the hoof wall, and at the laminar interface. Similarly, the laminitic condition was associated with altered stress and strain levels at all proximo-distal measurement sites, both at 0 and 100% HWD.

These potential pathological changes may have important functional consequences for the afflicted animal. Firstly, the increases in stress and strain levels within a compromised laminar interface, represents a potentially catastrophic scenario, which could threaten the functional integrity of the SADP. The material properties of the SADP for the donkey are not known. However ultimate strength values have been reported both for the horse (Hallab *et al.* 1991, Burt *et al.*1997), and for Cattle (Tarlton and Webster 2000a,b, 2002, Tarlton *et al.* 2002, Maierl *et al.* 2002a,b). Values range from ~2.5 to ~5MPa. Hood (1999a) stated that the ultimate strength of the equine SADP was reduced between 43-60%, as a consequence of the laminitic condition, whilst Burt et al. (1997) reported mean ultimate strength values of 1.8 and 1.2MPa for 'Treatable' and 'Untreatable' laminitic horse respectively. If ultimate strength data for the donkey SADP are similar to those reported for the horse and cattle, and a similar reduction in ultimate strength occurs in response to laminitis, then predicted Von Mises stress values for the inner aspect of the laminitic hoof wall (i.e. ~1MPa) approach potentially critical levels. Indeed, modelled stress levels for dynamic weightbearing, i.e. loading forces equivalent to 1xBwt predict stress levels at ~3 MPa (Collins 2003 – Unpublished data).

Elevated strain levels within the outer region of the hoof wall may also lead to increased degradation, and contribute to the anecdotal association of the condition with 'poor' quality

hoof horn. Similarly, increased strain levels at the BB would further threaten the structural integrity of the white line. This may be an important factor in the processes that result in the white line changes typically seen within the laminitic hoof capsule. Finally, elevated stress levels in the region of the coronary corium would potential leave the corium susceptible to traumatic damage, which may in turn, adversely affect the normal processes of hoof horn formation.

These collective changes may in part explain the viscous cycle of insult, poor quality horn production, lesion formation and functional compromise evident within the laminitic foot, and hence contribute directly towards the chronic pain and lameness associated with the laminitic condition.

The functional consequences of the relatively modest differences in Maximum Principle, and Von Mises stress at the laminar interface between the two respective laminitic groups (Group 1 levels > Group 2) are not known. However, given a scenario whereby the ultimate strength of the SADP is reduced in response to the laminitic condition, in line with that reported by Hood (1999a), then a situation may arise whereby small differences in stress and strain levels could have pronounced function consequences.

It is also important to note that differences in HPA and capsular shape, which were not investigated in this modelling exercise, will also affect stress/strain levels within the hoof wall, and the relative proportion of axial and bending stress. These issues may be of functional significance and are considered below.

It is appreciated that the performance effects described above will be modulated by inter-animal variation in bodyweight, HPA and capsular shape. In this regard, bodyweight variation will merely affect the absolute values of stress and strain at a given location and not the nature of their distribution within the hoof wall. The precise effects of differences in HPA are however more difficult to assess. Further work is required to establish appropriate rules to describe the effect of HPA on loading patterns within the donkey foot. The effects of variations in capsular shape upon force distribution within the hoof wall are similarly, poorly defined. First principle considerations suggest that DHWA will increase the degree of axial compression, whilst decreasing the contribution from bending within the capsule. It is therefore expected that bending forces within Laminitic Group 1, which is characterised by a relatively low DHWA, will be elevated, with a corresponding reduction in axial compression. Hence predicted strain levels are likely to represent an under-estimation of actual 'in vivo' levels. This may have important biomechanical consequences especially in respect of the compromised laminar interface. Likewise upright medial and lateral quarter are likely to increase axial resistance and

decrease lateral heel expansion. This is likely to reduce the degree of bending forces experienced by the MDC, and potential limit biaxial force generation at this site.

The application of Finite Element Analysis to describe the performance of the hoof wall extends and complements the range of experimental techniques that have been used formerly to evaluate hoof wall function. A better understanding of the function of the hoof as a loadbearing element can be obtained by a detailed evaluation of the possible contributions to its overall performance from the various components of the material. In this respect FEA provides a vehicle for assessing the gross anatomical, macro- and micromechanical performance of the hoof horn material, and the effects of pathological change upon performance.

7. INTERACTIONS, PROJECT APPRAISAL AND CONCLUSIONS, AND DIRECTIONS OF FUTURE WORK

7.1 INTERACTIONS

7.1.1 STATISTICAL ANALYSIS

A statistical analysis of the data generated during this project was conducted to further explore the interactions between the quantitative radiographic appearance of the foot (Chapter 3), the morphometric characteristics of hoof wall structure (Chapter 4), and its material properties (Chapter 5). The aim of this analysis was to test the assertion that degenerative anatomic changes within the laminitic foot are associated with changes in the materials characteristics of the hoof wall. The analysis of total degenerative anatomical change was restricted to the plane of maximum variance (see Chapter 3), that is to PC1 and PC2 data only.

In addition, the relationship between the morphometric characteristics of structure and the material properties of the hoof wall were investigated. In this way, a comprehensive materials characterisation was achieved and potential structure-function relationships identified.

An essential element of such an analytical approach is also to investigate the possibility of confounding covariate effects that are not fully controlled within the study design. This is of particular relevance with regard to this project. This is because the random nature of euthanased cases prevented the establishment of 'matched' pairs within the trial groups. Hence the potential effects of, for example, age and bodyweight were not controlled within the experimental design.

An initial Pearson product moment correlation analysis was performed at an alpha level of 0.05, to interrogate the data matrix to identify potential relationships. The resultant significant interactions were further assessed using regression analysis techniques. A series of single, multiple, Best Subset and Stepwise linear regression models were evaluated at an alpha level of 0.05, to describe, model and assess these inter-relationships.

Model evaluation was based upon the R^2 (adj.) statistic associated with each regression model. Models were rejected on an arbitrary basis as being inappropriate if they failed to account for more than 30% of the observed variation within a stated response, that is at an R^2 (adj.) <30%.

7.1.2 MORPHOMETRIC CHARACTERISTICS OF STRUCTURE

The correlation matrix for the morphometric parameters of structure is given in Appendix VI. Analysis of this data matrix revealed a complex pattern of inter-relationships.

These included: -

- Significant 'within zone' structural relationships in Zones 1, 2 and 3 ($P<0.05$)
- Zonal independence of individual structural parameter 'between zones' ($P>0.05$)
- Zonal relationships between different structural parameters ($P<0.05$)

7.1.3 COVARIATE EFFECTS

7.1.3.1 CORRELATIONS

There was no relationship between age and bodyweight within the study cohort ($P>0.05$). Similarly there was no relationship between age and the radiographic parameters of the normal and laminitic foot, nor between age and either the morphometric parameters of structure, or the material properties of the hoof wall within the laminitic group.

However there were significant correlations ($P<0.05$) between bodyweight and several of these parameters as follows: -

1. In the Normal Group

Radiographic Parameters

A significant positive correlation ($p<0.05$) was evident between bodyweight and PcaSco1. Significant negative correlations ($p<0.05$) also occurred between bodyweight and radiographic Integument Depth (Parameters A and B).

2. In the Laminitic Group

Radiographic Parameters

Significant positive correlations were present between bodyweight and PcaSco1, and dorsal hoof wall angle (Parameter S). Conversely significant negative correlations occurred between bodyweight and the linear and angular radiographic descriptors DP Displacement (Parameters D and D Ratio), Integument Depth (Parameters A, B, and STTM) and Capsular Rotation (Parameter Ang H).

Morphometric Characteristics of Structure

Significant positive correlations were present between bodyweight and the following linear and area 'feature' specific parameters Z1Ma(MA), Z1Ma(MI), Z1Tu(MA), Z1Co(MA), Z2Tu(MA), Z2Tu:Ma(MA) Z3Tu:Ma(MI) and also the 'field' specific parameters Z1Ma, Tu, and Co Area measurements, and Z1Tu and Co Area Fraction.

Material Properties

A significant positive correlation was present between bodyweight and Z1 E_C.

7.1.3.2 REGRESSION ANALYSIS

A summary of the modelled associations between bodyweight, and the significant correlates which exceeded the critical R^2 (adj.) level are given for the laminitic group in Table 7.1.

Table 7.1 Summary of linear regression R^2 (adj.) data exceeding the critical level of 30% by modelled parameter.

	Modelled Parameter					
	PcaSco1	**Z1Tu(MA)**	**Z1Co(MA)**	**Z1Ma Area**	**Z1Tu Area**	**Z1Co Area**
Bodyweight	34.2	51.2	44.6	34.7	32.0	30.0

7.1.3.3 ANALYSIS OF BODYWEIGHT VARIATION BY GROUP

Subsequent analysis of bodyweight variation between groups revealed that the laminitic group had a significantly lower bodyweight than the normal group ($P<0.05$). Similarly, Laminitic Group 1 had a significantly lower bodyweight than Laminitic Group 2. There was no significant difference in bodyweight between the Normal Group and Laminitic Group 2 ($P>0.05$), however the Normal Group had a significantly greater bodyweight than Laminitic Group 1.

7.1.3.4 CORRECTING FOR BODYWEIGHT EFFECTS

In order to remove bodyweight effects from the final data analysis, regression models which exceeded the critical R^2 (adj.) level were recalculated based upon residual data (Res). The residual data were established by regressing initially both the predictor, and the response parameter, against bodyweight. In this way a 'true' R^2 (adj.) statistic could be established, that reflected the degree to which variation in the response parameter, could be explained by variation in the predictor parameter.

7.1.4 RADIOGRAPHIC MORPHOMETRIC AND MATERIAL PROPERTY INTERACTIONS

7.1.4.1 CORRELATION ANALYSIS

1. PcaSco1

<u>Morphometric Characteristics of Structure</u>

Significant positive correlations were present between PcaSco1 and the following linear and area 'feature' specific parameters Z1Ma(MA), Z1Tu(MA), Z1Co(MA), Z3Tu:Ma(MI), Z3Tu:Ma(MA), and also the 'field' specific parameters Z1Ma Area measurement and the Z1Ma, Tu and Co Area Fraction data.

<u>Material Properties</u>

A significant positive correlation was present between PcaSco1and Z1 E_C, with a trend towards a positive correlation between full HWD E_C (P=0.07).

2. PcaSco2

Morphometric Characteristics of Structure

Significant positive correlations were present between PcaSco2 and the following linear and area 'feature' specific parameters Z2Ma(MA), Z2Ma(MI), Z3Tu(MA), Z3Tu(MI) and also the 'field' specific parameters Z2Ma, Co and Tu Area measurements, and Z3Tu and Co Area measurements.

Material Properties

There were no significant correlations (P>0.05) between PcaSco2 data and the respective material properties recorded for the laminitic hoof wall.

7.1.4.2 Regression Analysis

A summary of the modelled associations that exceeded the critical R^2 (adj.) for both PcaSco1 and 2, and their respective significant correlates are presented in Table 7.2 and Table 7.3.

Table 7.2 Summary of linear regression R^2 (adj.) data exceeding the critical level of 30% by modelled parameter for PcaSco1.

	Modelled Parameter			
	Z1Co(MA)	Z1TuAF	Z1CoAF	Z1 E_C
PcaSco1	30.0	33.2	30.2	50.4

Table 7.3 Summary of linear regression R^2 (adj.) data exceeding the critical level of 30% by modelled parameter for PcaSco2.

	Modelled Parameter				
	Z2Ma(MA)	Z2Ma Area	Z2Tu Area	Z3Tu(MA)	Z3Tu Area
PcaSco2	33.0	33.9	30.1	34.1	30.0

Secondary regression analyses in respect of PcaSco1, adjusted for the linear effect of bodyweight, revealed an R^2 (adj.) statistic for Z1 E_C of 38.8. All other modelled parameters fell below the critical level of 30%.

Best Subset and Stepwise Regression analyses of the morphometric characteristics of structure indicated that a two factor model of Z1TuAF and Z1Tu(MA) represented an optimal condition, with an R^2 (adj.) of 60%. With regard to PcaSco2, the optimal condition was achieved, at an R^2 (adj.) of 48% with a two factor model of Z1Ma(MA) and Z3Tu(MA).

Further analyses of the association between the morphometric characteristics of structure and the key radiographic parameters that contribute to PC1 and PC 2 exhibited a complex pattern of interactions.

Linear regression analyses revealed that different morphometric characteristics of structure gave significant associations with the radiographic anatomy of the laminitic foot. However the degree to which specific radiographic parameters of the foot were modelled varied considerably. Similarly the ability of the different morphometric parameters of hoof wall structure to model a given radiographic feature varied considerably.

The Z1 morphometric parameters exhibited strong modelled associations with Capsular Rotation within the laminitic foot (Parameter Ang H and A:B). Conversely, Phalangeal Rotation (Ang R and PAxis) and Distal Displacement events (Parameter D, D Ratio, STTM, and B) were poorly modelled by the morphometric characteristics of hoof wall structure investigated in this study.

The specific linear regression models exceeding the critical rejection threshold of 30% were: -

- Parameter D

  $D = 28.6 - 0.305\ Z1Ma(MA) - R^2\ (adj.) = 35.8\%$

- Parameter D Ratio

  $DRatio = 0.551 - 0.00534\ Z1Ma(MA) - R^2\ (adj.) = 31.1\%$

- Parameter Ang H

  $Ang\ H = 50.6 - 0.248\ Z1Tu(MA) - R^2\ (adj.) = 30.7\%$

  $Ang\ H = 36.7 - 123\ Z1TuAF - R^2\ (adj.) = 43.5\%$

  $Ang\ H = 33.5 - 129\ Z1CoAF - R^2\ (adj.) = 38.0\%$

- Parameter Ang R

  No modelled R^2 (adj.) >30%

- Parameter STTM

  $STTM = 34.1 - 58.2\ Z2CoAF - R^2\ (adj.) = 30.2\%$

- Parameter A:B

  $A:B = 1.32 - 1.10\ Z1CoAF - R^2\ (adj.) = 38.3\%$

  $A:B = 1.34 - 1.03\ Z1TuAF - R^2\ (adj.) = 41.1\%$

  $A:B = 1.39 - 0.00247\ Z1\ Co(Ma) - R^2\ (adj.) = 30.6\%$

- Parameter PAxis

  No modelled R^2 (adj.) >30%

Analyses of the interactions between material properties and the morphometric characteristics of hoof wall structure are summarised below: -

1. <u>Zone 1 Compressive modulus</u>
   - $Z1\ E_C = 106 + 0.630\ Z1Tu(MA) - R^2\ (adj.) = 46.4\%$
   - $Z1\ E_C = 120 + 3.19\ Z1Ma(MI) - R^2\ (adj.) = 33.3\%$
   - $Z1\ E_C = 129 + 0.729\ Z1\ Co(MA) - R^2\ (adj.) = 45.1\%$

- Z1 E_C = 154 + 0.0426 Z1 Ma – R^2 (adj.) = 31.5%
- Z1 E_C = 168 + 0.00514 Z1Tu – R^2 (adj.) = 36.2%
- Z1 E_C = 174 + 0.00530 Z1Co – R^2 (adj.) = 33.3%
- Z1 E_C = 164 + 1344 Z1MaAF – R^2 (adj.) = 32.6%
- Z1 E_C = 147 + 293 Z1TuAF – R^2 (adj.) = 72.6%
- Z1 E_C = 151 + 326 Z1CoAF – R^2 (adj.) = 72.5%

2. Zone 2 Compressive modulus

   No modelled R^2 (adj.) >30%

3. Zone 3 Compressive modulus

   No modelled R^2 (adj.) >30%

Secondary regression analyses in respect of Z1 E_C, adjusted for the linear effect of bodyweight, revealed the following corrected regression models: -

- Z1 E_C Res = - 5.99 + 0.621 Z1Tu(MA) Res – R^2 (adj.) = 30.2%
- Z1 E_C Res = - 6.21 + 0.668 Z1Co(MA) Res – R^2 (adj.) = 30.4%
- Z1 E_C Res = - 5.07 + 273 Z1TuAF Res – R^2 (adj.) = 66.5%
- Z1 E_C Res = - 5.31 + 306 Z1CoAF Res – R^2 (adj.) = 65.4%

All other modelled parameters fell below the critical R^2 (adj.) level of 30%.

7.1.5 DISCUSSION

The statistical analysis detailed above highlighted a highly complex and varied picture of interactions within the laminitic foot. These interactions indicate that important structure-function relationships may be present within the hoof wall, and that degenerative events linked with the laminitic condition may be associated with changes in the material characteristics of the hoof wall. These changes appeared to be 'event specific', and that different hoof horn parameters were affected differently, dependant upon the nature of the radiographic change evident within the foot.

Analysis of the correlation matrix of the morphometric parameters of structure revealed numerous associations in both linear and area, 'feature' and 'field' specific structural characteristics within the *SM* of the laminitic donkey. Such correlations suggest that a level of control exists in the process of hoof horn formation. However the marked independence of given structural features between the respective zones of the donkey hoof wall lends support to the hypothesis of a zonal pattern of structural organisation within the donkey *SM*, and further suggest that zonal differences in hoof horn production occur. This structural independence was balanced by a variable pattern of significant cross-correlations between the different structural features both 'within' and 'between' zones.

These correlations may represent 'chance', indirect associations, or conversely they may indicate the presence of specific mechanisms that regulate structure in a manner similar to that proposed by Reilly (2001). This author suggested that these structural and zonal inter-relationships may reflect a means of achieving 'diverse biological control' within the SM, whereby the functional requirements of the hoof wall may be achieved through a number of 'subtly different mechanisms'.

The zonal differences in structural cross-correlates might reflect distinct functional differences across the HWD, or alternatively, that contributions to hoof wall function, from other levels within the design hierarchy, differ between the respective zones. Zonal differences in the pattern of structural association were also recorded in the pony by Reilly (2001). In this author's four-fold zonal division of the pony *SM*, marked differences in structural correlates were evident within the inner region of the *SM* (Z4) compared to those observed in the other zones (Z1, 2 and 3).

The data analyses in this thesis reveal potential relationships which may be of fundamental importance in hoof function. Most notable are the significant positive correlations between bodyweight and the compressive modulus within Z1, and specific morphometric characteristics of structure within this zone. These findings support the assertion of Nickel (1938, 1939) that the structural organisation evident at the microscopic level of the design hierarchy contributes to the material properties of the hoof wall, and that these properties are linked to a supportive role in static weightbearing. These findings are consistent with structure-function correlates reported both for the pony (Reilly 2001), and the donkey (Hopegood 2002). In addition, these associations indicate that the material performance of Z1 of the donkey hoof wall can, by first approximation, be interpreted in terms of composite material theory.

The absence of a similar pattern of structure-function associations within Z2 and 3 is not readily explained. However the region-specific nature of the associations across the dorso-palmar depth of the hoof wall further supports the concept of zonation within the donkey *SM*.

This 'zone specific' nature of the associations may suggests that mechanisms responsible for static weightbearing is focused within the outer region of the donkey hoof wall, that other factors within the design hierarchy predominate within these zones, or that experimental errors were more pronounced within these regions of the hoof wall.

The bodyweight relationships that have been revealed, may be related to the supportive role of the hoof horn tissue, with the structural organisation and material properties of the *SM* directly relate to the magnitude of the forces imposed upon the hoof wall during weightbearing.

The mechanics of static weightbearing within the equid hoof wall is poorly defined, however, the positive correlation recorded between Z1 E_C and bodyweight would serve to further

concentrate stress within this region of the hoof wall in response to increased bodyweight. In addition, the resultant level of deformation within the hoof would also be reduced as consequence of the increase in E_C. This may represent an important compensatory mechanism whereby a state of 'comparable' strain is achieved within the hoof horn material, in face of the higher static stress associated with increasing bodyweight.

These effects would ensure that the structures deep within the hoof are protected from excess levels of stress and strain. This may be of importance both in maintaining the functional integrity of the SADP, and also in achieving smooth and painless force transfer within the foot.

Given the complexity of the design hierarchy evident within the hoof, it is not surprising that the functionality is achieved by contributions from the different hierarchical levels. Hence simple relationships involving single structural features, or indeed a given level of the design hierarchy considered in isolation, may not be present. Similar investigations of other biological material that display a hierarchical design, for example plant tissue (Niklas 1992, Spatz *et al.* 1999) and bone (Martin and Boardman 1993, Riggs *et al.* 1993) have revealed that complex multi-variable and multi-hierarchical interactions are commonplace within nature. It is possible that factors other than those recorded in this study may be important determinants of material properties. (For example: at a macroscopic level, by TD, at the microscopic level, by variations in the relative development of the different cortical regions, and/or at the ultrastructural level, by differences in keratin and lipid proportions and biochemistry). In addition, the mixed tubule morphology which characterised Z2 may further complicate the nature of the structure-function relationship within this particular zone. In this regard, significant associations between TD and bodyweight have been reported both for the pony (Reilly 2001) and the donkey (Hopegood 2002). Further work incorporating the objective characterisation at both the ultrastructural and molecular levels is required in order to provide an all encompassing structure-function model for the donkey hoof wall.

Chapter 4 commented upon the indistinct nature of the cortico-intertubular boundary of the Type 3 donkey tubule within Z2 and 3. This was in marked contrast to the distinct boundary of the Type 1 tubule in Z1. Hence it is possible that the measurement error within Z2 and 3 was greater than that within Z1.

Given the statistically significant associations reported above, it is not unreasonable to assume that biofeed-back mechanisms operate within the hoof wall to allow control and regulation of material properties in response to increased load, in a manner similar to that evident with other supportive tissues such as bone and tendon. In this way, the mechanism of hoof horn production from the coronary region may be under direct stress and/or strain level control to ensure that the morphometric characteristics of structure, and/or the material basis of the hoof horn, are

sufficient to accommodate the forces associated with weightbearing. Modelled stress and strain distribution within the donkey hoof wall, given in Section 6.9.1, predict maximal surface levels for the dorsal aspect of the hoof wall which are focused upon the proximal coronary region. This would represent an optimal condition for such a biofeed-back mechanism operating within Z1 at the MDC. Further work is however required to confirm the hypothesis of feed-back regulated horn production within this region of the donkey hoof wall. This could be achieved either through '*in vivo*' trials involving the stereometric assessment of material obtained from weight-matched animals subjected to different levels of mechanical stimuli. Conversely '*in vitro*' trials may be possible subjecting dermo-epidermal explants from the coronary region, to different levels of mechanical stress.

The findings of this present study highlighted a different pattern of structure-function associations to those reported by Reilly (2001) for the pony. Reilly (2001) reported statistically significant positive correlations between bodyweight and structural parameters across the entire dorso-palmar depth. Specifically this author reported highly significant correlations, with coefficients >0.7 for Z1Co, Z2 Co, Z3Tu, and Z4Ma area measurements. This may indicate important 'species specific' differences either in the manner in which the hoof wall accommodates forces and/or that difference modes of weightbearing are present. These 'species-specific' differences may in part account for the difference in structural organisation of the *SM* evident between the donkey and the equine.

Conversely differences in the pattern of association may have arisen as a consequence of laminitic change within the material investigated in this study. Indeed the correlation coefficients, which reflect the strength of the modelled association, revealed in this present study were consistently lower than the values reported by Reilly (2001). This may indicate that the laminitic condition results in the diminution of these associations, or that they become more variable.

The absence of an age related affect in respect of the morphometric characteristics of structure, or the material properties of the donkey hoof wall was in marked contrast to the age related associations reported for the equine by Schroth (2000) and Reilly (2001), and the excepted dogma that cortical size increases with age (Schummer *et al.*1981). The absence of an age effect may reflect the fact that the animals used in this present study represented a cohort of fully mature equids, whereas the animals investigated by Schroth (2000) and Reilly (2001) included individuals at different developmental stages. Commenting upon the effect of age upon hoof wall structure Reilly (2001) suggested that bodyweight, more so than age, dictated tubular morphometry within the pony *SM*. Similarly Hopegood (2002) reported limited age dependant effects on TD within the donkey hoof wall, and indeed no effect upon material properties of the

hoof wall. It is also possible that the absence of age related effects in this present study results is an indirect indicator of a laminitic effect. This would be consistent with the findings of Collins (1997) in the pony, and Mostafa and El-Ghoul (1999) in the horse, that the laminitic condition is associated with a decrease in Tu and Co Area and Area Fraction.

The evidence of a laminitic condition effect upon the morphometric characteristics of structure was variable. At a macroscopic level absolute values of HWD did not conform to the predictive bodyweight algorithm described for the normal donkey by Hopegood (2001). This departure, combined with the significant correlation that is evident both between actual HWD and PcaSco1, and between actual HWD and the respective radiographic parameters Ang H, A, B, and A:B suggests that Capsular Rotation within the laminitic foot exerts a direct effect upon hoof wall structure. This relationship is consistent with the assertion that this specific rotational event results in elongation of the dorso-palmar extent of the coronary corium, which leads to a corresponding increase in HWD, commensurate with the degree of rotation.

The absence of a similar association with regard to parameter Ang R is to be anticipated. This is because the normal anatomical relationship that exists between the DP and the hoof wall is largely unaffected by Phalangeal rotation. Hence the coronary corium is not subjected to anatomical dislocation in the same manner to that which occurs in association with Capsular rotation events.

The absence of a relationship between HWD and the specific radiographic parameters which assess DP displacement (i.e. Parameter D and D ratio) was, however, surprising. This is because dislocation of the coronary corium is to be expected as a consequence of this specific degenerative event. This may indicate that a degree of DP displacement may be possible within the laminitic foot, before anatomical dislocation of the coronary corium occurs.

A highly complex pattern of associations were evident between the radiographic anatomy of the laminitic foot, and structural characteristics of the hoof wall at the microscopic level of the design hierarchy. However the true nature of these relationships was difficult to establish given the confounding effect of bodyweight within the trial design. Partial correlation analyses, which correct the data in respect of the linear effects of bodyweight, provide a realistic picture of the 'true' level of association between parameters. These analyses highlighted the presence of several significant associations, albeit that the 'strength' of the specific associations were lower than those calculated in the initial analysis. These 'corrected' findings lend support to the possibility of a direct laminitic effect upon hoof wall structure.

The data analysis suggests that the laminitic effect upon structure at the microscopic level is both 'zone specific' and 'event specific'.

With regard to the 'zone specific' nature of the laminitic effect, the 'response' is most pronounced within Z1 both in terms of the absolute number of significant associations, and also in the magnitude of the R^2 (adj.) statistic. However the laminitic effect was related to the nature of the radiographic changes within the affected foot. In this regard, events associated with PcaSco1 were predominantly marked by significant associations with Z1 structure. Conversely, events associated with PC2 were characterised by structural associations in Z2 and Z3.

It was not possible, given the experimental design of this project, to further elucidate the precise nature of the zonal and event specific effects, nor to investigate their inter-relationships. This would require a complex factorial experimental design, with animals carefully selected on the basis of anatomical changes evident in the radiographic anatomy of the foot.

The precise mechanisms which account for these structural changes are not known. However the 'zone specific' nature of the response suggests that either the effect of the laminitic condition is more pronounced within the outer region of the coronary corium, or alternatively that this region is more susceptible to laminitic effects. The 'event specific' nature of the 'response' however indicates that the different degenerative events affect the process of hoof horn formation differently.

The potential functional consequence of these laminitic effects is further highlighted by the significant associations which occur both between PcaSco1 and the Z1 E_C, and between the structural characteristic of Z1and Z1 E_C. The modelled effect that this zonal change in material property has upon stress and strain distribution within the hoof wall has been detailed in Section 6.9.3, and its potential impact upon the functionality of the foot described in Section 6.10. These relationships suggest that degenerative events associated with PC1 have a pronounced upon Z1 structure, and that these structural changes adversely affect hoof wall function as a consequence of changing the material properties of this zone. Conversely, events associated with PC2 have a modest effect within this Z1, and therefore exert a modest effect upon the material property of this zone. Hence these events have a minimal effect upon normal hoof function.

Chapter 3 stated that PC1 was characterised by Capsular Rotation and DP Displacement, whereas PC2 was associated with Phalangeal rotation within the foot. These differences, combined with the changes in hoof wall structure and material property described above, may in part explain the empirical observation described in chapter 1 that the donkey is not tolerant of capsular rotation.

The significant correlations evident between Z1 E_C and the morphometric characteristic of structure, including Tu and Co AF data indicate that it is possible to interpret the material performance of this region of the laminitic hoof wall in terms of composite theory. This may

have important implications in terms of developing effective screening programs for the detection of potential hoof problems, and monitoring the efficacy of treatment protocols.

The relationships evident within this zone also offer an insight into possible failure modes within the structure. In this regard Z1 E_C was correlated with the relative thickness of the horn tubule only, and not the spatial distribution of the cortical material. This would suggest that Z1 horn tubules are potentially susceptible to Local as opposed to Euler buckling effects. This may be of particular significance given the association of the laminitic condition with tubule kinking, the classical sign of local buckling. This may provide an alternative explanation for the occurrence of this feature within laminitic hoof horn.

In conclusion, this statistical investigation suggests that the structural characteristics and material properties at the MDC sampling site of the laminitic donkey hoof wall are, in part, related to the anatomy of the laminitic foot, and in particular, to the degree of capsular rotation evident within the afflicted foot. These relationships are however restricted, at this sampling site, to Z1, and the respective 'strength' of these associations are variable.

Whilst the association between Z1 Ec and the radiographic anatomy of the laminitic foot is 'strong', the relative 'strength' of the associations between the individual structural parameters, and the radiographic anatomy, are relatively 'modest'. This difference in the relative strength of the association is however to be anticipated. This is because the material properties of the hoof wall are likely to be determined by both the hoof horn material, and the structural organisation of this material. Hence disruption to any one of the specific mechanisms that control hoof horn production, as a sequela to pathophysiological events within the foot, are likely to result in material property changes, irrespective of the specific mechanism which is affected.

Conversely, individual structural parameters are likely to be under the regulation of specific mechanisms of control. Hence changes in a given structural parameter will only occur if the specific regulating mechanism is affected by the pathophysiology of the condition. It is therefore conceivable, given the varied array of pathophysiology encountered within the laminitic foot, that material property changes occur in all cases, whereas changes in a given structural parameter are more varied.

7.2 PROJECT APPRASAL

The use of morbid hoof capsules offers several advantages over alternative modes of material sourcing. The materials characteristics of hoof horn material obtained in this way are minimally affected by mechanical and environmental degradation. This is of particular relevance to the assessment of laminitic hoof horn, where changes in both structure and material properties are likely sequelae of pathology. The physical constraints placed upon the size, and orientation of

test specimens that can be produced are minimal in comparison with other modes of material sourcing. This is of particular relevance with regard to the material testing of hoof horn. Samples of sufficient size can be produced such that the effects of structure upon the material properties of the hoof wall can be investigated.

Specimen geometry is a limiting factor in the testing of biological materials. Hence the use of morbid hoof capsules gives greater flexibility in the range of testing techniques that can be employed, and the manner in which these techniques can be applied in relation to the structural organisation of the hoof wall. This is importance as effective testing of biological materials is dependent upon the simulation of 'in vivo' conditions. These particular issues are discussed in detail in Chapter 5.

The use of morbid hoof capsules provides the unique opportunity to perform morphometric, material testing and moisture analyses, on both full HWD and zonal samples that has been obtained from concurrent hoof horn material within the same hoof. No other mode of material sourcing can do this.

Obtaining morbid source material that has not been altered pathologically represents a problem in the UK, given the high incidence of degenerative foot problems. Hence it is unlikely that effective control material can be obtained from UK donkeys, euthanased on medical grounds. Hence sourcing morbid material from donkeys living in their natural arid environment may be the only means of obtaining normal control material. Although this option was not available for this project, this represents a key area for future research.

The sectioning protocols detailed for the hoof wall represent the first reported methodology for the preparation of histology samples from untreated hoof horn material for morphometric assessment at the macroscopic and microscopic level. Indeed these techniques have proved successful in producing sections from pathologically altered material that is widely recognised as being difficult to work with.

Avoiding the need for fixation and embedding reduces the procedural time in sample preparation. It also minimises the risk of artefacts production occurring during section preparation. This further increases the likelihood that observed changes in structure are related to the prevailing pathology.

The successful production of untreated samples also favours the future use of immunohistochemical techniques. This is because, specimen fixation is known to decreases antigenicity (Budras *et al.* 2002). This is of particular relevance to hoof horn assessment at the ultrastructural level, where immunohistochemical techniques are often employed. These techniques have been used to conduct keratin characterisation within the hoof e.g. Pellmann *et al.* (1993), Wattle (1998, 2000, 2001), Patan (2001) and König (2001). This may be of particular

significance with regard to the laminitic condition, as changes in keratin expression are considered to be pathognomonic (Obel 1948).

The IAS offers the opportunity to place hoof horn assessment on a quantitative basis. It affords the opportunity to apply more sophisticated stereometric techniques. In particular 'feature' specific linear and area measurements can be achieved. This enables a more detailed characterisation of structure, and hence can lead to an effective elucidation of the structure-function interactions of the hoof.

Similarly the IAS afforded the opportunity to develop new approaches for the assessment of the radiographic anatomy of the donkey foot, and the objective characterisation of anatomical change within the laminitic foot.

The development of reliable methods for the evaluation of the material properties of both full HWD, and zonal laminitic hoof horn samples which give consistent and repeatable data, have enabled the further elucidation of the material properties of this pathologically altered material. Achieving this objective has enabled the further understanding of the structure-function relationships within the donkey hoof wall.

Finally, the successful application of computer modelling techniques have provided a means of investigating hoof wall function at the gross, macroscopic and microscopic level of the design hierarchy. In addition, these techniques offer new insights as to the potential functional consequences of change in the structural and material properties of the hoof wall associated with the laminitic condition.

The accuracy of any modelled solution is dependant upon the assumptions made in the development of the model. Confidence in the model can be taken from the fact that the predicted responses at the gross anatomical level are consistent with the recognised pattern of 'in vivo' hoof wall deformation, and that strain values are of a similar order of magnitude to previously reported 'in vivo' values.

7.3 PROJECT CONCLUSIONS

It is not possible at this stage to state whether these structural and material property 'response's are of a formational origin, resulting from pathological alteration to the normal process of hoof horn production. Conversely, they may arise as a consequence of a biofeed-back response to the alteration in the normal pattern of weightbearing which is characteristic of the laminitic condition. Further studies are required in order to elucidate the precise mechanism responsible for these 'responses'.

Given the unavoidable confounding effect of bodyweight present within this initial screening trial, caution must taken in drawing definitive conclusions as to the effects of the laminitic

condition upon the hoof wall. There is a need to repeat this study in a controlled manner, using weight-matched normal and laminitic animals. In addition the effect of the hydration status of the material must be considered before accurate 'in vivo' data can be achieved. This need to encompass an assessment of gross moisture levels, an elucidation of how water specifically interacts with the material, and an evaluation of the consequences of this interaction in terms of the modulation of material properties.

In this way, baseline models of the structure-function can be established based upon radiographic, morphometric and material property data, against which the effects of the laminitic condition can be assessed. If this achieved, it may be possible to derive robust predictive models for the condition that are of clinical importance both for the diagnosis of the condition, and also for monitoring response to therapy.

This thesis has highlighted the fact that the donkey must be viewed as a unique equid, and that the application of an equine model to the donkey hoof and is inappropriate and unsatisfactory.

This thesis gives evidence that supports the assertion that the laminitic condition is associated with structural and material property changes within the donkey hoof wall. Evidence is also presented that suggests that these changes in materials characteristics may affect normal process of hoof wall function. In addition, the material characteristics of the donkey hoof wall are related both to the nature and extent of the anatomical changes evident within the radiograph of the affected foot.

By further understanding the effect of the laminitic insult on the coronary corium, and the subsequent response within the *SM* it may be possible to break the cycle of insult of poor quality horn production, lesion formation and functional compromise to the hoof. In this way, it may ultimately be possible to reduce the incidence and severity of lameness.

Computer modelling of the *SM* at both the macroscopic and microscopic level may help resolve the functional consequences of any formational structural change within the *SM* associated with the factors discussed. Alternatively, computer modelling may provide an insight as to the origin of deformational changes within the *SM*.

By investigating the effects of laminitis upon the structural organisation of the *SM*, and by developing an understanding of the functional consequences of change, it may be possible to design enhanced screening and therapeutic regimes, and enable objective evaluation of their effects. Thus further understanding of hoof horn structure-function relationships will bring benefits to the welfare and management of the laminitic donkey.

7.3.1 ENUMERATED CONCLUSIONS

The work for thesis has made original contributions to scientific endeavour and to knowledge in the following ways: -

1. Protocols have been established for the collection, preparation, and objective assessment of structural and functional characteristics of laminitic donkey hoof horn, and methods for the investigation of the structure-function relationships within the donkey hoof wall.
2. New methods have been developed for the preparation of histology sections from this pathologically altered and friable material
3. Multivariate statistical techniques have been employed to characterise the radiographic anatomy of the donkey foot, and to assess the nature and the extent of anatomical change associated with the laminitic condition.
4. Baseline data has been obtained for the radiographic anatomy of the normal donkey hoof.
5. Comparison of these data, with that previously reported for the pony and the horse suggest that guidelines for diagnostic and prognostic interpretations should be revised for the donkey.
6. Two distinct Laminitic Sub-Groups have been identified, characterised by differences in the nature of the DP dislocation, and also the occurrence of roentogenic changes to the DP, evident within digital radiographs.
7. The morphological and morphometric characteristics of structure have been defined, and the zonal characteristics evaluated. A three-fold zonal division is suggested for the donkey based upon variation in tubular morphology. This zonation pattern differs from that reported for the horse, with regard to the relative dorso-palmar extent of the three respective zones.
8. Irregularities in structure at the microscopic level of the design hierarchy have been identified. These structural irregularities have been defined, and their zonal distributions within the *SM* have been detailed.
9. Significant 'between group' differences were recorded in various linear and area, 'feature' and 'field' specific structure parameters.
10. Preliminary investigations, reported in Hopegood *et al.* (2003a) established that there was no significant 'laminitic effect' upon the hydration characteristics of either full HWD or zonal material.
11. Material properties of perceived functional importance have been evaluated in response to compression, for full HWD and zonal material. The material's resistance to

deformation (E_C) and its energy absorbing characteristics have been defined. The strain rate dependency of E_C for full HWD samples has been elucidated, and ratio of axial to lateral E established. The effect of structure upon material properties has been elucidated, by controlling for the modulating effect of moistur.e

12. Full HWD E_C was strain rate dependent, a three order of magnitude change in strain rate resulted in a 29% increase in E_C. The material is characterised by mean axial to lateral E_C ratio of 1.5:1, and a dorso-palmar decrease in zonal E_C across the HWD. Significant 'between group' differences were recorded in Z1 E_C. There was no significant 'between group' difference in energy absorbing capacity.
13. Protocols have been developed to enable the application of the computer modelling technique of Finite Element Analysis. These included methods for the characterisation of hoof wall shape, structure and material properties. In this way the gross anatomical, macro and micro-mechanics of the hoof wall have been investigated, structure-function relationships have been explored, and hoof wall function has been elucidated. In addition, the potential effects of the laminitic condition upon hoof wall function have been modelled.
14. Modelled data indicates a pattern of hoof wall function consistent with 'in vivo' observations. The material properties of the hoof wall facilitate the smooth transfer of stress across the dorso-palmar HWD. Macromechanical investigations suggest that the material properties of the hoof wall can be explained in terms of composite material theory. Micromechanical modelling highlighted the effects upon stress and strain concentration within the hoof wall, resulting from the organisation of the hoof horn material into tubular and intertubular components.
15. Modelled data suggest that changes in material properties associated with the laminitic condition alter the normal pattern of stress and strain distribution with the hoof wall. These changes increase the level of stress and strain acting upon the laminar interface. This may contribute to the pain and lameness associated with the chronic laminitic condition, and can also explain the variation in lameness evident in clinical presentation of the laminitic animal.
16. These changes, combined with the reported decrease in the ultimate strength of the SADP may represent a viscious cycle of degenerative change which the affected foot. This may explain the progressive nature of the digital collapse seen within refractory exacerbative laminitic cases.
17. The significant associations evident between specific parameters of the radiographic anatomy of the laminitic foot, and the structural characteristics, and material property of

the hoof wall, may be of significance regarding condition severity, recovery outcome, and differences between refractory exacerbative and chronic remissive cases.

18. The modelled effect upon hoof wall function of material property changes, and the effects of structure upon material property, and their inter-relationships with the radiographic anatomy of the foot may explain the reported associations between DP dislocation and recovery outcome.

7.4 SUMMARY OF FUTURE WORK DIRECTIONS

A summary of suggested areas of future research is presented below: -

1. There is a need to build upon the radiographic baseline data for both normal and laminitic cases. In this way, unbiased mathematical models for the diagnosis and classification of the laminitic condition may be possible.
2. Further investigation of the inter-relationships between the radiographic anatomy of the foot and structure and material properties of the hoof wall are required. Detailed knowledge in this area may form a basis for differentiating between chronic remissive and refractory exacerbative laminitic cases.
3. There is a need for controlled and blinded trials to repeat the morphometric characterisation of structure within laminitic hoof wall, and compare these data with that obtained from weight-matched normal donkeys.
4. The materials characterisation presented in this thesis needs to be conducted at other sites within the hoof wall in order to effectively map the structural and material properties of this important weightbearing structure.
5. Techniques need to be developed to complete the materials characterisation at other levels within the design hierarchy. Only in achieving this, will the structure-function relationships that operate within the hoof wall be fully elucidated.
6. There is a need to obtain baseline data for the material properties of the SADP, and investigate the effects of the laminitic condition upon these properties.
7. There is a need to monitor changes in structure and material properties of the laminitic hoof wall over time, and in response to different treatment modalities.
8. In order to further develop an understanding of hoof wall function, the debilitating effects of the laminitic condition, and to improve treatment regimes, there is a need to further develop the computer modelling of the hoof wall. Important area of future modelling work include:
   - Functional evaluation of the effects of capsular geometry, and the changes in shape associated with the laminitic condition.

- Development of a model for the equid foot.
- Dynamic simulation of equid locomotion.
- Model remedial farriery effects.

9. Appropriate 'in vivo' methods for assessing hoof function need to be achieved to provide effective data for model validation. This will necessitate both kinetic and kinematic methods of investigation.
10. Finally, the effects of degenerative anatomical change within the laminitic foot also need to be investigated upon other capsular components, e.g. the white line and sole, in a similar multidisciplinary fashion. In this way, other important pathognomonic changes associated with the laminitic condition may be revealed.

REFERENCES

ACKERMAN, N., GARNER, H.E., COFFMAN, J.R. AND CLEMENT, J.W. (1975) Angiographic appearance of the normal equine foot and alterations in chronic laminitis. *J. Am. Vet. Med. Assoc.* **166**, 58-62.

ÅKERBLOM, E. (1934) Uber die Aetiology und Pathogenes der Futterrehe beim Pferdes. *Scand. Archiv. Physiol. Suppl.* **68** (Diss. med. vet., Stockholm).

ALBARANO, T. (1993) Der Einfluss der Umgebung auf die Zugfestigkeit und Harte des Klauenhorns von Rind und Schwein. Diss. med. vet., Zurich.

ALBERTS, B., BRAY, D., LEWIS, J., RAFF, M., ROBERTS, K. AND WATSON, J.D. (1994) *Molecular Biology of the Cell.* Ed: R. ADAMS, 3rd Edn., Garland Publishing Inc., London. pp 330-1046.

ALFORD, P., GELLER, S., RICHARDSON, B., SLATER, M., HONNAS, C., FOREMAN, J., ROBINSON, J., MESSER, M., GOBLE, D., HOOD, D. AND CHAFFIN, M (2001) A multicenter, matched case-control study of risk factors for equine laminitis. *Prev. Vet. Med.* **49**, 209-222.

ALLEN, D., KORTHUIS, R.J. AND CLARK, E.S. (1988) Starling forces in the equine digit. *J. Appl. Physiol.* **64**, 1580-1583.

ALT, M. (1990) *Exploring hyperspace: A non-mathematical explanation of multivariate analysis.* McGraw-Hill Book Co (UK) Ltd., London. pp. 139.

ANON (1992) *Integumentum commune.* In: *Illustrated Veterinary Anatomical Nomenclature.* Ed: O. SCHALLER, Vienna. pp 545-561.

ANON (1994) *Nomina Anatomica Veterinaria.* International Committee on Veterinary Anatomical Nomenclature. 2nd Edn., Ed: O. SCHALLER, R.E. HABEL and J. FREWEIN, Vienna.

ASTM D 695 – 96 (1996) Standard Test Method for Compressive Properties of Rigid Plastics. A.S.T.M., Philadelphia.

ASTM D 1621 – 00 (2000) Standard Test method for Compressive Properties of Rigid Cellular Plastics. American Society for Testing and Materials (ASTM), Philadelphia.

ASTM D 1576 – 90 (reapproved 1995) Standard Test Method for Moisture in Wool by Oven Drying. American Society for Testing and Materials (ASTM), Philadelphia.

ASTM D 3878 – 95c (1996) Standard Terminology of High-Modulus Reinforcing Fibres and Their Composites. American Society for Testing and Materials (ASTM), Philadelphia.

ASTM D 6108 – 97 (1998) Standard Test Method for Compressive Properties of Plastic Lumber and Shapes. American Society for Testing and Materials (ASTM), Philadelphia.

ASTM E 6 – 89 (1989) Standard Terminology Relating to Methods of Mechanical Testing. American Society for Testing and Materials (ASTM), Philadelphia.

ASTM E 9 – 89A$^{\varepsilon 1}$ (1989) Standard Test Methods of Compression Testing of Metallic Materials at Room Temperature. American Society for Testing and Materials (ASTM), Philadelphia.

ASTM E 111 – 82 (Reapproved 1998) Standard Test Method for Young's Modulus, Tangent Modulus and Chord Modulus. American Society for Testing and Materials (ASTM), Philadelphia.

BAILEY, S.R. (1998) *A study of the vascular effects and factors regarding the concentration of 5-hydroxytryptamine in the equine digital circulation.* PhD Thesis. RVC, London.

BAILEY, S.R. AND ELLIOTT, J. (1998) Plasma 5-hydroxytryptamine constricts equine digital blood vessels *in vitro*: implications for pathogenesis of acute laminitis. *Equine Vet. J.* **30**, 124-130.

BAILLIE, C., SOUTHAM, C., BUXTON, A. AND PAVAN, P. (2000) Structure and properties of bovine hoof horn. *Adv. Compos. Lett.* **9**, 101-113.

BALCH, O.K., WHITE, K. AND BUTLER, K. (1991) Factors involved in the balancing of equid hooves. *J. Am. Vet. Med. Assoc.* **198**, 1980-1989.

BALCH, O.K., BUTLER, D. AND COLLIER, M.A. (1997) Balancing the normal foot: hoof preparation, shoe fit and shoe modification in the performance horse. *Equine Vet. Educ.* **9**, 143-154.

BANKS, W.J. (1993) *Applied Veterinary Histology.* 3rd Edn., Mosby Yearbook, London. pp 311-325.

BARTEL, D.L., SCHRYVER, H.F., LOWE, J.E. AND PARKER, R.A. (1978) Locomotion in the horse: A procedure for computing the internal forces in the digit. *Am. J. Vet. Res.* **39**, 1721-1727.

BAXTER, G.M. (1986) Equine laminitis caused by distal displacement of the distal phalanx: 12 cases (1976-1985). *J. Am. Vet. Med. Assoc.* **189**, 326-329.

BAXTER, G.M. (1992a) Laminitis: In Current Therapy in Equine Medicine Ed: L. W. B. MILLS. Saunders, Philadelphia. pp 154-160.

BAXTER, G.M. (1992b) Equine laminitis. *In Practice.* **14**, 13-22.

BAXTER, G.M. (1994) Acute Laminitis. *Vet. Clin. N. Am.-Equine Pract.* **10**, 627-642.

BEEK, M., KOOLSTRA, J.H., van RUIJUVEN, L.J. AND Van EIJDEN, T.M. (2001) Three-dimensional finite element analysis of the cartilaginous structures in the tempromandibular joint. *J. Dent. Res.* **80**, 1913-1918.

BEKO, J. (1967) Trocknungsversuche und histologische Untersuchungen sowie Messungen der Stärke der Zehenwand am Klauenhorn vom Österreichischen Fleckvieh. *Wien Tierarztl. Mschr.* **54**, 562-563.

BENNETT, D.K. (1980) Stripes do not a zebra make, part 1: a cladistic analysis of *Equus*. *Syst. Zool.* **29**, 272-287.

BENNETT, D. (1992) The Evolution of the Horse. In: *World Animal Science C, Production-System Approach 7, Horse Breeding and Management.* Ed: J. WARREN
EVANS, Elsevier, Amsterdam. pp 1-80.

BERGSTEN, C. (1994) Haemorrhages of the Sole Horn of Diary Cows as a Retrospective Indicator of Laminitis: An Epidemiological Study. *Acta Vet. Scand.* **35**, 55-66.

BERTRAM, J.E.A. (1984) *Fracture toughness design in equine hoof wall.* MSc Thesis. University of British Columbia.

BERTRAM, J.E.A. AND GOSLINE, J.M. (1986) Fracture toughness design in horse hoof keratin. *J. Exp. Biol.* **125**, 29-47.

BERTRAM, J.E.A. AND GOSLINE, J.M. (1987) Functional design of hoof horse keratin: the modulation of mechanical properties through hydration effects. *J. Exp. Biol.* **130**, 121-136.

BIEWENER, A.A. (1992) *Biomechanics - Structures and Systems. A Practical Approach.* IRL Press, Oxford University Press, Oxford. pp 286.

BISCHOFF, J.E., ARRUDA, E.M. AND GROSCH, K. (2000) Finite element modeling of human skin using an isotropic, nonlinear elastic constitutive model. *J Biomech.* **33**, 645-652.

BOLBOL, A.E. AND SALEH, A.S. (1987) Survey on equine hoof affections in upper Egypt. *J. Egyptian Vet. Med. Assoc.* **47**, 545-553.

BOLLIGER, C.H. (1991) *The equine hoof: morphological and histochemical findings.* Diss. med. vet., Zurich.

BORDALAI, C.C. AND NIGAM, J.M. (1977) Angiographic studies of Donkey foot (Normal and Abnormal). *J. Am. Vet. Radiog. Soc.* **18**, 90-92.

BOWDEN, P.E., QUINLAN, R.A., BREITKREUTZ, D. AND FUSENIG, N.E. (1987) Expression and modification of keratins during terminal differentiation of mammalian epidermis. *Curr. Top. Dev. Biol.* **22**, 35-68.

BRADLEY, H.K., SHANNON, D.D. AND NEILSON, D.R. (1989) Subclinical laminitis in dairy heifers. *Vet. Rec.* **125**, 177-179.

BRAGULLA, H. (2003) Fetal Development of the Segment-Specific Papillary Body in the equine Hoof. *J. Morphol.* **258**, 207-224.

BRAGULLA, H., MÜLLING, C. AND BUDRAS, K-D. (1992) Light- and ultramicroscopic studies of hoof horn keratinization with special reference to aseptic inflammation of the bovine and equine digit. In: *Proceedings of the VII International Symposium on Disorders of the Ruminant Digit,* Rebild, Denmark. Ed: K. MORTENSEN.

BRIDGES, J. (1752) *No foot, No Horse: an Essay on the Anatomy of the foot of that Noble and Useful animal the Horse.* Brindley, London.

BRITISH STANDARD EN 20287 (1994) Paper and board - determination of moisture content - oven-drying method. 1-4. British Standards Institute.

BRITISH STANDARD EN 2746 (1998) Glass fibre reinforced plastics - flexural test - three point bend method. British Standards Institute.

BRUHNKE, J. (1931) Vergleichende Untersuchungen der Hornwandstruktur des Zehenendes bei Huf und Klauentieren. *Deutsche Tierarztliche Wochenschrift.***1**, 4-10.

BUCHER, K. (1987) *Zum mikroskopischen Bau der Epidermis an umschriebenen Stellen des Pferdehufes.* Diss. med. vet., Zurich.

BUDRAS, K.D. AND BRAGULLA, H. (1990) Besonderheiten des Membrane-Coating-Materials (MCM; Kittsubstanz zwischen Keratinozyten) im harten Horn des Pferdehufes. *Anat. Anz. Suppl.* **170**, 435-436.

BUDRAS, K-D. AND HUSKAMP, B. (1990) Normalisierung von Struktur und Qualität der Hufkapsel nach orthopädischer Behandlung der chronischen Hufrehe. *Arbeitstagung der Fachgruppe Pferdekrankheiten der DVG.* **11**, 174-181.

BUDRAS, K-D. AND HUSKAMP, B. (1999) Belastungshufrehe – Vergleichunde Betrachtungen zu anderen systemischen Hufreheerkrankungen. *Pferdeheilkunde.* **15**, 89-110.

BUDRAS, K-D. AND PATAN, B. (2003) Segmentspezifitäten am Pferdehuf – Teil I: Struktur- und Funktionsvarianten. *Pferdeheilkunde.* **19**, 58-64.

BUDRAS, K-D. AND SCHIEL, C. (1996) A comparison of horn quality of the white line in the domestic horse (*Equus caballus*) and the Przewalski horse (*Equus przewalskii*). *Pferdeheilkunde.* **12**, 641-645.

BUDRAS, K-D., HULLINGER, R.L. AND SACK, W.O. (1989) Light and electron microscopy of keratinization in the laminar epidermis of the equine hoof with reference to laminitis. *Am. J. Vet. Res.* **50,** 150-1159.

BUDRAS, K-D., HUSKAMP, B. AND BRAGULLA, H. (1992a) Normal and pathological structure of hoof horn and ways of improving its quality. In: *12 Arbeitsgagung der Fachgruppe Pferde krankheiten,* Wiesbaden, 9th – 10th April. pp 49-57.

BUDRAS, K-D., BRAGULLA, H., MÜLLING, C.H. AND REESE, S. (1992b) Concerning the structure of the healthy and laminitis affected equine hoof. In: *Proceedings of the VII International Symposium on Disorders of the Ruminant Digit,* Rebild, Denmark. Ed: K. MORTENSEN.

BUDRAS, K-D., SACK, W.O. AND RÖCK, S. (1995) *Anatomy of the horse, an illustrated guide.* 2nd Edn., Mosby-Wolfe, Hannover.

BUDRAS, K-D., BRAGULLA, H., PELLMANN, R. AND REESE, S. (1996) Das Hufbein mit Periost und Insertionszone des Hufbeinträgers. *Wien. Tierarz. Monats.* **84**, 241-247

BUDRAS, K-D., SCHIEL, C. AND MULLING, C. (1998a) Horn tubules of the white line: an insufficient barrier against ascending bacterial invasion. *Equine Vet. Educ.* **10**, 81-85.

BUDRAS, K.D., GEYER, H., MAIERL, J. AND MULLING, C.K.W. (1998b) Anatomy and structure of hoof horn (Workshop Report). In: *Proceedings of the X International Symposium on Lameness in Ruminants*, Lucerne, Switzerland, 7th – 10th September. Ed: CH. J. LISCHER and P. OSSENT. pp 176-188.

BUDRAS, K.D., SCHIEL, C., MULLING, C.K.W. AND PATAN, B. (2002) Method for preparing thin sections of untreated hoof horn for electron microscopic examination. *Microsc. Res. Tech.* **58**, 114-120.

BUTLER, K.D. (1976) *The effect of feed intake and gelatin supplementation on the growth and quality of the equine hoof.* PhD Thesis. Cornell University, Ithaca, New York.

BUTLER, K.D. (Jr) AND HINTZ, H. F. (1977) Effect of level of feed intake and gelatin supplementation on growth and quality of hoofs of ponies. *J. Anim. Sci.* **44**, 256-261.

BUTLER, J.A., COLLES, C.M., DYSON, S.J., KOLD, S.E. AND POULOS. P.W. (1998) *Clinical Radiography of the horse.* Blackwell Science, Oxford. pp 547.

CALLISTER, W.D. Jr. (1994) *Materials Science and Engineering: An Introduction.* 3rd Edn., J. Wiley & Sons Inc., New York. pp 811.

CHANDRA, I.S., NIGAM, J.M., SINGH, A.P. AND SINGH, K. (1982) Radiographical diagnosis of equine chronic laminitis (founder). *Indian Vet. J.* **59**, 640-641.

CHANG, Y.H., SHERRILL, J. AND BERTRAM, J.E.A. (1993) Hoof wall function in horses and donkeys - experimental alteration of surface strain. In: *Proceedings of the 1993 IEEE 19th Annual Northeast Bioengineering Conference,* 18th –19th March. Ed: J.K.J. LI and S.S. REISMAN, IEEE Service Centre, Piscataway, New Jersey. **98**, 64-65.

CHAPMAN, B. AND PLATT, G.W. (1984) Laminitis. In: *Proceedings of the Annual Meeting of American Association of Equine Practitioners.* **30**, 99-112.

CHAUVEAU, A. (1853) *La Structure et al Secretion de la Corne. Influence du systeme nerveux sur les proprietes nutritives et secretoires de la membrane keratogene et sur la nutrition et les secretions en general.* Lyon.

CLARK, B. (1817) *Stereoplea or the artificial defence of the horse's hoof considered.* London, printed for the author and sold at No 17, Giltspur St. In: *A series of original experiments on the foot of the living horse*. Sherwood, Nealy and Jones, London. pp 124-147.

CLARK, B. (1820) *A new exposition of the horse's hoof.* London.

COFFMAN, J.R., JOHNSON, J.H., FINOCCHIO, E.J. AND GUFFY, M.M. (1970a) Biomechanics of pedal rotation in equine laminitis. *J. Am. Vet. Med. Assoc.* **156**, 219-223.

COFFMAN, J.R., JOHNSON, J.H., GUFFY, M.M. AND FINOCCHIO, E.J. (1970b) Hoof circulation in equine laminitis. *J. Am. Vet. Med. Assoc.* **156**, 76-83.

COFFMAN, J.R. GARNER, H.E., HAHN, A.W. AND HARTLEY, J. (1972) Characterization Of Refractory Laminitis. In: *Proceedings of the 18th Annual Convention of the American Association of Equine Practitioners*. **18**, 351-358.

COLEMAN, E. (1805) *Grundsätze des Hufbeschlages.* Georg Freidrich Heyer, Darmstadt and Giessen.

COLLES, C.M. (1983) Interpreting radiographs 1: The foot. *Equine Vet. J.* **15**, 297-303.

COLLES, C.M. (1989) A technique for assessing hoof function in the horse. *Equine Vet. J.* **21**, 17-22.

COLLES, C.M. AND JEFFCOTT, L.B. (1977) Laminitis in the horse. *Vet. Rec.* **100**, 262-264.

COLLINS, S.N. (1997) *Effects of dietary biotin supplementation on morphometric properties of the hoof wall.* BSc (Hons) Diss. De Montfort University, Lincoln.

COLLINS, S.N. AND REILLY. J.D. (2004a) Irregularities in structure of the *Stratum medium* of laminitic donkey hoof horn. *Equine Vet. J.* (Submitted)

COLLINS, S.N. AND REILLY. J.D. (2004b). Radiographic anatomy of the normal and laminitic donkey foot. *Equine Vet. J.* (Submitted).

COLLINS, S.N., COPE, B.C., HOPEGOOD, L., LATHAM, R.J., LINFORD, R.G. AND REILLY, J.D. (1998) Stiffness as a function of moisture content in natural materials: Characterisation of hoof horn samples. *J. Mater. Sci.* **33**, 5185-5191.

COLLINS, S.N., WEALLEANS, H., HOPEGOOD, L., LATHAM, R.J., NEWLYN, H.A. AND REILLY, J.D. (2002) 'Foot, Hoof and Fancy FEA' – Current Studies on the Donkey Hoof. In: *Medicine and Surgery of the Donkey, Proceedings of the BEVA Congress 2nd CPD Course*, Glasgow, 11th September. pp 1-15.

COOK, J. AND GORDON, J.E. (1964) A mechanism for control of cracks in brittle systems. *Proc. Roy. Soc. Lon. Ser. A-Math. Phys. Sci.* **282**, 508-520.

COPE, B.C., HOPEGOOD, L., LATHAM, R.J. AND REILLY, J.D. (1998) Equine hoof horn: a natural engineering composite. In: *Materials Solutions to Natures Designs, Proceedings of the Institute of Materials Conference*, Cirencester, 6th – 8th April. pp 3-8.

CRANE, M. (2000) Care of the Geriatric Donkey. In: *The Donkey A Unique Equid, BEVA Conference Proceedings 1st CPD Course*, Langford, Bristol, 15th February. pp 34-42.

CRANE, M. (2001) Foot Problems in the Donkey. In: *Proceedings of the 4th Biannual Seminar BEVA and NAFB&AE Conference*, Stoneleigh, 22nd May. pp 21-22

CRANE, M. (2002a) Care of the Donkey's Foot. In: *Medicine and Surgery of the Donkey, Proceedings of the BEVA Congress 2nd CPD Course*, Glasgow, 11th September. pp 16-17.

CRANE, M. (2002b) The geriatric donkey. In: *Medicine and Surgery of the Donkey, Proceedings of the BEVA Congress 2nd CPD Course*, Glasgow, 11th September. pp 26-30.

CRANE, M. (2003) Further Thoughts On The Care Of Donkey Feet. In: *Proceedings of the 5th Biannual Seminar BEVA and NAFB&AE Conference*, Stoneleigh, 21st October. pp 12-22.

CRIPPS, P.J. AND EUSTACE, R.A. (1999a) Radiological measurements from the feet of normal horses with relevance to laminitis. *Equine Vet. J.* **31**, 427-432.

CRIPPS, P.J. AND EUSTACE, R.A. (1999b) Factors involved in the prognosis of equine laminitis in the UK. *Equine Vet. J.* **31**, 433-442.

CURTIS, S. (1999) *Farriery: From Foal to Racehorse.* R & W Publications (Newmarket), Newmarket. pp 194.

CURISKIS, J.I. AND FEUGHELMAN, M. (1983) Finite Element Analysis of the Composite Fiber, Alpha Keratin. *Text. Res. J.* **53**, 271-274.

DALSTRA, M., HUISKES, H.W.J. AND van ERNING, L. (1995) Validation of a Three-Dimensional Finite Element Model of the Pelvic Bone. *J. Biomech. Eng.* **117**, 272-278.

DAVIES, H.M.S. (2002) No hoof, no horse! The clinical implications of modelling the hoof capsule. *Equine Vet. J.* **34**, 646-647.

DELAFOND (1845) Bulletin de la Société central de Médecine véterinaire

DELLMAN, H.D. (1971) *Veterinary Histology - an Outline Text Atlas.* Lea and Febiger, Philadelphia. pp 262-265.

DEENE, J.S. (2000) *Multivariate Analysis: Principle Components and Calibration, Postgraduate Continuing Professional Training in Industrial Data Modelling.* Department of Biomedical Statistics, De Montfort University, Leicester.

DEENE, J.S. (2001) *Classification, Postgraduate Continuing Professional Training in Industrial Data Modelling.* Industrial Data Modelling Unit, De Montfort University, Leicester.

DEJARDIN, L.M., ARNOCZKY, S.P. AND CLOUD, G.L. (1999) A method for determination of equine hoof strain patterns using photoelasticity: an *in vitro* study. *Equine Vet. J.* **31**, 232-237.

DEJARDIN, L.M., ARNOCZKY, S.P., CLOUD, G.L. AND STICK, J.A. (2001) Photoelastic stress analysis of strain patterns in equine hooves after four-point trimming. *Am. J. Vet. Res.* **62**, 467-473.

DIETZ, O. (1977) *Hoof, Diseases of.* In: Encyclopaedia of Equine Medicine and Surgery. Ed: R. RUTHE, Verlag Paul Parey, Berlin. pp. 1210-1254.

DIETZ, O. AND PRIETZ, G. (1981) Klauenhornqualität, Klauenstatus. *Monatsh. Veterinarmed.* **36**, 419-422.

DIRKS, C. (1985) Makroskopische, licht- und elektronenmikroskopische Untersuchungen uber den Ruckenteil der Rinderklaue. Diss. med. vet., Freie Univ. Berlin.

DISTL, O., GRAF, F. AND KRÄUSLICH, H. (1982) Genetische Variation von morphologischen, histologischen und elektrophoretischen Parametern bei Rinderklauen und deren phänotypischen und genetischen Beziehungen. *Züchtungskunde.* **54**, 106-123.

DITTRICH, J.R., FLEMMING, J.S. AND MINARDI, I. (1994) Efeito de niveis suplementares de biotina no crescimento, estrutura e integridade dos cascos de potros de 1 a 2 anos de idade. *Agrarias Curitiba.* **13**, 135-144.

DOGUER, Y.S. (1943) Anatomical difference between hooves of local horses and donkeys. *Saya Ankara Yusek Ziraat Enstitusu.* **136**. pp 60.

DONEV, A.N. (2000) *Multivariate data Analysis: Lecture Notes.* Department of Biomedical Statistics, De Montfort University, Leicester. pp 127.

DOUGLAS, J. (1994) Mechanical aspects of equine hoof wall. In: *No Foot No Horse II.* Equine Research Centre, Restro Graphics, Mississauga. pp 32-40.

DOUGLAS, J.E. (1998) *Morphological and material properties of the equine hoof wall and laminar junction.* PhD Thesis. University of Guelph.

DOUGLAS, J.E., MITTAL, C., THOMASON, J.J. AND JOFRIET, J.C. (1996) The modulus of elasticity of equine hoof wall - implications for the mechanical function of the hoof. *J. Exp. Biol.* **199**, 1829-1836.

DYCE, K.M., SACK, W.O. AND WENSING, C.J.G. (1987) *Textbook of Veterinary Anatomy.* W.B. Saunders Co., Philadelphia. pp 547.

DYHRE-POULSEN, P., SMEDEGAARD, H.H., ROED, J. AND KORSGAARD, E. (1994) Equine hoof function investigated by pressure transducers inside the hoof and accelerometers mounted on the first phalanx. *Equine Vet. J.* **26**, 362-366.

EISENMANN, V. (1986) Comparative Osteology of Modern and Fossil Horses, Half-asses, and Asses. In: *Equids in the ancient world.* Ed: R. H. MEADOW and H-P. UERPMANN, Verlag Reichert, Wiesbaden. pp 67-116.

EKFALCK, A. (1991) *Studies On The Morphology And Biochemistry Of The Epidermis Of The Equine And The Bovine Hoof With Special Regard To Laminitis.* PhD Thesis. Uppsala.

ELEY, J.L. (1998) *Keeping your Donkey Healthy.* Donkey Breed Society, Kent.

ELEY, J.L. (2000) Foot Problems in the Donkey. In: *The Donkey A Unique Equid, BEVA Conference Proceedings 1st CPD Course*, Langford, Bristol. 15th February. pp 4-20.

ELEY, J. AND FRENCH, J.M. (1993a) Chronic Founder in the Donkey. (Abstract) In: *Proceedings of the BEVA Congress.*

ELEY, J.L. AND FRENCH, J.M. (1993b) Estimating the bodyweight of donkeys. *Vet. Rec.* **132**, 250

EMERY, L., MILLAR, J. AND VAN HOOSEN, N. (1977) *Horseshoeing theory and hoof care.* Lea and Feibiger, Philadelphia. pp 271.

EUSTACE, R.A. (1991) *Radiological measurements involved in the prognosis of equine laminitis.* RCVS Fellowship Thesis.

EUSTACE, R.A. (1992) *Explaining equine laminitis and its prevention.* J.W. Arrowsmith Ltd., Bristol. pp 71.

EUSTACE, R.A. (1993) Equine laminitis. In: *Equine Practice 2.* Ed: E. BODEN, Baillière Tindal, London. pp 150-164.

EUSTACE, R.A. (1995) What Happens Within The Foot In Laminitis? In: *Proceedings of Dodson & Horrell Ltd. 1st International Conference on Feeding Horses.* Scots Corner, 5th September.

EUSTACE, R.A. (1998) Significant Prognostic Parameters for Laminitis, Founder and Sinker Syndrome. In: *Proceedings of Dodson & Horrell Ltd. 1st International Research Conference on Equine Laminitis*, Stoneleigh, 9th September.

FERGUSSON, D. (1994) Defining Rotation. *Eur. Farrier's J.* **51**, 36-44.

FLEMING, G. (1871) Observations on the anatomy and physiology of the horse's foot. *Veterinarian.* **XLIV,** 522, 4th series, 198, 388-396.

FOWLER, J. (1995) Trimming donkeys feet. *Equine Vet. Educ.* **7**, 18-21.

FRENCH, J. (2000) The Donkey – A Small Horse? In: *The Donkey A Unique Equid, BEVA Conference Proceedings 1st CPD Course.* Langford, Bristol, 15th February, pp 2-8.

FROHNES, A. AND BUDRAS, K-D. (2001) Endogene Einflußfaktoren auf die Horn-qualität im Sohlen und Ballen-Strahlsegment des Pferdeshufes. Teil II: Intra- und Interzelluläre Faktoren. *Pferdeheilkunde.* **17**, 437-443.

GALVIN, S., LOOMIS, C., MANABE, M., DHOUAILLY, D. AND SUN, T-T. (1989) The major pathways of keratinocyte differentiation as defined by keratin expression: an overview. *Arch Dermatol.* **4**, 277-300.

GARNHAFT, R. (1925) *Vergleichende Messungen der Elastizität des Hornes gesunder und kranker Pferdehufe.* Diss. vet. med., Wien.

GATLIN, C.L., SCHABERG, E.S., JORDAN, W.H., KUYAT, B.L. AND SMITH, W.C. (1993) Point counting on the Macintosh a semiautomated image analysis technique. *Anal. Quant. Cytol. Histol.* **15**, 345-350.

GEARY, J.E. (Jr) (1975) *The dynamics of the equine foreleg.* Masters of Mechanical and Aerospace Engineering Thesis. University of Delaware.

GEORGE, M. AND RYDER, O.A. (1986) Mitochondrial DNA evolution in the genus *Equus. Mol. Biol. Evol.* **3**, 535-546.

GETTY, R. (1975) *Sisson and Grossman's The Anatomy of the Domestic Animals.* 5th Edn., W.B. Saunders Co., London.

GEYER, H. (1980) Zur mikroskopischen Anatomie der Epidermis an der Schweineklaue. *Anat. Histol. Embryol.-J. Vet. Med. Ser. C* **9**, 337-360.

GEYER, H. AND LEU, U. (1988) L'influence du traitement a la biotine sur la croissance et la qualite de la corne des sabots et sur le taux plasmatique de biotine chez le cheval. *J. Rech. Chevaline.* **14**, 92-202;

GEYER, H. AND SCHULZE, J. (1994) The long term influence of biotin supplementation on hoof horn quality in horses. *Schweiz Arch Tierheilk.* **136**, 137-149.

GEYER, H. AND TAGWERKER, F. (1986) *The pig's hoof. It's structure and alterations.* Hoffmann-La Roche, Basle, Switzerland. pp 27.

GILLETTE, E.L., THRALL, D.E. AND LEBEL, J.L. (1977) *Carlson's Veterinary Radiology.* 3rd Edn., Lea and Febiger, Philadelphia. pp 441-442.

GLÖCKNER, S. (2002) *Eine retrospektive Studie über die Hufrehe bei Pferden; dargestellt an den Patienten der Klnik für Pferde, Allgmenine Chirurgie und Radiologie der Freien Universität Berlin aus den Jahren 1976-1995.* Diss. med. vet., Freie Univ. Berlin.

GNIADECKA, M., NIELSEN, O. F., CHRISTENSEN, D.H. AND WULF, H.C. (1998) Structure of Water, Proteins, and Lipids in Intact Human Skin, Hair and Nail. *J. Invest. Dermatol.* **110**, 392-398.

GOODALL, G.P. (1997) Cutting large sections of horse foot. *Microsc. microanal.* March, 17.

GOETZ, T.E. (1987) Anatomic, hoof, and shoeing considerations for the treatment of laminitis in horses. *J. Am. Vet. Med. Assoc.* **190**, 1323-1332.

GOETZ, T.E. (1989) The treatment of laminitis in the horse. *Vet. Clin. N. Am.-Equine Pract.* **5**, 73-108.

GORDON, J.E. (1976) *The New Science of Strong Materials.* Penguin Books Ltd., Middlesex. pp 269.

GREENOUGH, P.R. (1978) The nomenclature of anatomical features of the bovine digits. In: *Report of the II Symposium on the Bovine Digit,* Skara, Sweden. pp 1-10.

GREENOUGH, P.R. (1982) Laminitis in review. In: *Proceedings of the IV International Symposium on Disorders of the Ruminant Digit,* Paris.

GREENOUGH, P.R. (1985) The subclinical laminitis syndrome. *Bovine Pract.* **20**, 144-149.

GREENOUGH, P.R., MACCALLUM, F.J. AND WEAVER, A.D. (1981) *Lameness in Cattle.* 3rd Edn., J. Wright & Sons, Bristol. pp 471.

GRIFFITH, A.A. (1921) The phenomena of rupture and flow in solids. *Phil. Trans. Roy. Soc.* **A221**, 163-198.

GROSENBAUGH, D.A. AND HOOD, D.M. (1992) Keratin and associated proteins of the equine hoof wall. *Am. J. Vet. Res.* **53**, 1859-1863.

GROSENBAUGH, D.A. AND HOOD, D.M. (1993) Practical Equine Hoof Wall Biochemistry. *Equine Pract.* **15**, 8-14.

GROSENBAUGH, D.A., HOOD, D.M., AMOSS, M.S., J.R. AND WILLIAMS, J.D. (1991) Characterisation and distribution of epidermal growth factor receptors in equine hoof wall laminar tissues: comparison of normal horses and horses affected with chronic laminitis. *Equine Vet. J.* **23**, 201-206.

GROSENBAUGH, D.A., MORGAN, S.J. AND HOOD, D.M (1999) The digital pathologies of chronic laminitis. *Vet. Clin. N. Am.-Equine Pract.* **15**, 419-436.

GROVES, C.P. (1974) *Horses, Asses and Zebras in the Wild.* David & Charles, London. pp 192.

GROVES, C.P. (1986) The Taxonomy, Distribution, and Adaptation of Recent Equids. In: *Equids in the ancient world.* Ed: R.H. MEADOW and H-P. UERPMANN, Verlag Reichert, Wiesbaden. pp 11-66.

GURTL, E.G. (1836) *Magazin für gesamte Tierheilkunden,* Berlin.

HAHN, M.V., McDANIEL, B.T. AND WILK, J.C. (1986) Rates of hoof horn growth and wear in holstein cattle. *J. Dairy Sci.* **69**, 2148-2156.

HALLAB, N.J., HOGAN, H.A. AND HOOD, D.M. (1991) Determining the Mechanical Properties of Equine Laminar Corium Tissue. In: *Proceedings from the 10th Annual Meeting of the Association for Equine Sports Medicine,* Reno, Nevada. 2nd – 3rd March. *Equine Athl.* **4**, 13-18.

HARRIS, B. (1980) The mechanical behaviour of composite materials. In: *The Mechanical Properties of Biological Materials, Symposia of the Society for Experimental Biology, Symposium XXXIV.* Ed: J.F.V. VINCENT and J.D. CURREY, Society for Experimental Biology, Cambridge University Press, Cambridge. pp 37-74.

HEMKER, S. (2001) *Die Bewertung der Meßmethoden bei der chronischen Hufrehe des Pferdes für den Grad und die Prognose.* Diss. med. vet., Freie Univ. Berlin.

HEMKER, S. AND HERTSCH, B. (2002) Zur röntgenologischen Auswertung bei chronischer Hufrehe. *Prakt. Tierartz.* **83**, 610-617.

HENDRY, K.A.K., MACCALLUM, A.J., KNIGHT, C.H. AND WILDE, C.J. (1997) Laminitis in the dairy cow: a cell biological approach. *J Dairy Res.* **64**, 475-485.

HENDRY, K.A.K., MacCALLUM, A.J., KNIGHT, C.H. AND WILDE, C.J. (1998) Keratin abundance and distribution in healthy and diseased bovine hoof tissue. In: *Proceedings of the X International Symposium on Lameness in Ruminants.* 7th – 10th September, Lucerne. Ed: CH.J. LISCHER and P. OSSENT. pp 212-213.

HERTHEL, D.AND HOOD, D.M. (1999) Clinical presentation, diagnosis, and prognosis of chronic lamiinitis. *Vet. Clin. N. Am.-Equine Pract.* **15**, 375-394.

HICKMAN, J. AND HUMPHREY, M. (1987) *Hickman's Farriery.* 2nd Edn., J. A. Allen, London. pp

HIFNY, A. AND MISK, N.A. (1983) Anatomy of the hoof in donkeys. *Assiut Vet. Med. J.* **10**, 3-6.

HILDEBRAND, M. (1959) Motions of the running cheetah and horse. *J. Mammal.* **40**, 481-495.

HILDEBRAND, M. (1987) The mechanics of horse legs. *Am. Scientist.* **75**, 594-601.

HINCKLEY, K.A., FEARN, S., HOWARD, B.R. AND HENDERSON, I.W. (1996) Near infrared spectroscopy of pedal haemodynamics and oxygenation in normal and laminitic horses. *Equine Vet. J.* **27**, 465-470.

HINTERHOFER, C. (1996) *Untersuchungen zum kleben von Hufhorn mit besonderer Berucksichtigung der Versorgung von Hornspalten beim Pferd.* PhD Thesis. Universität Wien.

HINTERHOFER, C., STANEK, C. AND HAIDER, H. (1997) Belastungssimulation an einem aus finiten elementen konstruierten computermodell der hornkapsel des pferdes. *Pferdeheilkunde.* **13**, 319-329.

HINTERHOFER, C., STANEK, C. AND BINDER, K. (1998) Elastic modulus of equine hoof horn, tested in wall samples, sole samples and frog samples at varying levels of moisture. *Berliner Munchener Tierarztl. Wochenschr.* **111**, 217-221.

HINTERHOFER, C., STANEK, C. AND HAIDER, H. (2000) The effect of flat horseshoes, raised heels and lowered heels on the biomechanics of the equine hoof assesed by Finite Element Analysis. *J. Vet. Med. Ser. A-Physiol. Pathol. Clin. Med.* **47**, 73-82.

HINTERHOFER, C., STANEK, C. AND HAIDER, H. (2001) Finite element analysis (FEA) as a model to predict effects of farriery on the equine hoof. *Equine Vet. J. Suppl.* **33**, 58-62.

HIROKAWA, S. AND TSURUNO, R. (2000) Three-dimensional deformation and stress distribution in an analytical/computational model of the anterior cruciate ligament. *J. Biomech.* **33**, 1069-1077.

HIRSCHBERG, R.M., MÜLLING, C.K.W. AND BUDRAS, K-D. (2001) Pododermal Angioarchitecture of the Bovine Claw in Relation to Form and Function of the Papillary Body: A Scanning Electron Microscopic Study. *Microsc. Res. Tech.* **54**, 375-385.

HOFSTETTER, B. (1985) Contribution à l.étude histologigue á but pratique de la corne des onglons des bovins. *Schweiz. Arch. Tierheilkd.* **127**, 417-432.

HOGAN, H.A. (1992) Micromechanics modelling of haversian cortical bone properties. *J. Biomech.* **25**, 549-556.

HOGAN H.A., WICHTMANN, A.D. AND HOOD, D.M. (1991) Finite element analysis of the internal deformation and stresses in the equine distal digit. In: *Proceedings from the 10th Annual Meeting of the Association for Equine Sports Medicine,* Reno, Nevada, 2nd – 3rd March. pp 43.

HOOD, D.M. (1984) *Studies on the pathogenesis of equine laminitis.* PhD Thesis. Texas A&M University.

HOOD, D.M. (1997a) Perspectives on Chronic Laminitis. In: *Proceedings of the Hoof Project.* Ed: D.H. HOOD, I.P. WAGNER and A.C. JACOBSON, Texas A&M University, Texas. pp 21-34.

HOOD, D.M. (1997b) Digital Instability as a Potential Prognostic Indicator in Horses with ChronicLaminitis. In: *Proceedings of the Hoof Project.* Ed: D.H. HOOD, I.P. WAGNER and A.C. JACOBSON, Texas A&M University, Texas. pp 106-115.

HOOD, D.M. (1999a) The mechanisms and consequences of structural failure of the foot. *Vet. Clin. N. Am.-Equine Pract.* **15**, 437-461.

HOOD, D.M. (1999b) Laminitis in the horse. *Vet. Clin. N. Am.-Equine Pract.* **15**, 287-294.

HOOD, D.M. (1999c) The pathophysiology of developmental and acute laminitis. *Vet. Clin. N. Am.-Equine Pract.* **15**, 321-343.

HOOD, D.M. AND STEVENS, K.A. (1981) Pathophysiology of Equine Laminitis. *Compend. Contin. Edu. Pract. Vet.* **3**, s454-s460.

HOOD, D.H. AND WICHTMANN, A.D. (1991) Finite element analysis of the internal deformation and stresses in the equine distal digit. In: *Proceedings from the 10th Annual Meeting of the Association for Equine Sports Medicine,* Reno, Nevada, 2nd – 3rd March. pp 43.

HOOD, D.M., HOGAN, H.A., HARDEN, W., TREADWAY, C., GROSENBAUGH, D.A. AND WILLLIAMS, J.D. (1991) Dorsal hoof wall deformation in static weight bearing. In: *Proceedings from the 10th Annual Meeting of the Association for Equine Sports Medicine,* Reno, Nevada, 2nd – 3rd March. pp 47.

HOOD, D.M., GROSENBAUGH, D.A., CHAFFIN, M.K., HONAS, C.M., SLATER, M.R. AND MORGAN, S.J. (1993a) The Role of Vascular Mechanisms in the Development of Acute Equine Laminitis. *J. Vet Intern. Med.* **7**, 228-234.

HOOD, D.M., GROSENBAUGH, D.A., MOSTAFA, M.B., MORGAN, S.J. AND THOMAS, B.C. (1993b) Pathophysiology of Chronic Laminitis. In: *Proceedings of the 39th Congress American Association of Equine Practitioners.* **39**, 199-200.

HOOD, D.M., GROSENBAUGH, D.A. AND SLATER, M.R. (1994) Vascular perfusion in horses with chronic laminitis. *Equine Vet. J.* **26**, 191-196.

HOOD, D.M. AND JACOBSON, A.C. (1997) The principles of equine hoof wall conformation. In: *Proceedings of the Hoof Project.* Ed: D.H. HOOD, I.P. WAGNER and A.C. JACOBSON, Texas A&M University, Texas. pp 2-20.

HOPEGOOD, L. (2002) Tubule Density, Moisture Content and Mechanical Properties of Donkey Hoof Horn. PhD Thesis. De Montfort University, Leicester.

HOPEGOOD, L., COLLINS, S.N., COPE, B., LATHAM, R.J. AND REILLY, J.D. (2003a) The Effect of Modulation of Moisture Content on Mechanical Properties of Full and Partial Hoof Wall Depth Samples of Donkey Hoof Horn Samples. *Comp. Biochem. Physiol. A-Mol. Integr. Physiol.* **134**, Suppl., s44.

HOPEGOOD, L., COLLINS, S.N., LATHAM, R.J. AND REILLY, J.D. (2003b) Analyses of the Moisture Content of Hoof Horn from Horses, Donkeys and Laminitic Donkeys. In: *Emerging Equine Science*, Proceedings of the British Society of Animal Science, Cirencester, 15th – 16th September. pp 28.

HULL, D. (1981) *An introduction to composite materials.* Cambridge University Press, London. pp 246.

HUNT, R.J. (1991) The Pathophysiology of Acute Laminitis. *Compend. Contin. Educ. Pract. Vet. (European Edition)* **13**, 401-409.

HUNT, R.J. (1993) A retrospective evaluation of laminitis in horses. *Equine Vet. J.* **25**, 61-64.

HUNT, R.J. (1996) Diagnosing and treating chronic laminitis in horses. *Vet. Med.* **91**, 1025-1032.

HUISKES, H.W.J. AND CHAO, E.Y.S. (1983) A survey of finite element analysis in orthopaedic biomechanics: the first decade. *J. Biomech.* **16**, 385-409.

IMOKAWA, G., KUNO, H. AND KAWAI, M. (1991) *Stratum corneum* Lipids as a Bound –Water Modulator. *J. Invest. Dermatol.* **96**, 845-851.

ISHIDA, N., OYUNSUREN, T., MASHIMA, S., MUKOYAMA, H. AND SAITOU, N. (1995) Mitochondrial DNA sequences of various species of the genus *Equus* with special refernce to the phylogenic relationship between the Przewalski's horse and the domestic horse. *J. Mol. Evol.* **41**, 180-188.

JACKSON, A.P. (1992) Bone, nacre and other ceramics. In: *Biomechanics Materials. A Practical Approach.* Ed: J.F.V. VINCENT, Oxford University Press, Oxford. pp 33-56.

JOHNSON, P.J., TYAGI, S.C., KATAWA, L.C., GANJAM, V.K., MOORE, L.A., KREEGER, J.M. AND MESSER, N.T. (1998) Activation of extracellular matrix metalloproteinases in equine laminitis. *Vet. Rec.* **142**, 392-396

JOHNSON, P.J., KREEGER, J.M., KEELER, M., GANJAM, A. AND MESSER, N.T. (2000) Serum markers of lamellar basement degradation and lamellar histopathological changes in horses affected with laminitis. *Equine Vet. J.* **32**, 462-468.

JOSSECK, H., ZENKER, W. AND GEYER, H. (1995) Hoof horn abnormalities in Lipizzaner horses and the effect of dietary biotin on macroscopic aspects of hoof horn quality. *Equine Vet. J.* **27**, 175-182.

KAMEYA, T. (1973) Clinical studies on laminitis in the Racehorse. *Exp. Rep. Equine Hlth. Lab.* **10**, 19-40.

KAMEYA, T., KIRYU, K., KANEKO, M. AND SATOH, H. (1980) Histopathogenesis of thickening of the hoof wall laminae in equine laminitis. *Jpn. J. Vet. Sci.* **42**, 361-371.

KASAPI, M.A. (1997) *Design for fracture control and the mechanical properties of the equine hoof wall.* PhD Thesis. University of British Columbia.

KASAPI, M.A. AND GOSLINE, J.M. (1996) Strain rate dependent mechanical properties of the equine hoof wall. *J. Exp. Biol.* **199**, 1133-1146.

KASAPI, M.A. AND GOSLINE, J.M. (1997) Design complexity and fracture control in the equine hoof wall. *J. Exp. Biol.* **200**, 1639-1659.

KASAPI, M.A. AND GOSLINE, J.M. (1998) Exploring the possible functions of equine hoof wall tubules. *Equine Vet. J. Suppl.* **26**, 10-14.

KASAPI, M.A. AND GOSLINE, J.M. (1999) Micromechanics of the equine hoof wall: optimizing crack control and material stiffness through modulation of the properties of keratin. *J. Exp. Biol.* **202**, 377-391.

KERSTING, J.A. (1777) *Unterricht Pferde zu beschlagen und die an dem Fuß der Pferde vorgetallenan Gebrechen zu heilen.* Göttingen.

KIND, H. (1961) *Vergleichende Untersuchungen uber die Abnutzung der Hufe einiget Equiden aufgrund der Struktur der Hufkapselwand.* Diss. med. vet., Humboldt-Univ. Berlin.

KITCHENER, A. (1987) Fracture toughness of horns and a reinterpretation of the horning behaviour of bovids. *J. Zool. Lond.* **213**, 621-639.

KITCHENER, A. AND VINCENT, J.F.V. (1987) Composite theory and the effect of water on the stiffness of horn keratin. *J. Mater. Sci.* **22**, 1385-1389.

KLEMA, E. (1937) *Untersuchung uber Tonofibrillen in der Hufledertiault des pferdes.* Diss. med. vet., Vienna.

KLEMOLA, V. (1933) Über keratoplastische Reaktion der Hufhornbildung durch einige physiologische Faktoren. *Biederm Zbl.* **V**, 657-675.

KOBLIK, P.D., O'BRIEN, T.R. AND COYNE, C.P. (1988) Effects of dorsopalmar oblquity on radiographic measurement of distal phalangeal rotation angle in horses with laminitis. *J. Am. Vet. Med. Assoc.* **192**, 346-349.

KÖNIG, B. (2001) *Struktur, Funktion und Qualität des Kronhornes im Pferdehuf.* Diss. med. vet., Freie Univ. Berlin.

KRAJCINOVIC, D., TRAFIMOW, J. AND SUMARAC, D. (1987) Simple Constitutive Model for a Cortical Bone. *J. Biomech.* **30**, 779-784.

KÜNG, M. (1991) *Die Zugfestigkeit des Hufhorns von Pferden.* Diss. med. vet., Zurich.

KÜNG, M., GEYER, H., WIGET, P. AND STEINMANN, W. (1991) Influence of localisation and environment on the tensile strength of horn in the horse. *Acta Anat.* **140**, 196.

KÜNG, M, BOLLIGER, CH., ALBARANO, T. AND GEYER, H. (1993) The assessment of hoof horn quality and the influence of environmental factors in horses compared to cattle and pigs. In: *Proceedings of the 3rd Geneva Congress of Equine Medicine and Surgery - 3rd Congress of the World Equine Veterinary Association (WEVA).* Geneva, 7th – 11th December. *Swiss Vet.* ***11-S/1993,*** 185.

KUNSEIN, L. (1882) *Über die Entwicklung des Hornufes bei einigen Ungulaten.* Diss. med. vet., Dorpat.

KUWANO, A. (1994) Preparation of thin ground section of resin-embedded hooves for histologic analysis. *J. Equine Sci.* **5**, 37-39.

KUWANO, A. (1996) Stain characteristics of thin ground sections of hydrophobic resin-embedded equine hooves. *J. Equine Sci.* **7**, 27-34.

KUWANO, A., YOSHIHARA, T., TAKATORI, K. AND KOSUGE, J. (1998)
Onychomycosis in white line disease in horses: pathology, mycology and clinical features. *Equine Vet. J. Suppl.* **26**, 27-35.

LAMBERT, F. (1966) The role of moisture in the physiology of the hoof of the harness horse. *Vet. Med. Small Anim. Clin.* **61**, 342-347.

LAMBERT, .F (1968) An experiment demonstrating rapid contraction of a Standardbred horse hoof from moisture loss during flooring. *Vet. Med. Small Anim. Clin.* **63**, 879-880.

LANDEAU, L.J., BARRETT, D.J. AND BATTERMAN, S.C. (1983) Mechanical properties of equine hooves. *Am. J. Vet. Res.* **44**, 100-103.

LANOVAZ, J.L., CLAYTON, H.M. AND WATSON, L.G. (1998) *In vitro* attenuation of impact shock in equine digits. *Equine Vet. J. Suppl.* **26**, 96-102.

LARSSON, B., OBEL, N. AND ABERG, B. (1956) On the biochemistry of keratinisation in the matrix of the horse's hoof in normal conditions and in laminitis. *Nord. Vet-Med.* **8**, 761-776.

LEACH, D.H. (1980) The structure and function of the equine hoof wall. PhD Thesis. University of Saskatchewan, Saskatoon.

LEACH, D.H. (1990a) Biomechanics of limb weightbearing. In: *Equine Lameness and foot conditions.* Refresher course for veterinarians, University of Sydney, 5th – 9th February. Ed: R. ROSE, **Proceedings 130**, 59-69.

LEACH, D.H. (1990b) Adaptation of Hoof to Weightbearing. In *Equine Lameness and foot conditions.* Refresher course for veterinarians, University of Sydney, 5th – 9th February. Ed: R. ROSE, **Proceedings 130**, 121-128.

LEACH, D.H. AND ZOERB, G.C. (1983) Mechanical properties of equine hoof wall. *Am. J. Vet. Res.* **44**, 2190-2194.

LEACH, K.A. (1996) *Lesions and microscopic structure of claw horn in dairy cows.* PhD Thesis. University of Edinburgh.

LEKEUX, P. AND ART, T. (1994) The respiratory system: Anatomy, physiology and adaptation to exercise and training. In: *The atheletic horse: Principles and practice of equine sports medicine.* Ed: D.R. HODGSON and R.J. ROSE, W.B. Saunders Co., Philidelphia. pp 88-127.

LEUENBERGER, W. P. AND MARTIG, J. (1979) *Ursachen des spezifischen traumatitischen Sohlengeschwürs beim Rind.* Schlussbericht über das Untersuchungsprojekt 012.77.7

LEY, W.B., SCOTT PLEASANT, R. AND DUNNINGTON, E.A. (1998) Effects of season and diet on tensile strength and mineral content of the equine hoof wall. *Equine Vet. J. Suppl.* **26**, 46-50.

LINDE, F. (1994) Elastic and viscoelastic properties of Trabecular Bone by compression testing approach. *Dan. Med. Bull.* **41**, 119-138.

LINDE, F., HVID, I. AND MADSEN, F. (1992) The effect of specimen geometry on the mechanical behaviour of trabecular bone specimens. *J. Biomech.* **25**, 359-368.

LINFORD, R.L. (1987) *A radiographic, morphometric, histological and ultrastructural investigation of lamellar funciton, abnormality and the associated radiographic findings for sound and footsore thoroughbreds and horses with experimentally induced traumatic and alimentary laminitis.* PhD Thesis. University of California, Davis.

LINFORD, R.L. (1990) Laminitis (founder). In: *Large Animal Internal Medicine.* Ed: B.P. SMITH, C.V. Mosby, St. Louis. pp 1158-1168.

LINFORD, R.L. (1996) Laminitis (founder). In: *Large Animal Internal Medicine.* Ed: B.P. SMITH, C.V. Mosby, St. Louis. pp 1300-1309.

LINFORD, R.L., O'BRIEN, T.R. AND TROUT, D.R. (1993) Qualitative and morphometric radiographic findings in the distal phalanx and digital soft tissues of sound Thoroughbred racehorses. *Am. J. Vet. Res.* **54**, 38-51.

LUNGWITZ, A. (1883) Der gegenwärtige Strandpunkt der mechanischen Verrichtungen des Pferdehufes. *Hufschmied.* **1**, 17-21.

LUNGWITZ, A. (1891) The Changes in the Form of the Horse's Hoof under the Action of the Body-Weight. *J. Comp. Path. Ther.* **4**, 191-211.

LUNGWITZ, A. AND ADAMS J.W (1913) *A Textbook of Horseshoeing*. 11th Edn., J.B. Lippincott Co., London. pp 216.

McCLINCHEY, H.L. (2000) *The effects of changing hoof shape variables analysed with a validated finite element model.* MSc Thesis. University of Guelph.

McCLINCHEY, H.L., THOMASON, J.J. AND JOFRIET, J.C. (2001) Mechanism of quarter and heel expansion in the equine hoof investigated by finite element. (Authors Draft).

MacFADDEN, B.J. (1988) Horses, the fossil record, and evolution. *Evol. Biol.* **22**, 131-158.

MACLEAN, C.W (1971a) The histopathology of laminitis in dairy cows. *J. Comp. Path.* **81**, 563-570.

MACLEAN, C.W. (1971b) The long-term effects of laminitis in dairy cows. *Vet. Rec.* **89**, 34-37.

McNEEL, S.V. (1986) The phalanges. In: *Textbook of Veterinary Diagnostic Radiology*. Ed: D.E. THRALL, W.B. Saunders Co., London. pp 176-197.

MAIERL, J., BÖHIMISCH, R., DICKOMEIT, M. AND LIEBICH, H-G. (2002a) A Method of Biomechanical Testing of the Suspensory Apparatus of the Third phalanx in Cattle: a Technical Note. *Anat. Histol. Embryol.-J. Vet. Med. Ser. C* **31**, 321-325.

MAIERL, J., BÖHIMISCH, R. AND METZNER, M. (2002b) Biomechanical testing of the suspensory apparatus of thephalanx distalis in the claw of beef bulls. *Wien Tierarztl. Mschr.* **89**, 203-210.

MAIR, F-J. (1974) Dehnungsmessungen an der Hornwand in Tragrandnähe und and der Hornsohle beim Pferd-Hinterhuf. *Wien. Tierarz. Monats.* **61**, 70-71.

MARKS, G. (1984) *Makroskopische, licht- und elektronenmikroskopische Untersuchungen zur Morphologie des Hyponichiums bei der Hufrehe des Pferdes.* Diss. med. vet., Freie Univ. Berlin.

MARKS, G. AND BUDRAS, K.D. (1985) Zusammenhangstennung im corium und der epidermis bei der chronischen hufrehe des pferdes. *Anat. Histol. Embryol.-J. Vet. Med. Ser. C* **14**, 187.

MARKS, G. AND BUDRAS, K.D. (1987) Licht und elektronenmikroskopische Untersuchungen uber die akute Hufrehe des Pferdes. *Berliner Munchener Tierarztl. Wochenschr.* **100**, 82-88.

MARKS, R. (1981) Mechanical properties of the Skin. In: *Physiological, Biochemical and Molecular Biology of the Skin*. Ed: A. GOLDSMITH, Academic Press, London. pp 602-621.

MARTIN, R.B. AND BOARDMAN, D.L. (1993) The Effects Of Collagen Fibre Orientation, Porosity, Density, And Mineralisation On Bovine Cortical Bone Bending Properties. *J. Biomech.* **26**, 1047-1054.

MATHEWS, N.S. (2000) Anaesthesia for Donkeys and Mules. In: *The Donkey A Unique Equid, BEVA Conference Proceedings 1st CPD Course,* Langford, Bristol. 15th February. pp 21-24.

MATHEWS, N.S. (2002) Therapeutics and anaesthesia in the donkey. In: *The Medicine and Surgery of the Donkey, BEVA Conference Proceedings 2nd CPD Course,* Glasgow, 11th September. pp 3-5.

MATHEWS, N.S., TAYLOR, T.S. AND HARTSFIELD, S.M. (1997) Anaesthesia of donkeys and mules. *Equine Vet. Educ.* **9**, 198-202.

MATTHECK, C. AND REUSS, S. (1991) The Claw of the Tiger: An Assessment of its Mechanical Shape Optimization. *J. theor. Biol.* **150,** 323-328.

MAUSKE, S. (1972) *Klauenhornstruktur - Histologische Untersuchungen am Bellen, an der Sohle und der Kronepidermis der Deutschen Schwarzbunten Niederungsrinder.* Diss. med. vet., Humboldt-Univ. Berlin.

MAY, H. (1924) *Über die Elastizität des gequellenen Hufhornes beim Pferd.* Diss. med. vet., Wien.

MAY, S.A. (1989) Lameness research in Europe – a review with comments on current research priorities. In: *The report of the workshop on Research into Equine Lameness.* Ed: E.J.L. SOULSBY, A.D. CARE, N.CHANDLER, W. PLOWRIGHT, P.D. ROSSDALE and J.R. WALTON, R & W Publications, Newmarket, Suffolk.

METTAM, A.E. (1896) On the Development and Histology of (1) the Hoof Wall and Subjacent Soft Structures of the Horse's Foot. *Veterinarian*, **69**, No 818, Fourth Series, No 494, 85-98.

MISHRA, P.C. AND LEACH, D.H. (1983a) Electron microscopic study of the veins of the dermal lamellae of the equine hoof wall. *Equine Vet. J.* **15**, 14-21.

MISHRA, P.C. AND LEACH, D.H. (1983b) Extrinsic and intrinsic veins of the equine hoof wall. *J Anat.* **136**, 543-559.

MOLYNEUX, G.S., HALLER, C.J., MOGG, K. AND POLLITT, C.C. (1994) The Structure, Innovation and Location of Arteriovenous Anastomoses in the Equine Foot. *Equine Vet. J.* **26**, 305-312.

MOORE, G.V. (1988) Digital image processing and analysis techniques. In: *Microcomputers in physiology a practical approach.* Ed: P.J. FRASER, IRL Press, Oxford. pp 129-155.

MOORE, J.N. AMD ALLEN, D. (1995) *A guide to equine acute laminitis.* VLS Books, London. pp 40.

MOORE, J.N., ALLEN, D. AND CLARKE, S.E. (1989) Pathophysiology of acute laminitis. *Vet. Clin. N. Am.-Equine Pract.* **5**, 67-72.

MORGAN, J.P. (1972) *Radiology in Veterinary Orthopaedics.* Lea and Febiger, Philadelphia. pp 364.

MORGAN, S.J., GROSENBAUGH, D.A. AND HOOD, D.M. (1999) The pathophysiology of chronic laminitis. *Vet. Clin. N. Am.-Equine Pract.* **15**, 395-417.

MOSTAFA, M.B. (1986) Studies on Experimental Laminitis in the Horse. PhD Thesis. Cairo University.

MOSTAFA, M.B. (1988) Acute laminitis in a donkey: a case report. *Indian Vet. J.* **65**, 348-349.

MOSTAFA, M.B. AND EL-GHOUL, W.S. (1999) Histometric studies of the equine hoof wall in normal and laminitic horse. In: *Proceedings Tagungsband-Symposium,* Cairo, 6th November. pp 183-191.

MÜLLER, F. (1936) Der Pferdehuf im sagittalen Axialschnitt. *Arch. Wiss. Prakt. Tierheilk.* **70**, 296-301.

MÜLLING, Ch. (1993) Struktur, Verhornung und Hornqualität in Ballen, Sohle und weisser Linie der Rinderklaue und ihre Bedeutung fur Klauenerkrankungen. Diss. med. vet., Freie Univ. Berlin.

MÜLLING, C., BRAGULLA, H. AND BUDRAS, K.D. (1994a) The significance of the intercellular cementing substance for the quality of hoof horn. *Anat. Histol. Embryol.-J. Vet. Med. Ser. C* **23**, 56.

MÜLLING, C., BRAGULLA, H., BUDRAS, K.D. AND REESE, S. (1994b) Structural factors influencing horn quality and sites of predilection for disease at the surface of the cattle hoof. *Schweiz. Arch. Tierheilk.* **136**, 49-57.

MULLING, C., BRAGULLA, H. AND REESE, S. (1994c) Histochemical and immunohistological studies of the horn quality of the cattle hoof. *Anat. Histol. Embryol.-J. Vet. Med. Ser. C* **23**, 76.

NAKADE, T., KOTANI, T., ANDO, Y., NUMATA, Y. AND UCHIDA, Y. (1992) Scanning electron and light microscope observations on the hoof in equine laminitis. *J. Jpn. Vet. Med. Assoc.* **45**, 305-311.

NEWLYN, H.A., COLLINS, S.N., COPE, B.C., HOPEGOOD, L., LATHAM, R.J. AND REILLY, J.D. (1998) Finite element analysis of static loading in donkey hoof wall. *Equine Vet. J. Suppl.* **26**, 103-110.

NEWLYN, H.A., COLLINS, S.N., COPE, B.C., HOPEGOOD, L., LATHAM, R.J. AND REILLY, J.D. (1999) Equid Hoof Horn: A Natural Composite. In: *Proceedings of the 5th International Conference on Deformation and Fracture of Composites*, 18-19 March 1999, IOM Communications Ltd., London. pp 231-240.

NEWLYN, H.A., COLLINS, S.N., LATHAM, R.J. AND REILLY, J.D. (2004) Donkey Hoof Horn: A natural Composite? *J. Mater. Sci.* (Submitted for Publication).

NICKEL, R. (1938a) Uber den Bau der Hufröhrchen und siene Bedeutung für den Mechanismus des Pferdehufes. *Dtsch. Tierarztl. Wochenschr.* **46**, 449-452.

NICKEL, R. (1938b) Uber den Bau der Hufröhrchen und siene Bedeutung für den Mechanismus des Pferdehufes *Morph. Jahrbuch.* **82**, 119-160.

NICKEL, R. (1939) Untersuchungen uber den Bau des Pferdehufes mit besonderer Berucksichtigung des Hufmechanismus und von Hufkrankheiten. *Dtsch. Tierarztl. Wochenschr.* **46**, 521-524.

NIKLAS, K.J. (1992) Voigt and Reuss Models for Predicting Changes in Young's Modulus in Dehydrating Plant Organs. *Annal. Bot.* **70**, 347-355.

NILSSON, S.A. (1963) Clinical, morphological and experimental studies of laminitis in cattle. *Acta Vet. Scand.* **4** (Suppl. 1).

O'BRIEN, T.R. AND BAKER, B.S. (1986) Distal extremity examination: how to perform the radiographic examination and interpret the radiographs. In: *Proceedings of the Annual Meeting American Association of Equine Practitioners.* **32**, 553-566.

O'GRADY, S.E. Managing chronic laminitis using 'glue-on' shoeing technology. *Equine Vet. Educ.* **14**, 152-162.

OBEL, N. (1948) *Studies on the histopathology of acute laminitis.* Diss. Stockholm Almqvist and Wiksell, Uppsala.

OKAMOTO, H. (1994) A dialogue on biomimetic design for natural technology. *Biomimetics* **2**, 1-13.

OLIVER, A. (1987) Interstial fluid pressure within the coronary dermis of the horse with chronic laminitis. PhD Thesis. College Station, Texas A&M University.

OSSENT, P. AND LISCHER, C.J. (2000) Bovine Laminitis: the lesions and the theories on their pathogenesis. In: *Proceedings of the XI International Symposium on Disorders of the Ruminant Digit, Parma, Italy, 3rd – 7th September.* Ed: C.M. MORTELLO, L. De VECCHIS and A. BRIZZI. pp 27-29.

OTT, E.A. AND JOHNSON, E.L. (2001) Effect of trace mineral proteinates on growth and skeletal and hoof development in yearling horses. *J. Equine Vet. Sci.* **21**, 287-291.

OTTAWAY, C.W. (1955) The Mechanism of Movement. In: *Progress in the Physiology of Farm Animals.* Vol. 2, Ed: J. HAMMOND, Butterworth's Scientific Publications, London. pp 395-743.

PARKER, R.A. (1973) The analysis of the forces and displacements in the digit of the horse during walk. MSc Thesis. Cornell University, Ithaca, New York.

PARKS, A.H., BALCH, O.K. AND COLLIER, M.A. (1999) Treatment of acute laminitis. *Vet. Clin. N. Am.-Equine Pract.* **15**, 363-375.

PARKS, A.H. AND O'GRADY, S.E. (2003) Chronic Laminitis: current treatment strategies. *Vet. Clin. N. Am.-Equine Pract.* **19**, 393-416.

PATAN, B. (2001) Saisonaler Einfluß auf Hornbuildungsrate, Hprnabrieb und Hornqualität in der Hufwand von Przewalkipferden (*Equus ferus przewalskii*). Diss. med. vet., Freie Univ. Berlin.

PATAN, B. AND BUDRAS, K-D. (2003) Segmentspezifitäten am Pferdehuf – Teil II: Zusammenhang zwichen Hornstruktur und mechanisch-physikalischen Horneigenschaften in den verschiedenen Hufsegmenten. *Pferdeheilkunde.* **19**, 177-184.

PAYNE, J.M. (1966). *Brit. Vet. J.* **122**, 183.

PELLMANN, R (1995) Struktur und Funktion desHufbeinträgers beim Pferd. Diss. med. vet., Freie Univ. Berlin.

PELLMANN, R., REESE, S. AND BRAGULLA, H. (1993) Relationship between the structure and quality of equine hoof horn and a potential procedure for studying disorders of keratinisation. *Monatsh. Veterinarmed.* **48**, 623-630.

PELLMANN, R., BURAS, K.D. AND BRAGULLA, H. (1997) Structure and function of the suspensory apparatus of the coffin bone in the horse. *Pferdeheilkunde.* **13**, 53-64.

PETERS, F. (1883) *Die Formveränderungen des Pferdeshufes bei der Einworkung der Last mit besonderrem Bezug auf die Ausdehungstheorie.* Verlag Paray, Berlin.

PEUCHE, F. AND LESBRE (1855) *Précis du pied du cheval et de ferrure.* Paris.

PFLUG, W. (1978) *Die Anpassung des Fleckviehs in Süd- und Südwestafrika unter besondere Berücksichtigung der Klauen.* Diss. med. vet., München.

PFLUG, W., OSTERHOFF, D.R., KRAUSELICH, H. AND OSTERKORN, K. (1980) The Adaptability of Simmentaler Cattle in South and South West Africa with specific reference to their Claws. *S Afr. J. Anim. Sci.* **10**, 91-97.

POLITIEK, R.D., DISH, O. AND FJELDAAS, T. (1986) Importance of claw quality in cattle: review and recommendations to achieve genetic improvement. Report of the EAAP working group on "claw quality in cattle". *Livest. Prod. Sci.* **15,** 133-152.

POLLITT, C.C. (1990a) The treatment of laminitis and founder. In: *Proceedings of a course in foot lameness in horses, Massey University. Vet. Cont. Educ.* **No. 129**, 83-90.

POLLITT, C.C. (1990b) The pathophysiology of equine laminitis. In: *Equine Lameness and foot conditions.* Refresher course for veterinarians, University of Sydney, Australia 5th – 9th February. Ed: R. ROSE. Proceedings 130, 221-226.

POLLITT, C.C. (1992) Clinical anatomy and physiology of the normal equine foot. *Equine Vet. Educ.* **4,** 219-224.

POLLITT, C.C. (1993) *Equine foot studies.* (Video) Television unit, Prentice Centre. The University of Queensland.

POLLITT, C.C. (1994) The basement membrane at the equine hoof dermal epidermal junction. *Equine Vet. J.* **26**, 399-407.

POLLITT, C.C. (1995) *Colour Atlas of the Horse's Foot.* Mosby-Wolfe, London. pp 208.

POLLITT, C.C. (1996) Basement membrane pathology - a feature of acute equine laminitis. *Equine Vet. J.* **28**, 38-46.

POLLITT, C.C. (1998a) The anatomy and physiology of the hoof wall. *Equine Vet. Educ.* **10**, 318-325.

POLLITT, C.C. (1998b) Understanding Laminitis: What Really Happens. In: *Proceedings of Dodson & Horrell Ltd. International Research Conference on equine laminitis,* Stoneleigh, 8th – 9th September. pp 15-21.

POLLITT, C.C. (2001) *Equine Laminitis: A report for the Rural Industries Research and Development Corporation, RIRDC Publication 01/129.* RIRDC, Kingston. pp 99.

POLLITT, C.C. (2002) Aetiology of fructan-induced laminitis; mechanism of fructan involvement, alteration of hindgut microflora and quantities required. In: *Proceedings of the Dodson & Horrell Ltd. 4th International Conference on Feeding Horses,* United Kingdom, 5th – 7th March. pp 3-6.

POLLITT, C.C. AND MOLYNEUX, G.S. (1990) A scanning electron microscopic study of the dermal circulation of the equine hind limb claw. *Equine Vet. J.* **22**, 79-87.

POLLITT, C.C. AND DARADKA, M. (1998) Equine laminitis basement membrane pathology: loss of *type IV* collagen, *type VII* collagen and laminin immunostaining. *Equine Vet. J. Suppl.* **26**, 139-144.

QUDDUS, M.A., KINGSBURY, H.B. AND ROONEY, J.R. (1978) A force and motion study of the foreleg of a standardbred trotter. *J. Equine Med. Surg.* **2**, 233-242.

RANTHER, L.T. (1966) Rudolf Virchow's views on pathology, pathological anatomy and cellular pathology. *Arch Pathol.* **82**, 197-204.

REDDEN, R.F. (1990) White line disease. *Equine Pract.* **12**, 14-18.

REDDEN, R.F. (1997) Shoeing the laminitic horse. In: *Proceedings of the American Association of Equine Practitioners.* **43**, 354-359.

REDDEN, R.F. (1998) Understanding Laminitis. The Blood-Horse Inc. pp 142.

REDDEN, R.F. (1999) Shoeing the Laminitic Horse. In*: Proceedings of the 6th Kongres für die Pferdesmedizin und Pferdeschirurgie*, Kongr. ber., S. 36-39.

REDDEN, R.F. (2002) *Radiography of the Equine Foot; Techniques for enhancing the quality of your films.* Equine Podiatry Monograph Series, Series One, Nanric Inc., Kentucky. pp 25.

REID, I.M. (1980) Morphometric methods in veterinary pathology: a review. *Vet. Pathol.* **17**, 522-543.

REILLY, J.D. (1995) No hoof no horse? *Equine Vet. J.* **27**, 166-168.

REILLY, J.D. (1997) The Donkey's Foot and Its Care. In: *The Professional Handbook of the Donkey.* Ed: E.D. SVENDSEN, 3rd Edn., Whittet Books Ltd., London. pp 71-92.

REILLY, J.D. (1998) Hail hoof science! *Equine Vet. J. Suppl.* **26**, 2-3.

REILLY, J.D. (2001) *Effects of Dietary Biotin on the Physiology, Anatomy and Mechanics of Pony Hoof Horn.* PhD Thesis. University of Edinburgh.

REILLY, J.D. AND KEMPSON, S.A. (1992) Towards an understanding of hoof horn quality. In: *Proceedings of the VII International Symposium on Diseases of the Ruminant Digit*, Denmark. Ed: K. MORTENSEN.

REILLY, J.D., COTTRELL, D.F., MARTIN, R.J. AND CUDDEFORD, D. (1996) Tubule density in equine hoof horn. *Biomimetics*. **4**, 23-35.

REILLY, J.D., COLLINS, S.N., COPE, B.C., HOPEGOOD, L. AND LATHAM, R.J. (1998a) Tubule density of the *Stratum medium* of horse hoof. *Equine Vet. J. Suppl.* **26**, 4-9.

REILLY, J.D., COLLINS, S.N., COPE, B.C., HOPEGOOD, L. AND LATHAM, R.J. (1998b) Laminitis and the hoof horn capsule. In: *Proceedings of Dodson & Horrell Ltd. 1st International Research Conference on equine laminitis,* Stoneleigh, 8th – 9th September. pp 1-6.

REILLY, J.D., NEWLYN, H., COPE, B., LATHAM, R.J., COLLINS, S. AND HOPEGOOD, L. (2002a) A novel method for assessing hoof horn tubule density (TD) and a comparison of TD in the hooves of ponies, horses, donkeys, cattle, sheep and pigs. In: *Proceedings of the XII International Symposium on Lameness in Ruminants*, Orlando, Florida, 9th – 13th January. Ed: J.K. SHEARER. pp 275.

REILLY, J.D., NEWLYN, H., COPE, B., LATHAM, R.J., COLLINS, S. AND HOPEGOOD, L. (2002b) A comparison of different moisture-loss methods for measuring hoof wall moisture content. In: *Proceedings of the XII International Symposium on Lameness in Ruminants*, Orlando, Florida, 9th – 13th January. Ed: J.K. SHEARER. pp 193.

REILLY, J.D., COLLINS, S.N., HOPEGOOD, L. AND LATHAM, R.J. (2003 – Submitted) Tubule density of Donkey Hoof Horn and comparison with Pony and Horse Hoof Horn.

RIGGS, C.M. AND KNOTTENBELT, D.C. (2000) Acute and Subacute Laminitis. In: *Metabolic and Endocrine Problems of the Horse.* Ed: T.D.G. WATSON, W B Saunders, London. pp 1-22.

RIGGS, C.M, VAUGHAN, L.C., EVANS, G.P. LANYON, L.E. AND BOYDE, A. (1993) Mechanical implications of collagen fibre orientation in cortical bone of the equine radius. *Anat. Embryol.* **187**, 239-248.

ROONEY, J.R. (1978) Studies in equine biomechanics. *J. Equine Med. Surg.* **2**, 107-145.

ROONEY, J.R. (1980) *The Mechanics of the Horse.* R.E. Krieger Publishing Co., Florida. pp 56-61.

RÖSSNER, G. (1940) *Untersuchungen über die verteilung von hornröhrchen und zwischenhorn in der schutzschicht bei verschiedenen wandstellungen am hufe des pferdes.* Diss. med. vet., Hannover.

RUSS, J.C. (1992) The image processing handbook, CRC Press Inc., Boca Ratan. pp 354.

RYAN, T. (1999) Laminitis: a new interpretation and a new form of treatment. In: *Proceedings of the 3rd Biannual BEVA and NAFB & AE Conference on Veterinary and Farriery Practice,* Stoneleigh, 5th September. pp 10-15.

RYAN, T. (2000a) Laminitis - A new interpretation. 2: The dorsal wall lifting theory of laminitis. *Forge.* December, 3-9.

RYAN, T. (2000b) Laminitis - A new interpretation. 1: Laminitis induced by heel trimming of upright feet. *Forge*. October, 14-16.

SACK, W.O. AND HABLE, R.E. (1977) *Rooney's guide to the dissection of the horse.* Veterinary Textbooks, Ithaca, New York. pp 203.

SAID, A.H., KHAMIS, Y., MAHFOUZ, M.F. AND EL-KEIEY, M.T. (1983) Angiographic appearance of the metacarpus, phalanges and foot of the donkey. *J. Vet. Med. Ser. A-Physiol. Pathol. Clin. Med.* **30**, 788-795.

SAID, A.H., FAHMY, L.S., HEGAZY, A.A. AND MOSTAFA, M.B.A.D. (1992) Studies on chronic hyperplastic laminitis in the horse. *Vet. Med. J. Giza.* **40**, 43-51.

SALIBA, J.E. (1996) Use of finite element in micromechanics of natural composites. *Comput. Struct.* **61**, 415-420.

SCHROTH, S. (2000) Anatomie und Histologische Untersuchungen an den Hufen von Connemara-Ponys, Irischen Huntern und Englischen Vollblütern. Diss. med. vet., Leipzig.

SCHUMMER, A., WILKENS, H., VOLLMERHAUS, B., HABERMEHL, K.H., SILLER, W.G. (TRANSLATOR), AND WIGHT, P.A.L. (TRANSLATOR) (1981) *The Circulatory System, the Skin and the Cutaneous Organs of the Domestic Animals*. Verlag Paul Parey, Berlin. pp 610.

SEEGMILLER, A. AND MILLER (1981) Ecological relationships of feral burros and desert bighorn sheep. *Wildl. Monogr.* **No 78**. pp 58.

SINGH, S.S., MURRAY, R.D. AND WARD, W.R. (1992) Histopathological and Morphometric Studies on the Hooves of Dairy and Beef Cattle in Relation to Overgrown Sole and Laminitis. *J. Comp. Path.* **107**, 319-328.

SLATER, M.R., HOOD, D.M. AND CARTER, G.K. (1995) Descriptive epidemiological study of equine laminitis. *Equine Vet. J.* **27**, 364-367.

SLATER, M.R. AND HOOD, D.M. (1997) A cross-sectional epidemiological study of equine hoof wall problems and associated factors. *Equine Vet. J.* **29**, 67-69.

SMITH, F. (1921) The foot. In: *A Manual of Veterinary Physiology*, 4th Edn., London.

SPATZ, H.-CH., KÖHLER, L. AND NIKLAS, K.J. (1999) Mechanical Behaviour of Plant Tissues: Composite Materials or Structures. *J. Exp. Bot.* **202**, 3296-3272.

SPITZLEI, S. (1996) *Untersuchung zur Zusammensetzung des Hufhorns beim Pferd, deren Bedeutung für die Stabilität und Beziehung zur Nährstoffversorgung.* Diss. med. vet., Hannover.

STASHAK, T.S., KLIMESH, R. AND OVNICEK, G. (2002) Trimming and Shoeing for Balance and Soundness. In: *Adams' Lameness in Horses.* 5th Ed'n., Ed: T. S. STASHAK, Lippincott Williams & Wilkens, Philadelphia. pp 1081-1142.

STICK, J.A., LANN, H.W., SCOTT, E.A. AND EDWARD ROBINSON, N. (1982) Pedal bone rotation as a prognostic sign in laminitis of horses. *J. Am. Vet. Med. Assoc.* **180**, 251- 253.

STUMP, J.E. (1966) *An electron microscopic study of the dermo-epidermal junction and basal cell layer of the secondary epidermal laminae of the equine hoof.* PhD Thesis. Purdie University, Lafayette, Indiana.

STUMP, J.E. (1967) Anatomy of the normal equine foot, including microscopic features of the laminar region. *J. Am. Vet. Med. Assoc.* **151**, 1588-1597.

SUTER, M.M., CRAMERI, F.M., OLIVRY, T., MUELLER, E., VON TSCHARNER, C. AND JENSEN, P.J. (1997) Keratinocyte biology and pathology. *Vet. Dermatol.* **8**, 67-100.

SVENDSEN, E.D. (1995) The Donkey Sanctuary and International Donkey Protection Trust. *Equine Vet. Educ.* **7**, 53-59.

SYMONS, D. (1994) Equus Asinus. *Eur. Farrier's J.* **49**, 54-59.

TACHIO, G., DAVIES, H.M.S., MORGATE, M. AND BERNARDINI, D. (2002) A radiographic technique to assess longitudinal balance in front hooves. *Equine Vet. J. Suppl.* **34**, 368-372.

TAKENOUCHI, M., SUZUKI, H. AND TAGAMI, M.D. (1986) Hydration Characteristics of Pathologic Stratum Corneum – Evaluation of Bound Water. *J. Invest. Dermatol.* **87**, 574-576.

TALUKAR, A.H., CALHOUN, M.L. AND STINSON, A.W. (1972) Microscopic anatomy of the skin of the horse. *Am. J. Vet. Res.* **33**, 2365-2390.

TARLTON, J.F. AND WEBSTER, A.J.F. (2000a) Biochemical, biomechanical and histological analysis of failure of supportive structures in cattle hooves. In: *Proceedings of the British Society of Animal Science.* pp. 126.

TARLTON, J.F. AND WEBSTER, A.J. (2000b) Biomechanical and biochemical analyses of changes in the supportive structure of the bovine hoof in maiden heifers and around the time of first calving. In: *Proceedings of the XI International Symposium of Disorders of the Ruminant Digit,* Parma, Italy, 3rd – 7th September. Ed: C.M. MORTELLO, L. De VECCHIS AND A. BRIZZI. pp 97-101.

TARLTON, J.F. AND WEBSTER, A.J. (2002) A Biochemical And Biomechanical Basis For The Pathogenesis Of Claw Horn Lesions. In: *Proceedings of the XII International Symposium on Lameness in Ruminants*, Orlando, Florida, 9th – 13th January. Ed: J.K. SHEARER. pp 395-398.

TARLTON, J.F., HOLAH, D.E., EVANS, K.H., JONES, S., PEARSON, G.R. AND WEBSTER, A.J.F. (2002) Biomechanical and Histopathological changes in the Support Structures of Bovine Hooves around the Time of First Calving. *Vet. J.* **163**, 196-204.

THOMASON, J.J. (1998) Variation in surface strain on the equine hoof wall at the midstep with shoeing, gait, substrate, direction of travel, and hoof shape. *Equine Vet. J. Suppl.* **26**, 86-95.

THOMASON, J.J., BIEWENER, A.A. AND BERTRAM, J.E.A. (1992) Surface strain on the equine hoof wall in vivo: implications for the material design and functional morphology of the wall. *J. Exp. Biol.* **166**, 145-165.

THOMASON, J.J., McCLINCHEY, H.L. AND JOFRIET, J.C. (2002) Analysis of strain and stress in the equine hoof capsule using finite element method: comparison with principle strain recorded '*in vivo*'. *Equine Vet. J.* **34**, 719-725.

THRALL, D.E. (1998) *Textbook of Veterinary Diagnostic Radiology.* 3rd Edn., W.B. Saunders, London. pp 663.

TOHARA, S. (1948) Study of the hoof quality of horses. 1. On the horn-tube. *Jpn. J. Vet. Sci.* **10**, 69-80.

TSCHERNE, L. (1910) *Über die beziehungen der qualität des wandhornes der pferdehufe zur histologischen einrichtung desselben.* Diss. med. vet., Hochschule zu Dresden, Univ. Leipzig.

TRAUTMANN, A. AND FIEBIGER, J. (1957) *Fundamentals of the Histology of Domestic Animals.* R.E. HABEL and E.L. BIBERSTEIN Translation and Revision, 1949 German Edn. Comstock Publishing Association, New York. pp 360-369.

TRAWFORD, A. (1998) Multi-Disciplinary collaboration for the world-wide benefit of working equines In: *Proceedings of the 3rd International colloquium on donkeys, mules and horses in tropical agricultural development,* Universidad Nacional Autonoma De Mexico, Mexico. pp 271-280.

TRAWFORD, A. AND CRANE, M. (1995) Nursing care of the donkey. *Equine Vet. Educ.* **7**, 36-38.

VERMUNT, J.J. AND GREENOUGH, P.R. (1995) Structural characteristics of the bovine claw: horn growth and wear, horn hardness and claw conformation. *B. Vet. J.* **151**, 157-179.

VINCENT, J.F.V. (1990) *Structural Biomaterials.* Revised Edn., Princeton University Press, New Jersey. pp 244.

VINCENT, J.F.V. (1992) *Biomechanics - Materials. A Practical Approach.* IRL Press, Oxford University Press, Oxford. pp 247.

VOGEL, S. (1988) *Life's Devices: the Physical World of Animal and Plants.* Princeton University Press, New Jersey. pp 367.

VOGEL, S. (1998) *Cats' Paw and Catapults: Mechanical Worlds of Nature and People.* Penguin Books Ltd., London. pp 375.

VOGEL, S. AND WAINWRIGHT, S.A. (1969) *A Functional Bestiary – laboratory studies about living systems.* Addison-Wesley Publishing Co., Reading, Massachusetts. pp 106.

VON BERGEN, W. (1963) *Wool Handbook.* Vol 1. 3rd enlarged Edn., Interscience Publications, London. pp 800.

WAGNER, I.P., HOOD, D.M. AND HOGAN, H.A. (2001) Comparison of bending modulus and yield strength between outer *Stratum medium* and *Stratum medium zona alba* in equine hooves. *Am. J. Vet. Res.* **62**, 745-751.

WAINWRIGHT, S.A., BIGGS, W.D., CURREY, J.D. AND GOSLINE, J.M. (1976) *Mechanical Design in Organisms.* Edward Arnold, London. pp 423.

WALKER, M., TAYLOR, T.S., SLATER, M., HOOD, D., WEIR, V. AND ELSLANDER, J. (1995) Radiographic Appearance Of The Feet Of Mammoth Donkeys And The Findings Of Subclinical Laminitis. *Vet. Radiol. Ultrasound* **35**, 32-37.

WALZ, J. (1979) *Histologische Untersuchungen zur Erfassung der Klauenhornqualität beim Rind.* Diss. med. vet., Ludwig-Maximilians Univ. München.

WATTLE, O. (1998) Cytokeratins of the equine hoof wall, chestnut and skin: bio- and immunohistochemistry. *Equine Vet. J. Suppl.* **26**, 66-80.

WATTLE, O.S. (2000) Cytokeratins of the *Stratum medium* and *Stratum internum* of the equine hoof wall in acute laminitis. *Acta Vet. Scand.* **41**, 363-379.

WATTLE, O.S. (2001) Cytokeratins of the matrices of the chestnut (torus carpeus) and periople in horses with acute laminitis. *Am. J. Vet. Res.* **62**, 425-432.

WARZECHA, C. (1993) *The ruminant hoof: Morphological and histochemical findings in cattle, sheep and goat.* Diss. med. vet., Zurich.

WEAVER, A.D. (1971) Review of disorders of the ruminant digit with proposals for anatomical and pathological terminology and recording. *Vet. Rec.* **108**, 117-120.

WEIBEL, E.R. (1979) *Stereological Methods. Vol I. Practical Methods for Biological Morphometry.* Academic Press, London. pp 542.

WEISS, D.J. (1997) Equine laminitis: a review of recent research. *Equine Pract.* **19**, 16-20.

WEISS, D.J., GEOR, R.J., JOHNSTON, G. AND TRENT, A.M. (1994) Microvascular thrombosis associated with onset of acute laminitis in ponies. *Am. J. Vet. Res.* **55**, 606-612.

WEISS, D.J., TRENT, A.M. AND JOHNSTON, G. (1995) Prothrombotic events in the prodromal stages of acute laminitis in horses. *Am. J. Vet. Res.* **56**, 986-991.

WEISS, D.J., EVANSON, O.A., McCLENAHAN, D., FAGLIARI, J.J. AND JENKINS, K. (1997) Evaluation of platelet activation and platelet-neutrophil aggregates in ponies with alimentary laminitis. *Am. J. Vet. Res.* **58**, 1376-1380.

WEISS, J.A. AND GARDINER, J.C. (2001) Computational modelling of ligament mechanics. *Crit. Rev. Biomed. Eng.* **29**, 303-371.

WESTERFELD, I. (2003) *Struktur und Funcktion des Bovinen Klauenbeinträgers.* Diss. med. vet., Freie Univ. Berlin.

WHITEHEAD, G., FRENCH, J. AND IKIN, P. (1991) Welfare and veterinary care of donkeys. *In Practice.* **13**, 62-68.

WICHTMANN, A.D., HOGAN. H.A. AND HOOD, D.H. (1990) Development of a two-dimensional finite element model for studying the internal mechanism of the distal digit of the horse. *Adv. Bioeng.* **17**, 331-334.

WILKENS, H. (1955) Zum mikroarchitektonischen Aufbau der Klauenepidermis. *Dtsch. Tierarztl. Wochenschr.* **62**, 437-442.

WILKENS, H. (1964) Zür makroskopischen und mikroskopischen Morphologie der Rinderklaue mit einem Vergleich der Architektur von Klauen- und Hufröhrchen. *Zbl. Vet. med.* **11**, 163-200.

WILLIAMS, .D. (1993) The Donkey's Foot and Its Care. In: *The Professional Handbook of the Donkey.* Ed: E.D. SVENDSEN, 2rd Edn., Whittet Books Ltd., London. pp 71-92.

WOODS, W. Jun, (1889) Laminitis. *Vet. J. Ann. Comp. Pathol.* **XXIX** 370-377.

WORTLEY-AXE, J. (1912) *The Horse: Its Treatment in Health and Disease.* Divisional Volume **IX**, Gresham Publishing Comp. London.

WU, J.Z. DONG, R.G., SMUTZ, W.P. AND SCHOPPER, A.W. (2003) Modeling of time-dependent force response of fingertip to dynamic loading. *J. Biomech.* **36**, 383-392.

XU, X., GULBERG, A. AND AMASON, U. (1996) The complete mitochondrial DNA (mDNA) of the donkey and mDNA comparisons among four closely related mammalian species-pairs. *J. Mol. Evol.* **43**, 438-446.

YELLE, M. (1986) Clinicians guide to equine laminitis. *Equine Vet. J.* **18**, 156-158.

ZENKER, W. (1991) *Hufprobleme bei Lipizzanern und ein Behandlungsversuch mit Biotin. Histologische Untersuchungen an veranderten Hafen und Bestimmung biotin - abhangiger Enzyme.* Diss. med. vet., Zurich.

ZENKER, W., JOSSECK, H. AND GEYER, H. (1995) Histological and physical assessment of poor hoof horn quality in Lipizzaner horses and a therapeutic trial with biotin and a placebo. *Equine Vet. J.* **27**, 183-191.

ZHANG, M. AND ROBERTS, C. (2000) Comparison of computational analysis with clinical measurement of stresses on below-knee residual limb in a prosthetic socket. *Med. Eng. Phys.* **22**, 607-612.

ZHOA, Y.F., WANG, X.Y., GLO, K.K., KANG, Z.L., SHEN, H., DAI, X. AND HUANG, S.H. (1989) The finite element analysis of the bicuspid and molar of mandible. *Hua Xi Yi Ke Da Xue Xue Bao.* **20**, 311-314.

ZOERB, G.C. AND LEACH, D.H. (1978) Mechanical properties of the hoof wall of the horse. *Am. Soc. Agric. Eng.* **ASAE Technical Paper No 78-3063**, 1-13.

ZSCHOKKE, E. (1885) Über das Absorptionsvermögel des Hornes und über die Hufsalben. *Schw. Arch. Tierheilk.* **4**, 151-165.

APPENDIX I
MATERIAL PROPERTIES

INTRODUCTION

Knowledge of how materials respond to externally applied forces is central to developing, and testing, theories of structure-function relationships within the hoof.

When a solid object is subjected to an external force or load, it deforms in accordance with Newton's third law of motion in order to oppose the force. The size of the deformation, for a given material under defined conditions, is dependent upon the magnitude of the applied force and the dimensions of the object.

STRESS

Stress (σ) is defined as a measure of the applied force normalised per unit area upon which the force is applied, hence: -

- Stress = force / area

This definition of stress is more correctly referred to as engineering stress, and represents a first approximation of the true stress within the material (ASTM E 6 – 89). True stress is calculated on the basis of cross sectional area at the moment of observation, and hence takes into account the deformational response of the sample to the applied load. The reader is referred to Callister (1994) for a comprehensive discussion of these issues.

The SI unit of Stress is the Pascal (Pa).

1 Pa = $1N/m^2$

1MPa = $1N/mm^2$ or $1MN/m^2$

PRINCIPLE STRESS

The principle (normal) stress is defined as the maximum or minimum value of stress perpendicular to the plane on which the loading force acts (ASTM E 6 – 89), with tensile forces ascribed a positive value, and compressive forces, a negative value.

There are three principle stresses on three mutually perpendicular (orthogonal) planes (ASTM E 6 – 89). Hence the state of stress in a sample can be described either as: -

- Uniaxual – A state of stress in which two of the principle stresses are zero
- Biaxial – A state of stress in which one of the principle stresses is zero
- Triaxial – A state of stress in which none of the principle stresses are zero

STRAIN

Strain (ε) is a measurement of the resultant deformation in the direction of the applied stress normalised against the original length of the object, thus: -

- Strain = change in length / original length

Hence strain is a dimensionless (unit-less) parameter expressed either in percentage terms, or as a relative fraction of the specimens original length (ASTM E 6 – 89).

Strain as defined here is more correctly referred to as engineering strain, and represents a first approximation of the true strain within the sample. True stain is calculated as the natural logarithm of the ratio of the specimen length at the moment of observation to the original length (Callister 1994).

STRESS-STRAIN INTERACTIONS – A MOLECULAR CONSIDERATION

The relationship between stress and strain is derived from the character of the forces acting at a molecular level within a material (Gordon 1976). In the unstressed state, an equilibrium position exists in which the inter-atomic distances are such that inter-atomic forces are balanced, at their lowest energy state. The application of an applied force alters the inter-atomic distances and increases the inter-atomic forces, which raises the energy level within the material.

STRESS-STRAIN RELATIONSHIP

Figure I.I illustrates the theoretical stress-strain relationship of a linear elastic material to failure. This plot illustrates the nature of deformation of this material with increasing load.

The initial part of the stress-strain curve reveals a linear or proportional relationship in which strain is directly proportional to the applied stress. Strain within the proportional range of the material is non-permanent. Once the loading stress has been removed, the material will return to its original equilibrium position.

This relationship is referred to as Hooke's law of linear elasticity (After R. Hooke 1635-1703). The linear relationship of the stress strain plot corresponds to the proportional range of the inter-atomic force curve.

Figure I.I Typical stress-strain relationship of a linear elastic material loaded to failure.

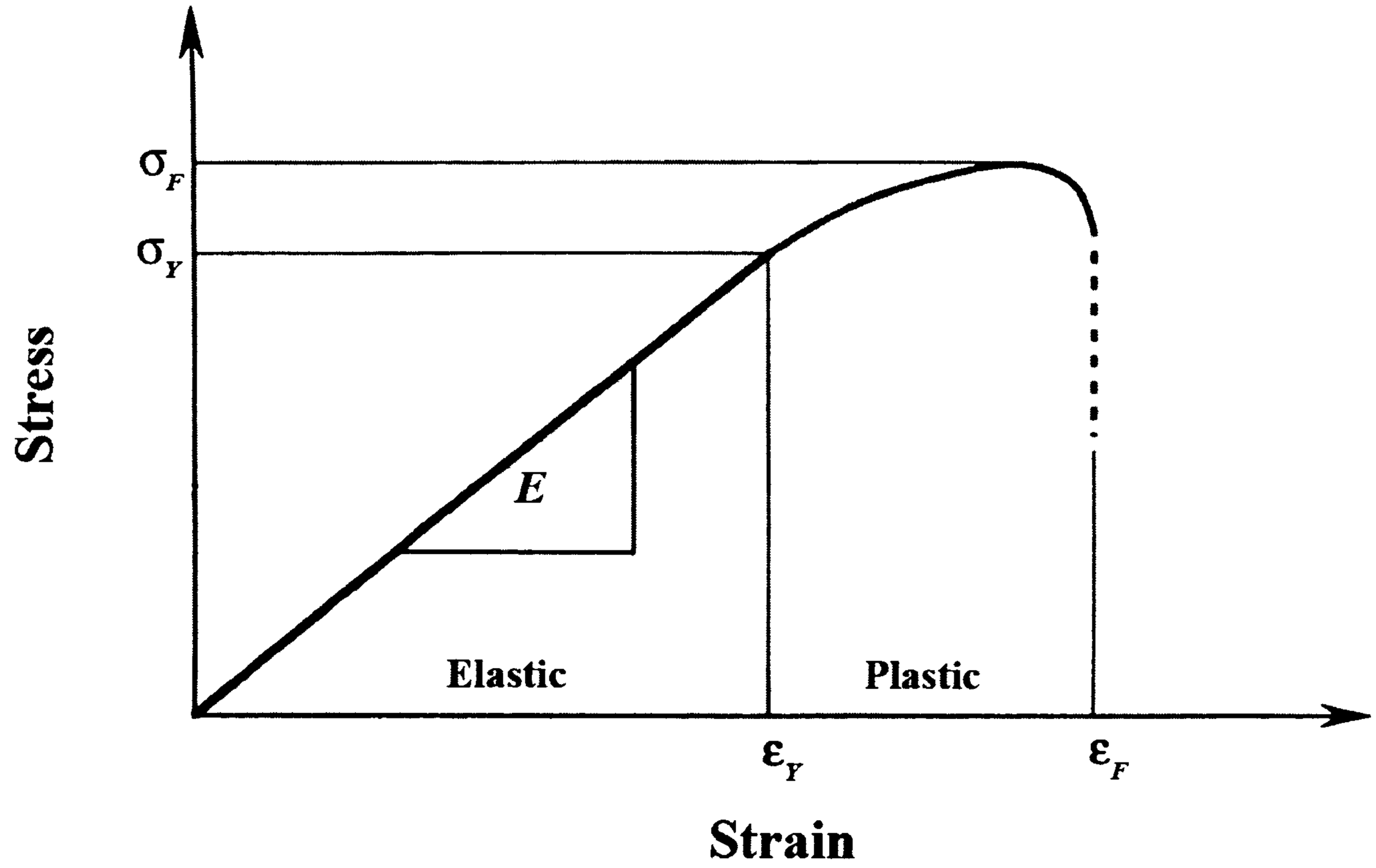

Key: Elastic, **Region of linear stress-strain relationship.** Plastic, **Region of non-linear stress-strain relationship.** σ_Y, **Yield stress – stress level at Bioyield.** σ_F, **Ultimate strength of the material.** ε_Y, **Strain at Bioyield.** ε_F, **Strain at failure.** *E*, **Modulus of Elasticity – gradient of linear region of stress-strain relationship. Note: Resilience = Area under the stress-strain plot within the elastic region. Toughness = Area under the stress-strain plot to failure.**

PAGE NUMBERING AS ORIGINAL

YOUNG'S MODULUS OF ELASTICITY

The gradient of the stress-strain plot within the linear or proportional region is defined by the constant *E* (ASTM E 111 – 82), or Young's modulus of elasticity (After R Young 1773-1829). Hence: -

- Stress = modulus of elasticity x Strain
- $\sigma = E\varepsilon$

This modulus is a measure of a material's rigidity or resistance to deformation (Wainwright *et al.* 1976). In this way, the greater the modulus the smaller is the resultant strain, or deformation, at a given stress level. Materials can be considered to be either rigid or pliant (Vogel 1988). Rigid materials are characterised by a high modulus and are therefore resistant to deformation when loaded. Conversely, pliant materials have a low modulus, and hence deform readily upon loading.

STIFFNESS AND MODULUS OF ELASTICITY - SYNONYMOUS MATERIAL PROPERTY TERMS?

It is important to recognise that modulus of elasticity and stiffness, are not equivalent terms. Stiffness (*K*) is correctly defined as the force per unit extension, and represents the slope of the force displacement plot for a material. Whereas, the modulus of elasticity, reflects the stress required, to achieve unit strain within a material.

Stiffness is not independent of the effect of test sample size. Doubling the sample length of a given material will reduce the stiffness by 50%, whereas the modulus, because it is normalised both in respect of the cross sectional area and sample length, will remain constant. Hence the modulus of elasticity is independent of sample geometry, and thus represents a defining characteristic of a material.

YIELD STRENGTH / BIOYIELD

A point is reached, the proportional limit, at which departure from stress-strain linearity occurs within the material (Mohsenin 1968, ASTM E 6 – 89). The stress level at this point (σ_Y) defines the material's yield strength, (Callister 1994), or bioyield (Vincent 1992), and represents a defining characteristic of the material.

σ_Y represents the greatest stress that a material is capable of sustaining without any deviation from proportionality of stress and strain (ASTM E 6 – 89).

Bioyield occurs at a strain value of ε_Y. This reflects the point at which the inter-atomic bonds of the material can no longer resist the applied stress (Gordon 1976). Thereafter, permanent non-

recoverable inelastic (plastic) deformation occurs within the material (Wainwright et al. 1976, ASTM E 111 – 82, ASTM E 6 – 89).

FAILURE

Plastic deformation continues until catastrophic failure of the material occurs. This occurs at a stress level of σ_F, and represents the ultimate strength of the material. The corresponding strain level at failure is defined as ε_F.

STRAIN ENERGY, RESILIENCE AND TOUGHNESS

Deformation results in the generation of strain energy within a material (Gordon 1976). Strain energy is determined by the product of the stress applied to the material, and the resultant strain generated within the material (Wainwright *et al.* 1976, Gordon 1976).

As strain within the proportional range of the material is non-permanent, removal of the loading stress results in dissipation or recycling of the accrued strain energy. Hence this is referred to as Elastic strain energy.

Thus the area under the proportional range of the stress-strain plot represents a measure of the total elastic strain energy absorbed by the material (Callister 1994), or resilience (Wainwright *et al.* 1976).

Hence: -

- Resilience (elastic strain energy of a linear elastic material to bioyield = 1/2 (Yield Stress x Yield Strain)
- Resilience = 1/2 ($\sigma_Y \varepsilon_Y$)

Resilience per unit volume of material is expressed in MJ/m^3.

Once the proportional limit of the material is exceeded non-recoverable, plastic strain energy absorption occurs within a material. The area under the stress strain plot to failure, represents the total energy absorbed by a material, or toughness (Callister 1994), and hence includes both elastic, and plastic, strain energy absorption.

CRACK INITIATION AND PROPAGATION

A material will fail if it can not readily absorb strain energy (Biewener 1992). High rigidity, or modulus, limits inter atomic displacement and hence limits strain energy storage within a material.

The inability to store strain energy results in stress concentration within the atomic bonds that immediately surround any defect present within the material (Callister 1994). This stress concentration may reach critical levels that exceed the inter-atomic bond strengths. This results

in crack initiation and propagation within the material leading to ultimate catastrophic failure (Griffith 1921, Gordon 1976, Vincent 1992).

Gordon (1976) argued that a lack of material toughness resulted from a low resistance to crack propagation. Hence, pliant materials are normally tougher than rigid materials (Wainwright *et al.*1976, Callister 1994) due to their inherent characteristic of readily deforming in an elastic manner, and thereby storing elastic strain energy.

This is a defining characteristic of most biological materials (Vogel 1988, 1998, Vincent 1990, 1992), and accounts for the ability of these materials both to accommodate and resist imposed forces (Vogel 1988).

COMPOSITE 'MATERIALS'

Biological materials can be classified as composites (Wainwright *et al.* 1976, Vogel 1988). Composites are composed of two or more distinct material phases, and display mechanical properties not possessed by its constituent material phases (ASTM D3878 – 95c). Composites are inhomogenous at a microscopic level, but can be considered, at a macroscopic level, to be homogenous. The constituent phases do not mix, and hence retain their identities within the resultant composite, although they act in concert to synergistic effect.

Many biological materials can be considered as fibre – reinforced composites (Vogel 1988), in which a certain volume fraction (relative proportion) of a rigid fibrous material, the dispersed phase, is contained within a pliant matrix, or continuous phase.

In this way, a material is formed which combines the high strength and rigidity of the fibre, with the energy absorbing capacity of the matrix. In this regard, the fibre phase serves to reinforce the matrix (ASTM D3878 – 95c).

This synergistic interaction between these distinct material phases produce,s at the macroscopic level, a relatively strong yet tough material, which has good crack resistant properties (Wainwright *et al.* 1976). Such materials are ideal in fulfilling a supportive or aggressive structural role within nature (Vogel 1988, 1998).

Fibre composites can be further sub-divided, dependent upon fibre orientation (ASTM D3878 – 95c), into unidirectional and multidirectional fibre composites. In the unidirectional fibre composite, all fibres are aligned in the single direction, whereas in multidirectional fibre composites, the fibres are orientated in several directions.

The elastic behaviour of a unidirectional fibre composite subjected to specific uniaxial loading conditions can be approximated by the Voigt and Reuss Estimates (Hull 1981) or "*Rule of mixtures*" (Callister 1994).

These specific loading conditions are illustrated in Figure I.II: -

1. Uniaxial loading in the axial (y) direction, parallel to the fibre orientation

$$\text{Axial Modulus } Ey = EfVf + EmVm$$

Where:

Ef = Modulus of Elasticity of the fibre phase

Vf = Volume fraction of the fibre phase

Em = Modulus of Elasticity of the matrix phase

Vm = Volume fraction of the martrix phase

2. Uniaxial loading in the lateral (x) direction, perpendicular to the fibre orientation

$$\text{Horizontal Modulus } (Ex)^{-1} = Vm / Fm + Vf / Ef$$

Or

$$Ex = \frac{EmEf}{Ef(1 - Vf) + EmVf}$$

The presence of voids within composites represents a special case in that the void has zero strength and stiffness (Wainwright *et al.* 1976). Voids also act as stress raisers by concentrating stress at their boundary (Gordon 1976). This may lead to 'Griffith Type' crack fracture (Gordon 1976). The shape of the void affects the nature of the stress concentration (Wainwright *et al.* 1976). The more elliptical the void, then the greater is the stress raising factor at the margin of the major elliptical axis (Wainwright *et al.* 1976).

AXIAL COMPRESSION – BUCKLING

Wainwright *et al.* (1976) stated that unidirectional fibre composites subjected to uniaxial compressive loading have a tendency to failure due to buckling effects. This arises due to the fact that the fibres subjected to an increased axial loading will, at a critical level, bend along their longitudinal axis. There are two distinct buckling phenomena. These are: -

- Euler buckling.
- Local buckling.

The type of the buckling response that occurs within a hollow cylinder, or tube, is dependent mainly upon the thickness of the walls of the tube (Vogel 1988).

Figure I.II Diagrammatic representation of axial (A) and lateral (B) loading cases for a unidirectional fibre composite.

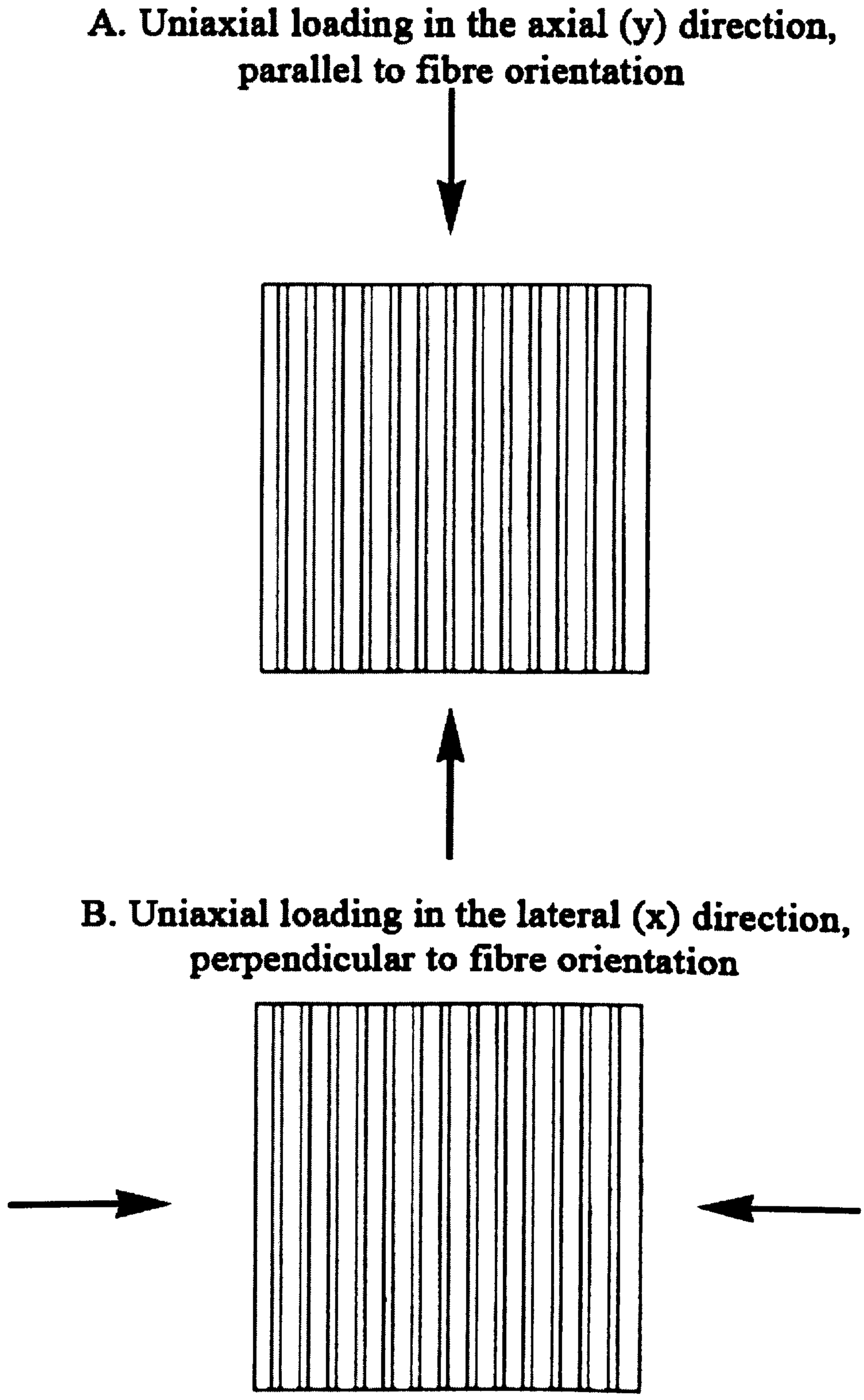

Key: Arrows indicate direction of applied force relative to the fibre oreientation

EULER BUCKLING

Euler buckling involves a smooth continuous bend, or series of bends, that course along the entire length of the column. This type of buckling, which ASTM D 6108 – 97 refers to as lateral buckling, induces compressive forces on the concave side of the deformed column, whilst tensile forces are initiated on the convex surface. Thus it is possible that a column subjected to axial compression can suffer tensile failure. Euler buckling is degenerative in nature, and once initiated, it will continue to propagate (Vogel 1988).

The critical load that initiates this type of buckling is dependent upon the column's second moment of area (Wainwright *et al.* 1976), which is often referred to as the initial moment of inertia of the cross section (ASTM E6 – 89).

The second moment of area, (I) accounts for material distribution effects upon column deformability, and represents a measure of the column's effective resistance to bending. Specifically, I reflects how the distribution of the material within the column affects its response to loading. The specific value of I, is determined both by the amount of material, and its spatial distribution in relation to the longitudinal, or centroidal axis of the column. It is this axis around which the bending moment occurs, and is therefore analogous to the neutral axis described in bending theory.

It is differences in the value of I alone that explain why the ultimate compressive strength of a composite, reinforced with large diameter fibres, is greater than that of a composite containing an equivalent volume fraction of small diameter fibres (Harris 1980).

LOCAL BUCKLING

Local buckling is marked by the presence of a localised failure or 'kink'. This type of buckling, which ASTM D 6108 – 97 refers to as, 'microbuckling' is most often encountered in hollow tubes. Unlike Euler buckling, it is the thickness of the tube walls *per se*, and not I, that is the critical factor in the initiation this type of buckling event (Wainwright *et al.* 1976).

REFERENCES

ASTM E6 – 89 (1989) Standard Terminology Relating to Methods of Mechanical Testing. American Society for Testing and Materials (ASTM), Philadelphia.

ASTM D3878 – 95c (1996) Standard Terminology of High-Modulus Reinforcing Fibres and Their Composites. American Society for Testing and Materials (ASTM), Philadelphia.

ASTM E 111 – 82 (Reapproved 1998) Standard Test Method for Young's Modulus, Tangent Modulus and Chord Modulus. American Society for Testing and Materials (ASTM), Philadelphia.

ASTM D 6108 – 97 (1998) Standard Test Method for Compressive Properties of Plastic Lumber and Shapes. American Society for Testing and Materials (ASTM), Philadelphia.

BIEWENER, A.A. (1992) Biomechanics - Structures and Systems. A Practical Approach. IRL Press, Oxford University Press, Oxford. pp 286.

CALLISTER, W.D. Jr. (1994) Materials Science and Engineering: An Introduction. 3rd Edn., J. Wiley & Sons Inc., New York. pp 811.

GORDON, J.E. (1978) The New Science of Strong Materials or Why You Don't Fall Through the Floor? Penguin Books Ltd., Middlesex. pp 269.

GRIFFITH, A.A. (1921) The phenomena of rupture and flow in solids. Phil. Trans. Roy. Soc. A221, 163-198.

HARRIS, B. (1980) The mechanical behaviour of composite materials. In: The Mechanical Properties of Biological Materials, Symposia of the Society for Experimental Biology, Symposium XXXIV. Ed: J.F.V. VINCENT and J.D. CURREY, Society for Experimental Biology, Cambridge University Press, Cambridge. pp 37-74.

HULL, D. (1981) An introduction to composite materials. Cambridge University Press, London. pp 246.

MOHSENIN, N.N. (1968) Physical properties of plant and animal materials. Vol I: Structure, Physical Characteristics and Mechanical properties. Gordon and Breach Science Publishers, London. pp 730.

VINCENT, J.F.V. (1990) Structural Biomaterials. Revised Edn., Princeton University Press, New Jersey. pp 244.

VINCENT, J.F.V. (1992) *Biomechanics - Materials. A Practical Approach.* IRL Press, Oxford University Press, Oxford. pp 247.

VOGEL, S. (1988) *Life's Devices: the Physical World of Animal and Plants.* Princeton University Press, New Jersey. pp 367.

VOGEL, S. (1998) *Cats' Paw and Catapults: Mechanical Worlds of Nature and People.* Penguin Books Ltd., London. pp 375.

WAINWRIGHT, S.A., BIGGS, W.D., CURREY, J.D. AND GOSLINE, J.M. (1976) *Mechanical Design in Organisms.* Edward Arnold, London. pp 423.

APPENDIX II
CLASSIFICATION OF THE LAMINITIC CONDITION – A CRITICAL REVIEW

An effective and fully comprehensive mode of classification for the laminitic condition is yet to be achieved. Classification of the laminitic condition has been variable based upon aetiological factors, clinical or radiographic presentation, and/or treatment and recovery outcome. Table 1.4 summarised the various classification systems that have been applied to the laminitic condition. This review highlights the advantages and disadvantages of the respective classification systems, both with regards to the horse and the donkey.

Dietz (1977) proposed a classification system based upon the aetiological factor inducing laminitis. This approach has been criticised due to the fact that the different aetiologic factors results in a 'common digital pathology' (Coffman and Garner 1972, Colles and Jeffcott 1977). In addition, this approach does not consider the severity of the condition, nor the likely prognosis. Recent research by Budras and Huskamp (1999) has however reported distinct differences in attendant digital pathology in laminitis of systemic and traumatic origin.

Obel (1948) proposed a classification system based upon the subjective grading of 'degree of lameness'. This classification approach, although selectively modified by various researchers including Hood (1997a), Pollitt and Daradka (1998) and Pollitt (2001), has provided the mainstay for the clinical assessment of the laminitic equid.

Obel (1948) suggested that lameness scoring could serve as a reliable prognostic indicator. Indeed Hunt (1993) reported a positive association between lameness grade and recovery in a retrospective case study of 202 laminitic equids.

Several authors including Stick *et al.* (1982) have however, expressed concerns regarding the value of lameness grading *per se* as an effective basis for classification. These authors argued that variations in the clinical presentation of lameness are also likely to reflect differences in individual stoicism, disease duration, concomitant systemic and digital pathologies, and/or therapeutic intervention. These issues question the effectiveness of a classification system based solely upon the lameness grade of the presented animal.

The specific issue of stoicism may be of particular relevance with regard to the donkey. Given the pharmacological evidence, reported by Mathews *et al.* (1997) and Mathews (2000, 2002), as to this species' stoical response to pain. Thus the adoption of a classification system based only upon overt signs of pain may be unwarranted in the donkey.

In light of the comments raised Stick *et al.* (1982), several researchers have variably used the occurrence and/or nature of digital collapse within the foot as a more appropriate basis for

classification. However, inconsistent use of the terms 'acute' and 'chronic', and 'founder' and 'sinker' have caused confusion and limited progress in this area.

Dietz (1977), Hood and Stevens (1981) and Marks (1984) distinguished between two forms of the laminitic condition based upon whether DP dislocation had occurred within the foot. These were referred to respectively as, the acute and chronic phases of the condition. In this regard, DP dislocation was considered as pathognomonic of the chronic phase of the condition, with the onset of dislocation marking progression from the acute phase into the chronic phase. Progression into the chronic phase was considered to be particular significance as this event results in irreversible anatomical change within the foot (Hood 1984).

However Colles and Jeffcott (1977) and Baxter (1992a,b) used these term to indicate the duration of the laminitic condition. According to this principle, 'acute' refers to a short standing condition, whilst chronic indicates a condition of long standing. There are however, inherent difficulties in establishing an accurate time line for the condition. This is dependent upon the prompt presentation, and effective diagnosis, of the affected animal. This is not always the case, even within domesticated herds of equids (Hood 1998 – Pers Com.). Owners are often reluctant to present an animal with low-grade lameness, and presentation may be delayed until severe signs of pain are evident. Thus the true time line for the condition can often only be speculated. These problems are further compounded by the propensity for the afflicted animal to experience recurrent bouts of laminitis. Hence it is possible to find in the animal presented for the first time, extensive degenerative damage within the foot which is consistent with a laminitic condition of long standing. Despite these facts, the terms acute and chronic have been widely employed, adding to the confusion surrounding classification of the laminitic animal. For example, Eustace (1991) distinguished between 'acute founder' and 'chronic founder' groups dependent upon the duration of the condition. Whereas Yelle (1986), stated that DP dislocation occurred during the acute phase of the condition, and is stabilised during the chronic phase. The use of the term 'acute founder' (Eustace 1991) and also, the linkage of DP dislocation to the acute phase of the condition (Yelle 1986), are both diametrically opposed to the rational advocated by Dietz (1977), Marks (1984) and Hood (1984). This is because Dietz (1977), Marks (1984) and Hood (1984) considered DP dislocation to be pathognomonic of the chronic phase of the condition, and that the dislocation event marks the division between the respective acute and chronic phases.

The terms 'acute' and 'chronic' have also been to used to differentiate laminitic animals based upon the severity of the condition, as judged by the level of pain. In this regard, acute is used to define severe digital pain, whilst chronic denotes low-grade pain.

The level of pain evident within the afflicted animal is however likely to determined by individual stoicism, inflammatory response, pharmacological intervention and therapeutic treatments. Hence this represents an inappropriate basis for classification. The importance of assessing the severity of the laminitic condition can not however be overlooked. These issues are covered in Section 1.11.4.

Hood and Stevens (1981) recommended the adoption of proposed a 4-fold classification system based upon that devised by Nilsson (1963) for the assessment of bovine laminitis. This system, subsequently refined by Hood (1997a) related the specific pathophysiologic and degenerative events that may occur within the foot, to the time line of the laminitic condition. Laminitic animals were classified into one of 4 mutually exclusive categories, each representing a distinct phase in the progression of the laminitic condition. Classification was based upon the clinical signs of laminitis, the incidence of digital collapse, and the duration of the condition. The terms acute and chronic were used in accordance with Dietz (1977). In addition, animals were classified as developmental within the initial 48 hours of the condition, and sub acute if the condition had lasted more than 72 hours without DP dislocation having occurred.

The nature of DP dislocation event has itself been used to classify laminitic cases. Historically 'founder' and 'sinker' were used to differentiate between DP rotation and DP displacement respectively (Butler *et al.* 1998). Particular emphasis has been placed upon the nature of the DP dislocation event due to guarded prognosis associated with distal displacement in the horse that was reported by Baxter (1985). However empirical evidence suggests this guarded prognosis is unwarranted for the donkey (Eley 2003 – Pers Com.).

This two-fold categorisation, which Hood *et al.* (1993a) referred to as Type I and II dislocation, however represents an over simplification as rotational and DP displacement events may occur concurrently within the foot (Baxter 1992b).

The inconsistent and *ad hoc* use of 'founder' and 'sinker' within the literature causes further confusion. For example, Chandra *et al.* (1982), Linford (1990, 1996), and Pollitt (1995) have variable used either 'founder' or 'sinker' as synonymous generic terms for the laminitic condition when they are not. This situation has been compounded by the work of Eustace (1991, 1992, 1995), and Cripps and Eustace (1999a,b). These authors refer to absolute linear measurement of DP displacement within the hoof capsule as 'founder distance'. This is in spite of the fact that these authors specifically differentiate between 'founder' and 'sinker' cases in accordance with the definition given by Butler *et al.* (1998).

The confusion surrounding the 'founder' and 'sinker' terms question both the merits, and desirability, for their continued usage as a basis for classifying DP dislocation events.

Baxter (1992a,b), Eustace (1992), Moore and Allen (1995), and Cripps and Eustace (1999a) have variably expanded upon the 2-fold 'founder'/ 'sinker' classification in order to provide a more complete system for classification. These systems reflect both the occurrence and the nature of DP dislocation within the foot. In addition, these systems directly link these events either to Obel lameness grades (Moore and Allen 1995), or to the clinical presentation of the afflicted animal (Eustace 1992, Cripps and Eustace 1999a,b).

Hood *et al.* (1993a,b) argued that it was important to consider the functional significance of the digital collapse. These authors stated that a full recovery, and a 'return to former athletic potential', was only possible so long as mechanical failure of the SADP had not occurred. This is because, the permanent anatomical changes that occurs within the foot following failure of the SADP, prevent the restoration of normal biomechanical function.

Hood *et al.* (1993a,b) stated that the degree to which former performance could be restored, was related to the extent of the mechanical failure within the SADP. This suggests that important links may exist between the extent of pathological change evident within the foot, and the degree of biomechanical impairment.

Eustace (1993) recognised two distinct chronic founder sub-groups based upon differences in response to therapy, which he referred to respectively as Type I 'rehabilatory' and Type II 'refractory'. The degree of degenerative change within these sub-groups differed, with marked anatomical change, and significant roentgenic change to the DP noted within the Type II sub-group. Coffman *et al.* (1972) and Linford (1990) similarly recognised distinct refractory, exacerbate laminitics (REL) or chronic remissive laminitics (CRL) subgroups, which they stated, differed in their respective 'likely return to former athletic performance'. Several researchers including Kameya (1973) and Stick *et al.* (1982) have attempted to objectively measure the nature and extent of DP dislocation associated with an ordinal scale of 'degree of return to former performance levels'. These issues are discussed within Chapter 3 of this thesis.

More recently, Hood (1997a,b, 1999) suggested an alternative two-way classification approach that takes into account both lameness severity and the change in the degree of lameness over time. In this classification system, an animal may be classified as either 'compensated' if it is not significantly lame, or 'uncompensated', if significantly lame. In addition, the animal may be considered as being either 'static' or 'progressive' dependent on whether the degree of lameness evident in the affected animal increases over time.

In conclusion, the search for an effective classification represents a key priority in laminitic research, if improvements in the management of the affected animal are to be achieved, and the welfare of the laminitic animal improved.

To achieve this end, appropriate diagnostic and prognostic criteria must be considered collectively. Whilst anatomic and/or pathologic alterations within the foot must form the basis for classification, the biomechanical consequences of these alterations must also be considered. Assessment of impaired biomechanical function by indirect methods alone is of questionable value. The degree of functional compromise evident within the foot is likely to be determined by the nature, and extent of the DP dislocation, and also, the attendant digital pathologies that arise as a consequence of digital collapse.

An effective classification system for the laminitic condition requires standardised terminology. The terminology adopted must then be consistently used in related research. Definitions must be unambiguous, and limit the possibility for confusion within the wider community. Thus colloquialism must be avoided. It is only through achieving these aims that progress can be made in improved management and welfare, to the ultimate benefit of the equid.

REFERENCES

BAXTER, G.M. (1986) Equine laminitis caused by distal displacement of the distal phalanx: 12 cases (1976-1985). *J. Am. Vet. Med. Assoc.* **189**, 326-329.

BAXTER, G.M. (1992a) Laminitis: In Current Therapy in Equine Medicine Ed: L. W. B. MILLS. Saunders, Philadelphia. pp 154-160.

BAXTER, G.M. (1992b) Equine laminitis. *In Practice.* **14**, 13-22.

BAXTER, G.M. (1994) Acute Laminitis. *Vet. Clin. N. Am.-Equine Pract.* **10**, 627-642.

BUDRAS, K-D. AND HUSKAMP, B. (1999) Belastungshufrehe – Vergleichunde Betrachtungen zu anderen systemischen Hufreheerkrankungen. *Pferdeheilkunde.* **15**, 89-110.

BUTLER, J.A., COLLES, C.M., DYSON, S.J., KOLD, S.E. AND POULOS. P.W. (1998) *Clinical Radiography of the horse.* Blackwell Science, Oxford. pp 547.

CHANDRA, I.S., NIGAM, J.M., SINGH, A.P. AND SINGH, K. (1982) Radiographical diagnosis of equine chronic laminitis (founder). *Indian Vet. J.* **59**, 640-641.

COFFMAN, J.R. AND GARNER, H.E. (1972) Acute laminitis. *J. Am. Vet. Med. Assoc.***161**, 280-1283.

COLLES, C.M. AND JEFFCOTT, L.B. (1977) Laminitis in the horse. *Vet. Rec.* **100**, 262-264.

CRIPPS, P.J. AND EUSTACE, R.A. (1999a) Radiological measurements from the feet of normal horses with relevance to laminitis. *Equine Vet. J.* **31**, 427-432.

CRIPPS, P.J. AND EUSTACE, R.A. (1999b) Factors involved in the prognosis of equine laminitis in the UK. *Equine Vet. J.* **31**, 433-442.

DIETZ, O. (1977) *Hoof, Diseases of.* In: Encyclopaedia of Equine Medicine and Surgery. Ed: R. RUTHE, Verlag Paul Parey, Berlin. pp. 1210-1254.

EUSTACE, R.A. (1991) *Radiological measurements involved in the prognosis of equine laminitis.* RCVS Fellowship Thesis.

EUSTACE, R.A. (1992) *Explaining equine laminitis and its prevention.* J.W. Arrowsmith Ltd., Bristol. pp 71.

EUSTACE, R.A. (1993) Equine laminitis. In: *Equine Practice 2.* Ed: E. BODEN, Baillière Tindal, London. pp 150-164.

EUSTACE, R.A. (1995) What Happens Within The Foot In Laminitis? In: *Proceedings of Dodson & Horrell Ltd. 1st International Conference on Feeding Horses.* Scots Corner, 5th September.

HOOD, D.M. (1984) *Studies on the pathogenesis of equine laminitis.* PhD Thesis. Texas A&M University.

HOOD, D.M. (1997a) Perspectives on Chronic Laminitis. In: *Proceedings of the Hoof Project.* Ed: D.H. HOOD, I.P. WAGNER and A.C. JACOBSON, Texas A&M University, Texas. pp 21-34.

HOOD, D.M. (1997b) Digital Instability as a Potential Prognostic Indicator in Horses with ChronicLaminitis. In: *Proceedings of the Hoof Project.* Ed: D.H. HOOD, I.P. WAGNER and A.C. JACOBSON, Texas A&M University, Texas. pp 106-115.

HOOD, D.M. (1999) The mechanisms and consequences of structural failure of the foot. *Vet. Clin. N. Am.-Equine Pract.* **15**, 437-461.

HOOD, D.M. AND STEVENS, K.A. (1981) Pathophysiology of Equine Laminitis. *Compend. Contin. Edu. Pract. Vet.* **3**, s454-s460.

HOOD, D.M., GROSENBAUGH, D.A., CHAFFIN, M.K., HONAS, C.M., SLATER, M.R. AND MORGAN, S.J. (1993a) Pathophysiology of Chronic Laminitis. In: *Proceedings of the 39th Congress American Association of Equine Practitioners.* **39**, 199-200.

HOOD, D.M., GROSENBAUGH, D.A., MOSTAFA, M.B., MORGAN, S.J. AND THOMAS, B.C. (1993b) The Role of Vascular Mechanisms in the Development of Acute Equine Laminitis. *J. Vet Intern. Med.* **7**, 228-234.

HUNT, R.J. (1993) A retrospective evaluation of laminitis in horses. *Equine Vet. J.* **25**, 61-64.

KAMEYA, T. (1973) Clinical studies on laminitis in the Racehorse. *Exp. Rep. Equine Hlth. Lab.* **10**, 19-40.

LINFORD, R.L. (1990) Laminitis (founder). In: *Large Animal Internal Medicine.* Ed: B.P. SMITH, C.V. Mosby, St. Louis. pp 1158-1168.

LINFORD, R.L. (1996) Laminitis (founder). In: *Large Animal Internal Medicine.* Ed: B.P. SMITH, C.V. Mosby, St. Louis. pp 1300-1309.

MARKS, G. (1984) *Makroskopische, licht- und elektronenmikroskopische Untersuchungen zur Morphologie des Hyponichiums bei der Hufrehe des Pferdes.* Diss. med. vet., Freie Univ. Berlin.

MATHEWS, N.S. (2000) Anaesthesia for Donkeys and Mules. In: *The Donkey A Unique Equid, BEVA Conference Proceedings 1st CPD Course,* Langford, Bristol. 15th February. pp 21-24.

MATHEWS, N.S. (2002) Therapeutics and anaesthesia in the donkey. In: *The Medicine and Surgery of the Donkey, BEVA Conference Proceedings 2nd CPD Course,* Glasgow, 11th September. pp 3-5.

MATHEWS, N.S., TAYLOR, T.S. AND HARTSFIELD, S.M. (1997) Anaesthesia of donkeys and mules. *Equine Vet. Educ.* **9**, 198-202.

MOORE, J.N. AMD ALLEN, D. (1995) *A guide to equine acute laminitis.* VLS Books, London. pp 40.

NILSSON, S.A. (1963) Clinical, morphological and experimental studies of laminitis in cattle. *Acta Vet. Scand.* **4** (Suppl. 1).

OBEL, N. (1948) *Studies on the histopathology of acute laminitis.* Diss. Stockholm Almqvist and Wiksell, Uppsala.

POLLITT, C.C. (1995) *Colour Atlas of the Horse's Foot.* Mosby-Wolfe, London. pp 208.

POLLITT, C.C. (2001) *Equine Laminitis: A report for the Rural Industries Research and Development Corporation, RIRDC Publication 01/129.* RIRDC, Kingston. pp 99.

POLLITT, C.C. AND DARADKA, M. (1998) Equine laminitis basement membrane pathology: loss of *type IV* collagen, *type VII* collagen and laminin immunostaining. *Equine Vet. J. Suppl.* **26**, 139-144.

STICK, J.A., LANN, H.W., SCOTT, E.A. AND EDWARD ROBINSON, N. (1982) Pedal bone rotation as a prognostic sign in laminitis of horses. *J. Am. Vet. Med. Assoc.* **180**, 251- 253.

YELLE, M. (1986) Clinicians guide to equine laminitis. *Equine Vet. J.* **18**, 156-158.

APPENDIX III
MULTIVARIATE STATISTICAL ANALYSIS

PRINCIPLE COMPONENT ANALYSIS (PCA)

This is a powerful variable-directed statistical analysis technique (Donev 2000) that is based upon the combined effect of all measured variables (i.e. multivariate). It is in this respect that this technique differs from traditional univariate statistical approaches. The analysis creates new orthogonal axes or principle components (PCs) according to maximum variance criterion, which maximise the variance within the data set. In this way, each successive PC is an orthogonal linear combination of the original variables such that it covers the maximum variance not accounted for by the previous PC (Donev 2000, Deene 2000). Hence the variance explained by PC1>PC2>....PCn.

The technique calculates the percentage of the total captured variance within the data set that is accounted for by each respective PC, and provides a statistical measure of importance (eigen-value) for each PC.

The relative contribution or loading (PcaLoa) of each variable in respect of each principle component (PC) is also expressed. In addition, PCA generates a value or score (PcaSco) for each animal in respect of each PC. In this way the technique facilitates readily the graphical representation of the data in respect of all measured variables (Deene 2000).

GRAPHICAL REPRESENTATION OF THE ANALYSIS

The Eigenvalue profile plot or Scree plot provides a valuable means of determining the number of significant PCs. This plots the calculated Eigenvalue against each respective PC, i.e. PC1, PC2...PCn. The points are connected thereby forming a decreasing curve. The presence of any pivot point, combined with the absolute Eigenvalue and the amount of explained variance are used to arrive at a reasoned number of significant components for the analysis.

The scatter plot of the variable loadings (PcaLoa) onto the corresponding PCs (loading plot) provide a means of exploring the effect of each variable in respect of the stated PCs. In this regard, the loadings can be considered to be vectorial in nature (Eigenvectors). Hence by connecting the variable loading co-ordinates to the scatter plot origin, the magnitude and the direction of influence of each variable can be elucidated. The respective lengths of the loading vectors approximates to the standard deviation of the corresponding variable. The angle between loading vectors is proportional to the 'between variable' correlation.

In a similar fashion, scatter plots of the PcaSco onto the corresponding PCs (score plots) can be used to examine the between object inter-relationships. The distances between object points on a given score plot, for example PcaSco1 Vs PcaSco2 gives a measure of their dissimilarity in

respect of those PCs. That is, the greater the distance between objects, the more dissimilar they are with respect to each other.

Combining the score plot and the loading plot for a given combination of PCs indicates which variables are responsible for the separation of the objects in the data-set, and also the relative importance of those particular variables.

The position of an object is therefore determined by the 'weighted average' of all variables (Donev 2000). It is important to note however, that two objects in a similar location in the scatter plot do not necessarily express similar values in all measured variables.

CLUSTER ANALYSIS

Cluster analysis is a type of object–directed analysis that is concerned primarily with the relationships between objects based upon multivariate observations (Deene 2001). It focuses upon how similar or dissimilar objects are to each other. This method allows a sample of objects to be divided into clusters (classes or groups) so that the objects that are similar are grouped together. A simple approach to identifying clusters is through the examination of PcaSco score plots in respect of the major principle components, and thereby visually identify clusters or groups.

The success of this approach will however intuitively depend upon the proportion of variance captured by those principle components that are selected for the analysis. Whilst this approach may be questioned on the basis of its subjective nature, Deene (2001) commented on its effectiveness due to the natural human ability to discern underlying patterns. Nevertheless such a subjective approach remains open to observer bias in its interpretation. In addition, it is difficult to establish the precise position of the cluster boundaries, especially if the clusters are not well separated (Deene 2001 – Pers Com.). In this regard there are a number of different multivariate techniques that use numerical algorithms to perform the cluster analysis. These algorithms are defined so as to cluster n objects each with measurements on p variables. One such technique is Hierarchical Cluster Analysis.

HIERARCHICAL CLUSTER ANALYSIS

Hierarchical techniques start by calculating the distances of each object to all other objects. Clusters may be formed either by agglomeration or division. Agglomerative clustering begins with all objects viewed as separate objects, each forming its own cluster. In the first step, the two objects which are closest are joined together to form a new cluster. In the next agglomerative step, either a third object is added to this cluster or two other objects join to

produce a new cluster. In this way, each iterative step results in one less cluster. The process continues until all the objects are combined into one cluster.

REGULARISED DISCRIMINATIVE ANALYSIS (RDA)

This analysis technique enables the recognition and prediction potential of proposed classification systems to be investigated theoretically. The technique models each group or class mathematically based upon the class centroid and the associated covariance matrix. This involves a two-stage approach.

Firstly, the analysis calculates an optimum mathematical model to describe the proposed groupings. In this way, classification rules and class boundaries are established, in addition to a critical 'no model' error and risk statistic. The 'no model' error statistic is a measure of the goodness of class recognition, whilst the no model risk is a measure of the predictive capabilities of the model. The validity of the model can be assessed by direct comparison of the resultant error and risk statistics with the associated no model statistics. The minimum requirement being that both statistics out-perform the 'no model' values.

In the second stage of the analysis, a mis-classification exercise is conducted, based upon the optimum model, in order to both test how well objects of known class are classified, and to test how well objects of unknown class will be predicted. In the first instance, objects are assigned to classes based upon the derived classification rules. In the second instance, a cross-validation class assignment analysis is performed in an iterative manner. In this way, assignment plots are generated of 'true' and 'assigned' classes.

REFERENCES

DEENE, J.S. (2000) *Multivariate Analysis: Principle Components and Calibration, Postgraduate Continuing Professional Training in Industrial Data Modelling*. Department of Biomedical Statistics, De Montfort University, Leicester.

DEENE, J.S. (2001) *Classification, Postgraduate Continuing Professional Training in Industrial Data Modelling*. Industrial Data Modelling Unit, De Montfort University, Leicester.

DONEV, A.N. (2000) *Multivariate data Analysis: Lecture Notes*. Department of Biomedical Statistics, De Montfort University, Leicester. pp 127.

APPENDIX IV
COMPUTER BASED IMAGE ANALYSIS, SYSTEM REQUIREMENTS AND DESIGN THEORY

OVERVIEW

The fundamental working premise of computer based image analysis is the conversion of optical images into an electronic form, so that all procedures in the analysis process can be conducted through a computer interface. The sequential series of image analysis processes involved in a morphometric assessment are summarised in Figure IV.I.

Figure IV.I Image analysis flowchart.

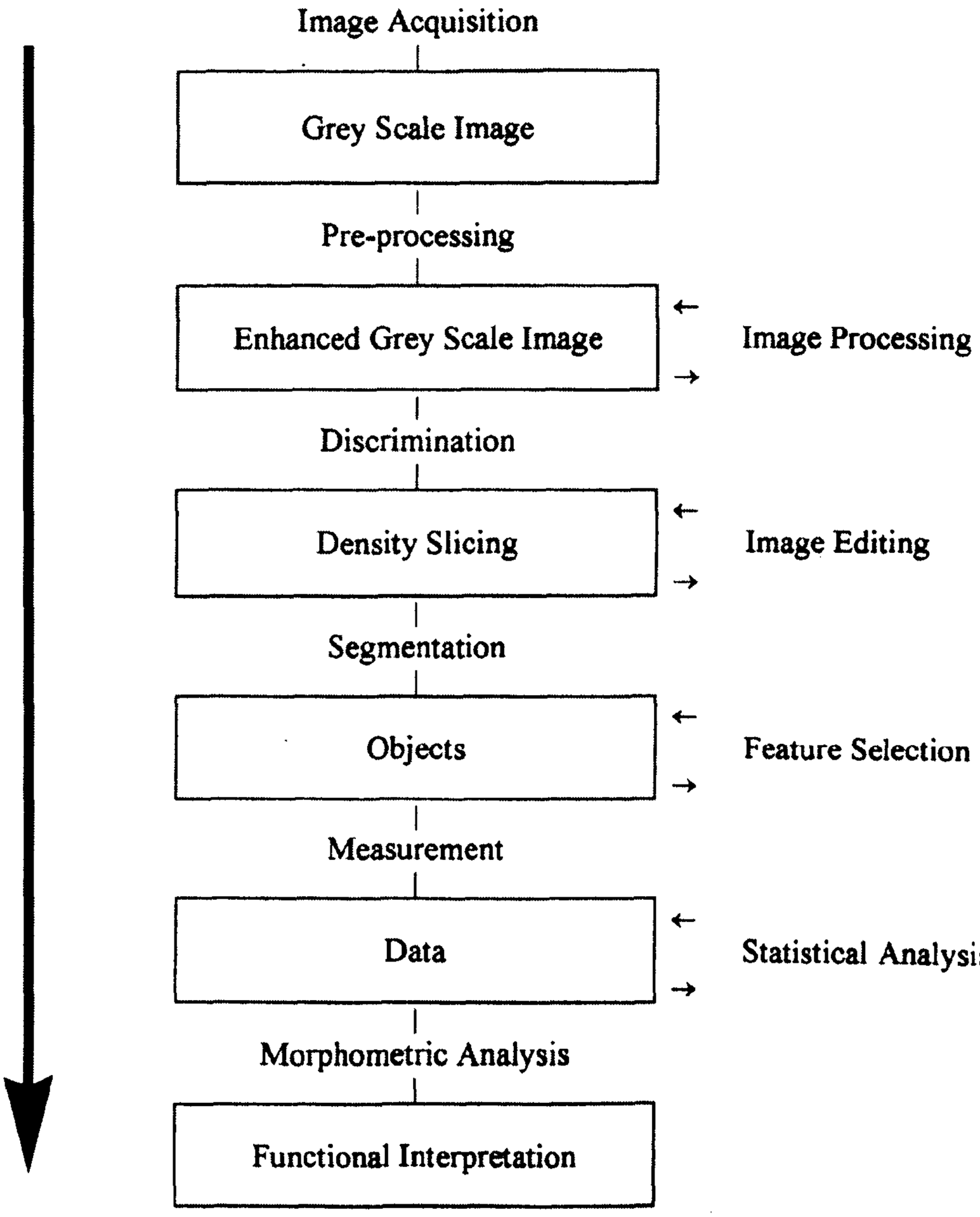

SYSTEM REQUIREMENTS

The basic hardware requirements include: -

- Imaging device to convert optical image into analogue electrical form
- Digitizing device to convert analogue image to digital form
- Memory unit to store image during processing
- Processor to manipulate the image
- Display generator to extract the processed image
- Display device to view the processed image

The basic software requirements are: -

- Programme capable of image enhancement, processing, discrimination and segmentation and measurement operations
- Flexibility to enable the automation of routine or customised procedures via 'macro' programming

The quality of the original optical image significantly affects all image analysis procedures, and ultimately determines the operational performance of the analysis system. Issues of optical quality and illumination are critical factors. Therefore a central issue in the design of any image analysis system is the means by which the optical image is produced.

DESIGN THEORY

The acquisition of the optical image is achieved via a solid state sensor chip or charge coupled device (CCD) contained within the video camera. Each chip is divided into an array of individual 'pixel' (picture elements) sensors that operate as discrete photon detectors. Each sensor receives illumination from the corresponding section of the original optical image. The resultant voltage produced by each sensor is directly proportional to the light intensity emanating from that pixel section of the image. Through the use of three such sensor chips (3CCD), each specific to the red (R), green (G) and blue (B) light respectively, 'pseudo-colour' (RGB) imaging is possible.

The resultant signal read out from each line of detectors produces an analogue voltage, which corresponds to the brightness at different points of the CCD. In greyscale imaging, each horizontal line of detectors is read out sequentially. The vertical timing clock selects each line of detectors in turn, then the horizontal clock shifts along each detector. The complete scan is normally composed of 480 scan lines per image, divided into 2 interlaced raster scans each containing ½ of the image information separated by $1/50^{th}$ second.

In order for the image to be processed by the computer, the analogue signal must be transformed into a digital format (digitization). This involves the sequential sampling of the signal along

each scan line. Each sampling point is converted into a numerical value that corresponds to the average brightness of that sampling site. This value is retained within memory store and the next site is sampled to give a sequential series of brightness values along each scan line. Thus the entire image is converted into an array of pixels, each with a discrete numerical value. From this, each pixel may be allocated a discrete brightness value or grey-scale level. By adjusting for the 'interlace' the image may be reconstructed by the computer and displayed by the monitor as a pixel array.

The ability to discriminate between objects in the resultant image is determined by the resolving power of the system. In grey-scale imaging this is governed by the number of grey-scale levels available, the lateral/spatial pixel resolution (the number of sampling sites along each scan lines) and the precision of pixel measurement. These factors are largely controlled by the working specifications of the 'analogue to digital converter' (ADC) or 'frame grabber'.

The number of grey-scale levels is dependent on the amount of memory allocated for its storage. The number of levels = $2^n - 1$ values, where n = number of bits of memory allocated to each pixel. Hence an 8 bit ADC permits 0-256 discrete levels of grey (256 greyscale).

The accuracy of object discrimination is greatly influenced by the boundary conditions. Pixels that straddle the boundary between two regions of different brightness will exhibit an intermediate grey level. The value is clearly related to how the pixel lies with respect to the boundary. It therefore follows that in order to achieve accurate and effective boundary definition; pixels must be relatively small (*i.e.* high spatial resolution) and the number of grey values, large.

In order to achieve an accurate representation of the original image without linear distortion it is essential to have square pixels. Square pixels are also desirable to achieve accurate measurements. This can only be achieved with a high precision acquisition clock. Furthermore as the standard video image is not square, possessing a width to height ratio of 4:3, only those ADC devices with a similar array configuration are capable of acquiring the complete field of view and yet maintain vital square pixel representation.

Achieving the desired level of high spatial / lateral pixel resolution and greyscale resolution necessary for effective imaging generates computer image files of considerable size, and this requires large memory storage space. It follows that subsequent image processing places significant demands on memory availability, computer processor speed and the interactive nature of the interface.

The quality of image displayed to the observer is central to subsequent image analysis. The number of scan lines in the raster ultimately limits image resolution. Hence the vertical resolution of the monitor is the major determinant of image quality.

SYSTEM DESIGN

The important system design considerations can be summarised as follows: -

- The quality of the optics involved in the generation of the optical image
- Number and size of CCD sensors - Mono and / or 'Pseudo colour' imaging
- Number of pixel sensors in the CCD
- The number and ratio of scan lines in the ADC
- Lateral and grey scale resolution of the ADC
- Accuracy of the acquisition clock
- Memory allocation and computing speed of the computer
- Capabilities of the software program
- Number of vertical scan lines in the monitor raster scan

In light of these key considerations the following system components were integrated to produce a high quality IAS capable of facilitating large-scale quantification. A diagrammatic representation of the imaging system is given in Figure IV. II and is illustrated in Figure IV.III. Central to the system is the Olympus 'B' series microscope. The high quality optics provides excellent image resolution for transmission light microscopy. The NIH-Image analysis software program was selected for image processing. This public domain share program produced by the National Institute of Health (Maryland USA) represents an industry standard. It provides the opportunity for both 8 bit (256 greyscale scale) and RGB 'Pseudo-colour' image acquisition. The program supports basic image-processing functions and allows customisation of processing functions to reduce procedural times. Standardised Image processing 'macros' can be designed to achieve consistent 'between sample' image manipulation, and thereby minimise observer error.

UPGRADING THE IMAGE ANALYSIS SYSTEM

Recent technological advances in image analysis have enabled continued enhancement of the IAS. This has included both hardware and software upgrades. The advent of

IEEE 'Firewire' technology has enabled direct acquisition of digital images. This negates the need for ADC, and has created the opportunity for increased levels of data transfer.

Improvements in CCD technology have made it possible for digital imaging to take advantage of these increased levels of data transference.

Figure IV.II Diagrammatic representation of the computer based image analysis system (IAS).

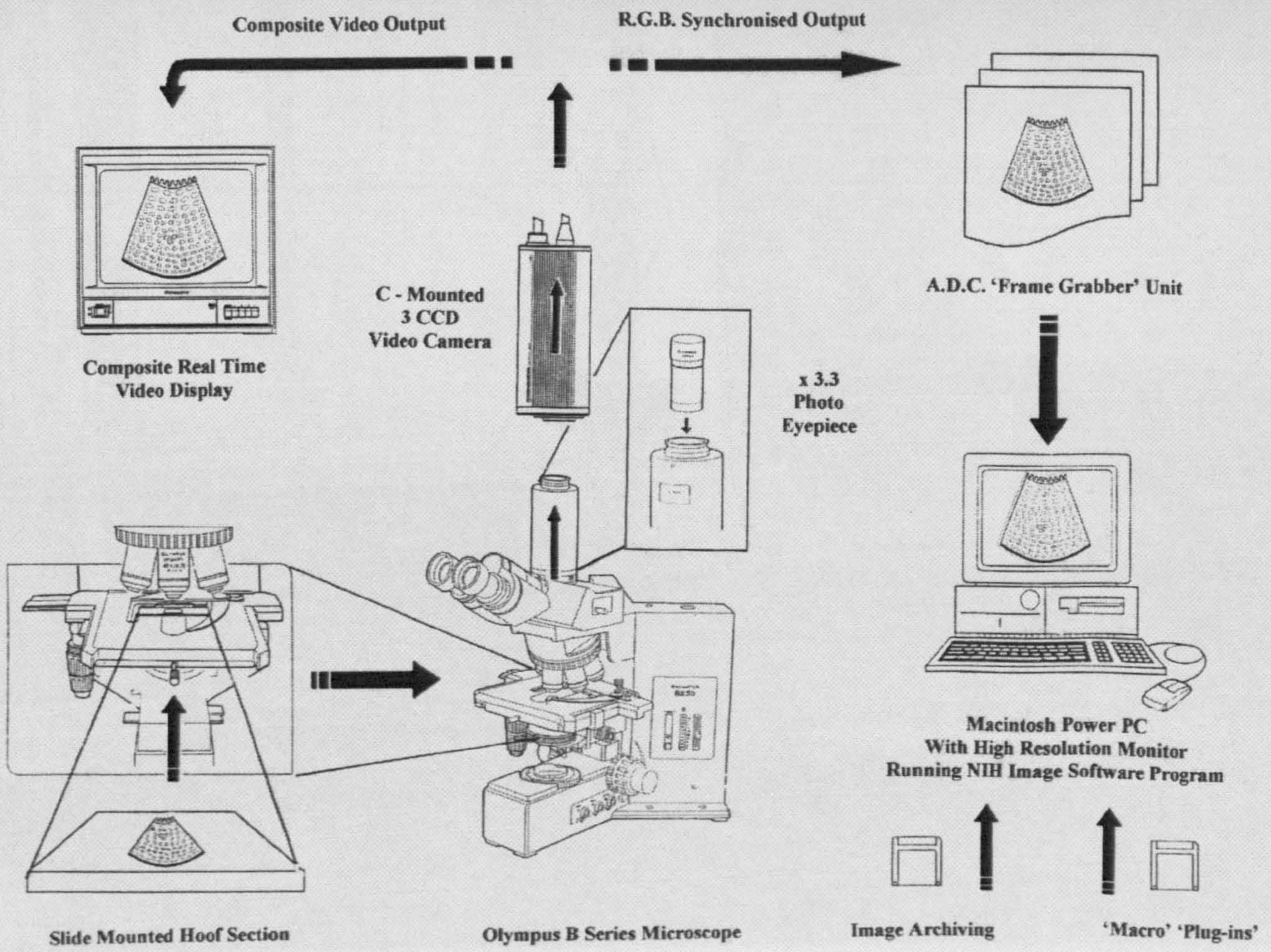

Figure IV.III Photograph of the computer based image analysis system.

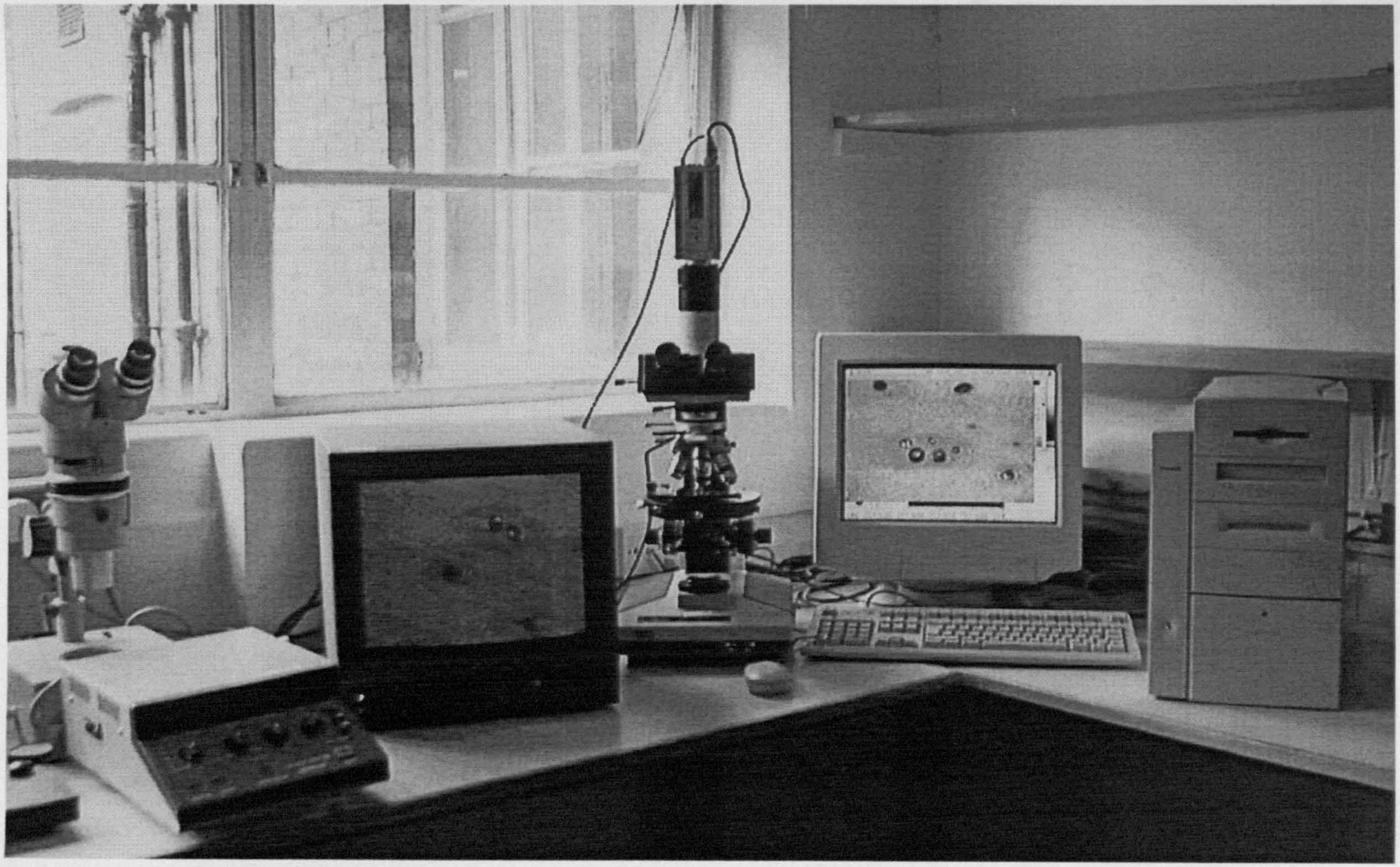

As a consequence, it is now possible to obtain digital images of 4.5 million pixels. The spatial resolution of these images approaches that which can be obtained using traditional, silver halide photographic methods.

Advances in computer processing power, memory storage capabilities, and levels of random access memory (RAM) have afforded greater sophistication in image processing and analysis techniques. This has resulted in the emergence of a new generation of image analysis software that surpasses the NIH standard. Proprietary algorithms have been developed which enable 2-dimmensional image tiling, in the horizontal plane, to be performed in real time, and also, real time image summation (montaging) in the vertical plane. This further enhances image quality, and leads to improvements in image discrimination capabilities.

The IAS was upgraded in line with these technical advances, with the acquisition of a digital 3CCD camera, and new generation image analysis software.

APPENDIX V
SUMMARY OVERVIEW OF THE HYDRATION CHARACTERISTICS OF LAMINITIC DONKEY HOOF HORN

Data presented in this appendix was derived from concurrent hydration studies performed on material obtained from the trial donkey population (Collins 2003 – Unpublished data).

Table V.I Zonal percentage Moisture Content and Moisture Regain data at '*in vivo*' Hydration levels for laminitic donkey hoof horn

Zone	Moisture Content (%)			Moisture Regain ($gH_2O/100gDM$)		
	Median	IQ Range	Min - Max	Median	IQ Range	Min - Max
HWD	33.4	31.8 – 34.3	29.3 – 36.3	50.2	46.6 – 52.6	41.4 – 57.0
Zone 1	22.3	21.0 – 23.8	16.7 – 25.5	28.7	26.6 – 31.2	20.0 – 34.2
Zone 2	29.7	27.8 – 30.6	19.7 – 34.5	42.1	38.4 – 44.1	24.5 – 52.7
Zone 3	37.3	35.1 – 38.4	28.8 – 41.4	59.7	54.5 – 63.0	40.4 – 70.8

Table V.II Zonal Percentage Moisture Content and Moisture Regain values at Maximal Hydration levels in laminitic donkey hoof horn

Zone	Percentage Moisture Content (%)			Moisture Regain ($gH_2O/100gDM$)		
	Median	IQ Range	Min - Max	Median	IQ Range	Min - Max
HWD	35.1	33.9 – 36.1	31.6 – 36.7	54.1	51.3 – 56.5	41.4 – 57.0
Zone 1	26.5	28.5 – 25.3	23.8 – 31.1	36.1	39.8 – 33.8	31.2 – 45.1
Zone 2	32.6	34.1 – 30.1	28.2 – 38.2	48.3	51.7 – 43.1	39.2 – 61.7
Zone 3	40.4	40.9 – 38.7	32.7 – 43.7	67.7	69.2 – 63.0	48.5 – 77.7

Table V.II Percentage Saturation ($\%S_R$) of laminitic donkey hoof horn at 'in vivo' Hydration Levels

	Full HWD	Zone 1	Zone 2	Zone 3
Median $\%S_R$	93.3	79.5	85.2	88.2

Key: $\%S_R$, Percentage Saturation.Subscript **R**, Moisture Regain.

Table V.III Zonal Percentage Moisture Content and Moisture Regain values at '*in vivo*' Hydration Levels by Laminitic Group

	Percentage Moisture Content (%)					
Zone	**Laminitic Group 1**			**Laminitic Group 2**		
	Median	IQ Range	Min - Max	Median	IQ Range	Min - Max
Zone 1	21.4	17.8 – 24.3	16.7 – 24.6	22.8	21.1 – 23.7	20.2 – 25.5
Zone 2	28.3	23.2 – 30.4	19.7 – 30.5	29.8	27.9 – 32.3	26.5 – 34.5
Zone 3	37.2	31.8 – 38.7	28.8 – 40.9	37.3	35.2 – 38.3	31.4 – 41.4
	Moisture Regain (gH2O/100g DM)					
	Laminitic Group 1			**Laminitic Group 2**		
	Median	IQ Range	Min - Max	Median	IQ Range	Min - Max
Zone 1	27.3	21.6 – 32.1	20.0 – 32.7	29.5	26.7 – 31.0	25.2 – 34.2
Zone 2	39.6	30.2 – 43.6	24.5 – 43.9	42.5	38.8 – 48.0	36.0 – 52.7
Zone 3	59.1	46.7 – 63.2	40.4 – 69.1	59.8	46.6 – 52.6	45.7 – 70.8

Table V.IV Zonal Percentage Moisture Content and Moisture Regain data by Laminitic Group at Maximal Hydration Levels

	Percentage Moisture Content (%)					
Zone	**Laminitic Group 1**			**Laminitic Group 2**		
	Median	IQ Range	Min - Max	Median	IQ Range	Min - Max
Zone 1	27.5	25.3 – 30.9	24.7 – 31.1	26.1	25.2 – 28.5	23.8 – 29.8
Zone 2	31.8	29.5 – 33.8	28.2 – 34.1	33.3	30.9 – 36.6	29.6 – 38.2
Zone 3	40.1	37.3 – 41.5	32.7 – 43.7	40.4	38.9 – 40.9	43.3 – 34.4
	Moisture Regain (gH2O/100g DM)					
	Laminitic Group 1			**Laminitic Group 2**		
	Median	IQ Range	Min - Max	Median	IQ Range	Min - Max
Zone 1	37.9	33.8 – 44.8	32.7 – 45.1	35.3	33.6 – 39.8	31.2 – 42.4
Zone 2	46.6	41.7 – 51.0	39.2 – 51.8	49.8	44.7 – 57.7	42.0 – 61.7
Zone 3	67.0	59.4 – 71.0	48.5 – 77.7	67.8	63.6– 69.1	52.3 – 76.4

Table V.V Summary table of full HWD and zonal water fraction partitioning in laminitic donkey hoof horn

Sampling Site	Bound Water			Free water		
	Median	IQ Range	Min - Max	Median	IQ Range	Min - Max
HWD	63.6	67.3 – 59.2	43.3 – 76.0	36.4	40.8 – 32.7	24.1 – 56.7
Zone 1	84.0	88.6 – 80.4	66.1 – 91.7	16.0	19.6 – 11.4	8.3 – 33.9
Zone 2	61.8	69.6 – 58.1	50.0 – 89.5	35.4	41.9 – 30.4	10.5 – 50.2
Zone 3	57.3	60.8 – 51.8	43.3 – 65.8	43.7	48.2 – 39.2	34.2 – 56.5

Table V.VI Water partitioning within the hoof wall of the laminitic donkey hoof horn, along with the theoretical Hydration Status at '*in vivo*' Hydration Levels

	Zone 1	Zone 2	Zone 3	HWD
$\%MC_M$	**26.5**	**32.6**	**40.4**	**35.1**
MR_M	**36.1** $gH_2O/100gDM$	**48.3** $gH_2O/100gDM$	**67.7** $gH_2O/100gDM$	**54.1** $gH_2O/100gDM$
Bound to Free Water Ratio at Maximal Hydration	**83.9:16.1**	**64.7:25.3**	**56.3:43.7**	**63.5 : 36.5**
Derived Bound Fraction at Maximal Hydration	**30.3** $gH_2O/100gDM$	**31.3** $gH_2O/100gDM$	**38.1** $gH_2O/100gDM$	**34.4** $gH_2O/100gDM$
Derived Free Water Fraction at Maximal hydration	**5.8** $gH_2O/100gDM$	**17.0** $gH_2O/100gDM$	**29.6** $gH_2O/100gDM$	**19.7** $gH_2O/100gDM$
MR at Bound Water Capacity	**30.3** $gH_2O/100gDM$	**31.3** $gH_2O/100gDM$	**38.1** $gH_2O/100gDM$	**34.4** $gH_2O/100gDM$
Theoretical %MC at Bound Water Capacity	**23.3**	**23.8**	**27.6**	**25.6**
$\%MC_F$	**22.3**	**29.7**	**37.3**	**33.4**
MR_F	**28.7** $gH_2O/100gDM$	**42.1** $gH_2O/100gDM$	**59.7** $gH_2O/100gDM$	**50.2** $gH_2O/100gDM$
Difference in H_2O between MR_F and MR at Bound Water Capacity	**-1.6** g/100gDM	**10.8** g/100gDM	**21.6** g/100gDM	**15.8** g/100gDM
% Bound Water Capacity at MR_F	**94.7%**	**134.5%**	**156.7%**	**145.9%**

Key: %MC, Percentage Moisture Content. **MR**, Moisture Regain. Subscript **F**, 'In vivo' Hydration level. Subscript **M**, Maximal Hydrated Hydration level.

Table V. VII Comparison of the water partitioning within the hoof wall of the two respective laminitic groups, along with the theoretical Hydration Staus at *in vivo* Hydration levels

	Laminitic Group 1				Laminitic Group2			
	Zone1	**Zone 2**	**Zone 3**	**HWD**	**Zone 1**	**Zone 2**	**Zone 3**	**HWD**
$\%MC_M$	**27.5**	**31.8**	**40.1**	**35.4**	**26.1**	**33.3**	**40.4**	**34.5**
MR_M	**37.9** gH_2O/ 100g DM	**46.6** gH_2O/ 100g DM	**67.0** gH_2O/ 100g DM	**55.0** gH_2O/ 100g DM	**35.3** gH_2O/ 100g DM	**49.8** gH_2O/ 100g DM	**67.8** gH_2O/ 100g DM	**52.7** gH_2O/ 100g DM
Bound to Free Water Ratio at Maximal Hydration	**81.5:18.5**	**64.0:36.0**	**54.7:45.3**	**61.5:38.5**	**85.4:14.6**	**65.1:34.9**	**57.3:42.7**	**64.7:35.3**
Derived Bound Fraction at Maximal Hydration	**30.9** gH_2O/ 100g DM	**29.8** gH_2O/ 100g DM	**36.6** gH_2O/ 100g DM	**33.8** gH_2O/ 100g DM	**30.1** gH_2O/ 100g DM	**32.4** gH_2O/ 100g DM	**38.8** gH_2O/ 100g DM	**34.1** gH_2O/ 100g DM
Derived Free Water Fraction at Maximal hydration	**7.0** gH_2O/ 100g DM	**16.8** gH_2O/ 100g DM	**30.4** gH_2O/ 100g DM	**21.2** gH_2O/ 100g DM	**5.2** gH_2O/ 100g DM	**17.4** gH_2O/ 100g DM	**29.0** gH_2O/ 100g DM	**18.6** gH_2O/ 100g DM
MR at Bound Water Capacity	**30.9** gH_2O/ 100g DM	**29.8** gH_2O/ 100g DM	**36.6** gH_2O/ 100g DM	**33.8** gH_2O/ 100g DM	**30.1** gH_2O/ 100g DM	**32.4** gH_2O/ 100g DM	**38.8** gH_2O/ 100g DM	**34.1** gH_2O/ 100g DM
Theoretical %MC at Bound Water Capacity	**21.4**	**28.3**	**37.2**	**33.0**	**22.8**	**29.8**	**37.3**	**33.4**
$\%MC_F$	**23.6**	**23.0**	**26.8**	**25.2**	**23.3**	**23.8**	**27.6**	**25.6**
MR_F	**27.3** gH_2O/ 100g DM	**39.6** gH_2O/ 100g DM	**59.1** gH_2O/ 100g DM	**49.3** gH_2O/ 100g DM	**29.5** gH_2O/ 100g DM	**42.5** gH_2O/ 100g DM	**59.8** gH_2O/ 100g DM	**50.2** gH_2O/ 100g DM
Difference in H_2O between MR_F and MR at Bound Water Capacity	**-3.6** gH_2O/ 100g DM	**9.8** gH_2O/ 100g DM	**22.5** gH_2O/ 100g DM	**15.5** gH_2O/ 100g DM	**-0.6** gH_2O/ 100g DM	**10.1** gH_2O/ 100g DM	**21.0** gH_2O/ 100g DM	**16.1** gH_2O/ 100g DM
% Bound Water Capacity at MR_F	**88.3%**	**132.9%**	**161.4%**	**145.9%**	**98.0%**	**131.2**	**154.1**	**147.2**

Key: %MC, Percentage Moisture Content. **MR**, Moisture Regain. Subscript **F**, 'In vivo' Hydration level. Subscript **M**, Maximal Hydrated Hydration level.

APPENDIX VI
PEARSON PRODUCT MOMENT CORRELATION MATRICES FOR THE MORPHOMETRIC CHARACTERISTICS OF STRUCTURE WITHIN THE *STRATUM MEDIUM* OF THE LAMINITIC DONKEY HOOF WALL

The correlation matrix presents the correlation for every possible pair of selected variables, and displays the lower triangle of the resultant matrix. The correlation coefficient (corr), that is the upper figure presented in each cell of the matrix, gives the degree of correlation between each respective pair of structural variables within the matrix. The correlation coefficient assumes a value between -1 and +1. If one variable tends to increase as the other decreases, the correlation coefficient is negative. Conversely, if the two variables tend to increase together the correlation coefficient is positive. A coefficient of 1 indicates a perfect linear relationship, whereas a value of zero indicates that is no evidence of a linear relationship between the two variables.

The p-value, the lower figure given in each cell of the matrix, is the statistical probability for the hypothesis that the correlation coefficient for the relationship between two given variables is zero, i.e. that there is no linear relationship.

Key:

Z1 – Zone 1 of the *SM*

Z2 – Zone 1 of the *SM*

Z3 – Zone 1 of the *SM*

Ma – Marrow

Tu – Tubule

Co – Cortex

Area – Absolute Area Measurement

AF – Area Fraction

MA – Major Axis

MI – Minor Axis

T - Thickness

% – Percentage

: – Ratio

(The use of these terms are additive)

Correlation matrix for the 'field' specific area morphometric characteristics of structure.

	Z1MaArea	Z1TuArea	Z1CoArea	Z1MaAF	Z1TuAF	Z1CoAF	Z2MaArea	Z2TuArea
Z1TuArea	0.570							
	0.017							
Z1CoArea	0.481	0.990						
	0.051	0.000						
Z1MaAF	0.724	0.097	0.006					
	0.001	0.712	0.981					
Z1TuAF	0.717	0.748	0.700	0.623				
	0.001	0.001	0.002	0.008				
Z1CoAF	0.661	0.813	0.778	0.498	0.987			
	0.004	0.000	0.000	0.042	0.000			
Z2MaArea	-0.517	-0.469	-0.447	-0.454	-0.633	-0.610		
	0.034	0.057	0.072	0.067	0.006	0.009		
Z2TuArea	-0.168	-0.026	-0.022	-0.088	-0.016	0.011	0.636	
	0.520	0.921	0.934	0.736	0.951	0.968	0.003	
Z2CoArea	0.039	0.123	0.119	0.025	0.156	0.183	0.491	0.934
	0.882	0.637	0.649	0.924	0.549	0.482	0.033	0.000
Z2MaAF	-0.146	-0.145	-0.135	-0.214	-0.254	-0.230	0.661	0.203
	0.575	0.578	0.605	0.410	0.325	0.374	0.002	0.404
Z2TuAF	0.206	0.315	0.305	0.332	0.425	0.412	0.323	0.590
	0.428	0.218	0.234	0.192	0.089	0.100	0.178	0.008
Z2CoAF	0.213	0.336	0.323	0.382	0.482	0.463	0.244	0.594
	0.411	0.187	0.207	0.130	0.050	0.061	0.313	0.007
Z3MaArea	-0.322	-0.402	-0.399	-0.134	-0.378	-0.406	0.513	0.195
	0.208	0.109	0.112	0.608	0.135	0.106	0.025	0.425
Z3TuAea	0.356	0.180	0.125	0.137	0.216	0.210	0.231	0.452
	0.160	0.490	0.633	0.599	0.404	0.418	0.342	0.052
Z3CoArea	0.378	0.216	0.160	0.135	0.243	0.241	0.199	0.449
	0.135	0.405	0.538	0.604	0.347	0.351	0.413	0.054
Z3MaAF	-0.404	-0.489	-0.477	-0.179	-0.517	-0.542	0.557	0.075
	0.108	0.047	0.053	0.491	0.034	0.025	0.013	0.760
Z3TuAF	-0.165	-0.271	-0.283	-0.159	-0.273	-0.264	0.466	0.292
	0.526	0.292	0.271	0.543	0.289	0.305	0.045	0.226
Z3CoAF	-0.164	-0.232	-0.245	-0.190	-0.245	-0.227	0.429	0.297
	0.530	0.369	0.344	0.464	0.344	0.381	0.067	0.216

	Z2CoArea	Z2MaAF	Z2TuAF	Z2CoAF	Z3MaArea	Z3TuAea	Z3CoArea	Z3MaAF
Z2MaAF	0.266							
	0.271							
Z2TuAF	0.585	0.400						
	0.009	0.080						
Z2CoAF	0.578	0.273	0.988					
	0.010	0.244	0.000					
Z3MaArea	0.058	0.359	0.154	0.120				
	0.812	0.131	0.530	0.625				
Z3TuAea	0.455	-0.006	0.278	0.264	0.206			
	0.050	0.979	0.250	0.275	0.398			
Z3CoArea	0.466	-0.026	0.268	0.256	0.124	0.996		
	0.045	0.916	0.268	0.289	0.612	0.000		
Z3MaAF	-0.068	0.480	0.047	-0.008	0.893	-0.151	-0.227	
	0.781	0.032	0.844	0.973	0.000	0.536	0.350	
Z3TuAF	0.213	0.337	0.168	0.117	0.585	0.555	0.517	0.374
	0.382	0.146	0.479	0.623	0.009	0.014	0.024	0.104
Z3CoAF	0.236	0.285	0.136	0.095	0.508	0.578	0.548	0.245
	0.332	0.223	0.567	0.690	0.026	0.010	0.015	0.297

	Z3TuAF
Z3CoAF	0.986
	0.000

Correlation matrix for the 'feature' specific linear and area morphometric characteristics of structure.

	Z1MaMA	Z1MaMI	Z1TuMA	Z1TuMI	Z1TuMA:M	Z1Tu:MaM	Z1Tu:MaM	Z1%MaTu
Z1MaMI	0.633							
	0.006							
Z1TuMA	0.638	0.709						
	0.006	0.001						
Z1TuMI	0.167	0.741	0.691					
	0.521	0.001	0.002					
Z1TuMA:M	0.347	-0.404	0.061	-0.655				
	0.173	0.107	0.817	0.004				
Z1Tu:MaM	-0.020	0.404	0.755	0.767	-0.241			
	0.941	0.107	0.000	0.000	0.352			
Z1Tu:MaM	-0.280	0.264	0.409	0.840	-0.640	0.770		
	0.275	0.306	0.103	0.000	0.006	0.000		
Z1%MaTu	-0.017	-0.558	-0.674	-0.867	0.492	-0.869	-0.812	
	0.949	0.020	0.003	0.000	0.045	0.000	0.000	
Z1CoMAT	0.466	0.646	0.979	0.749	-0.023	0.872	0.544	-0.770
	0.059	0.005	0.000	0.001	0.931	0.000	0.024	0.000
Z1CoMIT	-0.047	0.529	0.584	0.962	-0.663	0.805	0.955	-0.869
	0.858	0.029	0.014	0.000	0.004	0.000	0.000	0.000
Z2MaMA	-0.407	-0.638	-0.496	-0.511	0.311	-0.337	-0.239	0.545
	0.105	0.006	0.043	0.036	0.224	0.185	0.355	0.024
Z2MaMI	-0.435	-0.501	-0.473	-0.417	0.163	-0.281	-0.207	0.483
	0.081	0.041	0.055	0.096	0.531	0.274	0.425	0.050
Z2TuMA	0.283	0.304	0.232	0.176	0.019	0.039	-0.018	-0.102
	0.271	0.236	0.371	0.498	0.943	0.882	0.945	0.698
Z2TuMI	-0.250	-0.058	-0.029	0.102	-0.121	0.160	0.180	0.045
	0.332	0.826	0.913	0.696	0.644	0.540	0.490	0.864
Z2TuMA:M	0.215	-0.451	-0.108	-0.600	0.789	-0.334	-0.522	0.489
	0.407	0.069	0.679	0.011	0.000	0.190	0.031	0.046
Z2Tu:MaM	0.288	0.311	0.237	0.182	0.015	0.043	-0.015	-0.108
	0.263	0.224	0.359	0.484	0.955	0.869	0.955	0.679
Z2Tu:MaM	0.138	0.359	0.398	0.469	-0.246	0.419	0.380	-0.415
	0.597	0.157	0.113	0.058	0.341	0.094	0.133	0.098
Z2%MaTu	-0.236	-0.182	-0.335	-0.171	-0.066	-0.265	-0.101	0.188
	0.361	0.485	0.189	0.512	0.802	0.304	0.699	0.469
Z2CoMAT	0.285	0.306	0.233	0.178	0.018	0.040	-0.017	-0.104
	0.268	0.232	0.367	0.494	0.946	0.878	0.948	0.692
Z2CoMIT	-0.087	0.165	0.185	0.310	-0.214	0.313	0.302	-0.171
	0.741	0.528	0.476	0.226	0.410	0.221	0.239	0.512
Z3MaMA	-0.152	-0.505	-0.350	-0.522	0.382	-0.360	-0.342	0.451
	0.561	0.039	0.168	0.032	0.130	0.156	0.178	0.069

	Z1MaMA	Z1MaMI	Z1TuMA	Z1TuMI	Z1TuMA:M	Z1Tu:MaM	Z1Tu:MaM	Z1%MaTu
Z3MaMI	-0.180	-0.519	-0.371	-0.535	0.382	-0.361	-0.352	0.463
	0.489	0.033	0.142	0.027	0.130	0.155	0.165	0.061
Z3TuMA	-0.049	-0.387	-0.041	-0.420	0.579	-0.039	-0.309	0.205
	0.853	0.125	0.877	0.094	0.015	0.883	0.228	0.430
Z3TuMI	0.231	0.170	0.390	0.098	0.302	0.287	-0.030	-0.166
	0.372	0.515	0.122	0.708	0.239	0.263	0.908	0.524
Z3TuMA:M	-0.303	-0.572	-0.607	-0.556	0.150	-0.542	-0.320	0.472
	0.237	0.016	0.010	0.020	0.565	0.025	0.211	0.056
Z3Tu:MaM	0.116	0.231	0.333	0.251	0.013	0.354	0.159	-0.305
	0.658	0.372	0.191	0.331	0.960	0.164	0.541	0.233
Z3Tu:MaM	0.272	0.496	0.554	0.506	-0.107	0.504	0.304	-0.467
	0.290	0.043	0.021	0.038	0.683	0.039	0.236	0.059
Z3%MaTu	-0.187	-0.469	-0.488	-0.477	0.164	-0.495	-0.298	0.520
	0.473	0.057	0.047	0.053	0.529	0.043	0.246	0.032
Z3CoMAT	0.002	-0.232	0.081	-0.261	0.479	0.086	-0.206	0.059
	0.994	0.370	0.758	0.312	0.052	0.742	0.427	0.823
Z3CoMIT	0.291	0.353	0.516	0.288	0.159	0.411	0.096	-0.329
	0.256	0.165	0.034	0.263	0.541	0.101	0.713	0.197

	Z1CoMAT	Z1CoMIT	Z2MaMA	Z2MaMI	Z2TuMA	Z2TuMI	Z2TuMA:M	Z2Tu:MaM
Z1CoMIT	0.684							
	0.002							
Z2MaMA	-0.461	-0.385						
	0.062	0.127						
Z2MaMI	-0.427	-0.323	0.953					
	0.087	0.206	0.000					
Z2TuMA	0.191	0.099	-0.077	-0.079				
	0.463	0.706	0.748	0.740				
Z2TuMI	0.034	0.153	0.409	0.520	-0.221			
	0.897	0.558	0.074	0.019	0.349			
Z2TuMA:M	-0.182	-0.574	0.369	0.209	-0.032	-0.357		
	0.485	0.016	0.110	0.376	0.894	0.123		
Z2Tu:MaM	0.196	0.104	-0.091	-0.093	1.000	-0.226	-0.038	
	0.451	0.692	0.704	0.698	0.000	0.338	0.875	
Z2Tu:MaM	0.421	0.447	-0.533	-0.495	-0.154	0.475	-0.549	-0.146
	0.093	0.072	0.015	0.026	0.517	0.034	0.012	0.540
Z2%MaTu	-0.322	-0.142	0.494	0.495	0.563	-0.275	0.132	0.555
	0.208	0.587	0.027	0.027	0.010	0.240	0.580	0.011
Z2CoMAT	0.192	0.100	-0.081	-0.083	1.000	-0.222	-0.033	1.000
	0.460	0.702	0.736	0.729	0.000	0.346	0.890	0.000
Z2CoMIT	0.236	0.324	0.046	0.154	-0.220	0.924	-0.506	-0.220
	0.362	0.204	0.848	0.517	0.351	0.000	0.023	0.351

	Z1CoMAT	Z1CoMIT	Z2MaMA	Z2MaMI	Z2TuMA	Z2TuMI	Z2TuMA:M	Z2Tu:MaM
Z3MaMA	-0.362	-0.453	0.584	0.526	-0.144	-0.079	0.513	-0.152
	0.153	0.068	0.007	0.017	0.545	0.742	0.021	0.521
Z3MaMI	-0.378	-0.464	0.591	0.532	-0.154	-0.067	0.481	-0.162
	0.134	0.060	0.006	0.016	0.518	0.778	0.032	0.495
Z3TuMA	-0.034	-0.373	0.382	0.377	-0.226	0.395	0.236	-0.231
	0.898	0.141	0.096	0.102	0.338	0.084	0.316	0.327
Z3TuMI	0.387	0.055	0.147	0.178	0.182	0.275	0.020	0.180
	0.125	0.835	0.536	0.454	0.443	0.240	0.932	0.449
Z3TuMA:M	-0.616	-0.469	0.239	0.166	-0.058	-0.041	0.216	-0.061
	0.008	0.057	0.310	0.485	0.807	0.864	0.361	0.797
Z3Tu:MaM	0.352	0.223	-0.355	-0.317	-0.018	0.340	-0.292	-0.012
	0.166	0.390	0.125	0.173	0.941	0.143	0.211	0.959
Z3Tu:MaM	0.564	0.438	-0.408	-0.360	0.239	0.257	-0.347	0.245
	0.018	0.079	0.074	0.119	0.310	0.274	0.134	0.298
Z3%MaTu	-0.510	-0.411	0.445	0.368	-0.092	-0.283	0.513	-0.099
	0.036	0.101	0.049	0.111	0.699	0.227	0.021	0.679
Z3CoMAT	0.092	-0.235	0.200	0.216	-0.192	0.456	0.068	-0.194
	0.725	0.364	0.397	0.361	0.417	0.043	0.775	0.412
Z3CoMIT	0.515	0.220	-0.067	-0.015	0.238	0.300	-0.154	0.239
	0.034	0.397	0.780	0.951	0.313	0.198	0.517	0.311

	Z2Tu:MaM	Z2%MaTu	Z2CoMAT	Z2CoMIT	Z3MaMA	Z3MaMI	Z3TuMA	Z3TuMI
Z2%MaTu	-0.790							
	0.000							
Z2CoMAT	-0.152	0.561						
	0.523	0.010						
Z2CoMIT	0.771	-0.540	-0.220					
	0.000	0.014	0.351					
Z3MaMA	-0.591	0.319	-0.146	-0.327				
	0.006	0.170	0.538	0.159				
Z3MaMI	-0.581	0.321	-0.156	-0.316	0.995			
	0.007	0.167	0.512	0.174	0.000			
Z3TuMA	0.050	-0.204	-0.227	0.289	0.385	0.400		
	0.836	0.389	0.335	0.217	0.094	0.081		
Z3TuMI	0.117	-0.057	0.181	0.239	0.177	0.187	0.772	
	0.623	0.811	0.445	0.310	0.455	0.431	0.000	
Z3TuMA:M	-0.205	0.153	-0.059	-0.122	0.115	0.106	-0.150	-0.646
	0.387	0.519	0.804	0.609	0.630	0.657	0.529	0.002
Z3Tu:MaM	0.670	-0.515	-0.016	0.535	-0.791	-0.779	0.241	0.295
	0.001	0.020	0.945	0.015	0.000	0.000	0.307	0.206
Z3Tu:MaM	0.624	-0.364	0.241	0.459	-0.796	-0.795	0.101	0.424
	0.003	0.115	0.306	0.042	0.000	0.000	0.671	0.062

	Z2Tu:MaM	Z2%MaTu	Z2CoMAT	Z2CoMIT	Z3MaMA	Z3MaMI	Z3TuMA	Z3TuMI
Z3%MaTu	-0.644	0.401	-0.094	-0.492	0.837	0.825	-0.127	-0.329
	0.002	0.080	0.694	0.028	0.000	0.000	0.593	0.156
Z3CoMAT	0.269	-0.337	-0.193	0.432	0.052	0.069	0.942	0.771
	0.251	0.146	0.416	0.057	0.828	0.772	0.000	0.000
Z3CoMIT	0.328	-0.174	0.238	0.354	-0.183	-0.175	0.629	0.935
	0.158	0.464	0.312	0.126	0.440	0.460	0.003	0.000

	Z3TuMA:M	Z3Tu:MaM	Z3Tu:MaM	Z3%MaTu	Z3CoMAT
Z3Tu:MaM	-0.215				
	0.364				
Z3Tu:MaM	-0.488	0.908			
	0.029	0.000			
Z3%MaTu	0.349	-0.928	-0.927		
	0.132	0.000	0.000		
Z3CoMAT	-0.204	0.549	0.400	-0.443	
	0.389	0.012	0.081	0.050	
Z3CoMIT	-0.686	0.578	0.713	-0.629	0.747
	0.001	0.008	0.000	0.003	0.000

APPENDIX VII
PUBLICATIONS AND CONFERENCE PROCEEDINGS ASSOCIATED WITH WORK CONDUCTED FOR THIS THESIS

COLLINS, S.N. AND REILLY. J.D. (2004a) Irregularities in structure of the *Stratum medium* of laminitic donkey hoof horn. *Equine Vet. J.* (Submitted for Publication).

COLLINS, S.N. AND REILLY. J.D. (2004b) Radiographic anatomy of the normal and laminitic donkey foot. *Equine Vet. J.* (Submitted for Publication).

COLLINS, S.N., COPE, B.C., HOPEGOOD, L., LATHAM, R.J., LINFORD, R.G. AND REILLY, J.D. (1998) Stiffness as a function of moisture content in natural materials: Characterisation of hoof horn samples. *J. Mater. Sci.* **33**, 5185-5191.

COLLINS, S.N., WEALLEANS, H., HOPEGOOD, L., LATHAM, R.J., NEWLYN, H.A. AND REILLY, J.D. (2002) 'Foot, Hoof and Fancy FEA' – Current Studies on the Donkey Hoof. In: *Medicine and Surgery of the Donkey, Proceedings of the BEVA Congress 2nd CPD Course*, Glasgow, 11th September. pp 1-15.

CRANE, M. (2003) Foot Problems in the Donkey. In: *Veterinary and Farriery Practice: the Common Ground, Proceedings of the 5th Biannual Seminar BEVA and NAFB&AE Conference*, Stoneleigh, 21st October. pp 12-14.

HOPEGOOD, L., COLLINS, S.N., COPE, B., LATHAM, R.J. AND REILLY, J.D. (2003a) The Effect of Modulation of Moisture Content on Mechanical Properties of Full and Partial Hoof Wall Depth Samples of Donkey Hoof Horn Samples. *Comp. Biochem. Physiol. A-Mol. Integr. Physiol.* **134**, *Suppl.*, s44.

HOPEGOOD, L., COLLINS, S.N., LATHAM, R.J. AND REILLY, J.D. (2003b) Analyses of the Moisture Content of Hoof Horn from Horses, Donkeys and Laminitic Donkeys. In: *Emerging Equine Science, Proceedings of the British Society of Animal Science*, Cirencester, 15th – 16th September. pp 28.

NEWLYN, H.A., COLLINS, S.N., COPE, B.C., HOPEGOOD, L., LATHAM, R.J. AND REILLY, J.D. (1998) Finite element analysis of static loading in donkey hoof wall. *Equine Vet. J.* Suppl. **26**, 103-110

NEWLYN, H.A., COLLINS, S.N., COPE, B.C., HOPEGOOD, L., LATHAM, R.J. AND REILLY, J.D. (1999) Equid Hoof Horn: A Natural Composite. In: *Proceedings of the 5th International Conference on Deformation and Fracture of Composites*, 18-19 March 1999, IOM Communications Ltd., London. pp 231-240.

NEWLYN, H.A., COLLINS, S.N., LATHAM, R.J. AND REILLY, J.D. (2004) Donkey Hoof Horn: A natural Composite? *J. Mater. Sci.* (Submitted for Publication).

REILLY, J.D., COLLINS, S.N., COPE, B.C., HOPEGOOD, L. AND LATHAM, R.J. (1998a) Tubule density of the *Stratum medium* of horse hoof. *Equine Vet. J. Suppl.* **26**, 4-9.

REILLY, J.D., COLLINS, S.N., COPE, B.C., HOPEGOOD, L. AND LATHAM, R.J. (1998b) Laminitis and the hoof horn capsule. In: *Proceedings of Dodson & Horrell Ltd. 1st International Research Conference on Equine Laminitis*, Stoneleigh, 8th – 9th September. pp 1-6.

REILLY, J.D., NEWLYN, H., COPE, B., LATHAM, R.J., COLLINS, S. AND HOPEGOOD, L. (2002a) A novel method for assessing hoof horn tubule density (TD) and a comparison of TD in the hooves of ponies, horses, donkeys, cattle, sheep and pigs. In: *Proceedings of the XII International Symposium on Lameness in Ruminants*, Orlando, Florida, 9th – 13th January. Ed: J.K. SHEARER. pp 275.

REILLY, J.D., NEWLYN, H., COPE, B., LATHAM, R.J., COLLINS, S. AND HOPEGOOD, L. (2002b) A comparison of different moisture-loss methods for measuring hoof wall moisture content. In: *Proceedings of the XII International Symposium on Lameness in Ruminants*, Orlando, Florida, 9th – 13th January. Ed: J.K. SHEARER. pp 193.

REILLY, J.D., COLLINS, S.N., HOPEGOOD, L. AND LATHAM, R.J. (2003) Tubule density of Donkey Hoof Horn and comparison with Pony and Horse Hoof Horn. *The Veterinary Record.* (Submitted for Publication).

TRAWFORD, A (1998) Multi-Disciplinary collaboration for the world-wide benefit of working equines. In: *Proceedings of the 3rd International colloquium on donkeys, mules and horses in tropical agricultural development,* Universidad Nacional Autonoma De Mexico, Mexico. pp 271-280.

APPENDIX VIII
COPIES OF PUBLICATIONS AND CONFERENCE PROCEEDINGS ASSOCIATED WITH WORK CONDUCTED FOR THIS THESIS

BEST COPY

AVAILABLE

Poor text in the original thesis.

Tubule density of the *stratum medium* of horse hoof

J. D. REILLY*, S. N. COLLINS, B. C. COPE, L. HOPEGOOD and R. J. LATHAM

*Faculty of Applied Sciences, De Montfort University, Leicester LE1 9BH. UK and *Royal Army Veterinary Corps, DASU, Normandy Barracks, Sennelager, BFPO 16.*

Keywords: horse; Tubule density; *stratum medium*; hoof

Summary

The number of tubules/mm^2 (tubule density) of horse hoof horn was quantified in samples taken from the left forefeet of 8 randomly selected slaughterhouse horses in order to establish the normal tubule density characteristics at the midline dead centre (MDC) for the *stratum medium* of horse hoof. In the past the measurement of tubule distribution within the hoof has lacked objectivity. The horse hoof tubule density results are compared to a recent objective study carried out on pony hoof. A similar 4 zone pattern of tubule density was observed, although the precise zonal boundaries and tubule density values differed to those found for pony hoof. There were significant differences in tubule density between zones. Comparison with pony hoof revealed significant tubule density differences in zones 1, 2 and 4; however, there was no significant difference in zone 3. The existence of a 4 zoned pattern of tubule density for horse hoof, as for pony hoof, has been confirmed.

Introduction

Reilly *et al.* (1996) and Kasapi and Gosline (1997) noted that the hoof wall exhibits a structural hierarchy evident at the macroscopic, microscopic and ultrastructural level. At the macroscopic level, hoof wall is composed of 3 morphologically distinct layers (Trautmann and Feibiger 1957), namely the *stratum internum*, *stratum medium* and *stratum externum*. The *stratum medium*, which constitutes the bulk of the hoof wall (Nickel 1938, 1939), forms the basis of this study and is considered to be the principle component determining the load bearing capabilities of the hoof wall (Pollitt 1992; Kasapi and Gosline 1997). At the microscopic level the *stratum medium* exhibits a distinctive structural architecture composed of tubular and intertubular horn (Bruhnke 1931; Nickel 1938, 1939; Wilkens 1964).

Horn tubules are composed of a central medullary cavity, or marrow, surrounded by a cellular cortex. The individual horn tubules are surrounded and separated by intertubular horn. These horn tubules are assumed to be continuous from the coronary band to the bearing border (Pollitt 1995) and, in cattle, are said to be arranged parallel to the wall (Greenough *et al.* 1981). The hoof wall derives strength and form from the orderly proximodistal arrangements of tubular and intertubular horn (Balch *et al.* 1997). It is believed that this structural arrangement is responsible for the functional capacity of the hoof (Nickel 1939; Schummer *et al.* 1981) and the distribution of forces within the capsule (Bertram and Gosline 1987).

Tubule density of the *stratum medium* has been defined as the number of tubules/unit area (Reilly *et al.* 1996) and many workers have suggested that this parameter influences the macroscopic mechanical properties of hoof horn. For example, Gunther *et al.* (1983) and Geyer and Tagwerker (1986) for cattle and pig hoof, respectively, suggested that 'hardness' was related to tubule density. In an early study, Bruhnke (1931) stated that the tensile/shear force of the horn of cattle, sheep, pigs and horses decreased from the dorsal aspect towards the palmar/plantar aspect. Much later, Wilkens (1964) reported that the mechanical strength of the hoof wall was dependent upon tubule density. However, no data were given to support this statement. More recently, Geyer (1980) summarised the work of Kind (1961) as suggesting that the higher the tubular density the greater the loading to which the horn may be subjected without compromise. Schummer *et al.* (1981) suggested a relationship between tubule density and resistance to wear of the hoof horn capsule. Dittrich *et al.* (1994) believed that an increase in the number of tubules improved hoof horn integrity, although again no data were presented to support this argument. The precise nature of the implied relationship between tubule density and the mechanical properties of hoof still needs to be evaluated.

Reilly *et al.* (1996) suggested that a specific pattern of tubule density may exist which reflects the functional demands placed on equine hoof. A variation in tubule density in different locations around the equine hoof capsule has been described by Lungwitz and Adams (1913), Nickel (1938, 1939), Geyer (1980), Bolliger (1991), Pellman *et al.* (1993), Bragulla *et al.* (1994) and Reilly *et al.* (1996). Differences also occur across the depth of the hoof wall (Nickel 1938, 1939; Zoerb and Leach 1978; Reilly *et al.* 1996; Kasapi and Gosline 1997) and descriptions of morphological zonation within the hoof wall have been reported for the horse (Bruhnke 1931; Nickel 1938, 1939; Wilkens 1964; Stump 1967; Leach 1980; Bolliger 1991).

Reilly (1995) argued that there is a need to measure objectively hoof horn parameters and consequently Reilly *et al.* (1996) established a systematic method and provided a detailed protocol for ascertaining tubule density in pony hoof. This provided a quantitative and objective measurement of this anatomical feature within the hoof capsule. The existence of 4 separate zones of hoof horn within the *stratum medium* at the midline dead centre (MDC) was proposed by Reilly *et al.* (1996) (Fig 1); and it was further suggested that this may be an equine pattern.

The aim of this study was to establish the normal tubule density for the *stratum medium* of the hoof of the horse, and to compare the zonal arrangement of tubules reported by Reilly *et*

TABLE 1: Comparison of tubule density and zonation in the *stratum medium* at the midline dead centre (MDC) for horse and pony hoof

	Horse		Pony (Reilly *et al.* 1996)	
Zone	% HWD	Tubule density (tubules/mm^2)	% HWD	Tubule density (tubules/mm^2)
Zone 1	0–25	>22	0–26	>27
Zone 2	25–47	16–22	26–51	16–27
Zone 3	47–69	11–16	51–77	8–16
Zone 4	69–100	<11	77–100	<8

HWD = hoof wall depth.

TABLE 2: Mean and range tubule density values for equine hoof (tubules/mm^2)

Author	Tubule density
Kind (1961)	(5–9)
Leach (1980)	30
Bucher (1987)	8 and 14
Pellman *et al.* (1993)	7
Reilly *et al.* (1996)	16
	(3–61)
Kasapi and Gosline (1997)	(10–25)
Reilly *et al.* (1998)	16
	(5–48)

al. (1996) from a selected and controlled population of ponies, to the *stratum medium* obtained from a randomly selected slaughterhouse population of horses.

Materials and methods

The left fore feet of 8 randomly selected slaughterhouse horses were used to provide hoof samples. The sampling site was the midline dead centre of the *stratum medium* of the hoof wall after Reilly *et al.* (1996).

The centre point of the sample was taken as the mid point between the coronary band and the bearing border. The final block taken from the hoof capsule was 1 cm in height, 1 cm long (mediolaterally) and encompassed the full dorso-palmar extent of the stratum medium of the hoof wall. Reilly *et al.* (1996) referred to this as the full hoof wall depth of the *stratum medium* (HWD). The sample was taken at right angles to the direction of the tubules. A sledge microtome was used to cut a horizontal section of 12 µm from the centre of the block. Sections were stained in Haematoxylin and Eosin, dehydrated and mounted in DPX with a coverslip. Digitised images of each section were captured using a video camera and Global Laboratory software. Images were processed using NIH Image (Public domain software version 1.59) to enhance tubule definition. The digitised images were enlarged using Adobe Photoshop[1] to A4 format, prior to printing. A grid was then overlaid on the image and a tubule density count was carried out according to the method of Reilly *et al.* (1996).

Statistical analysis

The results were analysed using Minitab[2]. Graphs were produced using Minitab and Excel[3]. The normality of data was established using the Kolmogorov-Smirnov normality test. Differences between zones for transformed data were analysed using one way analysis of variance (ANOVA) and Tukey test. Zonal tubule density comparisons between horse and pony were evaluated by *t* test using transformed data.

Results

The frequency histograms for nontransformed and transformed horse tubule density data are shown in Figures 2a and 2b. The distribution in Figure 2a is skewed to the right such that the mean and median values are not the same. The normal probability plot indicated that the data were non-normally distributed ($P<0.01$). Square root (sqrt) transformation of the data after Reilly *et al.* (1996) gave a distribution that was normal ($P>0.01$) by the Kolmogorov-Smirnov normality test (Fig 2b).

The results for tubule density as a function of percentage hoof wall depth (%HWD) are illustrated in Figure 3. Subsequent analysis of the data follows the convention given by Reilly *et al.* (1996). Dividing the transformed data, by use of ± 1 and ± 2 s.d. about the mean (3.95 sqrt tubules/mm^2), gave divisions at 2.56, 3.26, 4.65 and 5.34 sqrt tubules/mm^2 which correspond to tubule densities of ~6.6, ~10.6, ~21.6 and ~28.5 tubules/mm^2, with a mean of ~15.6. The square root tubule density values, at conventional standard deviations about the mean, delimit the zonal boundaries. These values were used to establish the %HWD at which the zonal boundaries occurred. A simple regression equation defined the relationship between %HWD and sqrt tubule/mm^2 as:-

$$\%HWD = 172 - 31.7 \text{ sqrt tubule density}$$

This equation was used to determine the corresponding intercepts in terms of percentage hoof wall depth for each square root tubule density value.

In this way the *stratum medium* of the hoof wall at the MDC was divided into 4 zones at ~25%, ~47% and ~69% HWD. The corresponding tubule density ranges are shown in Table 1.

There were significant differences in transformed tubule density values between all zones ($P<0.05$ by one-way ANOVA and Tukey test).

In addition, zones 1 and 2 tubule density values for the horse were significantly lower than those for the pony ($P<0.05$), whereas those for zone 4 were significantly higher ($P<0.01$). There was no significant difference in zone 3 for tubule density values between horse and pony horn ($P>0.05$).

Discussion

The results reported in this paper resemble those obtained by Reilly *et al.* (1996) from a pony population and have been compared in Table 1. The dorso-palmar decrease in tubule density is not uniform across the hoof wall and a distinct zonal pattern is evident (Fig 3).

Although differing tubule densities occur in the different zones of the *stratum medium*, the mean tubule density based upon transformed data is the same for both horses and ponies (~16 tubules/mm^2). This may represent an optimal mean tubule density for this site within the hoof capsule. Although the zonal trends are similar in both cases, the absolute distribution of tubule density within the zones varies.

The scatter plot (Fig 3) reveals 2 regions of changing tubule density (zones 1 and 3) and one region of relatively consistent tubule density (zone 2). This is similar to the findings of Reilly *et al.* (1996). The tubule density trend in zone 4, however, was difficult to ascertain. Excessive take up of stain resulted in 27

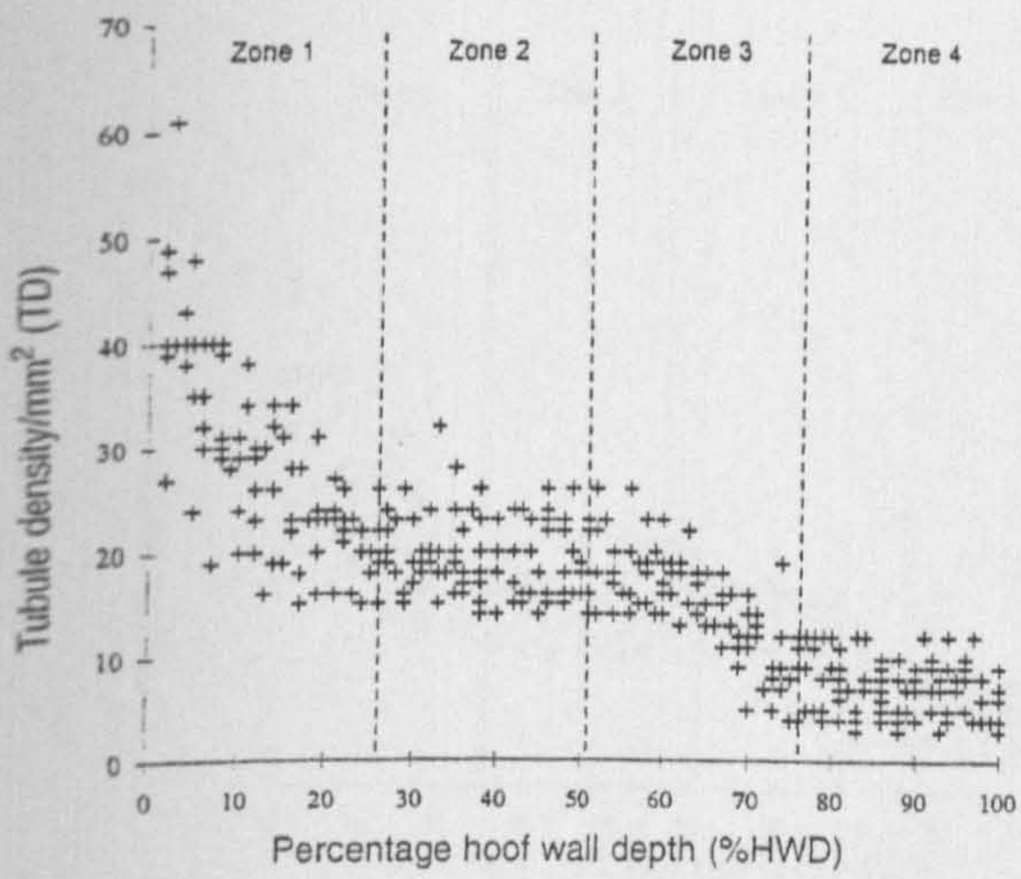

Fig 1: Tubule density (TD) by percentage hoof wall depth (%HWD) to show the 4 zones of the stratum medium *at the midline dead centre for ponies (after Reilly* et al. 1996).

incomplete cell counts from a total of 308. This occurred solely in zone 4. However, Reilly *et al.* (1996) successfully completed a tubule density count from this region and showed consistent tubule density values in this zone giving a similar pattern, but different objective values, to that seen in zone 2.

The adjusted means and scatter plots for both horse and pony tubule density indicate a significantly lower tubule density in zones 1 and 2 for horse *stratum medium* ($P<0.01$). This may represent a functional difference between horse and pony horn. However, this difference in tubule density may relate to the method of image analysis employed. It can be argued that a video based system cannot match the resolving power of conventional optics and photography. This may not have allowed very small tubules to be resolved. Another reason for the difference may be the use of slaughterhouse samples which may have been biased towards older animals. While the precise relationship between tubule density and age for horses is not known, both Gunther (1974) and Geyer (1980) have suggested that in cloven hooves the number of tubules diminishes with age. If a similar relationship exists in the horse, lower tubule density values could be anticipated if such a sampling bias occurred in this study.

The tubule density values within zone 3 for horse and pony (11–16/mm^2 and 8–16/mm^2 respectively) were not significantly different ($P>0.05$). However, significant differences occurred in zone 4 (<11/mm^2, <8/mm^2, horse and pony respectively). These may represent differences in optimal tubule density values in this zone between horse and pony respectively.

The boundaries of zones 1 and 2 are close to those determined by Reilly *et al.* (1996). Determination of the boundary between zones 3 and 4 based upon a simple regression line indicates a boundary at ~68% of the hoof wall depth for our horses compared with ~77% for the ponies. This may reflect a genuine difference between horse and pony hoof or may represent the influence of excessive uptake of stain in zone 4. The latter may contribute to the disparity in tubule density values between other authors. Under representation of the tubule density contribution from zone 4 would cause a shift to the left of the zonal boundaries on the scatter plot (Fig 3); with the shift at the zone 3/4 boundary being more pronounced.

Previously published tubule density values for horse hoof

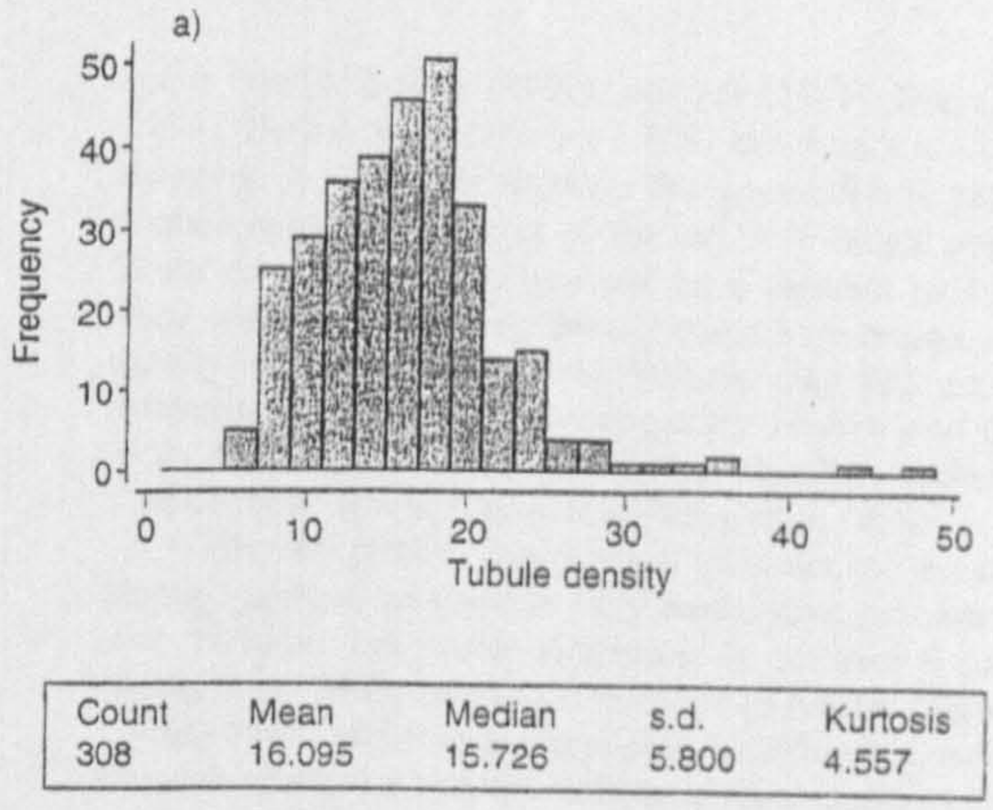

Count	Mean	Median	s.d.	Kurtosis
308	16.095	15.726	5.800	4.557

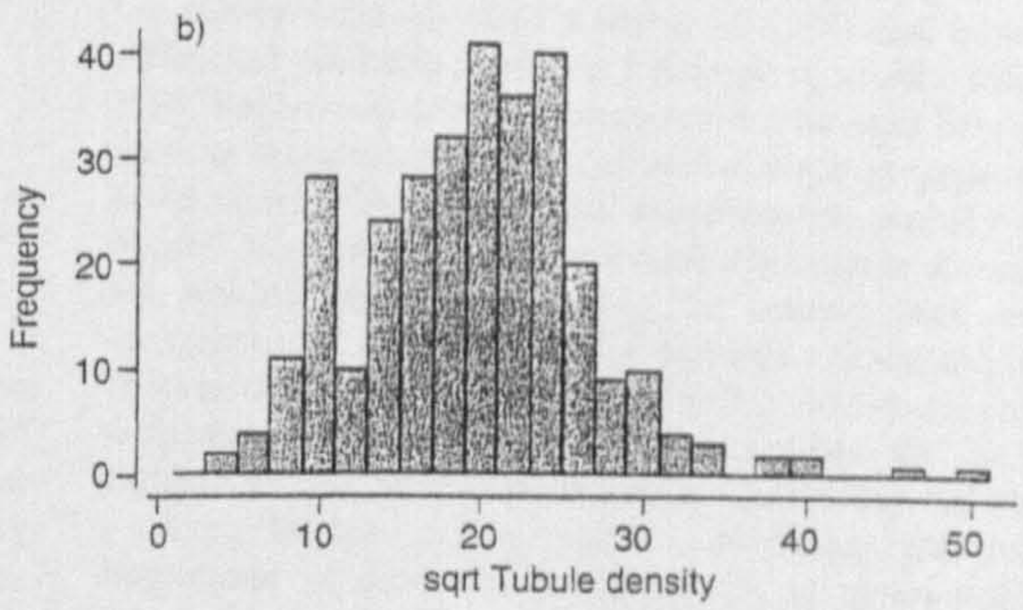

Count	Mean	Median	s.d.	Kurtosis
308	3.951	3.966	0.696	1.290

Fig 2: Frequency histograms for horse tubule density data; a) non transformed data and b) square root transformed data.

are shown in Table 2. These results show considerable variation between studies with several values differing from those reported in this study. However, direct comparisons are made difficult as details of methodologies and sampling areas have not been published by previous authors.

Reilly *et al.* (1996) demonstrated the potential overestimation of tubule density values if working with non-normal data. The tubule density data in this study displays a non-normal distribution which is consistent with that reported in the pony. Hence the true mean of tubular density should be calculated from the transformed data. In this case, the true mean of $(3.9513)^2$ tubules/mm^2 corresponds to 15.6 tubules/mm^2, which contrasts with a 'mean' of 16.1 tubules/mm^2 based upon untransformed data. This discrepancy highlights the slight overestimation that can occur if non transformed data is used for analysis. Reilly *et al.* (1996) emphasised the importance of this overestimation when interpreting work from different authors; and when subsequently relating tubule density to other physical properties.

A four zone division of the *stratum medium* of the hoof wall is proposed for the horse with an adjusted mean of >22, 16–22, 11–16 and <11 tubules/mm^2. This is in contrast to Bucher (1987) who divided the *stratum medium* into an 'inner' and 'outer' zone without clearly defining zonal boundaries. The tubule density of

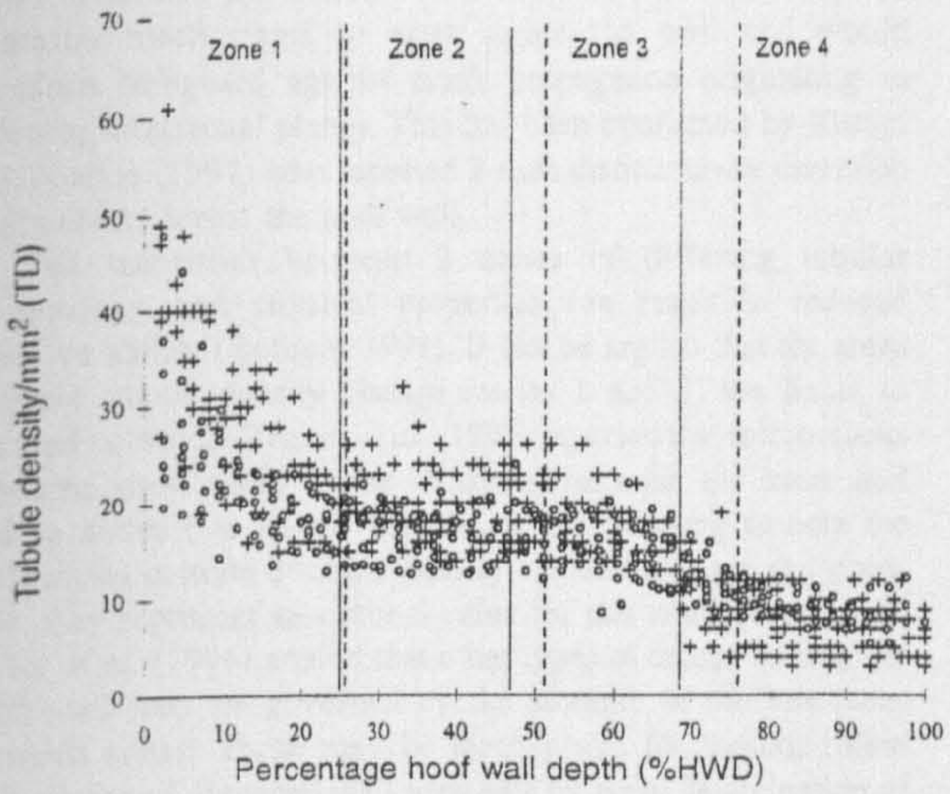

Fig 3: Comparison of tubule density (TD) and zonal boundaries by percentage hoof wall depth (%HWD) for the stratum medium *of ponies and horses.*

Bucher's (1987) 'inner' zone (8 tubules/mm^2) is slightly lower than that for zone 4 in this study and is similar to the results of Reilly *et al.* (1996) for pony hoof. The results from the outer zone from Bucher's study (14 tubules/mm^2) were considerably lower than either zone 1 or 2 for the pony hoof studies (>27/mm^2) by Reilly *et al.* (1996), or for horse hoof (>22/mm^2). The lower tubule density reported by Bucher (1987) may have arisen because the sample set included the *stratum medium* from hind feet. Both Reilly *et al.* (1996) and this study used left forefeet only. The relationship for tubule density and %HWD for hind feet is not known. The sample site used by Bucher (1987) also differed from that in this study.

A detailed methodology was not provided by Kasapi and Gosline (1997) when assessing the tubule density of the right fore hoof for a limited sample population of only 2 horses. They reported a palmaro-dorsal increase in tubule density across the hoof wall from 10 tubules/mm^2 in the 'inner wall' to 25 tubules /mm^2 towards the 'outer wall' which they refer to as a 'radial increase'. It is not possible to see whether a zonal pattern exists in their results, as only 6 equidistant sampling sites were selected. Nevertheless, the results are in broad agreement with this paper and those reported by Reilly *et al.* (1996).

The *stratum medium* of horse hoof has previously been divided into 3 zones ('outer', 'middle' and 'inner') based upon tubular morphology (Bruhnke 1931; Nickel 1938, 1939; Wilkens 1964). Stump (1967) agreed with this description, but also reported an 'intermediate' zone between the 'inner' and 'middle' zones containing tubule forms from both. Kasapi and Gosline (1997) found abrupt morphological changes in tubule form at 66% of the hoof wall depth which they interpreted as being the 'intermediate' zone first described by Stump (1967) and reported by Leach (1980). This area corresponds to zone 3 in this study. The transition between the low tubule density of zone 4 and the higher tubule density of zone 2 may account for the progressive change across zone 3.

Another population of tubules is reported to exist between zone 4 and the *stratum internum.* This has been described by Leach (1980), Bucher (1987), Bolliger (1991), Bragulla *et al.* (1994), Budras and Huskamp (1994) and Reilly *et al.* (1996). However, it is unclear whether this population is part of the *stratum medium* or is part of the cap horn tubule population. These tubules were not recorded as a separate entity in this study, either because their density made little impact upon the density values for zone 4 or because they fell outside the sampling area due to the curvature of the *stratum internum*. The method used in this investigation may therefore underestimate the true mean tubule density (see Reilly *et al.* 1996).

While the precise functional significance of zonal tubule density variation has yet to be fully investigated, it is possible that such variation will confer differences in mechanical properties (Reilly *et al.* 1996), modulated by moisture content (Bertram and Gosline 1987), and commensurate with the differential mechanical demands required across the wall (Kasapi and Gosline 1997). The hoof capsule plays a significant part in dampening concussive locomotory forces (Dyhre-Poulsen *et al.* 1994) and, in terms of athleticism, the horse represents a pinnacle of evolution (Bolliger 1991; Reilly *et al.* 1996). A compromise must exist between the need to accommodate forces, minimise crack propagation and avoid excessive deformation that would threaten dermal integrity. Vogel (1989) stated that the biomechanical properties of a structure are probably determined both by the material itself and the arrangement of that material. The distinctive tubule density and zonal tubule arrangement of the hoof wall of the horse is probably designed optimally in order to accommodate the functional demands of the hoof both at the level of the tubule and of the wall.

Considerable debate exists concerning the relative importance of the tubular architecture in determining the functional capacity of the hoof wall. For example, Leach (1980) suggested that, during weightbearing, ground reaction forces are transmitted proximally up the wall. Nickel (1938, 1939) and Wilkens (1964) believed the tubular and intertubular arrangement of hoof horn to be of importance in stress transfer and resilience, providing resistance to loading forces. The early work of Nickel (1938, 1939) considered that the tubules acted as vertical struts with the intertubular horn transferring stresses to the tubules. However, Thomason *et al.* (1992) reported no relationship between principal strain and the orientation of tubules and intertubular horn, although Chang *et al.* (1993) noted that the strain pattern was aligned with the major functional axes of the hoof wall tissue in horses and donkeys.

Reilly *et al.* (1996) suggested that the high tubule density in zone 1 may allow stress to be concentrated in the outer wall as a function of its load bearing properties and that the rapid decline in tubule density in zone 1, and the step like pattern of tubule density from zone 1 to zone 4, may be a mechanism for the smooth transfer of stress across the hoof wall to the axial skeleton. This mechanism of smooth energy transfer may work in conjunction with stiffness changes, mediated by changing hydration levels that have been reported by Leach (1980), Leach and Zoerb (1983) and Bertram and Gosline (1987). Reilly *et al.* (1996) concluded that the hoof wall is a multi-laminated composite structure. Transferring load as gradually as possible between interfaces is a guiding principle in composite technology and helps prevent failure. As well as transferring load, the presence of a large number of tubules per unit area in zone 1 may act to significantly increase the work of fracture and create a 'tortuous jagged path' to inward crack propagation. As energy is absorbed in the separation of 2 different phases (Gordon 1976; Vogel 1989) the tubular-intertubular interface may produce an effective crack stopping mechanism (Bertram

and Gosline 1986; Reilly *et al.* 1996; Kasapi and Gosline 1996, 1997). Distinct populations of tubules allow different crack diversion mechanisms to exist across the wall and would therefore safeguard against crack propagation originating in different directional planes. This has been confirmed by Kasapi and Gosline (1997) who reported 3 such distinct crack diversion mechanisms across the hoof wall.

The transition between 2 zones of differing tubular morphology and physical properties can result in reduced cohesive ability (Bolliger 1991). It can be argued that the areas of rapid tubule density change (zones 1 and 3) are liable to reduced cohesion. Zenker *et al.* (1995) reported that microcracks appeared most often at the transition between the inner and middle zones (i.e. in our zone 3). It is interesting to note the similarities in zone 3 tubule density values for horse and pony. This may represent an optimal value for this zone. In addition, Reilly *et al.* (1996) argued that other types of cracks seen in the hoof wall may be governed by the strength of the interfaces between zones. These may be mechanisms for the controlled elimination of damaged wall segments by zonal delamination of hoof wall layers along planes of designed inherent weakness. These would act as an effective means of preventing catastrophic failure (Bertram and Gosline 1986; Reilly *et al.* 1996; Kasapi and Gosline 1997). In this way, Reilly *et al.* (1996) suggested that the hoof wall may function as a quadrilaminar ply and Kasapi and Gosline (1997) a trilaminar ply.

Reilly (1995) emphasised that there is a need to develop an understanding of the anatomical and functional relationships between the various hoof horn parameters in normal equine hoof. In order to achieve this, these must be defined through objective measurements from recognisable anatomical sites. This study furthers the characterisation of one of these parameters, namely tubule density at the midline dead centre of the *stratum medium*. The results confirm a 4 zonal pattern similar to that reported for pony hoof by Reilly *et al.* (1996), and reinforces the suggestion that this is an equine pattern for construction of the hoof wall at this site. However, the differing tubule density values and zonal boundaries for horse and pony suggests a difference in finer detail between the two. It should also be noted that Hifney and Misk (1983) described tubular density differences between horse and donkey hoof. Reilly (1997) commented upon this, and presented photographic comparisons in support of these observations. However, these purported differences are still to be measured objectively.

Reilly *et al.* (1996) gave examples of the usefulness of a full understanding of hoof tubule density in research terms. Further work is required to establish tubule density values for equid populations and to test the precise mechanical consequences of this structural arrangement under controlled experimental conditions. It may then be possible to assess whether abnormal tubule density changes are associated with pathologically altered states, such as laminitis, and to evaluate the mechanical consequences of these changes.

Acknowledgements

The authors would like to thank Mike Ball (Department of Pharmaceutical Sciences, DMU) for advice on staining and microtomy, Dr Mark Bradshaw (Department of Textiles and Fashion, DMU) and Howard Freeman (Centre for Educational Technology and Development, DMU) for assistance with the image analysis and processing.

Manufacturers' addresses

[1]Adobe Photoshop, Adobe Systems Inc. California, USA.
[2]Minitab Minitab Inc. State College, Pennsylvania, USA.
[3]Microsoft Corp. USA.

References

Balch, O.K., Butler, D. and Collier, M.A. (1997) Balancing the normal foot: hoof preparation, shoe fit and shoe modification in the performance horse. *Equine vet. Educ.* **9**, 143-154.

Bertram, J.E.A. and Gosline, J.M. (1986) Fracture toughness design in horse hoof keratin. *J. expt. Biol.* **125**, 29-47.

Bertram, J.E.A. and Gosline, J.M. (1987) Functional design of horse hoof keratin: the modulation of mechanical properties through hydration effects. *J. expt. Biol.* **130**, 121-136.

Bolliger, C.H. (1991) *The Equine Hoof: Morphological and Histochemical Findings*. Diss. University of Zurich.

Bragulla, H., Reese, S. and Mulling, C. (1994) Histochemical and immunohistochemical studies of the horn quality of equine hoof. *Anat. Histol. Embryol.* **23**, 44-45.

Bruhnke, J. (1931) *Vergleichende Untersuchungen der Hornwandstruktur des Zehenendes bei Huf und Klauentieren*. Deutsche Tierarztliche Wochenschrift, **1**, 4-10.

Bucher, K. (1987) *Zum mikroskopischen Bau der Epidermis an umschriebenen Stellen des Pferdehufes*. Diss University of Zurich.

Budras, K.D. and Huskamp, B. (1994) Therapeutic measures to improve the horn quality of hoof of horses with laminitis. *Anat. Histol. Embryol.* **23**, 45.

Chang, Y.H., Sherrill, J. and Bertram, J.E.A. (1993) Hoof wall function in horses and donkeys - experimental alteration of surface strain. In: *Proceedings of the 1993 IEEE 19th Annual Northeast Bioengineering Conference*. Eds: J.K.J. Li and S.S. Reisman. IEEE Service Centre, Piscataway, New Jersey. **98**, pp 64-65.

Dittrich, J.R., Flemming, J.S. and Minardi, I. (1994) Efeito de niveis suplementares de biotina no crescimento, estrutura e integridade dos cascos de potros de 1 a 2 anos de idade. *Agrarias, Curitiba* **13**, 1-2, 135-144.

Dyhre-Poulsen, P., Smedegaard, H.H., Roed, J. and Korsgaard, E. (1994) Equine hoof function investigated by pressure transducers inside the hoof and accelerometers mounted on the first phalanx. *Equine vet. J.* **26**, 362-366.

Geyer, H. (1980) Zur mikroskopischen Anatomie der Epidermis an der Schweineklaue. Zentralblatt fur Veterinarmedizin Reihe C - Journal of Veterinary Medicine Series C - *Anatomia Histologia Embryologia*, **9**, 337-360.

Geyer, H. and Tagwerker, F. (1986) *The Pig's Hoof. Its Structure and Alterations*. Hoffmann-La Roche, Basle, Switzerland. p 27.

Gordon, J.E. (1976) *The New Science of Strong Materials*. Penguin Books, Middlesex. p 269.

Greenough, P.R., MacCallum, F.J. and Weaver, A.D. (1981) *Lameness in Cattle*. 2nd edn. Wright Scientechnica, Bristol. p 471.

Gunther, M. (1974) *Klauenkrankheiten*, VEB, Gustav Fischer Verlag Jena.

Gunther, M., Anton, W. and Kastner, R. (1983) *Klauenkrankheiten*. Gustav Fischer, Verlag.

Hifney, A. and Misk, N.A. (1983) Anatomy of the hoof in donkeys. *Assiut vet. med J.* **10**, 3-6.

Kasapi, M.A. and Gosline, J.M. (1996) Strain rate dependent mechanical properties of the equine hoof wall. *J. expt. Biol.* **199**, 1133-1146.

Kasapi, M.A. and Gosline, J.M. (1997) Design complexity and fracture control in the equine hoof wall. *J. expt. Biol.* **200**, 1639-1659.

Kind, H. (1961) *Vergleichende Untersuchungen uber die Abnutzung der Hufe einiget Equiden aufgrund der Struktur der Hufkapselwand*. Diss Humboldt-Universitat, Berlin.

Leach, D.H. (1980) *The Structure and Function of Equine Hoof Wall*. PhD thesis, University of Saskatchewan.

Leach, D.H. and Zoerb G.C. (1983) Mechanical properties of equine hoof wall. *Am. J. vet. Res.* **44**, 2190-2194.

Lungwitz, A. and Adams, J.W. (1913) *A Textbook of Horseshoeing*, 11th edn. J.B. Lippincott Co., London. p 216.

Nickel, R. (1938) Uber den Bau der Hufrohrchen und seine Bedeutung fur den Mechanismus des Pferdehufes. *Morph. Jahrbuch* **82**, 119-160.

Nickel, R. (1939) Untersuchungen uber den Bau des Pferdehufes mit besonderer Berucksichtigung des Hufmechanismus und von Hufkrankheiten. *Dtsch. tierarztl. Wschr.* **46**, 449-552.

Pelimann, R., Reese, S. and Bragulla, H. (1993) Relationship between the structure and quality of equine hoof horn and a potential procedure for studying disorders of keratinisation. *Monatshefte vet.* **48**, 11-12, 623-630.

Pollitt, C.C. (1992) Clinical anatomy and physiology of the normal equine foot. *Equine vet. Educ.* **4**, 219-224.

Pollitt, C.C. (1995) The anatomy of the inner hoof wall: new information. In: *Proceedings from the Annual Seminar of the Equine Branch of the NZVA*. Publication No 167. Veterinary Continuing Education. Massey University, Palmerston North, New Zealand. pp 97-106.

Reilly, J.D. (1995) No hoof no horse? *Equine vet. J.* **27**, 166-168.

Reilly, J.D., Cottrell, D.F., Martin, R.J. and Cuddeford, D. (1996) Tubule density in equine hoof horn. *Biomimetics*. **4**, 23-35.

Reilly, J.D. (1997) The donkey's foot and its care. In: *The Professional Handbook of the Donkey*. Ed: E.D. Svendsen. Whitet Books Ltd. London. pp 71-92.

Schummer, A., Wilkens, H., Vollmerhaus, B. and Habermehl, K.H., Siller, W.G. (translator), Wight, P.A.L. (translator) (1981) *The Circulatory System, the Skin and the Cutaneous Organs of the Domestic Animals*. Verlag Paul Parey, Berlin. p 610.

Stump, J.E. (1967) Anatomy of the normal equine foot, including microscopic features of the laminar region. *J. Am. vet. med. Ass.* **151**, 1588-1597.

Thomason, J.J., Biewener, A.A. and Bertram, J.E.A. (1992) Surface strain on the equine hoof wall in vivo: implications for the material design and functional morphology of the wall. *J. expt. Biol.* **166**, 145-165.

Trautmann, A. and Fiebiger, J. (1957) *Fundamentals of the Histology of Domestic Animals*. Eds: R.E., Habel and E.L. Biberstein. Translation and revision. 1949 German edn. Comstock Publishing Association, New York. pp 360-369.

Vogel, S. (1989) *Life's Devices: the Physical World of Animal and Plants*. New Jersey, Princeton University Press.

Wilkens, H. (1964) Zur makroskopischen und mikroskopischen morphologie der Rinderklaue mit einem Vergleich der Architektur von Klauen und Hufrohrchen. *Zbl. vet. Med.* **11a**, 163-234.

Zenker, W., Josseck, H. and Geyer, H. (1995) Histological and physical assessment of poor hoof horn quality in Lipizzaner horses and a therapeutic trial with biotin and a placebo. *Equine vet. J.* **27**, 183-191.

Zoerb, G.C. and Leach, D.H. (1978) Mechanical properties of the hoof wall of the horse. *American Society of Agricultural Engineers*. pp 1-13.

Equine vet. J., Suppl. **26** (1998) 103-110

Finite element analysis of static loading in donkey hoof wall

H. A. NEWLYN, S. N. COLLINS*, B. C. COPE*, L. HOPEGOOD*, R. J. LATHAM* and J. D. REILLY*†

Department of Mechanical and Manufacturing Engineering, Faculty of Applied Sciences, De Montfort University, Leicester LE1 9BH, UK and †Royal Army Veterinary Corps, UKSC(G), DASU, BFPO 16.

Keywords: horse; finite element analysis; donkey; hoof wall

Summary

A finite element model of donkey hoof wall was constructed from measurements taken directly from the hoof capsule of the left forefoot. The model was created with a 2 mm mesh and consisted of 11608 nodes. A linear elastic analysis was conducted assuming isotropic material properties in response to a 375 newton (N) load, to simulate static loading. The load was applied to the wall via 400 laminae in order to simulate the way in which the pedal bone is suspended within the donkey hoof capsule. Displacement, stress concentration, principal strain, and force distribution across the hoof wall were evaluated. The hoof wall model revealed loading responses that were in broad agreement with previously reported *in vivo* and modelled observations of the equid hoof. Finite element analysis offers the potential to model hoof wall function at the macroscopic and microscopic level. In this way, it could help to develop further our understanding of the functional relationship between the structural organisation and material properties of the hoof wall.

Introduction

Leach (1980) suggested that the functional demands placed upon the equid musculoskeletal system are immense as, during both static and dynamic loading, the entire weight of the equid is directed through the foot and the hoof in particular. During locomotion the hoof strikes the ground with great force and frequency. For example, in the galloping horse a vertical concussive force of approximately 9000 N (Quddus *et al.* 1978), equivalent to twice the bodyweight of the animal, is generated during a stance of 0.1 s (Geary 1975), and at a frequency of up to 120 strides/min (Lekeux and Art 1994). In this respect, Dyhre-Poulson *et al.* (1994) noted that the anatomical structures of the foot are particularly adapted to absorb energy. However, the hoof capsule is fundamental to equid performance and has largely been overlooked in terms of biomechanical modelling. Modelling studies have tended to focus upon the role of the dermal structures and the bones during load bearing. However, the hoof must afford protection to the underlying sensitive structures of the foot. Hence it is essential that it is capable of withstanding the forces generated by ground impact (Douglas *et al.* 1996) and it must also dissipate the resultant shock waves to dampen concussive forces (Dyhre-Poulson *et al.* 1994). This must be achieved without excessive deformation or failure (Leach 1980; Bertram and Gosline 1986), as this would threaten the sensitive structures of the foot (Leach and Zoerb 1983). In this way, smooth and painless force transfer between the ground and the axial skeleton can be achieved (Reilly and Kempson 1992). As a result of these capabilities, Pollitt (1990) and Reilly *et al.* (1996) have described the hoof as a miracle of bioengineering.

Vogel (1988) stated that a biological preference exists for accepting rather than preventing deformation and Sack and Gabel (1977) suggested that the hoof capsule yields under the pressure of impact to dissipate concussive forces. Distortion of a solid object in response to an applied load generates internal forces sufficient to counter the applied load (Gordon 1976). Hence, during normal weight bearing and locomotion, the hoof deforms in a consistent pattern (Douglas *et al.* 1996) which results from a compromise between the complex force changes occurring internally within the capsule, and those external compressive forces acting against the ground (Leach 1980).

The hoof wall represents the major functional load-bearing component of the hoof capsule (Nickel 1938, 1939; Parker 1973; Sack and Gabel 1977). However, considerable scientific debate exists as to the means by which the hoof wall achieves its functional requirements. Rooney (1978) proposed that the structural design of the hoof reflects the need for force resistance and energy absorption. Therefore, an interpretation of hoof wall function necessitates an understanding not only of the structure and morphology of the wall, but also the complexities of the external and internal forces affecting the capsule, and the response of the wall to these forces (Leach 1980). There is, however, a distinct lack of scientific information regarding the nature and distribution of forces within the hoof wall during loading.

Studies dating back to the last century have attempted to evaluate hoof deformation in response to loading (Miles 1856; Lechner 1881; Bayer 1886; Förringer 1889). However, many of these earlier studies were significantly restricted by the technology available at that time. Nevertheless, Lungwitz (1883, 1891) was able to arrive at a model of hoof wall deformation that has, in the main, been substantiated by later workers including Fischerleitner (1974), Leach (1980), Colles (1989) and Thomason *et al.* (1992). Lungwitz (1883, 1891) recorded an inward movement of the anterior aspect of the hoof wall at the height of the coronary band that Leach (1980) referred to as a dorsoconcavity. In addition, Lungwitz (1891) recorded a concurrent expansion at the heels, flattening of the sole, and sinking of the heels which decreased the hoof wall height (Fig 1).

Bartel *et al.* (1978) proposed a model for the sagittal plane of the distal limb illustrating force transmission within the foot. A

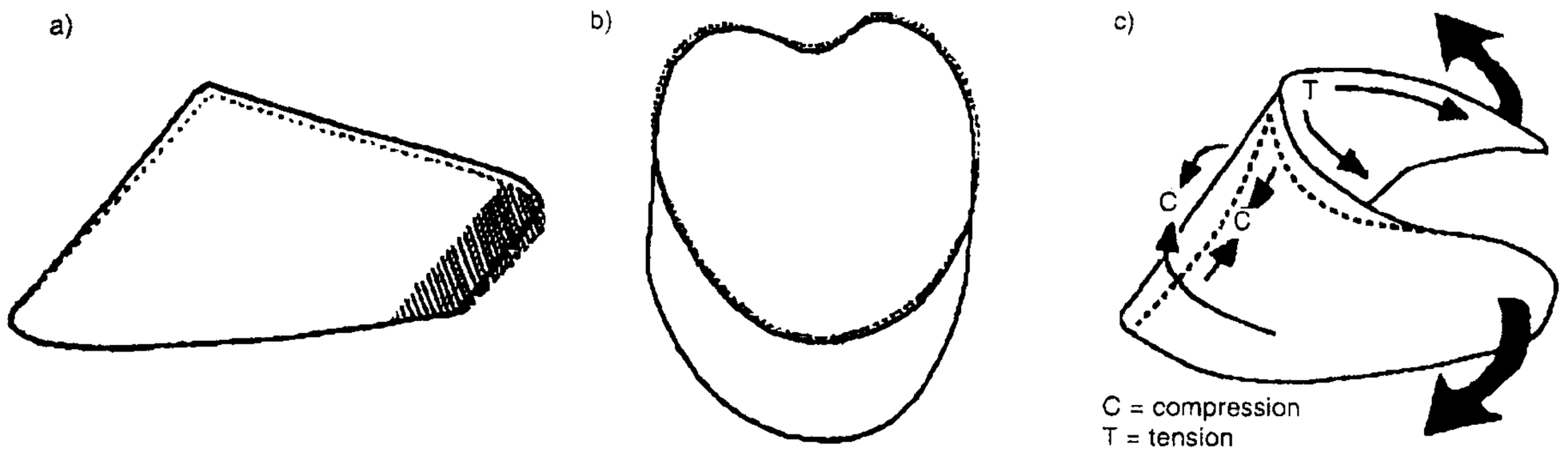

(a) The unbroken line indicates the original shape of the hoof in the free loaded state. The dotted line illustrates the retraction of the coronary edge and the sinking of the heels. The shaded area indicates expansion at the heels. (b) The dotted line shows the geometric change in form of the hoof wall during load-bearing. (c) The unbroken line represents the shape of the unloaded hoof wall and the dotted line shows the change in form that occurs during loading.

Fig 1: Diagram to show the deformation of the hoof wall during loading, illustrating the expansion of the heels, the retraction of the leading edge of the hoof and the sinking of the heels (after Lungwitz 1891) and the force inter-action according to Leach (1980).

TABLE 1: Basic geometric measurements at the 10 hoof wall measurement sites in the lateral half of the hoof capsule

Site	y, z coordinates[a]	Tubule inclination (°degrees)[b]	Tubule length (mm)	Wall thickness at bearing border (mm)
1	0,0	40	57	10
2	10,2	40	58	10
3	20,6	40	57	10
4	30,15	40	56	10
5	35,28	40	56	10
6	36,38	40	54	10
7	36,48	40	52	10
8	39,58	40	48	10
9	39,68	40	43	10
10	38,78	40	40	10

[a]y,z Coordinates. y = distance in mm from the plane of the midline dead centre (MDC) at the bearing border (BB), along the y axis. z = distance in mm from the dorsal aspect of the midline dead centre (MDC) at the bearing border (BB), along the z axis.
[b]Tubule inclination from the axis in the x, z plane, expressed in °degrees.

vertically orientated ground reaction force was considered to act through the centre of the hoof capsule, counteracted by the downward force of the bodyweight acting through the distal phalanx. Components of this ground reaction force acted throughout the whole of the distal bearing border of the hoof wall, with a resolved force vector directed parallel to the hoof wall. An inwardly directed tensile force was suggested on the inner surface of the wall, orientated in an orthogonal direction. The former being resisted by the hoof wall itself while the latter was countered by the laminar junction. Leach (1980) suggested that the concussive wave is dampened as it travels vertically through the hoof wall, and that the internally directed tensile force is possibly increased by the action of the deep digital flexor tendon on the distal phalanx. The action of the flexor tendon would cause posterioventral rotation of the phalanx and a synchronous displacement of the hoof wall (Fischerleitner 1974; Leach 1980; Thomason *et al.* 1992) resulting in the observed dorsoconcavity.

Leach (1980) and Thomason *et al.* (1992) argued however, that such a model did not adequately take account of the 3 dimensional nature of the hoof capsule. They suggested that the compressive forces directed through the wall would result in tensile strain at right angles to these forces. Expansion of the heels in response to the posterioventral movement of the distal phalanx results in horizontally directed compressive forces at the toe - at right angles to those generated by the ground reaction forces. This would subject the wall to biaxial compression (Mair 1974). Furthermore, Geary (1975) observed that the extent of the laminar junction varies throughout the capsule resulting in tensile components being centred upon the anterior half of the hoof. Thomason *et al.* (1992) suggested that this results in the quarters being pulled inwards and downwards.

These studies have initiated debate regarding the precise nature of forces acting upon the hoof wall and have raised questions regarding its function (Nickel 1938, 1939; Rooney 1978; Leach 1980). Leach (1980) concluded that the hoof wall is likely to experience forces originating from 3 sources, namely compressive stress from the ground, tensile stress from the laminae and stress resulting from the change in form.

Various techniques have been employed to evaluate force distribution in the hoof wall. Strain gauges attached to the outer surface of the hoof have been used to monitor capsular deflections during loading (Mair 1974; Colles 1989; Thomason *et al.* 1992). However, it is important to appreciate the limitations of these studies - for example, sensors are restricted to monitoring deflections upon the outer surface of the capsule only. Also, the information provided is only site specific and may not be representative of capsule dynamics, and the location of the sampling sites themselves are often ill defined. In general, these studies have provided evidence that supported the proposals of Leach (1980), with compression predominating at all monitored sites. Strain patterns vary however between studies. Mair (1974) and Chang *et al.* (1993) detected biaxial compression at the dorsum, which is the anatomical site referred to as the midline dead centre (MDC) by Reilly *et al.* (1996), suggesting horizontal compression within the hoof. However, Thomason *et al.* (1992) recorded such strain patterns only in proximal MDC sites. Furthermore, strain patterns recorded at the quarters indicate that heel expansion does not occur in a simple horizontal manner (Thomason *et al.* 1992). Rather, the heel expands more at the distal margin than the proximal edge (Douglas 1994). This results in an outward and upward

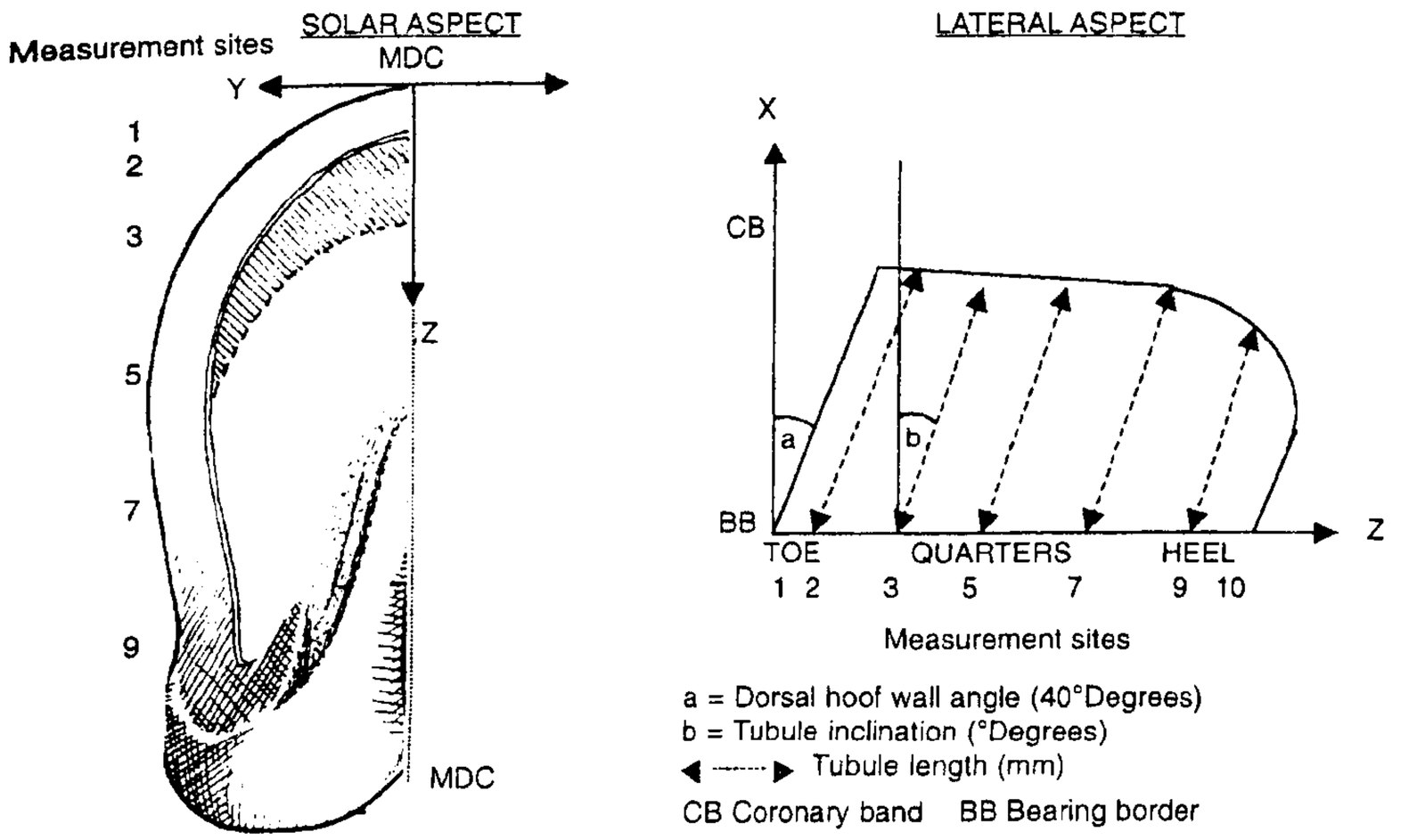

Fig 2: Diagrammatic representation of the basic geometric measurements used to construct the basal template and bounding curves of the donkey hoof wall Finite Element model.

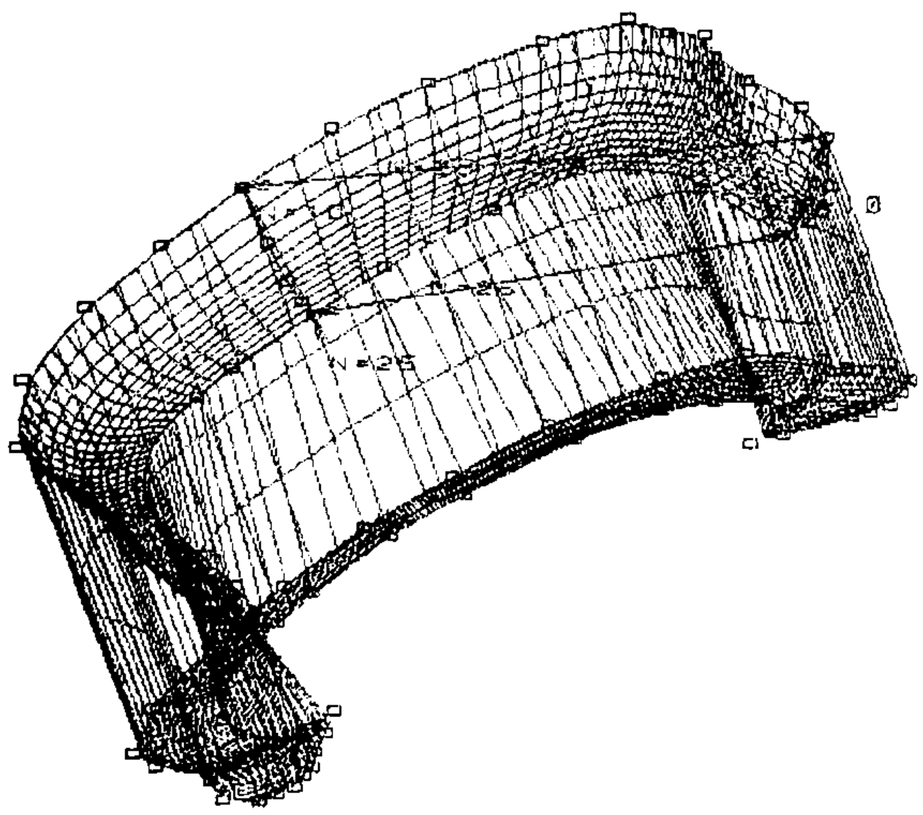

Fig 3: Surface model of the donkey hoof wall showing the initial mapping of the control points, splines and bounding curves.

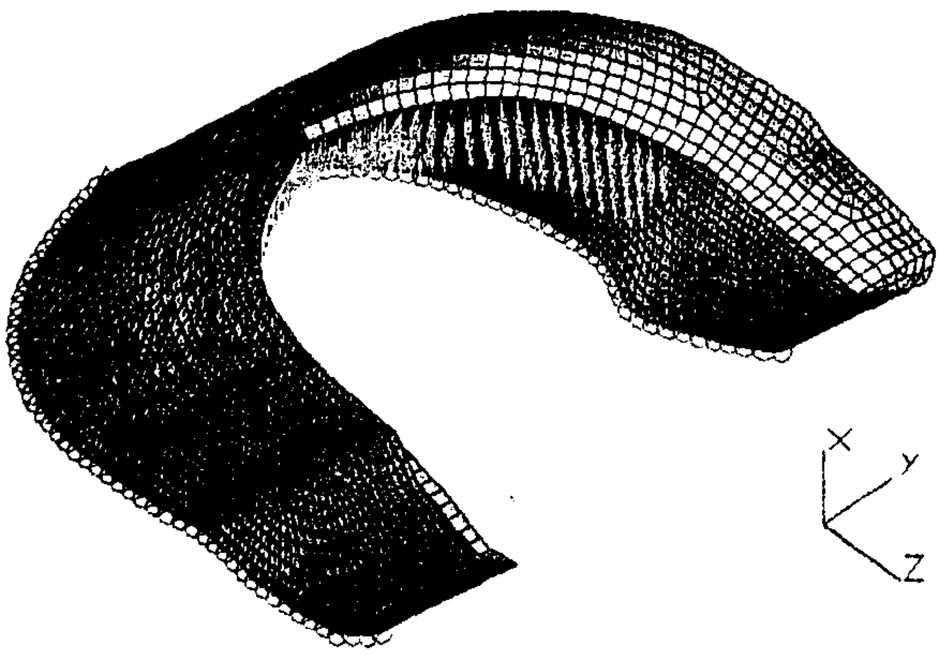

Fig 4: Finite element net construction model of hoof wall using a 2 mm mesh size, showing loading conditions (yellow arrows) and boundary restraints (red circles).

expansion of the hoof wall, generating compressive forces directed towards the coronary band at the MDC (Douglas 1994).

Davies (1997) and Dejardin *et al.* (1997) utilised photoelastic stress analysis techniques to document the distribution and magnitude of shear stress occurring on the outer surface of the hoof capsule in response to loading. This technique facilitates monitoring of the entire hoof capsule, therefore overcoming the 'site specific' limitation of conventional strain gauge analysis. However, this analysis is restricted to recording surface conditions only, and cannot objectively elucidate the nature of force distribution across the entire hoof wall depth.

Nickel (1938, 1939) assumed that the hoof wall was subjected to compressive forces alone, whereas Thomason *et al.* (1992) argued that the inner aspect of the hoof capsule was likely to be subjected to tensional forces, thereby intimating the occurrence of bending forces. In this respect, Hood *et al.* (1992) evaluated force generation in the hoof wall during loading using transducers capable of discriminating between bending and compressive deformation. They observed that the dorsal hoof wall (MDC) was subjected to either pure bending, or compression and bending. Pure compression alone within the wall, was not recorded.

Reilly (1995) argued that there is a need to further develop our knowledge of the mechanical functioning of the hoof wall as the mechanisms by which the hoof wall successfully achieves its function are not fully understood. The relationship between the forces generated during loading and the structural organisation and biomechanical and material properties of the hoof need to be established. Computer assisted 3 dimensional modelling of the hoof wall using finite element analysis (FEA) may serve as a means of elucidating the complex interaction of forces generated during loading, and provide essential information that is required to unravel the functional complexity of the hoof wall.

Several authors have used this mathematically based modelling technique to investigate internal deformations and stress distribution in different biological structures including bone and tendon. However, its application to the hoof has been limited. Wichtmann *et al.* (1990) and, Hood *et al.* (1991) used this technique to produce a 2 dimensional model of the equine foot in the sagittal plane in order to evaluate the theoretical

force distribution within the various structures of the digit in response to static loading. Hinterhofer *et al.* (1997) employed FEA to investigate the effect of dynamic loading upon a 3 dimensional model of the hoof capsule. This paper represents a logical progression to these former FEA studies and marks the first in depth 3 dimensional simulation of the major load bearing element of the hoof capsule, namely the hoof wall during static loading.

Materials and methods

Application of finite element analysis to the hoof wall

The Finite Element Analysis (FEA) method is widely used in the engineering industry and associated fields, and can be applied to static, dynamic, thermal, electrostatic and fluid flow problems. Used in static analysis it essentially relies upon developing mathematical equations that relate the displacements created, to the forces applied to small discrete subregions of the structure or 'Finite Elements'. These Finite Elements can be of various geometrical configurations i.e. rod, brick, or plate-shaped. The ends or corners of the element are called nodes. When these elements are assembled to represent the structure, the occurrence of common nodes, i.e. those which are common to adjoining finite elements, allow mathematical equations to be assembled to determine how the structure reacts theoretically to the applied forces. The derived displacements can then be used to determine strains and stresses. In order to restrain the structure and prevent free body movement, boundary conditions need to be applied. These have to be carefully considered in order to recreate accurate *in vivo* conditions.

The application of Finite Element Analysis to the structural performance of the hoof wall extends and complements the range of experimental techniques that have formerly been used to evaluate hoof wall function. Confidence in such an analytical technique should always be developed by comparison with experimental work, although care must be taken that like is compared with like. For example, the application of photoelastic material to the surface of a hoof in order to assess stress levels with unavoidably reinforce and stiffen the structure that is being assessed and, if bending is the major stress developing process, this may critically alter results. The aims of this study were to design a finite element model of the hoof wall of a donkey, and to model the effect of static loading upon the structure. This assumed linear elastic stress - strain relationships and isotropic material properties within the hoof wall. The study also aimed to evaluate the potential application of finite element techniques to hoof wall mechanics by comparison of simulated loading responses with previously reported *in vivo* observations and modelled data in the equid hoof capsule.

Developing the model

The model was based upon measurements of a hoof capsule obtained from the left forefoot of a donkey, which had no apparent signs of disorders related to the feet, that had been humanely destroyed on medical grounds. Immediately after destruction, the hoof capsule was sealed in Parafilm[1] to prevent shrinkage resulting from moisture loss, and was stored in a fridge until autolytic degradation of the dermal/epidermal junction allowed removal of the intact hoof capsule. Measurements were taken immediately after capsular removal to minimise the effect of moisture loss.

In order to create a successful model of a shape, such as the hoof wall that is composed of many intersecting curved surfaces, the use of a surface modeller is required. In this case, the initial shape of the bounding curves was developed. To this end the solear aspect (bearing border) of the hoof wall was accurately measured and mapped into the computer. In this way a basal template was constructed to which all subsequent measurements could be related spatially (Fig 2). The position of the coronary band was established by measuring the heights along the longitudinal axis of the horn tubules, from the bearing border to the coronary band, at ten sites from the MDC to the heels in the lateral half of the capsule (Table 1). The angle of inclination from the x axis was measured in the x, z plane. In this way, a series of control points were created and splines, a form of mathematical curve, fitted to the control points to form the bounding curves. These splines were transferred to the surface modeller and with the addition of some connecting lines, the bounding areas were created. Once this had been completed for one half of the hoof wall model it was mirrored about the plane of the MDC to form the complete hoof wall structure. These were then patched to create the surfaces of the model (Fig 3). These were subsequently meshed to form a finite element net construction on the surfaces of the wall model. Specific attention was given to ensure that the mesh size was small enough to allow the development of modelling detail, yet large enough to avoid an excessive computer file size.

This surface mesh was then enhanced to generate a more regular model, and brick elements generated to fill the volume using a finite element software package[2]. Once more, mesh size selection was critical, as not only does the mesh size affect the accuracy and detail of the final results, it also governs the processing time required for the analysis. This ultimately determines the feasibility of the analysis. For example, although a 1 mm mesh size provides a model capable of generating exceptional detail, the mesh enhancement process alone would require 16 h computer processing time on a Pentium 75 mHz PC to create ~45,000 elements. Therefore a 2 mm mesh size was selected. This required 4 h to generate and gave a respectable model with adequate detail, consisting of 18305 elements and 11608 nodes. A general arrangement, light shaded view, of the 2 mm mesh models is shown in Figure 4, with arrows indicating the loading surfaces and red circles indicating the boundary restraints.

A vertical static load of 375 N was used for the model. This represents a static loading force equivalent to a 150 kg bodyweight animal distributed equally between the 4 hooves. One hundred and fifty kg is a typical bodyweight for a donkey (Chang *et al.* 1993). This force was applied uniformly around the wall in a manner designed to simulate the suspension of the axial skeleton within the hoof capsule (Sack and Gabel 1987), via 400 laminae (Hifney and Misk 1983). The bearing border of the hoof wall was restrained vertically to simulate *in vivo* ground contact conditions. In addition the bearing border at the MDC was fully restrained preventing displacement at this anatomical site in any direction. These boundary conditions were consistent with the observations of Lungwitz (1883, 1891) and video footage published by Pollitt (1993) for the horse. The hoof wall was assumed to be isotropic with a Young's Modulus of 0.5×10^3 N/mm^2 (Wichtmann *et al.* 1990) and a Poisson's ratio of 0.4 (Chang *et al.* 1993). The analysis required the solution to 34,261 equations which took approximately 2 h computer processing time on a Pentium 75 mHz PC.

Results

Figure 5 illustrates the deformation of the hoof wall model in response to loading and boundary restraints. A comparison of the displaced shape with the original unloaded structure revealed an outward displacement at the heels, which progressively increased towards the palmar aspect attaining a maximum value of 2.36 mm. A dorso-concave deformation of the dorsal aspect of the MDC was indicated with the proximal region experiencing an inward deflection of 0.3 mm. The 'total deflection' at any point around the hoof wall model in the loaded state is shown in Figure 6. The maximum principal strain in the outer aspect varied around the hoof wall. In general strain values increased from the heels towards the MDC, attaining a maximum value in the order of 2500 με at the proximal region of the MDC (Fig 7). The direction of the principal strains indicates that the maximum principal strain at the MDC was aligned along the x axis both proximally and distally, and that the hoof wall at this site was subjected to biaxial compression. The biaxial compression was greater proximally than distally.

A modelled sagittal section taken along the plane of the MDC (Fig 8) revealed that the dorsal aspect of the hoof wall was subjected to compressive forces which increased progressively in a proximal direction from the bearing border. These compressive forces decreased across the hoof wall, in the dorso-palmar direction, with the development of tensile forces towards the inner margin of the wall section. The greatest tensile force was generated in the proximal half of the wall.

Discussion

The displacement diagram and displaced shape projections reported in this paper predicts a pattern of donkey hoof wall deformation, in response to static loading, which is in broad agreement with *in vivo* observations for the horse as reported by Lungwitz (1889, 1891) and Pollitt (1993). The simulated loading, resulting in an outward expansion of the heels and a simultaneous dorsoconcavity of the proximal MDC suggests that the mode of mechanical functioning of the donkey hoof wall may be similar to that of the horse. The displacement diagram illustrates that, in the region of the quarters and heel, the displacement value is greater proximally than distally. This contradicts *in vivo* observations in the horse where lateral expansion is greatest at the bearing border reported by Thomason *et al.* (1992). However, it is important to note that the displacement values are nominal, that is they give absolute displacement values only, and are not vector quantities giving directional information. The displaced space plot indicates a uniform outward expansion. Therefore, the predicted values suggest that the proximal region of the quarters may be subjected to a combination of different compressive, tensile, bending and torsion forces. Thomason *et al.* (1992) suggested that the proximal region of the heels in the horse were subjected to an inwardly directed tensile force that results in an outward and upward movement of the heel distally. However, the displacement plot in the y direction for the donkey (Fig 9) predicts uniform outward expansion proximally and distally and, therefore, it suggests that axial compressive forces may be contributing to the displacement at this site. This may reflect the sophistication of the model and the assumptions made in this respect, or may represent a genuine difference between horse and donkey. Reilly (1997) commented upon the anatomical differences between horse and donkey hoof capsule, and suggested that there may be different amounts of movements within the 2 capsules during loading. It can be argued in terms of mechanical principles, that geometrical differences are likely to affect displacement under loading. In this case, heel expansion is likely to be less in the more upright donkey capsule due to increased axial resistance. In addition, tapering of the hoof wall depth in the heel region of the horse (Reilly 1997) presents less material to resist displacement, and increases the tendency to accommodate such movement.

The theoretical distribution of principal strain around the outer surface of the hoof wall indicates the occurrence of maximum principal strain centred upon the proximal region of the MDC. This is consistent with experimental observations using surface strain gauges for the horse (Thomason *et al.* 1992; Chang *et al.* 1993; Kasapi and Gosline 1996) and for the donkey (Chang *et al.* 1993). This suggests that this FEA model is reproducing *in vivo* conditions. In addition, the principal strain distribution in the hoof wall model was comparable with that reported in the donkey hoof by Chang *et al.* (1993).

The stress distribution at the surface of the capsule that is derived from the strains using the stated Young's Modulus and Poisson's ratio can be displayed in various forms. The magnitude of the Maximum Principal stress can be plotted as can the Minimum Principal stress, or, a combination of these related to various failure theories. However, given the complexity of the structural hierarchy evident in the hoof wall (Reilly *et al.* 1996; Kasapi and Gosline 1997), and our limited knowledge of the material properties of hoof horn (Reilly 1995), it is difficult to say which failure mode is applicable. However, 2 stress states may be of interest, (i) The Maximum shear stress (Tresca) and (ii) The Von Mises Stress (Shear strain energy theory). Both of these are usually related, in engineering applications, to failure in ductile materials. Such a mode of failure may be applicable to hoof wall modelling due to the potential plasticising effect of the material's inherent moisture content (Cope *et al.* 1998). However, as the material is non isotropic and possibly behaves in a nonlinear fashion when loaded at high speed, these values can only give an indication of the resultant conditions. The accuracy of the results can be as accurate only as the assumptions made in developing and resolving the model. The Shear stress plot is also interesting in that it relates to the isochromatic fringes produced in photoelastic analysis. A plot of 2x the Tresca stress is used to simulate photoelastic surface strain and is used as a comparison (Fig 10).

The accuracy of FEA is dependent upon contributions from the geometrical modelling of the structure, the selected mesh size, the specified material properties, the defined boundary conditions, and the chosen load and means of loading. Whilst confidence can be expressed in terms of the geometric modelling and the boundary restraints, several important assumptions and compromises have had to be made with respect to the other factors.

The accuracy of the solution is related to the mesh size. The software used in these simulations can provide an indication of accuracy by calculating a precision value. It takes the values of the quantity of interest, for example stress, and compares the values derived at a node from all the elements connected at that node. These will differ depending on the mesh size and the local stress/strain gradients. The precision is defined as the maximum difference between these values divided by the maximum stress in the body. In this way it can be seen where the mesh needs to be refined to improve future accuracy.

Accurately inputting material properties into the model represents more of a challenge because there is a distinct lack of

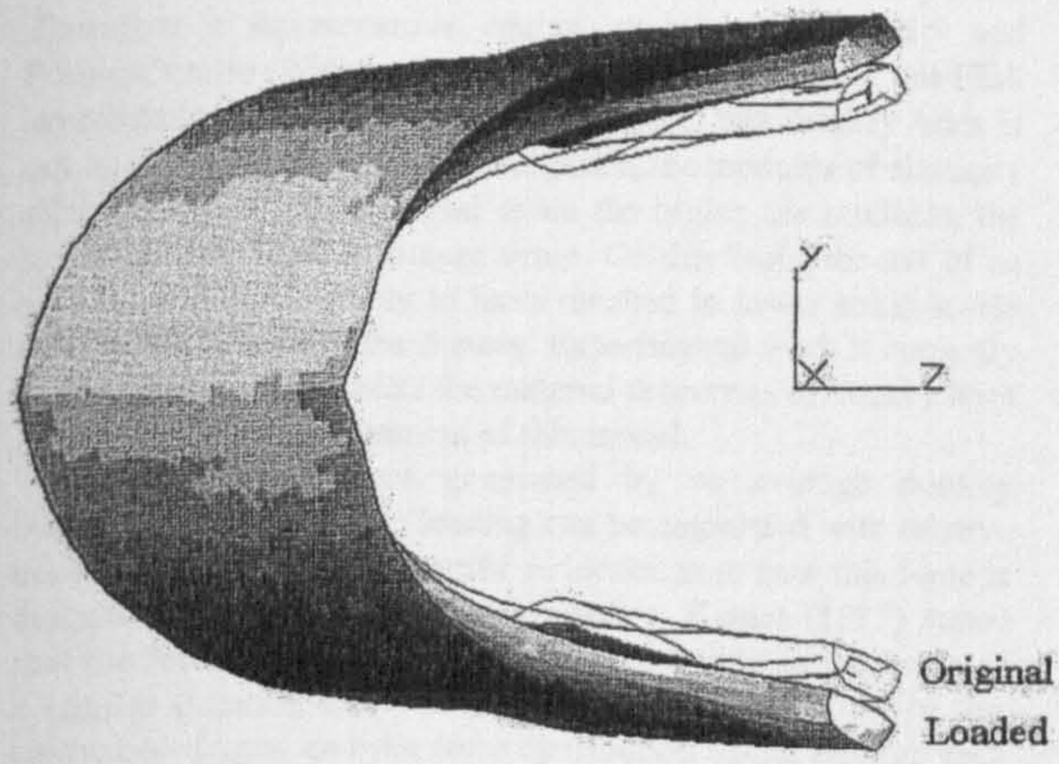

Fig 5: Displaced shape diagram of modelled hoof wall deformation in response to loading, illustrating the deformed/displaced wall section compared to the original unloaded net construction model.

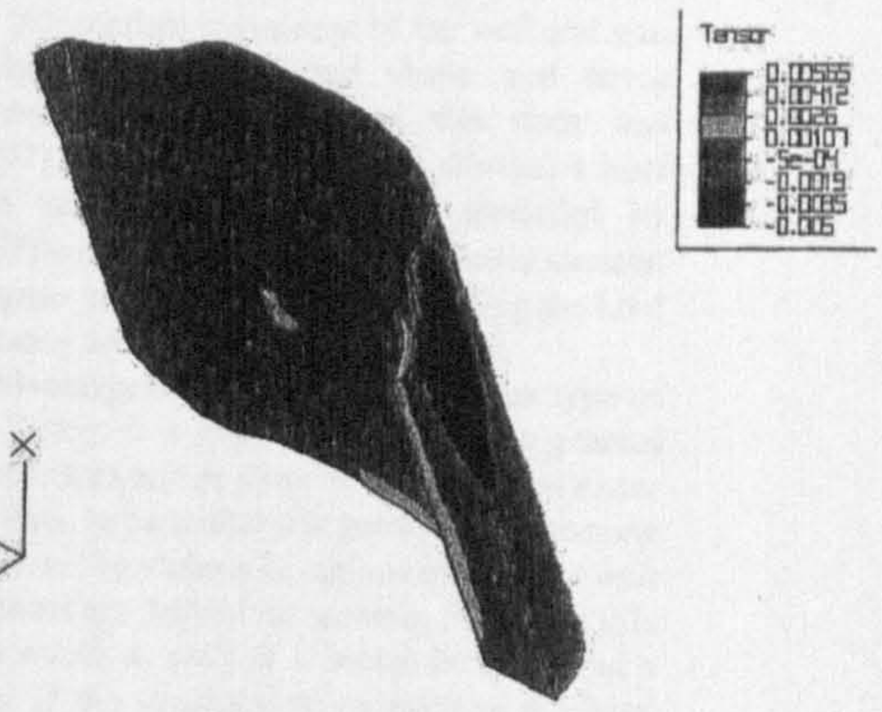

Fig 8: Force distribution along the sagittal plane in the region of the midline dead centre (MDC) during static loading.

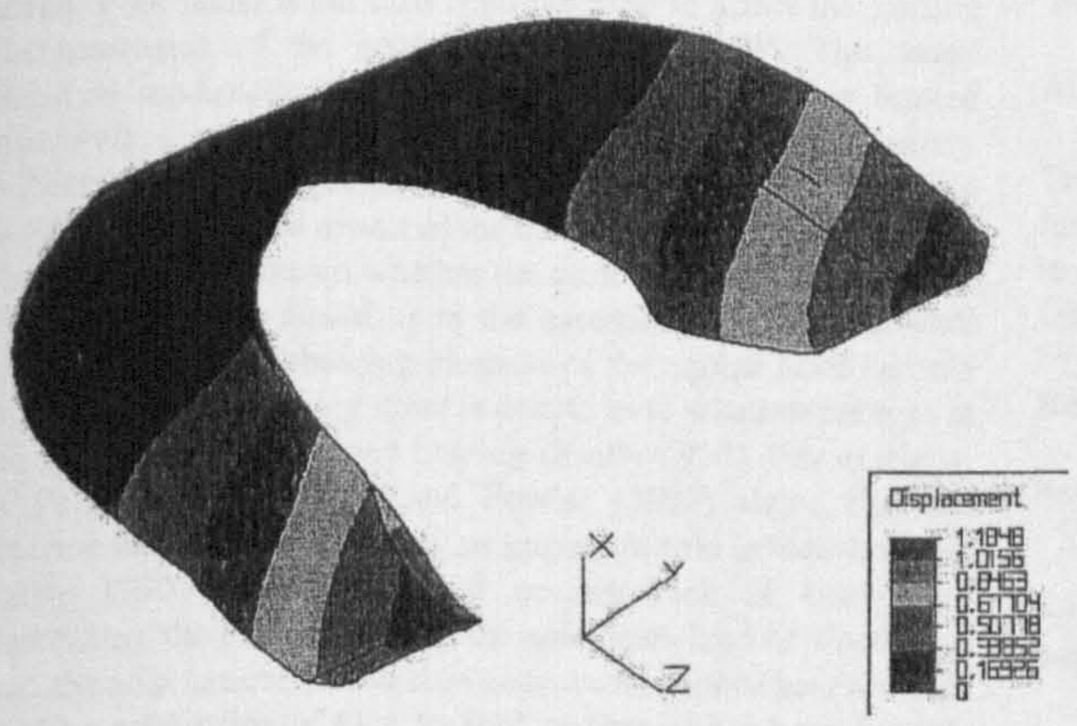

Fig 6: Displacement plot of total displacement (mm) at all points around the loaded hoof wall model.

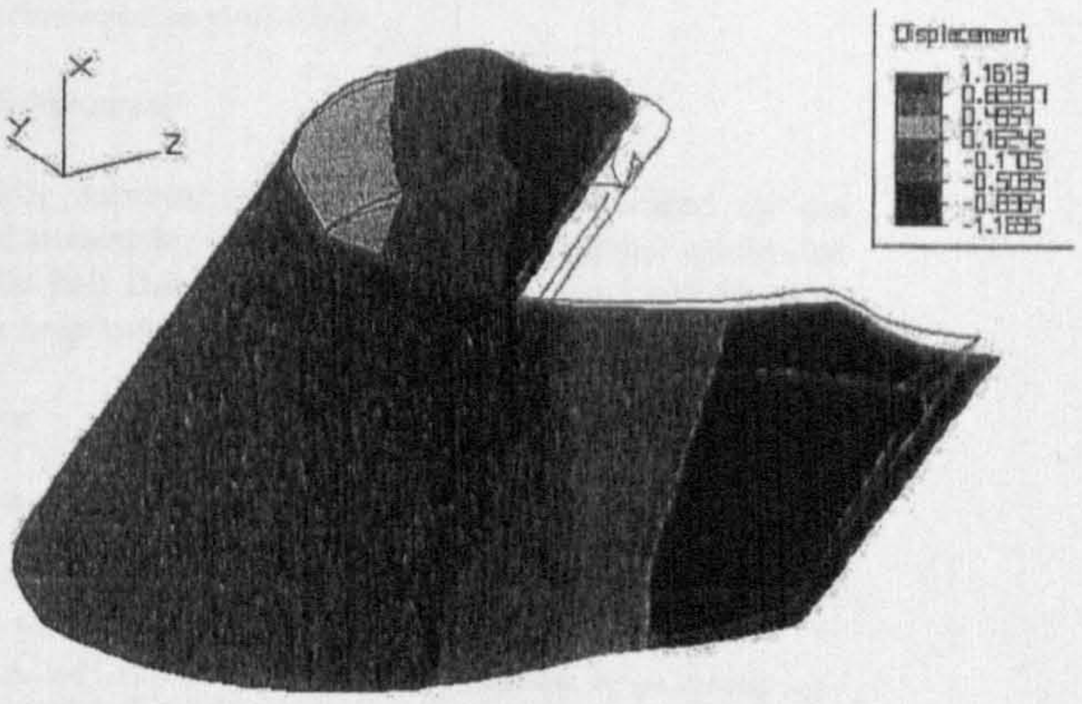

Fig 9: Projection of hoof wall displacement along the y axis in response to loading onto the original net construction.

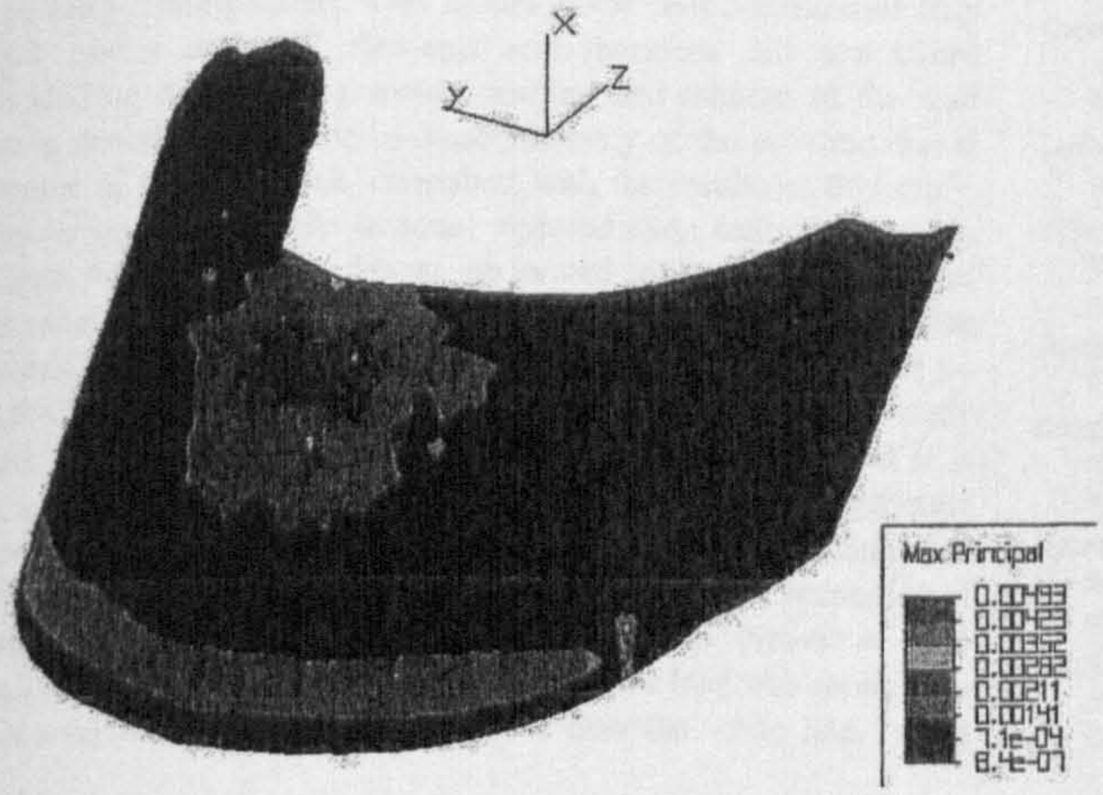

Fig 7: Shaded plot representation of Maximum Principal Strains generated in the hoof wall model in response to loading.

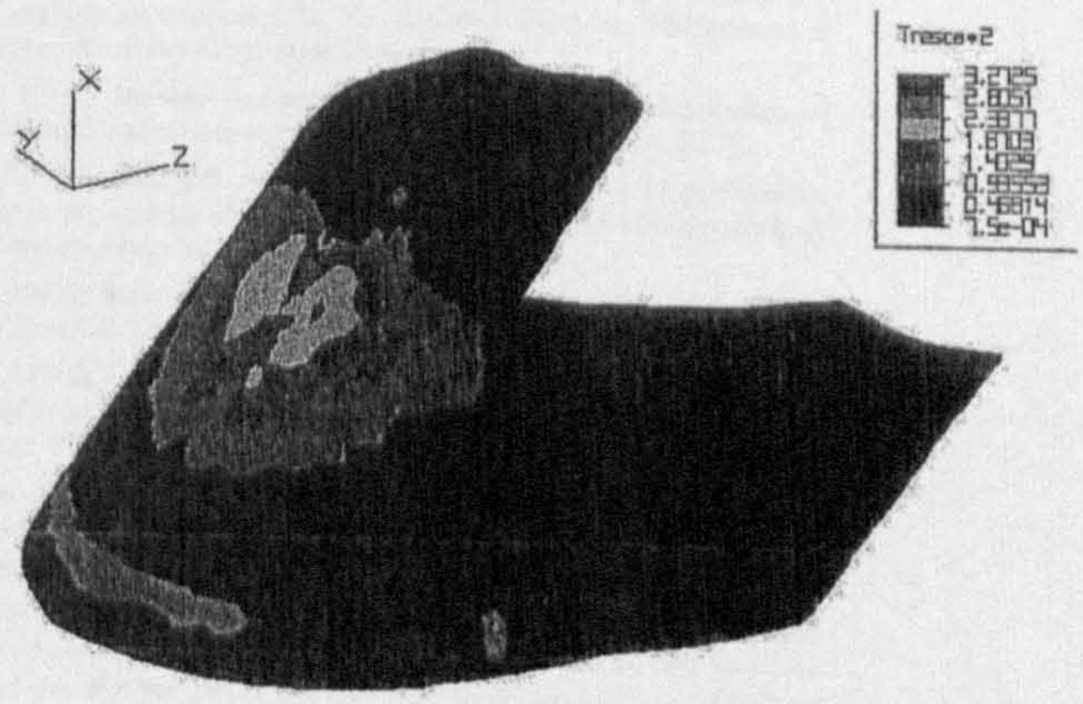

Fig 10: Plot of 2x tresca stress during loading to simulate photoelastic surface strain analysis.

information regarding the material characteristics of donkey horn. Therefore a representative equine modulus of elasticity and Poisson's ratio (Wichtmann *et al.* 1990) was selected for this FEA investigation. Anecdotal evidence suggests that donkey horn is not as stiff as that from the horse. Since, the modulus of elasticity affects the resultant principal strain the higher the modulus, the lower the principal maximum strain. On this basis, the use of an equine modulus is likely to have resulted in lower strain levels than occur *in vivo* for the donkey. Experimental work is currently in progress to characterise the material properties of donkey hoof in order to enable refinement of this model.

Although the force generated by an average donkey bodyweight during static loading can be calculated with relative ease, there is a lack of scientific evidence as to how this force is distributed between the 4 hoof capsules. Kainer (1987) stated that the forefeet support 60% of the bodyweight of the horse. If a similar situation exists in the donkey then the results of this study, based upon an even force distribution acting through each hoof, under-represents the effect of static loading upon the deformation and stress distribution in the forelimb donkey hoof wall. In addition, there is limited information regarding the means by which the force is transferred from the axial skeleton to the ground via the hoof capsule. It is not known if the load is transferred equally via the 400 laminae or whether more weight is taken at the MDC as suggested by Douglas *et al.* (1996) in the horse. Foot balance has also been reported to affect the loading characteristics of the hoof (Chang *et al.* 1993). This study assumes mediolateral foot balance, although there is limited information regarding natural foot balance in the donkey. Williams (1993) suggested that the donkey naturally takes more weight on the medial aspect of the bearing border in the hindfoot, however it is not known whether the same is true for the forefoot. This study is also based upon the assertion that the hoof wall constitutes the load-bearing element of the equine hoof capsule (Nickel 1938, 1939), but there is debate as to whether the sole in the donkey should be load-bearing (Reilly 1997). For example, Whitehead *et al.* (1991) and Fowler (1995) stated that the anterior third of the sole plays an important role in load-bearing. Reilly (1997) referred to the present lack of knowledge concerning the extent to which the sole bears load or whether in fact, the sole naturally should be concave and hence bear no load.

The application of FEA to hoof mechanics has been limited. The different modelling techniques employed, and the working assumptions made, make direct comparison difficult. Wichtmann *et al.* (1990) and, Hood and Wichtmann (1991) modelled a 2 dimensional sagittal section at the MDC of the equine foot, loaded via the second phalanx. This model of the foot consisted of only 964 nodes and 457 elements and therefore did not afford modelling detail. Compression bending and rotation of the wall were described resulting in dorsoconcavity of the proximo dorsal aspect of the hoof wall, consistent with the results of this study. However, such a 2 dimensional representation cannot model the effect of compressive forces generated at the MDC by heel expansion, nor the tensile forces generated orthogonal to the tubular axis as described by Leach (1980) and Thomason *et al.* (1992). Consistency of dorsoconcavity between this present study and Wichtmann *et al.* (1990) supports our assumption that it is possible to model the hoof wall in isolation and still generate accurate *in vivo* simulation. Hinterhofer *et al.* (1997) working with a more sophisticated model in terms of the material properties of the capsular components, were not able to create *in vivo* deformation within the wall, unless part of the load was applied via the sole/frog. However it is not clear how the white line, which forms the wall sole junction was modelled. It is believed that the white line allows for independent movement of the wall and sole (Reilly 1997). Comparison of displaced shape and stress concentration plots reveal similarity between this study and Hinterhofer *et al.* (1997). However it is uncertain whether a hoof capsule subjected to forces of ~30000 N, as modelled by Hinterhofer *et al.* (1997) would function in a linear elastic manner. Further work is in progress to validate whether modelling the hoof wall in isolation accurately simulates *in vivo* conditions.

There are many advantages in applying FEA to this type of mechanical problem. Firstly, it is possible to generate a general understanding of the structure and analyse how it performs under various loading conditions. In particular it is possible to determine with reasonable confidence, conditions in regions of the hoof wall where experimental results are difficult to achieve. Secondly, it is possible to work on a micro as well as a macro level so that a more detailed analysis of the structural complexity of the hoof wall, and its performance, can be achieved. Finally, FEA provides an ideal focus for bringing together the information derived from a multidisciplinary approach to investigating hoof function, as advocated by Reilly (1995).

Manufacturers' addresses

[1]American National Can, Connecticut, USA.
[2]Algor Inc., Pittsburgh Pennsylvania, USA.

Acknowledgements

The Donkey Sanctuary, Sidmouth, Devon is thanked for the funding of studentship for SNC and LH. The authors would like to thank Dr Ralf Dahm (Department of Chemistry and Physics, DMU) for help and assistance with German translations.

References

Bartel, D.L., Schryver, H.F., Lowe, J.E. and Parker, R.A. (1978) Locomotion in the horse: A procedure for computing the internal forces in the digit. *Am. J. vet. Res.* **39**, 1721-1727.

Bayer (1886) *Experimentales uber Hufmechanisma Oesterr Monatschrift.*

Bertram, J.E.A. and Gosline, J.M. (1986) Fracture toughness design in horse hoof keratin. *J. expt. Biol.* **125**, 29-47.

Chang, Y.H., Sherrill, J. and Bertram, J.E.A. (1993) Hoof wall function in horses and donkeys - experimental alteration of surface strain. In: *Proceedings of the 1993 IEEE 19th Annual Northeast Bioengineering Conference* Ed: J.K.J. Li and S.S. Reisman. IEEE Service Centre, Piscataway, New Jersey. pp 64-65.

Colles, C.M. (1989) A technique for assessing hoof function in the horse. *Equine vet. J.* **21**, 17-22.

Cope, B.C., Hopegood, L., Latham, R.J. and Reilly, J.D. (1998) Equine hoof horn: a natural engineering composite. In: *The Materials Congress, Proceedings of the Institute of Materials Conference.* Cirencester.

Davies, H.M. (1997) Non-invasive photoelastic method to show distribution of strain in the hoof wall of a living horse. *Equine vet. J., Suppl.* **23**, 13-15.

Dejardin, L.M., Arnoczky, S.P. and Fox, D.B. (1997) The use of photoelastic technology in the analysis and localisation of strain on the loaded equine hoof - an *in vitro* pilot study. *Vet. Surg.* **26**, 413.

Douglas, J.E. (1994) Structure and function: anatomy of the equine foot. In: *No Foot - No Horse II.* Equine Research Centre, Guelph. pp 32-40.

Douglas, J.E., Mittal, C., Thomason, J.J. and Jofriet, J.C. (1996) The modulus of elasticity of equine hoof wall - implications for the mechanical function of the hoof. *J. expt. Biol.* **199**, 1829-1836.

Dyhre-Poulson, P., Smedegaard, H.H., Roed, J. and Korsgaard, E. (1994) Equine hoof function investigated by pressure transducers inside the hoof and accelerometers mounted on the first phalanx. *Equine vet. J.* **26**, 362-366.

Fischerleitner, F. (1974) *Röntgenographischhe Untersuchungen über den Einfluss der Lageveränderungen des Huf, strahl- und Kronbeines auf die Mechanik der Hornkapsel des Pferdes im Belastungsgerät.* Inaugural Diss., Tierärtzliche

Hochschule Wien.

Förringer, H. (1889) Studies on the draught force of horses. *Acta. Agric. Scand. (Suppl).* **4**, 109.

Fowler, J. (1995) Trimming donkeys feet. *Equine vet. Educ.* 7, 18-21.

Geary, J.E., Jnr. (1975) *The Dynamics of the Equine Foreleg.* Masters of Mechanical and Aerospace Engineering, University of Delaware.

Gordon, J.E. (1976) *The New Science of Strong Materials.* Penguin Books, UK. p 269.

Hifney, A. and Misk, N.A. (1983) Anatomy of the hoof in donkeys. Assiut vet. Med. J. **10**, 3-6.

Hinterhofer, C., Stanek, C. and Haider, H. (1997) Belastungssimulation an einem aus finiten elementen konstruierten computermodell der hornkapsel des pferdes. *Pferderheilkunde* **13**, 319-329.

Hood, D.M. and Witchtmann, A.D. (1991) Finite element analysis of the internal deformation and stresses in the equine distal digit. In: *Proceedings of Tenth Annual Meeting of the Association for Equine Sports Medicine.* Brilig Hill Inc., California. p 43

Hood, D.M., Hogan, H.A., Harden, W., Treadway, C., Grosenbaugh, D.A. and Williams, J.D. (1991) Dorsal hoof wall deformation in static weight bearing. In: *Proceedings from the Tenth Annual Meeting of the Association for Equine Sports Medicine*, Brillig Hill Inc. California. p 47.

Kainer, R.A. (1987) Functional anatomy of equine locomotor organs. In: *Adams' Lameness in Horses*, 4th Edn. Ed: T.S. Stashak. Lea & Febiger. Philadelphia. pp 1-18

Kasapi, M.A. and Gosline, J.M. (1996) Strain rate dependent mechanical properties of the equine hoof wall. *J. expt. Biol.* **199**, 1133-1146.

Kasapi, M.A. and Gosline, J.M. (1997) Design complexity and fracture control in the equine hoof wall. *J. expt. Biol.* **200**, 1639-1659.

Leach, D.H. (1980) *The Structure and Function of the Equine Hoof Wall.* PhD Thesis, University of Saskatchewan, Saskatoon.

Leach, D.H. and Zoerb, G.C. (1983) Mechanical properties of equine hoof wall. *Am. J. vet. Res*, **44**, 2190-2194.

Lechner, J. (1882) Beitrag zum Hufmechanismus. *Dtsch. Z. Tiermed.* **8**, 179-199.

Lekeux, P. and Art, T. (1994) The respiratory system: Anatomy, physiology and adaptation to exercise and training. In: *The Atheletic Horse: Principles and Practice of Equine Sports Medicine*. Ed: D.R. Hodgson and R.J Rose. W.B. Saunders Company. Philadelphia, USA. pp 88-127.

Lungwitz, A. (1883) Der gegenwärtige Strandpunkt der mechanischen Verrichtungen des Pferdehufes. *Der Hufschmied.* **1**, 4-7, 17-21.

Lungwitz, A. (1891) The changes in the form of the Horse's Hoof under the action of the body-weight. *J. comp. Path. Therap.* **4**, 191-211.

Mair, F.J. (1974) Dehnungsmessungen an der Hornwand in Tragrandnähe und and der Hornsohle beim Pferd-Hinterhuf. *Wiener Tierärz. Monatssch.* **61**, 70-71.

Miles, W.J. (1856) *The Horse's Foot.* Longman, Brown, Green and Longman, London.

Nickel, R. (1938) Uber den Bau der Hufröhrchen und siene Bedeutung für den Mechanismus des Pferdehufes (The construction of horn tubules and its significance for the mechanics of the equine hoof). *Morph. Jahrbuch.* **82**, 119-160.

Nickel, R. (1939) Untersuchungen uber den Bau des Pferdehufes mit besonderer Berucksichtigung des Hufmechanismus und von Hufkrankheiten. *Deutsche Tierarz. Wochenschrift.* **46**, 449-452.

Parker, R.A. (1973) *The Analysis of the Forces and Displacements in the Digit of the Horse During Walk. MSc Thesis, Cornell University, Ithaca, New York.*

Pollitt, C.C. (1990) An autoradiographic study of equine hoof growth. *Equine vet. J.* **22**, 366-368.

Pollitt, C.C. (1993) Video equine foot studies. Television Unit, Prentice Centre. The University of Queensland.

Quddus, M. A., Kingbury, H.B. and Rooney, J.R. (1978). A force and motion study of the foreleg of a standardbred trotter. *J. equine med. Surg.* **2**, 233-242.

Reilly, J.D. (1995) No hoof no horse? *Equine vet. J.* **27**, 166-168.

Reilly, J.D. (1997) The donkey's foot and its care. In: *The Professional Handbook of the Donkey*, 3rd edn. Ed: E.D. Svendsen. Whittet Books Ltd. London. pp 71-92.

Reilly, J.D., Cottrell, D.F., Martin, R.J. and Cuddeford, D. (1996) Tubule density in equine hoof horn. *Biomimetics* **4**, 23-35.

Reilly, J.D. and Kempson, S.A. (1992) Towards an understanding of hoof horn quality. In: *Proceedings of the 7th International Symposium on Diseases of the Ruminant Digit.* Ed: K Mortensen, Denmark.

Rooney, J.R. (1978) Studies in equine biomechanics. *J. equine Med. Surg.* **2**, 107-145.

Stashak, F.S. (1987) *Adams' Lameness in Horses.* 4th edn. Lea and Febiger, Philadelphia.

Sack, W.O. and Gabel, R.E. (1977) *Rooney's Guide to the Dissection of the Horse.* Veterinary Textbooks, Ithaca, New York.

Thomason, J.J., Biewener, A.A. and Bertram, J.E.A. (1992) Surface strain on the equine hoof wall *in vivo*: implications for the material design and functional morphology of the wall. *J. expt. Biol.* **166**, 145-165.

Vogel, S. (1989) *Life's Devices: the Physical World of Animal and Plants.* New Jersey, Princeton University Press.

Whitehead, G., French, J. and Ikin, P. (1991) Welfare and veterinary care of donkeys. *In Pract.* **13**, 62-68.

Wichtmann, A.D., Hogan, H.A. and Hood, D.H. (1990) Development of a two-dimensional finite element model for studying the internal mechanism of the distal digit of the horse. *Advances Bioengin.* **17**, 331-334.

Williams (1993) The donkey's foot and its care. In: *The Professional Handbook of the Donkey*, 1st edn. Ed: E.D. Svendsen. Sovereign Print Co, England. pp 121-127.

JOURNAL OF MATERIALS SCIENCE 33 (1998) 5185–5191

Stiffness as a function of moisture content in natural materials: Characterisation of hoof horn samples

S. N. COLLINS, B. C. COPE, L. HOPEGOOD, R. J. LATHAM, R. G. LINFORD
Solid State Research Centre, School of Applied Sciences, De Montfort University, Leicester, LE1 9BH, UK
E-mail: bcope@dmu.ac.uk

J. D. REILLY
Royal Army Veterinary Corps, Defence Animal Centre, Melton Mowbray, Leicestershire, LE13 0SL, UK

Hoof horn, which forms the capsule at the lower part of the legs of many grazing animals including equids (horses, donkeys and mules), is a composite natural material based on α-keratin. Its function is influenced by the tubular and intertubular material and is modulated by the moisture content. There is a requirement to adopt a standard approach to drying regimes and sampling protocols in order to make progress in understanding how the biomechanical properties of hoof horn are related to its structure. In this work the stiffness of donkey hoof has been examined using a three point bending technique and the effect of hydration has been investigated. Also the tubule density properties of this hoof horn material are reported. © *1998 Kluwer Academic Publishers*

1. Introduction

The study of hoof horn provides materials scientists with a challenging insight into natural materials, but why approach the study of hoof horn from the materials science base? Hoof horn may be described as a naturally occurring composite material which includes keratin arranged in a tubular and intertubular form [1]. Its biofunctional role is not yet completely understood. Each tubule consists of a medulla (possibly hollow) which is surrounded by a cortex of keratinised cells [2]. Thus materials scientists may think of hoof horn as a mixed morphology material whose mechanical properties are very dependent on the structure [3]. The properties of hoof horn are of potential interest to conservators and restorers, but much more importantly to those concerned with animal husbandry and welfare. Hoof management has tended historically to be a skill rather than a science and consequently there is a paucity of information concerning structure-property relationships in the scientific and veterinary literature. The need to assess critically the scientific information that has been reported is highlighted in a recent review by Reilly [3] who comments also on such issues as the inadequate numbers in sample populations together with a lack of funding for focussed research.

Materials science provides a platform for investigating the effects of environment, nutrition and management on hoof horn structure and aspects of genetic influences can be included by careful experimental design. Is equine hoof different from bovine hoof in its structural aspects; do other equids such as donkey have the same hoof horn structure as horse? In order to answer these and other related questions it is important to generate a sound knowledge base of hoof horn characteristics for different species based on controlled trial situations [3], and in this respect materials scientists have a role to play alongside veterinary practitioners and biochemists [4]. Baillie and Fiford [5], for example, have analysed hoof structure-property relationships in order to understand the nature of cattle hoof horn as a material. Animals are reliant on the hoof horn capsule for effective locomotion and the mechanical properties of hoof horn are therefore important [1]. The mechanical properties of hoof horn and other biomaterials can be routinely investigated by using tensile, compression and hardness testing methods and this is recognised in the materials science approach to biomechanics outlined by Vincent [6], and Fraser and Macrae [7]. Hoof horn is designed to cope with different types of natural impact and an understanding of its structure-property relationships will facilitate in biomimetic design as envisaged by Vincent [6]. For example, measurement of stiffness of horn sheath keratin by three point bending experiments have been reported by Kitchener and Vincent [8], and Kitchener [9]. Stiffness, which is the resistance to deformation, can be measured by the deformation of a material in uniaxial tension or compression using strain gauges or extensometers, and also by bending. Three point bending measurements are of particular relevance to hoof horn material because the technique mimics the *in vivo* situation in the hoof capsule as compression occurs in the

hoof wall resulting from its reaction with the ground [10, 11].

Examination of samples by various forms of microscopy is also important. For example, the nature of tubules and the intertubular matrix can be examined by scanning electron microscopy (SEM) and elemental mapping by energy dispersive X-ray analysis. The tubular density within the hoof horn matrix is important and it has been shown that there is a zonal arrangement [12] for horse hoof horn and that the type of tubule varies according to position in the hoof wall [11, 13]. Wilkens [14] has described the tubular nature of bovine hoof horn but did not quantify the distribution of tubules. An alternative to the tried and tested staining of microtomed sections followed by manual counting methods is to develop computer imaging techniques.

The properties of keratinous materials are strongly influenced by their state of hydration [8] and it is well established that water will modulate many of the properties of hoof horn. For example, the effect of water on the stiffness and viscoelasticity of horn sheath material has been reported by Kitchener [9]. Similarly, the mechanical properties of hoof horn have been shown to vary with hydration by Bertram and Gosline [15] and it has been reported that the variation in tensile stiffness of hoof keratin with hydration level may be more important than its anisotropy [16]. Definition of moisture content before assessment of material properties is therefore important as the subjective "quality" of the hoof horn and the mechanical function of the material are likely to be influenced by this property. Moisture contents in the range 25–35.5% have been reported but the results depend strongly on the drying method used and the sampling protocol adopted. Moisture content is dependent on relative humidity and the reports in the literature [8, 15] for the results of mechanical testing of biological samples at particular relative humidities suggest an exponential uptake of water with time.

Whilst it is possible to examine morbid hoof samples, the most readily available samples come from clippings associated with routine hoof management which are noninvasive to the animal. The materials science knowledge base needs to be built up from a range of clipped samples which have been collected and stored according to a clearly specified set of protocols, and samples for scientific study must come from defined points on the macrosample. Throughout the scientific and veterinary literature there is a lack of detailed information regarding experimental methodologies and comparative studies are therefore difficult. Weaver [17] reported that the physical properties of hoof horn from cattle are not easy to measure and that difficulties multiply when attempts to make comparisons are hampered by both the lack of standard approaches and by variables such as the selection of test sample from the hoof and the environment of the stock.

There are approximately 41 million donkeys[1] in the world compared with about 65 million horses [18] and despite the fact that there are obvious differences in hoof size and angle of hoof wall [19], and sole thickness [20] there is little reported work on donkey hoof. The Donkey Sanctuary, Sidmouth, UK houses a large donkey population which is generally unshod, from which a representative sample has been identified. This paper reports the initial results for selected techniques from experiments on donkey hoof horn samples.

[1] Horses and donkeys both belong to the generic category of equids but donkeys are physiologically different from horses. Only the latter are equines.

2. Experimental

2.1. Samples

Suitable clippings of hoof horn from the right foreleg were obtained by farriers during regular hoof maintenance and sharp hoof cutters were used in order to prevent tearing of the sample. The samples were wrapped immediately in three overlapping layers of Parafilm (Parafilm "M" Laboratory Film, American National Can™, CT 06836, USA) to make an airtight seal which moulded to the shape of the sample. The labelled, wrapped samples were then stored at 4 °C prior to examination. The portions removed for testing were from the midline dead centre site (MDC) [12] as shown in Fig. 1.

2.2. Determination of moisture content and effect of relative humidity

Clippings were obtained from an identified population of 31 donkeys from Sidmouth. The following drying regimes were employed:

- Room temperature
- Drying under vacuum at room temperature
- Placing over phosphorus pentoxide
- Freeze drying
- Oven drying at 90, 100, 105, 110 and 120 °C.

Masses were recorded daily until a constant level was observed and moisture contents were determined as a percentage of the dry mass.

Similar samples were prepared and subjected to different environments having relative humidities in the range 6.5–93% by suspending them over saturated solutions of specified salts. Again, masses were monitored daily until constant and then the samples were dried over phosphorus pentoxide at room temperature.

In an alternative approach to investigating the effect of relative humidity, samples were initially dried over phosphorus pentoxide and then subjected to environments having relative humidities in the range 3.2–99.2% provided by aqueous sulphuric acid solutions.

2.3. Tubule density

Transverse sections (thickness 10–12 μm) from the MDC samples were obtained using a microtome/cryostat at −20 °C. Typically, the sections were stained using haematoxylin, eosin and alcian blue-PAS. A tubule count per unit area to give a tubule density was then carried out on photographs taken of the slides by macrophotography using the principle outlined by Reilly *et al.* [12].

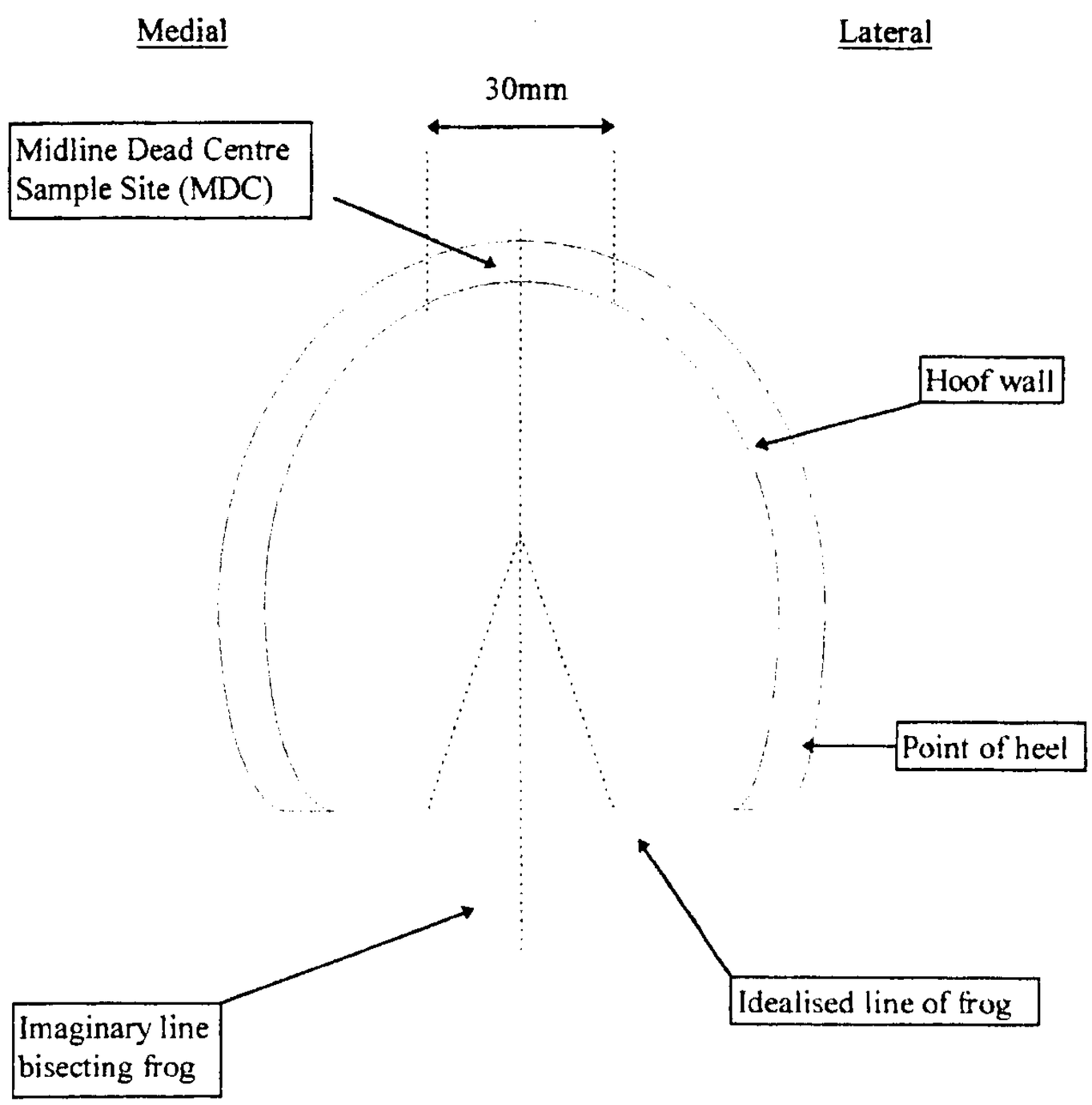

Figure 1 Position of sample sites on clipping (As seen from the underside of the donkey foot. Note to scale).

2.4. Three point bending

In order to avoid possible differences in stiffness due to tubular orientation, samples were taken from the MDC of clippings and milled into beams (hoof wall width × 30 mm × 2 mm) cut perpendicular to the line of the tubules. Samples were subjected to three point bending at 20 °C and 60% relative humidity using an Instron 4302 with a 100 N loadcell and a crosshead speed of 2 mm min^{-1} [6]. Samples with a span of 24 mm were tested to a deflection of 0.5 mm following preloading to ~0.04 N in order to minimise the effects of backlash and specimen curvature. Samples were tested as follows: fresh (stored as described previously to prevent loss of water); dried over P_2O_5 to constant mass; fully hydrated (placed in distilled water until constant mass); subjected to an environment of 75% relative humidity (until constant mass).

Compliance for the testing system was determined by carrying out an experiment with a rigid aluminium specimen which had a stiffness greater than that of the load frame. A correction factor was then applied to the results for the stiffness measurements on the hoof horn samples.

3. Results

3.1. Determination of moisture content and effect of relative humidity

Constant sample masses for 31 samples were obtained after about 5 days using freeze drying and 24 hours using oven drying regimes, whereas similar observations were made after about 10 days for room temperature drying and drying over phosphorus pentoxide. Moisture contents were in the range 25–35% and are summarised in Fig. 2. In both approaches the moisture content at room temperature rapidly increased with increasing relative humidity and this is shown in Fig. 3.

3.2. Tubule density

A photograph of a typical stained microtomed section of donkey hoof wall is shown in Fig. 4. For the purposes of comparison with the results for pony hoof previously reported by Reilly [12] the hoof wall was divided into four zones. A mean tubular density of 19 tubules mm^{-2} was obtained for zone 1 of the outer hoof wall with the remaining three zones having 8–9 tubules mm^{-2}. The results are summarised in Table I which includes a comparison with pony hoof.

3.3. Three point bending

The plots of stress vs deflection show a Hookean relationship. Typical stress-deflection plots for samples stored under different environments are shown in Fig. 5. The results for the modulus of elasticity calculated from these plots are summarised for the different storage regimes in Fig. 6. In some cases after drying over P_2O_5 the samples were too curved for the experiment to be performed effectively. The data set for samples tested

TABLE I Tubule density within the donkey hoof wall of MDC samples

Samples	Outer wall			Inner wall	
Donkey $n = 7$	Zone 1 Tubules mm^{-2}	Zone 2 Tubules mm^{-2}	Zone 3 Tubules mm^{-2}	Zone 4 Tubules mm^{-2}	Tubules mm^{-2} (full wall width)
Mean	19	8	8	9	11
Range	7–41	3–14	3–12	4–14	3–41
Ponies*	>27	16–27	8–16	<8	16

*The zones used by Reilly [12] do not relate exactly to the zones used above but provide a general guideline. Ponies are usually defined as horses under 14.2 hands at the withers.

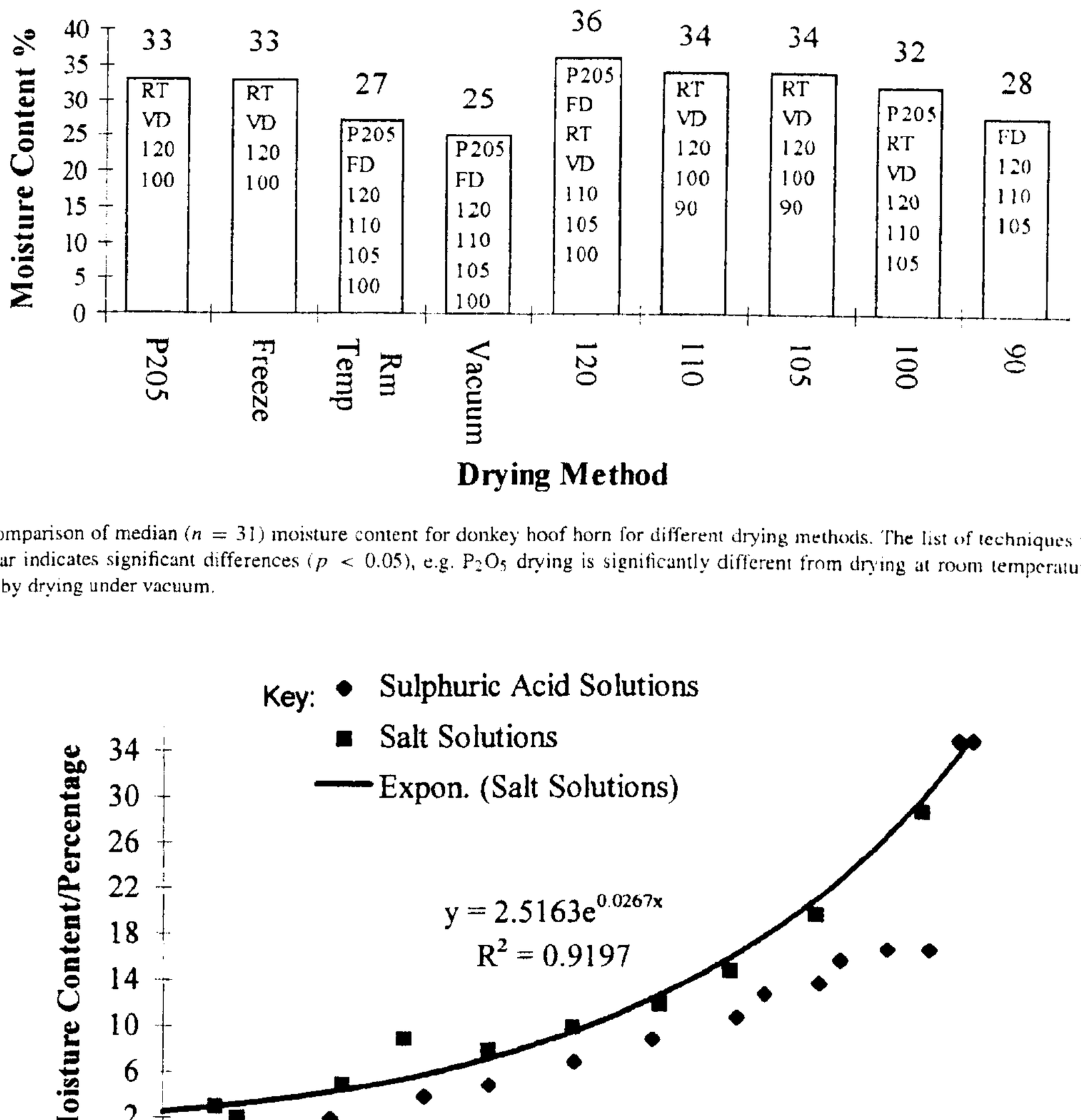

Figure 2 Comparison of median ($n = 31$) moisture content for donkey hoof horn for different drying methods. The list of techniques within each individual bar indicates significant differences ($p < 0.05$), e.g. P_2O_5 drying is significantly different from drying at room temperature, 100 and 120 °C, and by drying under vacuum.

Figure 3 Plots of moisture content vs relative humidity for donkey hoof horn samples.

with a fresh moisture content showed a non-normal distribution ($p < 0.05$) but the data set after correction for moisture showed a normal distribution. Mann Whitney U tests showed differences between all data sets ($p < 0.0001$) except for the comparison of data from the measurements of stiffness on fresh and fully hydrated samples ($p > 0.05$).

4. Discussion

To understand the biomechanical function of hoof horn material it is important to establish the relationships between moisture content, relative humidity, tubular density, structure and mechanical properties. In order to make progress the fundamental issues associated with each of these areas of interest must be fully examined.

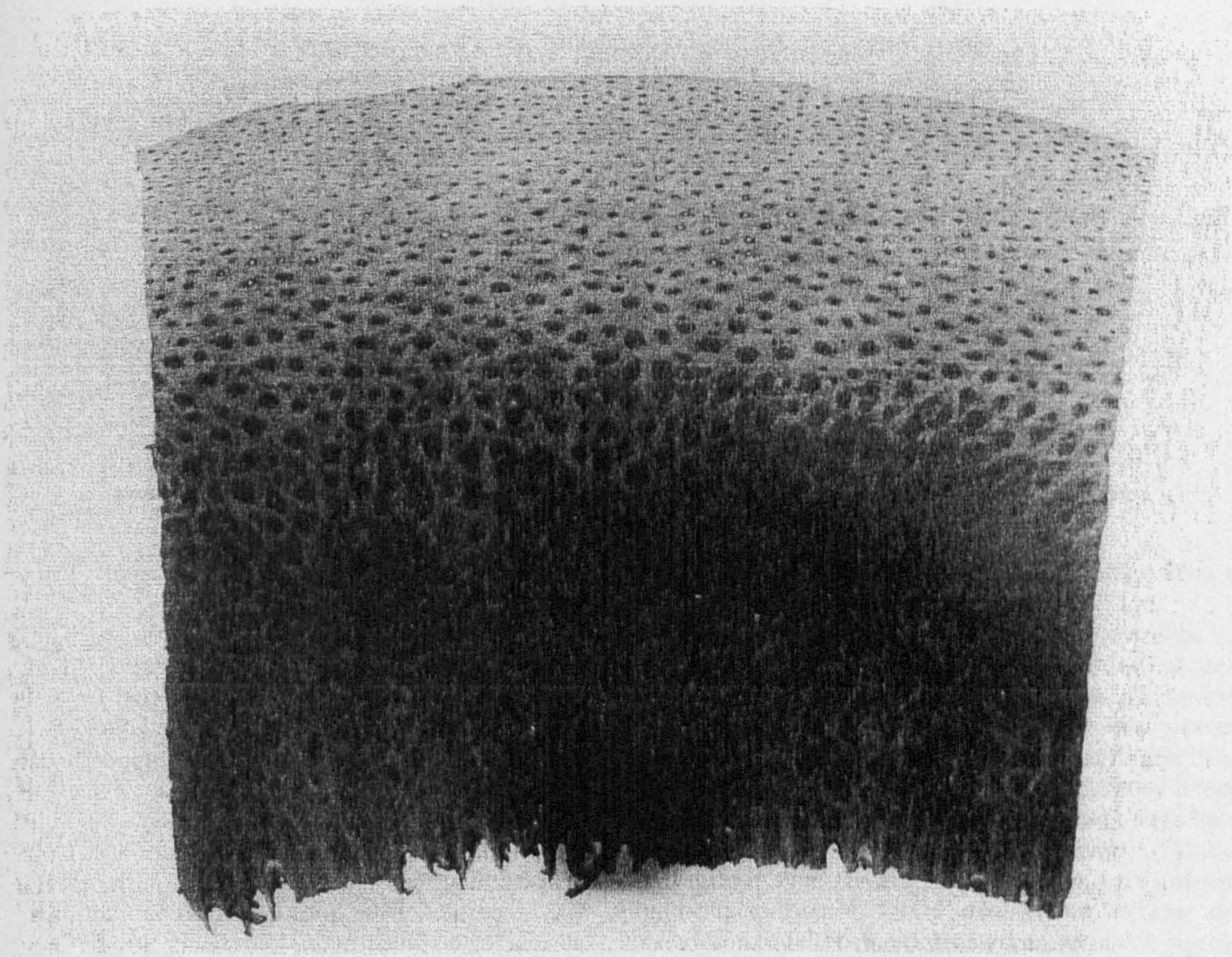

Figure 4 Photograph of stained transverse section of donkey hoof horn taken from a mid wall midline dead centre (MDC) section. Scale: |———| 1 mm.

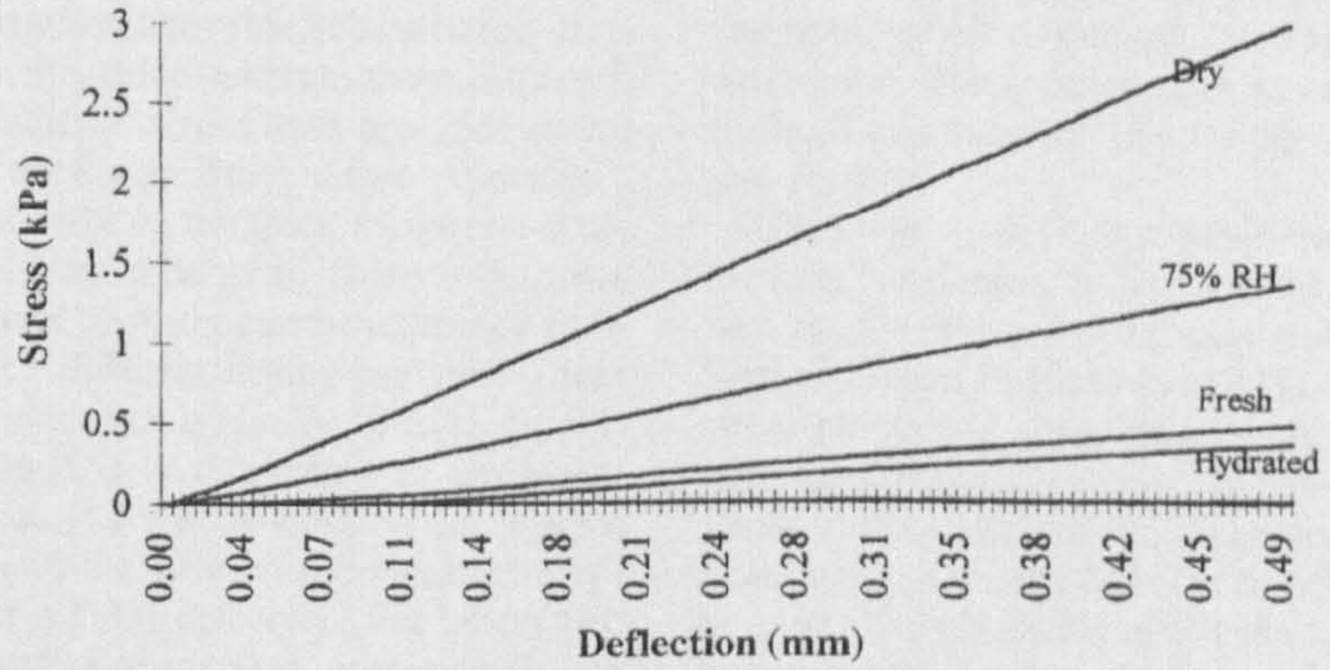

Figure 5 The effect of moisture on plots of stress vs deflection for donkey hoof horn.

Comparison with previously reported work on moisture content is difficult as a variety of different drying techniques have been employed. Reported moisture contents for horse hoof include 27.1% by Miyaki *et al.* [21], 27.9% (outer wall), 35.5% (inner wall) by Douglas *et al.* [22] and 17–24% by Leach [11] but there appear to be no reported comparisons with moisture content in donkey hoof horn. The results for the donkey hoof samples examined in this work broadly agree with those reported for horse hoof, although the experimental approaches and sampling protocols used by different workers vary.

The level of hoof wall hydration can be adjusted internally by fluids from within the dermis, from direct contact with water [15] or possibly by the relative humidity of the environment. Bertram and Gosline [15] deduced that the *in vivo* moisture content of the horse hoof was in the range 65–83% relative humidity and that maximum fracture toughness existed at this level. Using the principle outlined by Bertram and Gosline

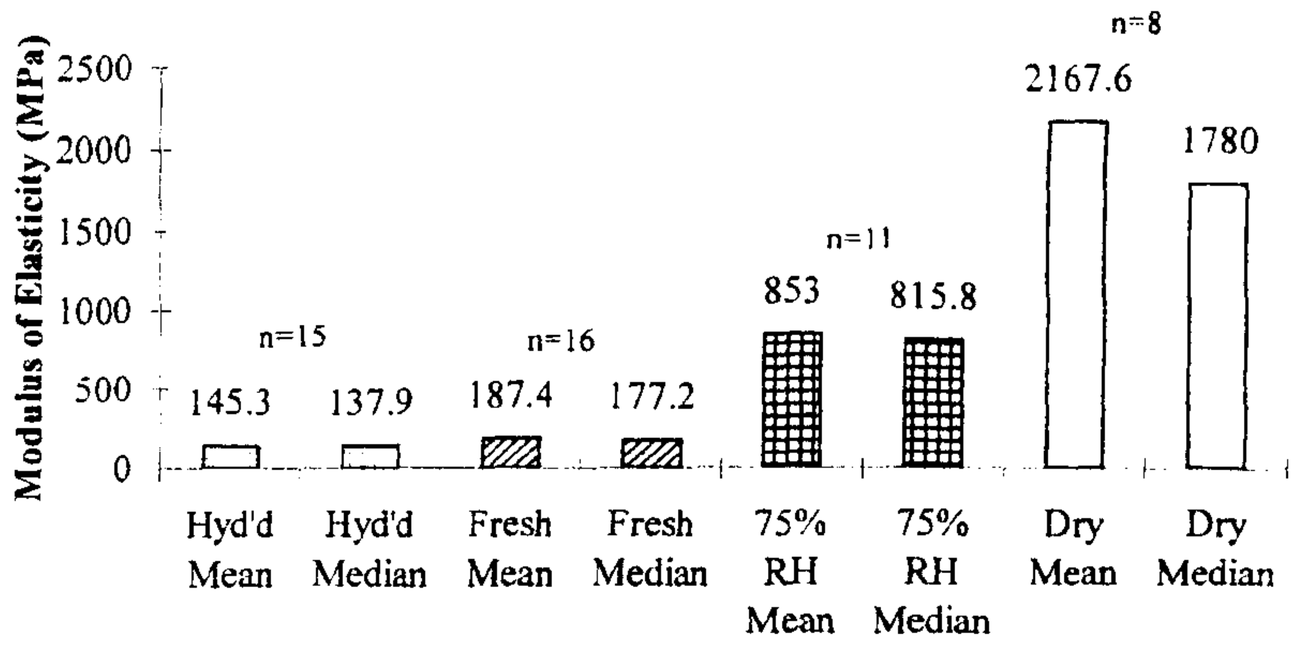

Figure 6 Comparison of mean and median modulus of elasticity for samples of donkey hoof horn having different moisture contents.

[15] for a hoof moisture sorption isotherm, the results shown in Fig. 3 indicate that a moisture content of 33% in donkey hoof corresponds to a relative humidity environment of about 96%. It is possible, however, that differences are due to different drying techniques and/or sample sites from the hoof clippings. The apparent negative result for the donkey hoof sample equilibrated in the 3.2% relative humidity environment provided by the vapour above sulphuric acid is because after drying of the sample over P_2O_5 there was a mass loss rather than a mass gain. Thus there must have been a transpiration of water vapour from the sample to the atmosphere in the humidity chamber in order to preserve the equilibrium state. Hysteresis effects are well known in absorption/desorption experiments carried out on the same sample and the differences between the two sets of data on Fig. 3 may well be a consequence of this phenomenon: samples equilibrated in relative humidity environments provided above the saturated salt solutions were subsequently dried, whereas those subjected to the relative humidity environments provided above sulphuric acid solutions were dried before exposure.

It is clear that in order to compare samples a standard drying approach must be used. This study shows that different amounts of water can be extracted from the hoof material by different drying regimes. There is a longer equilibrium time, typically 10 days, associated with drying over P_2O_5. Air drying leads to a larger variation and the results are dependent on the relative humidity. Fig. 2 shows the difference between air drying and drying over a P_2O_5 desiccant. For laboratory approaches to the drying of samples, processing times may be of importance. Techniques such as oven drying at high temperatures to ensure a fast drying time may lead to volatilization or decomposition of the sample. The loss of mass in these instances may, however, represent a loss of very tightly bound water or possibly some other volatile component of the tissue [15, 23]. This may not therefore be the ideal method to attain dry samples if mechanical testing is to follow as fibres in the drier outer layers may be torn apart and splitting may occur internally or externally if the moisture gradient becomes too steep. This phenomenon has previously been demonstrated for wood [24]. Mechanical testing following this drying may then yield results from an already stressed material.

Tubular density within hoof horn is alleged to be important in hoof "quality" and to influence hoof hardness [25]. Tubule densities have been reported for several species but details of the sampling methodologies are not always clear. These initial results suggest that there may be differences between the zonal tubular densities of pony and donkey hoof horn although both have higher tubular densities in the outer hoof wall. Tubular density may well have an influence on the mechanical properties of the hoof horn material and thus the difference between hydration effects between equine and donkey hoof horn may be a consequence of the differences in tubular characteristics. The tubular density pattern for pony hoof previously reported by Reilly *et al.* [12] showed a distinct arrangement of four zones and this zonal arrangement was not seen in these donkey hoof samples although there are similarities in the outer zone. These differences in tubule density across the hoof wall may be linked to the differences in moisture content.

The stress vs deflection plots show a Hookean relationship for donkey hoof horn, which is in agreement with results of work previously reported by Leach and Zoerb [26] and Landeau *et al.* [27]. From their work on stress-relaxation compression tests, Landeau *et al.* [27] concluded that equine hoof horn material behaves as a linear viscoelastic material. The results of the bending experiments reported here confirm that samples should be controlled for moisture content as there are clear differences in the force vs extension plots, shown in Fig. 5, for samples which have been subjected to different environments. Bertram and Gosline [15] have reported that horse hoof exists with a moisture content corresponding to ~75% relative humidity and yet for this study on donkey hoof it can be seen from Fig. 6 that there are considerable differences in stiffness between samples having a fresh moisture content and those at 75% relative humidity ($p < 0.0001$). In comparison, there is no significant difference between the results for samples with a fresh moisture content and those which have been hydrated ($p > 0.05$). This observation reinforces the fact that the results from moisture content studies

indicate that donkey hoof has an *in vivo* moisture content which corresponds to a relative humidity environment of ~ 96%. As expected, moisture content clearly has an influence on the stiffness of hoof horn and this is seen in Fig. 6 where stiffness of dry samples is about 10–15 times greater than those with fresh moisture content. Similar trends have been reported by other workers [8, 15, 22]. For example, Kitchener and Vincent [8] reported an increase in stiffness by a factor of about 40 for gemsbok horn when fresh and dried samples were compared. The level of difference between fresh and dried samples may be due to the use of different drying regimes (gemsbok horn was dried at 110 °C for 24 hours) but it may also be associated with the different anatomy and functionality of the horn material. As with moisture content studies, comparison with other studies reported in the literature is difficult as the descriptions of sampling, sample preparation and testing are unclear. Variables include: the type of mechanical test used to evaluate the modulus of elasticity, E, as it is not uncommon for the tensile strength in bending to be considerably higher than that in direct tension; the level of hydration of the sample; the area of hoof tested – different areas of the hoof may have different levels of hydration; the cross head speed used in bending measurements.

The experimental work reported in this paper has been focussed on the specific property of stiffness as a function of moisture content and the tubular structure of the hoof wall has been discussed in relation to mechanical properties and moisture content. Clearly the way forward involves a more detailed structure-property analysis which takes account of the composite nature of this natural material. Thus, not only the tubules, but other structural features should be considered in further work.

5. Conclusions

Hoof horn material is a composite natural material whose normal characteristics have not yet been properly defined. The interdependence of moisture content and role of water, morphology and biomechanical properties can only be explored by investing in links between veterinary science and materials science to provide a better understanding of the structure-function relationships.

- It is important to establish the sampling protocols in order to investigate moisture content and the effects of relative humidity.
- The results from tubular density measurements indicate that there may be differences between the morphology of hoof horn from different equids.
- The results from three point bending experiments show that stiffness is a function of moisture content.

Acknowledgements

The Donkey Sanctuary is thanked for financial support to SNC and LH.

References

1. J. D. REILLY and S. A. KEMPSON, in Proc. of 7th Int. Symp. on Diseases of the Ruminant Digit, edited by K. Mortensen, Denmark, 1992.
2. C. C. POLLITT, *Equine Vet. Ed.* **4** (1992) 219.
3. J. D. REILLY, *Equine Vet. J.* **27** (1995) 166.
4. A. GROSENBAUGH and D. M. HOOD, *Equine Pract.* **15** (1993) 8.
5. C. BAILLIE and R. FIFORD, *Biomimetics* **4** (1996) 1.
6. J. F. V. VINCENT, "Biomechanics-Materials: A Practical Approach" (IRL Press, Oxford, 1992) p. 247.
7. R.D.B. FRASER and T. P. MACRAE, in "The Mechanical Properties of Biological Materials, Symposium XXXIV," edited by J. F. Vincent and J. D. Currey (Cambridge University Press, Cambridge, 1980) p. 211.
8. A. D. KITCHENER and J.F.V. VINCENT, *J. Mater. Sci.* **22** (1987) 1385.
9. A. D. KITCHENER, *J. Mater. Sci. Lett.* **6** (1987) 321.
10. J. J. THOMASON, A. A. BIEWENER and J. E. BERTRAM, *J. Exper. Biol.* **166** (1992) 145.
11. D. H. LEACH, Ph.D. thesis, Univ. of Saskatchewan, Canada, 1980.
12. J. D. REILLY, D. F. COTTRELL, R. J. MARTIN and D. CUDDEFORD, *Biomimetics* **4** (1996) 23.
13. M. A. KASAPI and J. M GOSLINE, *J. Exper. Biol.* **200** (1997) 16393.
14. H. WILKENS, *Zbl. Vet. Med. Ser. A* **11** (1964) 163.
15. J. E. A. BERTRAM and J. M. GOSLINE, *J. Exper. Biol.* **125** (1986) 1721.
16. J. J. THOMASON, A. A. BIEWENER and J. E. BERTRAM, *ibid.* **166** (1992) 145.
17. A. D. WEAVER, *Vet. Record* **108** (1981) 117.
18. D. FIELDING, in International Colloquium on Donkeys, Mules and Horses in Tropical Agricultural Development, CTVM, Edinburgh, 1990.
19. J. FOWLER, *Equine Vet. Ed.* **7** (1995) 18.
20. A. HIFNY and N. A. MISK, *Assiut Vet. Med. J.* **10** (1983) 3.
21. H. MIYAKI, OHNISHI and T. YAMAMOTO, *Exp. Rep. Eq. Hlth. Lab. (Japanese)* **11** (1974) 15.
22. J. E. DOUGLAS, C. MITTAL, J. J. THOMASSON and J. C. JOFRIET, *J. Exp. Biol.* **199** (1996) 1829.
23. C. O. WILLITS, *Anal. Chem.* **23** (1951) 1058.
24. G. H. PRATT, "Timber Drying Manual," 2nd edition (Building Research Est., DoE, 1986) p. 26.
25. R. D. POLITIEK, O. DISH and T. FJELDAAS, *Livestock Prod. Sci.* **15** (1986) 133.
26. D. H. LEACH and G. C. ZOERB, *Amer. J. Vet Res.* **44** (1983) 2190.
27. L. J. LANDEAU, D. J. BARRETT and S. C. BATTERMAN, *Amer. J. Vet Res.* **44** (1983) 100.

Received 4 December 1997
and accepted 18 September 1998

LAMINITIS AND THE HOOF HORN CAPSULE

J.D Reilly[1,2], S.N. Collins[2], B.C. Cope[2], L. Hopegood[2], R.J. Latham[2].

1. **Royal Army Veterinary Corps.**

2. **De Montfort University, Faculty of Applied Sciences. Leicester.**

Laminitis poses a significant threat to all domestic equidae. It is a serious and painful condition that results in acute or chronic lameness, which may lead to humane destruction of the afflicted animal. As a result laminitis raises many welfare and management concerns. In addition, many owners of sporting equids will have suffered the frustration of not being able to realise the animal's true athletic potential.

Although the predisposing causes of laminitis are varied, they trigger a systemic disturbance that manifests itself at the level of the foot. This results in disruption to normal blood supply leading to vascular compromise, tissue damage and degenerative changes within the foot.

Research into laminitis has predominantly focused on the impact of the condition on the dermal tissues, the *laminae*, which lend their name to the condition. However the progression of the disease is also associated with changes to the visual appearance of the hoof capsule, most notably to the hoof wall and white line. These changes may include irregular thickening of the hoof wall, divergent growth rings on the outer hoof capsule, irregularities in the shape of the hoof capsule, thickening of the periople, and widening of the white line. Production of horn of 'inferior quality' is also said to occur with laminitis, but scientific ways of assessing this, as well as the response of the hoof wall to different nutrients either in the normal or in the diseased states, are in their infancy in scientific terms.

Our research group is interested in quantifying these changes in a non-invasive research programme which studies samples of normal and diseased hoof horn. The existence of the group has been made possible by generous funding from the Horserace Betting Levy Board, The Donkey Sanctuary and from Dodson and Horrell Ltd.

The subject is anatomy based and so it is necessary to cover complex areas of the hoof capsule architecture. The intricacies of it may surprise the reader who always thought that the hoof was a monolithic slab of rather 'dull' material!

Hoof Capsule anatomy

The hoof is a highly evolved locomotor organ of epidermal origin. It has a complex three-dimensional structure and consists of a horny capsule made of epidermal tissue, which encases bones, joints, ligaments, tendons, bursae, nerves, blood vessels, and connective and fatty tissues. The tissue in which nerves and blood vessels run is called dermal tissue and this supplies the epidermal hoof horn capsule with its nutrients.

The hoof horn capsule and its contents are collectively known as the 'foot'.

The visual parts of the hoof capsule can be divided into wall, sole frog and white line:

The Hoof wall

The wall is that part of the hoof that is visible in the standing animal. It makes up the largest part of the hoof capsule and it has a major function in weight bearing. It is divided regionally into toe, quarters and heel and at the bearing border it is reflected at the heels to form the 'bars'. The major part of the wall grows downwards from the coronary band and it has a cellular architecture, composed of horn tubules and intertubular horn, which can be seen microscopically when the hoof wall is cut in cross section. The horn tubules are produced by cells overlying dermal papillae, which protrude for short distances into the hoof wall at the coronary band and the intertubular horn, is produced from cells lying in the interpapillary regions. The full thickness of the hoof wall can be divided into three layers; *stratum externum*, the *stratum medium* and *stratum internum*:

The *stratum externum*, or periople, is also composed of tubular and intertubular horn. It is believed to have high lipid content and to act in water control and in protection. This part of the hoof turns milky white when wet.

The *stratum medium*, comprises the largest part of the wall. It has a well-defined tubular and intertubular architecture. In the pony and the horse it can be further sub divided into distinct layers or zones based on the distribution of these horn tubules.

The *stratum internum*, is composed of interlocking leaves of dermal and epidermal tissue known as laminae. This arrangement forms a large surface area of contact to allow firm bonding between the hoof wall and, ultimately, the pedal bone via the dermal connective tissue.

These anatomical features of the wall allow it to effectively deal with multidirectional forces during weight bearing and locomotion.

The sole

Solear horn is also composed of tubular and intertubular horn and is produced from tissue overlying the base of the pedal bone.

The frog

This is a readily recognisable 'v' shaped structure on the underside of the hoof capsule with its narrowest part pointing forward. In the middle of the frog is a groove referred to as the central sulcus. On either side of the frog, between it and the respective bar for that side, is another groove called the collateral sulcus. The frog is made of a rubbery form of horn, which is thought to function as an anti-concussive device, a non-slip device and possibly as an aid to blood circulation within the foot and limb. It may also help facilitate expansion of the heel under load. However, the frog is not the only 'expansion device' within the hoof capsule:

The white line

This forms a junction between wall and sole at a point below the internal dermal laminae. It is thought to allow some independent movement between the wall and sole during loading, thus preventing catastrophic failure of the hoof capsule.

The white line is an important indicator for the farrier and for the veterinary surgeon. The position of the white line determines the placement of nails during shoeing. German research workers also

recognise the importance of the white line as it reflects the state of the "suspensory apparatus of the pedal bone".

The white line is a complex three-dimensional anatomical structure, formed by horn contributions originating from the epidermis overlying the dermal or 'sensitive' laminae. Horn production from different parts of the *stratum internum* produce the components that make up the white line. These are: Lamellar horn of the epidermal or 'insensitive' lamellae, Terminal horn, and Cap horn.

Lamellar horn

Horn production from the basal cells overlying each adjacent pair of dermal or 'sensitive' laminae combine to form the lamellar horn. This horn is produced along the entire extent of the laminae from near the coronary band to near the bearing border. It forms the horny or 'insensitive' lamellae which interdigitate with the dermal laminae to form the "suspensory apparatus of the pedal bone".

Cap horn

This is produced by the basal cells overlying the papillae that bud from the crest of each individual dermal or 'sensitive' lamina.

Terminal Horn

The lowermost edge of each dermal lamina is marked by the formation of terminal papillae and it is this region of the dermal laminae that generates the terminal horn. This is produced by the basal cells overlying the distal margin of each dermal or 'sensitive' lamina. It is also composed of tubular elements originating from the cells overlying the terminal papillae. This material occupies the area between the adjacent lamellar horn and extends from the lowermost margin of the dermal laminae to the bearing border.

In this way the components of lamellar, cap and terminal horn combine distally to form the functional complex that is the white line.

Little is known about the precise effects of laminitis upon the structural organisation of the hoof capsule. Following laminitis, it has been suggested that the white line widens as the laminae are stretched following inflammation of the dermal laminae. In addition, the horn material produced following this laminar damage is said to be altered and inferior in nature, thereby predisposing the hoof to microbial invasion. In severe cases of total failure of the "suspensory apparatus of the pedal bone", a second white line may be formed. It is also possible that changes occur to the *stratum medium* of the hoof wall that are yet to be discovered. What is already known is that the rotation of the pedal bone causes an abrupt change to the orientation of the horn tubules at the level of the coronary band, and a simultaneous compression of the dermal papillae. The precise effects of these changes upon horn production are yet to be quantified. Hence the objective assessment of horn changes within the wall, white line and other areas of the hoof capsule, at the microscopic level, represents an important area for study in order to advance our knowledge and understanding of the laminitic condition.

The hoof capsule may provide us with valuable sources of evidence of laminitic change and allow us to investigate the effects of the disease still further. It is time to carry out this investigation in an objective manner by identifying and measuring critical structural and functional components of the hoof capsule that are changed by laminitis. By comparing these with clinically normal animals under appropriate control conditions, it may be possible to establish differences that occur as a result of laminitic insult.

In this way it will be possible to establish:

- Normal anatomical parameters for different parts of the hoof capsule.
- The parameters that are affected by laminitis.
- The progression of the disease at the level of the hoof capsule.
- Whether different parameters are affected in different stages of the disease.
- Whether there is variation between individual animal's capsular response to laminitis.
- The effect of individual variation in recovery.

The potential opportunities afforded by such an approach are considerable. These include the identification and/or establishment of:

- Diagnostic markers for the disease.
- A cost-effective adjunct to X-rays.
- A means of monitoring the progression of the disease and response to therapy.
- A method for rapid and widespread screening for laminitic change.
- Prognostic markers.

By investigating the effects of laminitis upon the hoof and by developing an understanding of the functional consequences of such changes, we will be in a better position to be able to recognise markers for the condition, screen for it, design enhanced management regimes and therapeutic strategies, and objectively evaluate the effects of implementing them. This will undoubtedly benefit the animal's welfare and management and help those that require it, to return to top form.

Funding bodies and sponsors must now recognise that this is an important and neglected area of veterinary research.

Further Reading:

BRAGULLA, H., BUDRAS, K.-D. AND REILLY, J.D. (1998) Foetal development of the white line (Zona alba) of the equine hoof. Equine Veterinary Journal Supplement **26.** In press.

BUDRAS, K.-D., SCHIEL, C., AND MÜLLING,C. (1988) Horn tubules of the white line: an insufficient barrier against ascending bacterial invasion. Equine Veterinary Education **10** (2) 81-85.

GOETZ, T.E. (1987) Anatomic, hoof and shoeing considerations for the treatment of laminitis in horses. *Journal of the American Veterinary Medical Association.* **190** (10) 1323-1332.

REILLY, J.D. (1995) 'No hoof no horse?' *Equine Veterinary Journal* **27** (3) 166-168.

3er Coloquio Internacional sobre Equidos de Trabajo

Tercer Coloquio Internacional sobre Equidos de Trabajo
México
1998

México, 1998

División Educación Continu

MULTI-DISCIPLINARY COLLABORATION FOR THE WORLD-WIDE BENEFIT OF WORKING EQUINES.

TRAWFORD, A. F.

Director of Veterinary Services
The International Donkey Protection Trust
Sidmouth
Devon, EX10 ONU, UK

ABSTRACT

The introduction to this paper summarises the objectives of the two previous colloquiums and highlights how the results should form the framework of project development based on a multi-disciplinary approach to epidemiological survey.

Information from many countries suggests that the demise of the working equine will slow down or stop in situations where the terrain, politics or economic pressures extend the popularity of 'our beasts of burden' as a source of draught power. This may act as an incentive to improve the welfare of working equines, thus providing an appropriate environment for equine health, welfare and management projects.

Project development is discussed in terms of cost effectiveness, feasibility and sustainability with education at the primary level being highlighted. The importance of a clear and concise extension message for the diverse populations that work with equines is also mentioned.

The conclusion of the paper gives examples from the International Donkey Protection Trust where research projects combine with hands on animal welfare projects to address the key points. These include "the thin equine, the lame or wounded equine and the diseased equine". Strategic use of modern day drugs and/or traditional/alternative medicines and the use of improved husbandry techniques form part of the future project programmes.

INTRODUCTION

The initial step in collaboration between and within disciplines started at the first colloquium held in Edinburgh in September 1990 (Donkeys, Mules and Horses in Tropical Agricultural Development, Fielding and Pearson, 1991). According to the organisers the end result was a most stimulating and interesting colloquium that also proved to be a lot of fun. The material presented was based on delegates' own experiences and individual research work. This formed a good base for information exchange, but needed to be developed.

The second colloquium held in Morocco in 1994 was another important opportunity for research workers, clinicians, extension officers, educators and project administrators to gather together. It provided a comprehensive review of the current knowledge and experience of all aspects of the working equine and reviewed progress since Edinburgh, also looking at the needs and opportunities for the future.

As a result of these two colloquiums it is proposed that future project development be of a multi-disciplinary research nature, based on epidemiological survey.

Andrew Prentis (1994) in his keynote address in Morocco cited mechanisation as a cause for the demise of the working equine population with the transition phase being particularly difficult for individual animals and the loss of and neglect of traditional husbandry methods leading to some of the worst conditions for equidae.

Whilst there is no doubt that the invention of the wheel has led to the demise of the working equine I suggest that the wheel is about to turn full circle.

One day fossil fuels will run out, but before that their value will increase, making fossil fuels inaccessible to the ever increasing population. Draught equines will continue to play a major role into the 21st century.

In 1970 I treated up to 20 mules and donkeys a day in Trench Town, Jamaica. Today you will find but one cart in Trench Town and yet the government of Jamaica is supporting a mule breeding programme. IDPT is also trying to address the acute shortage of donkeys still required by the coffee and sugar cane industries of Jamaica. This is not subsistence farming; this is big business.

The donkeys proven drought and disease resistance has led to their use in Northern Zimbabwe as draught power to replace the oxen which perished during the drought of the early 1990s (Barrett, O'Neill and Pearson, 1992; Morriss, 1995)

In countries like Yemen and Eritrea the donkey will remain a key working equine due to the terrain and continual use of terraced agriculture (the hanging gardens of Yemen).

The politics of Eastern Europe have led to a revival in the fortunes of the working equine that will not be reversed during my working life. Bulgaria, Albania and Romania use many more working equines today than five years ago.

THE BASIS OF PROJECT DEVELOPMENT

At the TAWS (World Association for Transport Animal Welfare and Studies) seminar (1998) it was suggested that the following protocol be adopted for project development.

- Epidemiological Research.
- Provide beneficiaries with their requirements (not what <u>you</u> think they want!)
- Inclusion of project evaluation costs.
- Cost effective evaluations.

Better to spend money on project evaluation and epidemiological research than waste money on a pet project.

IMPLEMENTATION OF PROJECT DEVELOPMENT

Initially any form of treatment which gains the confidence of the recipient is useful as long as it is followed by a programme designed to implement the results of epidemiological research for future generations of equines.

Education methods aimed at today's equine owners by television and other media coverage

are short term. These should be supplemented with specific equine information and technical books to Veterinary Universities and Agricultural schools. (for example Svendsen, E.D. 1997b - Professional Handbook of the Donkey).

Long term benefit should be aimed at introducing equine health and welfare programmes into the school curriculum by lobbying policy makers. Dr Svendsen has written several children's books which are country specific and written in the local language and English; to date books have been written for Ethiopia, Jamaica and Mexico (Svendsen, 1996, 1997a and 1998). This is a very gentle approach to improve animal welfare, the results of which will not become apparent for several years.

In the Bible, Matthew 19, verse 30 'But many that are first shall be last; and the last shall be first'. In the past, projects have come first and beneficiaries last. Now, beneficiaries need to be considered first so they can contribute to project planning and development.

ECONOMICAL AND SUSTAINABLE VETERINARY MEDICINE

Economical and sustainable veterinary medicine requires emphasis on traditional medicine.

At the ATNESA(Animal Traction Network for Eastern and Southern Africa) workshop in Ethiopia in May 1997 (Improving Donkey Utilisation and Management), one of the most popular evening workshops focused on the use of traditional medicines but specific information was hard to come by. Examples were (Starkey, 1998):-

- Wound healing - ash (universal), salt, papaya leaves (Zimbabwe), peach leaf poultice (South Africa), maggots (Jamaica, Pakistan, South Africa, UK).
- Worms - tobacco extract (Ghana, Namibia), aloe (South Africa), garlic (Ghana).
- Diarrhoea - chimney soot (Kenya).
- Skin disease - used engine oil (universal), sulphur and coconut oil (Jamaica), vaseline (Zimbabwe).

This was highlighted by Cheryl McCrindle at TAWS seminar in April 1998 in London when Dr McCrindle talked about the use of traditional and affordable treatment in traction animals. Examples of utilising normal household materials were:

- sugar or honey - stop bleeding, loosen dirt, facilitate cleaning and promote granulation.
- salt solution - clean wounds, acts as a mild disinfectant and used in an eye wash mixture for rehydration.
- Flowers of sulphur - used topically against dermatophytes, mites and lice.

EVALUATION OF BASIC HEALTH PROBLEMS

The need to evaluate on an internal country specific basis the epidemiology of basic health problems, as identified by Andrew Prentis (1994) in these key points:

- The thin equine
- The lame equine
- The wounded equine
- Equines in respiratory distress (not necessarily coughing)
- Welfare

In Garissa, Kenya, several male donkeys were presented for castration, but the procedure was not carried out due to their poor body condition. The initial advice was to worm the donkeys in preparation for a future operation, but during a general examination of these

donkeys to determine their age it was discovered that all had dental abnormalities which were contributing to their condition.

By good judgement and planned hard work the thin donkey has been almost eliminated from Lamu.

The secondary effects have been a marked reduction in body sores from ill fitting harness and less beating of the animals as they have the energy to perform their tasks willingly. The negative effect however is increased libido in the stallions causing behavioural problems and threatening the social fabric of the local community.

The introduction of a controlled breeding programme is now long overdue, but with cultural difficulties arising from the traditional beliefs of the Muslim donkey owners it is proving difficult to implement. The demonstration of a modern castration technique and the resultant improvement in behaviour and body condition in donkeys in Garissa, Kenya, has convinced future owners to castrate their donkeys.

Perhaps the most neglected area of research in donkeys is the phenomena of in-breeding. In closed populations such as the donkeys on the Turks and Caicos Islands poor physique based on lack of skeletal development appears to be the main problem although poor hoof development may also be a consideration.

It is vitally important that genetic research be carried out to identify areas of countries with an inbreeding problem. Ethiopia may provide good examples of this regional variation.

Through collaboration it may be possible to identify a primary cause for poor body condition in Kenya, lameness in Ethiopia and body sores in Egypt.

RESEARCH DIRECTIVES

Although the conditions may be inter-related researchers tend to analyse one aspect which relates to their training as a nutritionist or parasitologist rather than the overall epidemiology.

Single Discipline

The prohibitive cost of anthelmintics and increased publicity on anthelmintic resistance initiated a research project at the Donkey Sanctuary.

The first project presented as a paper at the WAAVP meeting in South Africa in 1997 was entitled "The use of Ivermectin for the control of strongyle species in the donkey; *Equus asinus*, using the egg reappearance period (ERP) as the parameter for assessment of efficacy".

Many modern day anthelmintic programmes for the control of endoparasites in equidae are based on the use of broad spectrum anthelmintics every 4-8 weeks - a regime that may be encouraging the development of resistance.

Research was undertaken at The Donkey Sanctuary to investigate the possibility of slowing down the development of resistance to anthelmintics and the possible reduction in the incidence of cyathostomiasis using faecal ERP as the criteria for periodic anthelmintic dosing.

The trial was conducted at four of The Donkey Sanctuary farms in Devon. The donkeys were given Eqvalan (Ivermectin) at a dose rate >200µg/kg prior to spring turnout. The faecal egg count (eggs per gram - EPG) was then monitored using the Modified McMaster technique by random sampling 15% of the herd. A total of 1521 donkeys were chosen using a randomisation programme and faecal sampling commenced eight weeks post worming and then fortnightly until the ERP reached the level of, 25% of the herd having a faecal egg count of more than 200epg (Uhlinger, 1992).

The results of this trial show that with good pasture management and favourable climatic conditions the periodicity of dosing can be extended to allow anthelmintic dosing at spring turnout and prior to winter housing (up to 22 weeks) by closely monitoring the ERP.

This regime is now policy at The Donkey Sanctuary and will hopefully reduce the onset of anthelmintic resistance and produce a cost saving on purchase of anthelmintics that will exceed the increased costs of laboratory labour and materials producing a real financial benefit.

How does this benefit the rural donkey in Ethiopia or anywhere else in the world.

The development of these trials allows the development of better strategic worming policies based on local weather conditions (predictable rainy seasons) and grazing patterns. Unfortunately El Niño has rather disrupted these predictable conditions

The lack of information on products available specifically for donkeys led to research on the specific problem of liver fluke in donkeys. Trawford and Tremlett, 1996 found that of 60 post-mortem examinations performed on Irish donkeys transferred to The Donkey Sanctuary *Fasciola hepatica* was identified in 17%. More recently of 200 faecal samples 8.5% were positive for *Fasciola hepatica* eggs. Blood samples taken from these donkeys before death indicated liver enzyme levels within normal range and it was noted at post-mortem examinations that there was very little reaction to the presence of the flukes in the bile ducts or liver tissue of the donkey.

Patent liver fluke infection does occur in the donkey and control of the parasite is therefore recommended, as good pasture management includes grazing sheep on donkey pastures to reduce pasture larvae burdens.

Since clinical symptoms of the disease are rarely seen, diagnosis is based entirely on faecal examination for fluke eggs by modified sedimentation techniques.

Treatment - although not licensed for use in equines triclabendazole (Fasinex) at a dose rate of 12mg/kg bodyweight is effective.

Collection and Collation of Information

Initial investigation often begins with a questionnaire, that relies on owner knowledge or even anecdotal information and observations. Evaluation of this information and the observations channels the researcher.

<u>Collaboration on Body Scores</u>
At the present time at least two systems are used for assessing body condition (scoring). It is important that one system be universally adopted. Other examples relate to estimations of body weight and blood biochemical parameters.

Universal Language

Experience at The Donkey Sanctuary in Devon has shown that even within one organisation the employment of three veterinary surgeons has resulted in failure of data retrieval due to the diversity in terminology used. This must inevitably be happening to a greater extent between and within international bodies.

Funding

Charities, Universities and pharmaceutical companies provide funds or are funded by organisations that demand certain disciplines be evaluated. The benefits of multi-source funding would lead to the removal of individual bias.

Multi-disciplinary

A multi-disciplinary approach to research and health and welfare allows the maximum use of resource with a minimum amount of expenditure.

Trypanosomiasis

Through work at KETRI which Dr N'dungu has presented in more detail in his paper on trypanosomiasis in the donkey, we are just beginning a new venture to evaluate epidemiological factors using multi-disciplinary groups.

Donkeys show a variable degree of resistance to trypanosomiasis making them a major source of draught power in tsetse areas. The following trypanosome species are found in equidae:-

- *T. brucei*
- *T. congolense*
- *T. equiperdum* (Dourine)
- *T. evansi* - equinum
- *T. vivax*

Pathogenicity for horses is recorded as highly pathogenic for *T. brucei* and *T. evansi* and less pathogenic for *T. congolense*, *T. vivax* and *T. equiperdum*. Donkeys follow a similar pattern with *T. congolense* often presenting as a chronic form of the disease.

The International Donkey Protection Trust has sponsored work on trypanosomiasis at KETRI (Kenya Trypanosomiasis Research Institute). Results have indicated that mixed infections are the most common and seasonal variation in pathogenicity may occur due to "trypanosome challenge" (the number of bites in a unit time). Further research includes investigation into evidence for or against trypano-tolerance in donkeys and possible regional differences in pathogenicity and incidence. Also addressed is how to reduce the incidence of trypanosomiasis in donkeys to further promote their use in tsetse infested areas. Methods under investigation include:

- Treatment of infected animals.
- Control of contact with potential reservoirs of infection (wildlife and other livestock).
- Control of tsetse fly populations.
- Improved resistance through improved management and welfare.
- Breeding for trypano-tolerance.

Although the paper compares tne incidence of trypasomiasis in two districts of Kenya Dr Githiori has carried out general health evaluation of all donkey in these areas. In Nguraman for example the Masai only use their donkeys for four months of the year. Some of these very fit healthy donkeys have worm burdens in excess of 6000epg, but adequate nutrition and natural immunity allow these animals to maintain body weight during this working period. Other village donkeys used on a daily basis do not fare so well but this more likely a combination of nutritional deficit, work and parasitic burden.

Harnessing

The Kenya Society for the Protection and Care of Animals (KSPCA) treats an average of 6,000 donkeys annually, 90% of which suffer from severe harness sores. The International Donkey Protection Trust (IDPT) and KSPCA with the help of saddlery consultants from The International League for the Protection of Horses (ILPH) are addressing the harnessing problem in Kenya. A pilot study has designed and produced a harness made from locally available materials. Beneficiaries have been involved at all stages of project development. The project will provide people with the skills to produce an effective cheap harness using local materials. The course also includes education in health, welfare and management of the donkey.

Population Control

In the Turks and Caicos Islands a population control programme was carried out to alleviate a human social problem and control in-breeding. The project was a combination of both old and new techniques and a good example of a multi-disciplinary approach. Since castration of all male donkeys was not feasible for logistical reasons some form of female sterilisation was envisaged.

Collaboration with Jay F. Kirkpatrick at Zoomontana led to the use of immunocontraception with porcine zona pellucidae (PZP). The technique required the periodic injection of PZP vaccine which had been tried in feral horses (Kirkpatrick and Turner, 1991; Kirkpatrick and Turner, 1994). For political reasons the project failed, but the concept proved useful.

"No Hoof, No Donkey"

The Donkey Sanctuary is sponsoring non-invasive research at De Montfort University, Leicester, headed by Major John Reilly and Professor Roger Latham to unravel the functional/design complexity of this locomotor structure. This investigation has adopted a novel multi-disciplinary approach which has brought together the professional knowledge and expertise of veterinarians, chemists, material scientists, animal scientists and mechanical engineers. This collaboration is proving extremely productive and is bringing new thoughts to old problems(Cope *et al*, 1998a; Cope *et al*, 1998b; Newlyn *et al*, 1998; Reilly, 1998 Collins, 1998; Newlyn *et al*, awaiting publication).

The research group at Leicester is employing a variety of scientific techniques both to characterise the normal hoof horn parameters of the donkey and to compare these with other equid species. Donkey hoof horn from diseased conditions such as laminitis is also investigated. Objective measurements are directed towards evaluating the degree of association of observed differences evident in abnormal horn. If there is a strong association with specific disease conditions then such horn parameters may serve as a powerful adjunct to traditional diagnostic and prognostic techniques such as x-rays.

Image analysis techniques have been developed to establish the distribution of horn tubules across the hoof wall in terms of tubule density (the number of tubules per mm^2)(Reilly *et al*, 1998). In addition further work is in progress to determine the way in which the size and shape of the horn tubules varies across the hoof wall and around the hoof capsule. These structural arrangements are considered to be important determinants of the functional capabilities of the hoof capsule and the way in which forces are transmitted between the ground and the skeleton across the hoof wall.

Different drying techniques are being used to establish the normal hydration levels within the hoof and the different ways in which the water interacts with the structure. Moisture levels are of particular interest, as it is believed that the mechanical properties and finer functioning of the hoof wall is modulated by water (Cope *et al*, 1998a; Collins *et al* (In press)).

SUMMARY

Exchange Information

The importance of any message must be based on consideration of each equine in its own unique environment, as the variation both between and within countries is enormous. This can be best accomplished by collaboration between owner, extension worker, project developer, researcher and funding organisation towards a common goal. A good example would be that harness wounds may result from poor equipment, poor nutrition, overwork or a combination of all three.

Collaborate on projects

Collaboration of information is needed on treatment, education and research as the learning curve from one country may be fully utilised, partially adopted or even improvised on for use in other countries.

Benefit the people by improving the animals

A small investment in improving the working equines health and welfare whether by improving the mechanisation of the cart it pulls, the load it carries or improving the nutrition is a practical way in which the owner utilises the varied multi-disciplinary information supplied by the project.

Acknowledgements

The International Donkey Protection Trust, The Donkey Sanctuary and De Montfort University.

I personally wish to thank Simon Collins and Danny Bryan for their contribution towards the production of slides and Catherine Morriss for compilation of the text and its production.

REFERENCES

BAKKOURY, M. and PRENTIS, R.A. 1994. Working Equines. Proceedings from the Second International Colloquium, Rabat (Morocco) April 20th - 22nd 1994. Actes Editions, 1994 - Insitut Agronomique et Veterinaire Hassan II B.P. 62002 - Insituts, 10101 Rabat (Mavoc).

BARRETT, J.C., O'NEILL, D.H. and PEARSON, R.A. 1992. Strategic needs relating to draught animal power: A diagnostic study in Zimbabwe. Working Paper of the Draught Animal Working Group, ODA Livestock Production Programme, ODA, London.

COLLINS, S.N., COPE, B.C., HOPEGOOD, L., LATHAM, R.J., LINFORD, R.G. and REILLY, J.D. Stiffness as a function of moisture content in natural materials: Characterisation of hoof horn samples. *Journal of Material Science* (In Press)

COPE, B.C., HOPEGOOD, L., LATHAM, R.J. and REILLY, J.D. 1998. Equine hoof horn: a natural engineering composite. In: The Materials Congress, Proceedings of the Institute of Materials Conference, Cirencester, 6-8 April, 1998.

COPE, B.C., HOPEGOOD, L., LATHAM, R.J., LINFORD, R.G., REILLY, J.D., SYMONS, M.C.R. and TAIWO, F.A. 1998. Studies of equid hoof horn material by electron paramagnetic resonance. *Journal of Materials Chemistry*. **8** (1) 43-45.

FIELDING, D. and PEARSON, R.A. 1991. Donkeys, Mules and Horses in Tropical Agricultural Development. Proceedings of a Colloquium organised by the Centre for Tropical Veterinary Medicine of the University of Edinburgh and held in Edinburgh, Scotland 3rd-6th September, 1990.

GITHIORI, J.B., WAITHANJI, E.M., OKECH, G.O. and NDUNG'U, J.M 1997. Trypanosomiasis, helminthiasis and other conditions of donkeys in Lamu and Mwingi districts, Kenya. In proceedings of the 23rd International Scientific council for Trypanosomosis Research and control, Banjul, Gambia. p210-216.

KIRKPATRICK, J.F. and TURNER, J.W. 1991. Reversible contraception in nondomestic animals. Journal of Zoo and Wildlife medicine 22(4): 392-408.

KIRKPATRICK, J.F. and TURNER, J.W. 1994. Immunocontraception of free-roaming and captive exotic wildlife: New approaches to old problems. Verh.ber.Erkrg.Zootiere (1994) 36.

MORRISS, C.J. 1995. A baseline survey of donkey management, health, reproduction and uses in Mashonaland Central, North Zimbabwe. MSc Thesis, Centre for Tropical Veterinary Medicine, University of Edinburgh.

NEWLYN, H.A., COLLINS, S.N., COPE, B.C., HOPEGOOD, L., LATHAM, R.J. and REILLY, J.D. 1998. Finite element analysis of static loading in donkey hoof wall. *Equine vet. J.* Suppl. **26** 103-110.

NEWLYN, H.A., COLLINS, S.N., COPE, B.C., HOPEGOOD, L., LATHAM, R.J. and REILLY, J.D. Equine Hoof Horn: A natural composite. (awaiting publication)

PRENTIS, R.A. 1994. Issues for Working Equines Keynote Address. Proceedings from the Second International Colloquium, Rabat (Morocco) April 20th - 22nd 1994. Actes Editions, 1994 - Insitut Agronomique et Veterinaire Hassan II B.P. 62002 - Insituts, 10101 Rabat (Mavoc).p 9-16.

REILLY, J.D. 1998. Hail hoof science! *Equine vet. J.* Suppl. **26** 2-3.

REILLY, J.D COLLINS, S.N., COPE, B.C., HOPEGOOD, L. and LATHAM, R.J. 1998. Tubule density of the stratum medium of horse hoof. *Equine vet J.* Suppl. **26.**

STARKEY, P. 1998. Improving donkey utilisation and management. Report of the international ATNESA workshop held 5-9 May 1997, Debre Zeit, Ethiopia.

SVENDSEN, E.D. 1996. The story of Dusty, the little Ethiopian donkey. Whittet Books Limited.

SVENDSEN, E.D. 1997a. The story of Joe, the donkey who flew to Jamaica. Whittet Books Limited.

SVENDSEN, E.D. 1997b. The Professional Handbook of the Donkey. Whittet Books Limited.

SVENDSEN, E.D. 1998. The story of Pepe, the donkey who went to Market. Whittet Books Limited.

TRAWFORD, A.F. and TREMLETT, J.G. 1996. Efficacy of triclabendazole against *Fasciola hepatica* in the donkey (*Equus asinus*). Veterinary Record (1996) 139, 142-143.

TRAWFORD, A.F., MORRISS, C.J., REID, S.W.J., and SVENDSEN, E.D. The use of Ivermectin for the control of strongyle species in the donkey; *Equus asinus*, using the egg reappearance period (ERP) as the parameter for assessment of efficacy. WAAVP (1997).

UHLINGER, C. 1992. Preliminary studies into factors affecting the variability of egg reappearance period and anthelmintic treatment intervals in the control of equine cyathostomes. *Equine Infectious Diseases VI.* 157-161. Proceedings of the Sixth International conference 7th - 11th July 1991, edited by W. Plowright, P. D. Rossdale and J. F. Wade. R & W Publications (Newmarket) Limited.

Composites

18-19 March 1999
The Institution of Mechanical Engineers,
London, UK

ISBN 1 86125 096 7
PUBLISHED BY

IOM Communications Ltd
A subsidiary of
The Institute of Materials
1 Carlton House Terrace
London SW1Y 5DB

Tel: +44 (0) 171 451 7300 Fax: +44 (0) 171 839 2:

IOM Communications Ltd is a registered Charity, number: 1059475
And is committed to "Investors in People".

Printed by The Chameleon Press Limited

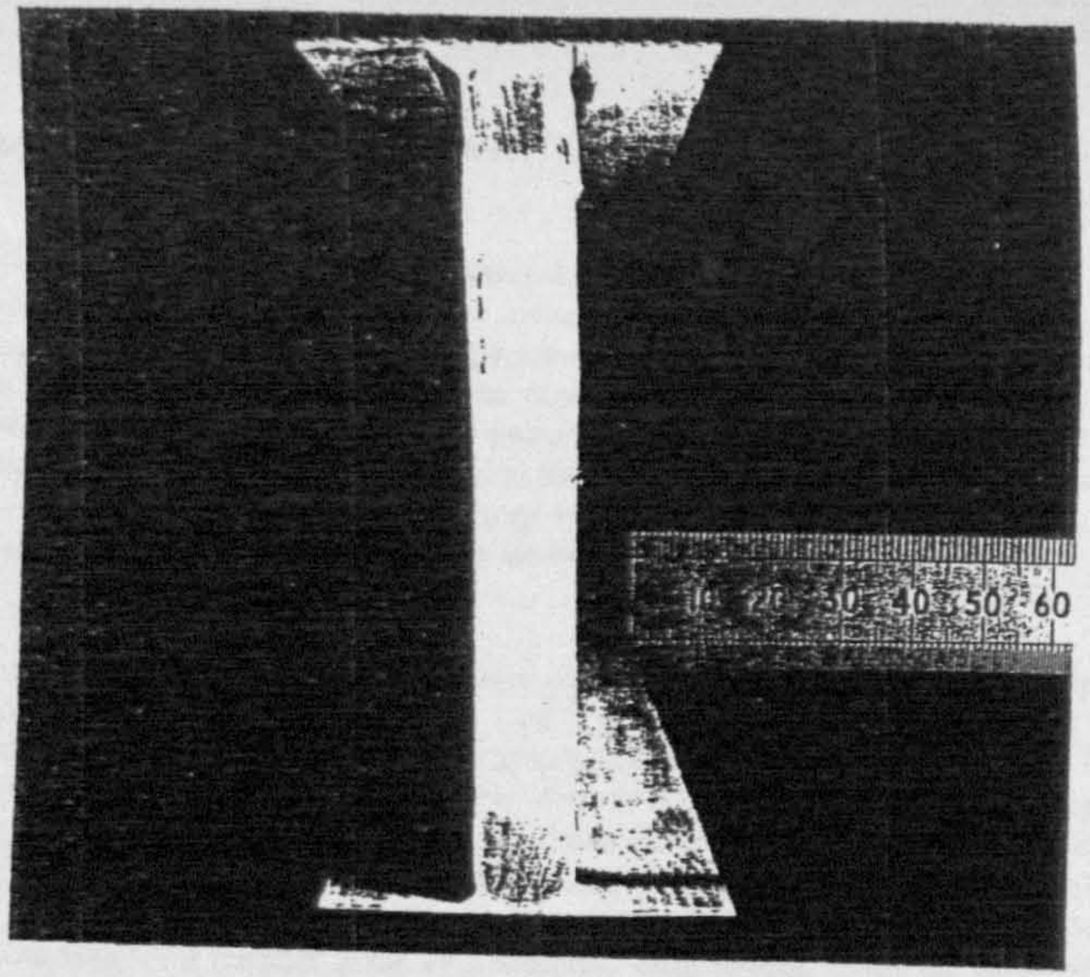

(a)

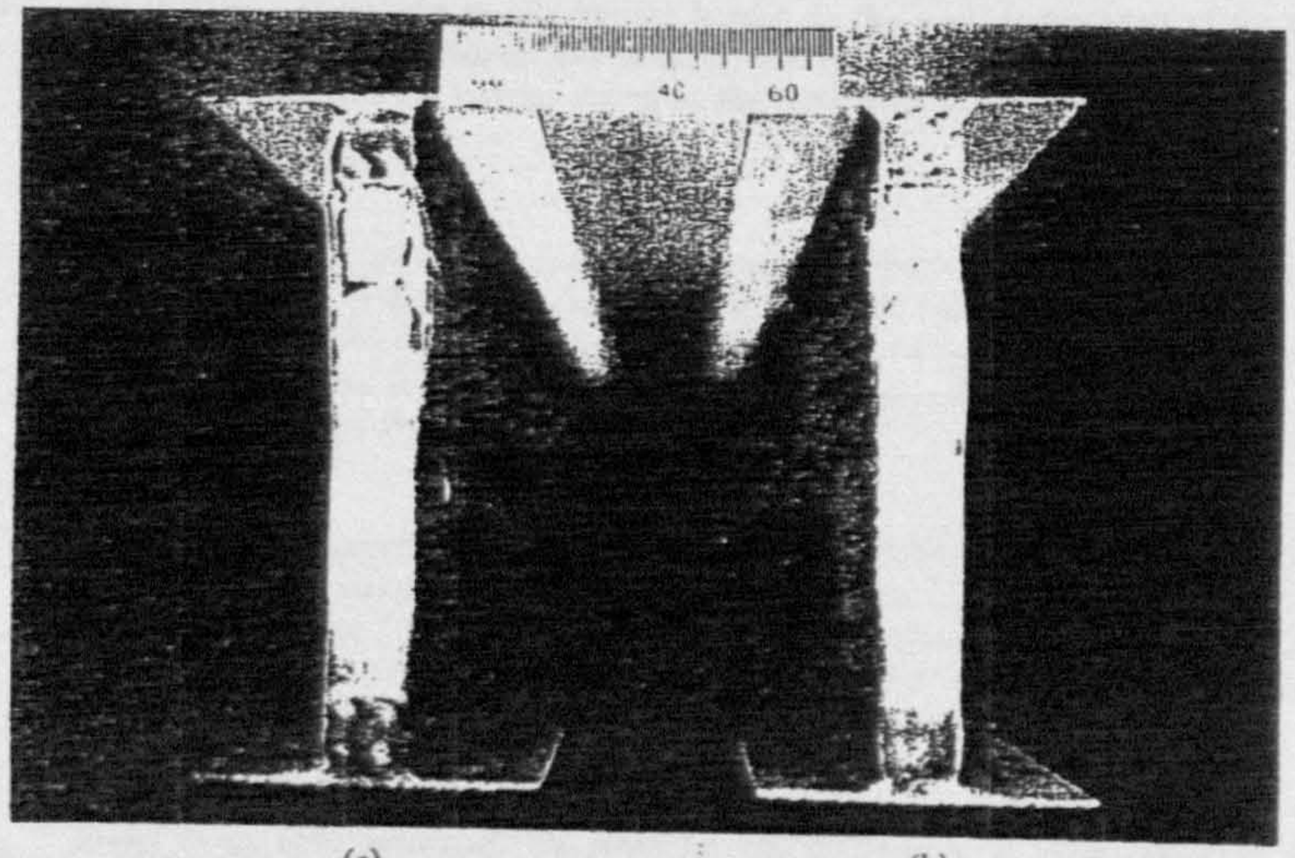

(c) (b)

Figure 11 Cross-sectional view at mid-span from three failed specimens
(a) intact, (b) with remote debonds and (c) with remote BVID

EQUID HOOF HORN: A NATURAL COMPOSITE

H.A. Newlyn[a], S.N. Collins[b], B.C. Cope[b], L. Hopegood[b], R.J. Latham[b] J.D. Reilly[b,c].
a Department of Mechanical and Manufacturing Engineering, De Montfort University, Leicester LE1 9BH.
b Faculty of Applied Sciences, De Montfort University, Leicester LE1 9BH.
c Royal Army Veterinary Corps, UKSC(G), DASU, BFPO 16.

ABSTRACT
A finite element model for the stratum medium of the equid hoof was developed at the microscopic level of its structural hierarchy based upon a morphometric analysis of the 'outer' region of the hoof wall at the midline dead centre of the donkey hoof capsule. A 2-dimensional plain strain finite element analysis (FEA) was conducted assuming isotropic material properties to generate mean modulus values in the lateral directions over a range of tubule to matrix stiffness ratios. Axial modulus values were also obtained based upon the ' rule of mixtures'. Solutions obtained from the FEA closely correspond with those obtained by the modified Hull equation, and, at a tubule to matrix modulus ratio of ~3.5- 4.0, the axial to lateral modulus ratios were in broad agreement with experimental data reported for the hoof. These results lend support to the assertion that the stratum medium may act as a unidirectional fibre composite at this level of the structural hierarchy, with the horn tubules acting as a fibre phase dispersed within a matrix of intertubular horn. The tubule and matrix strain concentration may be of significance with regard to energy absorption and crack propagation.

INTRODUCTION
The equid hoof is a natural biological composite composed of keratinised material Cope et al (1) that serves to suspend the skeleton and protect the sensitive structures of the foot. It must therefore be capable of accommodating and resisting high loads (up to 600 kg) on uneven surfaces and at high speeds without excessive deformation or catastrophic failure Leach (2). Consequently it is essential that it is capable of withstanding the forces generated by ground impact Douglas et al (3) and it must also have the ability to dissipate the resultant shock waves in order to dampen the concussive forces Dyhre-Poulson et al (4). Vogel (5) stated that a biological preference exists for accepting rather than preventing deformation. Hence during normal weight bearing and locomotion, the hoof deforms in a consistent pattern Douglas et al (3) thereby generating internal forces sufficient to counter the applied load. In this way, smooth and painless force transfer between the ground and the axial skeleton can be achieved Reilly et al (6). With respect to these capabilities, Pollitt (7) and Reilly et al (8) have described the hoof as a miracle of bioengineering.

However there is considerable scientific debate concerning the precise means by which the hoof wall achieves its functional requirements. Reilly et al (6) argued that a compromise must exist between the need to accommodate forces, minimise crack propagation and avoid excessive deformation that would threaten capsular integrity. Rooney (9) proposed that the structural design of the hoof reflects the need for force resistance and energy absorption. Thus, an interpretation of hoof function necessitates an understanding of the structure and morphology of the hoof, the complexities of the external and internal forces affecting the

capsule, and its response to these forces Leach (2).

Vogel (5) stated that the biomechanical properties of a structure are likely to be determined both by the material itself and the arrangement of that material. In addition Reilly et al (6) argued that the hoof is likely to be optimally designed in order to meet the functional demands placed upon it. In this respect, the equine hoof displays a complex hierarchical structural organisation evident at the gross anatomical, macroscopic, microscopic, ultrastructural and molecular level. Reilly et al (8) stated that the finer functional properties of the hoof are likely to be dictated by contributions from the structural organisation operating at many levels within the hierarchy, and these may be modulated by moisture content.

At the gross anatomical level the hoof capsule can be divided topographically into three main regions namely the wall, sole and frog. The hoof wall represents the major functional load-bearing component of the hoof capsule Nickel (10), Sack and Habel (11). Of the three morphologically distinct layers that form the hoof wall at the macroscopic level of the structural hierarchy, the stratum medium is considered to be the principal component responsible for determining its load bearing capabilities Pollitt (7), Kasapi and Gosline (12). At the microscopic level the stratum medium exhibits a distinct structural architecture consisting of a parallel array of keratinised horn tubules dispersed in a keratinised cellular matrix of intertubular horn Nickel (10), Wilkens (13). The horn tubules are comprised of a central void or medullary cavity, surrounded by a cellular keratinised cortex and extend from the coronary band to the weight-bearing border. In this way, at this level of the structural hierarchy the stratum medium has been considered as a unidirectional fibrous composite Reilly et al (8) with the tubules acting as the reinforcing material of the continuous phase Cope et al (1).

The relative importance of the tubular architecture in determining the functional capabilities of the hoof wall is unknown. However, if the hoof wall functions as a fibre composite then composite theory dictates that the mechanical properties of the structure will be determined by the material properties of the respective components, their volume fraction, and the orientation, size and shape of the reinforcing fibres.

Estimates of the mechanical properties of the hoof wall have been directly attained from a number of studies using compressive, tensile and bend test techniques Leach (2), Douglas (3), Kasapi and Gosline (12). However these tests have provided a wide range of values. These differences may reflect upon differences in testing protocol, moisture content of the material, sampling sites and inherent variability between individual animals.

Reilly et al (14) explained the need for careful control in experimentation and also emphasised the need to develop an understanding of the anatomical and functional relationships between the various hoof horn parameters in normal equine hoof. In order to achieve this, these must be defined by objective measurements from recognised anatomical sites. In addition, as there is a distinct lack of scientific information regarding the nature and distribution of forces within the hoof wall during loading, there is also a need to further develop our knowledge of the mechanical functioning and material properties of the hoof

wall

Various theoretical modelling techniques have been successfully applied to synthetic composites in order to predict mechanical performance both at a macroscopic and microscopic level. Traditional macromechanical techniques, such as 'simple rule of mixtures', deal only with the overall response of the material to an applied load and deal specifically with the resultant gross stiffness of the structure. On the other hand more advanced techniques, such as the finite element approach, can also evaluate the specific interactions of the respective components at the microscopic level. In this way a micromechanical approach can provide a means of evaluating the effect of local geometric and morphometric properties such as tubule distribution, tubule shape and size, and porosity effects arising from the medullary cavity. In this respect Hogan (15) argued that modelling and analysis techniques which incorporate the distinctive microstructural components should provide a more accurate and deterministic understanding of gross mechanics and function. In this way, computer assisted modelling of the hoof wall using finite element analysis (FEA) may serve as a means of further elucidating the complex interaction of forces generated during loading, and provide essential information that is required to unravel the functional complexity of the hoof wall.

A finite element model of the donkey hoof wall has already been used to develop an understanding of the stress and strain distribution generated within the structure during static loading Newlyn et al (16), and the resultant deformation. Modelling at the gross anatomical level of the structural hierarchy has predicted results that are in broad agreement with '*in vivo*' observations of capsular deformation and surface strain values given in the literature Thomason et al (17).

This study aims to build upon our former work by objectively measuring the morphometric properties of the donkey hoof wall at the microscopic level and to use this information to model the hoof wall at microscopic level of the structural hierarchy. In this way, the relationship between structural organisation and mechanical behaviour of equid hoof horn can be investigated and the assertion that the hoof wall acts as a unidirectional fibre composite tested

MATERIALS AND METHODS

Morphometric determination of the hoof wall

Histological sections were prepared from hoof wall samples taken from the midline dead centre (MDC) sampling site of the left forefoot of 6 donkeys, according to Reilly et al (8). Digitised images of each section were captured using a microscope-mounted video camera. Initial image acquisition was performed with a 4 x objective and a 3.3 x photo-eyepiece. This combined with a 1.25 x gain arising from the configuration of the trinocular microscope head, resulted in a total magnification of ~ 20 x. The captured images were imported into a computer based image analysis system and subsequently analysed using the NIH-Image software program. A three stage semi-automated method has been developed that provides both dimensional and area measurements, and area fraction data. Measurement criteria were selected to include length of the major and minor axes, and area measurements. By this means absolute dimensional measurements of marrow, cortex and tubule, and area fraction information for the tubular and intertubular components were determined. Measurements

and allowing poisson contraction. The mid-point of the restrained edge was fully restrained such that no displacement was possible in any directional plane. All other nodes were free to move. Plain strain 2-dimensional elements were used. The modulus was then determined by assessing the force in the boundary elements and the overall displacement in the chosen direction. This analysis was performed over a range of ratios of Et/Em from ~0.28 to 3.5. The FEA results derived from the analysis and the calculated values from the modified Hull equations have a restriction placed on strain in the x direction, and at a fibre to matrix modulus ratio of unity, indicate an axial to lateral modulus ratio >1. As the results are to be compared with modulus ratios obtained from tensile, compression and bend tests, where there is no strain restriction, the results were factored to pass through unity at a fibre to matrix ratio of 1.

FEA Micromechanics

Further interpretation of the FEA was conducted to investigate the micro stress/strain concentration developed as a consequence of the microstructural organisation. In this way, the effects of tubular shape upon the mechanical properties of the hoof could be further elucidated. Whilst it is appreciated that this approach cannot be used directly to assess possible failure, given that the tubular and intertubular components are likely to possess differing material properties, it may indicate areas of potential weakness. Such weaknesses may be of significance in crack initiation and stopping phenomena.

RESULTS

Morphometry results

The results of the morphometric analysis are summarised in Table II. The 'outer' hoof wall region was characterised by the presence of small, highly elliptical tubules, whose major axes were aligned parallel to the y or lateral axis. The tubular area fraction within this 'outer' region was 17%.

Table II – Morphometric analysis of the 'outer' hoof wall region

Hoof Wall Region	Percentage hoof wall depth (%HWD)	Tubule area fraction	Minor to major axes ratio	Mean tubule area measurement μm^2	Calculated tubule density Tubules mm^{-2}
Outer	5	0.17	1 : 3.07	6899	24.9

FEA Results

Figure III shows modulus ratios for the 5%HWD model for a range of ratios of Et/Em from 0.2857 to 3.5. The axial modulus (Ex), was derived from the 'rule of mixtures' relationship. It can be seen that the ratio of lateral to axial moduli Ey/Ex reduces consistently as the reinforcing in the axial direction becomes more dominant. At an Et/Em ratio of 3.5 the Ey/Ex ratio is 0.9. This indicates that there is a relative stiffness of this order between the keratinous material in the two respective phases, and that it is the structural organisation of this material alone, that accounts for the difference in moduli. At this K value the axial modulus is ~3% stiffer than the matrix material.

The stress strain concentration factors resulting from loading in the y direction are given in Figures IV. Analysis of this data revealed that in the matrix, the maximum stress and strain

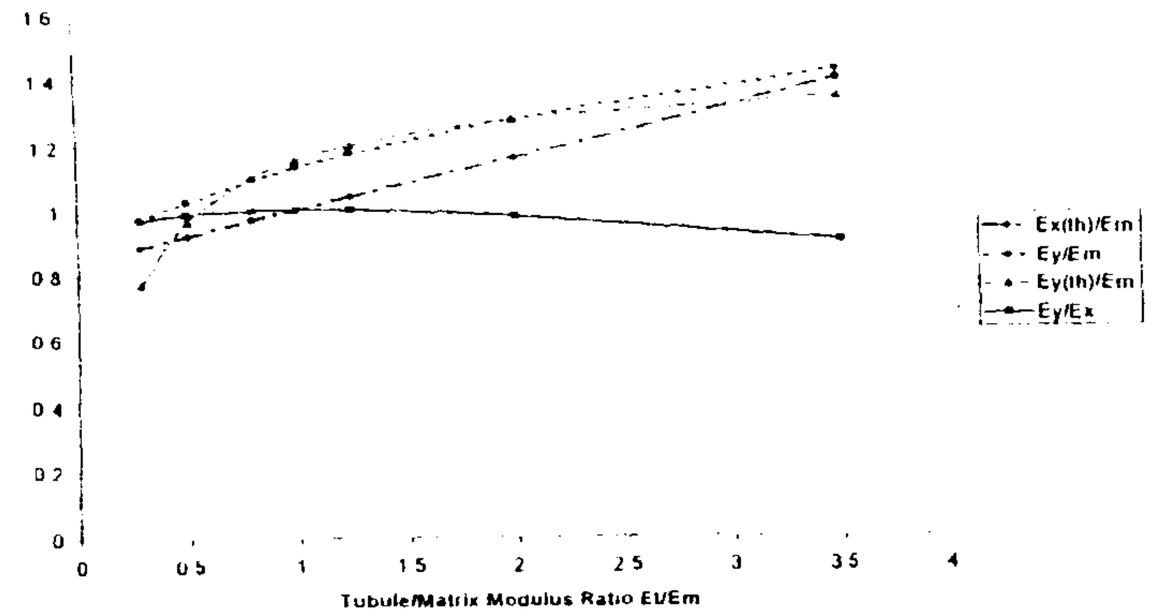

Figure III Comparison of modulus ratios for the 'outer' hoof wall model.
Ey - derived from FEA. Ey(th) – derived from the modified Hull equation. Ex - derived from 'rule of mixtures'. Em - matrix modulus.

concentration factors did not exceed twice the mean values at the maximum Et/Em ratio of 3.5. However within the tubular component, the maximum strain is up to three times the mean at Et/Em of 1 and progressively reduces as the tubule modulus increases. By extrapolating the results it would seem that at Et/Em of ~ 4 - 4.5 the ratio of maximum to mean strain value would be the same in the tubule as in the matrix at ~ 2.25.

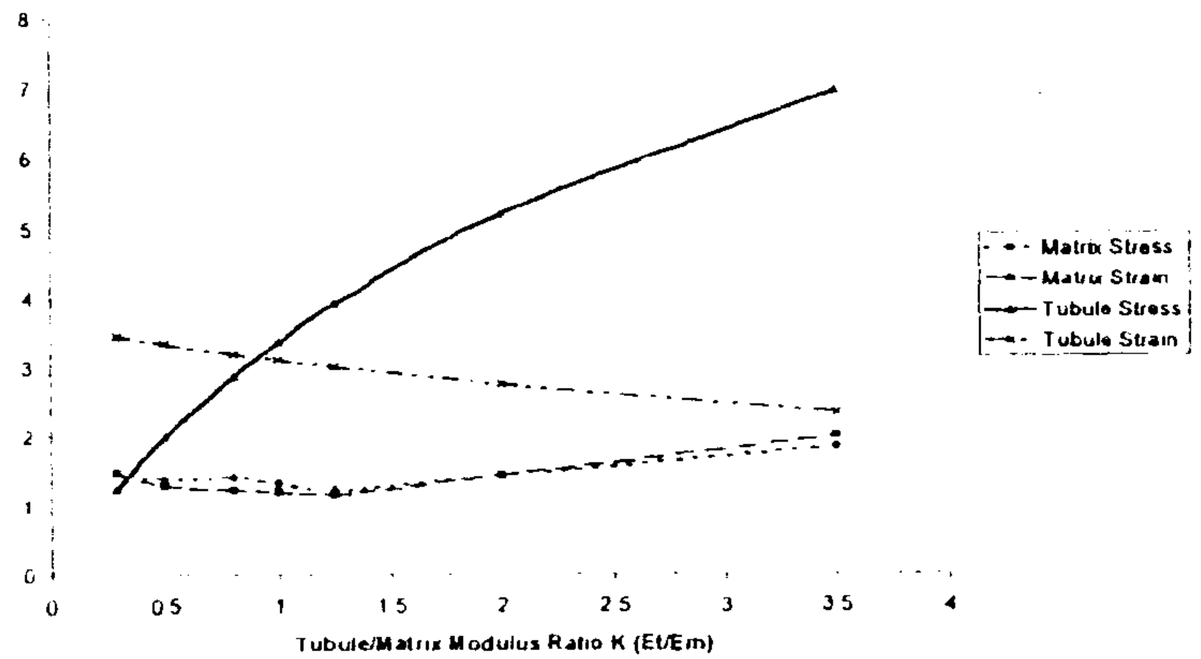

Figure IV Variation in the stress/ strain concentration factors in the tubule and matrix components of the 'outer' hoof wall model with increasing tubule/matrix modulus ratio.

The distribution of the regions of maximum strain within the matrix was dependent upon the K value. When loaded in the y direction, the point of maximum strain moved as the relative stiffness of the tubule increased from unity, from a position at the tubular-intertubular interface

were conducted at 5% hoof wall depth of the stratum medium (HWD). This site was considered to represent the 'outer' hoof wall region referred to by Douglas et al (3) and Kasapi and Gosline (12)

Development of the FEA microstructural model

The morphometric analysis provided the data to construct a finite element model (see Figure I) of the structural and geometric arrangement of the hoof wall. In developing this model, the microstructure of the hoof wall was considered as a 2 component (phase) hollow fibre reinforced composite. Each phase was treated as an isotropic linearly elastic component with perfect bonding assumed at the interface between the horn tubules and the intertubular horn. The geometric structure was simplified by assuming a hexagonal array of repeating horn tubule units each possessing an elliptical cross section in line with the mean major to minor axis ratio. The absolute dimensions of the horn tubule, cortex and medullary cavity were similarly based on the mean recorded values. The inter-fibre spacing combined with the absolute tubule dimensions, was used to generate a fibre density (tubule density) consistent with the area fraction data recorded

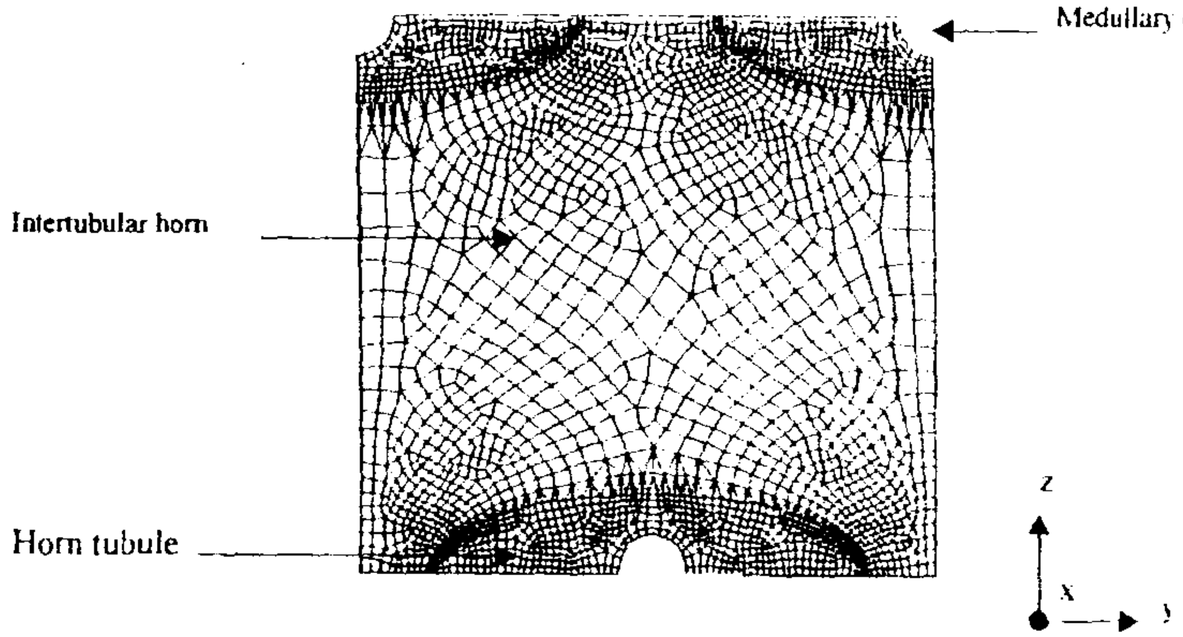

Figure I - A simplified 2-phase finite element microstructural model of a transverse section of the 'outer' hoof wall region to show the structural and geometric organisation of the horn tubules and the intertubular horn

Determination of the possible Moduli

The Youngs modulus (E) for the composite can be approximated using the simplified equations for unidirectional laminae as explained in Hull (18). There are difficulties in applying these equations directly to equine hoof, as neither the modulus of the tubule nor the intertubular matrix modulus is known. However, if a modulus ratio (K) of E tubule to E matrix (Et/Em) is introduced then an assessment of the possible variation in moduli for a range of E ratios is possible. This can then be used to investigate experimentally determined values of modulus with a view to extracting a tubule and matrix modulus

Table I - Axial and lateral modulus values reported for the equine hoof

Source	Hoof Wall Region	Axial modulus (Ex) N/mm^2	Lateral modulus (Ey) N/mm^2	Axial to lateral moduli ratio	Moisture content
Douglas et al (1996)	Outer	998	912	1 : 1.09	27.9%
Kasapi and Gosline (1997)	Outer	560	310	1 : 1.81	35.0%

A range of values for the Modulus ratio K, (Et/Em) was selected based upon previously reported mechanical testing data as shown in Table I. From this information it can be seen however, that the ratio of axial modulus (Ex) to lateral moduli (Ey) is not well defined. Figure II shows that if equations for axial and lateral modulus are used, at a tubular volume fraction of 0.2 (mean value for donkey hoof wall - Collins unpublished data), then K values between 0.28 – 3.50 provide data that lies within the range of experimental results reported for equid hoof horn.

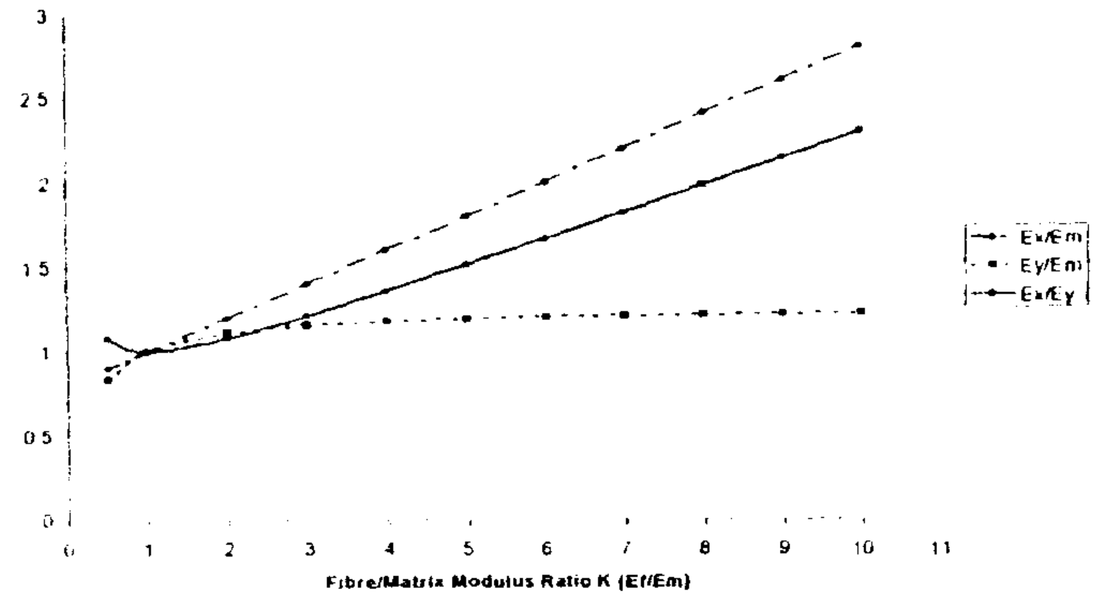

Figure II Variation in the theoretical modulus ratios in the x and y direction with increasing tubule/matrix modulus ratio as determined by 'rule of mixtures'.

Based upon these values and the area fraction data obtained from the morphometric analysis, the axial and lateral moduli were determined using 'rule of mixtures' and the modified Hull equations. In this way, theoretical moduli were determined for the 'outer' hoof wall region.

It was assumed that the volume fractions of tubular and intertubular horn were the same as the area fraction values determined experimentally. In addition by expressing the predicted moduli in Ex and Ey directions by convention as a ratio to the matrix modulus Em, the reinforcing effect of the structural organisation upon the matrix material can be evaluated for different values of K. By this means, it can be anticipated that a fibre composite structure reinforced in a given directional plane would display an E modulus in that direction > Em.

FEA Macromechanics

FEA was used to determine the lateral (Ey) modulus by a fixed displacement approach. This was achieved in each direction by applying a unit displacement on one edge in the direction required, and restraining the other edge with stiff boundary elements of known stiffness constant

adjacent to the apex of the tubule minor axis to the apex of the major axis. With regards to the strain distribution within the tubular elements, the position of maximum strain was located at the boundary of the medullary cavity normal to the direction of loading.

DISCUSSION

This paper represents a logical progression to our former FEA modelling studies conducted at the gross anatomical level Newlyn et al (16). It represents the first study to use this technique to investigate the macromechanical and micromechanical behaviour of the equine hoof wall, during loading, at the microscopic level of the structural hierarchy. The information provided enables further refinement of our hoof wall model and will help unravel the function / design complexity of the equine hoof capsule.

Confidence in modelling techniques should always be tested by comparing the output with the results from experimental work. In this respect the results of FEA combined with simplified theoretical composite equations are consistent with the experimental data from mechanical tests reported by Douglas et al (3). Such an agreement, in itself, does not confirm that hoof horn is truly a composite material but the findings reported here do lend further support to the assertion of Reilly et al (8) and Cope et al (1) that it may operate as a unidirectional fibre composite.

Whilst the value of the ratio of axial to lateral modulus at < 2 may appear to be very small in comparison with those regularly encountered in synthetic composites it is not unexpected as both the tubular and intertubular horn are essentially different structural arrangements of the same cellular material. This is typical of many biocomposites. Consequently the ratios of Ef to Em are typically low in comparison with synthetic composites. Although no previously published values exist for equid hoof horn Hogan (15) cites Ef/Em estimates for cortical bone ranging from 1:1 to 10:1.

Similarly, the tubule volume fraction values may be considered to be relatively low when compared to synthetic composites. However, Saliba (19) stated that natural composites are optimum structures best suited to an organism in its natural environment. In this respect, the hoof wall may be optimised naturally to achieve a balance between accommodation and resistance of loading forces so as to dampen concussive forces without failure. It is also important to note that material in the MDC of the hoof wall is subjected to biaxial compression during static loading Thomason et al (17), Newlyn et al (16). In this respect a material that exhibits a modest Ex/Ey may be adaptive. In addition, Curiskis and Feughelam (20) modelling composite fibres reported that the greatest rate of change in Ey/Ex for a given fibre volume fraction increase, occurred in the range of 0-25%. Thus, the volume fraction of the hoof wall may be optimised in order to achieve the greatest potential modulation of the mechanical properties at least cost to the animal.

The results of this study demonstrate that the use of FEA with models derived from the morphometric analysis of the hoof wall can predict values of E moduli consistent with those obtained from theoretical expressions and experimental results. On this basis, FEA represents a valuable modelling technique that can be further employed to developing our understanding

of the structural mechanical relationship at this level of the hoof wall hierarchy.
Given that the FEA modelling technique provides results consistent with those from the modified Hull equation at the macromechanical level, reasonable confidence can be expressed in the theoretical predictions at the micromechanical level. This assertion is further supported by work of Hull (18) and Saliba (19) who recorded stress concentration factors in synthetic composite materials at a volume fraction of .25 and below, similar to those predicted for the hoof wall models at ~2 even in the case of high Ef/Em ratios.

The stress concentration factors predicted within the tubular components are significantly affected by the presence of the medullary cavities. These cavities act as stress concentrators within the structure during loading and their presence results in the generation of stress in the direction of loading. The stiffer the tubular cortex, the lower the stress concentration at these sites due to the reinforcing effect of the cortex. This structural arrangement may serve to protect the medullary cavity from strain and thereby protect the capsule from failure.

The predicted results indicate that at an Et/Em value > (4 - 4.5) the strain is transferred from the tubule to the matrix, i.e. away from the medullary cavity. At this point the matrix is taking the majority of the deformation; this may represent a means of increasing and preserving the integrity of the structure. The pattern of strain gradient may be instructive in determining the susceptibility to crack production and deviation. However, it is appreciated that perfect bonding at the tubular-intertubular interface has been assumed in these models. If the structural organisation of this boundary were such that a compliant or viscous interface is formed, then, the resultant stress concentration would be significantly reduced.

The presence of a large number of tubules per unit area in the 'outer' region may significantly increase the work of fracture by creating a 'tortuous jagged path' to inward crack propagation Reilly et al (6). As energy is absorbed in the separation of two different phases Vogel (5), the tubular-intertubular interface may produce an effective crack stopping mechanism Bertram and Gosline (21) Reilly et al (8) Kasapi and Gosline (12). Conversely it may be argued that localised stress concentrations jeopardise the material by reducing the total energy required to cause fracture Griffith (22). Thus the tubular density in the 'outer' hoof wall might serve to concentrate stress in this part of the hoof wall, so as to achieve the controlled elimination of damaged hoof wall and protect the capsule from catastrophic failure.

The accuracy of the model is highly dependent upon the assumptions made. The assumptions made in this model were, a hexagonal geometric array, isotropic material properties, linear elasticity, perfect bonding, and ignoring the effects of other levels within the structural hierarchy.

Work is in progress to model this complex material using finite element analysis at the microscopic level of the structural hierarchy, in response to the stress distribution predicted by the gross anatomical model. An accurate model for the hoof wall will enable prediction of changes in the macro and micromechanical performance due to changes in the microstructure, which can occur in certain pathological states and in response to nutrition.

The application of Finite Element Analysis to the structural performance of the hoof wall extends and complements the range of experimental techniques that have formerly been used to evaluate hoof wall function. A better understanding of the function of the hoof as a load-bearing component can be provided by a detailed evaluation of the possible contribution of the various components of the material to its overall performance. In this respect FEA provides the means to assess both the macromechanical and micromechanical performance of the hoof.

ACKNOWLEDGEMENTS
The Donkey Sanctuary, Sidmouth, Devon is thanked for the funding of studentship for SNC and LH

REFERENCES

1 Cope BC, Hopegood L, Latham RJ, Reilly J D, In 'The Materials Congress, Proceedings of the Institute of Materials Conference, Cirencester, 6-8 April 1998.
2 Leach DH, The structure and function of the equine hoof wall PhD Thesis, University of Saskatchewan, (Saskatoon), 1980.
3 Douglas JE, Mittal C, Thomason JJ, Joftiet JC, Journal of Experimental Biology 199 (1996) 1829
4 Dyhre-Poulson P, Smedegaard HH, Roed J, Korsgaard E, Equine Veterinary Journal, 26 (1994) 362.
5 Vogel S, 'Life's Devices', Princeton University Press (New Jersey), 1988
6 Reilly JD, Collins SN, Cope BC, Hopegood L, Latham RJ, Equine vet. J. Suppl. 26 (1998) 4.
7 Pollitt CC, Equine Veterinary Education 4, (1992) 219
8 Reilly JD, Cottrell DF, Martin RJ, Cudderford D, Biomimetics 4 (1996) 23.
9 Rooney JR, Journal of Equine Medicine and Surgery 2 (1978) 107
10 Nickel R, Morph. Jahrbuch. 82 (1938) 119.
11 Sack WO, Hable RE, 'Rooney's guide to the dissection of the horse', Veterinary
12 Textbooks, (Ithaca, N Y) 1977
13 Kasapi MA, Gosline JM The Journal of Experimental Biology 200 (1997) 1639.
14 Wilkens H, Zentralblatt fur Veterinarmedizin, 11 (1964) 163
15 Reilly JD, Equine Veterinary Journal 27 (1995) 166
16 Hogan H A, Journal of Biomechanics 25 (1992) 549
17 Newlyn HA, Collins SN, Cope BC, Hopegood L, Latham RJ, Reilly JD, Equine vet. J. Suppl. 26 (1998) 103
Thomason JJ, Biewener AA, and Bertram JEA, Journal of Experimental Biology 166 (1992) 145
18 Hull D, 'An introduction to composite materials' Cambridge University Press (Cambridge) 1981
19 Saliba JF, Computers and Structures 61 (1996) 415
20 Curiskis JI, Feughelman M, Textile Research Journal 153 (1983) 271
21 Bertram JEA, Gosline JM, Journal of Experimental Biology 125 (1986) 29
22 Griffith AA, Philosophical Transactions of the Royal Society, Ser A, (1921) 221

OFF-AXIS COMPRESSIVE BEHAVIOR OF UNIDIRECTIONAL AND CROSS-PLY POLYMER MATRIX COMPOSITES

P N. MICHELIS and P D NICOLAOU
IMMG S.A
22 Askiton Str., Penteli, GR 15236, Greece

ABSTRACT

A series of uniaxial compression tests were conducted on two different PMC lay-ups i.e. unidirectionally reinforced and cross-ply [0° / 90°] in order to determine their response under compressive loading conditions, with the loading axis be at different orientation angles with respect to the fiber axis. The unidirectional one comprised an epoxy resin matrix reinforced with carbon fibers (15 plies), while the constituents of the cross-ply composites were rovimat 1200 and synolite 288 (also 15-plies). The test results revealed that the compressive strength of UD composites is quite sensitive to the orientation angle θ between the fiber and the loading axis. As θ increases, the compressive strength decreases very rapidly, however at an angle θ of approximately 30° it reaches a plateau. The experimental results allowed the establishment of the "maximum stress" criterion as being appropriate in predicting the compressive behavior. Similar trends were found for the variation of the elastic modulus of the composites versus the orientation angle. Contrary to the above, the cross-ply composites proved to be much less sensitive to the variation of the angle θ. In particular, the strength drop with the increase of the orientation angle is much smaller, likewise the elastic modulus. However, the gain of the strength insensitivity on θ was achieved in expense of the composite strength, which was fount to be quite lower in this case

1. INTRODUCTION

Polymer matrix composites (PMCs) represent an important class of materials for structural applications because of their high specific stiffness and strength. Usually, this type of materials comprises a polymeric matrix which is reinforced with long, high strength ceramic fibers, and because of their mechanical properties, they have established themselves as engineering structural materials. This came about not only because of the introduction of high performance fibers such as carbon, boron, and Kevlar, but also because of some new and improved matrix materials[1,2].

Because of the presence of the fibers, PMC materials possess highly anisotropic mechanical properties. The degree of anisotropy depends upon the fiber architecture and evidently the degree of anisotropy is reduced when the fibers are placed in different orientations in the plies[3]. Most common lay-ups comprise [0°], [0°/90°], and [0° / (+45°) / 90° / (-45°)] composites. In this study, the first two geometries were investigated, i.e. unidirectionally reinforced, and cross-ply [0° / 90°]. The former consisted of an epoxy resin matrix reinforced with carbon fibers (15 plies), while the latter comprised rovimat 1200 matrix synolite 288 fiber, 15-ply composites. In both cases the total fiber volume fraction

PROCEEDINGS OF THE

12th INTERNATIONAL SYMPOSIUM ON LAMENESS IN RUMINANTS

9th – 13th JANUARY 2002

Marriott World Center
Orlando, Florida, USA

Symposium Coordinator:

J.K. Shearer
Gainesville, FL, USA

Organizing Secretary:

Leslie C. Shearer
Gainesville, FL, USA

Preparation of Proceedings:
Linda F. Rose

Edited by:
J.K. Shearer

DISCLAIMER: Papers were printed as received from the author(s). Only format was changed where necessary to conform with proceedings guidelines.

A COMPARISON OF DIFFERENT MOISTURE-LOSS METHODS FOR MEASURING HOOF WALL MOISTURE CONTENT

Reilly J.D.,1 Newlyn H., Cope B., Latham R.J., Collins S. and Hopegood L
Faculty of Applied Sciences, De Montfort University, Leicester, England

It is well known that, in broad terms, the elastic modulus of hoof horn has a direct relationship with its moisture content (Leach 1980, Kitchener 1987, Bertram and Gosline 1987). In view of the high mechanical demand made on the hoof capsule, an understanding of the amount, type and control of moisture content within it are pre-requisites for further investigation of potential functional relationships between hoof horn moisture content and other objective parameters.

However, the methods by which moisture content in hoof horn is determined are not standardised. Different drying methods can cause differing moisture and volatile losses from hoof horn samples. This can make the determination of the moisture content of hoof horn variable and can make comparison between research results difficult.

The aim of this work was to determine the moisture-loss performance of wall horn samples using different moisture-loss methods. The methods tested were freeze-drying, vacuum drying, phosphorus pentoxide desiccation, room temperature drying and drying to 90, 100, 105, 110 and 120°C.

The different drying methods gave different absolute median values for hoof horn moisture content. Although each method has its specific advantages and disadvantages, the implications of the method used for drying hoof horn must be fully understood before the absolute result for moisture content is then used in the investigation, or interpretation, of further correlations with other functional hoof horn parameters.

A complete list of figures and references will be given on request by the authors.

A NOVEL METHOD OF ASSESSING HOOF HORN TUBULE DENSITY (TD) AND A COMPARISON OF TD IN THE HOOVES OF PONIES, HORSES, DONKEYS, CATTLE, SHEEP AND PIGS

Reilly J.D.,[1] Newlyn H., Cope B., Latham R.J. and Collins S.
Faculty of Applied Sciences, De Montfort University, Leicester, England.

The number of hoof horn tubules per unit area (tubule density TD) is thought to be an important determinent of "horn quality" in the cow (Politiek et al 1986) and in the pig (Geyer and Tagwerker 1986). 'Hardness' of horn is believed to be directly related to TD in cows (Gunther et al 1983) and in pigs (Geyer and Tagwerker 1986).

In this work TD was assessed using a simple but novel method. This involved dividing the hoof wall stratum medium using a grid. Previous workers have not taken this approach and have their quoted TDs for the whole or part of the hoof wall depth or have simply given descriptive reports of the way tubules are perceived to be distributed in the hoof wall. The new TD-counting method has revealed that the hoof wall of horses and ponies exhibit a unique four-zoned and stepped pattern, which is believed to have an important functionality and aids in preventing crack propagation (Reilly et al 1996, 1998).

Interestingly, this same method of TD assessment reveals that the stratum medium of donkey hoof horn exhibits a different pattern and the pig, sheep and dairy cow also have differing patterns of TD within their hoof walls. Objective information about this important and basic hoof horn parameter will enable further investigations of potential functional relationships within hoof wall to take place.

A complete list of figures and references will be given on request by the authors.

'Foot, Hoof and Fancy Fea'
A multidisciplinary approach to donkey hoof research

SN Collins[a], H Wealleans[a], L Hopegood[a,b], RJ Latham[a] , HA Newlyn[c], and JD Reilly[a,d]

a School of Molecular Sciences, De Montfort University, Leicester, UK.
b Dept Land Based Studies, Nottingham Trent University, Southwell, Nottingham, UK.
c Faculty of Engineering, Loughborough University, Loughborough, UK.
d Royal Army Veterinary Corps, Defence Animal Centre, Melton Mowbray, UK.

As the hoof capsule serves to suspend the skeleton and protect the sensitive structures of the foot, it is likely that the structural organisation of the hoof ultimately affects the animal's ability to achieve the painless transfer of locomotory forces and prevent infection[1]. Hoof related defects may lead to overt lameness and pose significant welfare and practical husbandry problems to the animal and its keeper[2]. In this respect, the adage *'no hoof no horse'* equally applies to the donkey. It has also been incorrectly assumed that the donkey hoof differs from that of the horse only in terms of size[3].

In order to rectify this situation there is a need to develop an objective understanding of the anatomical and functional relationships present within the normal donkey hoof. By achieving this it is possible to establish the interactions associated with the abnormal hoof [2]. This will lead to a scientific basis for improved hoof management regimes that will benefit the welfare of the donkey.

Effective hoof management is essential to the maintenance of economically important species such as the donkey and the horse, and such activity has hitherto been a skill rather than a science[2,4]. Traditional approaches to hoof pathologies have not yielded satisfactory results. In addition research into the equid hoof has traditionally focused on the horse. There is now a need for new thoughts and reasoning from other disciplines.

The Donkey Sanctuary is sponsoring non-invasive research within the Faculty of Applied Sciences at De Montfort University, Leicester, headed by Lt. Col J.D. Reilly RAVC MRCVS and Professor R.J. Latham to unravel the functional / design complexity of this locomotor structure. This investigation has adopted a novel multidisciplinary approach which allows the cross fertilisation of ideas across traditional departmental areas of interest. This approach has brought together the expertise of veterinarians, chemists, material scientists, animal scientists and mechanical engineers. This collaboration is proving extremely productive and is bringing new thoughts to old problems[4,5,6,7,8,9].

The hoof research group at Leicester is employing a variety of scientific techniques both to characterise the normal hoof horn parameters of the donkey and to compare these with other equid species. Donkey hoof association with diseased states such as laminitis is also being studied. Objective measurements are directed towards evaluating the degree of association of observed differences evident in abnormal horn. If there is a strong association with specific disease states then such horn parameters may serves as important markers and represent a powerful adjunct to traditional diagnostic and prognostic techniques such as x-rays.

Image analysis techniques have been developed to establish the distribution of horn tubules across the hoof wall in terms of tubule density (the number of tubules per mm^2)[1,10,11,12]. In addition further work is in progress to determine the way in which the size and shape of the

horn tubules varies across the hoof wall and around the hoof capsule. The structural arrangement of tubules is considered to be an important determinant of the functional capabilities of the hoof capsule (for example in limiting the propagation of cracks[1]) and the way in which forces are transmitted between the ground and the skeleton across the hoof wall[1].

The pony and the horse have different zones of tubule density, which change from outer to inner hoof wall[1,10]. For the donkey, however, there is no distinct zonation throughout the hoof wall, apart from the initial change in the curve at approximately 25% of the hoof wall depth. For the remaining hoof wall, the tubule density is fairly constant for the donkey[11]. Hoof horn tubule density patterns have also been studied in other species to reveal interesting differences[12].

The objective hoof horn parameters outlined above are being evaluated in relation to the material properties of the hoof. The modulus of elasticity and resilience of donkey hoof horn has been measured using material testing techniques and these important mechanical properties have been found to be highly modified by moisture content [4,8] .

Different gravimetric and thermo-gravimetric techniques are being used to establish the normal hydration levels within the hoof and the different ways in which the water interacts with the structure.

The objective differences outlined above may reflect important functional differences between the donkey and the horse. Perhaps differences in the way that they are grossly constructed, negates the need for the same mechanisms for stress transfer through the wall. This would bring into question the assertion that 'the donkey is but a small horse'.

A summary of the known differences between the properties of horse and donkey feet is given in the Table below. It is likely that with continued research, further interesting differences will be revealed.

Summary of Horse verses Donkey Comparisons

Parameter	**Horse** Equus caballus	**Donkey** ***Equus asinus***
Environmental adaptation	Adapted to the grassland plains of the temperate Steppe environment Trickle feeding on quality grasses	Adapted to the Arid plains Browsing on low quality herbage
Survival strategy	Highly evolved locomotor flight response Athleticism	Locomotor flight response? Stoical nature. Tendency to 'freeze' Sure footedness
Hoof Pastern Axis (HPA)	Straight HPA	Straight / broken forward HPA? – Axis masked by highly developed CB? HPA is more upright
Capsular shape	Circular solear profile Capsule inclined	'U' shaped solear profile with flare at heels. Capsule of upright, 'boxy' / quadrilateral appearance.

	Truncated cone?	Proportionally narrower than the horse Truncated cylinder?
Dorsal Hoof Wall Angle	Fore 45-50° Hind 55-60°	More upright by 5-10° Fore @ ~55° Hind @ ~62.5°
Lateral/medial angles	Inclined Lateral 101.57° Medial 101.37°	Almost perpendicular Lateral 91° Medial 88.5°
Capsular Dimensions Height ratio	MDC: Quarters: Heel 3:2:1	MDC: Quarters: Heel 3:3:1.5
Heel	Sloping heel	Strongly developed in the donkey – (Heel buttress) to give upright appearance
Solear weight bearing	Sole does not normally bear weight Sole height up to 10mm	Evidence of solear weight bearing? Sole height up to 13mm
Hoof wall depth (HWD)	Tapers from the MDC to the heel HWD at MDC ~ 10mm	Does not appear to taper significantly. HWD at MDC greater than the horse?
Perioplic groove	Merges with coronary groove	Widens at heel and fuses with frog
Frog	Intimate association with the hoof capsule. Contained within the other structures of the capsule.	Frog appears to be separate from the other structures of the capsule.
Suspensory Apparatus of the Distal Phallanx	Approx 600 laminae	Approx 350 laminae Laminae are broader than those of the horse
White line	2 - 3.5mm depth depending upon bwt	Normally not greater than 1 mm
Zona Nonpigmentosa	Evident within the horse Functional significance unknown	Not present?
Tubule Density	4 Zone Stepped pattern Zonal boundaries @ 25, 50, and 75% HWD	3 Zone? Curvilinear pattern Zonal boundaries @ ~ 30, and 50% HWD
Tubular horn organization	Distinct types of horn tubules present within the hoof wall. Tubule types vary 'across and around' the hoof wall. Arranged into distinct zonal populations	Broadly similar tubule types. Distribution of tubule types is markedly different from the horse
Moisture content In temperate climate	Physiological Moisture content in the order of ~ 25% Zonal variation across the HWD is unknown	Appears to be greater than the horse? @ ~33% Zonal variation across the HWD Z1 23% Z2 33% Z3 38%

Moisture Regain (gH_2O/100gDM)	Physiological Values Full HWD @ 33 g/100gDM Zonal values are unknown	Physiological Values Appears to be greater than the horse? @ ~49.25 g/100gDM Zonal values Z1 29.8 g/100gDM Z2 49.3 g/100gDM Z3 61.2 g/100gDM
Mechanical Properties	HWD: Modulus of elasticity at physiological moisture levels @ ~ 450 MPa Zonal moduli unknown	Comparable values for the donkey are markedly lower @ ~170 MPa, indicating that donkey hoof horn is more pliant. Modulus decreases across HWD Zonal moduli Z1 1223 MPa Z2 597 MPa Z3 397 MPa
Hoof Function	Recognized pattern of deformation during load bearing	Pattern not known Deformation not as pronounced?

Fundamental hoof horn measurements are being analysed in the context of how stresses and strains associated with loading are accommodated within the structure and how these forces are transmitted within the hoof capsule. Advances in our understanding of how the hoof wall may function are being made using the computer modelling technique of finite element analysis (FEA)[6].

As the baseline information is expanded, by establishing objective values for some of the important defining characteristics of hoof horn, the model will be further refined. In this way, it will be possible eventually to accurately predict the likely effect on capsular functioning of those changes brought about by nutritional or husbandry manipulation or by diseased states.

In order to achieve this aim, there is a need for a continued supply of basic information from fundamental studies of normal and abnormal horn production, associated with diseased states, and from controlled nutritional trials[2] and differing therapeutic regimes[5]. The advantages afforded by such a multidisciplinary approach will ensure continued progress in this vital yet often neglected area of animal science.

This will have far reaching effects in the world of farriery, veterinary medicine and animal welfare to the benefit of the donkey.

References

1 REILLY JD, COTTRELL DF, MARTIN RJ AND CUDDEFORD D (1996) Tubule density in equine hoof horn. *Biomimetics* **4** (1) 23-35.

2 REILLY, J.D. (1995) No hoof no horse? *Equine Veterinary Journal* **27**(3) 166-168.

3 REILLY, J.D. (1997) The donkey's foot and its care. In: *The Professional Handbook of the Donkey.* Ed: E.D. Svendsen. Whittet Books Ltd, London, pp.71-92.

4 COPE, B.C., HOPEGOOD, L., LATHAM, R.J., AND REILLY, J.D. (1998) Equine hoof horn: a natural engineering composite. In: The Materials Congress, Proceedings of the Institute of Materials Conference, Cirencester, 6-8 April, 1998.

5 COPE, B.C, HOPEGOOD, L., LATHAM, R.J., LINFORD, R.G., REILLY, J.D., SYMONS, M.C.R. AND TAIWO, F.A. (1998) Studies of equid hoof horn material by electron paramagnetic resonance. *Journal of Materials Chemistry.* **8** (1) 43-45.

6 NEWLYN, H.A., COLLINS, S.N.,COPE, B.C., HOPEGOOD, L., LATHAM, R.J. AND REILLY, J.D. (1998) Finite element analysis of static loading in donkey hoof wall. *Equine vet. J.* Suppl. **26** 103-110.

7 REILLY, J.D. (1998) Hail hoof science! *Equine vet. J.* Suppl. **26** 2-3

8 COLLINS, S.N., COPE, B.C., HOPEGOOD, L., LATHAM, R.J., LINFORD, R.G. AND REILLY, J.D.(1998) Stiffness as a function of moisture content in natural materials: Characterisation of hoof horn samples. *Journal of Material Science,* **33** 5185-5191.

9 NEWLYN, H.A., COLLINS, S.N.,COPE, B.C., HOPEGOOD, L., LATHAM, R.J. AND REILLY, J.D. Equid Hoof Horn: A natural engineering composite. In: Materials Solutions to Natures Designs. Conference Proceedings of the Institute of Materials. Cirencester, 6-8 April. Pp3-8.

10 REILLY, J.D., COLLINS, S.N., COPE, B.C., HOPEGOOD, L. AND LATHAM, R.J.(1998) Tubule density of the stratum medium of horse hoof. *Equine vet. J.* Suppl. **26** .

11 HOPEGOOD, L., COLLINS, S.N.,COPE, B.C., LATHAM, R.J AND REILLY, J.D. Tubule Density of the Stratum Medium of Donkey Hoof Horn. (In preparation).

12 REILLY, J.D., NEWLYN, H.,COPE, B., LATHAM,R.J., COLLINS, S AND HOPEGOOD, L (2002)
A novel method for assessing hoof horn tubule density (TD) and a comparison of TD in the hooves of ponies, horses, donkeys, cattle, sheep and pigs. In: Proceedings of the Twelfth International Symposium on Lameness in Ruminants, Orlando, Florida, Jan 9-13, p240.

Analyses of the moisture content of hoof horn from horses, donkeys and laminitic donkeys

L. Hopegood[1], S. N. Collins[2], R. J. Latham[2], J. D. Reilly[3]
1 The Nottingham Trent University, School of Land-based Studies, Brackenhurst, Southwell, Notts, NG25 OQF,Email: lyn.hopegood@ntu.ac.uk
2 De Montfort University, Faculty of Health and Life Sciences,The Gateway, Leicester, LE1 9BH, rjlatham@dmu.ac.uk, Email: scollins@dmu.ac.uk
3 Royal Army Veterinary Corps, Defence Animal Centre, Melton Mowbray, LE13 OSP

Introduction The moisture content of keratinous materials such as hoof horn is important as the presence of moisture has an inverse relationship on the mechanical properties of hoof horn and may have a subsequent effect on the function of the hoof. Methods previously used to dehydrate samples to calculate the moisture content of hoof horn vary considerably (Hopegood 2002). Subsequent comparison of results is therefore unreliable. A comparison of different methods of dehydrating hoof horn was therefore carried out to establish a standardised protocol for dehydrating hoof horn to assess its moisture content. The moisture content of donkey hoof horn from normal animals and those with laminitis has not been reported. Maclean (1971) established that the moisture content of cattle suffering from laminitis was significantly higher than normal hooves. The resultant standardised protocol from the first part of this study was then used to compare the moisture content of hoof horn samples taken from horses, donkeys and those donkeys that had suffered from laminitis.

Materials and methods Samples for comparison of different methods of dehydrating donkey hoof horn to ascertain the moisture content were taken from clippings removed from the left forelimb of 31 donkeys during regular farrier treatment at The Donkey Sanctuary, Sidmouth, Devon. Samples were immediately wrapped to prevent moisture loss. Nine adjacent samples, encompassing the full hoof wall depth (HWD), were removed from the Midline Dead Centre (MDC) of the clipping. Samples were randomly allocated to one of the drying methods: room temperature, vacuum drying, freeze-drying, drying over phosphorus pentoxide, oven drying at 90, 100, 105, 110, 120°C. Samples were weighed daily until they established equilibrium mass. The moisture contents were calculated with reference to the original mass of samples. Samples of horse hoof horn were obtained from the clippings removed from the left forelimb of 16 unshod animals at the Friends of Bristol Horses Society. The laminitic samples of donkey hoof horn were obtained from the left fore hoof capsules from 15 donkeys from The Donkey Sanctuary that had been euthanased for reasons other than this study. Samples were removed from the MDC of the capsules at 50% hoof wall height. One full HWD sample was removed from the horse and laminitic donkey hoof samples. All samples were then dehydrated over phosphorus pentoxide.

Results The moisture contents of samples dried by the different methods varied between 250-360 g/kg. The results for each technique were significantly different to those from at least 4 other methods ($p<0.05$, Mann-Whitney *U* tests). As samples dried over phosphorus pentoxide avoided both the unknown effect of high and low temperatures on hoof horn, showed a normal distribution and low variability (Coefficient of Variation (CV) of 6%) compared to other results (ranging 4-44%) this technique was then used to compare the moisture contents of further samples of hoof horn.

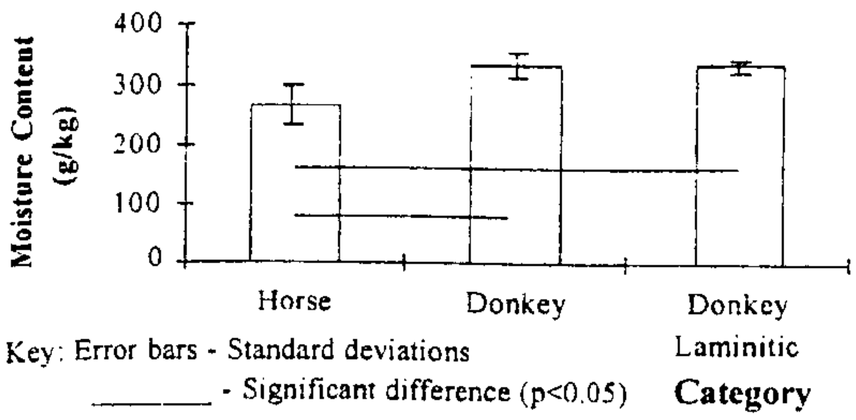

Figure 1 Comparison of Moisture Contents

There were significant differences between mean moisture contents from each data set (ANOVA, $p<0.05$). The moisture content for horse hoof horn was significantly lower than that for both donkey clippings and from laminitic hoof horn (Tukey Test, $p<0.05$) (Figure 1). There was no significant difference between the moisture content of donkey clippings and laminitic hoof horn (Tukey Test, $p<0.05$).

Conclusions A comparison of results of moisture contents of hoof horn in the literature should not be carried out unless the same drying techniques are used as different drying techniques result in different moisture contents. The moisture contents of donkey hoof horn, for both clippings (332 g/kg) and laminitic samples (332 g/kg) are higher than for horse hoof horn (264 g/kg). This may have implications for the practical management of both donkey and horse hoof horn and may be the reason why donkeys appear to suffer particular hoof problems. Laminitis may not affect the moisture content of hoof horn samples although it should be borne in mind that different sample sites were used.

References

Hopegood, L. (2002) *Tubule Density, Moisture Content and Mechanical Properties of Donkey Hoof Horn.* PhD Thesis, De Montfort University.
Maclean, C.W. (1971) The histopathology of laminitis in dairy cows. *J. Comp. Path.* **81**, 563-570.

VETERINARY & FARRIERY PRACTICE
THE COMMON GROUND

TUESDAY – 21 OCTOBER 2003

BRITISH EQUINE VETERINARY ASSOCIATION
in association with
NAFB & AE

STONELEIGH PARK
KENILWORTH

Sponsored by
Janssen Animal Health

Adequan
Imavérol

N.A. F.B.A.E.

British Equine Veterinary Association Trust

JANSSEN

FURTHER THOUGHTS ON THE CARE OF DONKEY'S FEET

Michael Crane BVSc, MRCVS

Objective information on the specific problems of the donkey hoof is scarce. In order to rectify this situation The Donkey Sanctuary is sponsoring non-invasive research within the Faculty of Applied Sciences at De Montfort University, Leicester. The hoof research group at Leicester is employing a variety of scientific techniques to characterise the normal hoof horn parameters of the donkey and to compare these with other equid species and disease states.

Further results of these ongoing studies will be published in the near future. Three areas of practical significance are highlighted here. I am particularly indebted to Simon Collins, Lyn Hopegood and Heidi Wealleans for their contribution to this work and permission to use some of their results.

1. Structure

It is well recognised that the donkey hoof is grossly different from that of the horse, being more upright, "U" shaped in profile with well developed heels. It can be described more as a truncated cylinder rather than the truncated cone of the horse/pony hoof. Through the use of computer modelling techniques one can analyse these differences and look at how these different structures may function when loaded. As more information is gained it may be possible to predict the impact on capsular function of disease states and changes in husbandry and farriery practice.

At a microscopic level the "composite" type structure is suggested. Differences exist in tubular density and distribution between the donkey and the horse. In the donkey tubules of a broadly similar type decline in density from a maximum of ~35 tubules/mm^2 in the outer hoof wall until ~50% hoof wall depth then remain constant at approximately 9 tubules/mm^2. The horse shows a more "stepped 4 zone pattern". It has been proposed that this reflects a species adaptation related to differing natural lifestyles that impose different demands on the foot, or differences in the way the hoof functions.

2. Moisture content and mechanical properties

Moisture content is believed to be important for the function, quality and mechanical properties of hoof horn. Water acts to plasticise keratin making it more pliant, the moisture content accounts for over 90% of the variation in the stiffness of donkey hoof horn. The moisture content of the hoof increases in a dorso-palmar direction across the hoof wall ("out to in") with a resultant decrease in "stiffness" (modulus of elasticity). This gradient may contribute to accommodating the necessary stress transfer across the hoof wall helping to protect the inner sensitive tissue.

The moisture content of donkey hoof is significantly greater than the horse and it is therefore more pliant, with laminitic horn being even more deformable.

The hoof horn would actually appear to be at levels of almost maximum hydration in the living animal. Small changes in this moisture content potentially have a significant impact on the structural characteristics of the hoof capsule.

3. Radiography

Evaluation of radiographic parameters has been used to assess the nature and extent of changes to the distal skeleton subsequent to laminitis in the horse. Radiographs from donkeys with apparently normal feet with no history of laminitis have been compared to both the horse and with donkeys affected by changes consistent with laminitis. Initial results suggest that some of the guidelines advocated for the interpretation of radiographs of the horse/pony should be revised for the donkey. "The founder distance" (the perpendicular linear distance between the proximal limit of the dorsal hoof marker and the proximal margin of the extensor process) being of particular note – with no significant difference between the two populations.

It must be noted that these studies have been conducted on donkeys from a temperate climate. Future work will endeavour to extend these studies to include animals from a more arid natural environment.

However there is little doubt that keeping donkeys in the UK predisposes them to foot problems. Both farriers and vets will hopefully benefit from an awareness of the common disorders encountered.

Trimming the overlong foot

- Assess for evidence of "chronic laminitis" (consider lateral weight bearing radiographs with markers if in doubt).
- Attend to "bearing surface" first (incremental sole trimming guided by "thumb pressure" test).
- Dress back toe/wall (guided by pastern axis and angle of proximal hoof wall at mid line).
- Check balance and gait post trim (consider advice on management, bedding and analgesia post farriery).

Pedal sepsis

- Commonest cause of acute severe lameness.
- Abscesses frequently track proximally from the white line – may rupture at coronary band.
  Consider: Resecting overlying hoof wall.
  Tetanus prophylaxis
  Analgesia and appropriate management to avoid hyperlipaemia.
  Abaxial sesamiod nerve block.
- Sub-solar abscesses often associated with terminal founder and pedal bone degeneration.

arrangement of the structural elements and could therefore be limited to two spatial dimensions. Input of the model is the activation of the muscle fibre system and the structural arrangements and tissue mechanical properties, output is the movement of an array of distributed masses that are accelerated by fibre forces (muscle and connective tissue) and pressure gradient within the tissue. The model demonstrates that the suggested elastic projection mechanism is indeed quantitatively feasible as similar projection performances are obtained as observed on high-speed videos.

A7.4–The effect of manupulation of the moisture content on the mechanical properties of full and partial hoof wall depth samples of donkey hoof horn

L. Hopegood, Nottingham Trent University; S. Collins, B. Cope, R. Latham, De Montfort University; H. Newlyn, Loughborough University; J. Reilly, Royal Army Veterinary Corps

The inverse relationship between moisture content and the mechanical properties of keratinous materials has not been reported for donkey hoof horn. This study examined, using three point bending tests, the effect of moisture content on the mechanical properties of full and partial hoof wall depth (HWD) samples of donkey hoof horn. A standardised method was used to assess the moisture content of the samples. Full HWD samples were tested at four different levels of hydration: at an in vivo moisture content, following drying over phosphorus pentoxide, fully hydrated and following equilibration at 75% relative humidity. The results indicated that there was an inverse relationship between moisture content and the mechanical properties of donkey hoof horn. There was a significant difference between all data sets ($p < 0.01$) except between those samples tested at an in vivo moisture content and those that were fully hydrated ($p > 0.05$). This may indicate there is a level of hydration beyond which there is no further change in hoof stiffness, thus providing a 'fail safe' mechanism. A stiffness gradient is believed to exist across the full HWD for horse hoof horn. However, previous studies did not control for changes in moisture content across the HWD. A lower moisture content exists in the outer hoof wall compared with the inner hoof wall. In this experiment the full HWD was divided into four sections and samples were tested at the same level of hydration. The results indicated that the mechanical properties did not vary across the four areas tested.

A7.5–Mechanical properties of the solear hoof horn of heifers before and during the first lactation – a prediction of lameness susceptibility

Betina Winkler, Jean K. Margerison and Charles Brennan, University of Plymouth

Mechanical tests were completed on samples of sole hoof horn taken from 20 heifers at 2 months before parturition (p1) and 100 days postpartum (p2). Simultaneously, all claws were assessed for the lesions score (LS) in the sole horn. Heifers were kept at pasture prepartum and housed loose in a straw bedded yard postpartum. Hoof samples were collected from all claws and analysed for elastic modulus (ELM) and puncture resistance (PR), each measurement was replicated five times on the same area of each claw. Data was analysed by ANOVA – GLM using period and claw as fixed effects. PR force of the sole horn was significantly greater in front claws (FC) when compared to hind claws (HC) ($P < 0.05$) (p1- FC 8.2, HC 7.4N, p2- FC 11.1, HC 10.3N). The PR force and ELM significantly increased postpartum compared with prepartum ($P < 0.01$) (p1- 7.8, p2- 10.7N and p1- 86.9, p2- 118.0N mm^{-2}), while the LS of the claw horn increased between periods ($p < 0.001$) (p1- 73.1, p2- 186.5). No significant difference in LS was found between FC and HC in the prepartum period, however LS was significantly greater in the HC compared with the FC in the postpartum period ($p < 0.001$) (HC 223.7, FC149.3). Prepartum ELM and PR force were not correlated with lesion score either pre or postpartum. However, postpartum ELM and PR force were significaly negatively correlated ($p < 0.01$) to the increase in lesion score between periods ($R = 0.651$). Mechanical tests reflected the changes in housing and in haemorrhage levels that occurred between p1 and p2.

A7.6–Bone strain in the goat radius throughout ontogeny: How in vivo bone strains relate to bone geometry and tissue microstructure

R.P. Main and A.A. Biewener, Harvard University

For years researchers have examined how the skeletal system accommodates the large size range seen among extant and extinct tetrapods. However, most of these studies have only been concerned with interspecific comparisons. Consequently, little work has examined intraspecific, or ontogenetic, changes in the skeleton as an animal increases in size and mass with age. The goal of the present study was to examine how in vivo bone strain magnitudes and cross-sectional strain distributions compare across different age groups within a species and how these strain patterns reflect the concomitant onto-